

FINAL REPORT

DO NOT DESTROY
RETURN TO LIBRARY

FRACTURE CONTROL OF H-O ENGINE COMPONENTS

by
J. T. Ryder

February 1977

PREPARED UNDER CONTRACT NO. NAS3-18896
FOR
NATIONAL AERONAUTICS AND SPACE ADMINISTRATION
LEWIS RESEARCH CENTER
CLEVELAND, OHIO

5 MAY 1977
MCDONNELL DUGLAS
RESEARCH & ENGINEERING LIBRARY
ST. LOUIS



LOCKHEED-CALIFORNIA COMPANY • BURBANK
A DIVISION OF LOCKHEED AIRCRAFT CORPORATION

M77-13098

NASA-CR-135137

1

1. REPORT NO. NASA CR-135137		2. GOVERNMENT ACCESSION NO.		3. RECIPIENT'S CATALOG NO.	
4. TITLE AND SUBTITLE FRACTURE CONTROL OF H-O ENGINE COMPONENTS				5. REPORT DATE February 1977	
				6. PERFORMING ORG CODE	
7. AUTHOR(S) J. T. Ryder				8. PERFORMING ORG REPORT NO. LR 27810	
9. PERFORMING ORGANIZATION NAME AND ADDRESS LOCKHEED-CALIFORNIA COMPANY P.O. BOX 551 BURBANK, CALIFORNIA 91520				10. WORK UNIT NO.	
				11. CONTRACT OR GRANT NO. NAS3-18896	
12. SPONSORING AGENCY NAME AND ADDRESS National Aeronautical and Space Administration Lewis Research Center Cleveland, Ohio 44135				13. TYPE OF REPORT AND PERIOD COVERED Contractor Report	
				14. SPONSORING AGENCY CODE 4423	
15. SUPPLEMENTARY NOTES					
16. ABSTRACT- The results of an experimental investigation designed to obtain the material characterization and fatigue crack propagation data necessary to establish the salient characteristics of a Ti-6Al-2.5Sn(ELI) alloy fuel pump impeller to be used in a cryogenic service environment are described. The primary objectives of the program were to: determine allowable initial defect sizes; define nondestructive inspection requirements; suggest a proof spin test procedure capable of assuring the design operating life of the bore region of a highly stressed rotor operating in a cryogenic environment. Among the different testing variables considered were: coupon orientation, frequency, load range ratio, and temperature. Data analysis correlated crack propagation data from conventional laboratory coupons with data from a parallel sided rotating disk used to model rotor stresses. Analysis results led to four major design recommendations when bore regions of fuel pump impellers to be operated in cryogenic environments are to be relatively highly stressed (ratio of hoop stress to yield stress at the bore >0.5). These conclusions are: 1) a proof cycle to assure rotor design life can not be conducted at room temperature without bore region plasticity; 2) similarly, a proof cycle at -253°C (-423°F) cannot be conducted without bore region plasticity; 3) potential claims that establishment of a NDI flaw screening program can assure rotor design life should be regarded with caution; 4) the most promising procedure to assure rotor design life is to develop and verify the concept of a proof cycle which will induce in the rotor appropriate post-proof cycle residual stress distributions.					
17. KEY WORDS (SUGGESTED BY AUTHOR(S)) titanium alloy life prediction fatigue crack proof testing propagation analytical cor- rotating component relation cryogenic temperature				18. DISTRIBUTION STATEMENT UNCLASSIFIED - UNLIMITED	
19. SECURITY CLASSIF. (OF THIS REPORT) UNCLASSIFIED		20. SECURITY CLASSIF. (OF THIS PAGE) UNCLASSIFIED		21. NO. OF PAGES 502	
				22. PRICE*	

FOREWORD

This applied research report describes an investigation of procedures necessary to develop a fracture control program for a fuel pump impeller component to be operated in cryogenic environments. The investigation was conducted by the Lockheed-California Company at the Rye Canyon Research Laboratory from 17 June 1974 through 5 August 1976 in fulfillment of National Aeronautics and Space Administration Contract NAS3-18896.

The contract was originally funded on 17 June 1974 to include only Tasks I through IV, described in the Introduction. As a result of technical progress, additional funding was granted on 12 May 1975 to conduct Tasks V through VII. Throughout the program, the work was sponsored by the NASA-Lewis Research Center, Cleveland, Ohio, under the constructive management and leadership of Mr. G. T. Smith and Mr. J. A. Misencik.

The program was successfully performed by the Fatigue and Fracture Mechanics Laboratory of the Lockheed-California Company. Throughout the program, the Lockheed engineering project leader was Dr. J. T. Ryder. Major portions of the work were conducted in exemplary manner by three subcontractors: The Ladish Company, Cudahy, Wisconsin; the Convair Division of General Dynamics Corporation; the Solar Division of International Harvester.

The engineering project leader acknowledges the major contributions of several individuals. Foremost among these is Dr. G. E. Bowie whose contributions were so large as to have been invaluable. They are often referenced throughout this report. Dr. Bowie's help, knowledge and encouragement are gratefully acknowledged by the project leader. The many technical discussions with this colleague are warmly remembered as is the guidance of Mr. W. E. Krupp, Group Leader of the Fatigue and Fracture Mechanics Laboratory and the technical support of Mr. D. E. Pettit. Kind appreciation is extended to Mr. R. E. Ashcraft for his skill in detailed design of the high-pressure hydraulic precrack unit used in this project. The significant contribution of the author's long-time colleague, Dr. A. F. Grandt, of the United States Air Force, Air Force Materials

Laboratory, Wright-Patterson AFB, Ohio is pleasantly acknowledged because the quality of this report would have been greatly impaired without his assistance.

The author is pleased to thank Mr. Wm. D. Bauman and Dr. K. R. Kondas, NAVSEC, Washington, D. C. for finding the time to critique the manuscript. Special thanks is extended to Ms. H. Bozarth for typing and preparing the manuscript for print. Finally the efforts of the several technicians who worked on this project, especially those of Mr. F. M. Pickel, are gratefully acknowledged.

Several individuals of the various subcontractors are singled out for appreciation. They are: Mr. A. F. Hayes and Mr. A. J. Vasquez of Ladish for exacting production of the forgings and for material characterization; Mr. W. E. Witzell of Convair for the generation of mechanical property data; Mr. L. Whittler of Solar for accomplishing the spin pit work with meticulous care.

More than a decade ago, a team of applied mechanics and materials engineers at the Turbine Division, Boeing Airplane Company, Seattle, Washington, performed studies on low cycle fatigue of impellers. The work was led by J. Brunso, with contributions by K. Meisl, R. Schedin, R. Bergstrom, H. Moreen, C. Lewis, R. Varanasi and others. Elements of the present study, such as unflawed disk burst speed prediction, parallel sided disk spin arbor design, and elastic-plastic stress analysis methods were influenced strongly by their work. The present study was performed to a large extent from a fracture mechanics rather than low cycle fatigue viewpoint. Yet a practice of causing bore yield prior to final impeller machining, developed by J. Brunso and his colleagues through experience, proved to be a major recommendation of the present fracture mechanics study. This report is respectfully dedicated to the farsighted work of the above individuals.

SUMMARY

The program described in this report was directed towards providing material characterization data, tensile and fracture toughness data, as well as crack propagation data necessary to establish the salient characteristics of a Ti-5Al-2.5Sn extra-low-interstitial (ELI) alloy fuel pump impeller to be used in a cryogenic service environment. A major objective was to correlate crack propagation data from conventional laboratory coupons with data from a parallel sided rotating disk used to model rotor stresses. Based on this correlation, the overall objectives were to determine allowable initial defect sizes, to define nondestructive inspection requirements, and to suggest a proof spin test procedure capable of assuring the design operating life of the bore region of a highly stressed rotor operating in a cryogenic environment.

Tensile and static fracture toughness properties in different parent forging orientations were obtained at room temperature in laboratory air and at -253°C (-423°F) in liquid hydrogen. Additional variables studied in the fatigue crack growth testing were load ratio and frequency effects. Static test results showed a large increase in yield and ultimate tensile strength at -253°C (-423°F), compared to room temperature, as well as a reduction in fracture toughness properties. Fatigue crack growth behavior was independent of coupon orientation or of frequency, but depended on load ratio and, at high stress intensity levels, on temperature.

Parallel sided disk fatigue crack growth and burst phenomena were studied in a room temperature spin pit test phase of the program. Traditional burst speed predictions were found to be satisfactory for unflawed disks. Provided that flaws in pre-cracked disks were sufficiently small, the prediction of burst speed on the basis of laboratory coupon fracture data was also found to be satisfactory. Fatigue crack propagation behavior observed for rotating disks was similar morphologically to that for laboratory coupons tested at the same stress intensity levels.

Analysis and correlation of the laboratory and spin pit results led to four major design recommendations when bore regions of fuel pump impellers to be operated in cryogenic environments are to be relatively highly stressed (ratio of hoop stress to yield stress at the bore $\sigma_{\theta\max} / \sigma_{ys} > 0.5$). These recommendations are: 1) a proof cycle to assure rotor design life cannot be conducted at room temperature without bore region plasticity; 2) similarly, a proof cycle at -253°C (-423°F) cannot be conducted without bore region plasticity; 3) potential claims that establishment of a NDI flaw screening program can assure rotor design life should be regarded with caution; 4) the most promising procedure to assure rotor design life is to develop and verify the concept of a proof cycle which will induce in the rotor appropriate post-proof cycle residual stress distributions.

Further conclusions based on the results of this program are: 1) establish that the maximum rotor bore stress of interest is or is not greater than $0.5 \sigma_{ys}$; 2) if $\sigma_{\theta\max} < 0.5 \sigma_{ys}$, assure design life by establishing a reliable NDI flaw screening program (preferably ultrasonic) for flaws greater than 2.54 mm (0.1 in.); 3) if $\sigma_{\theta\max} > 0.5 \sigma_{ys}$, verify by experiment and analysis the adequacy of a proof test cycle which upon unloading induces compressive residual bore stresses; 4) if $\sigma_{\theta\max} > 0.5 \sigma_{ys}$, and Conclusion 3 is found to be unworkable or unacceptable, then an extensive low cycle fatigue analysis and experiment program should be initiated in order to assure rotor design life by means of an extremely conservative approach.

TABLE OF CONTENTS

<u>Section</u>	<u>Page</u>
FOREWORD	iii
SUMMARY	v
LIST OF ILLUSTRATIONS	ix
LIST OF TABLES	xvii
1.0 INTRODUCTION	1
1.1 Program Objectives	1
1.2 Program Outline	2
2.0 PROGRAM OVERVIEW	7
2.1 Material Selection Background	7
2.2 Program Test Matrix	8
2.2.1 Material Characterization	8
2.2.2 Specimen Fabrication	10
2.2.3 Mechanical Properties Test Matrix	18
2.3 General Test Procedure	25
2.3.1 Tensile Test Procedures	30
2.3.2 Fracture Toughness Test Procedures	31
2.3.3 Compliance Calibration Procedures	32
2.3.4 Fatigue Crack Propagation Test Procedures	38
2.4 Rotational Specimen Test Procedures	38
2.4.1 Stress Analysis	43
2.4.2 Prediction of Burst Speed	44
2.4.3 Test Procedures	61
3.0 MATERIAL CHARACTERIZATION	61
3.1 Material Fabrication	77
3.2 Tensile Properties	92
3.3 Fracture Toughness Properties	94
3.4 Compliance Calibration Results	107
4.0 FATIGUE CRACK PROPAGATION RESULTS	107
4.1 Orientation Effects	112
4.2 Frequency Effects	112
4.3 Effect of Range Ratio	133
4.4 Effect of Temperature	133
4.5 Effect of Lot to Lot Variation	133
4.6 Summary of Results	144
4.7 Prediction of Life Analysis	

TABLE OF CONTENTS (Continued)

<u>Section</u>		<u>Page</u>
5.0	ROTATIONAL DISK STUDY RESULTS	151
5.1	Burst Tests	152
5.2	Crack Growth Tests	166
5.3	Discussion	176
6.0	PREDICTION OF DISK LIFE	195
6.1	Fracture Control Concepts	195
6.2	Proof Test Concepts	196
6.3	Rotor Design Life Analysis Procedures	199
6.4	Example of Rotor Design Life Analysis Procedure	201
6.5	Applications to Practical Rotor Design	212
7.0	CONCLUSIONS AND RECOMMENDATIONS	215
7.1	Conclusions	215
7.2	Recommendations	217
	REFERENCES	219
	APPENDIX	
	DISTRIBUTION LIST	

LIST OF ILLUSTRATIONS

<u>Figure</u>		<u>Page</u>
1	Program Flow Chart	3
2	Program Considerations for Fracture Control of H-O Engine Components	4
3	Specimen Layout Drawing for Pancakes 1 through 11	11
4	Specimen Layout Drawing for Pancakes 12 and 13	12
5	Specimen Layout Drawing for Pancakes 14 and 15	13
6	Specimen Layout Drawing for Pancake 16	14
7	Layout Drawing for Rotating Disk Specimens, Pancakes 19 - 28	15
8	Tensile Specimen Geometry	16
9	Compact Tension (WOL Type) Specimen Geometry	17
10	Disk Configuration for Precracking	19
11	Photograph of Disk Ready for Precracking	20
12	Final Configuration for Rotating Disk Specimens	21
13	Cryostat for Tensile Testing in a Tinius-Olsen Tensile Machine	29
14	Fatigue Crack Growth Coupon Being Tested in Laboratory Air	33
15	Fatigue Crack Growth Testing Equipment for -253°C Tests	35
16	Fatigue Crack Propagation Data for Ti-5Al-2.5Sn (ELI) at Room Temperature, R = 0.5, F = 10 Hz, Showing 2 σ Band Curves, Median Curve, and 1 σ Band (Design) Curve	39
17	Normalized Stress Intensity vs a/R_1 Showing the Function, f.	41

LIST OF ILLUSTRATIONS (Continued)

<u>Figure</u>		<u>Page</u>
18	Non-Dimensionalized Stress Intensity vs a/R_1 Showing the Function, g	42
19	Schematic of High Pressure Hydraulic Precracking System	45
20	Schematic of Frame Assembly Used to Preload Disks for Precracking	46
21	Spin Pit and Associated Control Equipment	48
22	Speed Spectrum from Rotational Crack Growth Test of Disk 25 which was Typical of all Rotationally Induced Fatigue Crack Growth Tests	49
23	Precrack Hole and Notch of Disk 19	50
24	Surface Crack of Disk 19 after Fatigue Precracking	50
25	Surface Crack of Disk 28 after Fatigue Precracking	51
26	Spin Shaft Used for Rotating Disks	52
27A	Spin Arbor and Associated Parts	53
27B	Spin Arbor and Associated Parts	54
27C	Spin Arbor and Associated Parts	55
28	Schematic Drawing of Disk Mounted on Spin Shaft and Arbor Assembly	56
29	Schematic of Cross-Section Through Assembly Used to Retain Disk in Case of Shaft Failure	58
30	Schematic of Spin Pit	59
31A	Top View of Pancake 17	66
31B	Edge View of Pancake 17	66
32	Macrostructure of Diametrical Cross-Section of Pancake No. 1, Etchant 10% HNO_3 , 8% HF	67

LIST OF ILLUSTRATIONS (Continued)

<u>Figure</u>		<u>Page</u>
33	Macrostructure of Diametrical Cross-Section of Pancake No. 9, Etchant 10% HNO_3 , 8% HF	68
34	Macrostructure of Diametrical Cross-Section of Pancake No. 16, Etchant 10% HNO_3 , 8% HF	69
35	Pancake Disk Forging	73
36	Typical Rotor Forging, Nominal Dimensions in mm (in.)	74
37	Photoelastic Study of Rotor Forging	75
38	Photoelastic Study of Pancake Forging	76
39	Microstructures (100X) from the Mid-Radius, Mid-Height Position of Pancake No. 1 in the Annealed Condition, Krolls Etchant	78
40	Microstructure (100X) from the Mid-Radius, Mid-Height Position of Pancake No. 9 in the Annealed Condition, Kroll's Etchant	79
41	Microstructure (100X) from the Mid-Radius, Mid-Height Position of Pancake No. 16 in the Annealed Condition, Kroll's Etchant	80
42	Microstructure (100X) from the Mid-Radius, Mid-Height Position of Pancake No. 18 in the Annealed Condition, Kroll's Etchant	81
43	Percent Difference between Experimental and Analytical Stress Intensity Calibration Function, C_3 , versus Normalized Crack Length, a/W , Based on Compliance Data of Coupons 11CR-2, 11RC-2, and 11SC-1	103
44	Effect of Orientation on Fatigue Crack Propagation Behavior of Ti-5Al-2.5 Sn (ELI) at Room Temperature $R = 0.05$, $F = 10$ Hz	108
45	Effect of Orientation on Fatigue Crack Propagation Behavior of Ti-5Al-2.5 Sn (ELI) at Room Temperature $R = 0.05$, $F = 0.1$ Hz	109

LIST OF ILLUSTRATIONS (Continued)

<u>Figure</u>		<u>Page</u>
46	Effect of Orientation on Fatigue Crack Propagation Behavior of Ti-5Al-2.5 Sn (ELI) at Room Temperature, R = 0.5, F = 10 Hz	110
47	Effect of Orientation on Fatigue Crack Propagation Behavior of Ti-5Al-2.5 Sn (ELI) at Room Temperature, R = 0.5, F = 0.1 Hz	111
48	Effect of Orientation on Fatigue Crack Propagation Behavior of Ti-5Al-2.5 Sn (ELI) at -253°C (-423°F), R = 0.05, F = 10 Hz	113
49	Effect of Orientation on Fatigue Crack Propagation Behavior of Ti-5Al-2.5 Sn (ELI) at -253°C (-423°F), R = 0.05, F = 0.1 Hz	114
50	Effect of Orientation on Fatigue Crack Propagation Behavior of Ti-5Al-2.5 Sn (ELI) at -253°C (-423°F), R = 0.5, F = 10 Hz	115
51	Fatigue Crack Propagation Behavior of Ti-5Al-2.5 Sn (ELI) at -253°C (-423°F), R = 0.5, F = 0.1 Hz, Specimen 5SR-2	116
52	Comparison of Fatigue Crack Propagation Behavior of Ti-5Al-2.5 Sn (ELI) at F = 10 and 0.1 Hz, R = 0.05, Room Temperature	117
53	Comparison of Suggested 1 σ Design Curves for Ti-5Al-2.5 Sn (ELI) at F = 10 and 0.1 Hz, R = 0.5, Room Temperature	118
54	Comparison of Fatigue Crack Propagation Behavior of Ti-5Al-2.5 Sn (ELI) at F = 10 and 0.1 Hz, R = 0.5, Room Temperature	119
55	Comparison of Suggested 1 σ Design Curves for Ti-5Al-2.5 Sn (ELI) at F = 10 and 0.1 Hz, R = 0.5, Room Temperature	120
56	Comparison of Fatigue Crack Propagation Behavior of Ti-5Al-2.5 Sn (ELI) at F = 10 and 0.1 Hz, R = 0.05, -253°C (-423°F)	121

LIST OF ILLUSTRATIONS (Continued)

<u>Figure</u>		<u>Page</u>
57	Comparison of Suggested 1σ Design Curves for Ti-5Al-2.5 Sn (ELI) at $F = 10$ and 0.1 Hz, $R = 0.05$, -253°C (-423°F)	122
58	Comparison of Fatigue Crack Propagation Behavior of Ti-5Al-2.5 Sn (ELI) at $F = 10$ and 0.1 Hz, $R = 0.5$, -253°C (-423°F)	123
59	Comparison of Suggested 1σ Design Curves for Ti-5Al-2.5 (ELI) at $F = 10$ and 0.1 Hz, $R = 0.5$, -235°C (-423°F)	124
60	Comparison of Fatigue Crack Propagation Behavior of Ti-5Al-2.5 Sn (ELI) at $R = 0.05$ and 0.5 , $F = 10$ Hz, Room Temperature	125
61	Comparison of Suggested 1σ Design Curves for Ti-5Al-2.5 Sn (ELI) at $F = 10$ Hz, $R = 0.05$ and 0.5 , Room Temperature	126
62	Comparison of Fatigue Crack Propagation Behavior of Ti-5Al-2.5 Sn (ELI) at $R = 0.05$ and 0.5 , $F = 0.1$ Hz, Room Temperature	127
63	Comparison of Suggested 1σ Design Curves for Ti-5Al-2.5 Sn (ELI) at $F = 0.1$ Hz, $R = 0.05$ and 0.5 , Room Temperature	128
64	Comparison of Fatigue Crack Propagation Behavior of Ti-5Al-2.5 Sn (ELI) at $R = 0.05$ and 0.5 , $F = 10$ Hz, -253°C (-423°F)	129
65	Comparison of Suggested 1σ Design Curves for Ti-5Al-2.5 Sn (ELI) at $F = 10$ Hz, $R = 0.05$ and 0.5 , -253°C (-423°F)	130
66	Comparison of Fatigue Crack Propagation Behavior of Ti-5Al-2.5 Sn (ELI) at $R = 0.05$ and 0.5 , $F = 0.1$ Hz, -253°C (-423°F)	131
67	Comparison of Suggested 1σ Design Curves for Ti-5Al-2.5 Sn (ELI) at $F = 0.1$ Hz, $R = 0.05$ and 0.5 , -253°C (-423°F)	132
68	Comparison of Fatigue Crack Propagation Behavior of Ti-5Al-2.5 Sn (ELI) at Room Temperature and -253°C (-423°F), $R = 0.05$, $F = 10$ Hz	134

LIST OF ILLUSTRATIONS (Continued)

<u>Figure</u>		<u>Page</u>
69	Comparison of Suggested 1σ Design Curves for Ti-5Al-2.5 Sn (ELI) at Room Temperature and -253°C (-423°F), $R = 0.05$, $F = 10$ Hz	135
70	Comparison of Fatigue Crack Propagation Behavior of Ti-5Al-2.5 Sn (ELI) at Room Temperature and -253°C (-423°F), $R = 0.05$, $F = 0.1$ Hz	136
71	Comparison of Suggested 1σ Design Curves for Ti-5Al-2.5 Sn (ELI) at Room Temperature and -253°C (-423°F), $R = 0.05$, $F = 0.1$ Hz	137
72	Comparison of Fatigue Crack Propagation Behavior of Ti-5Al-2.5 Sn (ELI) at Room Temperature and -253°C (-423°F), $R = 0.5$, $F = 10$ Hz	138
73	Comparison of Suggested 1σ Design Curves for Ti-5Al-2.5 Sn (ELI) at Room Temperature and -253°C (-423°F), $R = 0.05$, $F = 10$ Hz	139
74	Comparison of Fatigue Crack Propagation Behavior of Ti-5Al-2.5 Sn (ELI) at Room Temperature and -253°C (-423°F), $R = 0.5$, $F = 0.1$ Hz	140
75	Comparison of Suggested 1σ Design Curves for Ti-5Al-2.5 Sn (ELI) at Room Temperature and -253°C (-423°F), $R = 0.5$, $F = 0.1$ Hz	141
76	Fatigue Crack Propagation Data for Ti-5Al-2.5 Sn (ELI) at Room Temperature, $R = 0.05$, $F = 10$ Hz, Disk 29	142
77	Comparison of Fatigue Crack Propagation Data for Ti-5Al-2.5 Sn (ELI) Obtained from Pancake 29 and Pancakes 2, 7, 12, 13, 14 and 15, Room Temperature, $R = 0.05$, $F = 10$ Hz	143
78	Fracture Surface of Disk 27	155
79	Disk 19 after Burst Test	156
80	Fracture Surface of Disk 19	157
81	Fracture Surface of Disk 21	159

LIST OF ILLUSTRATIONS (Continued)

<u>Figure</u>		<u>Page</u>
82	Top Surface of Disk 21 After Being Spun to 66,850 rpm	160
83	Crack Tip on Top Surface of Disk 21 After Test	161
84	Crack Tip on Top Surface of Disk 21 After Test	162
85	Crack Tip on Bottom Surface of Disk 21 After Test	163
86	Crack Tip on Bottom Surface of Disk 21 After Test	163
87	One Half of Disk 24 After Burst	164
88	Fracture Surface of Disk 24	165
89	Fracture Surface of Disk 25	169
90	Fracture Surface of Disk 28	171
91	Fracture Surface of Disk 20	174
92	Fatigue Crack Growth Rate Data for Disks Compared to WOL Coupon Data	175
93	Comparison of Data for Coupon 5CR-2 and Previously Extrapolated WOL Data	177
94	Fracture Surface of WOL Coupon 5CR-2	179
95	High Stress Intensity Fatigue Crack Growth Rate Data for WOL Coupons at $R = 0.5$, Room Temperature	181
96	Comparison of High Stress Intensity Fatigue Crack Growth Rate Data to Previously Extrapolated WOL Data at $R = 0.5$, Room Temperature	183
97	Comparison of Ordered Fatigue Crack Growth Data for WOL Coupons to Rotating Disks	184
98	Fracture Surface of WOL Coupon 8CR-2	185
99	Fracture Surface of WOL Coupon 10CR-2	186
100	Fracture Toughness at Burst as a Function of a/R_1	189

LIST OF ILLUSTRATIONS (Continued)

<u>Figure</u>		<u>Page</u>
101	Fatigue Crack Growth Curves at Room Temperature for Use in Predicting Disk Life	192
102	Fatigue Crack Growth Curves at -253°C (-423°F) for Use in Predicting Disk Life	193
103	Relationship Between Flaw Size and Estimated Life for an Assumed Maximum Operating Stress	200
104	Establishment of Minimum Flaw Size by Proof Testing	200
105	Tangential and Radial Stress Distributions of Example Disk During Room Temperature Proof Cycle at 90,000 rpm	208
106	Tangential and Radial Stress Distribution of Example Disk at 0 rpm After Proof Cycle	209
107	Tangential and Radial Stress Distributions of Example Disk at -253°C (-423°F) and at 88,983 rpm Without Prior Proof Cycle	210
108	Tangential and Radial Stress Distributions of Example Disk at -253°C (-423°F) and at 88,983 rpm after Prior Proof Cycle at 90,000 rpm at Room Temperature	211

LIST OF TABLES

<u>TABLE</u>		<u>Page</u>
1	List of Number and Location of Rotating Disk Precrack Starter Holes	22
2	Mechanical Property Tests-Tensile	23
3	Static Fracture Toughness Tests	24
4	Cyclic Crack Growth Tests	26
5	Rotating Disk Test Matrix	27
6	Chemical Composition of Ti-5Al-2.5Sn(ELI)	62
7	Finished Dimensions of Ti-5Al-2.5Sn(ELI) Forged Pancakes	64
8	Hardness Survey Results for Top Surface Ti-5Al-2.5 Sn (ELI) Pancakes	65
9	Hardness Results for Tensile Coupons	82
10	Hardness Results for Compact Specimens	83
11	Tensile Properties of Ti-5Al-2.5Sn(ELI) Pancake Forgings at Room Temperature	85
12	Tensile Properties of Ti-5Al-2.5Sn(ELI) Pancake Forgings at -253°C (-423°F)	89
13	Fracture Toughness Test Results	93
14	Experimental Compliance Calibration Results Based on Equation (3) for Coupon 11CR-2 Tested at Room Temperature	96
15	Experimental Compliance Calibration Results Based on Equation (3) for Coupon 11RC-2 Tested at Room Temperature	97
16	Experimental Compliance Calibration Results Based on Equation (3) for Coupon 11SC-1 Tested at Room Temperature	98
17	Experimental Compliance Calibration Results Based on Equation (3) for Coupons 11CR-2, 11RC-2, and 11SC-1 Tested at Room Temperature	99

LIST OF TABLES (Continued)

<u>Table</u>		<u>Page</u>
18	Comparison of Compliance Derivative Calibrations Based on Equation (3) and Experimental Data of Coupons 11CR-2, 11RC-2 and 11SC-1	101
19	Comparison of Relative Crack Length Based on Optical Readings and on Compliance Measurements at -253°C (-423°F)	104
20	Parameters Used in Equation (6) for Calculating Compliance Based a/w Ratios for Crack Growth Coupons	106
21	Test Conditions and Numerical Analysis Summary	145
22	Comparison Between Predicted and Actual Fatigue Lives for WOL Coupons 29CR-1, 29CR-2	147
23	Comparison Between Predicted and Actual Fatigue Lives for WOL Coupons Tested at Room Temperature, $R = 0.05$, $f = 10$ Hz	148
24	Burst Speed Study	153
25	Fatigue Crack Growth Results for Disk 25	168
26	Fatigue Crack Growth Results for Disk 28	170
27	Proof and Fatigue Crack Growth Test Results for Disk 20	173
28	Comparison Between Predicted and Observed Disk Lives	188
29	Steps in Applying Fracture Mechanics Concepts to Fatigue-Crack Propagation Analysis	197
30	Flaw Detectability Limits for Various NDT Techniques	198
31	Effect of Maximum Rotor Design Operating Speed on Initial and Critical Crack Lengths	204
32	Effect of Load Range Ratio, R , on Initial and Critical Crack Lengths	207

1.0 INTRODUCTION

1.1 Program Objectives

The recent development of reusable upper stage spacecraft high pressure rocket engines for such applications as the space shuttle and space tug represents a significant extension of previous propulsion component design. The reusable nature of such components has necessitated careful consideration of procedures for insuring design life. The development of adequate procedures is severely influenced by the fact that these high pressure components must be of small size and weight which can only be achieved by employing high tip speed turbines and accepting the concomitant highly stressed impeller and turbine disks. The problem is aggravated for fuel pump impellers because the high stresses exist in rotor disks operated in the low temperatures of liquid hydrogen or oxygen.

At such high stresses and in the cryogenic environments of interest, titanium alloys such as Ti-5Al-2.5Sn(ELI) are used because of their low density and high strength. However, also due to the high stresses, rotor disks can be extremely sensitive to small initial defects. This problem is intensified by the reduction of an alloy's fracture toughness at cryogenic temperatures[1].

In order to adequately assure the design life of fuel pump disks subjected to the severe load and environment state described above, two primary analysis procedures are of interest: 1) low cycle fatigue and 2) fracture mechanics of fatigue crack growth. Only the latter procedure was considered in this program. In theory, fracture mechanics can be used to determine the critical defect size, a_c , which can cause premature disk failure as well as ascertaining the maximum initial flaw size allowable, a_i , for a required design life. Based on these flaw sizes and combined with crack growth data, inspection procedures or a proof cycle or both can be specified in principle to ensure that initial flaws are less than a_i and thus design life assured.

The program described in this report was directed towards providing material characterization data, tensile and fracture toughness data, as well as crack propagation data necessary to establish the salient characteristics of Ti-5Al-2.5Sn(ELI) alloy to be used in a fuel pump impeller in a cryogenic environment. A major objective was to correlate crack propagation data from conventional laboratory coupons with data from a parallel sided rotating disk used to model the rotor stresses. Based on this correlation, the overall objective was determination of allowable initial defect sizes, definition of non-destructive inspection requirements, and the design of a proof spin test capable of assuring the design operating life of the bore region of a highly stressed impeller rotor operating in a cryogenic environment.

1.2 Program Outline

Primary program flow features of the investigation are outlined in Fig. 1. The initial step was development and production of forgings and fabrication of test coupons and disks. Two lots of one heat were used in accordance with program support schedules. Tasks I, II and III established material, mechanical, static fracture toughness, and cyclic crack growth properties at the two temperatures (room temperature and -253°C) to be investigated. The results of these tasks were analyzed and correlated in Task IV.

Rotating disks were fabricated in Task V and tested in Task VI. Correlation of disk and laboratory coupon data was conducted in Task VII as was analysis of the proof spin test concept. The analysis results, material, load history and environmental considerations and fracture control concepts were combined to perform the design of the spin proof test, as illustrated in Fig. 2.

The results of Task VII provided the important link between the more conventional laboratory data and the proof spin test designed for the fuel pump rotor component. The final task of the program was delineation of the design recommendations based on the data and analysis and specific recommendations for procedures to be used to assure the structural integrity of a fuel pump impeller for use at cryogenic temperatures.

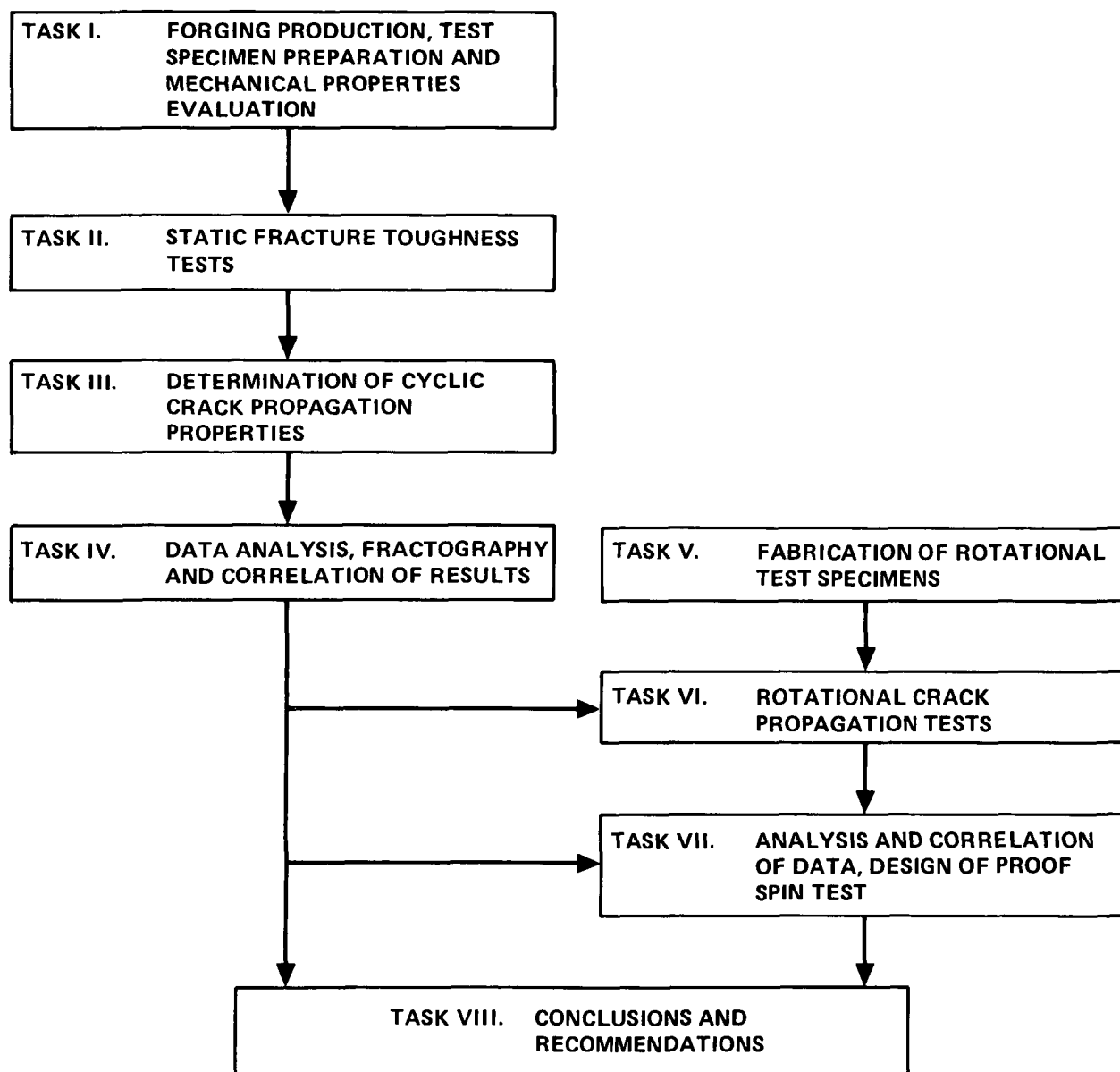


Figure 1.- Program Flow Chart

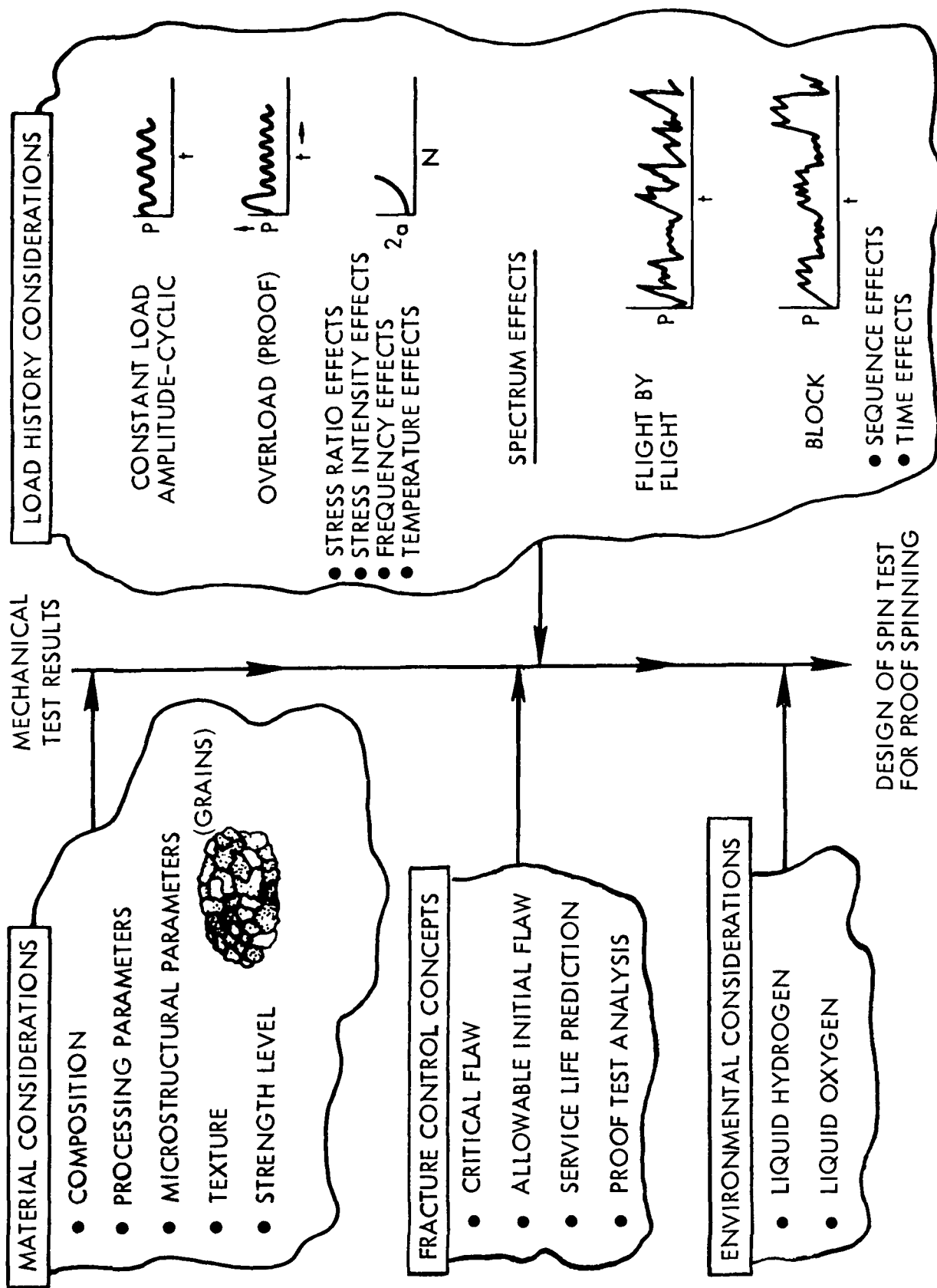


Figure 2. - Program Considerations for Fracture Control of H-O Engine Components

The pancake forgings were produced and all tensile, fracture toughness, and fatigue crack growth test coupons were machined at the Ladish Company, Cudahy, Wisconsin. Tensile, fracture toughness, and fatigue crack growth testing was conducted by the Convair Division of General Dynamics Corporation, San Diego, California, except for a few specialized tests conducted at the Lockheed-California Company's Rye Canyon Research Laboratory. Disks were spun at the Solar Division of International Harvester Company, San Diego, California.

Page Intentionally Left Blank

2.0 PROGRAM OVERVIEW

This program emphasized the delineation of the fracture control criteria necessary for design of a liquid hydrogen rotor component proof test and reduction of the incidence of service failure. This section presents a discussion of the material selection, program test matrix, general test procedures, and rotational specimen test procedures.

2.1 Material Selection Background

The Ti-5Al-2.5Sn(ELI) alloy was chosen by the NASA program administrator for this study. The alloy was selected specifically for use at cryogenic temperatures. This alloy is essentially an all-alpha phase alloy with excellent weldability. Presence of small beta stabilizer content (Fe and Mn) as an impurity can be detrimental to extreme low-temperature properties. The beta content in the alloy is therefore kept small and causes enough beta stabilization to be seen metallographically in the standard grade, but is not visible metallographically in the extra low interstitial (ELI) grade. This alloy is a non-heat treatable material and the ELI grade has somewhat lower properties than the standard grade [1, 2]. The microstructure at room temperature is essentially all-alpha with traces of beta phase from the residual iron content in the sponge. The alpha will have two forms: equiaxed or acicular.

The equiaxed structure is produced by mechanical working and annealing at temperatures in the alpha phase field while the acicular structure results from cooling from the beta phase field, i.e., at temperatures above the beta transus, approximately 1050°C (1920°F). Rapid cooling will produce a sharp, martensitic structure and slow cooling will produce a coarser, rounded acicular alpha grain structure. Holding in the beta field will also cause beta grain coarsening, and heating in the beta field, with no subsequent working in the alpha field lowers the ductility of the alloy.

Detrimental presence of ordered phases in the Ti-5Al-2.5Sn alloy is usually minimal [3]. The hexagonal close packed ordered compound Ti_3Al phase in titanium-aluminum alloys has virtually no solid solubility range, has a closed maximum at about 875°C, and on either side of the compound all ($\alpha + \text{Ti}_3\text{Al}$) two-phase fields exist. Some lowering of fracture toughness and stress corrosion resistance (K_{Isc}) has been attributed to Ti_3Al in other alloys [4].

Several investigations have reported on the effect of impurities and temperature on Ti-5Al-2.5Sn tensile properties. A Convair study [5] indicated that tensile properties are drastically reduced at -253°C (-423°F) by high iron and oxygen levels. Work at Convair and elsewhere [6] also indicated that the ultimate and tensile strengths of this titanium alloy are approximately doubled at -253°C (-423°F) as compared to room temperature properties.

Hydrogen reaction with titanium alloys has been rather extensively investigated (See Reference [7] for one summary). The summary report [7] indicates that Ti-5Al-2.5Sn has a high tolerance of, but readily reacts with, hydrogen. Normally, hydrogen embrittlement is not observed for this alloy when hydrogen concentrations are less than 250 ppm. A NASA Manned Spacecraft Center supported study indicated hydrogen can react with Ti-5Al-2.5Sn at room temperature and hydrogen embrittling can occur under certain conditions [8]. Another study [9] showed that very little reaction occurred in high pressure (1.72 MPa (250 psig)) hydrogen gas environment over a two-month storage period at temperatures of -73°C (-100°F).

2.2 Program Test Matrix

2.2.1 Material Characterization

The Ladish Company, Cudahy, Wisconsin, prepared twenty (20) press-forged pancake disks from a first billet of material and twelve (12) from a second lot. Each pancake was approximately 457 mm (18 in.) in diameter and 76 mm (3 in.) thick. Specimens were drawn from sections of the first 18 pancakes for tensile, fracture toughness and fatigue crack propagation behavior characterization. From the remaining pancakes of lot 1 and those of lot 2, disks for the spin pit investigation were manufactured as well as a few coupons for tensile, fracture toughness and fatigue crack propagation characterization.

The Ti-5Al-2.5Sn (ELI) material was completely characterized as follows:

1. Complete chemical analysis on the two lots of titanium used.
2. Cleanliness rating (according to the appropriate AMS specification) on the first lot of titanium used.
3. Two forging model studies, one for the pancake forging and one for a rectilinear rotor forging.
4. Texture results (pole figures) at the mid-radius, center position of the number one pancake forging.
5. Typical grain size determinations on the first, ninth, sixteenth and eighteenth pancakes.
6. Typical macrostructural and microstructural photographs of the RS plane (cut along the pancake diameter) of the first, ninth, and sixteenth pancake forgings. Microstructural photographs taken at the mid-radius, center of the pancakes and in three planes.

Each pancake was also characterized as follows:

1. Forging dimensions for each pancake (thickness, bulge and flat dimensions).
2. Hardness survey (BHN) of the top of each pancake forging consisting of three readings 120° apart at mid-radius. In addition, readings were taken on the tensile, fracture toughness, and fatigue crack growth coupons.

Grain size was determined in accordance with ASTM Standard E112-63, and macro-grain size was determined and rated in accordance with AMS 2380. The macro- and micro-structures and grain flow or orientation were fully described in three grain directions for the mechanical property test forging to assure consistency and uniformity of structures and grain flow throughout the lot.

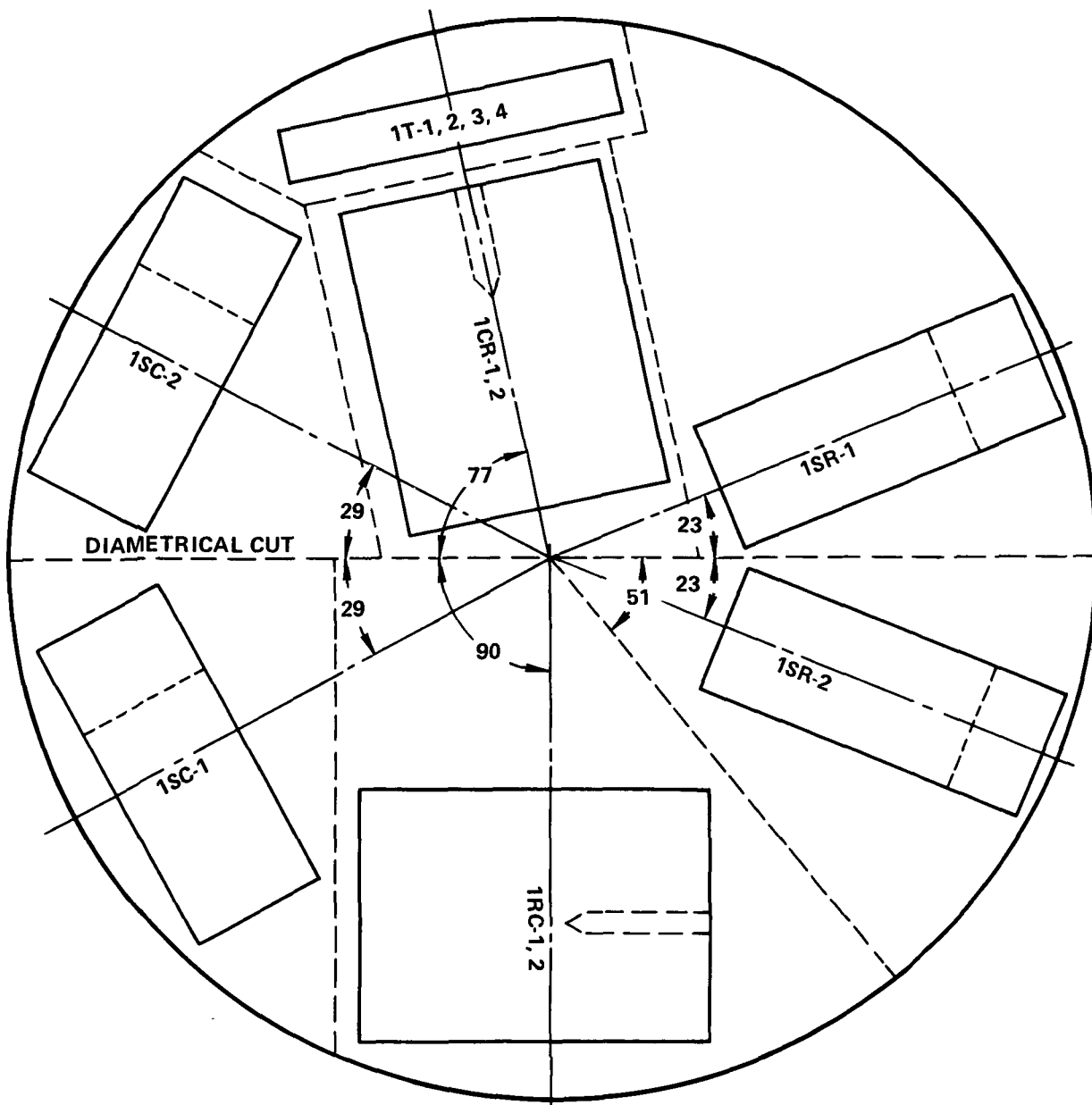
2.2.2 Specimen Fabrication

Layout drawings for the pancake forgings are presented in Figs. 3 thru 7. For tensile, fracture toughness, and fatigue crack propagation coupons, specimen locations and orientations and the specimen code stamped on each specimen are shown on the appropriate layout drawing. The code indicated the pancake (numbered 1 through 32) from which the specimen was machined, the orientation of the specimen (tensile - C, R, or S; compact tension, CR, RC, SR, RS, SC, CS) and the specimen number. The purpose of this code was to allow for completely cross indexed traceability of the specimen coupons to the layout drawings and the pancake microstructure.

The specimens were machined by the Ladish Company. Tensile specimen geometry is shown in Fig. 8 and the compact specimen (WOL) geometry is shown in Fig. 9. Sufficient specimens were machined to allow for losses during testing. Specimens were distributed among the pancakes as follows:

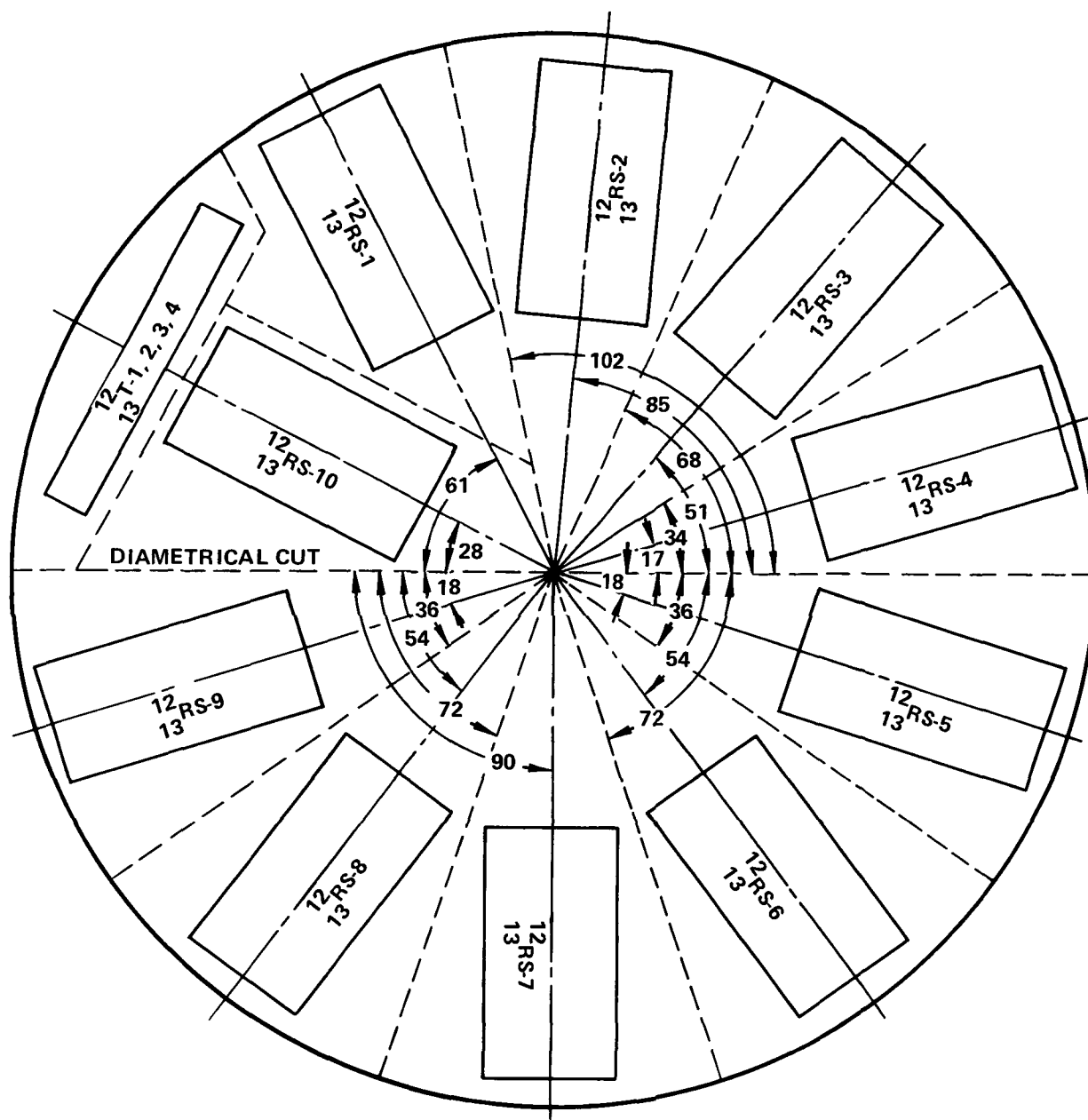
1. 76 tensile specimens from 16 pancakes
 - (a) 4 tensile specimens from each of Pancakes No. 1 thru 15 and 29; all specimens oriented circumferentially.
 - (b) 12 tensile specimens for Pancake No. 16, 4 each circumferential, radial and thickness.
2. 138 compact (WOL) specimens from 17 pancakes: 48 circumferential (26 CR, 22 CS), 45 radial (23 RC, 22 RS) and 45 thickness (23 SR, 22 SC).
 - (a) 8 WOL from Pancakes No. 1 through 11 (2 CR, 2 RC, 2 SR, 2 SC).
 - (b) 10 WOL from Pancakes No. 12 and 13 (10 RS)
 - (c) 11 WOL from Pancakes No. 14 and 15 (11 CS)
 - (d) 6 WOL from Pancake No. 16 (2 CR, 2 RS, 1 RC, 1 SR)
 - (e) 2 WOL from Pancake No. 29 (2 CR)

3. Ten rotating disk coupons from Pancakes 19 thru 28. Pancake 18 was used to replace three WOL coupons and one tensile coupon because of damage during machining or presence of forging cracks.



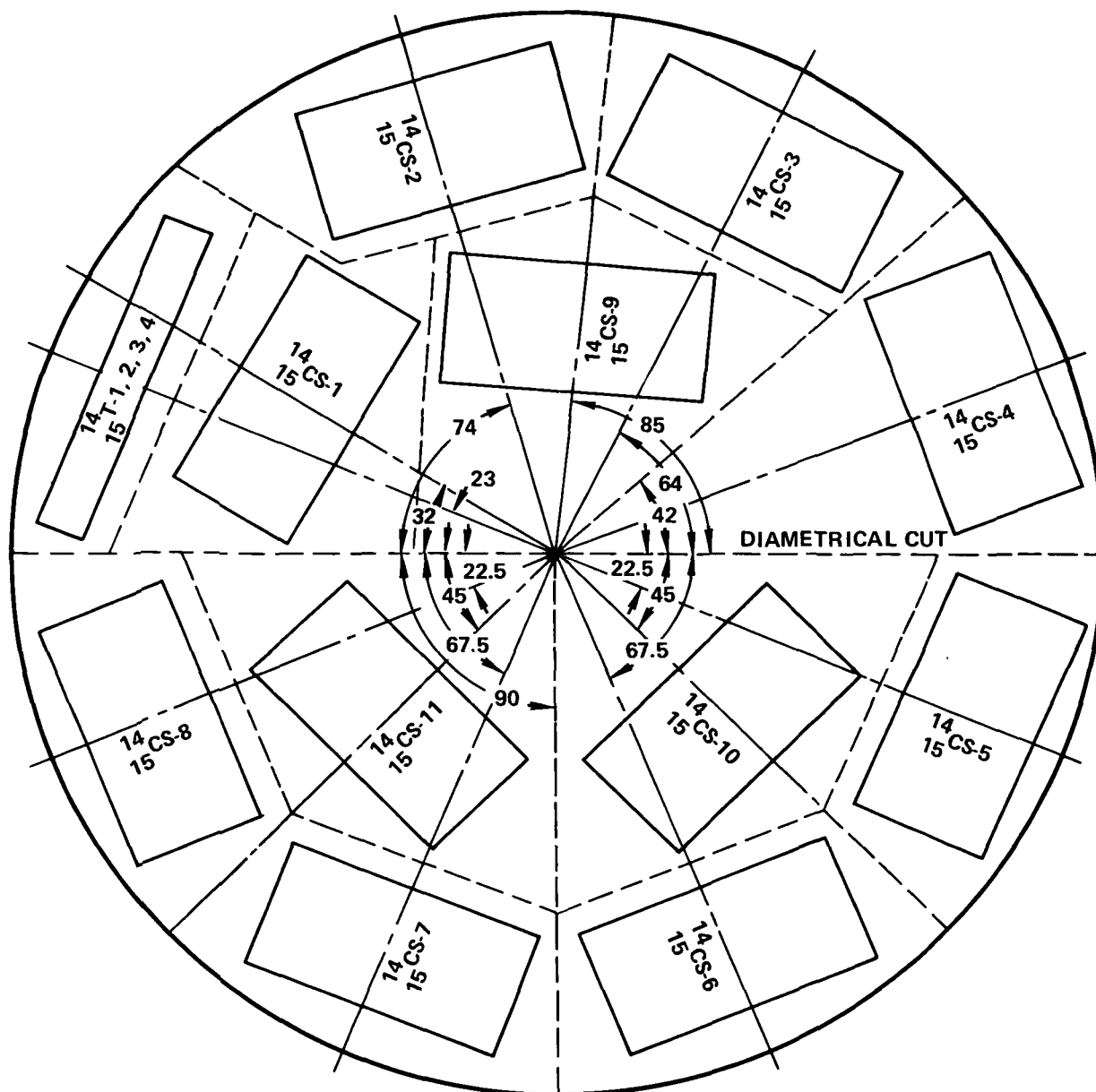
- NOTE:**
1. DASHED LINES INDICATE SAW CUTS
 2. THE FIRST NUMBER OF THE SPECIMEN CODE REFERS TO THE NUMBER OF THE PANCAKE FORGING
 3. ALL ANGLES ARE IN DEGREES

Figure 3.- Specimen Layout Drawing for Pancakes 1 through 11



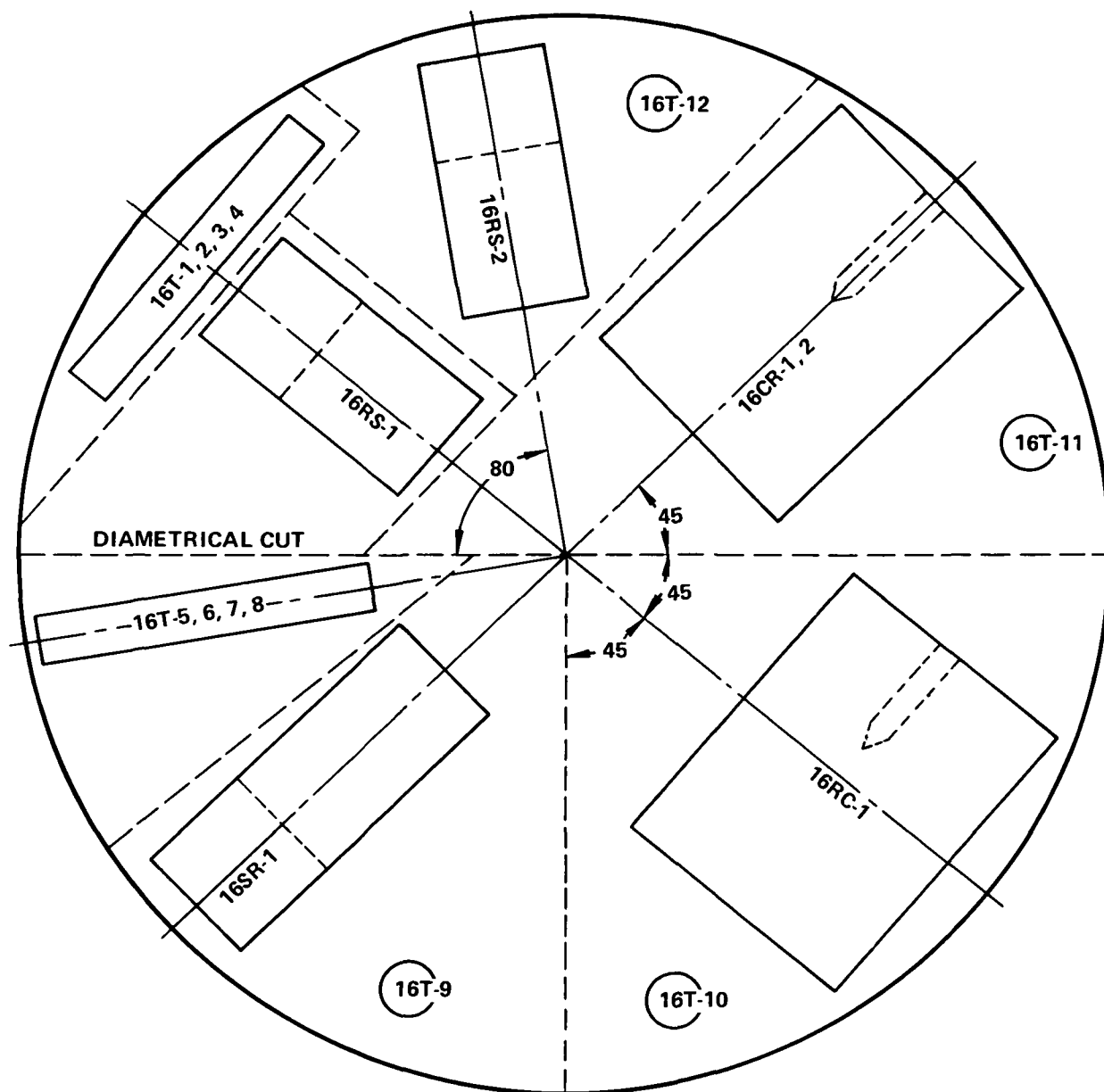
- NOTE: 1. DASHED LINES INDICATE SAW CUTS
2. THE FIRST NUMBER OF THE SPECIMEN CODE REFERS TO THE NUMBER OF THE PANCAKE FORGING
3. ALL ANGLES ARE IN DEGREES

Figure 4.- Specimen Layout Drawing for Pancakes 12 and 13



- NOTE: 1. DASHED LINES INDICATE SAW CUTS
 2. THE FIRST NUMBER OF THE SPECIMEN CODE REFERS TO THE NUMBER OF THE PANCAKE FORGING
 3. ALL ANGLES ARE IN DEGREES

Figure 5.- Specimen Layout Drawing for Pancakes 14 and 15



- NOTE: 1. DASHED LINES INDICATE SAW CUTS
2. THE FIRST NUMBER OF THE SPECIMEN CODE REFERS TO THE NUMBER OF THE PANCAKE FORGINGS
3. ALL ANGLES ARE IN DEGREES

Figure 6. - Specimen Layout Drawing for Pancake 16

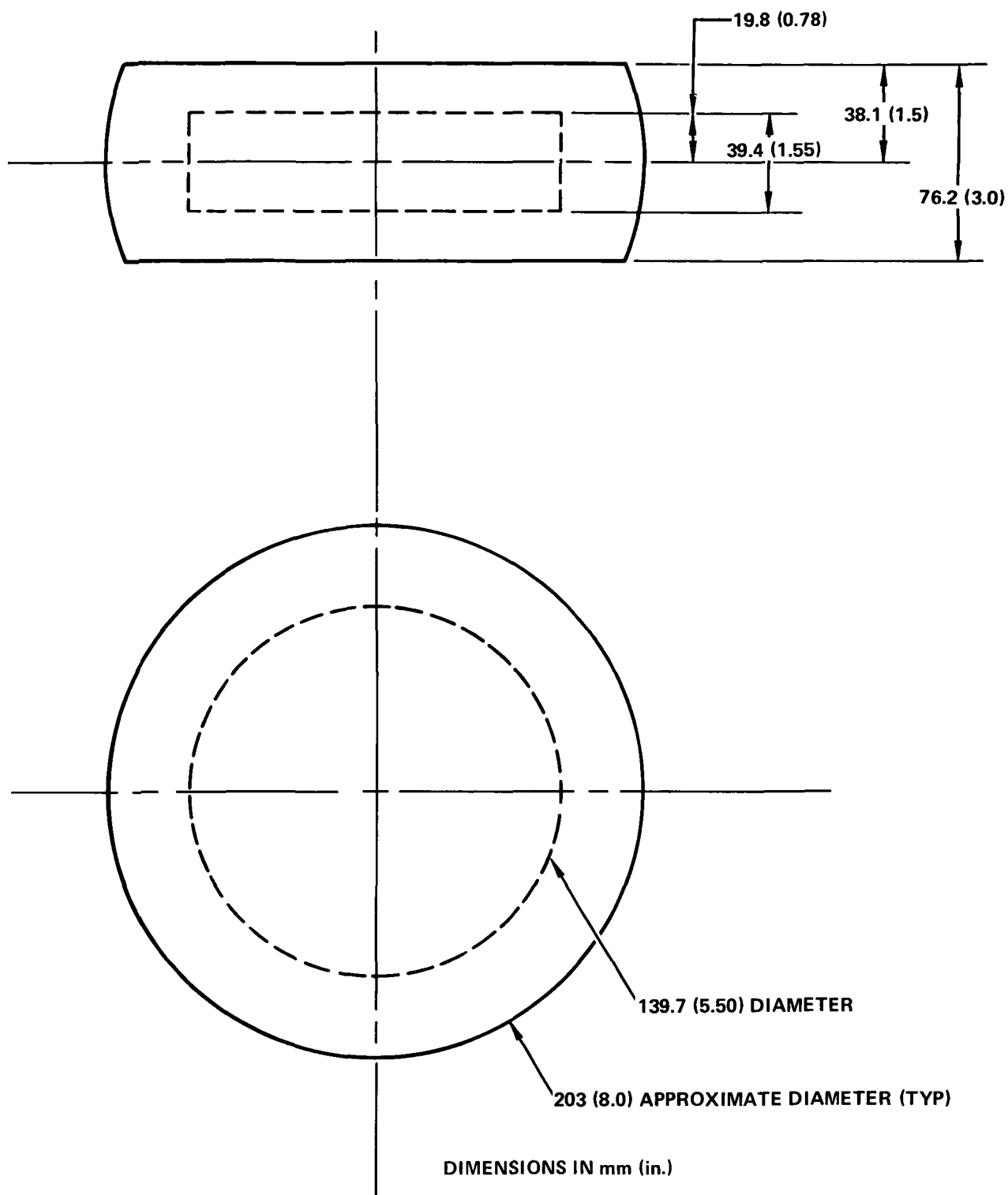


Figure 7. - Layout Drawing for Rotating Disk Specimens,
Pancakes 19 - 28

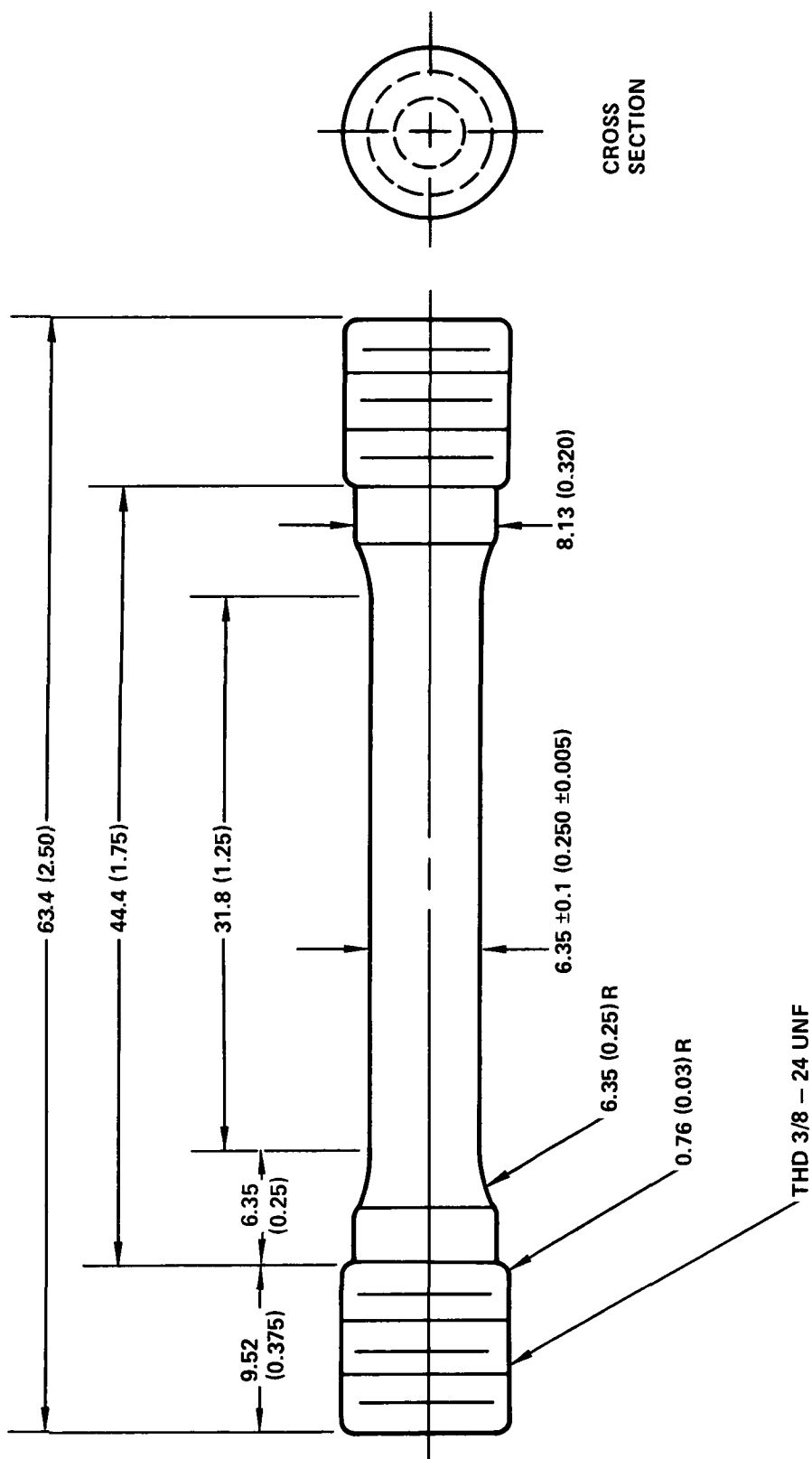


Figure 8. - Tensile Specimen Geometry

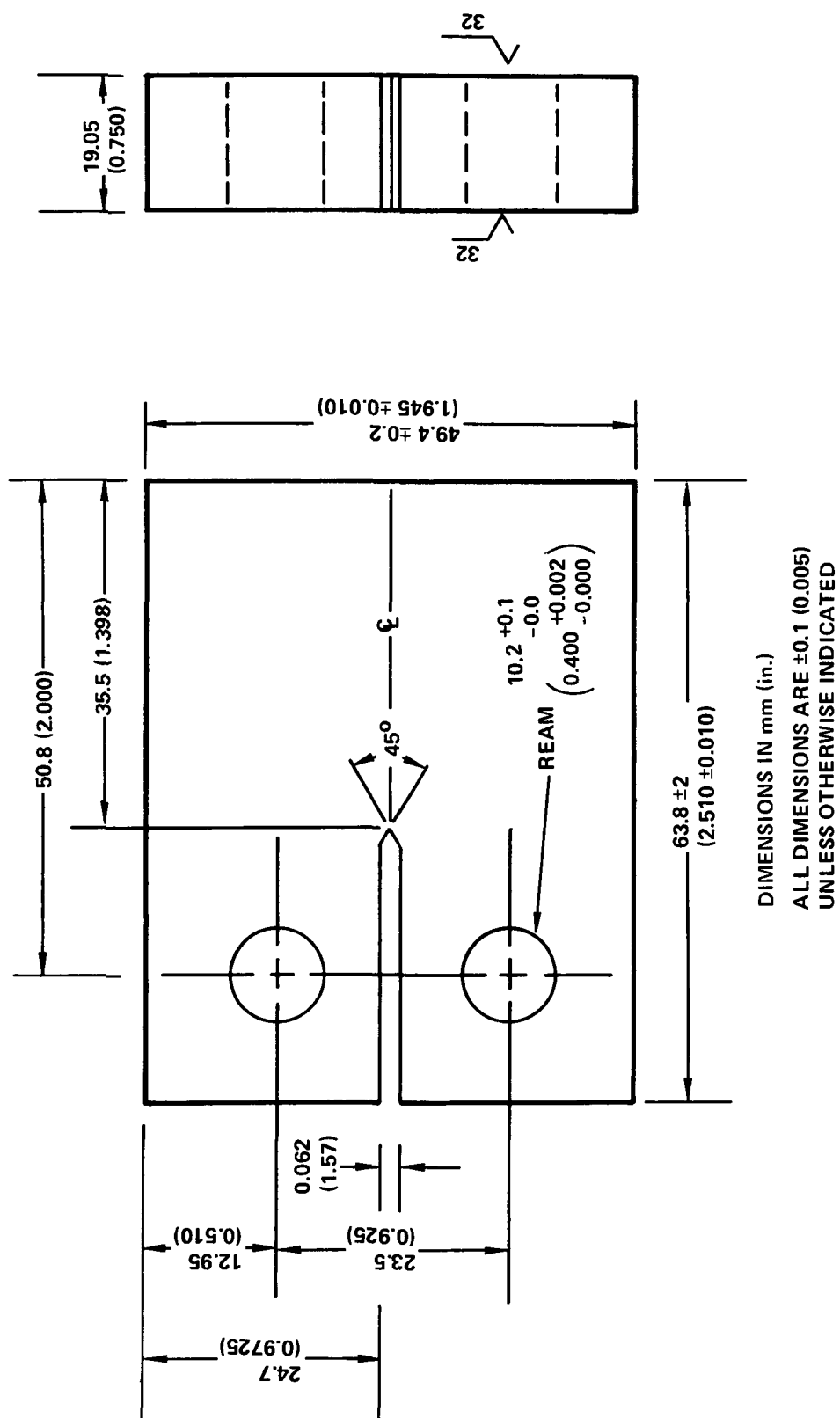


Figure 9. - Compact Tension (WOL Type) Specimen Geometry

Rotating disk coupons were first machined to the configuration shown schematically in Fig. 10 and photographically in Fig. 11. The number of holes (1 or 2) and the A and B dimensions were individually determined for each disk, based upon the particular test for which that disk was intended. Table 1 lists the A and B dimensions for each disk. After precracking one of the holes, disks were final machined to the configuration shown in Fig. 12 except that disks 19, 27, and 28 did not have notches.

2.2.3 Mechanical Properties Test Matrix

Tensile Tests - Tensile properties (F_{tu} , $0.2\% F_{ty}$, percent elongation, percent reduction in area) were determined in the circumferential, radial and thickness directions at room temperature and at -253°C (-423°F). Table 2 lists the tensile tests conducted.

Static Fracture Toughness Tests - Static fracture toughness properties were determined for the Ti-5Al-2.5Sn(ELI) pancake forgings at room temperature and at -253°C (-423°F). Duplicate specimens were tested at each condition. Specimens were of the WOL geometry shown in Fig. 9, with a thickness of 19 mm (.75 in.). Tests were conducted from specimens machined in three orientations; hoop, radial, and thickness. Specimens were machined such that: for the hoop direction, toughness was obtained for cracks in both the radial and thickness directions; for the radial direction, toughness was obtained for cracks in both the hoop and thickness directions; for the thickness direction, the toughness was obtained for cracks in both the hoop and radial directions. The fracture toughness tests conducted are shown in Table 3.

Crack Propagation Tests - Specimen geometry was identical to that used for the static fracture toughness tests (Fig. 9). The fatigue crack growth characteristics of this alloy were investigated using compact (WOL) specimens oriented in the hoop, radial, and thickness directions relative to the pancake forgings. Specimen orientations and respective crack propagation

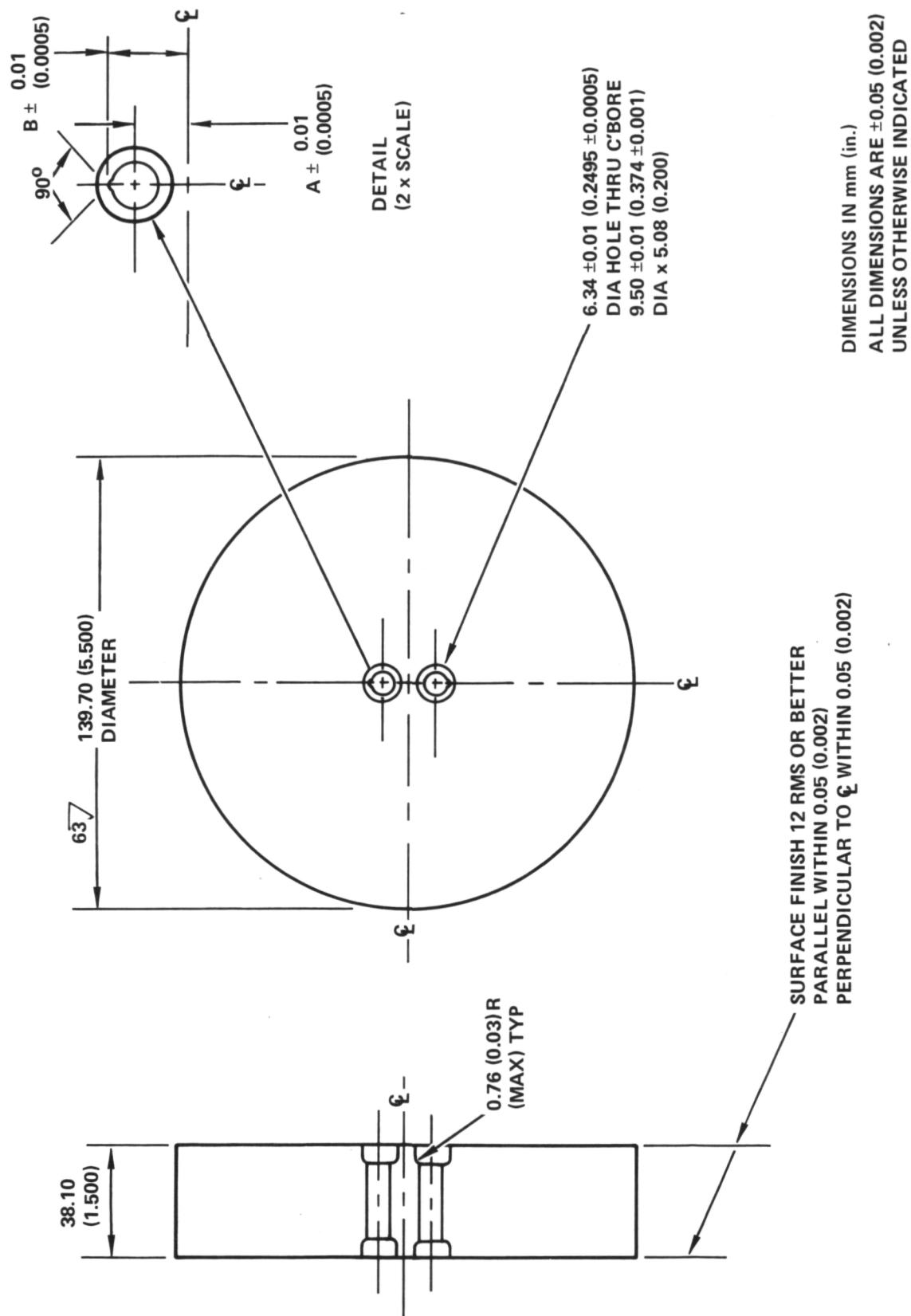


Figure 10. - Disk Configuration for Precracking

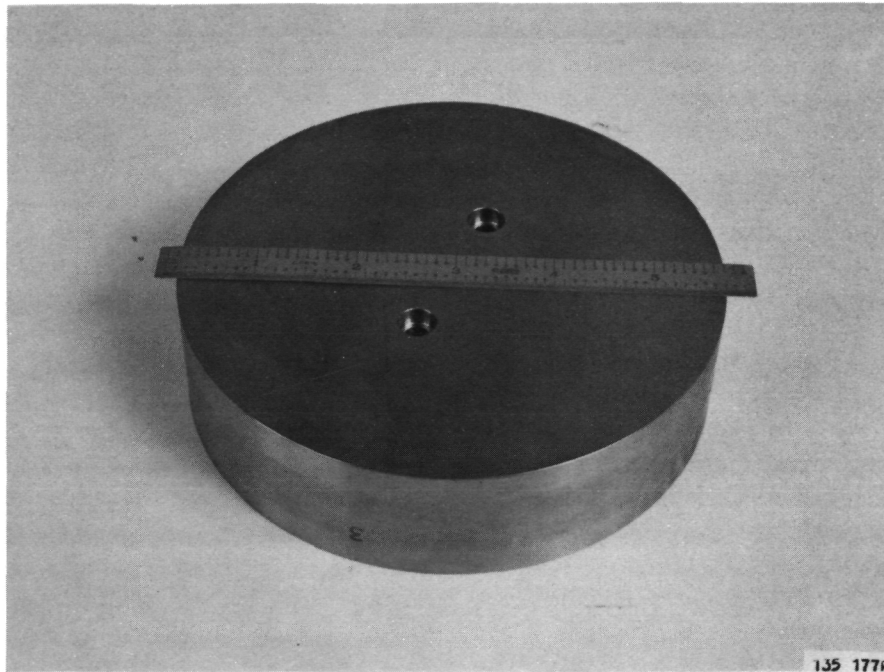
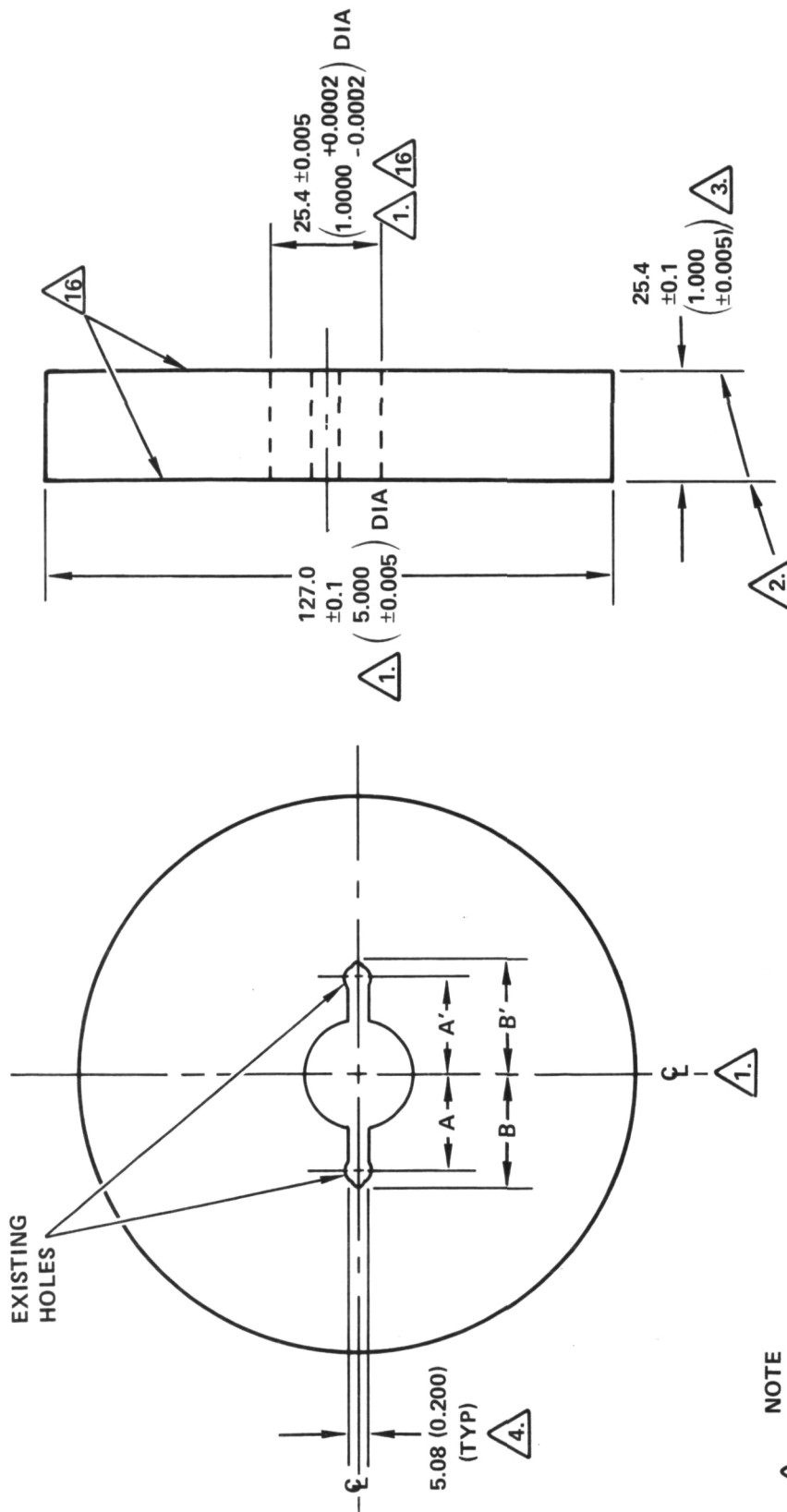


Figure 11.- Photograph of Disk Ready for Precracking



- NOTE
- 1. ϕ EQUALLY CENTERED BETWEEN EXISTING HOLES WITHIN 0.005 (0.0002) (B = B' WITHIN 0.005 (0.0002) CONCENTRIC WITHIN 0.005 (0.0002) T.I.R. TO ϕ PARALLEL WITHIN 0.01 (0.0005)
 - 2. OBTAIN DIMENSION BY REMOVING MATERIAL EQUALLY FROM BOTH SIDES TO ELIMINATE COUNTERBORES
 - 3. ϕ EQUALLY CENTERED ON EXISTING HOLE CENTERS WITHIN 0.005 (0.0002) SLOT WIDTH 0.200 CENTERED TO ϕ WITHIN 0.005 (0.0002)
 - 4.

Figure 12. - Final Configuration for Rotating Disk Specimens

TABLE 1

LIST OF NUMBER AND LOCATION OF
ROTATING DISK PRECRACK STARTER HOLES

Disk No.	No. of Precrack Starter Holes	Hole Location, Position A, mm (in.)	Slot Location, Position B, mm (in.)
19	1	8.51 (0.335)	12.4 (0.49)
20	2	21.21 (0.835)	25.1 (0.99)
21	2	21.21 (0.835)	25.1 (0.99)
22	2	28.83 (1.135)	32.8 (1.29)
23	2	28.83 (1.135)	32.8 (1.29)
24	2	28.83 (1.135)	32.8 (1.29)
25	2	23.75 (0.935)	27.7 (1.09)
26	0	0	0
27	1	8.51 (0.335)	12.4 (0.49)
28	1	8.51 (0.335)	12.4 (0.49)

TABLE 2

MECHANICAL PROPERTY TESTS-TENSILE

<u>Test Direction</u>	<u>Test Temperature °C(°F)</u>	<u>Number of Tests</u>
Circumferential (C)	22(72)	36 ^a
	-253(-423)	32 ^b
Radial (R) ^c	22(72)	2
	-253(-423)	2
Thickness (S) ^c	22(72)	2
	-253(-423)	<u>2</u>
Total Tests		76

- a. Two coupons each from Pancakes 1-16 and 4 from Pancake 29.
Coupon 16T-8 was damaged during machining due to a forging crack and replaced with 18T-8.
- b. Two coupons each from Pancakes 1-16.
- c. All radial and thickness direction coupons were from Pancake 16.

TABLE 3
STATIC FRACTURE TOUGHNESS TESTS^a

<u>Specimen Direction</u> ^b	<u>Test Temperature</u> <u>°C(°F)</u>	<u>Number of Tests</u>
Circumferential		
(CR & CS)	22(72)	5 ^c
(CR & CS)	-253(-423)	4
Radial		
(RC & RS)	22(72)	4
(RC & RS)	-253(-423)	4
Thickness		
(SR & SC)	22(72)	4
(SR & SC)	-253(-423)	4
	Total Tests	25

a. Precracked - WOL Specimens

b. C - Circumferential Direction

R - Radial Direction

S - Short Transverse or Thickness Direction

Crack plane is normal to direction of first letter with propagation in direction of second letter.

c. One CR direction fatigue crack propagation coupon from Pancake 29 was used to obtain K_{IQ} for the second lot of material.

directions were identical to the combinations used for the static fracture toughness tests.

Two stress ranges, $R = \frac{\text{minimum load}}{\text{maximum load}} = + 0.05$ and $+0.5$, and two frequencies (10, 0.1 Hz) were investigated. The test matrix was designed on the assumption that for the 0.1 Hz tests, at least a one order of magnitude increase in crack propagation rates would occur as compared to 10 Hz data. However, no such increase was noted in early tests and therefore many of the 0.1 Hz tests were deleted. A sinusoidal loading waveform was used throughout the test program. Tests at 22°C (72°F) were conducted in laboratory air (~40% R.H.) while tests at -253°C (-423°F) were conducted in liquid hydrogen (LH₂). Duplicate specimens were tested at each condition. The original cyclic crack growth test program is shown in Table 4.

Rotating Disk Tests - The rotational disk test program consisted of ten disks distributed over the test matrix shown in Table 5. Three types of tests were conducted: burst, fatigue crack growth, and proof spin. Tests 1 to 4 were designed to determine the effect of flaw length on burst speed. Initial flaws from 1.52 mm (0.06 in.) to 37.3 mm (1.47 in.) were chosen to insure that burst speeds would occur after onset of bore yielding for two disks and before onset of bore yielding for the other two disks. Test 5 was a burst test using an unflawed disk so that test results could be compared with traditional turbo-machinery experience. The results of the burst tests were compared to predictions based on linear elastic fracture mechanics and to the laboratory coupon data.

Tests 6, 7, and 8 were designed as rotating disk fatigue crack growth rate studies at various starting crack lengths. Disk and WOL coupon crack growth rate data were compared. Tests 9 and 10 were designed as evaluation of the proof test concept.

2.3 General Test Procedure

2.3.1 Tensile Test Procedures

A total of 72 tensile tests were conducted by Convair, half at room temperature

TABLE 4
CYCLIC CRACK GROWTH TESTS^a

Specimen ^b Direction	Test Temperature °C(°F)	Stress Range (+0.05, +0.5)	Cyclic Rate (10, 0.1 Hz)	Number of Tests
Circumferential				
(CR & CS)	22(72)	2	2	18 ^c
(CR & CS)	-253(-423)	2	2	16
Radial				
(RC & RS)	22(72)	2	2	16
(RC & RS)	-253(-423)	2	2	16
Thickness				
(SC & SR)	22(72)	2	2	16
(SC & SR)	-253(-423)	2	2	<u>16</u>
			Total Tests	98

a. Precracked WOL Specimens

b. C - Circumferential Direction

R - Radial Direction

S - Short or Thickness Direction

Crack plane is normal to direction of the first letter with propagation in direction of second letter.

c. Two of the coupons were from Pancake 29 to check uniformity of the crack propagation behavior of the second lot of material compared to the first lot.

TABLE 5
ROTATING DISK TEST MATRIX

<u>Test No.</u>	<u>Type of Test</u>	<u>Disk No.</u>
1	Burst	19
2	Burst	21
3	Burst	24
4	Burst	27
5	Burst	26
6	Crack Growth	23
7	Crack Growth	25
8	Crack Growth	28
9	Proof Spin	20
10	Proof Spin	22

and half at -253°C (-423°F). Tests were performed in Instron and Tinius-Olsen tensile test machines using Class B-1 extensometers for measuring the strain. Stress-strain curves were obtained for all tests as well as: ultimate strength, F_{tu} ; yield strength, $0.2\% F_{ty}$; percent elongation, $\%e$; percent reduction in area, $\%RA$; and apparent elastic modulus, E_A . All testing was conducted according to ASTM E8 requirements. Four tensile tests of coupons from Pancake 29 were conducted at the Lockheed-California Company similar to the Convair tests and also according to ASTM E8 requirements, but in a Baldwin 0.267 MN (60,000 lb.) Universal test machine.

Tests at -253°C (-423°F) were conducted in liquid hydrogen cryostats installed in the Convair tensile test machines. Extensometers used with liquid hydrogen testing consisted of rod-in-tube extensions that transmitted the strain from the specimen test section to a transducer located outside of the liquid hydrogen cryostat. The output of the transducer was transmitted to the drum recorder of the test machine in a conventional manner. Machine controls and readout equipment for the LH_2 tests were located in another room completely isolated from the area in which LH_2 was used, so that accidental arcing from electrical equipment could not pose a safety problem. The LH_2 was transferred from a storage tank outside of the test building via a double-walled, evacuated pipe to the cryostat on the test frame and then vented to the atmosphere. The test facility was subjected to continual monitoring for the presence of H_2 gas during any H_2 test. Figure 13 shows a cryostat installed in a static tensile test machine.

One batch of the round tensile specimens were improperly machined in the threaded grip area. In those cases where the threads were oversize, the specimens were remachined by Convair until they could be mated with existing load clevises. In some cases, the threads were undersize to the extent that they could not be successfully tested. After one test specimen failed in the thread area, an additional set of clevises was fabricated by Convair and the testing continued in a normal manner.

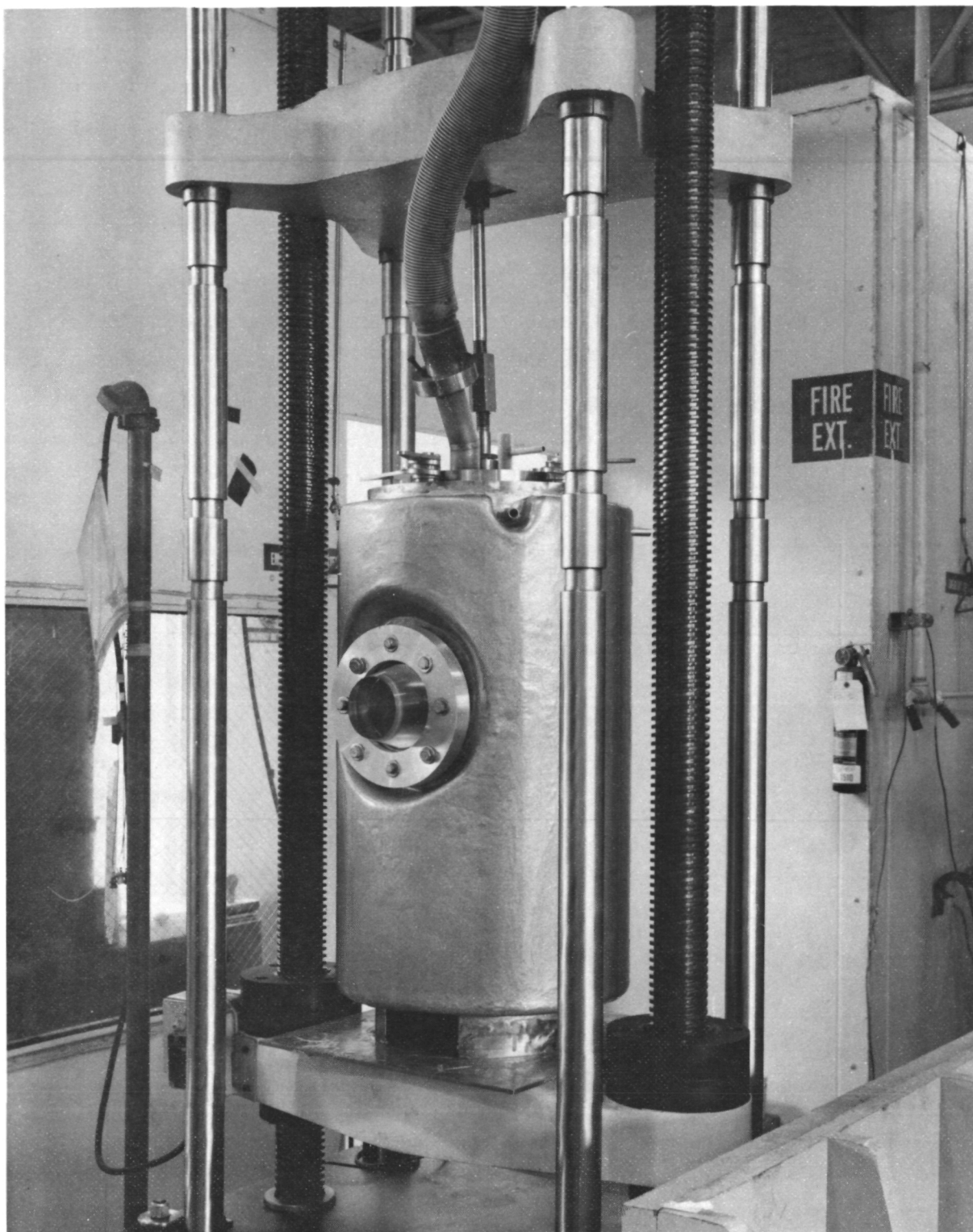


Figure 13. - Cryostat for Tensile Testing in
a Tinius-Olsen Tensile Machine

2.3.2 Fracture Toughness Test Procedures

A total of 24 compact specimens from material Lot 1 were tested at Convair. In addition, one of the two coupons from Pancake 29, material Lot 2, was tested at Lockheed-California Company. The tensile test equipment discussed in the previous section was used for static fracture toughness tests.

All fracture toughness specimens tested at Convair were precracked at room temperature in Baldwin SF-1N fatigue machines using a three-step fatigue loading sequence. All cyclic precracking was performed using a stress ratio, R , of 0.1 at a constant frequency of 30 Hz. The maximum loads were used in the following order:

- (1) 15.6 kN (3500 lbs)
- (2) 13.3 kN (3000 lbs)
- (3) 4.4 kN (1000 lbs)

The final load was equivalent to a stress intensity less than 60% of the expected K_{IQ} value. Specimens were instrumented with an ASTM E399 type crack opening displacement (COD) gage and a monotonic tensile load applied to produce failure. The resulting load-displacement curves were analyzed to determine plane strain fracture toughness values. If any of the K_{Ic} validity criteria were not met, appropriate K_Q values and residual strength ratios were calculated for each specimen per ASTM E399-74 requirements.

The following requirements of ASTM Standard E399 were met:

- (1) The length of the fatigue crack was not less than 5% of the length "a" and was not less than 1.27 mm (0.05 in.).
- (2) The ratio of the maximum stress intensity to the Modulus of Elasticity was less than $0.010 \text{ mm}^{1/2}$ ($0.002 \text{ in.}^{1/2}$).

$$\frac{K_f}{E} \leq 0.010 \text{ mm}^{1/2} (.002 \text{ in.}^{1/2})$$

- (3) The maximum fatigue stress intensity (K_f) did not exceed 60 percent of the conditional static stress intensity factor determined in the subsequent tests.

2.3.3 Compliance Calibration Procedures

Compliance calibration of three samples was obtained at room temperature in laboratory air and one sample at -253°C (-423°F) in LH_2 . Coupon 11SC-1, tested at room temperature, and coupon 7CR-2, tested at -253°C (-423°F) were used for calibration at Convair. Coupons 11CR-2 and 11RC-2 were tested at Lockheed-California Company at room temperature. The data were analyzed such that the results could be used to interpret the compliance data obtained from the fatigue crack propagation tests as well as to obtain an experimental compliance calibration. The primary purpose of the experimental compliance calibration was to determine if the compliance calibration of the material changed as a function of temperature.

The analytical and experimental basis of the compliance analysis procedure employed is described in detail in a Lockheed-California Company report, [10]. In essence, normalized compliance, CEB, was derived from experimental data as a three parameter function of a/W . This function was then used to determine crack length during subsequent fatigue crack propagation testing.

In addition, CEB was used to evaluate the term C_3 in the equation for stress intensity for this WOL geometry [11]:

$$K = \frac{P \sqrt{a}}{B a} C_3 \quad (1)$$

$$\text{where } C_3 = \frac{1}{2} \left[\frac{a}{w} \frac{d(\text{CEB})}{d(a/W)} \right]^{1/2} \quad (2)$$

This result was then compared to an analytically derived boundary value collocation expression for C_3 which, for this geometry, is given as [12]:

$$\begin{aligned} C_3 = & 30.96(a/W) - 195.8(a/W)^2 \\ & + 730.6(a/W)^3 - 1186.3(a/W)^4 \\ & + 754.6(a/W)^5 \end{aligned} \quad (3)$$

Calculated values of CEB were obtained from best fits of an equation originally suggested by Dr. G. E. Bowie and reduced to practice by Ryder [10]:

$$CEB = \text{Exp} \left\{ \text{Exp} \left[f(a/W) \right] \right\} - \text{Exp} (1) \quad (4)$$

$$\text{where} \quad f(a/W) = e + (v - e) \left[-\ln(1 - a/W) \right]^{1/k} \quad (5)$$

where k , e , and v are numerical parameters.

From Equation (4), experimentally based CEB was then known as a function of a/W . Equation (4) can be inverted to obtain a/W as a function of CEB such that a/W can be directly obtained from a compliance measurement.

$$a/W = 1 - \text{Exp}(-z^k) \quad (6)$$

where z , the reduced variate, is given by:

$$z = \frac{\ln(\ln(CEB + \text{Exp}(1))) - e}{v - e} \quad (7)$$

For the specimens tested at the Lockheed-California Company, the compliance measurement was the average of five readings taken at each a/W value. Compliance curve readings were made approximately every 1.3 mm (0.050 in.). For coupon 7CR-2, compliance readings were taken at irregular intervals to check if the compliance curve was a function of temperature.

2.3.4 Fatigue Crack Propagation Test Procedures

Precracking of fatigue crack propagation specimens was accomplished in the same manner as for static fracture toughness specimens. Testing was performed in such a manner as to provide a reasonable spread of data when plotted as cyclic crack growth (da/dN) versus the applied stress intensity range (ΔK). Generally, an attempt was made to obtain 20 data points for each specimen.

Tests, as discussed in detail in Section 2.2, were conducted at $R = 0.05$ and 0.5 , $F = 10$ and 0.1 Hz, and at room temperature (RT) and -253°C (-423°F). Tests at room temperature were conducted in laboratory air using a closed loop electrohydraulic testing machine; Fig. 14 shows a typical room temperature

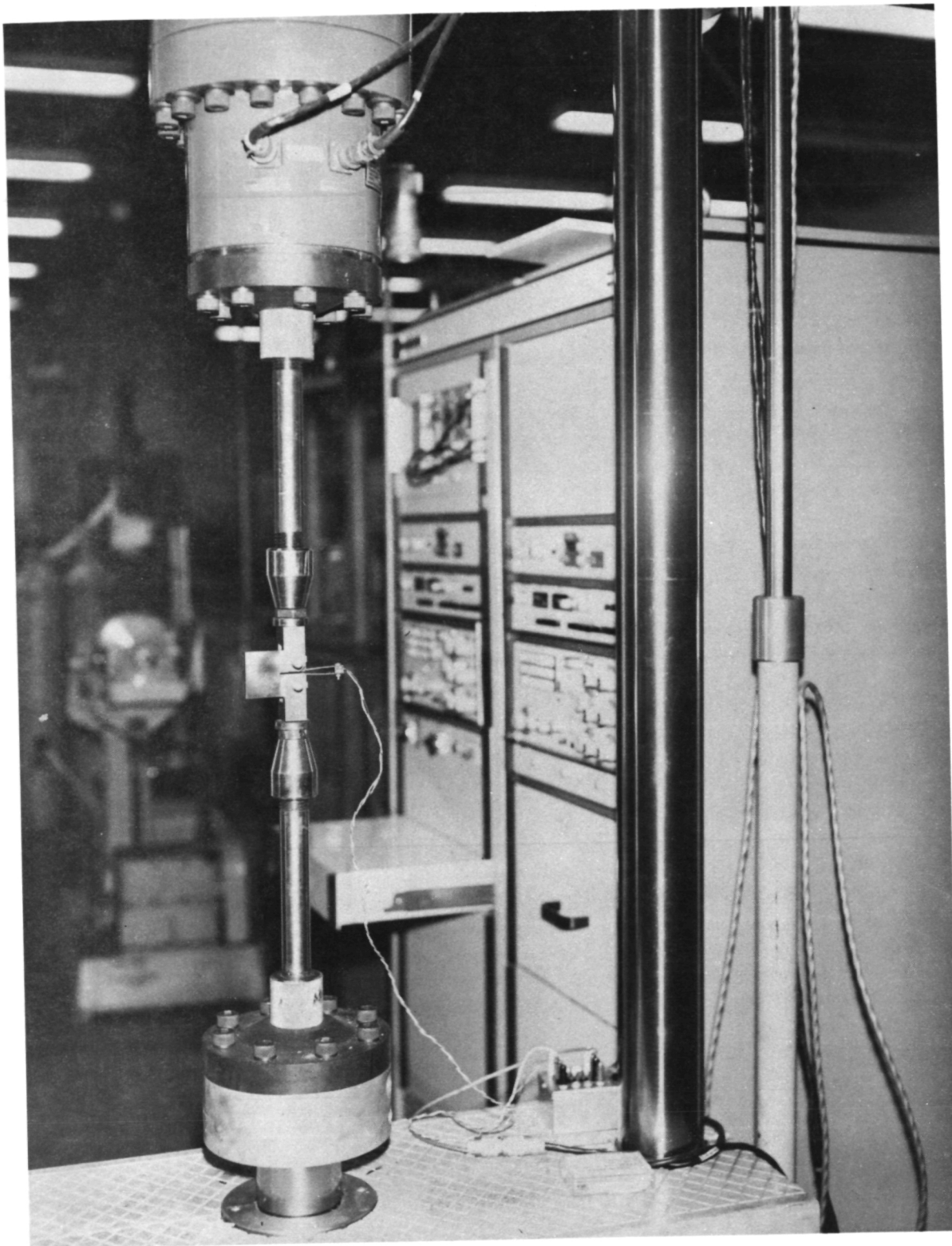


Figure 14. - Fatigue Crack Growth Coupon Being Tested in Laboratory Air

test. Coupons were tested at -253°C (-423°F) in a Tatnal servo-controlled test system equipped with a liquid hydrogen cryostat containing a clear plastic window, see Fig. 15.

An attempt was made to initiate crack growth at a rate of 5×10^{-9} m/cycle (2×10^{-7} in./cycle). Loads were applied in three steps with each load larger than the previous one (ascending order). Initially, marker bands were induced in the specimens for the purpose of enhancing post test fractography. However, the data reduction technique was adequate such that accurate growth readings were produced without the marker bands so they were discontinued.

Crack length of coupons tested at room temperature was measured optically on both sides of the room temperature coupons. The two surface measurements were averaged. For tests in LH_2 , optical readings could be taken on only one side, but this was not a critical omission because the crack front remained symmetrical throughout the tests as shown by post-test observation of the fracture surface.

A check of the crack length was obtained from COD data by expressing a/W as a function of CEB, using Equation (4), and comparing the results to those obtained optically. The optical crack length measurements, after adjustment for crack bowing, agreed closely to compliance based measurements (see Appendix). An adjustment length of 1.27 mm (0.050 in.) was added to each average optical surface crack length measurement to account for the bow in subsurface crack extension. This was justified by post-test observation of coupon fracture surfaces which showed that the crack length based upon the two surface readings and three subsurface measurements ($1/4$, $1/2$, $3/4$ thickness) was 1.01-1.52 mm (0.040-0.060 in.) longer than the average of the two surface measurements. The adjustment length of 1.27 mm (0.050 in.) was a good average value; the effect on ΔK due to a 1.01 mm (0.040 in.) or 1.52 mm (0.060 in.) adjustment was less than 1% while the effect on da/dN was zero.

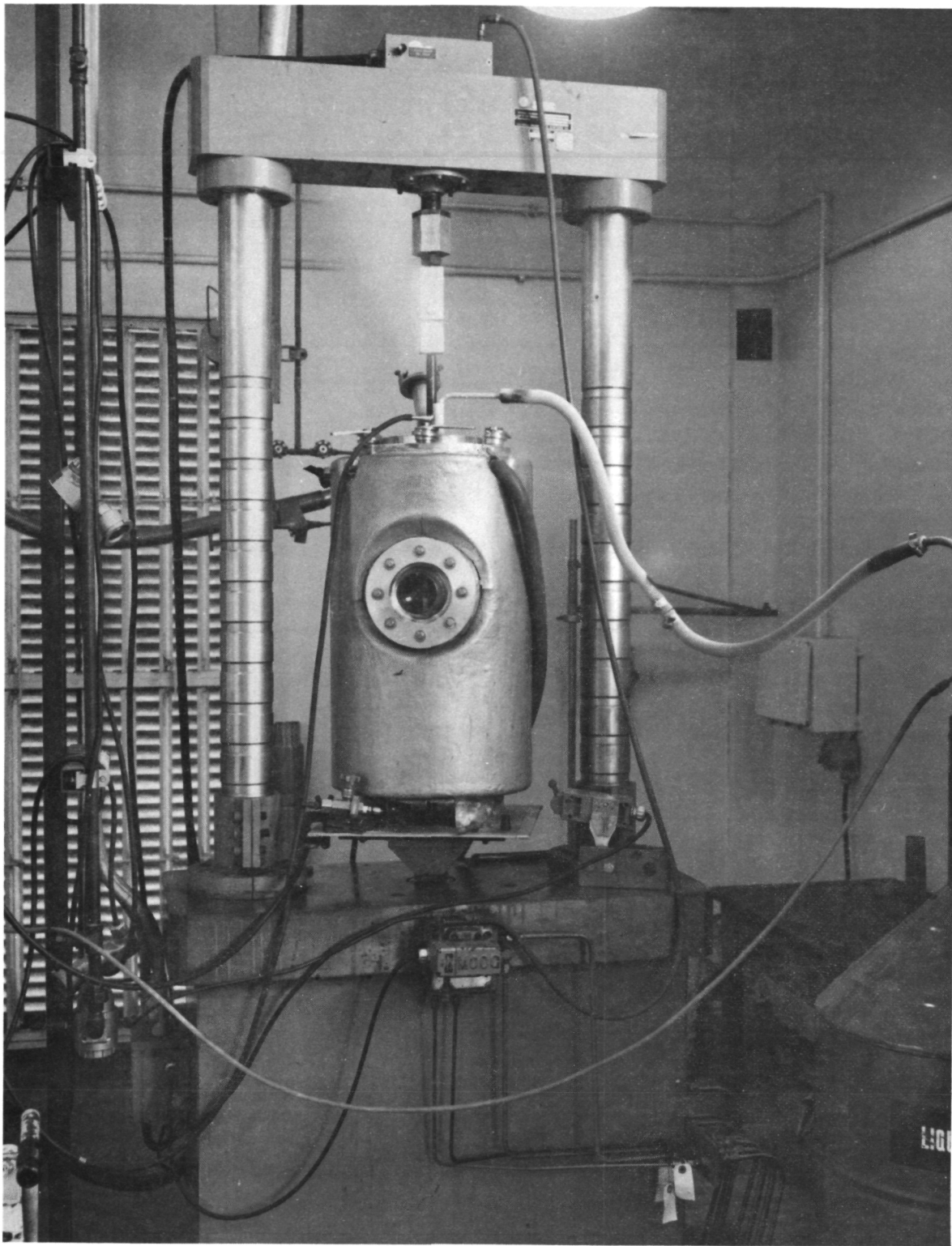


Figure 15. - Fatigue Crack Growth Testing
Equipment for -253°C Tests

Crack growth rate, da/dN , was defined simply as the change in crack length, Δa , divided by the change in cycles, ΔN , where Δa was based on the optical Measurement. Stress intensity was calculated using Equations (1), (2), and (4).

Data analysis was performed employing Calac computer programs using as input the measured crack length versus cycles data, the specimen geometry, loading conditions and the appropriate stress intensity expression. The computer analysis computed incremental crack growth rates, da/dN , and the stress intensity parameters at the average crack length in the specific crack length interval. A tabulation of the results was printed out and a plot of da/dN versus the alternating stress intensity factor, ΔK , printed. The tabulated data of all tests is presented in Appendix A, along with computer plots showing the data for each specimen plotted separately, but with the scatter bands for all data obtained at the same test condition.

All fatigue crack propagation data discussed in subsequent sections is presented in a graphical format. Plotted data are shown along with a curve fit scatter bands. The crack growth data taken at one test condition was combined and empirically fit using the following expression developed by Sandifer and Bowie [13]; after the well-known form of the Gumbel double exponential distribution [14]

$$da/dN = \text{Exp} \left\{ u - \ln \left[-\ln(1-\Delta K/K_d) \right] / \alpha \right\} - 1 \quad (8)$$

Where α and u are constants for a particular data set and K_d , also a constant for a particular data set, is the K_{\max} value at fracture of a crack growth coupon.

Equation (8) is based on several related investigations [15, 16, 17] at Lockheed-California Company into curve fitting algorithms which were inspired by Dr. G. E. Bowie and reduced to practice by the author of this report. Essentially the relation is of the form:

$$\begin{aligned}
& Y = bX + a & (9) \\
\text{where } & Y = \ln [-\ln(1 - \Delta K/K_d)] & (10) \\
& X = -\alpha [\ln(da/dN - 1) - u] & (11) \\
\text{and } & \alpha = -b & (12) \\
& u = -a/b & (13)
\end{aligned}$$

As a matter of laboratory practice, input data and calculations were performed in U.S. customary units. Results were converted to SI units for presentation purposes after curve fitting parameters were computed. In the computer routines, regression plane calculations were made of the sample correlation coefficient (R_o), standard deviation (σ), and sum of squared deviations in the Y-direction (D^2). In general, for a given set of (da/dN , ΔK) data, a value of K_d was selected in the range of the largest value of ΔK in the data set by maximizing the sample correlation coefficient, R_o . Computation for a given value of K_d amounted to straightforward linear regression analysis. For completeness, one should be aware that Equation (8) has the advantage that the stress intensity at which the crack growth rate rapidly decreases, K_{th} , is determined by the data rather than arbitrarily chosen. For the final value of K_d selected, the threshold stress intensity can be extrapolated as [13]:

$$K_{th} = K_d \left\{ 1 - \text{Exp}[-\text{Exp}(\alpha u)] \right\} \quad (14)$$

The determination of K_{th} was not of significant importance in this program because of the low cycle lives anticipated.

In keeping with practice established when crack growth data trends were approximated by means of hand drawn curves, the stress intensity range at the transition from slow to fast growth (ΔK_{sf}) [15, 16] was determined by calculating the ΔK value at the minimum value of the risk function (r) which is defined as:

$$r = \frac{d \ln(da/dN)}{d\Delta K} = \frac{1}{da/dN} \frac{d(da/dN)}{d\Delta K} \quad (15)$$

The stress intensity range parameter, ΔK_{sf} , is effectively the highest ΔK at which a crack can be said to be in slow propagation. Beyond ΔK_{sf} , no usable fatigue crack life remains except in a low cycle fatigue case, due to high growth rates. The advantage of calculating ΔK_{sf} is in precisely defining the ΔK value above which the life of the component is in the low cycle fatigue regime.

In this study, K_d was found by R_0 optimization for the room temperature, RT, $R = 0.05$, $F = 10$ Hz test condition. The same K_d was used for the RT, $R = 0.05$, $F = 0.1$ Hz because of convenience. This practice made no plotable difference in the curve fits. At room temperature, $R = 0.5$, $F = 10$ and 0.1 Hz test conditions, K_d was chosen by:

$$K_d \bigg|_{R = 0.5} = \left(\frac{1 - 5}{1 - 0.5} \right) K_d \bigg|_{R = 0.05} \quad (16)$$

in the hope the choice would be conservative. At -253°C (-423°F) for $R = 0.05$ data, K_d was chosen as $65.9 \text{ MPa}\sqrt{\text{M}}$ ($60.0 \text{ ksi}\sqrt{\text{in.}}$) which is approximately equal to $(1 - R)K_{IC}$. For $R = 0.5$ data at -253°C , K_d was found by means of Equation (16).

Based on Equation (8), a median crack growth curve was defined as that corresponding to the α and u values found by linear regression. The 2σ limit scatter bands were found by substituting $u = -(\alpha \pm 2\sigma)/b$ into Equation (8). A curve suggested by Bowie [18] as a useful design curve to give a conservative life estimate was defined by substituting $u = -(a - \sigma)/b$ into Equation (8) which resulted in a left side 1σ scatter band curve. Figure 16 shows the 2σ scatter bands, median curve and suggested design curve.

2.4 Rotational Specimen Test Procedures

2.4.1 Stress Analysis

Stress intensity analysis of the parallel sided disks was based on a linear superposition/weight function method [19 - 23] using unflawed disk stresses

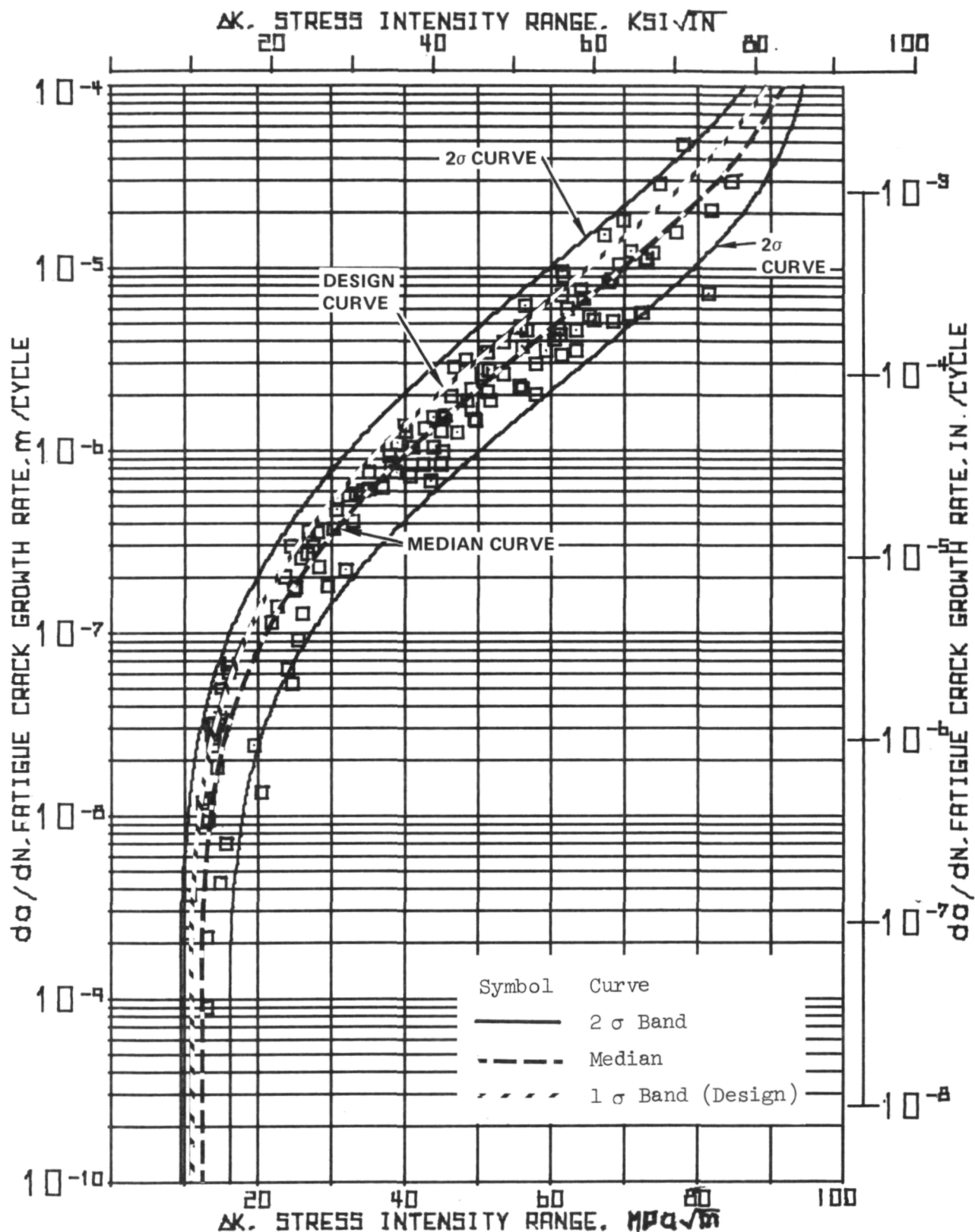


Figure 16.-Fatigue Crack Propagation Data for Ti-5Al-2.5 Sn (ELI) at Room Temperature, $R = 0.5$, $F = 10$ Hz, showing 2σ Band Curves, Median Curve, and 1σ Band (Design) Curve

as per Timoshenko [24]. The method is described in detail in Reference [25] where an application is shown to a rotating disk. A correction was used to allow for the finite diameter. The analysis for this particular disk was kindly performed by Dr. A. F. Grandt, Jr. [20] and resulted in two equivalent non-dimensionalized expressions for stress intensity:

$$K_I = f \rho \omega^2 R_i^2 \sqrt{\pi a} \quad \text{for } \nu = 0.31 \quad (17)$$

$$R_o/R_i = 5$$

where $f = f(a/R_i)$

and $a =$ crack length measured from edge of disk
 $R_i =$ inner radius of disk after final machining
 $R_o =$ outer radius of disk after final machining
 $\rho =$ mass density
 $\omega =$ angular velocity

$$\text{or} \quad K_I = g [(3 + \nu) \rho \omega^2 R_o^2 \sqrt{\pi a}] \quad (18)$$

for any ν

$g = g(a/R_i)$

The functions f and g (see Figs. 17 and 18) were obtained numerically for specific a/R_i values and graphically plotted for one and two equal radius cracks [26]. The crack length, a , given in Figs. 17 and 18 was equal to the B dimension of Figs. 10 or 12 (Section 2.2.3) plus the length of the fatigue precrack. Figure 18 shows that the function g agreed closely to the results of Bueckner and Giaever [27]. Equation (17) was used in this investigation. A polynomial expression for f , useful for calculating K_I in disk life analysis and found to be a good approximation for the analytically derived values of single radial crack curve shown in Fig. 17, was found to be given by:

$$f = 22.7818 - 23.7312(a/R_i) + 18.8487(a/R_i)^2 - 6.7494(a/R_i)^3 + 0.87477(a/R_i)^4 \quad (19)$$

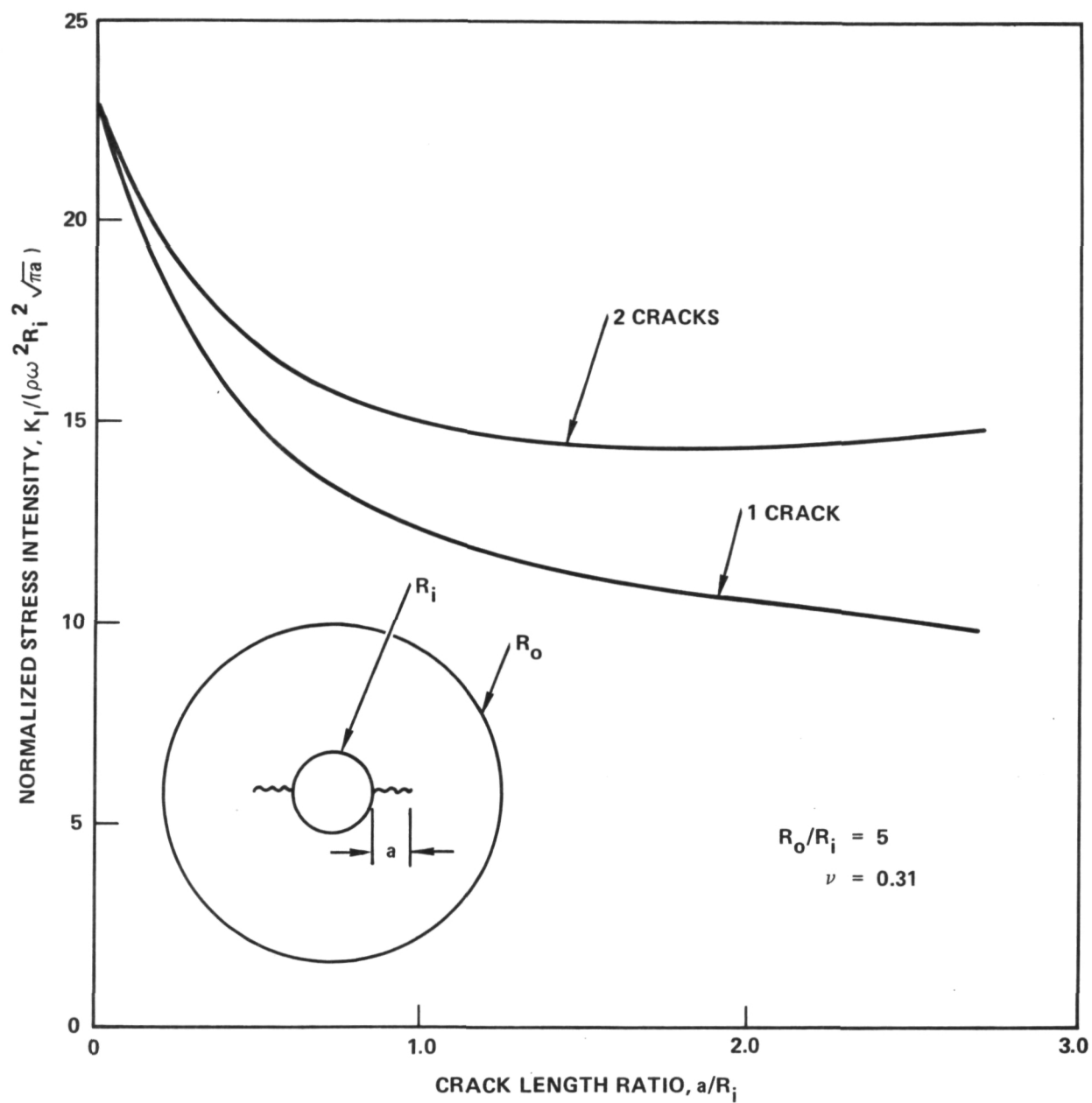


Figure 17. - Normalized Stress Intensity vs a/R_i Showing the Function, f .

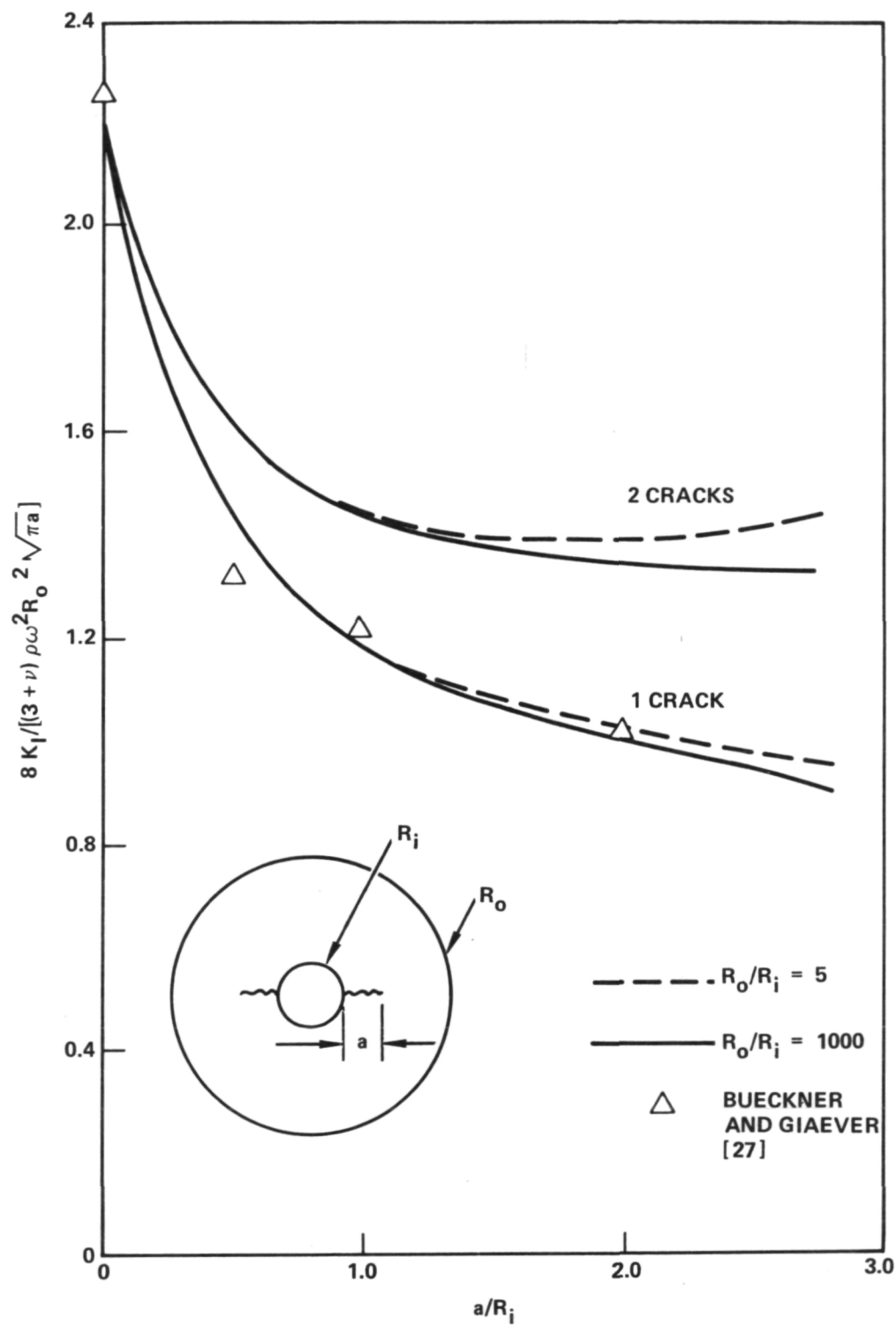


Figure 18.- Non-Dimensionalized Stress Intensity vs a/R_i Showing the Function, g

For this program, K_I was calculated using a single radial crack even though most disks had two notches of equal length in opposite directions. This assumption was made because only one of the notches had a fatigue precrack and this crack was long enough that the crack length, a , was much longer than the un-precracked notch. In addition, the disk was assumed to be less sensitive to the blunt un-precracked notch. Finally, the function $f(a/R_i)$ was used in the range $0 \leq a/R_i \leq 2.8$ even though the most reliable range is up to $a/R_i = 1.0$ [26]. The validity of these assumptions will be discussed in Section 5.

2.4.2 Prediction of Burst Speed

To allow for possible correlation between the results of this program's investigation of precracked rotating disk behavior to any other research work using "unflawed" disks, an unnotched disk was used in one of the burst tests. The predicted burst speed for this disk was calculated from the equation:

$$N_{\text{burst}} = N_1 [0.9 (\sigma_{\text{ult}}/\sigma_{\theta\text{avg}})]^{1/2} \quad (20)$$

The term N_1 is any speed below N_{burst} and $\sigma_{\theta\text{avg}}$ is the average tangential stress. Equation (20) is based on collective experience in the rotating disk technology field [28]. The stress, $\sigma_{\theta\text{avg}}$, was found by using the elastic stress analysis for rotating disks by Timoshenko [24]. The predicted burst speed based on Equation (20) was compared to that obtained from an equation due to Robinson [29]. He assumed that burst occurs when the nominal average tangential stress equals the tensile strength of the material. For a uniformly thick disk, σ_{ult} would be found by the following equation.

$$\sigma_{\text{ult}} = \frac{1}{3} \rho \omega_b^2 \left[\frac{R_o^3 - R_i^3}{R_o - R_i} \right] \quad (21)$$

where ρ is the density, ω_b is the angular velocity at burst, R_i is the internal radius, and R_o is the external radius. Plastic deformation analysis of rotating disks has also been used to predict burst speed. Such analyses are based on the Tresca yield criteria and associated flow rule or on the Hencky [30] deformation theory of plasticity. Predictions of burst speed based on the Hencky theory are usually somewhat higher than those based on Equation (20) or 21 [31]. See Reference [31] for a more complete discussion of these equations.

2.4.3 Test Procedures

After disks were machined to the configuration of Fig. 10, one hole was precracked using a high pressure hydraulic precrack unit. This machine was designed at Lockheed-California Company based on a general approach by Clark and Aschini [32]. The precrack unit is schematically shown in Fig. 19. Alternating pressures from 20.7 to 517 MPa (3000 to 50,000 psi) at up to 5 Hz could be generated by the precracking unit. The precracking system consisted of low and high pressure hydraulic units. Referring to Fig. 19, the low pressure system operated by pumping oil from a 0.028 m³ (5 gallon) reservoir into an accumulator until a pressure of 20.7 MPa (3000 psi) was reached. The low pressure valve was closed which cut off the reservoir and maintained 20.7 MPa (3000 psi) in the low pressure system through the high pressure intensifier check valve and into the lower manifold. Operation of the hydraulic actuator moved the piston of the high pressure intensifier and increased the pressure in the disk to the level desired. The actuator was operated in the stroke control mode while the high pressures were monitored using a pressure transducer. System operation was closed loop since the pressure readout was fed back to limit the stroke such that the desired pressure limits were maintained. Any over or under pressure resulted in system shutdown.

A disk to be precracked was placed between two high strength steel manifolds, see Fig. 20, which were fitted with metallic "O" ring seals and with protrusions for centering of the disk. The manifold and disk assembly was kept in contact with a hand-operated screw jack which was loaded to about 133 kN (30 kips). The possibility that near surface residual stress induced by the preload

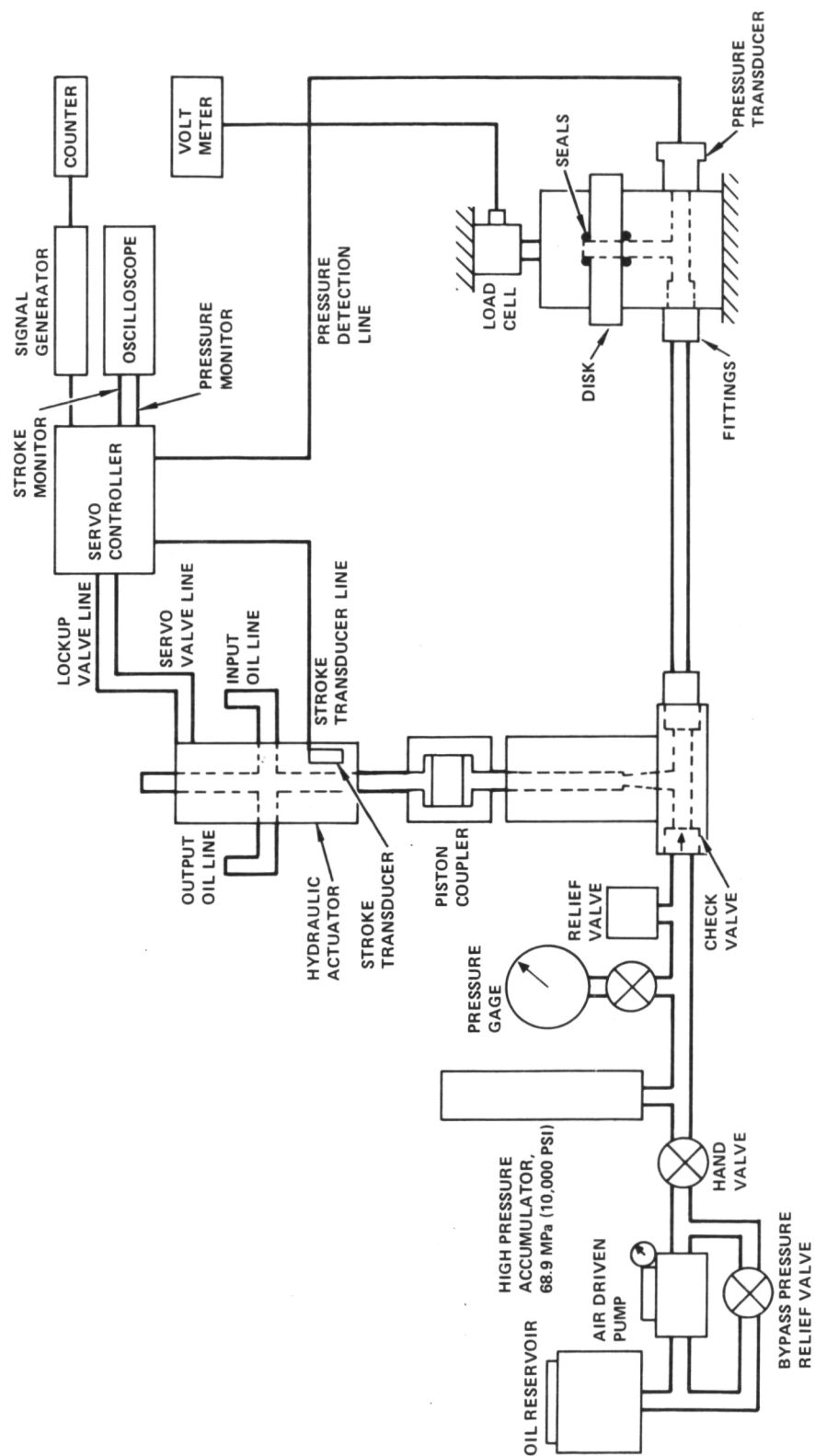


Figure 19. - Schematic of High Pressure Hydraulic Precracking System.

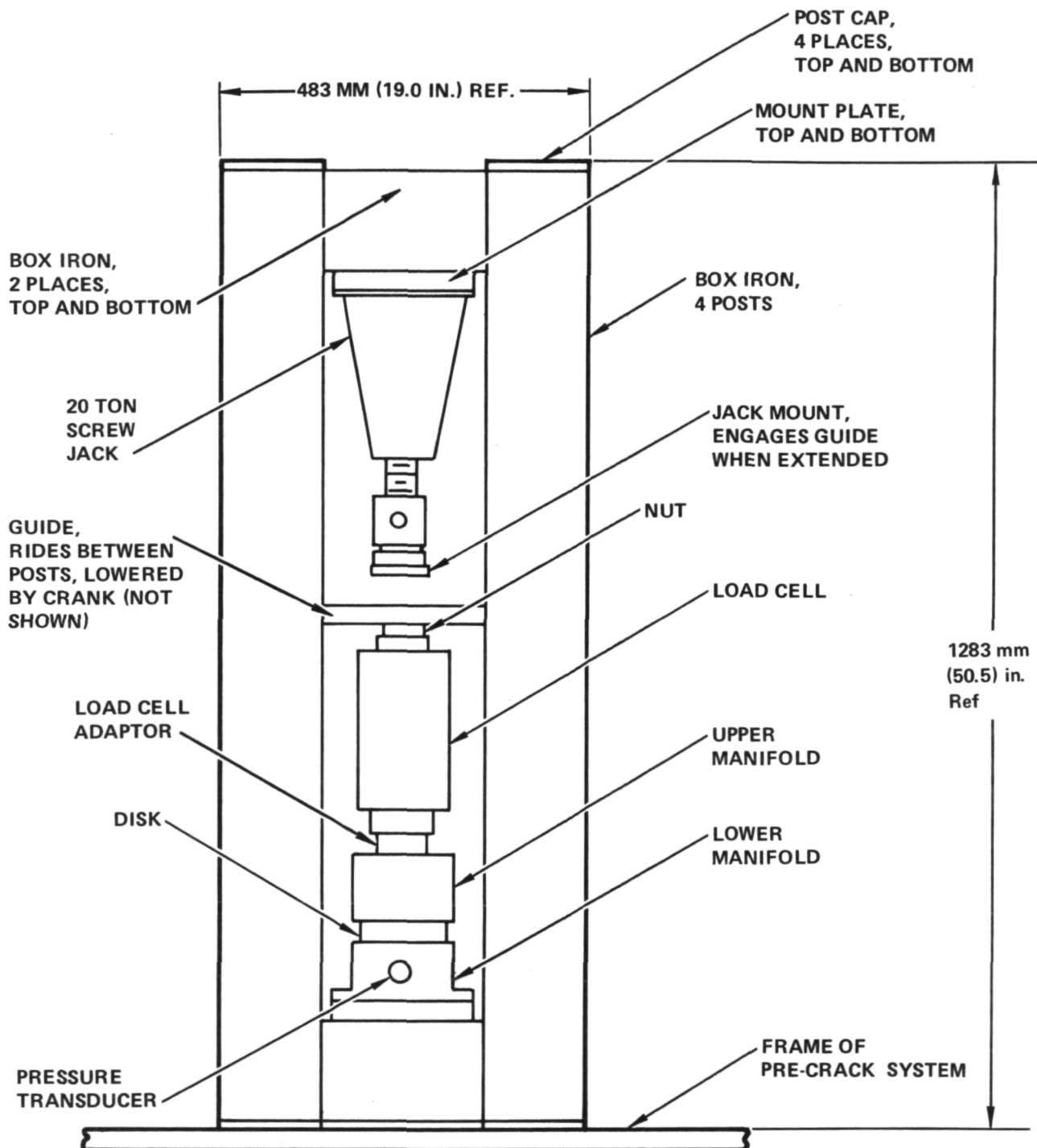


Figure 20. - Schematic of Frame Assembly Used to Preload Disks for Precracking

could effect growth of the crack during subsequent spin pit cycling was eliminated by the fact that disks were ~ 38 mm (1.5 in.) thick during pre-cracking and were machined down to 25.4 mm (1.0 in.) thickness prior to rotational induced loading.

In this program, disks were precracked at 34.5 to 206.8 MPa (5000 to 30,000 psi) or 34.5 to 275.8 MPa (5000 to 40,000 psi) at 2-3 Hz. These pressures resulted in maximum stress intensities at the notch root of approximately 27.5 to 38.5 MPa \sqrt{m} (25 to 35 ksi $\sqrt{in.}$), depending on the maximum pressure, and a minimum stress intensity of approximately 4.4 MPa $\sqrt{in.}$ (4.0 ksi $\sqrt{in.}$). These maximum stress intensities were well below those induced by the rotational stresses during spin pit testing.

Testing was conducted at the Solar Division of International Harvester Company. The spin pit (see Fig. 21) was capable of reaching 120,000 rpm and used a high pressure air system to spin the shaft. For burst tests, shaft speed was simply increased until burst occurred. The duration of a burst test was approximately 2 to 5 minutes. For fatigue crack growth tests, the air speed drive automatically shut-off at the maximum desired speed; a hand operated brake was applied until the lower speed was reached at which point the brake was released and the air speed driver reactivated. This semi-automatic system resulted in the wave shape shown in Fig. 22 and in a cycle time of approximately 0.75 min. Test cycles were automatically counted.

Figure 23 shows the hole and notch before precracking of disk 19 while Fig. 24 shows the final surface precrack of disk 19 prior to final machining. The outer indented ring seen in Figs. 23 and 24 was caused by the pressure of the hydraulic sealer ring. In the case of disk 19, the crack grew until the seal was reached at which time system pressure loss occurred. Fig. 25 shows a precrack for disk 28 which was terminated prior to reaching the seal.

Figures 26 and 27 show the spin shaft and arbor assembly used to rotate the disks in the spin pit while Fig. 28 is a schematic of a disk on the assembly.

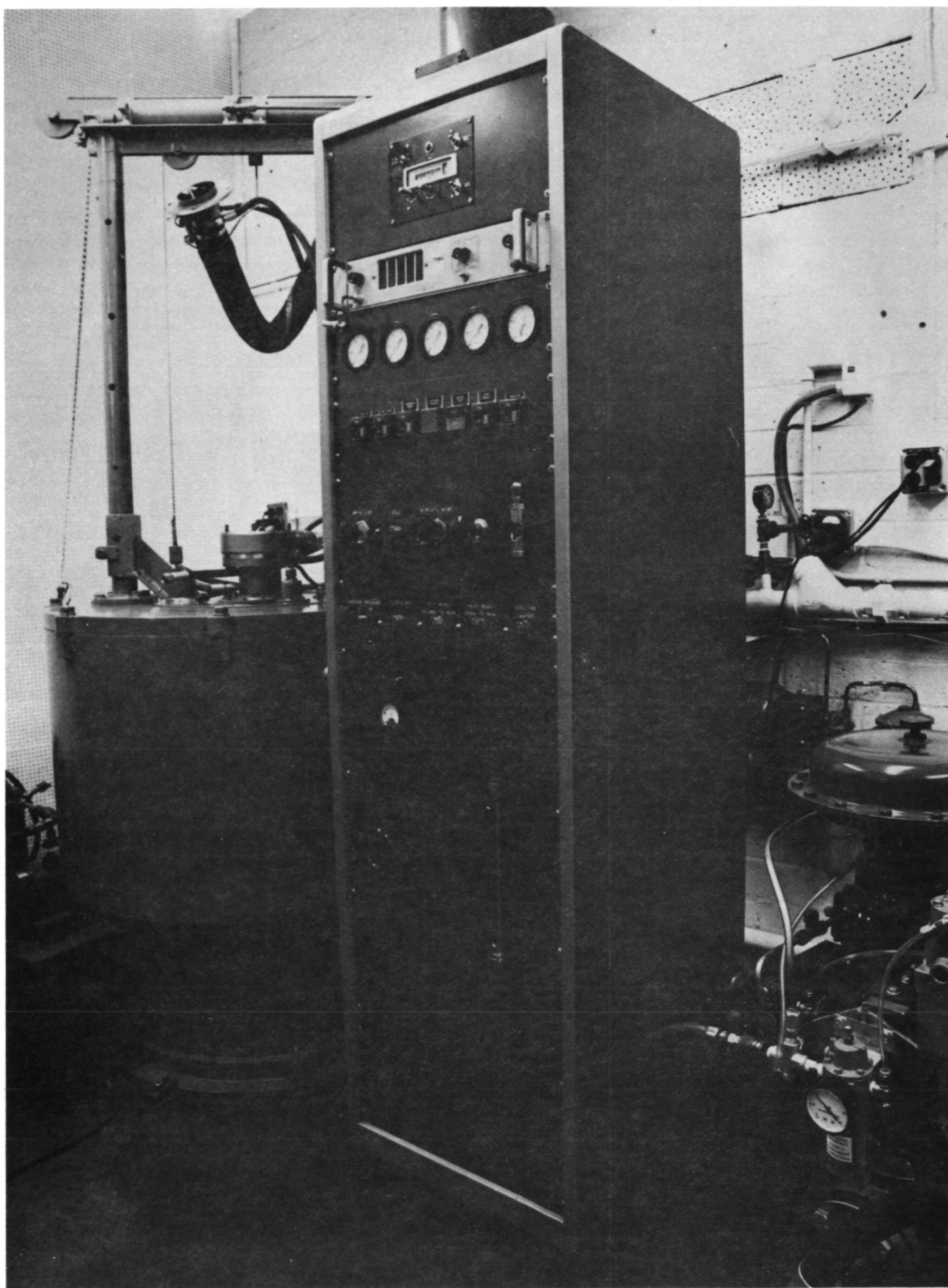


Figure 21. - Spin Pit and Associated Control Equipment

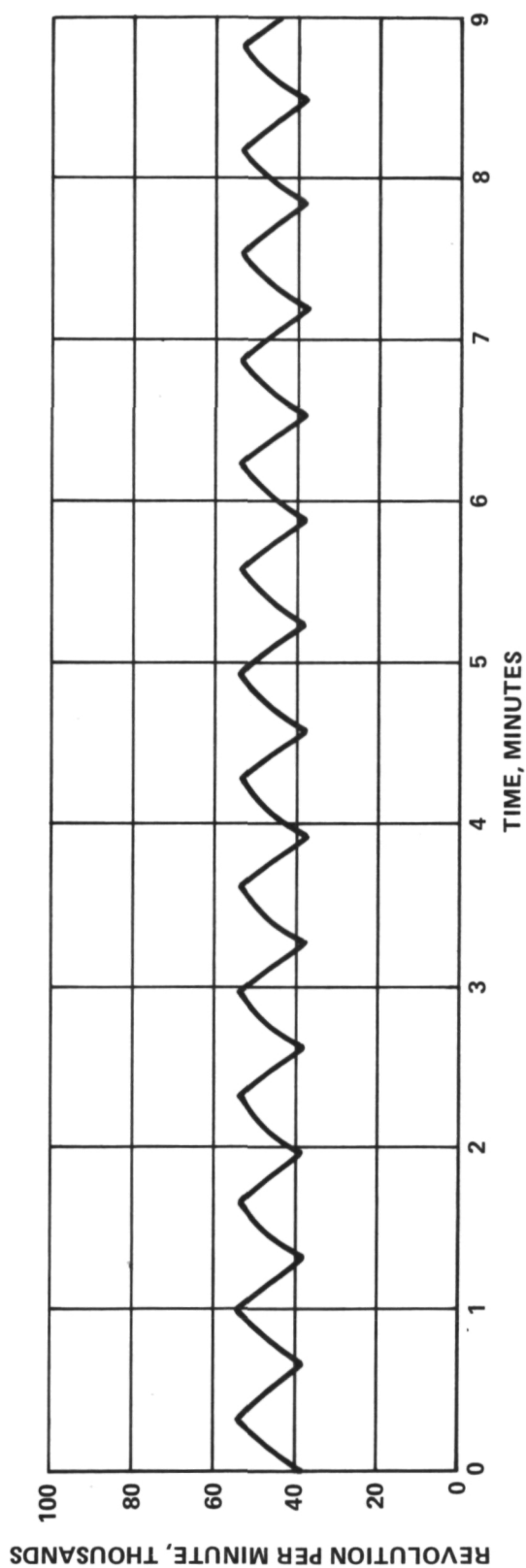


Figure 22. - Speed Spectrum from Rotational Crack Growth Test of Disk 25 which was Typical of all Rotationally Induced Fatigue Crack Growth Tests

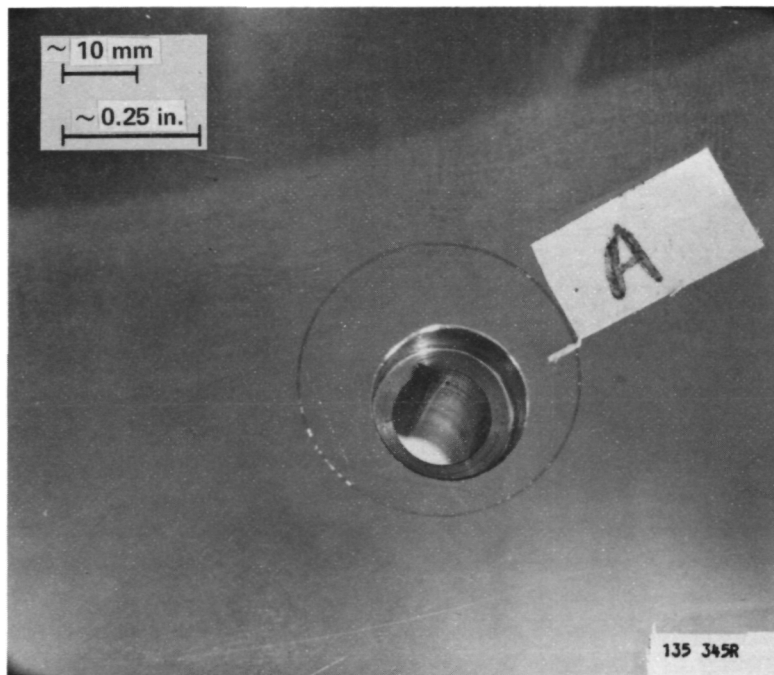


Figure 23. Precrack Hole and Notch of Disk 19

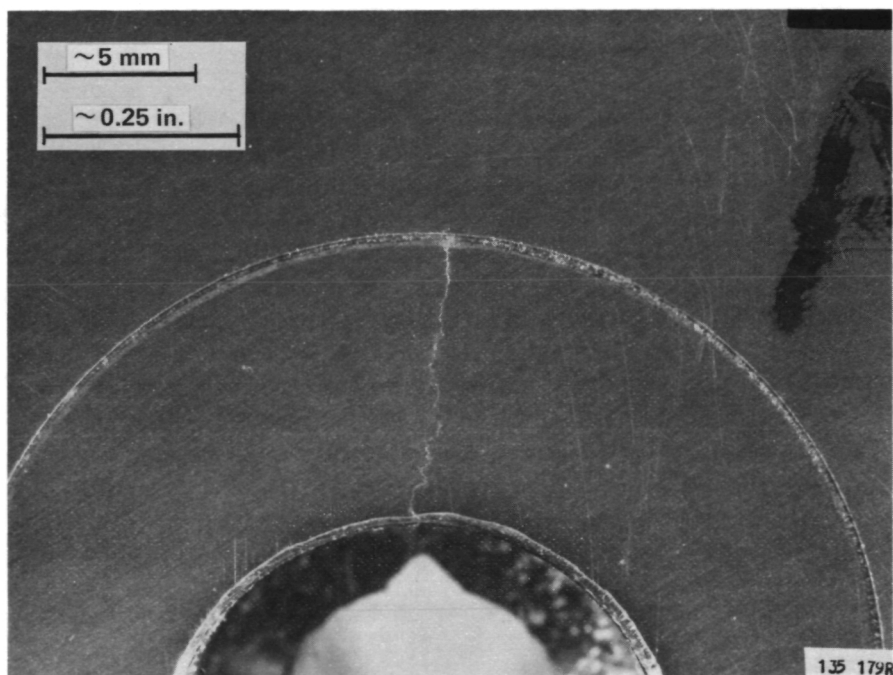


Figure 24.- Surface Crack of Disk 19 After Fatigue Precracking

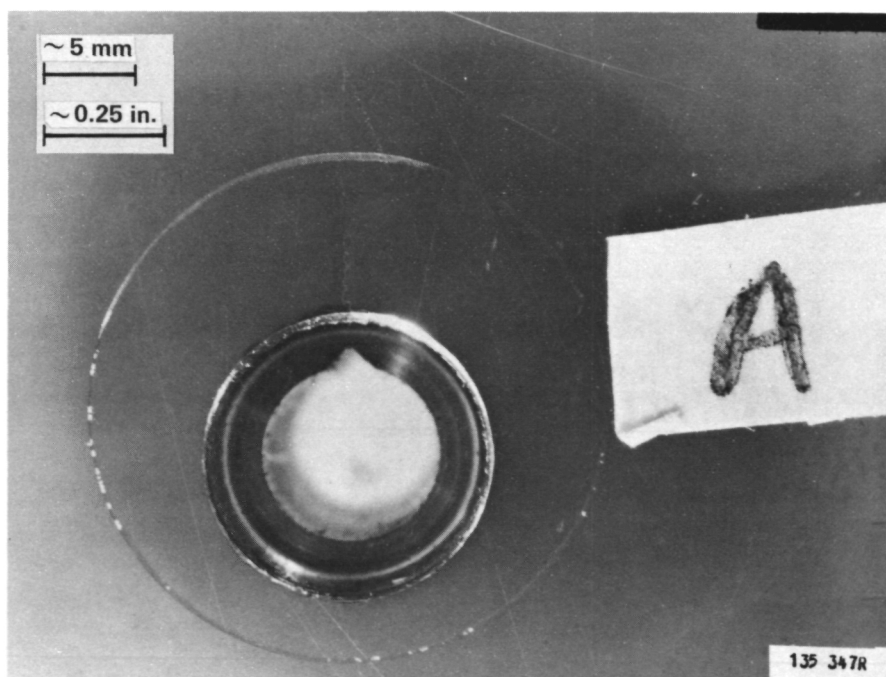
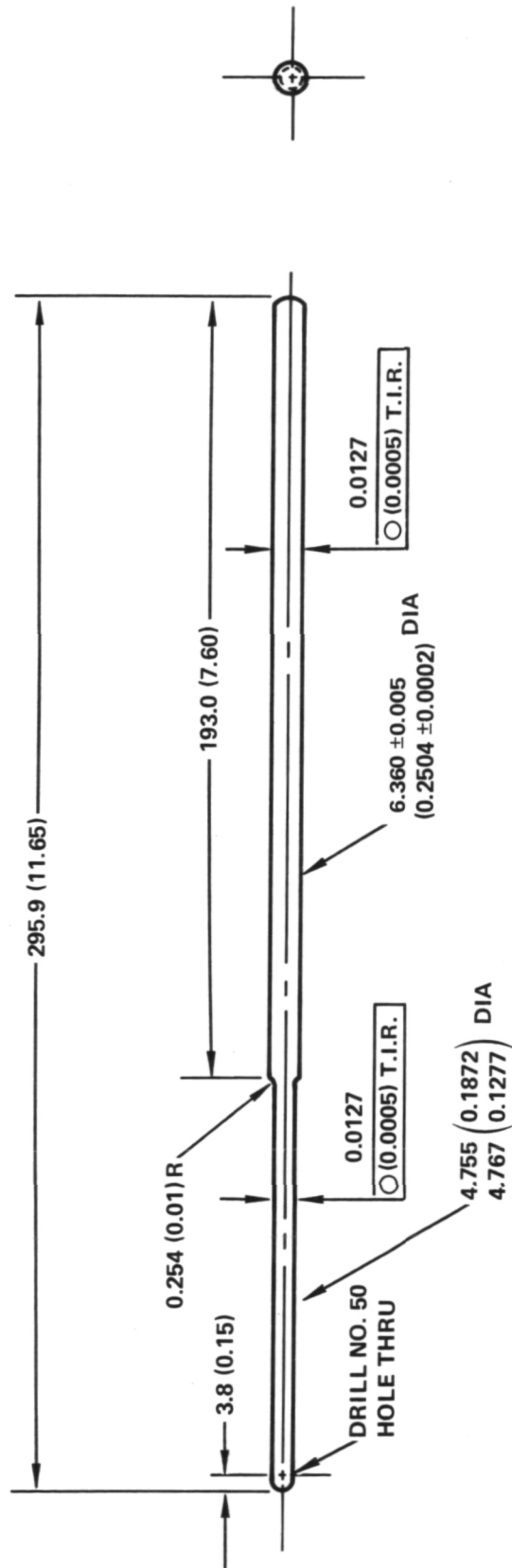


Figure 25.- Surface Crack of Disk 28 After Fatigue Precracking



DIMENSIONS IN mm (in.)

Figure 26.- Spin Shaft Used for Rotating Disks

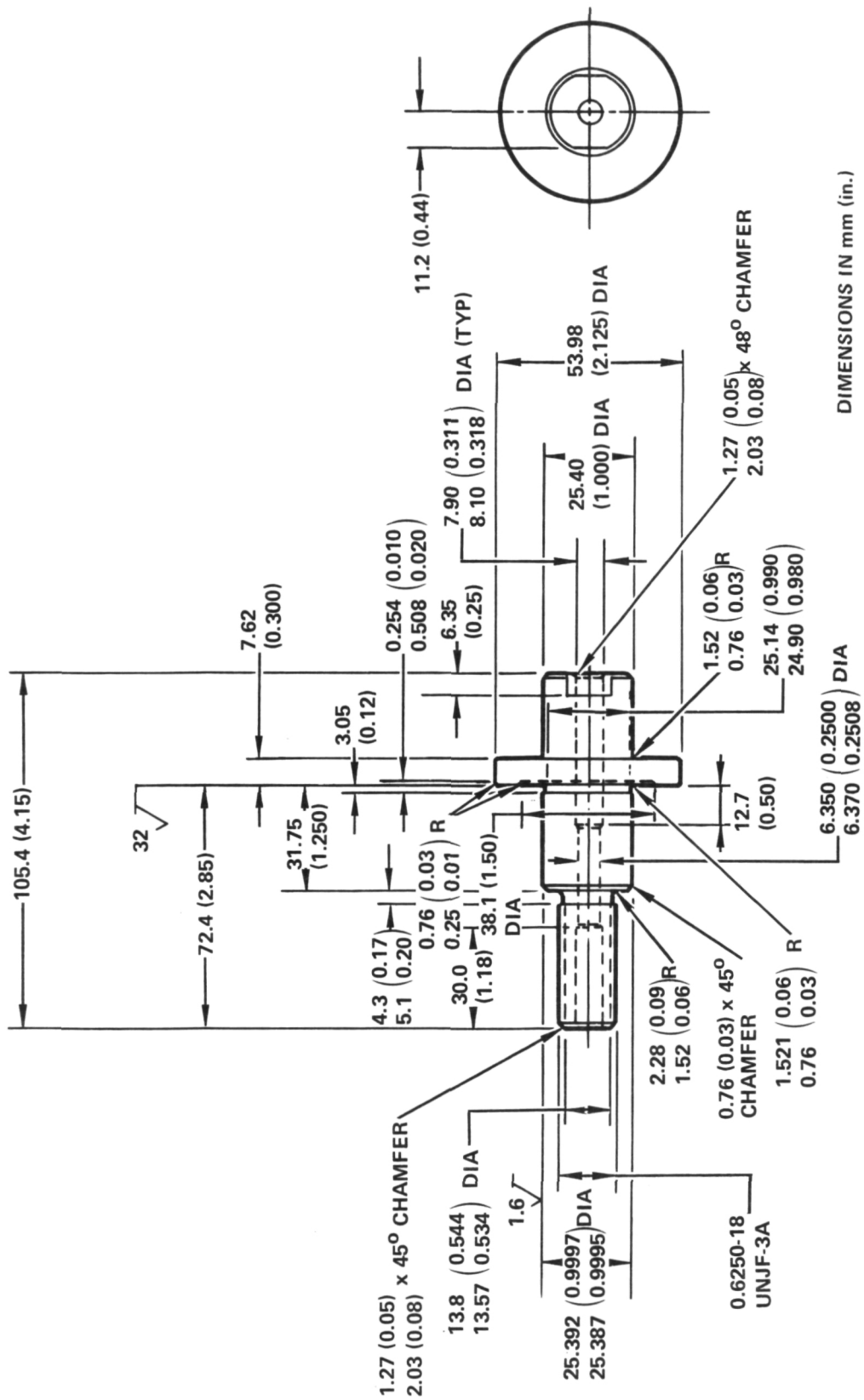
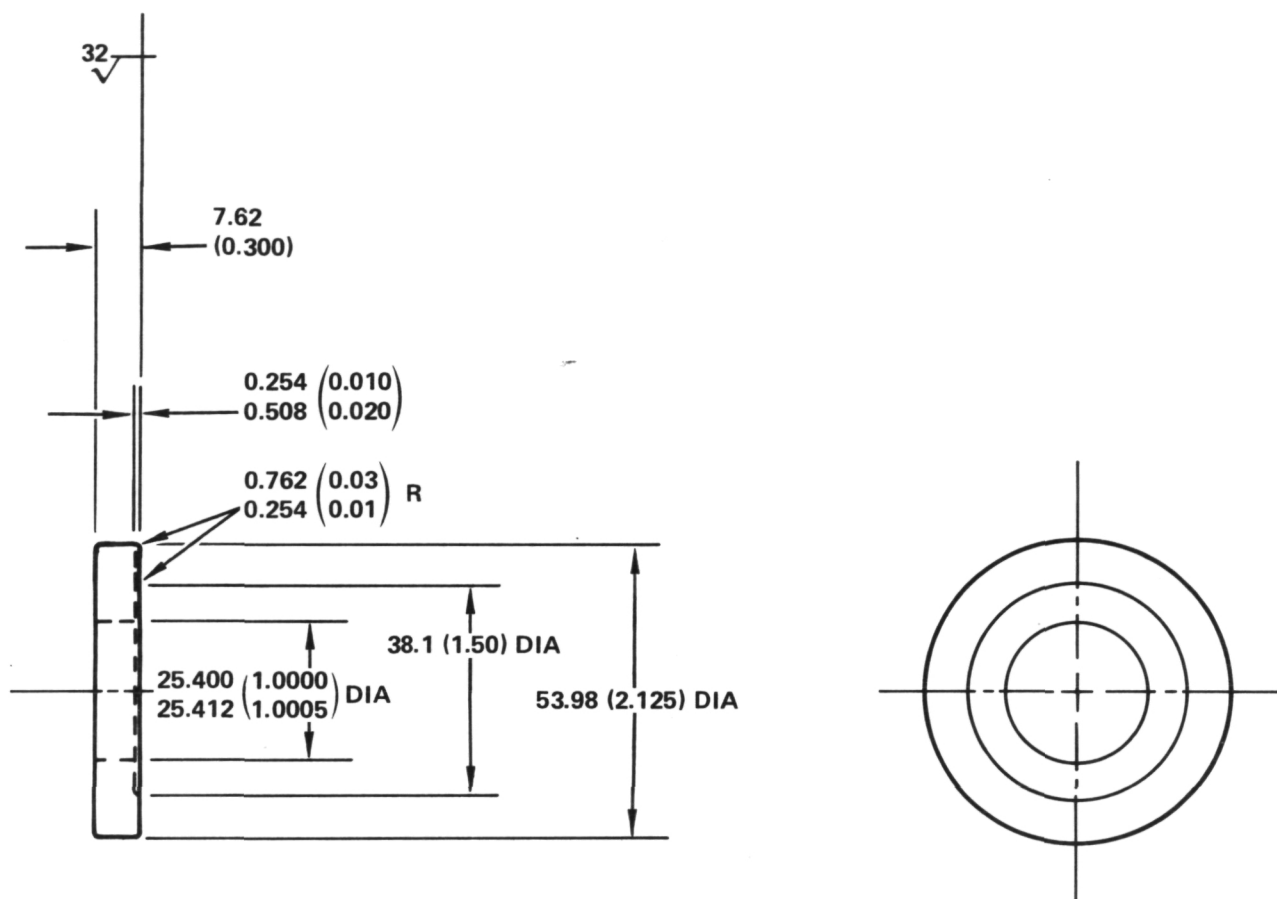


Figure 27A. - Spin Arbor and Associated Parts



DIMENSIONS IN mm (in.)

Figure 27B. - Spin Arbor and Associated Parts

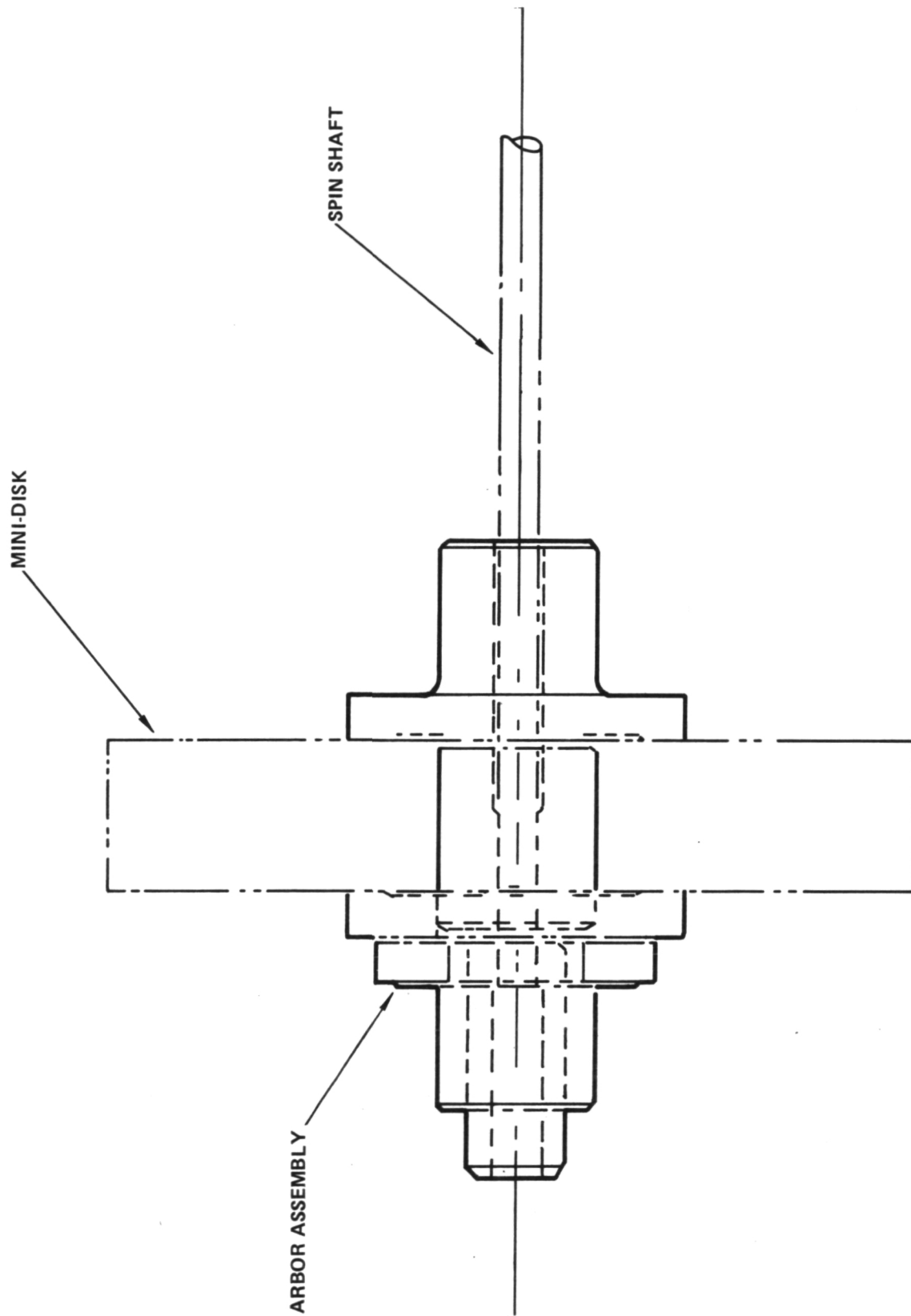


Figure 28. - Schematic Drawing of Disk Mounted on Spin Shaft and Arbor Assembly

The top end of the shaft was placed through the set of spin pit bushings and held in place by a small steel pin. The spin arbor was held on by a steel pin through the arbor and shaft. No balancing of the disks or arbor assembly was found necessary because the restricted machining tolerances for the disks eliminated the possibility of any imbalance to a non-detrimental level.

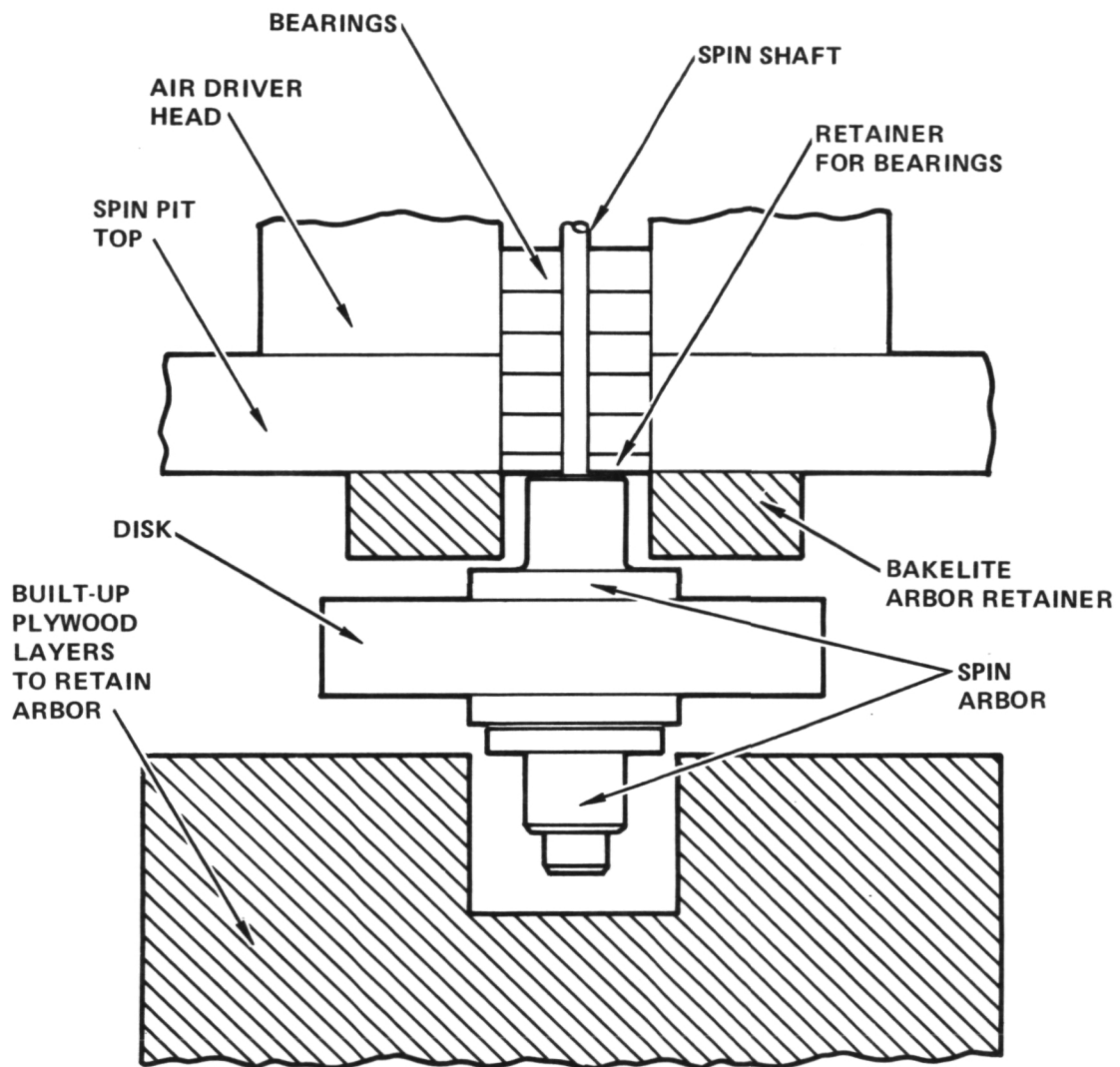
Throughout the test, the spin shaft was lubricated with oil which slowly flowed past the shaft and into the spin pit. This resulted in oil flowing onto the spin arbor and disk assembly which, of course, spun the oil off due to the high revolution speeds. During testing, disk temperature increased to the temperature range of 55° to 70°C (130° to 160°F). If failure of the spin shaft occurred prior to disk burst, damage to the disk was prevented by wood and bakelite restraining blocks around the spin arbor as shown schematically in Fig. 29. Containment of the disk pieces after burst was achieved by both wood and lead alloy liners, see Fig. 30.

The specific crack growth testing procedure varied for each disk. Prior to testing, the initial crack length from the bore was estimated, the stress intensity range ratio was chosen as $R = 0.5$, and test speeds calculated from

$$N = \omega \frac{60}{2\pi} \quad (22)$$

where ω was calculated from Equation (17) using the specific minimum and maximum K values chosen. Rotating crack growth tests were cycled, without hold time, between the minimum and maximum speeds at a frequency of approximately 1 cycle/min. No hold time was used because laboratory coupon tests indicated no effect of frequency. If a disk did not fail during fatigue crack growth testing, then a burst test was conducted.

Fatigue crack growth tests were periodically stopped and the disk removed. Crack length was measured on both sides using micrometer calipers and a 10X lens. Surface crack readings were estimated to be ± 0.127 mm (.005 in.). After bursting of the disk, the subsurface crack lengths were measured. The crack length used for calculating crack growth rate was an average of the



NOTE: NOT TO SCALE

Figure 29. - Schematic of Cross-Section Through Assembly
Used to Retain Disk in Case of Shaft Failure

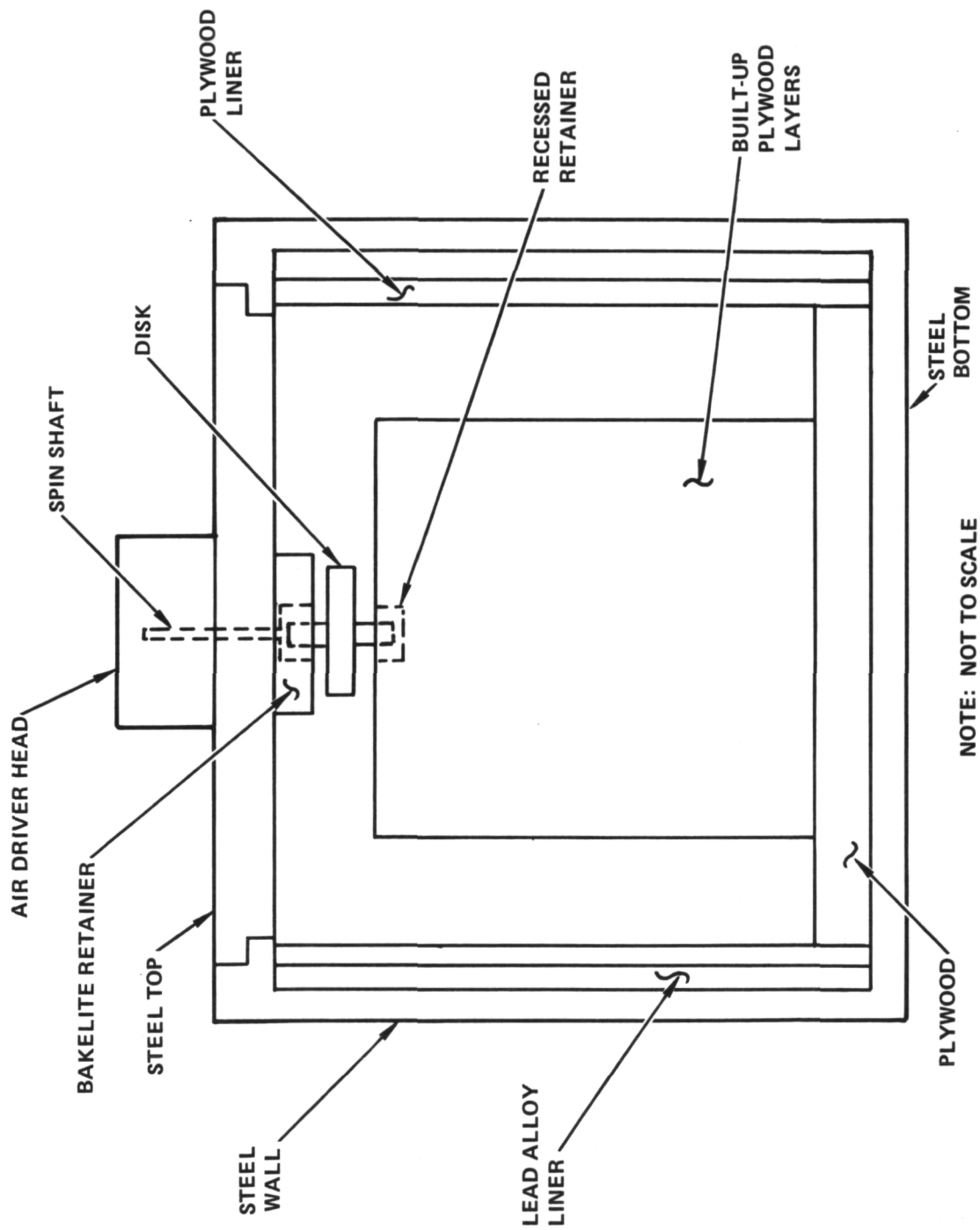


Figure 30. - Schematic of Spin Pit

two surface and three subsurface crack measurements. Crack growth rate was defined as the change in crack length divided by the number of cycles between readings. Stress intensity was calculated using Equation (17) and the average crack length within the test interval.

3.0 MATERIAL CHARACTERIZATION

3.1 Material Fabrication

Two lots of Ti-5Al-2.5Sn(ELI) were purchased from the Rocketdyne Division of Rockwell International. Both lots were from RMI Heat No. 891389 and were purchased to the ELI requirements of AMS4924B as well as appropriate Rocketdyne specifications. Lot 1 was a 3567 N (802 lbs) billet, 1090 mm (43 in.) long and 305 mm (12 in.) in diameter while Lot 2 was a 2002 N (450 lbs) billet, 610 mm (24 in.) long and 305 mm (12 in.) in diameter.

Chemical analysis results of the two lots of material is shown in Table 6. As can be seen in this table, both lots of material met both specifications. An element not listed in Table 6 is yttrium. Conversations with Rocketdyne personnel confirmed that this RMI Heat of Ti-5Al-2.5Sn(ELI) was one of numerous heats of titanium produced by RMI to which yttrium was added during the melt. Yttrium in small amounts and finely distributed can be used to reduce grain size and improve the forgeability of titanium and other alloys [33]. An analysis [34] of available data [35,36,37] on the effect of yttrium on the mechanical properties of titanium alloys indicated for Ti-6Al-4V somewhat lower longitudinal and short transverse tensile properties and a decrease in resistance to stress corrosion cracking. For Ti-6Al-2.5Sn, the addition of yttrium appeared to result in a reduction of K_{IC} by 13.2 to 22 MPa \sqrt{m} (12 to 20 ksi $\sqrt{in.}$) [34]. These reductions in mechanical properties were apparently due to both the addition and poor segregation of the yttrium [34-37]. The amount of segregation of yttrium in this alloy is unknown and thus the effects on properties is also unknown. Future users of this alloy must consider this potential problem.

The starting stock material of Lot 1 was cut into two pieces labeled 1-Top and 2-Bottom. These two pieces received Ladish Lot No. H4-2046 and H4-2180 while Lot 2 of the starting stock material received Ladish Lot No. H5-834.

TABLE 6

CHEMICAL COMPOSITION^a of Ti-5Al-2.5Sn(ELI)

Heat No. 891389

Chemical	Lot 1 H4-2046 H4-2180	Lot 2 H5-834	AMS4924 Specification Min. Max.	RB0170-152 ^b Specification Min. Max.
Aluminum (Al)	5.08	5.08	4.70 5.60	4.60 5.60
Tin (Sn)	2.37	2.37	2.00 3.00	2.00 3.00
Carbon (C)	0.01	0.02	- 0.08	- 0.05
Iron (Fe)	0.07	0.06	- 0.25	- 0.20
Hydrogen (H)	0.006	0.005	- 0.0125	- 0.010
Manganese (Mn)	<0.01	<0.01	- 0.10	- 0.030
Nitrogen (N)	0.01	0.01	- 0.07	- 0.04
Oxygen (O)	0.08	0.07	- 0.12	- 0.10
Other Elements, Each	<0.01	<0.01	- 0.05	- 0.05
Other Elements, Total	<0.15	<0.15	- 0.40	- 0.20
Titanium	Remainder	Remainder	Remainder	Remainder

a. All values in weight percent.

b. Rocketdyne Specification

All three pieces were drawn down to 152 mm (6 in.) diameter billets after which 152 mm (6 in.) long pieces were cut off for the pancake forgings. The Lot 1 billet yielded approximately 3025 N (680 lbs) of material after draw down while Lot 2 yielded approximately 1846 N (415 lbs) after draw down.

Forging reductions, to a total of 50%, were started above the beta transus temperature, T_{β} , determined to be 1010°C (1850°F) and finished in the alpha field. The billets were upset twice during forging. Forgings were annealed at $788 \pm 14^{\circ}\text{C}$ ($1450^{\circ}\text{F} \pm 25^{\circ}\text{F}$) for two hours and furnace cooled. The 152 mm (6 in.) diameter billets after draw down were found acceptable to level 30 according to Figure 3 of AMS Specification 2380. Sonic testing per AMS 2631 showed no apparent defects or flaws. The aluminum rating was met. While no specific AMS specification for microcleanliness is known to exist for this material, Ladish examination of the forged microstructure showed the material to be apparently free of microstructural segregation, porosity, or material nonuniformities.

From Lot 1, 10 pancakes from each piece were produced numbered 1 to 20 from the top down; the first 10 from piece 1-Top. Lot 2 produced 12 pancakes numbered 21 to 32. Pancakes 1 to 18 were forged on November 10, 1974, while pancakes 19 to 32 were forged on November 7, 1975. Finished pancake weight was approximately 151 N (34 lbs). Pancake 11 was slightly underweight and had to be machined carefully while pancakes 15 and 18 were discovered by sonic inspection to have small center cracks. During machining, pancake 16 was also discovered to have a small crack at the location of the two tensile blanks. Table 7 gives the finished dimensions of each forged pancake while Fig. 31 shows a typical finished pancake.

Figures 32, 33, and 34 show macrostructures of pancakes 1, 9, and 16 taken from a diametrical cut. Grain size appeared to be uniform. The photomicrographs showed that their macroetch grain size was acceptable per Figure 15 of the AMS 2380 Specification. The etchant used was Krolls: 10% nitric and 8% hydrofluoric acid in water. Some indication of grain flow was evident, but

TABLE 7

FINISHED DIMENSIONS OF Ti-5Al-2.5Sn(ELI) FORGED PANCAKES

Serial No. ^a	Top Face ^b Diameter, mm		Bulge Diameter, mm		Bottom Face Diameter, mm		Thickness, mm
1	179 ^c	184 ^c	232	236	200	210	76.2
2	203	208	236	238	179	187	75.9
3	203	208	237	240	192	195	75.2
4	210	213	239	241	194	197	75.2
5	210	214	241	245	190	197	74.4
6	210	214	240	242	194	195	76.2
7	211	216	237	217	198	203	74.9
8	210	211	236	240	197	202	74.9
9	210	213	240	241	195	200	75.4
10	206	208	236	238	192	195	75.4
11	192	195	217	222	182	197	75.4
12	205	210	233	236	194	198	75.2
13	206	211	238	240	198	203	75.4
14	206	210	239	240	197	198	75.7
15 ^d	210	211	236	238	202	208	75.4
16 ^d	208	211	237	238	206	210	74.9
17 ^d	211	213	240	240	205	208	74.4
18	210	216	237	242	205	208	75.9
19	204	198	236	232	206	201	81.0
20	203	198	240	237	216	210	78.6
21	210	201	217	238	209	206	79.4

TABLE 7 (Concluded)

Serial No. ^a	Top Face ^b Diameter, mm		Bulge Diameter, mm		Bottom Face Diameter, mm		Thickness, mm
22	206 ^c	265 ^c	240	239	209	206	81.8
23	205	204	239	236	209	204	78.6
24	206	205	239	236	209	204	77.9
25	197	191	233	233	207	201	81.0
26	209	204	237	233	204	202	77.9
27	202	199	234	230	202	198	80.2
28	202	197	203	229	201	196	79.4
29	201	198	233	228	197	195	81.0
30	202	200	236	233	204	201	77.0
31	204	200	237	233	206	201	77.0
32	205	197	237	231	206	200	77.9

a. Denotes sectioning of multiples in sequential order starting with top of ingot

b. Denotes face toward top of ingot, stamped face

c. First dimension is minimum value, second dimension is maximum value.

d. Denotes cracked pancake.

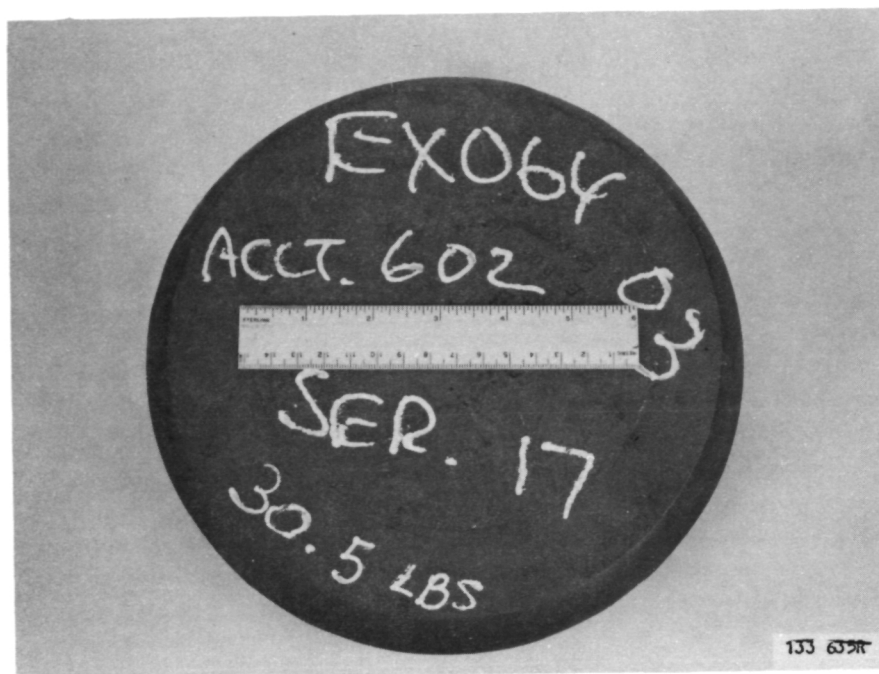


Figure 31A. -Top View of Pancake 17

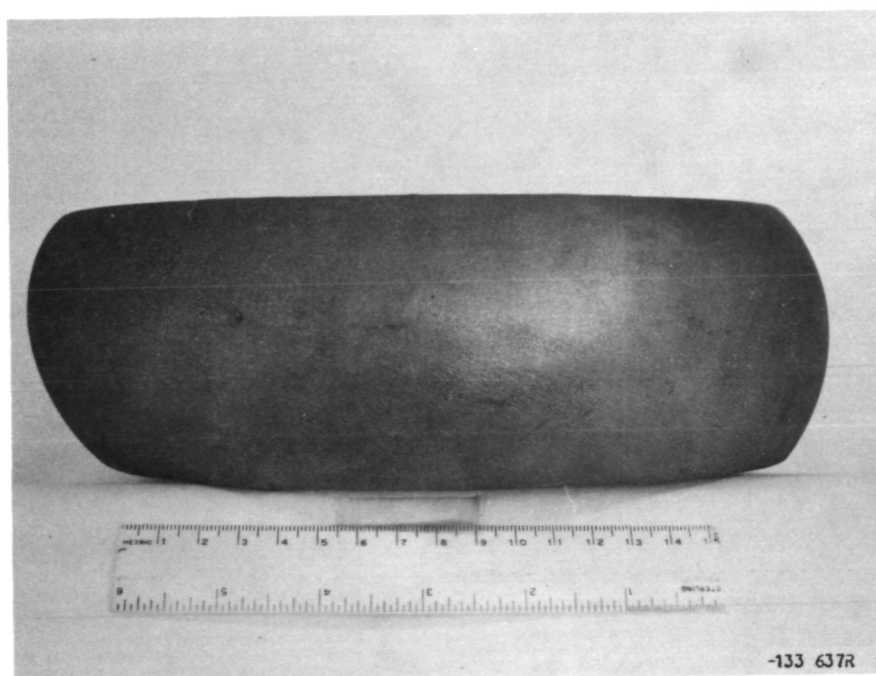


Figure 31B.- Edge View of Pancake 17

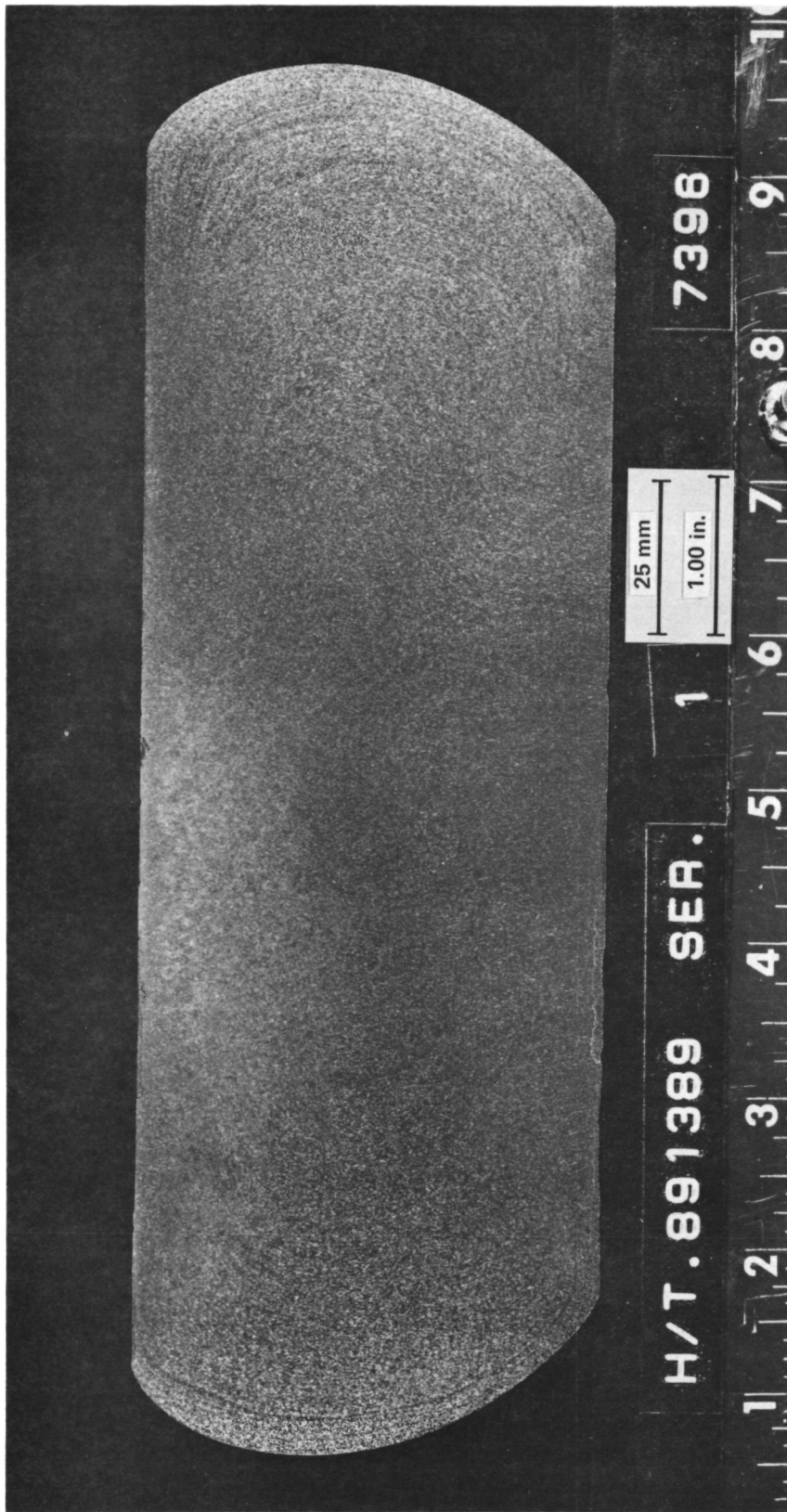


Figure 32. - Macrostructure of Diametrical Cross-Section of Pancake No. 1, Etchant 10% HNO_3 , 8% HF



Figure 33. - Macrostructure of Diametrical Cross-Section of Pancake No. 9, Etchant 10% HNO_3 , 8% HF

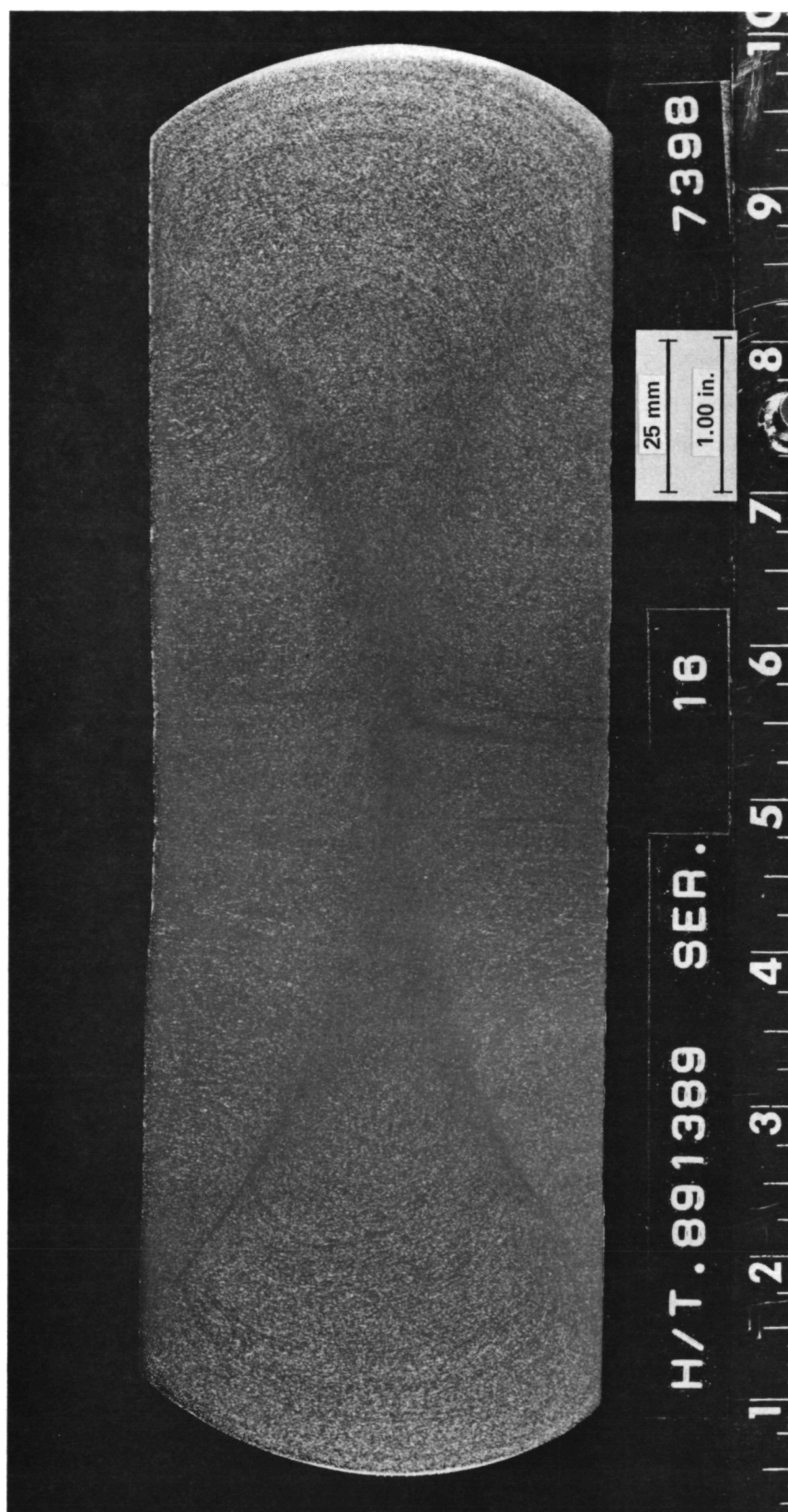


Figure 34. - Macrostructure of Diametrical Cross-Section of Pancake No. 16, Etchant 10% HNO_3 , 8% HF

this did not become pronounced until the higher serial numbered pancakes, numbers 15 through 18, as shown for number 16 in Fig. 34.

Ti-5Al-2.5Sn is potentially susceptible to a flow problem during forging caused by extreme friction between the die and material, called die lock, which can result in cracked forgings. Since T_p for these material lots was lower than that usually observed (T_p usually is $\approx 1032^\circ\text{C}$ (1890°F)), pancakes were forged at a lower temperature to remain below T_p . This lower forging temperature would result in greater resistance to flow and thus enhanced susceptibility to die lock. Usually thin cone-shaped lines observed in macrographs of forging grain flaws, such as those evident in Fig. 34, are an indication of some extent of die lock. Cracks which were found in pancake forgings 15, 16, and 18 were probably associated with this more pronounced flow pattern indicative of die lock.

The possibility of the occurrence of die lock was anticipated especially after determination of this materials low T_p , 1010°C (1850°F). Therefore, during the forging operation, each pancake was upset twice and more than one forging hit applied. This procedure reduced the total amount of reduction for each hit thus reducing the amount of flow per hit and hopefully minimizing the possibility of die lock and subsequent cracking. Unfortunately, cracking still occurred. The flow pattern evident in Fig. 34 was difficult to explain because such a phenomenon is normally associated with insufficient heating of the die. Therefore, this flow pattern would normally be more pronounced early in a forging series, and become less obvious later as the die temperature increased. This explanation was apparently inadequate in this case.

Because forging of pancakes 19 to 32 was conducted much later than pancakes 1 to 18, more extensive upset operations were considered for these pancakes. However, to prevent possible material changes due to a change in forging practice, pancakes 19 to 32 were forged in the same manner as pancakes 1 to 18. No cracks were found in the pancakes used in the spin pit test program, pancakes 19 to 29, which came from lot 2.

Even though a complete understanding of the causes of the cracking was not achieved, the above discussion indicates the possible causes. In any case, a potential problem appears to exist for any production run of rotors made from this material. The problem appears to be primarily one of a possibly greater loss of components during forging than is normally acceptable as well as the necessity of careful post-forging NDI inspection for forging flaws.

Table 8 lists the hardness results for the top surface of each pancake. All hardness readings were Brinell taken using a standard 2.942 kN (3000 kg) load and the standard 10 mm diameter steel ball. The entries in Table 8 are the Brinell hardness diameter (BHD). All pancake surface readings were taken at small polished areas. Brinell hardness was obtained because titanium sticks to the diamond tip used in Rockwell C hardness testing often resulting in false readings. In addition, although not a serious problem for Ti-5Al-2.5Sn which is an all alpha alloy, Brinell hardness is an average over a large area as opposed to the small diamond tip of Rockwell C testing which would detect differences in the two phases of titanium platelets, alpha and beta, which is not always desirable. Table 8 shows that the BHN of pancakes 19 to 32 was slightly lower than for pancakes 1 to 18.

A two-dimensional forging model study was conducted to compare flow characteristics of the pancakes during forging to that expected for the rotor forgings. The purpose of this study was to aid in establishing that the material characteristics of the pancakes due to the reduction steps during forging were similar to those to be expected in the bore region of the rotor. Figure 35 shows a schematic of a typical finished pancake forging while Fig. 36 shows a similar sketch of the rotor forging. Results of the forging model studies are shown in Figs. 37 and 38. As can be seen in these two figures, the pancake forging flow pattern was similar only to the flow pattern of the largest diameter of the rotor forging.

Two texture examinations (pole figures) were performed on pancake number 1, one at mid-radius, center position and one at 90° from the initial position,

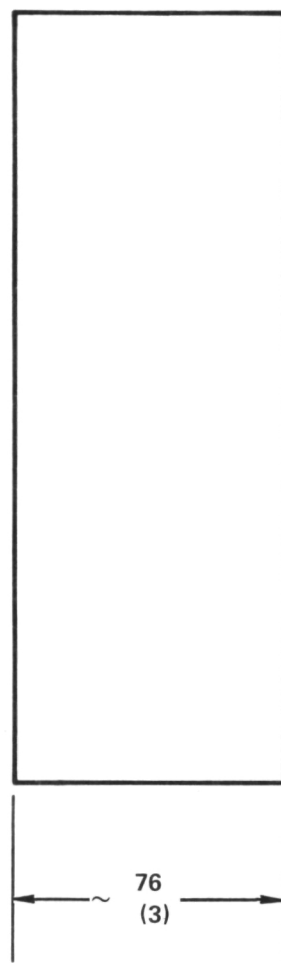
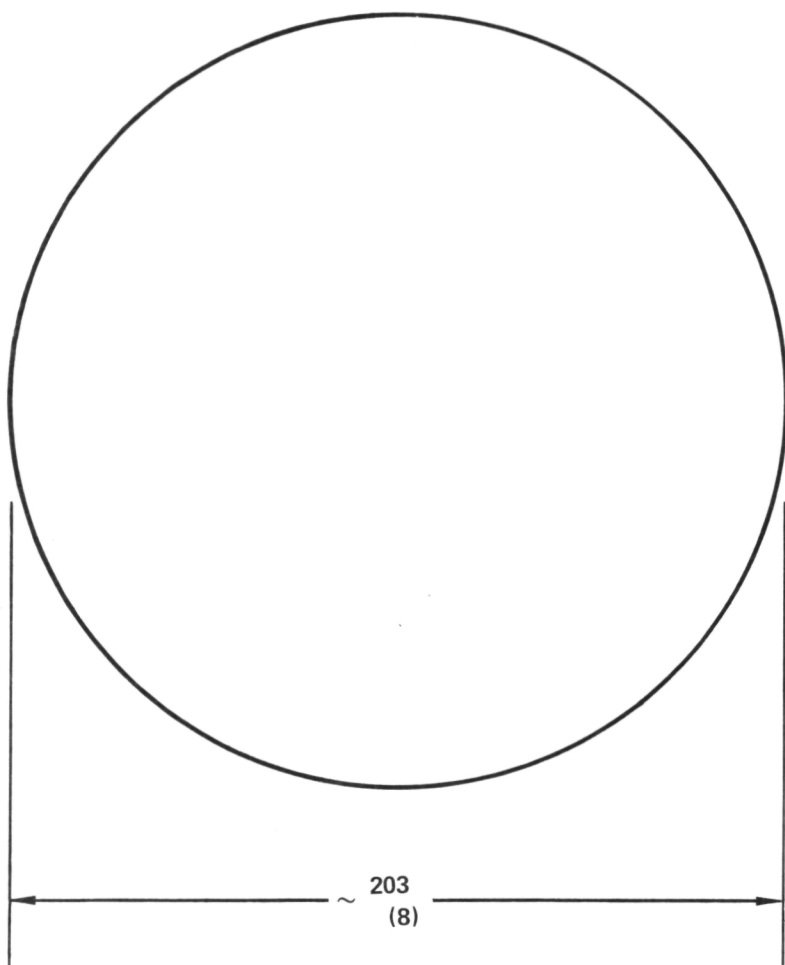
TABLE 8

HARDNESS SURVEY RESULTS FOR TOP SURFACE Ti-5Al-2.5Sn(ELI) PANCAKES

Serial No.	Brinell Diameter, ^a Hardness, BHD, mm		
1	3.70 ^b	3.70	3.70
2	3.70	3.70	3.70
3	3.70	3.70	3.70
4	3.70	3.70	3.70
5	3.70	3.70	3.70
6	3.70	3.70	3.70
7	3.70	3.70	3.70
8	3.70	3.70	3.70
9	3.70	3.70	3.70
10	3.70	3.70	3.70
11	3.70	3.70	3.70
12	3.70	3.70	3.70
13	3.70	3.70	3.70
14	3.70	3.70	3.70
15	3.70	3.70	3.70
16	3.70	3.70	3.70
17	3.70	3.70	3.70
18	3.70	3.70	3.70
19	3.60	3.60	3.70
20	3.60	3.60	3.70
21	3.60	3.70	3.60
22	3.70	3.60	3.65
23	3.70	3.70	3.60
24	3.60	3.60	3.60
25	3.60	3.70	3.70
26	3.60	3.60	3.60
27	3.60	3.60	3.70
28	3.60	3.60	3.70
29	3.60	3.65	3.70
30	3.55	3.60	3.70
31	3.60	3.70	3.70
32	3.60	3.65	3.70

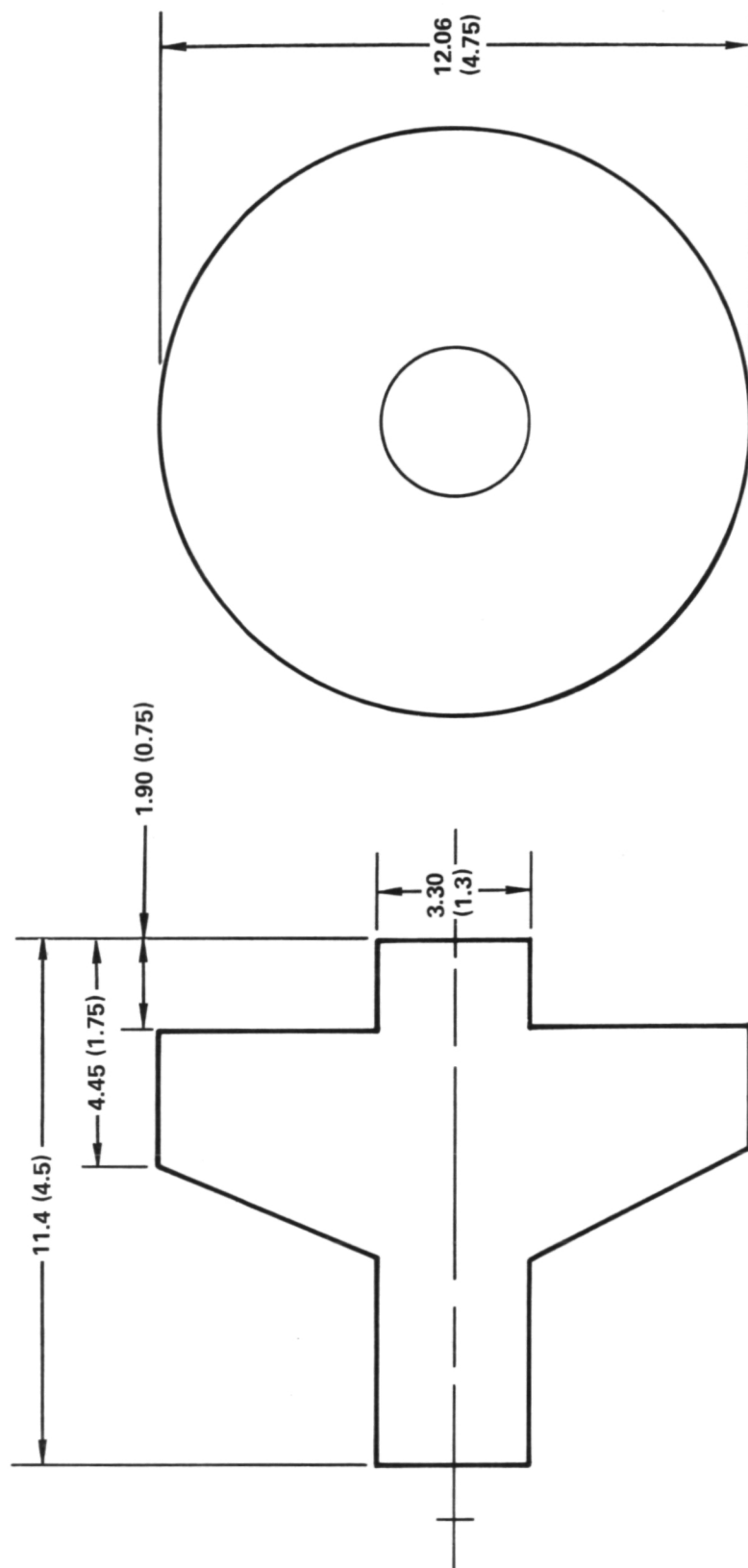
a. Readings taken at mid-radius, 120 degrees apart.

b. Brinell hardness diameter of 3.70 converts to 269 BHN.



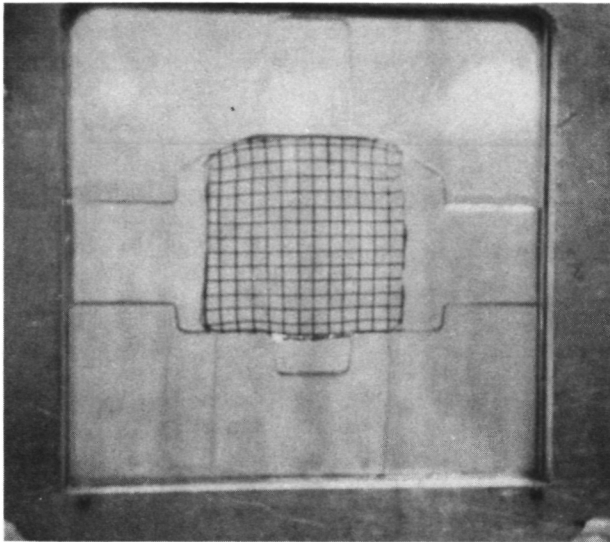
DIMENSIONS IN mm (in.)

Figure 35. - Pancake Disk Forging

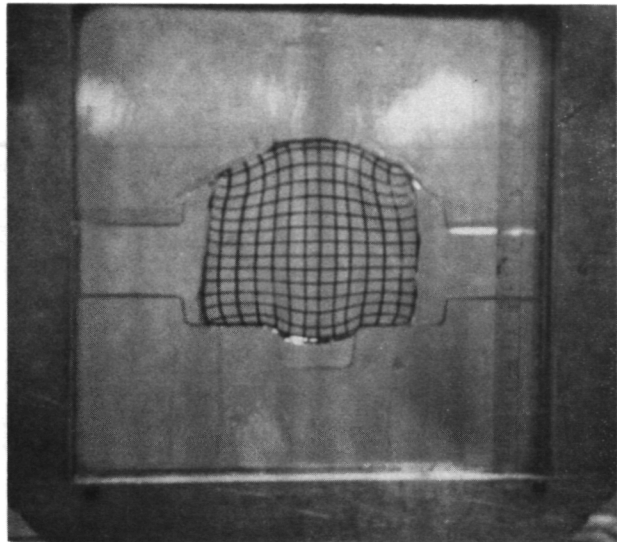


DIMENSIONS IN mm (in.)

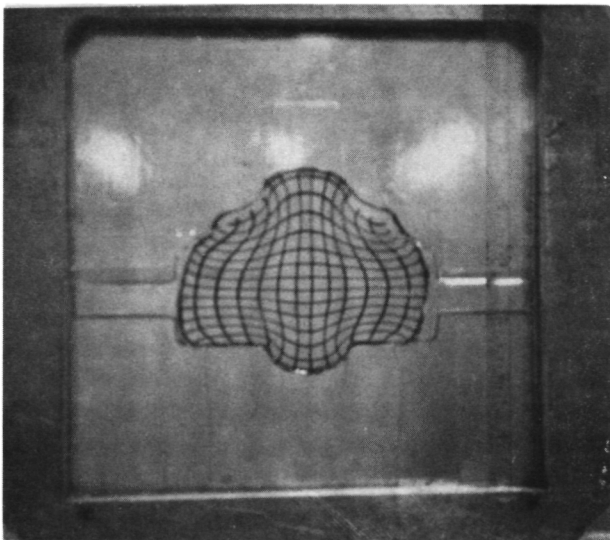
Figure 36. - Typical Rotor Forging, Nominal Dimensions in mm (in.)



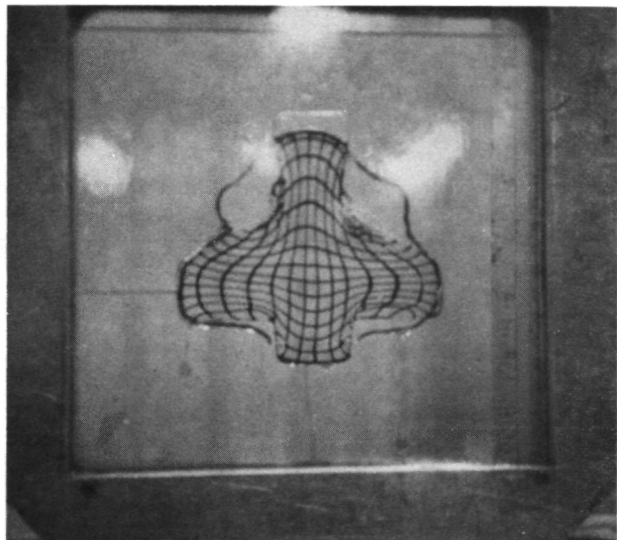
Reduction 0%



Reduction 50%

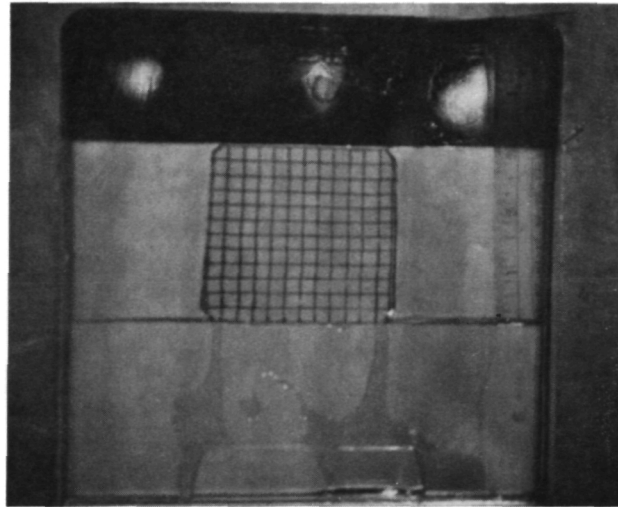


Reduction 75%

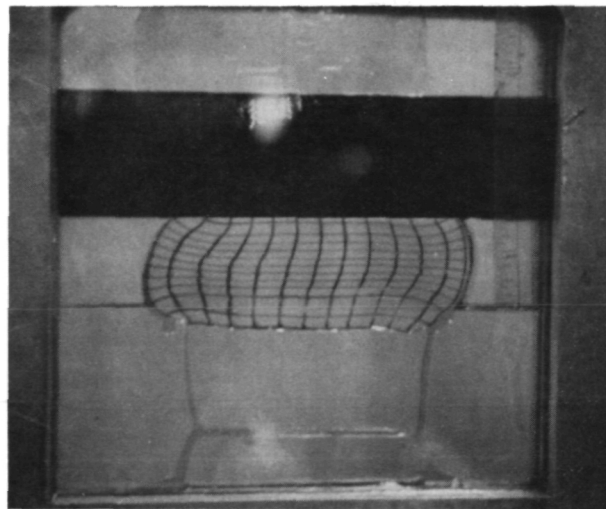


Closed Dies

Figure 37.-Photoelastic Study of Rotor Forging



Reduction 0%



Reduction 50%

Figure 38.-Photoelastic Study of Pancake Forging

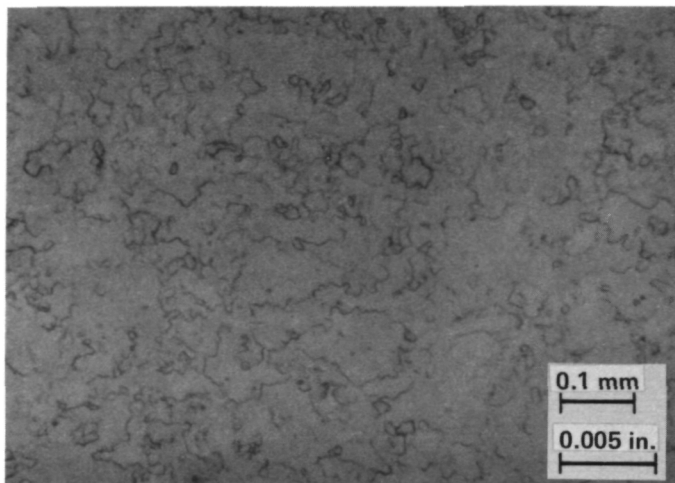
but at one-quarter radius from the pancake center. Both examinations showed no evidence of preferred orientation. This result helped confirm the forging model study results. Essentially, the mid-section of the pancake forgings are "dead" areas, but as indicated in Fig. 37, this should be similar to the center of the rotor forgings where the bore is located, the region of primary importance in this program.

Figures 39 through 42 show three micrographs for pancakes 1, 9, 16, and 18, taken from the same RS plane cut along the pancake diameter as the macrographs of Figs. 32 to 34. Although the standard does not actually apply to titanium alloys, ASTM Recommended Practice E112-63 was used to estimate the average grain size for the microstructures. Pancake No. 1 exhibited an estimated average grain size of 6 at 100X while pancakes number 9, 16, and 18 exhibited a grain size of 7 at 100X. A comparison of Figs. 39 through 42 indicated that the microstructure in all four pancakes was similar. However, there appeared to be a somewhat more oriented grain flow in pancakes number 9, 16, and 18 than in number 1 as well as more secondary particle segregation.

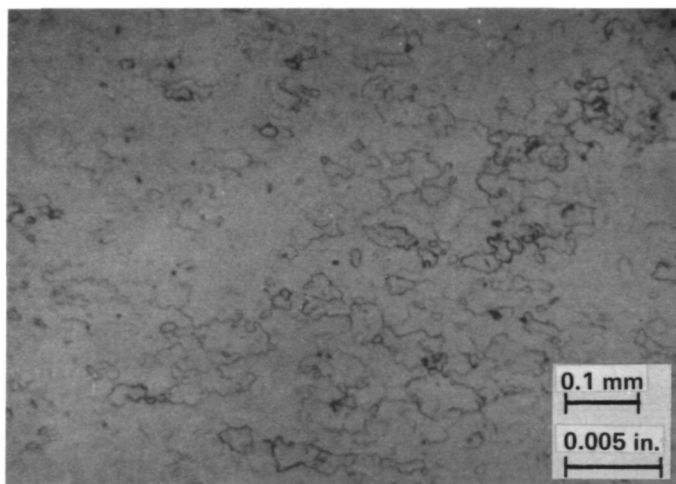
Hardness readings were taken of tensile, fracture toughness, and fatigue crack propagation test coupons. Hardness readings taken on tensile specimens are shown in Table 9 while those for each fracture toughness or fatigue crack growth specimen are shown in Table 10. The hardness survey results of Tables 8, 9, and 10 varied over a small range, from 3.60 BHD (285 BHN) to 3.90 BHD (241 BHN). According to approximate tensile ultimate tables and Rockwell C conversion tables these results convert to tensile ultimates from 800 to 896 MPa (116 to 130 ksi) and R_c values from 30 to 23. Hardness results for tensile coupons varied from 2.70 to 3.80 BHD which converts to 827 to 862 MPa, (120 to 125 ksi) tensile ultimate which appears to compare reasonably well to tensile results at room temperature, presented in detail below, where tensile ultimates varied from 800 to 841 MPa (112 to 116 ksi).

3.2 Tensile Properties

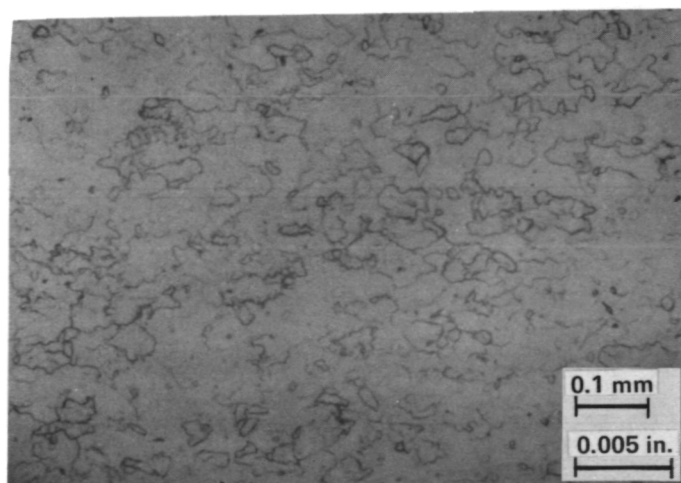
Tables 11 and 12 list tensile test results. All coupons from pancakes number 1 through 15 were in the circumferential direction and used for checking



**AXIAL VIEW OF THE RADIAL
CIRCUMFERENTIAL PLANE**

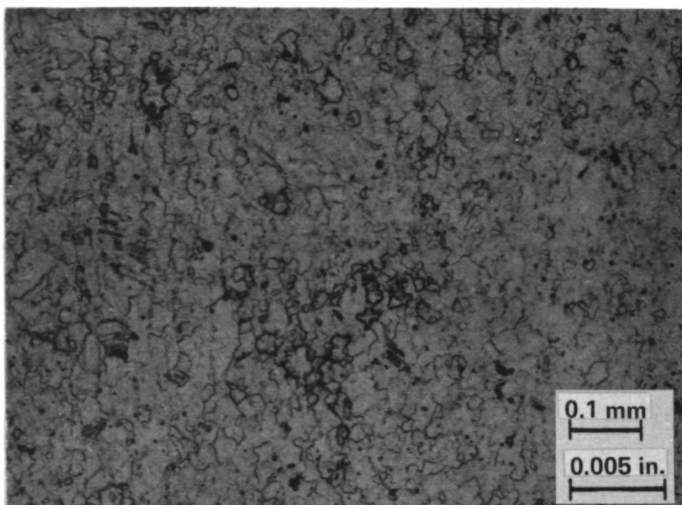


**CIRCUMFERENTIAL VIEW OF
AXIAL RADIAL PLANE**

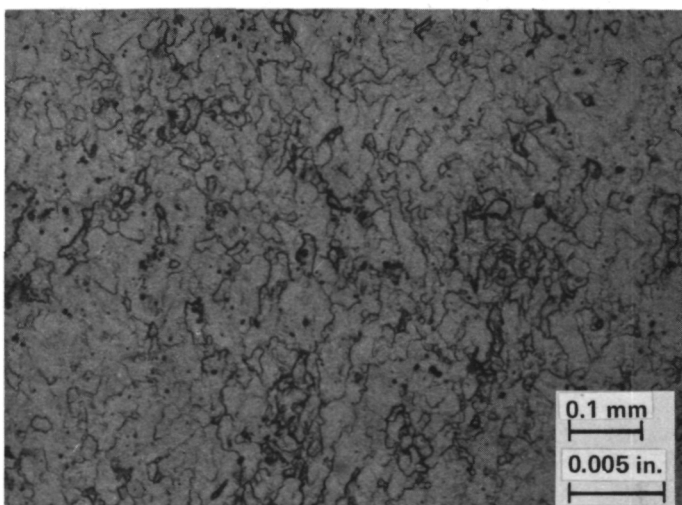


**RADIAL VIEW OF THE AXIAL
CIRCUMFERENTIAL PLANE**

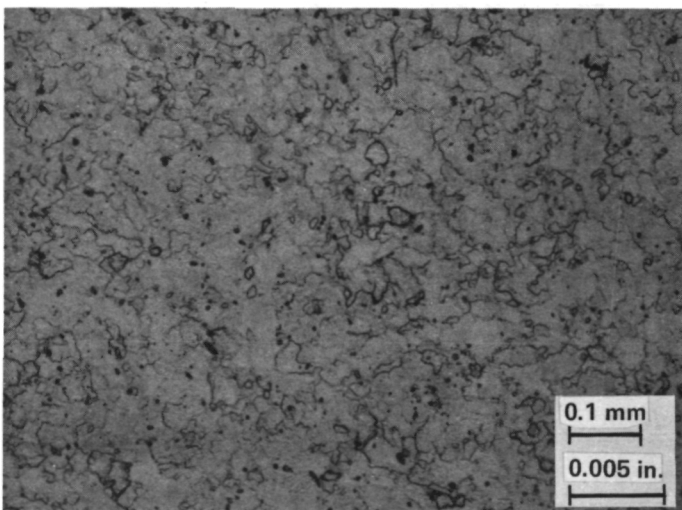
Figure 39. - Microstructures (100X) from the Mid-Radius, Mid-Height Position of Pancake No. 1 in the Annealed Condition, Krolls Etchant



**AXIAL VIEW OF THE RADIAL
CIRCUMFERENTIAL PLANE**

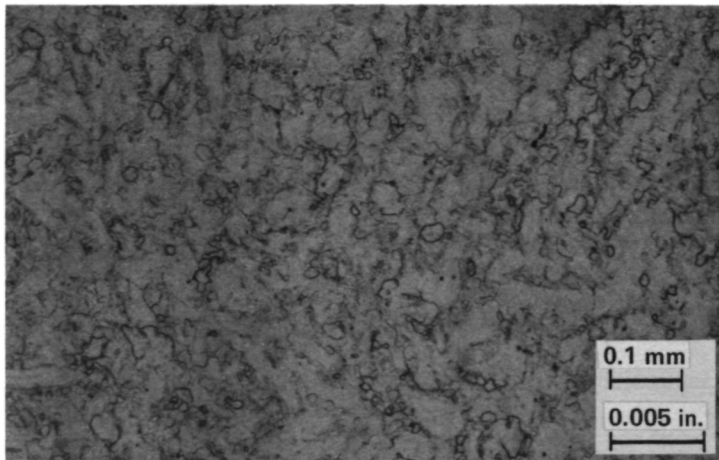


**CIRCUMFERENTIAL VIEW OF
AXIAL RADIAL PLANE**

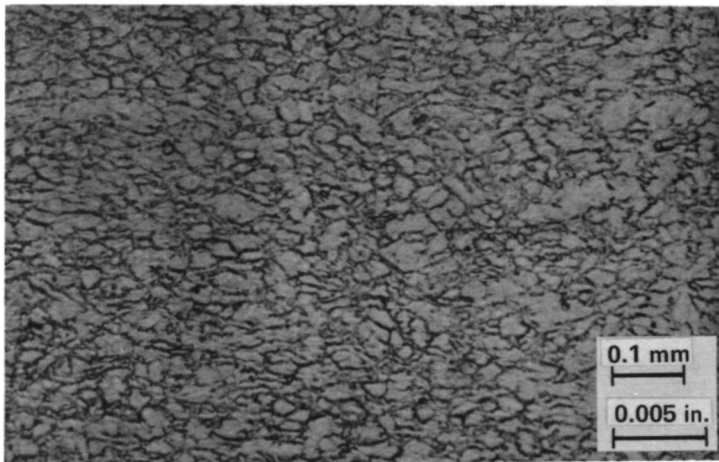


**RADIAL VIEW OF THE AXIAL
CIRCUMFERENTIAL PLANE**

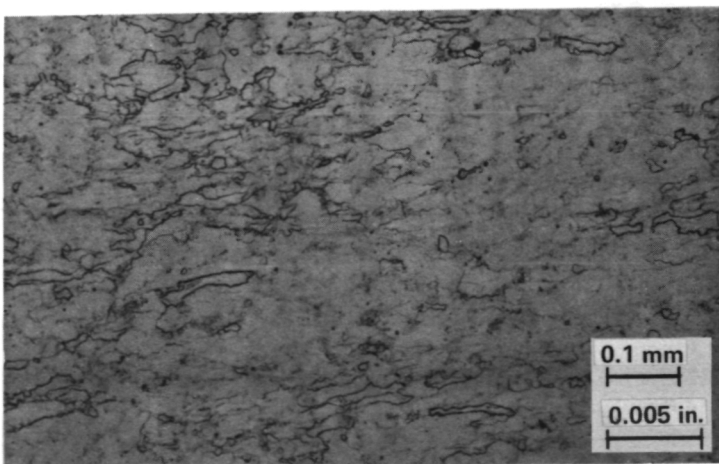
Figure 40.-Microstructure (100X) from the Mid-Radius, Mid-Height Position of Pancake No. 9 in the Annealed Condition, Kroll's Etchant



**AXIAL VIEW OF THE RADIAL
CIRCUMFERENTIAL PLANE**

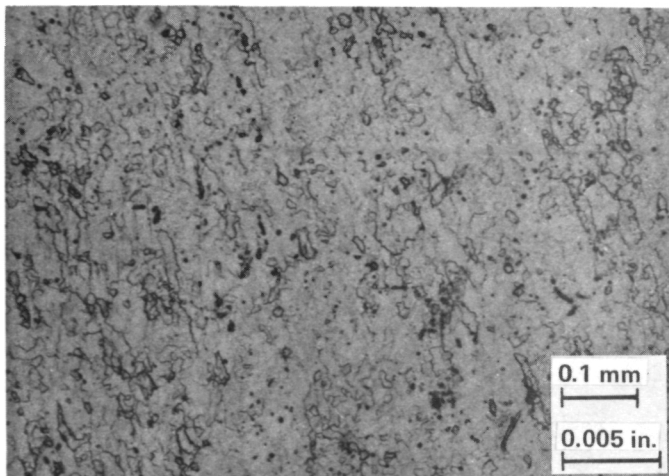


**CIRCUMFERENTIAL VIEW OF
AXIAL RADIAL PLANE**

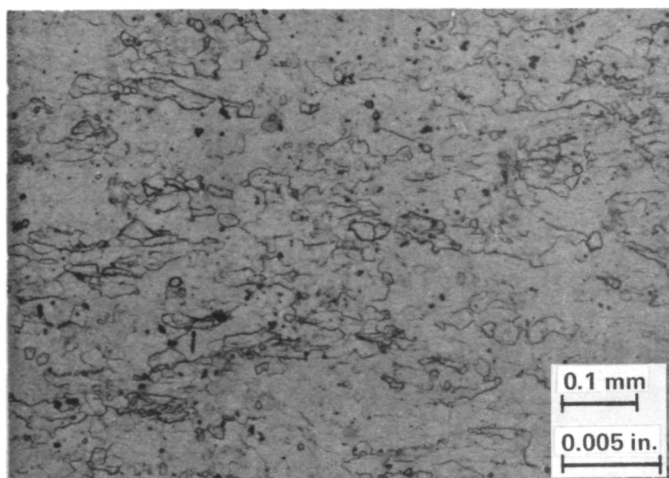


**RADIAL VIEW OF THE AXIAL
CIRCUMFERENTIAL PLANE**

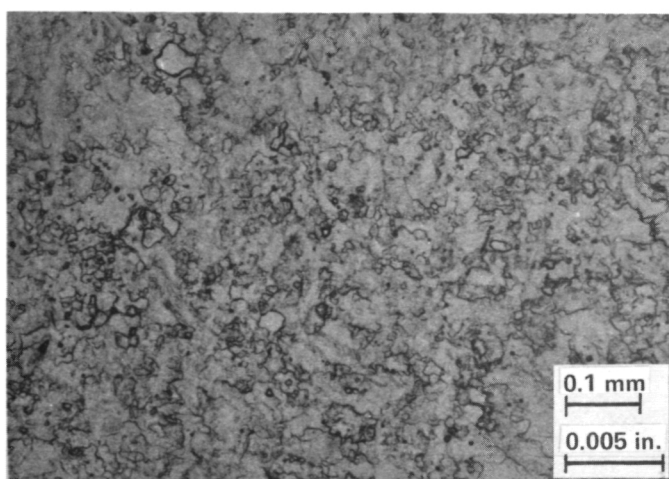
Figure 41.-Microstructure (100X) from the Mid-Radius, Mid-Height Position of Pancake No. 16 in the Annealed Condition, Kroll's Etchant



**AXIAL VIEW OF THE RADIAL
CIRCUMFERENTIAL PLANE**



**CIRCUMFERENTIAL VIEW OF
AXIAL RADIAL PLANE**



**RADIAL VIEW OF THE AXIAL
CIRCUMFERENTIAL PLANE**

Figure 42. -Microstructure (100X) from the Mid-Radius, Mid-Height Position of Pancake No. 18 in the Annealed Condition, Kroll's Etchant

TABLE 9
HARDNESS RESULTS FOR TENSILE COUPONS

Serial No.	Coupon No.	Brinell Hardness Diameter, BHD, mm	Brinell Hardness Number, BHD
1	T1	3.80	255
	T2	3.80	255
	T3	3.80	255
	T4	3.80	255
2	T1	3.70	269
	T2	3.70	269
	T3	3.70	269
	T4	3.70	269
3	T1	3.70	269
	T2	3.80	255
	T3	3.80	255
	T4	3.80	255
4	T1	3.70	269
	T2	3.70	269
	T3	3.70	269
	T4	3.70	269
5	T1	3.70	269
	T2	3.70	269
	T3	3.70	269
	T4	3.70	269
6	T1	3.70	269
	T2	3.70	269
	T3	3.70	269
	T4	3.70	269
7	T1	3.80	255
	T2	3.80	255
	T3	3.80	255
	T4	3.80	255
8	T1	3.70	269
	T2	3.70	269
	T3	3.70	269
	T4	3.70	269
12	T1	3.70	269
	T2	3.70	269
	T3	3.70	269
	T4	3.70	269
14	T1	3.70	269
	T2	3.75	262
	T3	3.80	255
	T4	3.80	255

TABLE 10
HARDNESS RESULTS FOR COMPACT SPECIMENS

Serial No.	Coupon No.	Brinell Hardness Diameter, BHD, mm	Brinell Hardness Number, BHN	Serial No.	Coupon No.	Brinell Hardness Diameter, BHD, mm	Brinell Hardness Number, BHN
1	CR1	3.70	269	6	CR1	3.70	269
	CR2	3.70	269		CR2	3.70	269
	RC1	3.70	269		RC1	3.70	269
	RC2	3.70	269		RC2	3.70	269
	SR1	3.70	269		SR1	3.80	255
	SR2	3.70	269		SR2	3.70	269
	SC1	3.70	269		SC1	3.70	269
	SC2	3.70	269		SC2	3.70	269
2	CR1	3.70	269	7	CR1	3.90	241
	CR2	3.65	277		CR2	3.70	269
	RC1	3.70	269		RC1	3.80	255
	RC2	3.70	269		RC2	3.70	269
	SR1	3.80	255		SR1	3.70	269
	SR2	3.70	269		SR2	3.80	255
	SC1	3.70	269		SC1	3.80	255
	SC2	3.70	269		SC2	3.60	285
3	CR1	3.80	255	8	CR1	3.70	269
	CR2	3.70	269		CR2	3.70	269
	RC1	3.70	269		RC1	3.80	255
	RC2	3.70	269		RC2	3.70	269
	SR1	3.70	269		SR1	3.70	269
	SR2	3.70	269		SR2	3.70	269
	SC1	3.70	269		SC1	3.70	269
	SC2	3.70	269		SC2	3.70	269
4	CR1	3.70	269	9	CR1	3.70	269
	CR2	3.70	269		CR2	3.70	269
	RC1	3.70	269		RC1	3.70	269
	RC2	3.70	269		RC2	3.70	269
	SR1	3.70	269		SR1	3.70	269
	SR2	3.75	262		SR2	3.70	269
	SC1	3.70	269		SC1	3.75	262
	SC2	3.70	269		SC2	3.70	269
5	CR1	3.70	269	10	CR1	3.70	269
	CR2	3.70	269		CR2	3.75	262
	RC1	3.70	269		RC1	3.70	269
	RC2	3.70	269		RC2	3.70	269
	SR1	3.70	269		SR1	3.80	255
	SR2	3.70	269		SR2	3.80	255
	SC1	3.80	255		SC1	3.70	269
	SC2	3.65	278		SC2	3.70	269

TABLE 10. (Concluded)

Serial No.	Coupon No.	Brinell Hardness Diameter, BHD, mm	Brinell Hardness Number, BHN	Serial No.	Coupon No.	Brinell Hardness Diameter, BHD, mm	Brinell Hardness Number, BHN
11	CR1	3.65	277	14	CS1	3.80	255
	CR2	3.70	269		CS2	3.75	262
	RC1	3.70	269		CS3	3.70	269
	RC2	3.65	277		CS4	3.75	262
	SR1	3.70	269		CS5	3.80	255
	SR2	3.65	277		CS6	3.70	269
	SC1	3.70	269		CS7	3.80	255
	SC2	3.70	269		CS8	3.70	269
12	RS1	3.70	269		CS9	3.70	269
	RS2	3.70	269		CS10	3.75	262
	RS3	3.70	269		CS11	3.80	255
	RS4	3.70	269	15	CS1	3.80	255
	RS5	3.70	269		CS2	3.70	269
	RS6	3.70	269		CS3	3.65	277
	RS7	3.75	262		CS4	3.75	262
	RS8	3.80	255		CS5	3.75	262
	RS9	3.70	269		CS6	3.75	262
	RS10	3.70	269		CS7	3.65	277
13	RS1	3.70	269		CS8	3.75	262
	RS2	3.70	269		CS9	3.75	262
	RS3	3.70	269		CS10	3.80	255
	RS4	3.70	269		CS11	3.80	255
	RS5	3.70	269	16	CR1	3.70	269
	RS6	3.70	269		CR2	3.70	269
	RS7	3.70	269		RC1	3.70	269
	RS8	3.70	269		RS1	3.70	269
	RS9	3.70	269		RS2	3.70	269
	RS10	3.70	269		SR1	3.70	269

TABLE 11

TENSILE PROPERTIES OF Ti-5Al-2.5Sn(ELI) PANCAKE FORGINGS AT ROOM TEMPERATURE

Specimen ^a Identification Number	Ultimate Tensile Strength, F_{tu} , MPa (ksi)	Yield Strength, 0.2% Offset, F_{ty} , MPa (ksi)	% Elongation in 25.4 mm, %e (1 in.)	% Reduction in Area, %RA	Apparent Tensile Modulus, E_A , GPa ($\text{psi} \times 10^6$)
1T-1	843.9 (122.4)	828.7 (120.2)	18.5	45.6	125.5 (18.2)
1T-3	821.2 (119.1)	781.2 (113.3)	17.5	45.2	118.6 (17.2)
2T-1	832.2 (120.7)	807.4 (117.1)	19.0	44.2	125.5 (18.2)
2T-3	815.6 (118.3)	761.2 (110.4)	17.5	43.2	131.0 (19.0)
3T-1	835.6 (121.2)	802.5 (116.4)	17.5	46.8	127.6 (18.5)
3T-3	827.4 (120.0)	792.9 (115.0)	15.0	39.1	122.0 (17.7)
4T-1	838.4 (121.6)	813.6 (118.0)	18.0	42.0	120.7 (17.5)
4T-3	815.0 (118.2)	770.8 (111.8)	16.5	44.8	120.7 (17.5)
5T-1	835.6 (121.2)	806.7 (117.0)	18.0	44.4	127.6 (18.5)
5T-3	817.7 (118.6)	766.7 (111.2)	20.5	40.8	122.7 (17.8)
6T-1	825.3 (119.7)	792.9 (115.0)	16.0	42.8	121.3 (17.6)
6T-3	823.2 (119.4)	783.9 (113.7)	18.0	44.4	135.1 (19.6)
7T-1	830.8 (120.5)	801.2 (116.2)	17.0	41.0	119.3 (17.3)
7T-3	813.6 (118.0)	765.3 (111.0)	16.0	44.0	117.9 (17.1)
8T-1	840.5 (121.9)	805.3 (116.8)	15.5	46.8	121.3 (17.6)
8T-3	843.2 (122.3)	815.0 (118.2)	15.5	48.1	130.3 (18.9)

TABLE 11 (Continued)

Specimen ^a Identification Number	Ultimate Tensile Strength, F _{tu} , MPa (ksi)	Yield Strength, 0.2% Offset, F _{ty} , MPa (ksi)	% Elongation in 25.4 mm, %e (1 in.)	% Reduction in Area, %RA	Apparent Tensile Modulus E _A , GPa, 10 ⁶ (psi x 10 ⁶)
9T-1	842.5 (122.2)	801.2 (116.2)	14.0	49.8	104.8 (15.2)
9T-3	821.8 (119.2)	766.7 (111.2)	18.0	44.4	103.4 (15.0)
10T-1	832.9 (120.8)	791.5 (114.8)	15.0	42.8	113.8 (16.5)
10T-3	841.2 (122.0)	796.3 (115.5)	15.0	39.6	114.4 (16.6)
11T-1	- _b	-	-	-	-
11T-3	852.9 (123.7)	756.3 (109.7)	17.0	31.9	119.3 (17.3)
12T-1	823.2 (119.4)	788.1 (114.3)	17.0	46.8	121.3 (17.6)
12T-3	813.6 (118.0)	766.7 (111.2)	15.0	39.6	124.8 (18.1)
13T-1	842.5 (122.2)	790.8 (114.7)	17.0	48.7	116.5 (16.9)
13T-3	818.4 (118.7)	769.4 (111.6)	16.0	37.6	116.5 (16.9)
14T-1	829.4 (120.3)	798.4 (115.8)	15.0	48.1	122.7 (17.8)
14T-3	816.3 (118.4)	771.5 (111.9)	16.5	42.8	122.7 (17.8)
15T-1	808.1 (117.2)	759.8 (110.2)	17.0	48.3	115.1 (16.7)
15T-3	801.2 (116.2)	747.4 (108.4)	17.0	32.1	115.1 (16.7)
16T-1	804.6 (116.7)	769.4 (111.6)	18.0	45.9	118.6 (17.2)
16T-3	801.9 (116.3)	737.0 (106.9)	17.0	43.6	108.2 (15.7)

TABLE 11(Continued)

Specimen ^a Identification Number	Ultimate Tensile Strength, F _{tu} , MPa (ksi)	Yield Strength, 0.2% Offset F _{ty} , MPa (ksi)	% Elongation in 25.4mm, %e (1 in.)	% Reduction in Area, %RA	Tensile Modulus, E _A , GPa, 10 ⁶ (psi x 10 ⁶)
16T-5	810.8 (117.6)	757.0 (109.8)	18.5	39.6	112.4 (16.3)
16T-7	801.2 (116.2)	755.7 (109.6)	15.5	46.3	117.2 (17.0)
16T-9	836.3 (121.3)	792.2 (114.9)	15.5	39.6	115.8 (16.8)
16T-11	851.5 (123.5)	811.5 (117.7)	15.0	40.4	128.2 (18.6)
29T-1	848.0 (123.0)	790.8 (114.7)	18.0	40.3	123.4 (17.9)
29T-3	842.5 (122.2)	773.6 (112.2)	17.0	41.0	125.5 (18.2)
29T-2	839.1 (121.7)	768.8 (111.5)	18.0	41.2	122.7 (17.8)
29T-4	845.3 (122.6)	786.7 (114.1)	16.0	39.7	123.4 (17.9)
Average Values Pancakes 1-18	830.1 (120.4)	784.3 (115.2)	16.9	44.9	116.5 (16.9)
	821.8 (119.2)	772.9 (112.1)	16.6	41.6	120.7 (17.5)
Average Values Pancake 29	843.2 (122.3)	779.8 (113.1)	18.0	40.8	122.7 (17.8)
	843.9 (122.4)	780.5 (113.2)	16.5	40.4	124.1 (18.0)
Average of All Tests AMS4924B Spec. RB0170-152 Spec.	827.4(120.0) 689.5(100.0) 689.5(100.0)	783.2(113.6) 620.5(90.0) 620.5(90.0)	16.8 10.0 10.0	42.9 - -	119.3(17.3) 103.4(15.0) 137.9(20.0)

TABLE 11 (Concluded)

Specimen ^a Identification Number	Ultimate Tensile Strength, F_{tu} , MPa (ksi)	Yield Strength, 0.2% Offset F_{ty} , MPa (ksi)	% Elongation in 25.4 mm, %e (1 in.)	% Reduction in Area, %RA	Apparent Tensile Modulus, E_A , GPa, 10^6 (psi $\times 10^6$)
Nachtigall (38)	861.8(125.0)	827.4(120.0)	-	-	-
Sullivan (39)	779.1(113.0)	723.9(105.0)	18.0	43.0	-
Stone, et al (1)	744.6(108.0)	681.9(98.9)	-	-	-

a. The first number refers to the pancake number; T refers to tensile coupon; and the second number denotes location within the pancake (1-top, 3-middle)

b. Coupon 11T-1 was not tested due to forging crack found during machining.

TABLE 12

TENSILE PROPERTIES OF Ti-5Al-2.5Sn(ELI) PANCAKE FORGINGS AT -253°C (-423°F)

Specimen ^a Identification Number	Ultimate Tensile Strength, F _{tu} , MPa (ksi)	Yield Strength, 0.2% Offset, F _{ty} , MPa (ksi)	% Elongation in 25.4 mm, %e (1 in.)	% Reduction in Area, %RA	Apparent Tensile Modulus, E _A , GPa (psi x 10 ⁶)
1T-2	1457 (211.3)	1373 (199.2)	12.5	33.3	120.0 (17.4)
2T-2	1475 (214.0)	1354 (196.4)	16.5	35.8	160.9 (24.5)
3T-2	1434 (208.0)	1389 (201.4)	12.5	30.1	156.5 (22.7)
4T-2	1470 (213.2)	1375 (199.4)	15.5	33.4	120.6 (17.5)
5T-2	1471 (213.3)	1382 (200.5)	15.0	31.9	180.0 (26.1)
6T-2	1457 (211.3)	1356 (196.6)	13.5	23.8	151.0 (21.9)
7T-2	1491 (216.2)	1390 (201.6)	17.5	28.5	152.4 (22.1)
		1384 (200.8)	13.0	34.6	106.9 (15.5)
		1505 (218.3)	17.8	23.8	103.4 (15.0)
		1388 (201.3)	22.0	31.9	113.8 (16.5)
		1440 (208.8)	23.8	30.1	117.2 (17.0)
		1393 (202.1)	18.9	28.7	103.4 (15.4)
		1467 (212.8)	22.4	30.1	96.5 (14.0)

TABLE 12 (Continued)

Specimen ^a Identification Number	Ultimate Tensile Strength, F _{tu} , MPa (ksi)	Yield Strength, 0.2% Offset, F _{ty} , MPa (ksi)	% Elongation in 25.4 mm, %e (1 in.)	% Reduction in Area, %RA	Apparent Tensile Modulus, E _A , GPa (psi x 10 ⁶)
8T-2	1442 (209.1)	1371 (198.9)	23.0	30.8	96.5 (14.0)
8T-4	1437 (208.4)	1384 (200.8)	18.1	33.4	96.5 (14.0)
9T-2	1499 (217.4)	1392 (201.9)	12.5	25.2	155.1 (22.5)
9T-4	1478 (214.3)	1401 (203.2)	15.0	23.8	130.3 (18.9)
10T-2	1437 (208.4)	1375 (199.4)	16.0	23.8	137.9 (20.0)
10T-4	1429 (207.2)	1356 (196.6)	16.0	32.4	137.2 (19.9)
11T-2	1500 (217.6)	1393 (202.1)	14.0	23.0	137.9 (20.0)
11T-4	1452 (210.6)	1359 (197.1)	14.5	24.4	137.9 (20.0)
12T-2	1484 (215.3)	1405 (203.8)	21.5	27.4	72.4 (10.5)
12T-4	1477 (214.2)	1352 (196.1)	21.4	25.2	96.5 (14.0)
13T-2	1466 (212.6)	1393 (202.0)	13.5	28.7	166.5 (24.0)
13T-4	1471 (213.4)	1379 (200.0)	14.0	25.2	112.4 (16.3)
14T-2	1434 (208.0)	1392 (201.9)	18.6	26.2	89.6 (13.0)
14T-4	1469 (213.0)	1367 (198.3)	17.8	23.2	65.5 (9.5)
15T-2	1485 (215.4)	1398 (202.8)	11.5	19.6	138.6 (20.1)
15T-4	1453 (210.8)	1418 (205.7)	12.5	22.3	155.8 (22.6)

TABLE 12 (Concluded)

Specimen ^a Identification Number	Ultimate Tensile Strength, F _{tu} , MPa (ksi)	Yield Strength, 0.2% Offset, F _{ty} , MPa (ksi)	% Elongation in 25.4 mm, %e (1 in.)	% Reduction in Area, %RA	Apparent Tensile Modulus, E _A , GPa 10 ⁶ (psi x 10 ⁶)
16T-2	1475 (214.0)	1407 (204.0)	13.5	20.2	155.1 (22.5)
16T-4	1480 (214.6)	1417 (205.5)	12.5	17.5	139.3 (20.2)
16T-6	1395 (202.4)	1344 (194.9)	13.0	30.6	155.1 (22.5)
16T-10	1433 (207.9)	1364 (197.9)	18.0	23.8	155.1 (22.5)
16T-12	1406 (204.0)	1389 (201.5)	16.0	35.3	156.5 (22.7)
18T-8	1326 (192.4)	1313 (190.4)	15.5	34.6	146.8 (21.3)
Average Values Pancakes 1-18	1460 (211.8)	1386 (201.0)	15.8	28.1	133.1 (19.3)
Average of All Tests RB0170-152 Spec.	1455(211.1) 1310(190.0)	1373 (199.1)	16.2 8.0	27.9 -	130.3(18.9) -
Nachtigall [38] Sullivan [39] Stone, et al [1]	1475(214) 1565(227) 1411(204.7)	1413(205) 1462(212) 1306(189.4)	- 7 -	- - -	- - -

a. The first number refers to the pancake number; T refers to tensile coupon;
and the second number denotes location within the pancake (2-top, 4-middle).

tensile properties of these pancakes. The four tensile coupons from these pancakes were from a small chordal section, shown in Figs. 3 through 6, and numbered 1 through 4 from the top surface. Tensile coupons T1 and T3 from each pancake were tested at room temperature while coupons T2 and T4 were tested at -253°C (-423°F). This procedure allowed for some comparison between surface and interior properties in addition to ascertaining the effect of temperature.

Table 11 lists the tensile results and test averages for coupons tested at room temperature and Table 12 for those tested at -253°C (-423°F). Included in the tables are the minimum properties from two standards, AMS4924B (dated 1 November 1969) and the more stringent Rocketdyne standard, RB0170-152 (dated 8 October 1973). In addition, results of three other studies are given for comparison. The work by Nachtigall [38] was conducted using 16.13 mm (0.635 in.) diameter coupons, that by Sullivan [39] was for coupons from 2.54 mm (0.1 in.) sheet while that by Stone, et al, [1] was for 25.4 mm (1 in.) thick plate. Stone, et al, [1] compared air cooled and furnace cooled tensile properties and found no significant difference.

Tables 11 and 12 clearly showed that tensile properties varied little from pancake to pancake. All minimum specifications except for the apparent tensile modulus at room temperature were exceeded and results compared quite favorably to results of other investigations. At both room temperature and -253°C (-423°F), tensile results of surface coupons slightly exceeded those of subsurface specimens. Encouragingly, percent elongation essentially did not change with decreased temperature while percent RA was still quite good at -253°C (-423°F).

3.3 Fracture Toughness Properties

Table 13 lists the results of the 25 fracture toughness tests conducted using coupons from pancakes 1-18, and 29. All coupons tested at -253°C (-423°F) met all of the plane strain criteria of ASTM E399-74 while all coupons tested at room temperature failed to meet the criteria.

TABLE 13

FRACTURE TOUGHNESS TEST RESULTS

Coupon No.	Test Temperature	Fracture Toughness, K_Q , MPa \sqrt{m} (ksi $\sqrt{in.}$)	Residual Strength Coefficient, R_{SC}	P_{max}/P_Q < 1.10	$B > 2$ K_Q $2.5(\frac{Q}{\sigma_y})$	$a > 2$ K_Q $2.5(\frac{Q}{\sigma_y})$	Valid K_{Ic}
1CR-1 6CR-1 29CR-2 1RC-1 6RC-1 1SR-1 6SR-1 1SC-1 6SC-1 12RS-1 13RS-1 14CS-1 15CS-1	RT	91.6(83.4) 89.8(81.7) 92.7(84.4) 91.4(83.2) 91.1(82.9) 84.7(77.1) 79.8(72.6) 93.4(85.0) 87.5(79.6) 80.3(73.1) 78.3(71.3) 85.6(77.9) 96.9(88.2)	0.950 0.932 1.35 0.955 0.940 0.866 0.818 0.884 0.911 0.886 0.843 1.03 1.07	X ^a			
1CR-2 6CR-2 1RC-2 6RC-2 1SR-2 6SR-2 1SC-2 6SC-2 12RS-6 13RS-6 14CS-6 15CS-6	-253°C (-423°F)	61.8(56.2) 63.5(57.8) 63.7(58.0) 65.5(59.6) 58.2(53.0) 57.7(52.5) 60.0(54.6) 54.4(49.5) 70.5(64.2) 67.0(61.0) 71.6(65.2) 75.3(68.5)	0.312 0.342 0.339 0.327 0.310 0.307 0.312 0.276 0.341 0.335 0.365 0.376	X X X X X X X X X X X X	X X X X X X X X X X X X	X X X X X X X X X X X X	X X X X X X X X X X X X

a. An X indicates that this requirement was met.

A review of the $-253^{\circ}\text{C} (-423^{\circ}\text{F})$ results showed a dependence of K_{Ic} on direction. Samples in which the crack was aligned in the thickness direction (RS, CS) had the highest toughness. This apparent dependence of K_{Ic} on orientation existed in spite of the fact that no crystallographic texture was observed as discussed in Section 3.1. Sample 29CR-2 from Lot 2 material was used primarily as a fatigue crack propagation test specimen, but was pulled as a fracture toughness specimen when the a/w reached the required ASTM E399-74 length. The result of this test is also shown in Table 13 and indicates that the pancakes used for the rotating disks had the same toughness as pancakes 1 to 18.

Fracture toughness properties of Ti-5Al-2.5Sn(ELI) alloy are known to vary with temperature consistent with these results. Values of $49.5 \text{ MPa } \sqrt{\text{m}}$ ($45 \text{ ksi } \sqrt{\text{in.}}$) at $-253^{\circ}\text{C} (-423^{\circ}\text{F})$ have been reported [40] for ELI grade and 49.5 to $66 \text{ MPa } \sqrt{\text{m}}$ (45 to $60 \text{ ksi } \sqrt{\text{in.}}$) [39] for thin sheet material. Other data has indicated a wide range of fracture toughness values depending on microstructure and specimen orientation [41]. Stone, et al [1] found that although fracture toughness properties at room temperature were similar for air and furnace cooled plate, at $-253^{\circ}\text{C} (-423^{\circ}\text{F})$, the toughness of the air-cooled material greatly exceeded that of the furnace-cooled material; 89 as compared to $73 \text{ MPa } \sqrt{\text{m}}$ (81 to $66.1 \text{ ksi } \sqrt{\text{in.}}$). This result suggests that in the future, Ti-5Al-2.5Sn(ELI) should possibly be air cooled, not furnace cooled as is the more typical practice.

3.4 Compliance Calibration Results

The purpose of compliance calibration was to determine: 1) if the normally used expression for the C_3 [12] used in determining stress intensity, given as Equation (3), is adequate for this material; 2) if the compliance behavior was a function of temperature; 3) an expression for crack length, or relative crack length, a/w , as a function of normalized compliance, CEB. The last purpose is a check on the optically based a/w discussed previously in Section 2.3.4.

Tables 14 to 16 list the calculated normalized compliance results for coupons 11CR-2, 11RC-2 and 11SC-1, obtained by fitting Equation (4) to the experimental data, compared to measured values. For the data from these three coupons, R correlations were in excess of 0.9993 as indicated in the tables. Because all three of these coupons were tested at room temperature and their geometries were identical, the three data sets were combined to obtain the normalized compliance calibration fit, averaged for orientation, for a large data set. Results are listed in Table 17 along with the parameters used in Equation (4) k, e, v . The compliance data in all of these tables is corrected to the load line.

Using Equation (4) and the appropriate k, e , and v values for the combined room temperature data set (see Table 17), the compliance derivative was calculated and used in Equation (2) to evaluate C_3 experimentally. Tabulated results are listed in Table 18. In Fig. 43 the percent differences, listed in Table 18, between the polynomial based C_{3w} , Equation (3), and experimentally based C_{3e} , Equations (2) and (4) are shown graphically. Table 18 and Fig. 43 show that the absolute percent difference between C_{3w} and C_{3e} was less than 2.2 percent for $0.33 \leq a/w \leq 0.65$ which confirmed the validity of Equation (3) over this region of a/w and affirmatively answered the first purpose of this compliance calibration study. For $a/w > 0.65$ deviation between C_{3w} and C_{3e} become large. Although most coupons used for fatigue crack propagation testing and all of those used for fracture toughness testing were used at $a/w < 0.653$, Equations (2) and (4) and the associated k, e , and v parameters for this combined data set were used in Equation (1) calculated stress intensity because a few coupons need a/w ratios up to 0.76.

To determine if compliance was a function of temperature, WOL coupon 7CR-2 was used to periodically record compliance at several crack lengths while the coupon was at -253°C (-423°F). Additionally, compliance at two of these crack lengths was also recorded with the coupon at room temperature. Table 19 lists the results of this investigation of temperature effect on compliance using coupon 7CR-2. The table shows the optically based a/w ratios, corrected

TABLE 14

EXPERIMENTAL COMPLIANCE CALIBRATION RESULTS BASED ON
EQUATION (3) FOR COUPON 11CR-2 TESTED AT ROOM TEMPERATURE

$R > 0.9994$

Index	Measured Crack ^a Length/Width Ratio, a/w	Measured ^b Normalized Compliance, CEB	Calculated ^b Normalized Compliance, CEB	Percent Deviation
1	0.304	17.70	18.25	3.15
2	0.335	22.89	22.13	-3.32
3	0.360	25.81	25.60	-0.82
4	0.385	29.83	29.46	-1.23
5	0.411	34.12	33.83	-0.86
6	0.436	38.32	38.61	0.78
7	0.461	43.82	44.07	0.56
8	0.486	50.13	50.05	-0.16
9	0.511	55.42	56.76	2.42
10	0.536	64.33	64.30	-0.03
11	0.560	72.49	72.80	0.45
12	0.585	80.75	82.46	2.12
13	0.610	93.80	93.48	-0.34
14	0.636	108.99	106.31	-2.46

Average Absolute
Percent Deviation = 1.34

a a/w is based on optical measurements and is uncorrected
for crack bow

b CEB is corrected to the load line

TABLE 15
EXPERIMENTAL COMPLIANCE CALIBRATION RESULTS BASED ON
EQUATION (3) FOR COUPON LLRC-2 TESTED AT ROOM TEMPERATURE

$R > 0.9994$

Index	Measured Crack ^a Length/Width Ratio, a/w	Measured ^b Normalized Compliance, CEB	Calculated Normalized Compliance, CEB	Percent Deviation
1	0.304	16.19	17.81	9.96
2	0.329	20.18	20.12	-0.40
3	0.354	22.98	22.69	-1.28
4	0.378	26.52	25.60	-3.49
5	0.404	29.64	28.89	-2.55
6	0.429	33.29	32.63	-1.98
7	0.454	37.36	36.89	-1.24
8	0.479	42.84	41.81	-2.41
9	0.504	50.30	47.51	-5.55
10	0.528	55.48	54.15	-2.40
11	0.553	63.41	61.93	-2.34
12	0.578	71.79	71.18	-0.85
13	0.603	81.92	82.26	0.42
14	0.628	96.20	95.67	-0.55
15	0.653	109.79	112.02	2.03
16	0.678	128.83	132.41	2.78
17	0.702	149.59	158.16	5.73
18	0.727	177.88	191.31	7.54
19	0.752	225.27	234.73	4.20
20	0.778	288.70	295.04	2.20
21	0.802	373.30	378.00	1.26
22	0.827	493.72	496.06	0.48
23	0.852	682.66	679.82	-0.42
24	0.877	967.28	984.78	1.81
25	0.902	1728.99	1544.33	-10.68

Average Absolute
Percent Deviation = 2.98

a a/w is based on optical measurements and is uncorrected for crack bow

b CEB is corrected to the load line

TABLE 16

EXPERIMENTAL COMPLIANCE CALIBRATION RESULTS BASED ON
EQUATION (3) FOR COUPON 11 SC-1 TESTED AT ROOM TEMPERATURE

$R > 0.9993$

Index	Measured Crack ^a Length/Width Ratio, a/w	Measured ^b Normalized Compliance, CEB	Calculated ^b Normalized Compliance, CEB	Percent Deviation
1	0.329	19.69	19.78	0.45
2	0.333	19.80	20.17	1.85
3	0.336	20.00	20.49	2.45
4	0.338	19.79	20.66	4.37
5	0.348	21.41	21.69	1.31
6	0.365	24.10	23.50	-2.46
7	0.380	26.08	25.24	-3.20
8	0.400	29.27	27.72	-5.30
9	0.425	32.61	31.39	-3.76
10	0.500	46.20	45.51	-1.49
11	0.599	75.60	77.72	2.81
12	0.704	148.59	155.01	4.32
13	0.804	346.15	374.00	8.05
14	0.856	770.61	708.71	-8.03

Average Absolute
Percent Deviation = 3.56

a a/w is based on optical measurements and is uncorrected for crack bow

b CEB is corrected to the load line.

TABLE 17

EXPERIMENTAL COMPLIANCE CALIBRATION RESULTS BASED ON
EQUATION (3) FOR COUPONS 11CR-2, 11RC-2, AND 11SC-1
TESTED AT ROOM TEMPERATURE

$$R > 0.998$$

$$k = 7.8417398876059$$

$$e = -2.0891721165336$$

$$v = 1.5020268401739$$

Index	Measured Crack ^a Length/Width Ratio, a/w	Measured ^b Normalized Compliance, CEB	Calculated ^b Normalized Compliance, CEB	Percent Deviation
1	0.334	18.33	18.21	-0.63
2	0.334	16.76	18.26	8.97
3	0.359	20.22	20.74	2.55
4	0.359	20.77	20.79	0.09
5	0.363	20.31	21.17	4.23
6	0.365	23.56	21.45	-8.96
7	0.366	20.50	21.56	5.15
8	0.368	20.28	21.72	7.11
9	0.377	21.91	22.81	4.09
10	0.384	23.58	23.63	0.21
11	0.390	26.46	24.36	-7.93
12	0.395	24.60	24.99	1.60
13	0.409	27.12	26.81	-1.12
14	0.410	26.56	26.96	1.52
15	0.415	30.48	27.64	-9.32
16	0.430	29.74	29.74	0.00
17	0.434	30.23	30.39	0.55
18	0.440	34.77	31.44	-9.58
19	0.455	33.04	33.89	2.58
20	0.459	33.86	34.46	1.79
21	0.465	38.94	35.65	-8.45
22	0.484	37.90	39.09	3.15
23	0.491	44.43	40.55	-8.73
24	0.508	43.38	44.40	2.33
25	0.516	50.73	46.07	-9.19
26	0.530	46.51	49.63	6.71
27	0.533	50.84	50.47	-0.73
28	0.541	56.00	52.43	-6.37

TABLE 17. (Concluded)

Index	Measured ^a Crack Length/Width Ratio, a/w	Measured ^b Normalized Compliance, CEB	Calculated ^b Normalized Compliance, CEB	Percent Deviation
29	0.558	56.00	57.52	2.73
30	0.566	64.90	59.80	-7.86
31	0.583	63.91	65.75	2.88
32	0.590	73.04	68.42	-6.33
33	0.598	71.89	71.34	-0.76
34	0.615	81.27	78.57	-3.33
35	0.623	81.97	82.02	0.06
36	0.629	75.69	84.84	12.08
37	0.640	94.30	90.62	-3.90
38	0.653	96.19	97.54	1.41
39	0.666	109.46	105.47	-3.64
40	0.673	109.72	110.02	0.27
41	0.698	128.67	128.61	0.02
42	0.734	148.02	164.35	11.03
43	0.737	150.20	168.33	12.07
44	0.762	178.47	201.95	13.16
45	0.787	225.84	245.69	8.79
46	0.812	289.30	305.29	5.53
47	0.832	373.20	368.04	-1.38
48	0.833	344.35	370.95	7.72
49	0.857	493.34	474.66	-3.79
50	0.886	765.84	681.39	-11.03
51	0.887	676.61	683.22	0.98
52	0.911	966.98	987.44	2.12
53	0.936	1727.70	1582.19	-8.42

Average Absolute
Percent Deviation = 4.81

a a/w is based on optical measurements and is corrected for the crack bow

b CEB is corrected to the load line

TABLE 18

COMPARISON OF COMPLIANCE DERIVATIVE CALIBRATIONS BASED ON
EQUATION (3) AND EXPERIMENTAL DATA OF COUPONS
11CR-2, 11RC-2 AND 11SC-1

Index	Measured ^a Crack Length/Width Ratio, a/w	Calculated ^b Compliance Calibration, C _{3w}	Experimental ^c Compliance Calibration, C _{3e}	Percent Deviation
1	0.3338	4.090	4.003	-2.17
2	0.3343	4.098	4.011	-2.17
3	0.3587	4.473	4.386	-1.99
4	0.3592	4.481	4.394	-1.98
5	0.3627	4.538	4.451	-1.95
6	0.3652	4.578	4.492	-1.93
7	0.3662	4.594	4.508	-1.92
8	0.3677	4.619	4.533	-1.90
9	0.3772	4.777	4.692	-1.80
10	0.3841	4.894	4.812	-1.70
11	0.3901	4.997	4.918	-1.62
12	0.3951	5.085	5.008	-1.53
13	0.4090	5.335	5.268	-1.28
14	0.4101	5.356	5.289	-1.26
15	0.4150	5.447	5.385	-1.15
16	0.4295	5.723	5.677	-0.82
17	0.4338	5.808	5.767	-0.71
18	0.4405	5.942	5.910	-0.54
19	0.4554	6.251	6.243	-0.13
20	0.4587	6.322	6.319	-0.04
21	0.4654	6.468	6.478	0.15
22	0.4836	6.886	6.931	0.65
23	0.4908	7.061	7.121	0.84
24	0.5085	7.516	7.613	1.27
25	0.5157	7.714	7.824	1.41
26	0.5301	8.133	8.269	1.64
27	0.5333	8.232	8.372	1.68
28	0.5406	8.463	8.613	1.75
29	0.5582	9.066	9.231	1.79
30	0.5655	9.337	9.504	1.75
31	0.5831	10.052	10.205	1.50
32	0.5904	10.376	10.515	1.32
33	0.5980	10.733	10.852	1.09
34	0.6153	11.627	11.673	0.39

TABLE 18. (Concluded)

Index	Measured Crack ^a Length/Width Ratio, a/w	Calculated ^b Compliance Calibration, C _{3w}	Experimental ^c Compliance Calibration, C _{3e}	Percent Deviation
35	0.6229	12.060	12.060	0.00
36	0.6288	12.414	12.373	-0.33
37	0.6402	13.147	13.009	-1.06
38	0.6527	14.032	13.760	-1.98
39	0.6657	15.052	14.607	-3.05
40	0.6726	15.639	15.086	-3.66
41	0.6975	18.051	17.018	-6.07
42	0.7339	22.569	20.561	-9.77
43	0.7373	23.062	20.947	-10.10
44	0.7622	27.095	24.142	-12.23
45	0.7871	31.974	28.153	-13.57
46	0.8124	37.949	33.418	-13.56
47	0.8323	43.480	38.769	-12.15
48	0.8331	43.719	39.012	-12.06
49	0.8567	51.405	47.521	-8.18
50	0.8864	63.006	63.645	1.00
51	0.8866	63.092	63.784	1.08
52	0.9114	74.685	86.204	13.36
53	0.9363	88.310	127.444	30.71

a a/w is based on optical measurements and is corrected for the crack bow

b C₃ results calculated using Equation (3) which is derived from a fit to boundary value collacation results [12]

c C₃ results based on experimental evaluation of Equation (2) employing Equation (4) and k, e, and v from Table 17

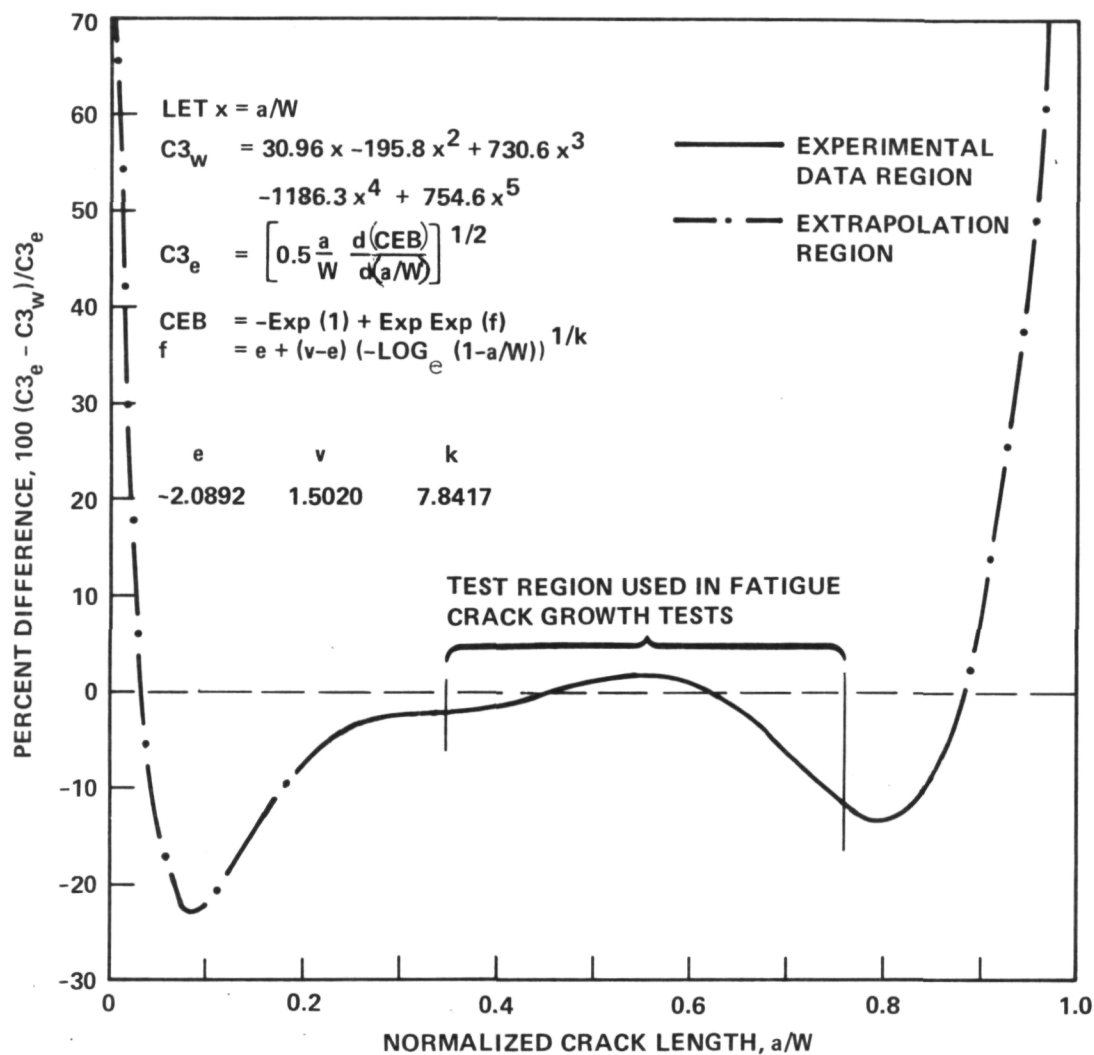


Figure 43. - Percent Difference Between Experimental and Analytical Stress Intensity Calibration Function, C_3 , versus Normalized Crack Length, a/W , Based on Compliance Data of Coupons 11CR-2, 11RC-2, and 11SC-1

TABLE 19

COMPARISON OF RELATIVE CRACK LENGTH BASED ON OPTICAL READINGS
AND ON COMPLIANCE MEASUREMENTS AT -253°C (423°F)

Coupon 7 CR-2

Calculation Based on Optical Measurement	Measured Crack Length/Width a/w Calculation ^a Based on Compliance Data at -253°C (-423°F)	Calculation Based on Compliance Data at Room Temperature
0.432	0.435	0.431
0.447	0.463	-
0.462	0.468	-
0.507	0.497	0.500
0.537	0.528	-
0.557	0.561	-
0.622	0.600	-

a Calculation made by assuming no effect of temperature on compliance except for change in apparent modulus in CEB calculation

after fracture for crack bowing, compared to a/w based upon the normalized compliance readings corrected to the load line of the coupon.

The crack lengths based on normalized compliance shown in Table 19 were determined by using Equation (6), the apparent elastic modulus obtained at -253°C (-423°F), and the k , e , and v values of the combined room temperature compliance data set. This procedure assumed that compliance at -253°C (-423°F) would be unchanged compared to that obtained at room temperature. If the assumption was correct, close agreement between optical and compliance based a/w should have resulted. This assumption was supported by the excellent agreement between optical and compliance based a/w data observed for all crack propagation coupons tested at room temperature (see Appendix). Table 19 clearly shows the excellent agreement between optical and compliance based a/w calculations regardless of the temperature at which the compliance calibration was conducted. In summary, calculation of a/w using low temperature based compliance data and k , e , v parameters obtained from room temperature based compliance data is correct provided the correction for apparent modulus due to temperature is taken into account. Compliance calibration and the associated calculation of a/w was not affected by low temperature except for allowance of a modulus change.

To obtain calculated values of a/w for each crack growth coupon, the associated compliance data for comparison to the a/w data (corrected for the crack bow) obtained optically, Equation (6) was used along with k , e , v parameters based on normalized compliance data measured at the crack mouth. These k , e , v , values are given in Table 20. By using these k , e , and v values, a/w was calculated from Equation (6) using the data taken directly from the load versus COD curves, since all clip gages were at the crack mouth. As mentioned previously, comparison between optical and compliance based a/w calculations was excellent as can be observed by careful scrutiny of the data in the Appendix to this report.

TABLE 20

PARAMETERS USED IN EQUATION (6) FOR CALCULATING
COMPLIANCE BASED a/w RATIOS FOR CRACK GROWTH COUPONS

Parameter	Numerical Value
k	2.1840630491827
e	0.71927792637216
v	1.6103577859161

4.0 FATIGUE CRACK PROPAGATION RESULTS

The experimental variables studied were: orientation, stress range ratio (0.05, 0.5), frequency (10 Hz, 0.1 Hz) and environment (room temperature laboratory air and -253°C liquid hydrogen). The results of these tests are summarized in this section. Summary figures only are presented since data for each individual specimen is presented in the Appendix.

Throughout the fatigue crack growth tests, crack length was measured optically as well as with a compliance gage. A comparison of a/w based upon the optical and COD measurements is given in the Appendix for most coupons tested at room temperature. The difference between optical and COD measurements was less than ± 8 percent for all of the crack length measurements for all of the coupons compared. The difference was always greatest for the smaller a/w ratios. The vast majority of the differences for all of the data points compared was less than ± 4 percent.

4.1 Orientation Effects

The effects of specimen orientation within the pancake forgings on the fatigue crack propagation behavior of Ti-5Al-2.5Sn(ELI) at room temperature are shown in Figs. 44 to 47. Careful study of this data using the individual plots of Appendix A showed no significant effect of coupon orientation on the fatigue crack growth behavior. Coupons 2CR-1 and 2RC-1 were not included because no crack growth data was recorded for these two coupons.

Variation in growth rates within a coupon were often as large as the variation from one orientation to another. The curves shown in Figs. 44 to 47 are the 2σ scatter bands discussed in Section 2.3.4; extrapolations are indicated by dashed lines. When the location of the data for each individual specimen was compared to the 2σ band for all data (see Appendix), then for Fig. 44 the CS and RS orientation data were found to be more in the lower half of the data band. However, for Figs. 45 to 47 the same trend for CS and RS data was not discernable. Differences in propagation rates for cracks growing in the R or C direction were not observed.

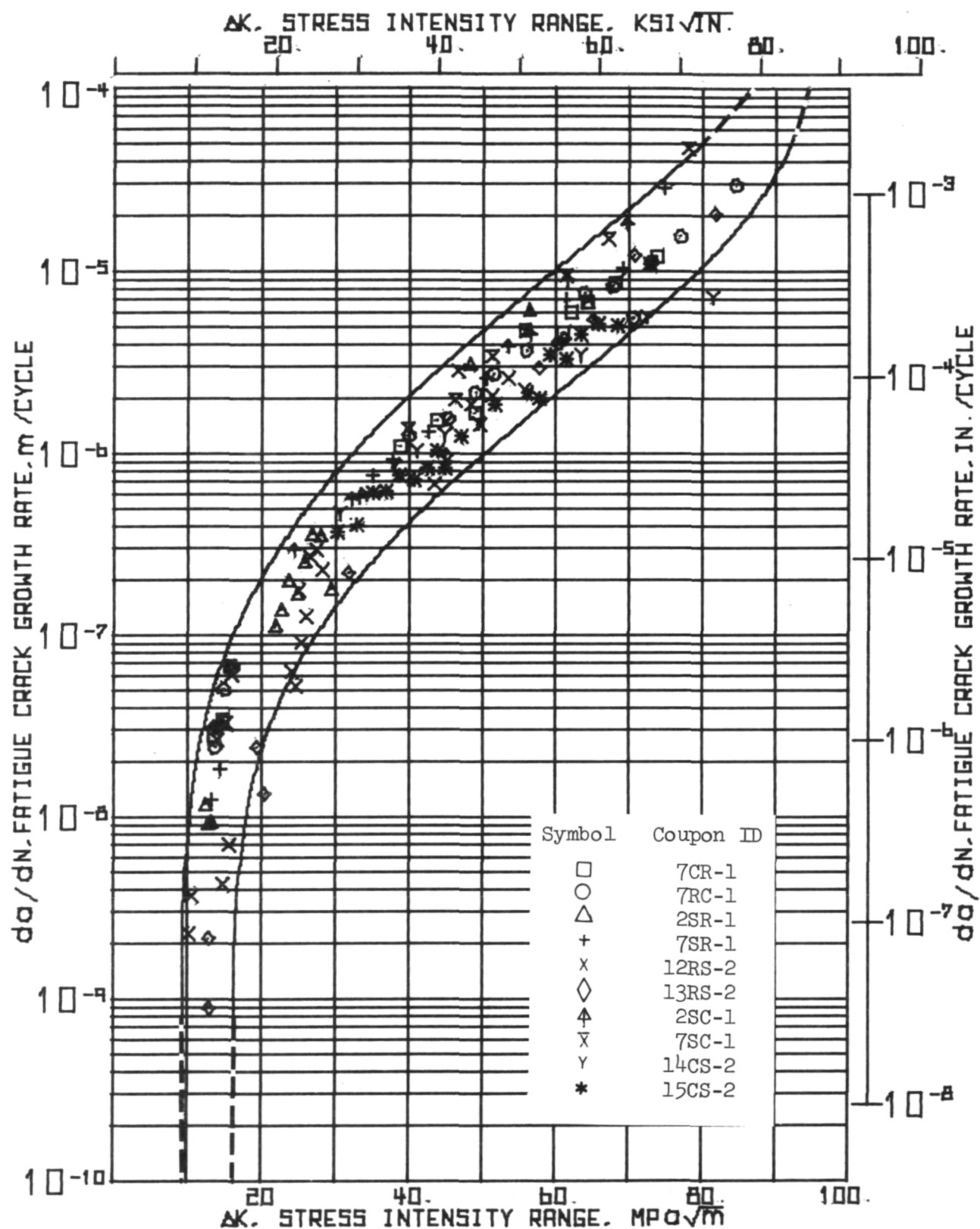


Figure 44.- Effect of Orientation on Fatigue Crack Propagation Behavior of Ti-5Al-2.5 Sn (ELI) at Room Temperature, $R = 0.05$, $F = 10$ Hz

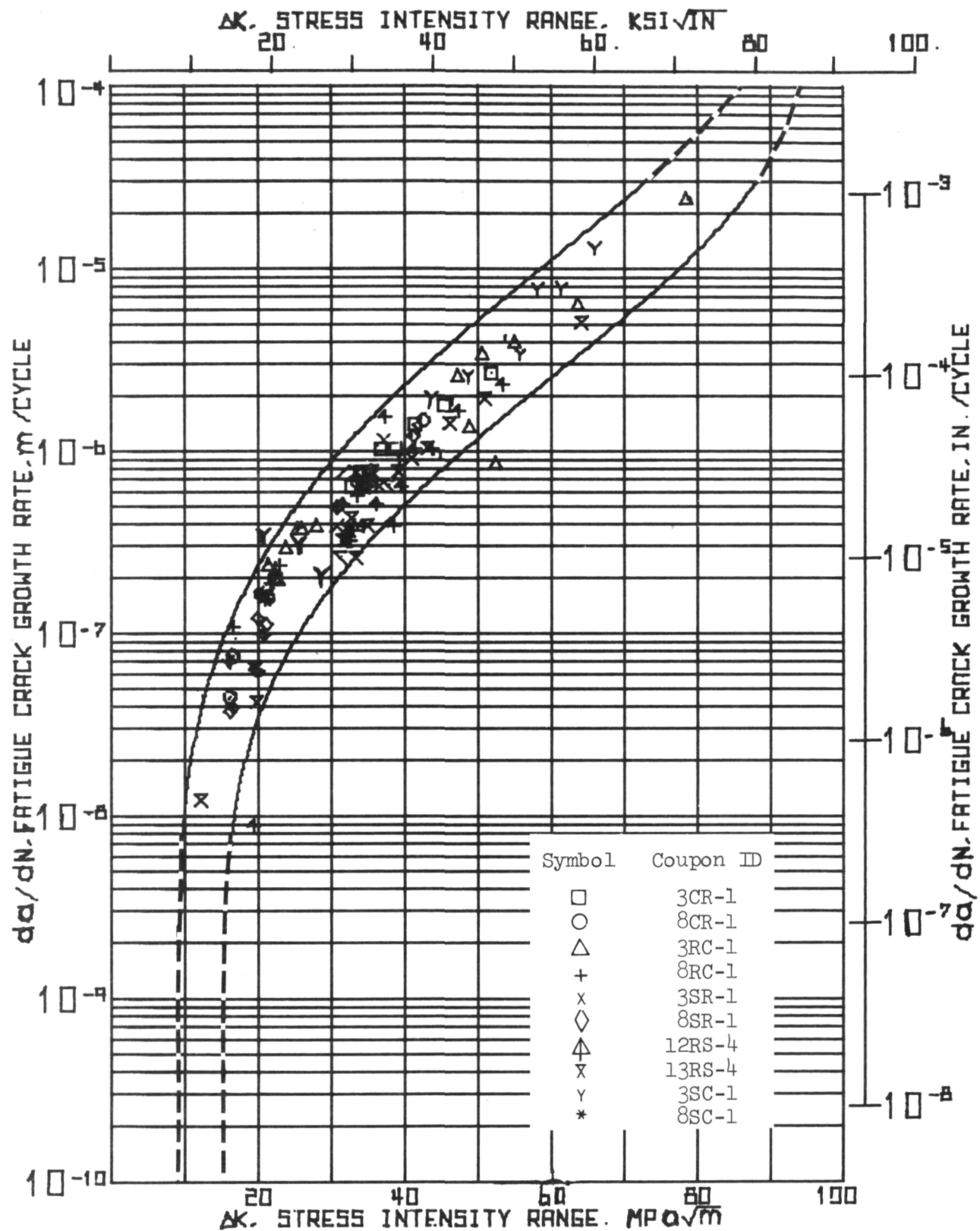


Figure 45.- Effect of Orientation on Fatigue Crack Propagation Behavior of Ti-5Al-2.5 Sn (ELI) at Room Temperature, $R = 0.05$, $F = 0.1$ Hz

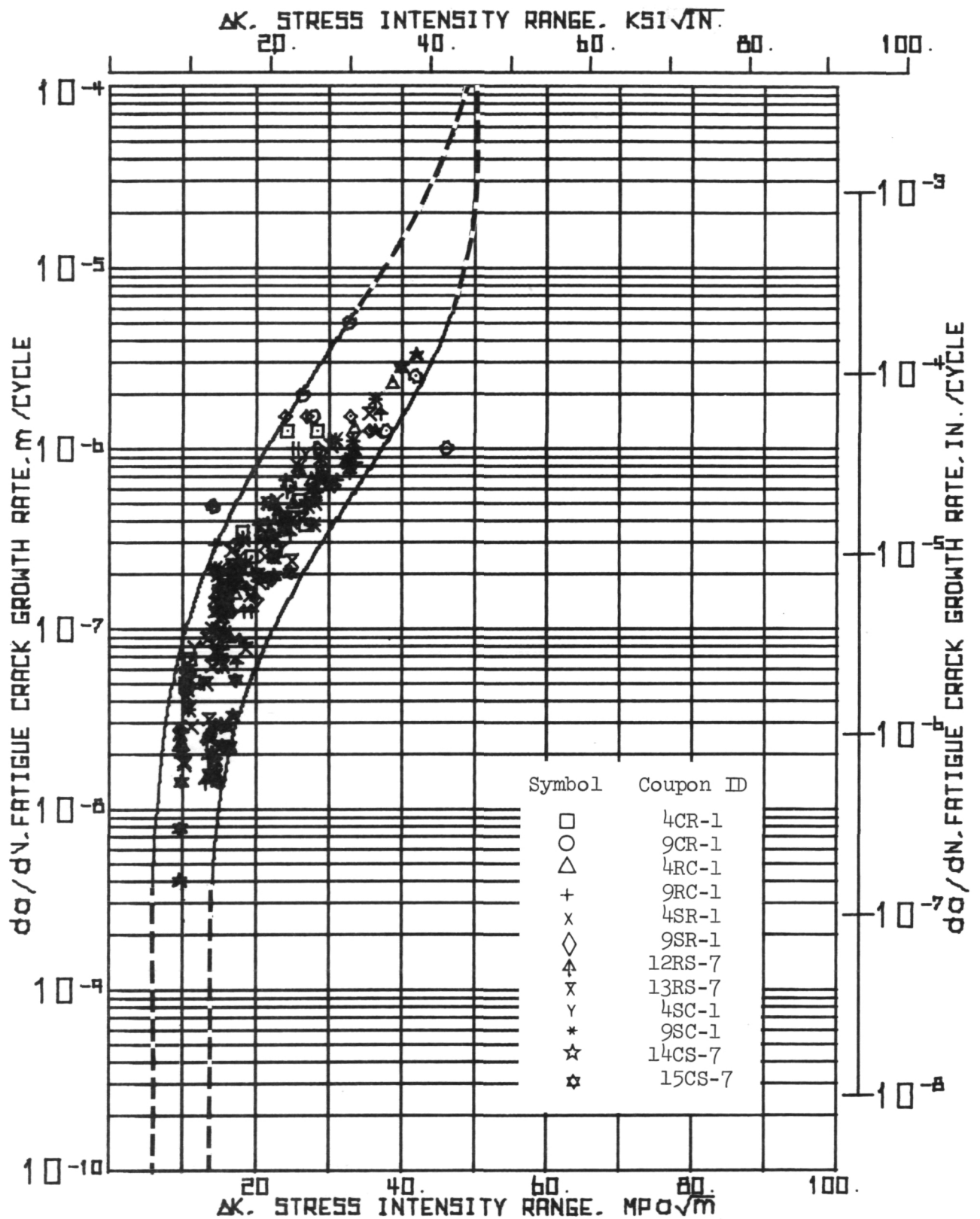


Figure 46. - Effect of Orientation on Fatigue Crack Propagation Behavior of Ti-5Al-2.5 Sn (ELI) at Room Temperature, $R = 0.5$, $F = 10$ Hz

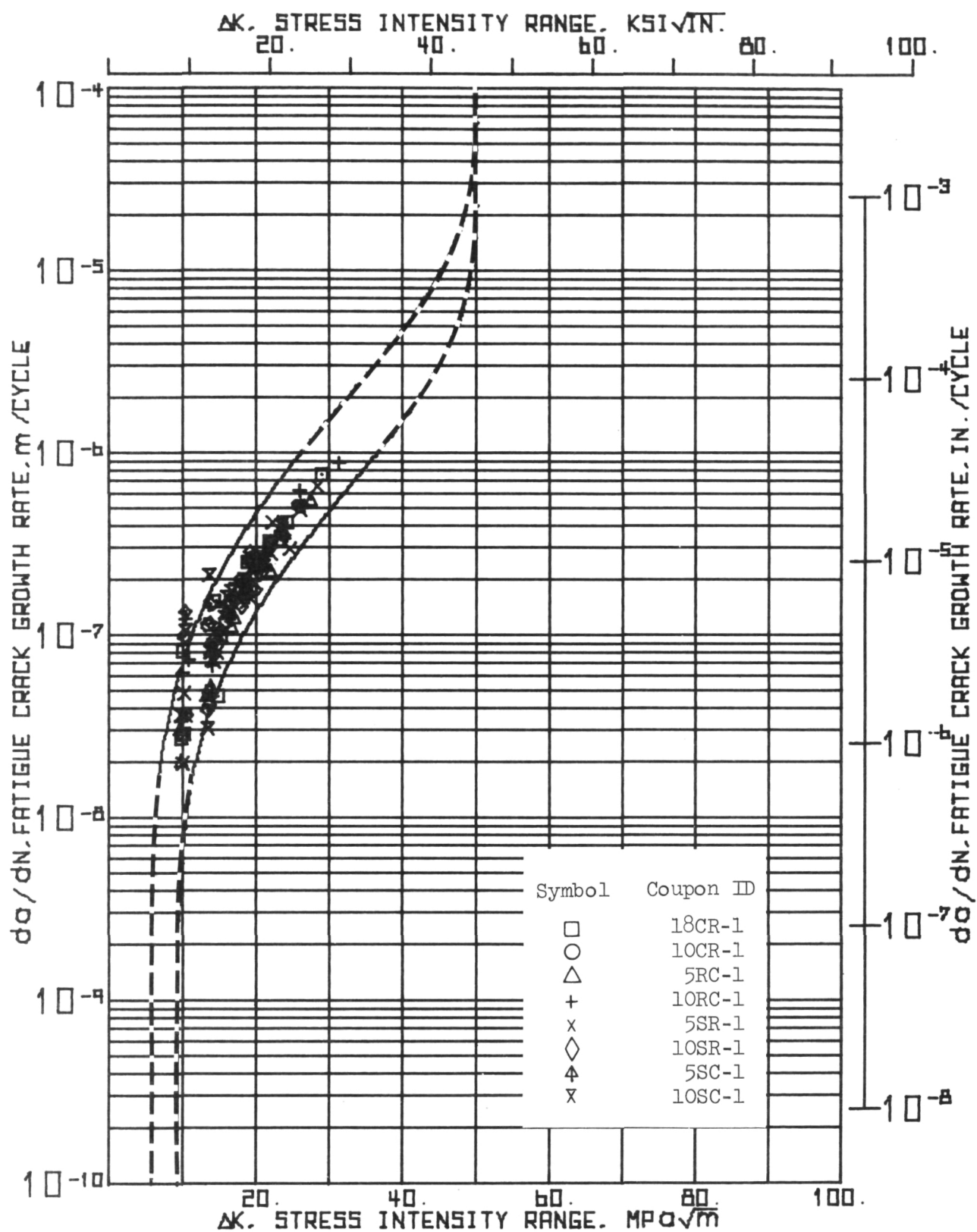


Figure 47. - Effect of Orientation on Fatigue Crack Propagation Behavior of Ti-5Al-2.5 Sn (ELI) at Room Temperature, R = 0.5, F = 0.1 Hz

Data scatter within any specimen was generally small except for specimens from disk 9, see Fig. 46. For this disk, data scatter was greater than that for specimens from other disks. No valid reason for this has been discerned.

Figures 48 to 50 show the effects of orientation on fatigue crack growth behavior at -253°C (-423°F). Study of this data again showed no detectable orientation effect. Figure 51 is included for reference since only one specimen was tested at $R = 0.5$, $F = 0.1$ Hz at -253°C (-423°F).

4.2 Frequency Effects

The effect of frequency on fatigue crack growth rate is shown in Figs. 52 to 55 for room temperature data and in Figs. 56 to 59 for -253°C (-423°F) data. Figs. 52, 54, 56 and 58 compare the results using 2σ bands while Figs. 53, 55, 57 and 59 compare them using the 1σ band suggested design curves.

The data clearly showed that no effect of frequency was observed at $R = 0.05$ at either room temperature or -253°C (-423°F). Curve shapes and thresholds were essentially identical, see Figs. 52, 53, 56 and 57. The same lack of a frequency effect was also true at $R = 0.5$ although at room temperature, Figs. 54 and 55 curve shapes were not identical, although this could be an artifact of the manner in which the data was extrapolated.

4.3 Effect of Range Ratio

Figures 60 to 67 show the effect of load ratio, R , on the fatigue crack growth behavior of this alloy. At both temperatures and both frequencies, the data at $R = 0.5$ was shifted to left or higher growth rates which can be easily seen in the Figures. The amount of the data shift was about the same for each temperature. This result was consistent with other fatigue crack growth studies (see for example Reference [42]) and was expected. The only other observation was that except under 10 Hz conditions at room temperature, data at $R = 0.5$ appeared to have somewhat less scatter, hence tighter 2σ data scatter bands, than the $R = 0.05$ data.

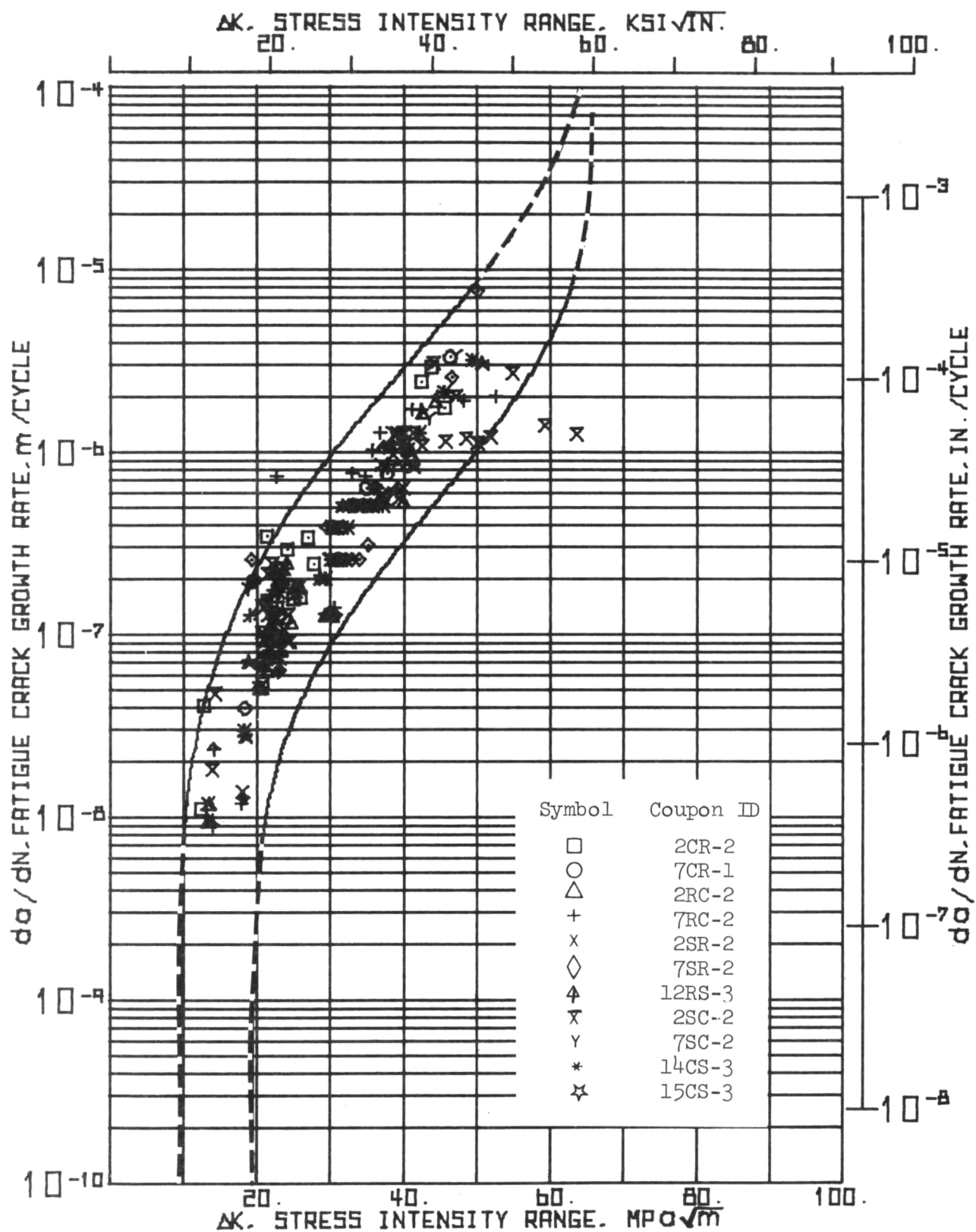


Figure 48. - Effect of Orientation on Fatigue Crack Propagation Behavior of Ti-5Al-2.5 Sn (ELI) at -253°C (-423°F), $R = 0.05$, $F = 10$ Hz

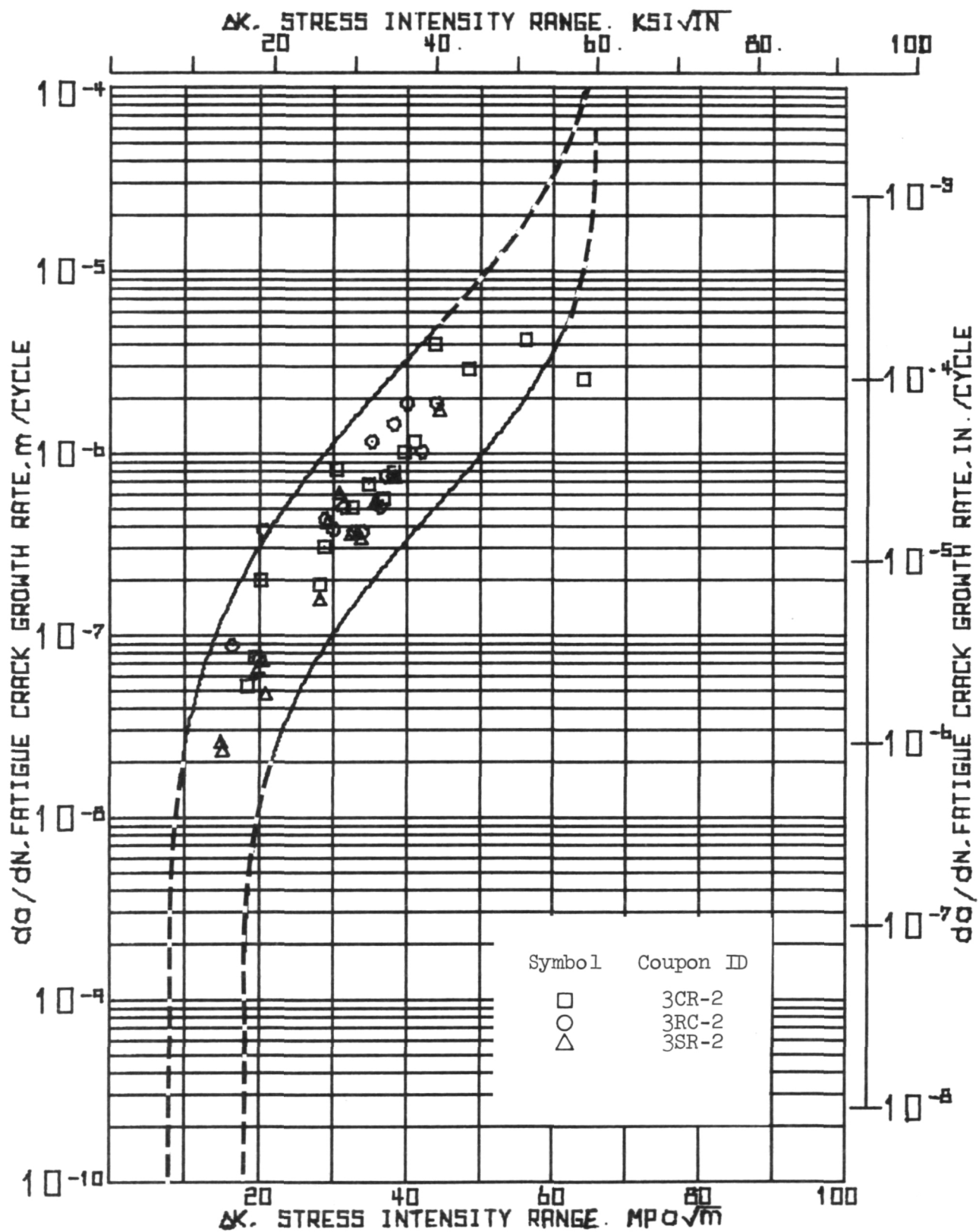


Figure 49.- Effect of Orientation on Fatigue Crack Propagation Behavior of Ti-5Al-2.5 Sn (ELI) at -253°C (-423°F), R = 0.05, F = 0.1 Hz

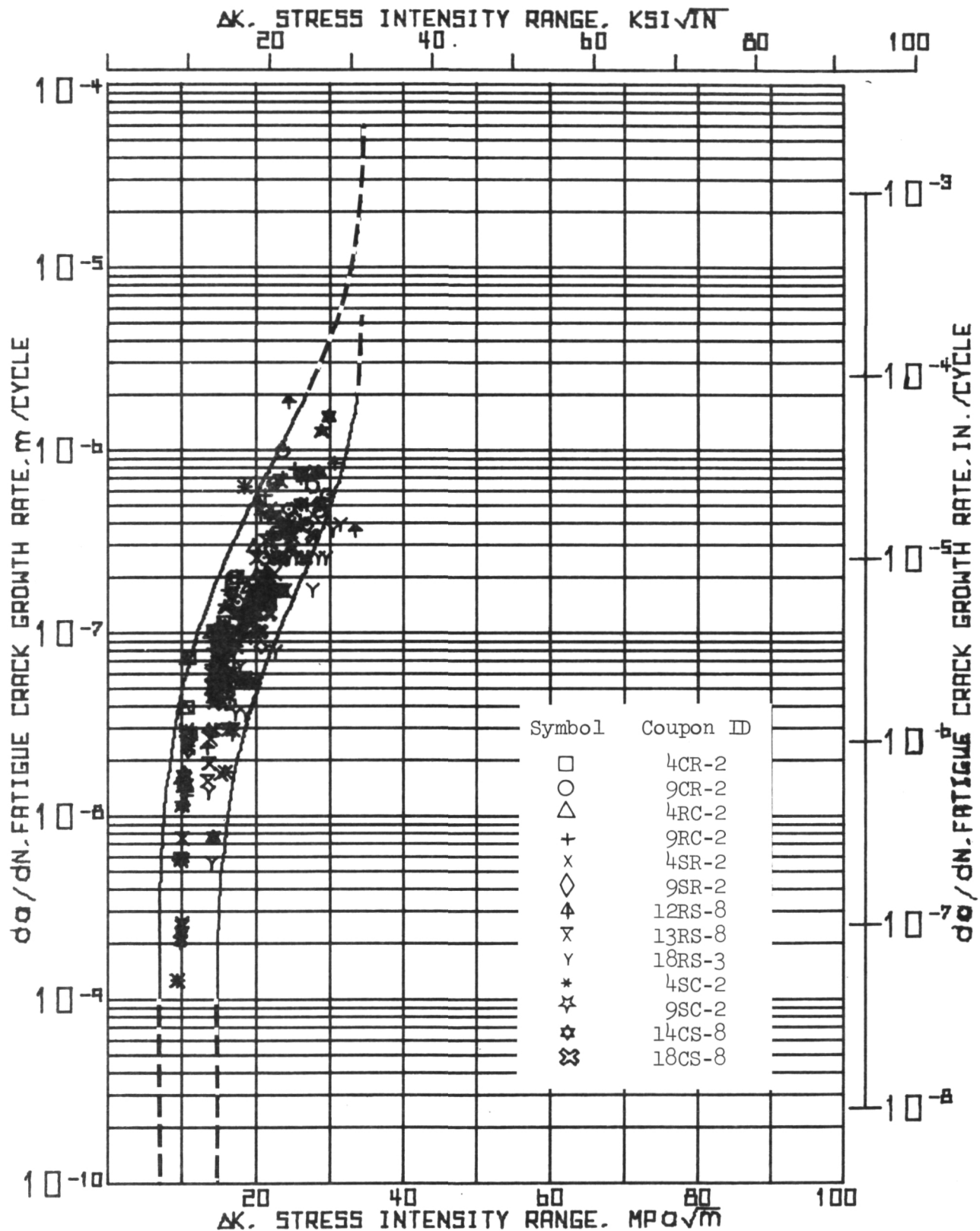


Figure 50.- Effect of Orientation on Fatigue Crack Propagation Behavior of Ti-5Al-2.5 Sn (ELI) at -253°C (-423°F), R = 0.5, F = 10 Hz

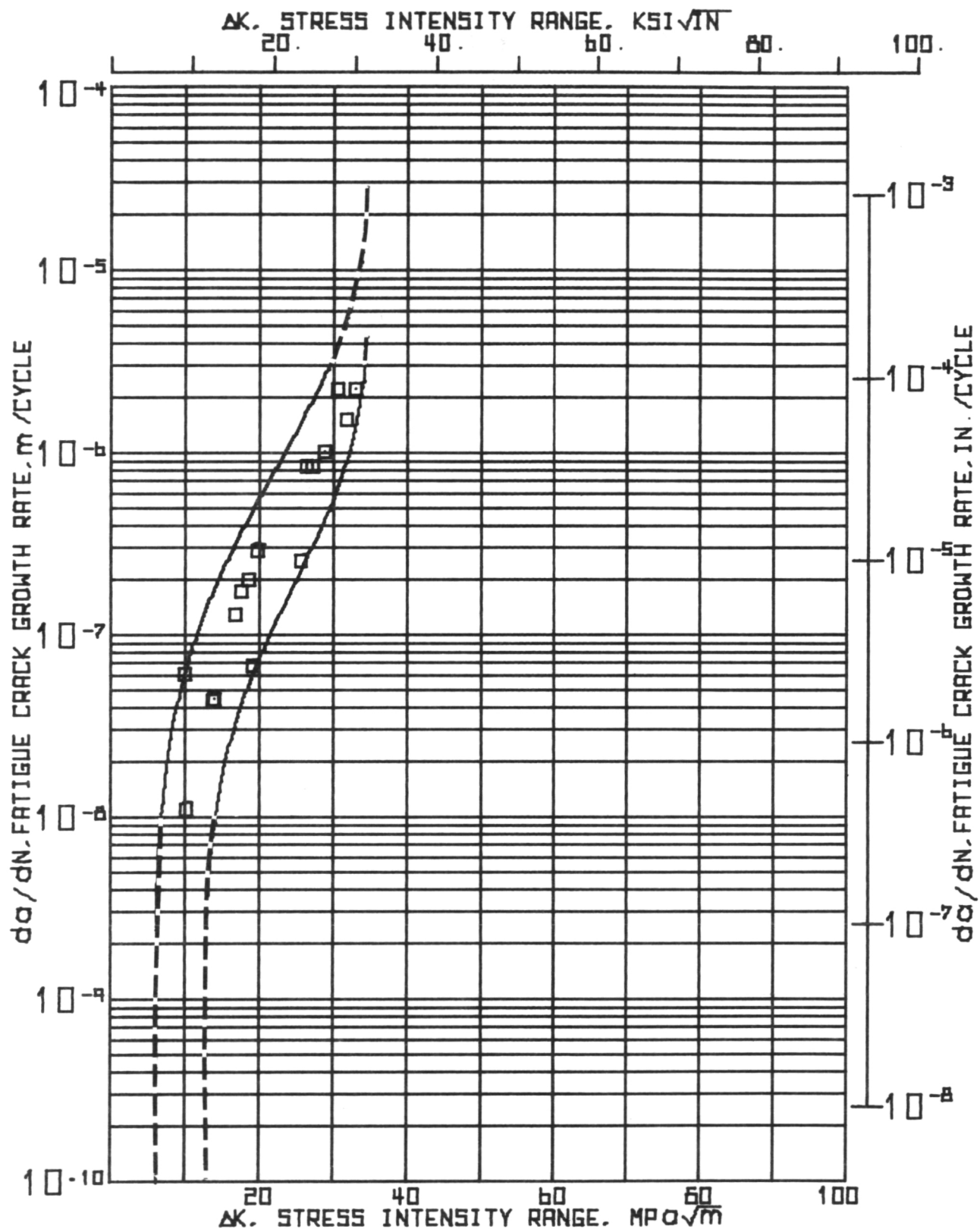


Figure 51.- Fatigue Crack Propagation Behavior of Ti-5Al-2.5 Sn (ELI) at -253°C (-423°F), R = 0.5, F = 0.1 Hz, Specimen 5SR-2

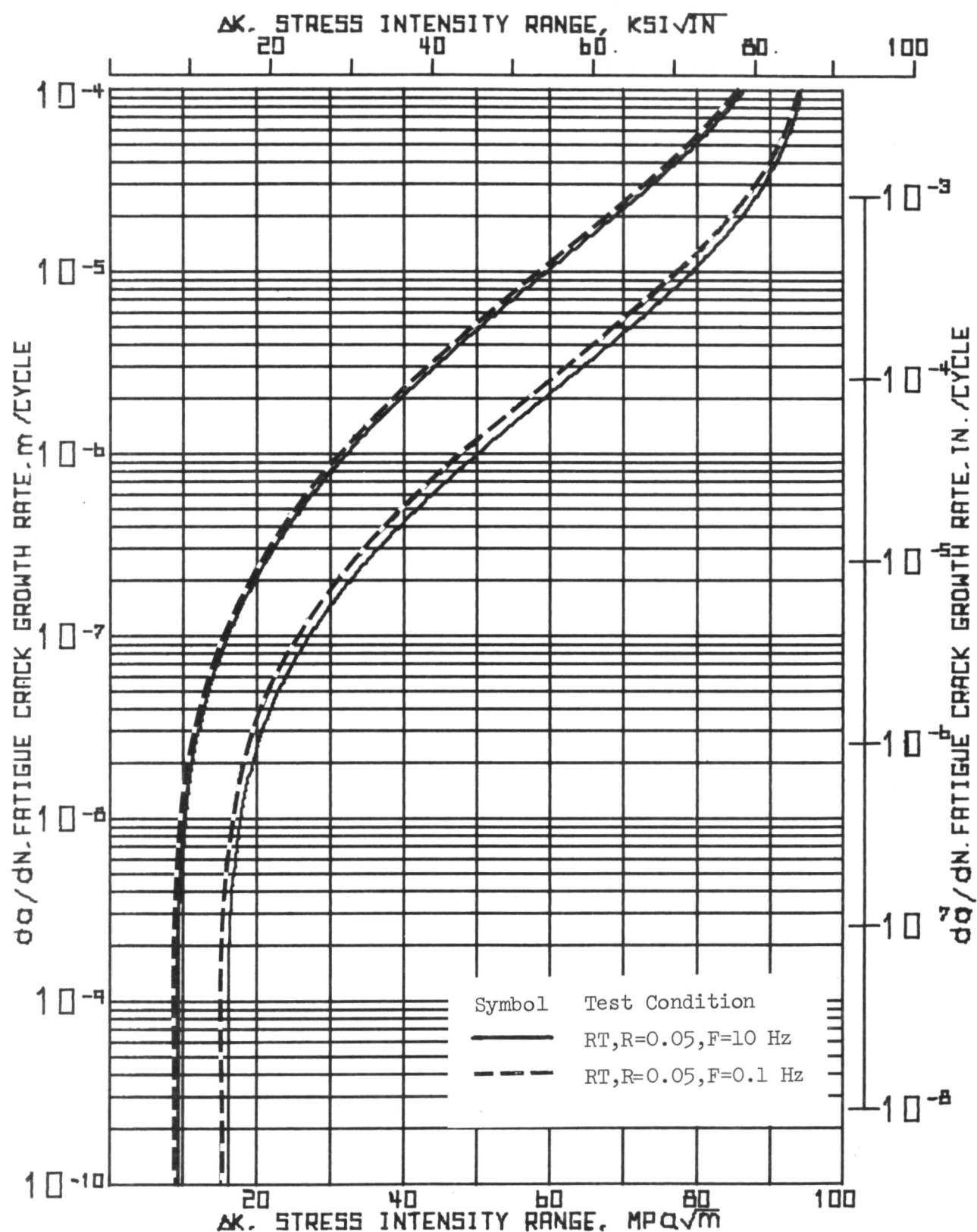


Figure 52.- Comparison of Fatigue Crack Propagation Behavior of Ti-5Al-2.5 Sn (ELI) at F = 10 and 0.1 Hz, R = 0.05, Room Temperature

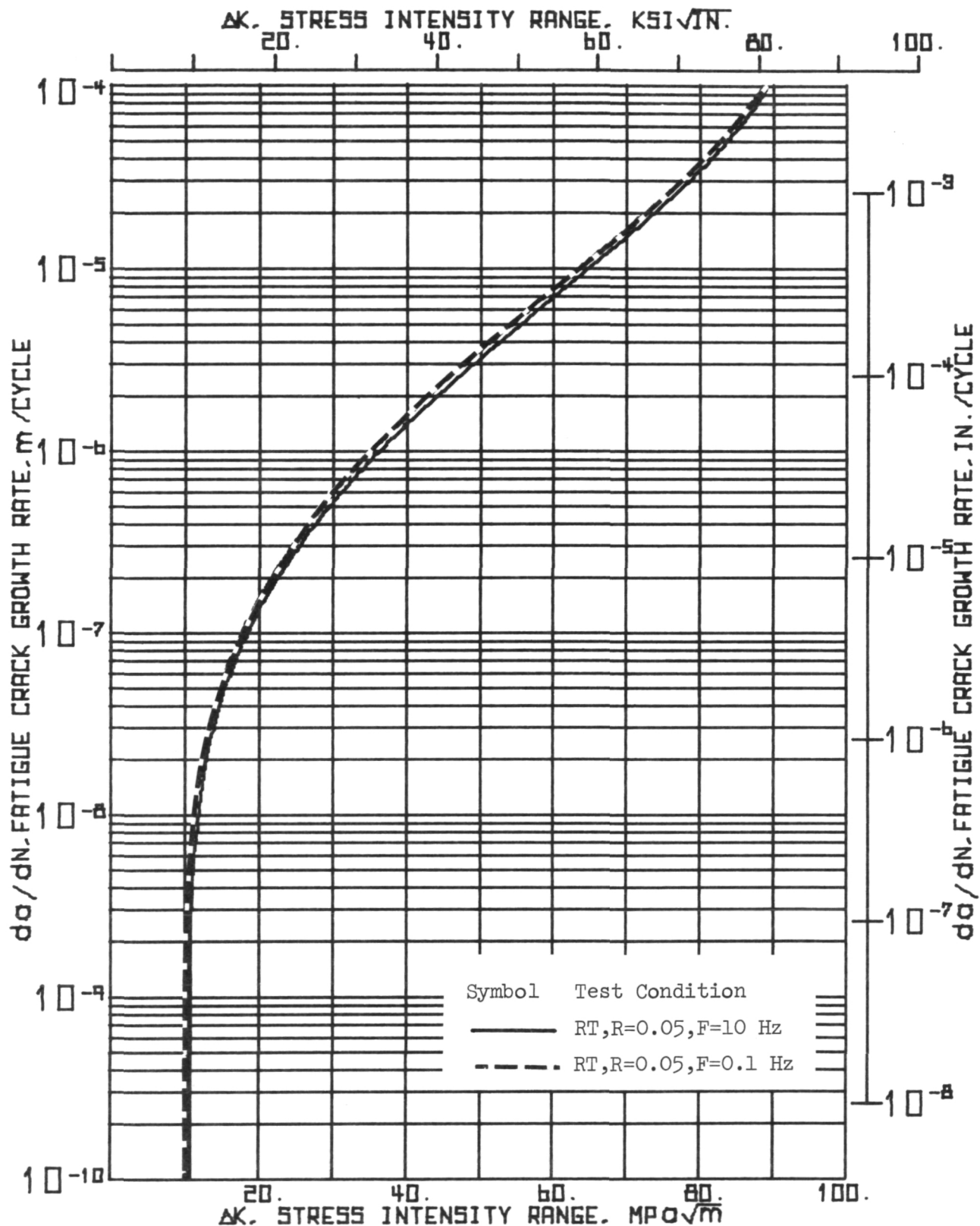


Figure 53.- Comparison of Suggested da/dN Design Curves for Ti-5Al-2.5 Sn (ELI) at $F = 10$ and 0.1 Hz, $R = 0.05$, Room Temperature

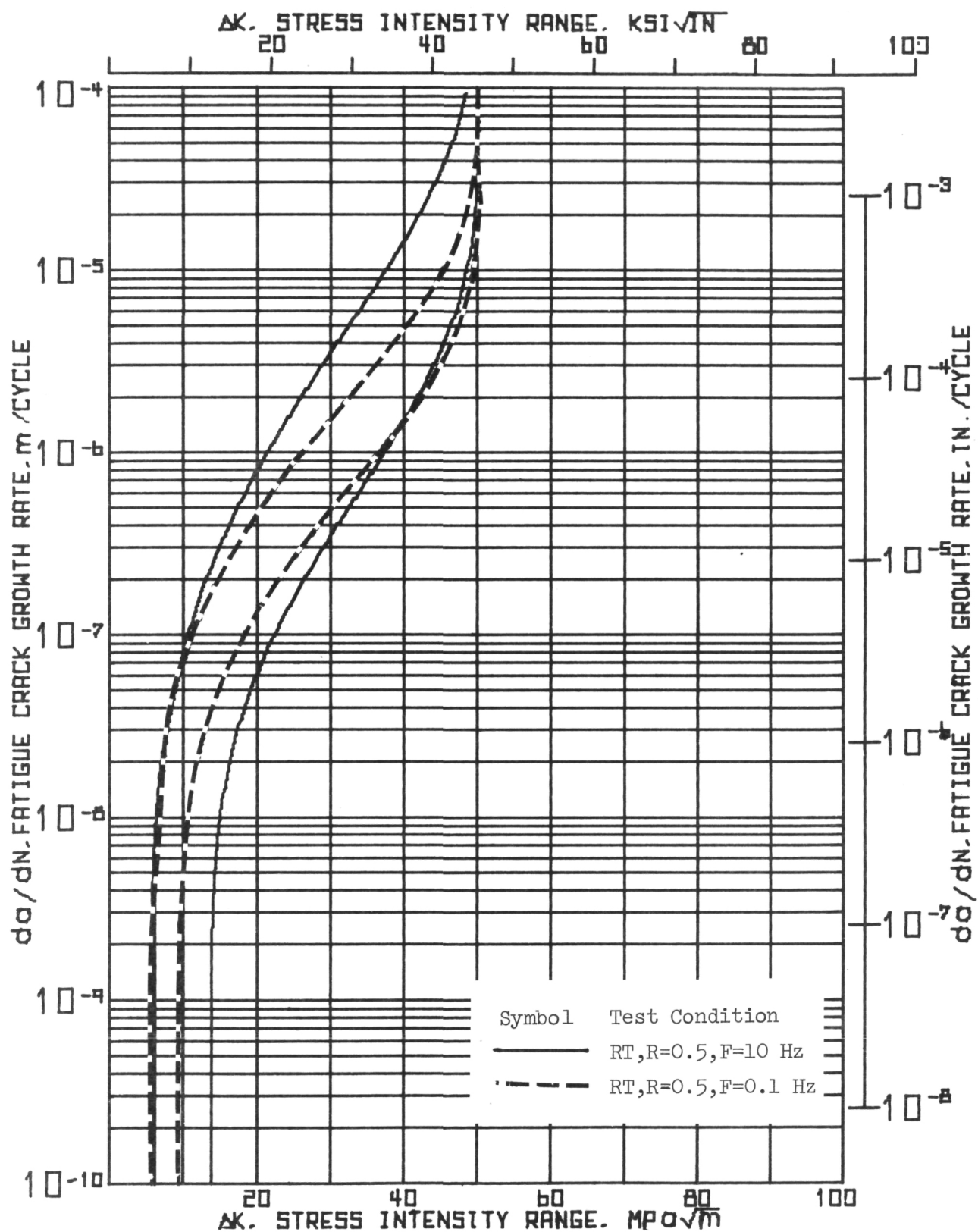


Figure 54.- Comparison of Fatigue Crack Propagation Behavior of Ti-5Al-2.5 Sn (ELI) at F = 10 and 0.1 Hz, R = 0.5, Room Temperature

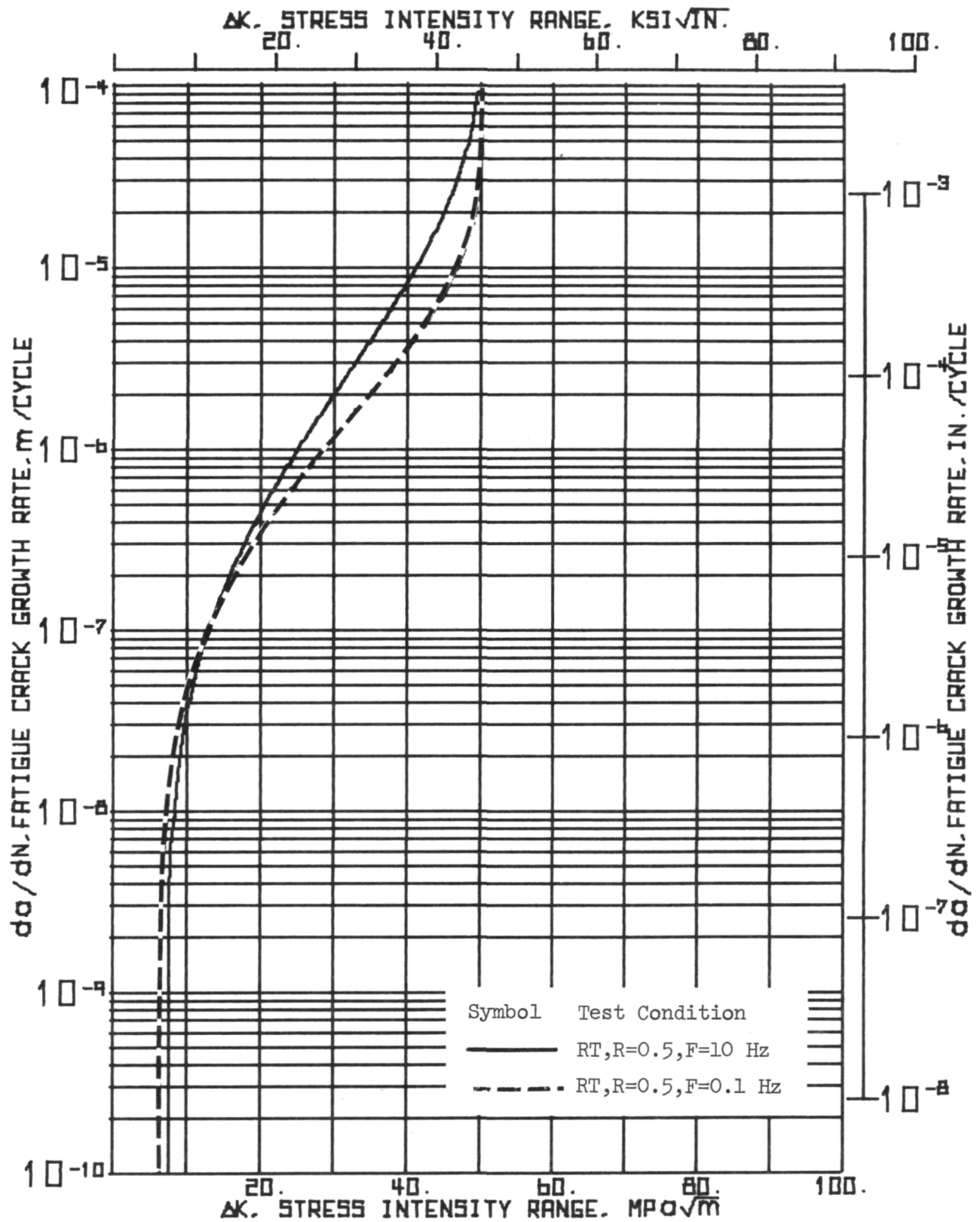


Figure 55.- Comparison of Suggested 1σ Design Curves for Ti-5Al-2.5 Sn (ELI) at $F = 10$ and 0.1 Hz, $R = 0.5$, Room Temperature

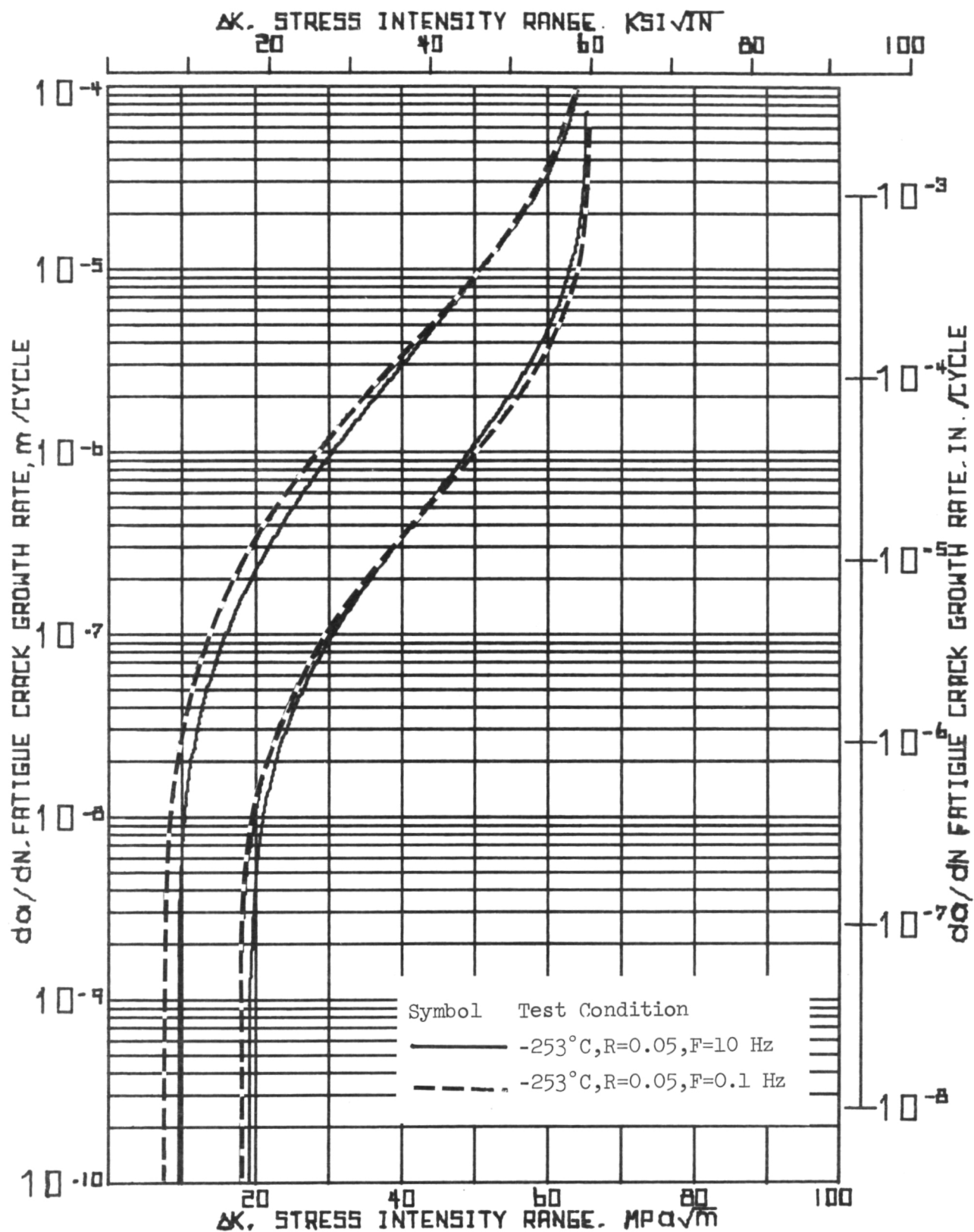


Figure 56.- Comparison of Fatigue Crack Propagation Behavior of Ti-5Al-2.5 Sn (ELI) at F= 10 and 0.1 Hz, R = 0.05, -253°C (-423°F)

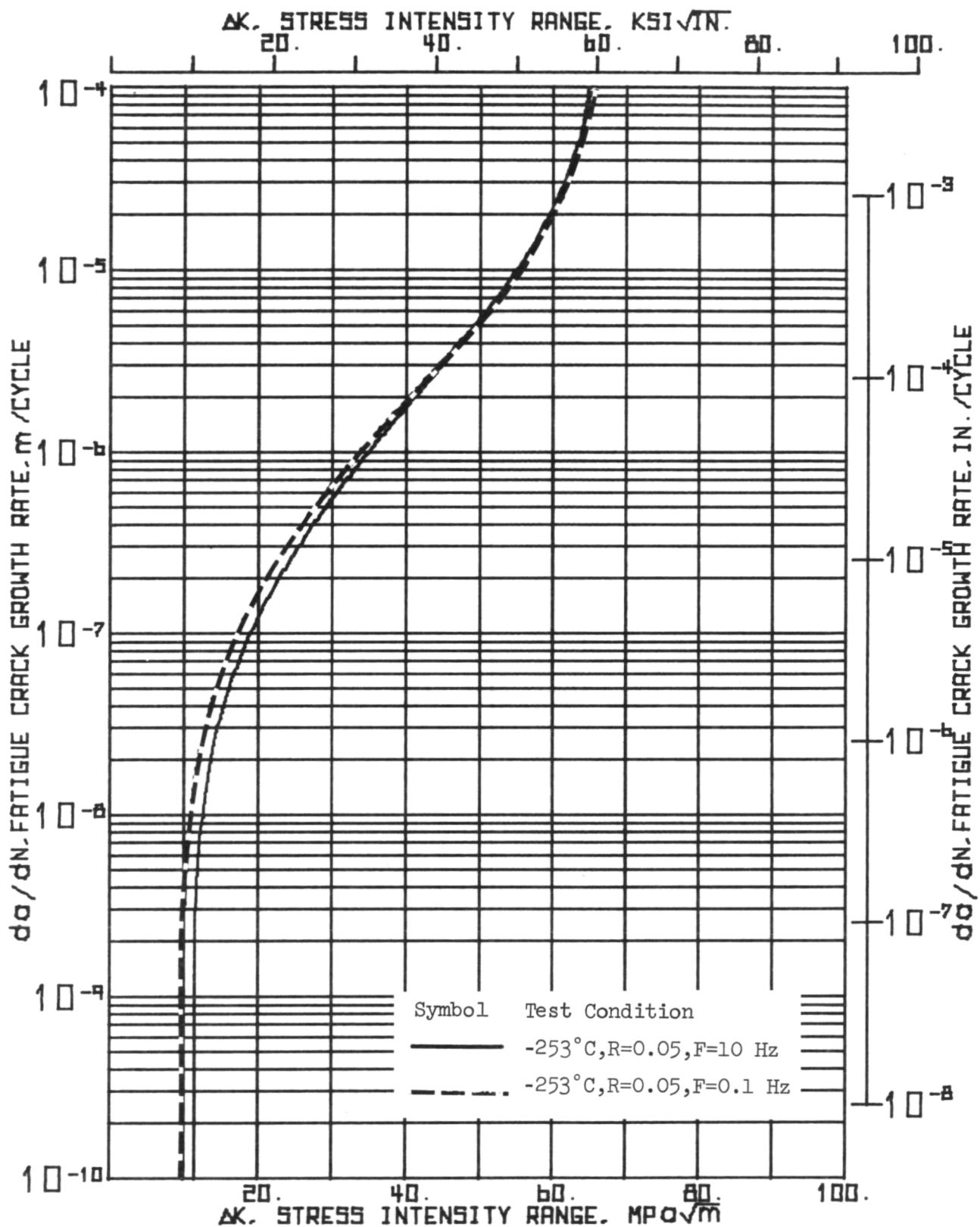


Figure 57.- Comparison of Suggested 1σ Design Curves for Ti-5Al-2.5 Sn (ELI) at $F = 10$ and 0.1 Hz, $R = 0.05$, -253°C (-423°F)

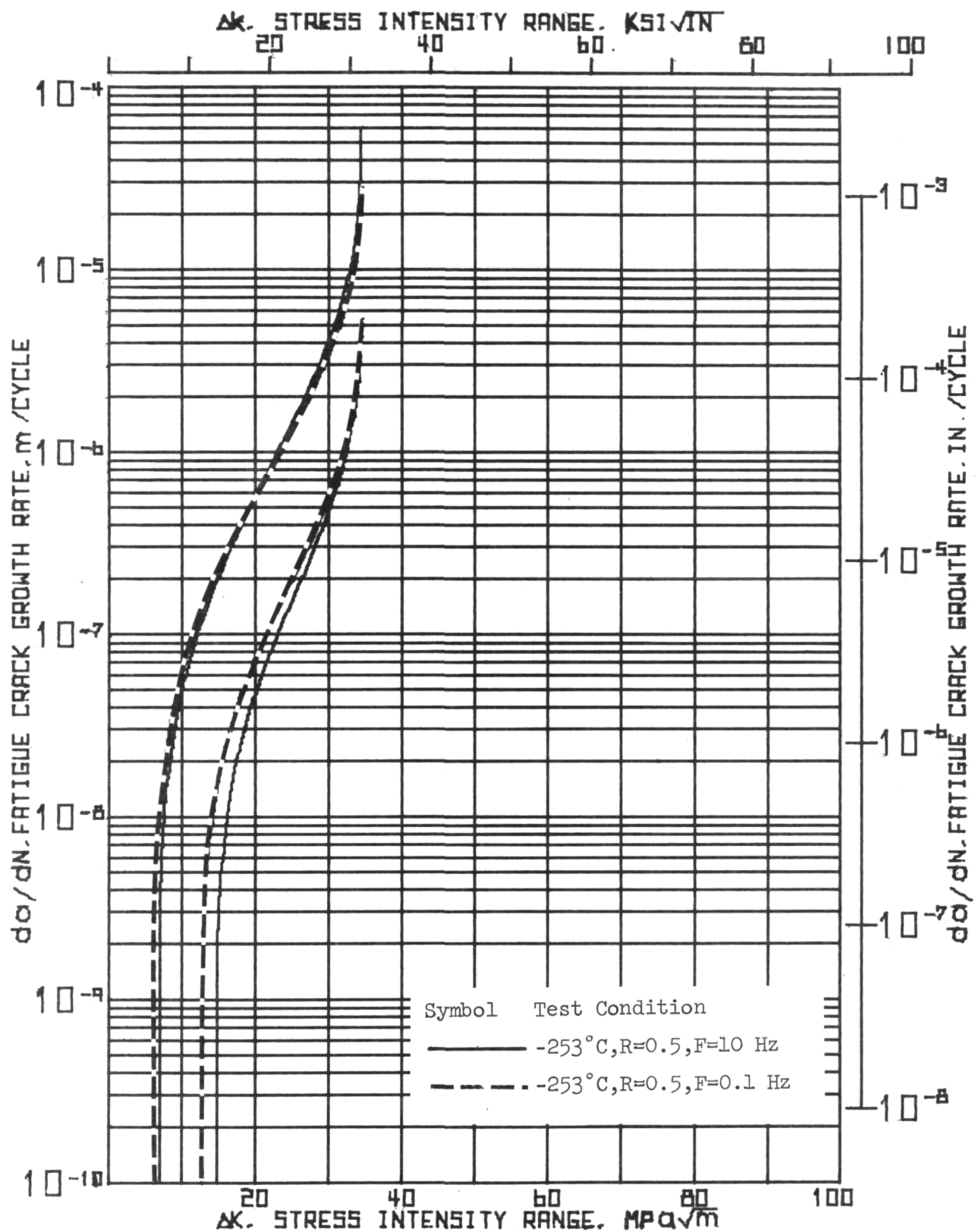


Figure 58.- Comparison of Fatigue Crack Propagation Behavior of Ti-5Al-2.5 Sn (ELI) at F = 10 and 0.1 Hz, R = 0.5, -253°C (-423°F)

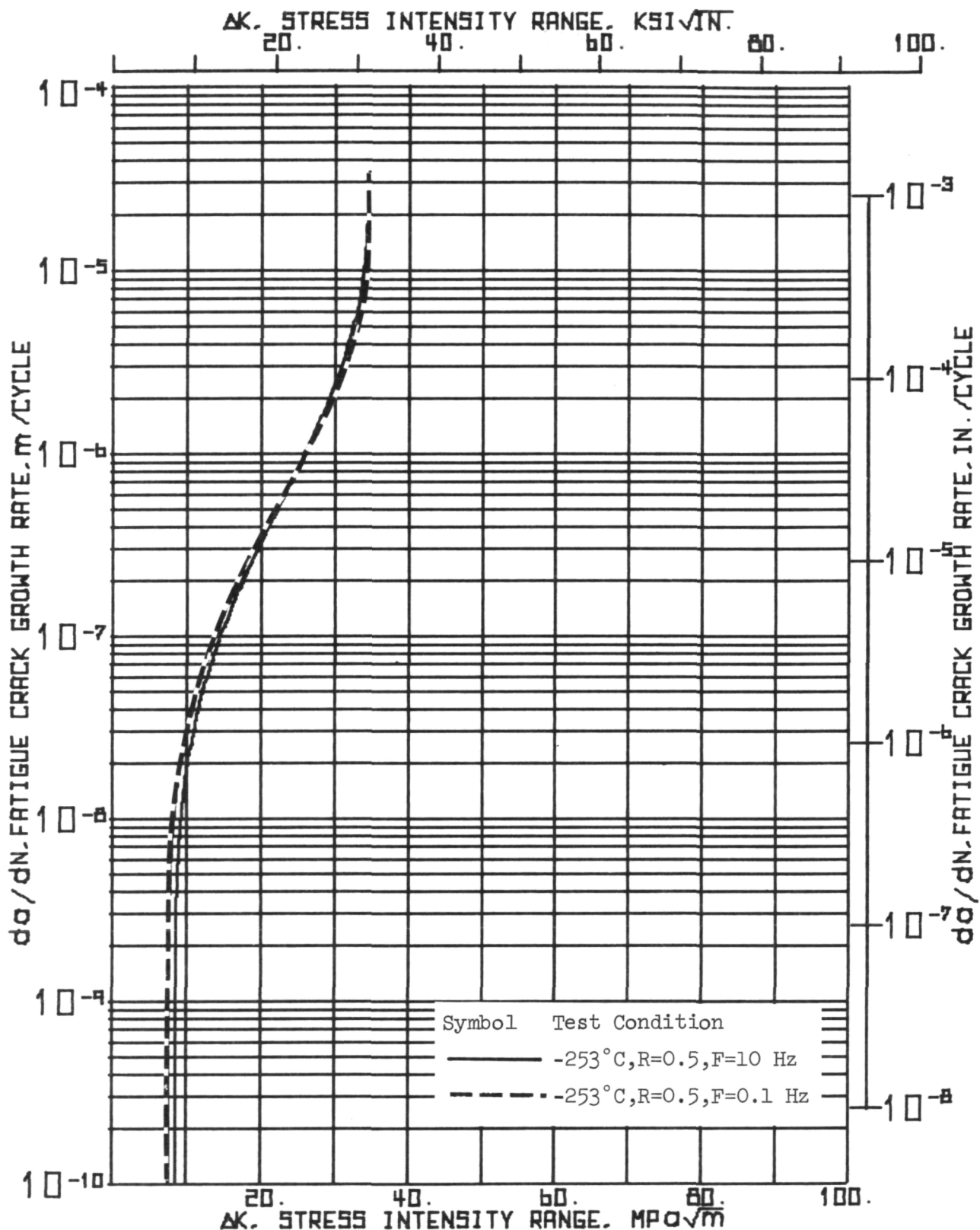


Figure 59.- Comparison of Suggested 1σ Design Curves for Ti-5Al-2.5 (ELI)
at $F = 10$ and 0.1 Hz, $R = 0.5$, -253°C (-423°F)

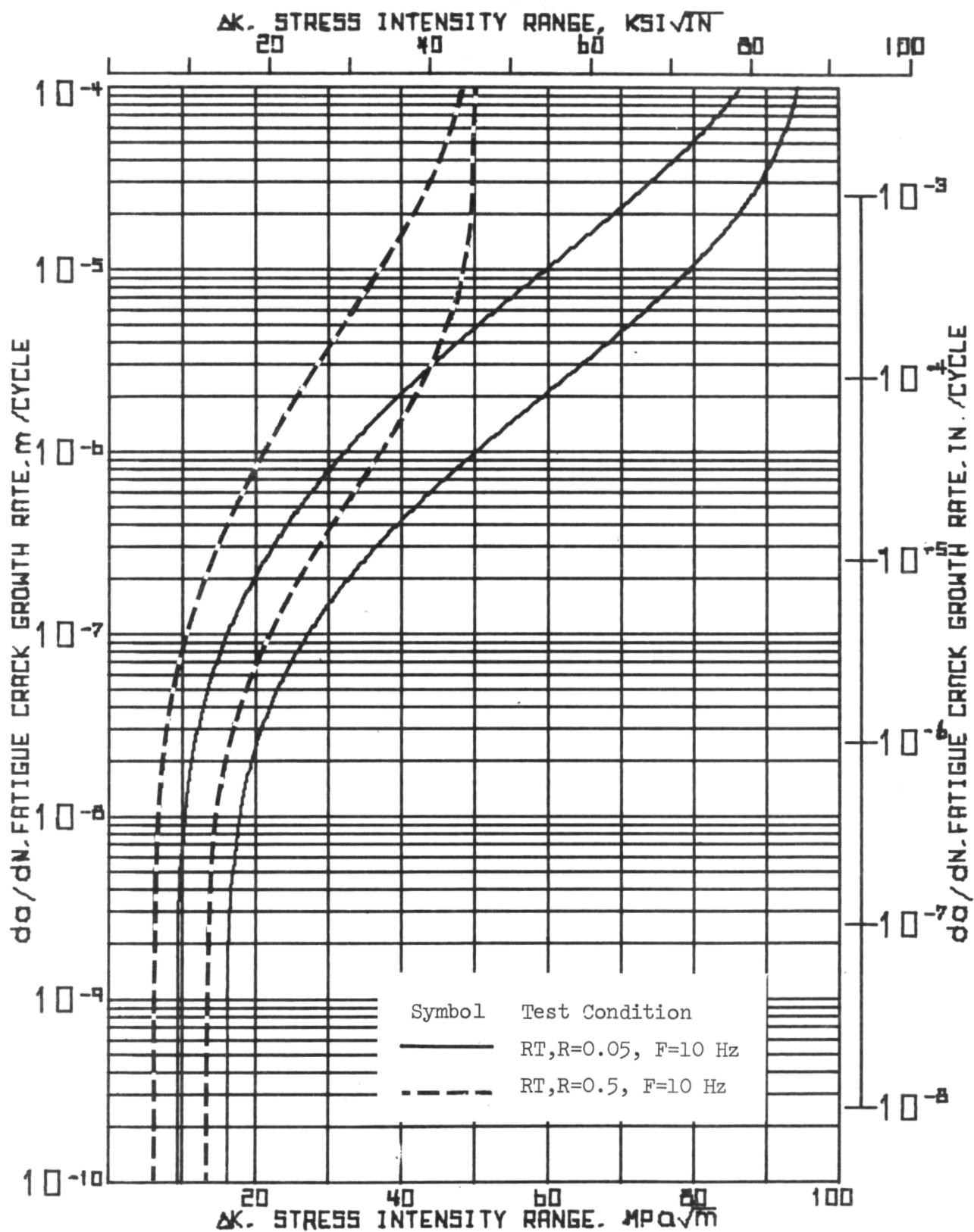


Figure 60.-Comparison of Fatigue Crack Propagation Behavior of Ti-5Al-2.5 Sn (ELI) at R = 0.05 and 0.5, F = 10 Hz, Room Temperature

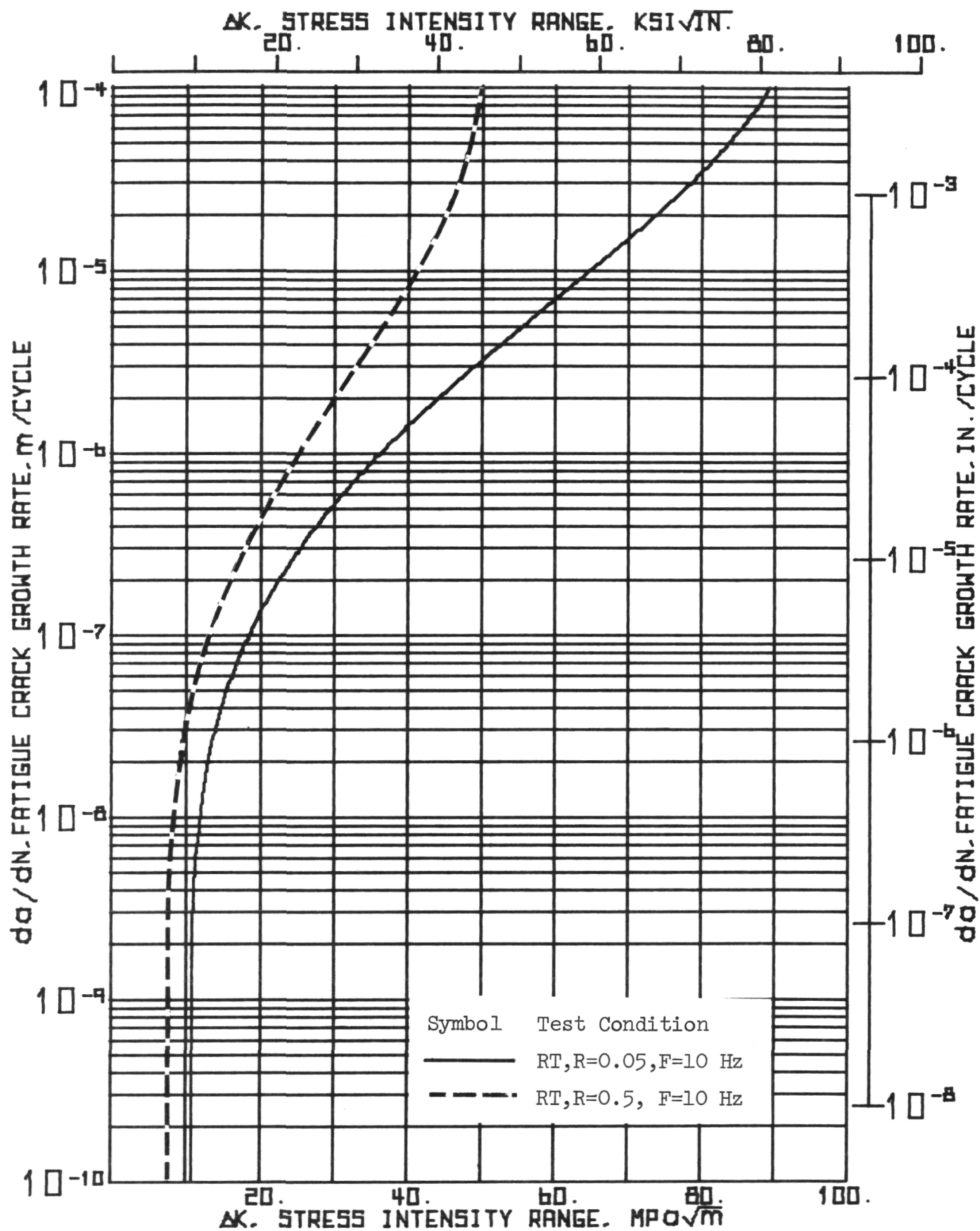


Figure 61.-Comparison of Suggested 1σ Design Curves for Ti-5Al-2.5 Sn (ELI) at $F = 10$ Hz, $R = 0.05$ and 0.5 , Room Temperature

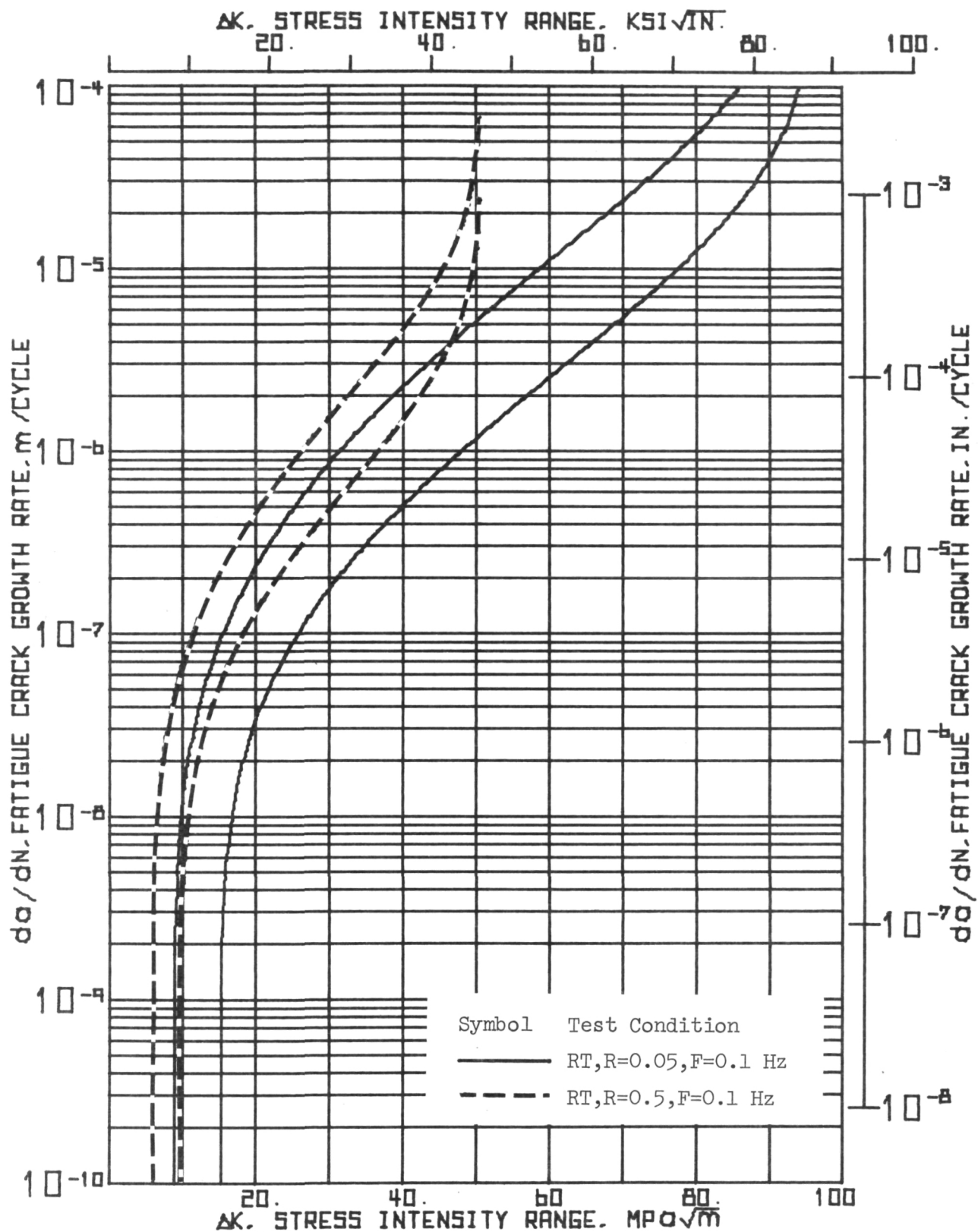


Figure 62.- Comparison of Fatigue Crack Propagation Behavior of Ti-5Al-2.5 Sn (ELI) at R = 0.05 and 0.5, F = 0.1 Hz, Room Temperature

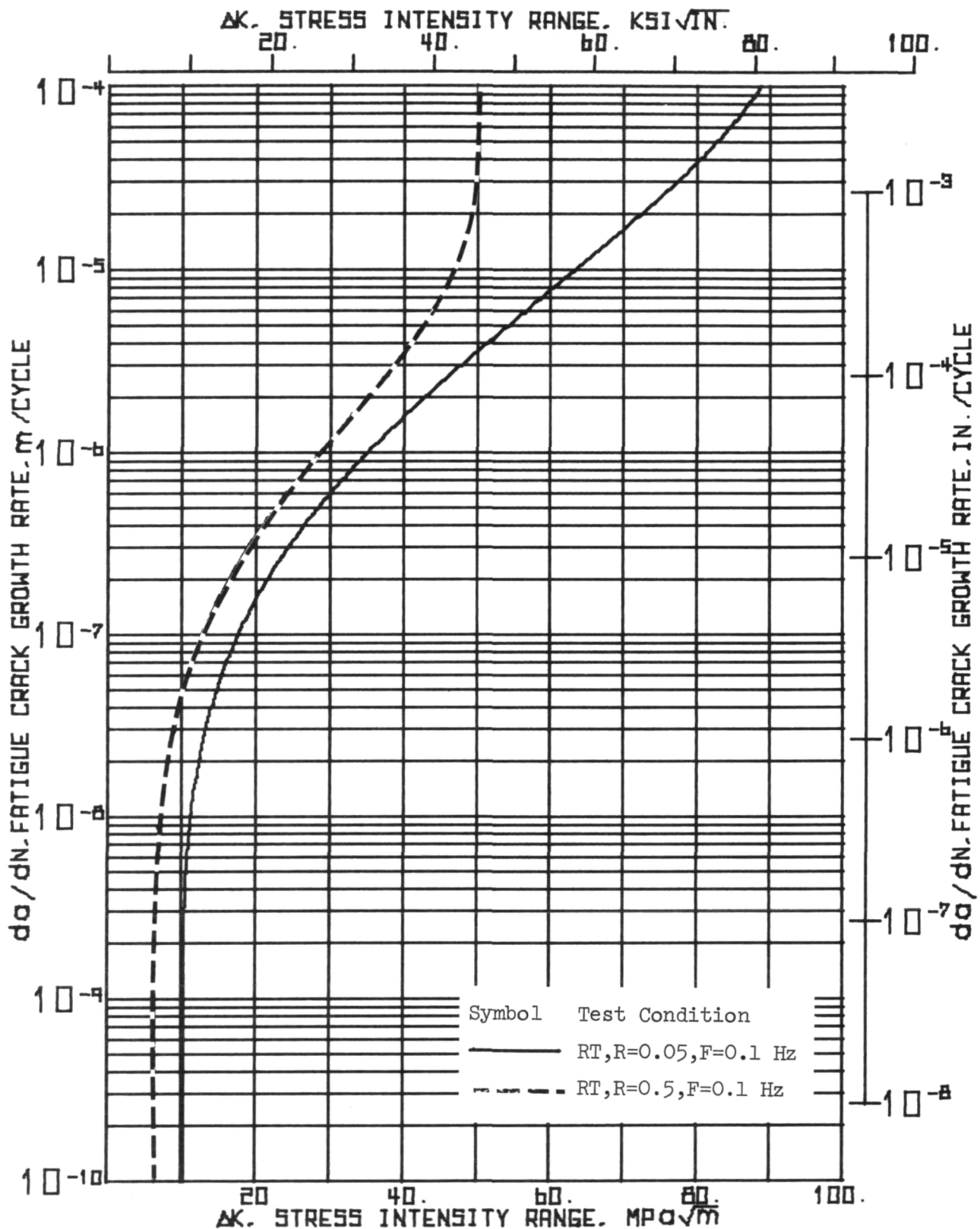
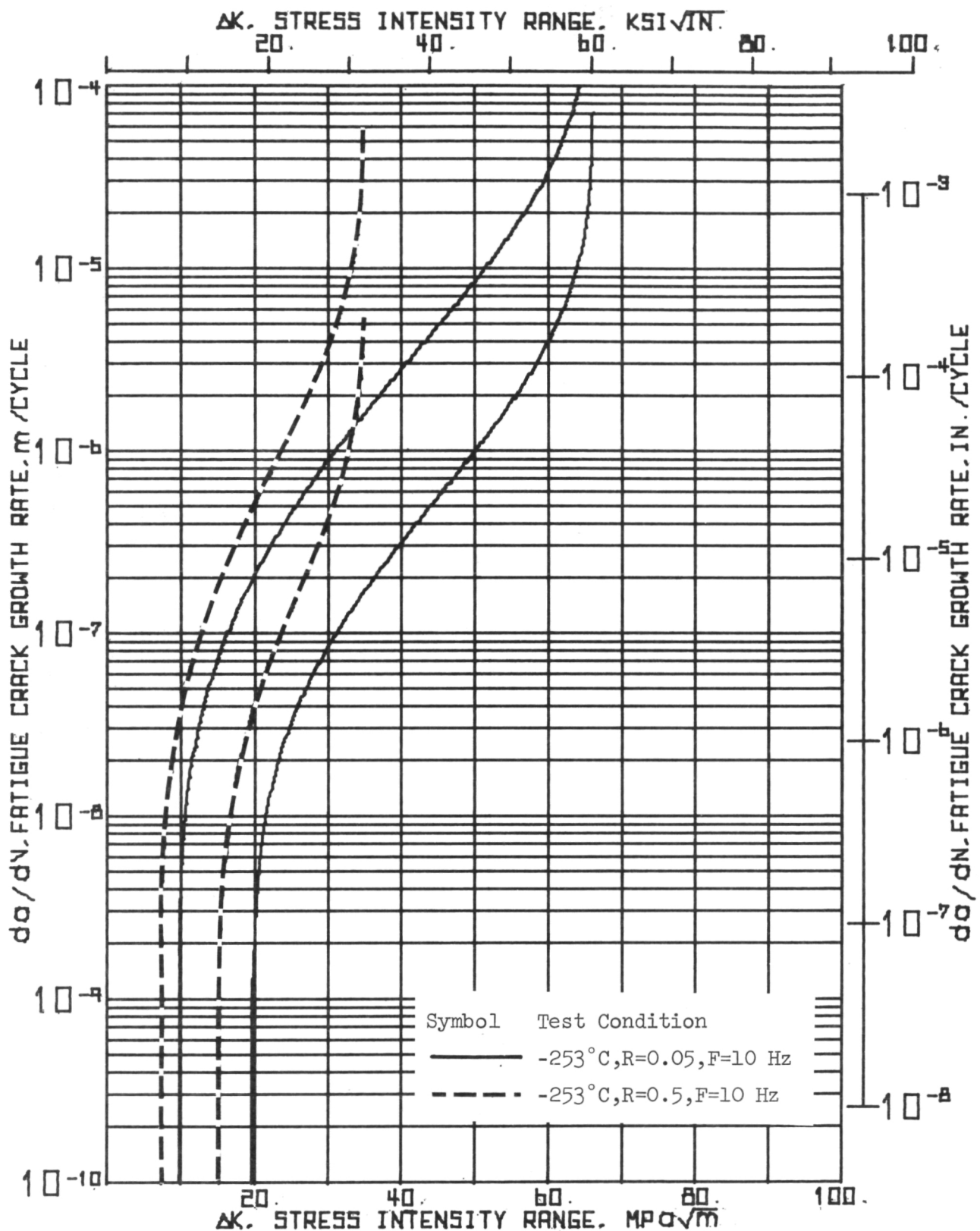


Figure 63.- Comparison of Suggested 1σ Design Curves for Ti-5Al-2.5 Sn (ELI) at $F = 0.1$ Hz, $R = 0.05$ and 0.5 , Room Temperature



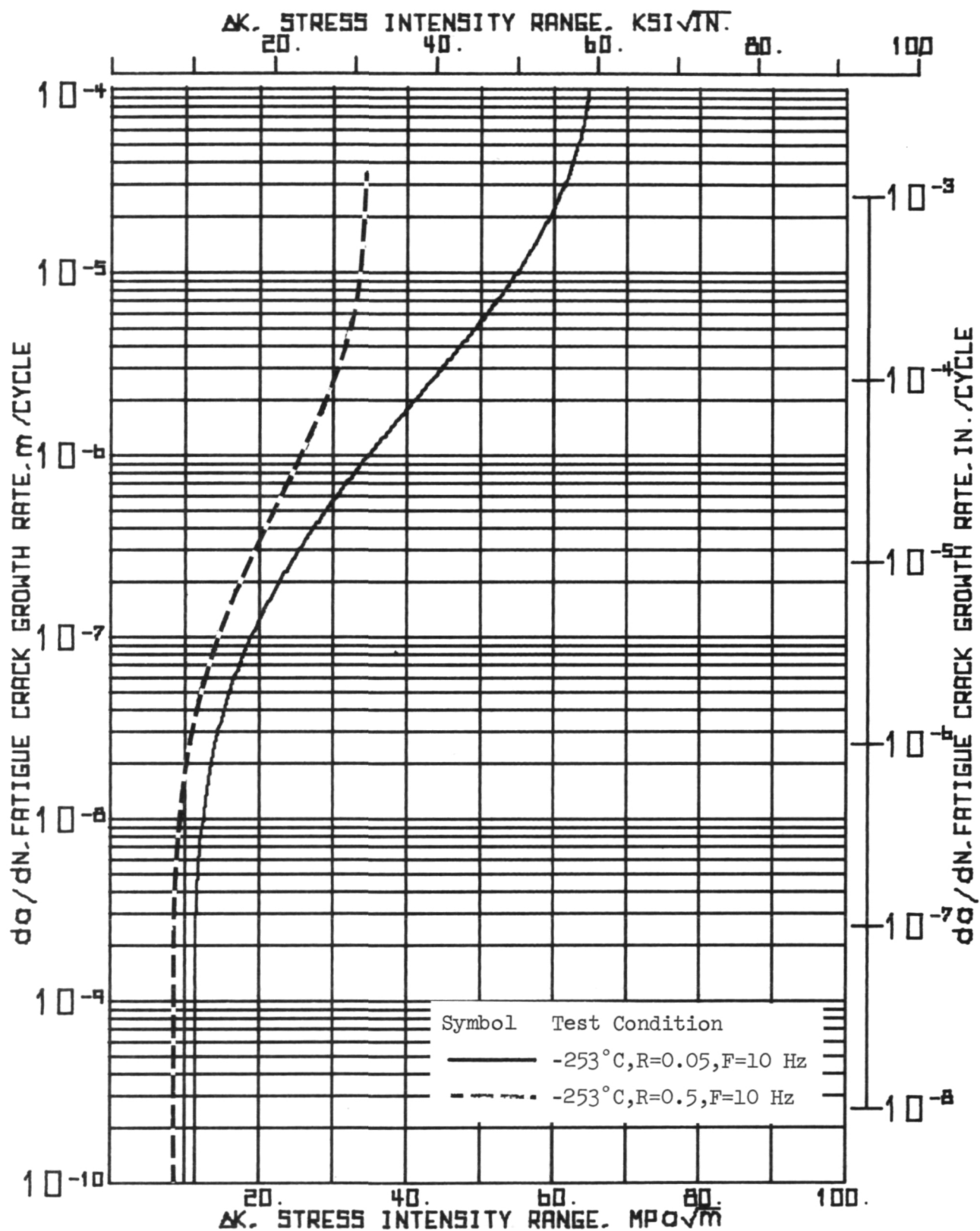


Figure 65.-Comparison of Suggested 1σ Design Curves for Ti-5Al-2.5 Sn (ELI) at $F = 10$ Hz, $R = 0.05$ and 0.5 , -253°C (-423°F)

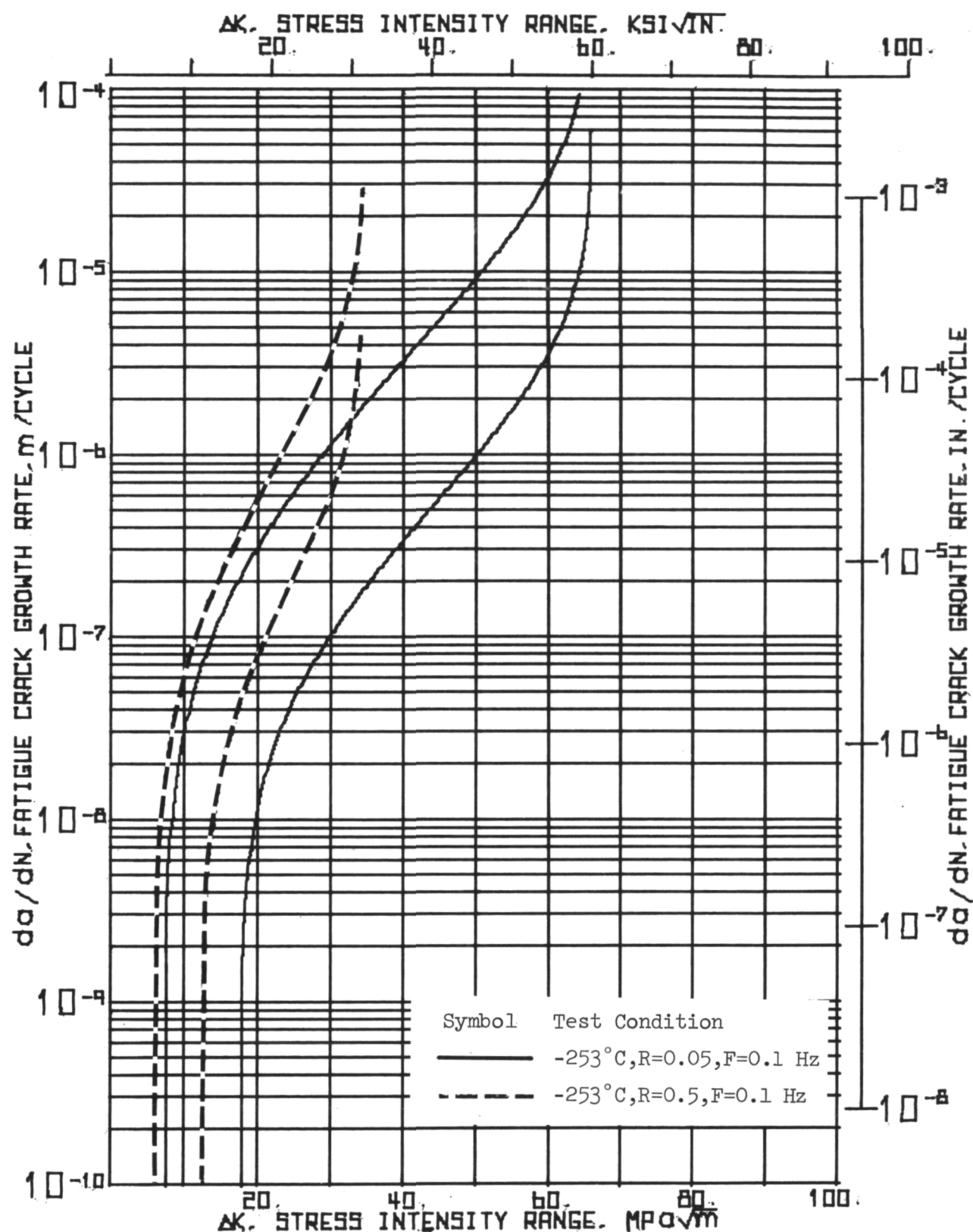


Figure 66.-Comparison of Fatigue Crack Propagation Behavior of Ti-5Al-2.5 Sn (ELI) at R = 0.05 and 0.5, F = 0.1 Hz, -253°C (-423°F)

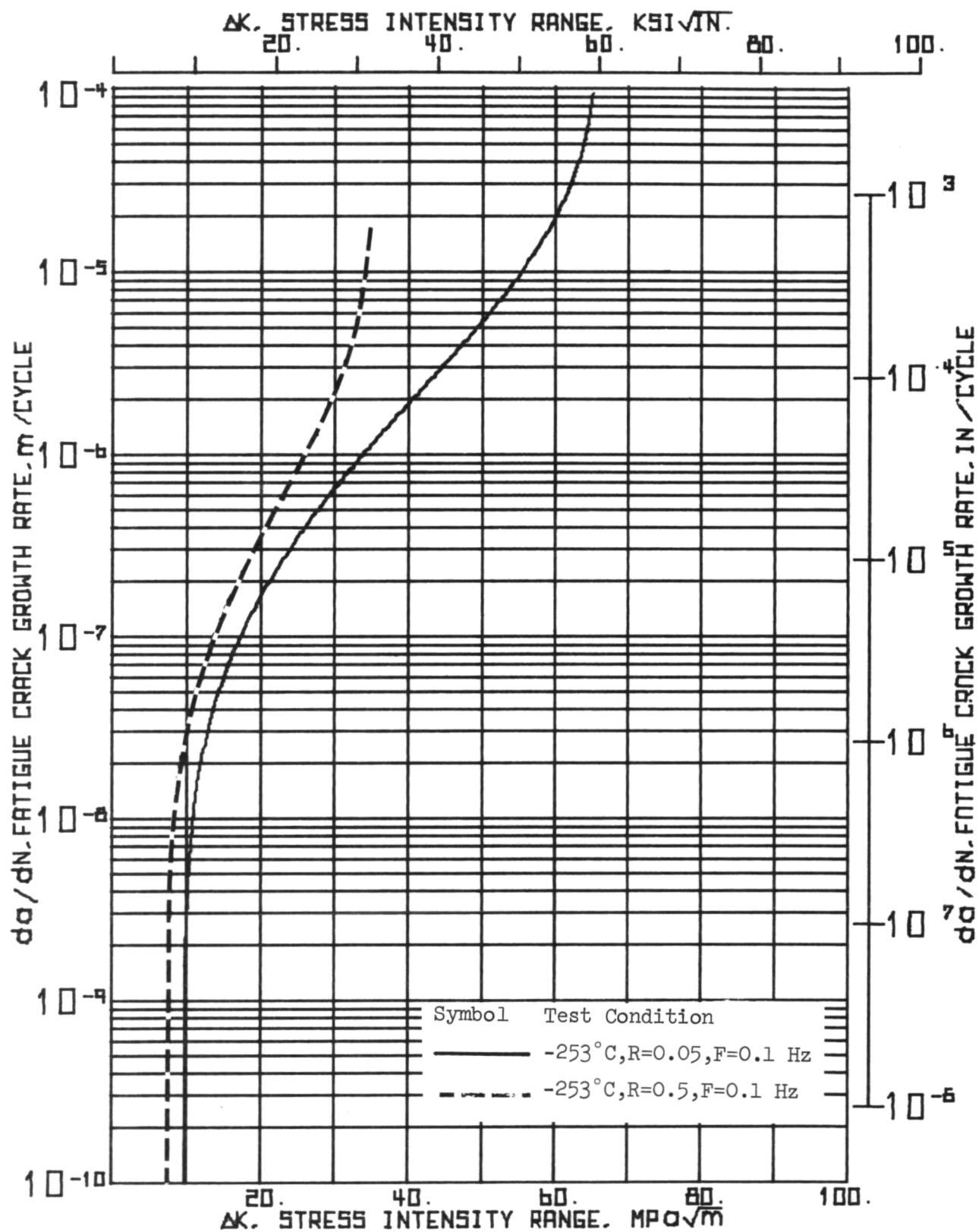


Figure 67.-Comparison of Suggested 1σ Design Curves for Ti-5Al-2.5 Sn (ELI) at $F = 0.1$ Hz, $R = 0.05$ and 0.5 , -253°C (-423°F)

4.4 Effect of Temperature

The effect of temperature at $R = 0.05$ is shown in Figs. 68 to 71 and at $R = 0.5$ in Figs. 72 to 75. At both R ratios, the extent of scatter was essentially the same at each temperature and frequency combination. In addition, there was no temperature effect at lower ΔK levels below $\Delta K = 44 \text{ MPa } \sqrt{\text{m}}$, ($40 \text{ ksi } \sqrt{\text{in.}}$) at $R = 0.05$ and below $33 \text{ MPa } \sqrt{\text{m}}$ ($30 \text{ ksi } \sqrt{\text{in.}}$) at $R = 0.5$. At higher ΔK levels, -253°C (-423°F) crack growth rates were faster than room temperature rates only because of the lower fracture toughness at -253°C (-423°F).

4.5 Effect of Lot to Lot Variation

As discussed in detail in the material characterization Section 3.2, some of the material used for the rotational disks was from Lot 2 material (pancakes 21 - 28), but of the same heat as coupons from pancakes 1 to 18 and disks from pancakes 19 and 20 which were from Lot 1 material. To investigate possible differences in fatigue crack growth behavior between the two lots, tests of two CR direction coupons from pancake 29 were conducted at Calac at $R = 0.05$, $F = 10 \text{ Hz}$, at room temperature. Results are shown in Fig. 76 and compared to previous results in Fig. 77.

Test results for specimens 29CR-1 and 29CR-2, Lot 2, produced crack growth rate data with small scatter. Growth rates were somewhat faster than the data from Lot 1. The Lot 2 data fell in the left half of the 2σ scatter bands of the Lot 1 data, see Fig. 77. The results of this study give an indication of the extent of the effect of forging parts at different times.

4.6 Summary of Results

This alloy had a remarkable lack of sensitivity to the various test conditions. No effect of frequency was found at any combination of R ratio or temperature. A load ratio effect was observed, but was manifested only by a small shift to higher rates of the $R = 0.5$ Hz data. No effect of temperature was found at low ΔK levels and at high ΔK levels the effect was dominated by the particular toughness value at that temperature.

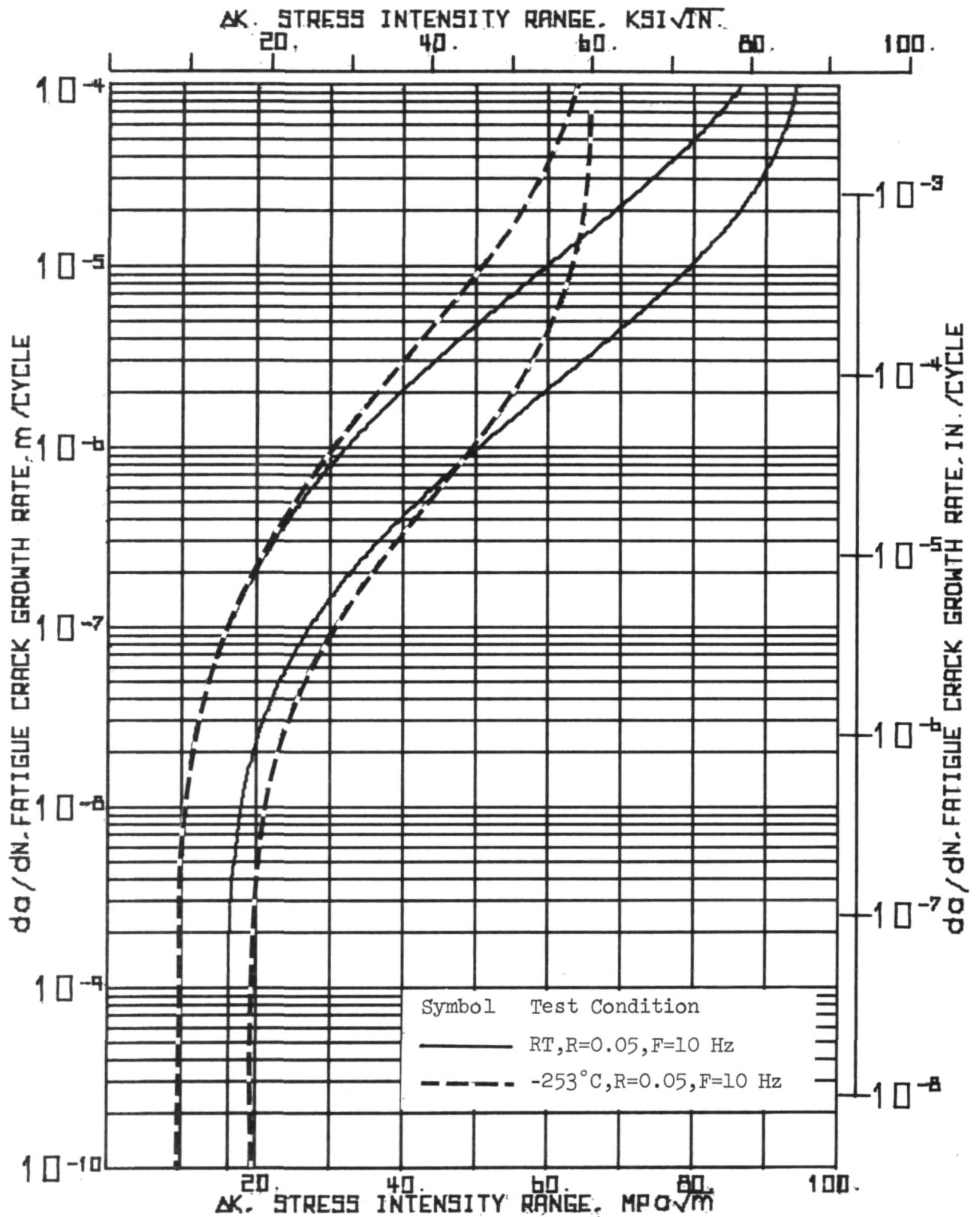


Figure 68.-Comparison of Fatigue Crack Propagation Behavior of Ti-5Al-2.5 Sn (ELI) at Room Temperature and -253°C (-423°F), R = 0.05, F = 10 Hz

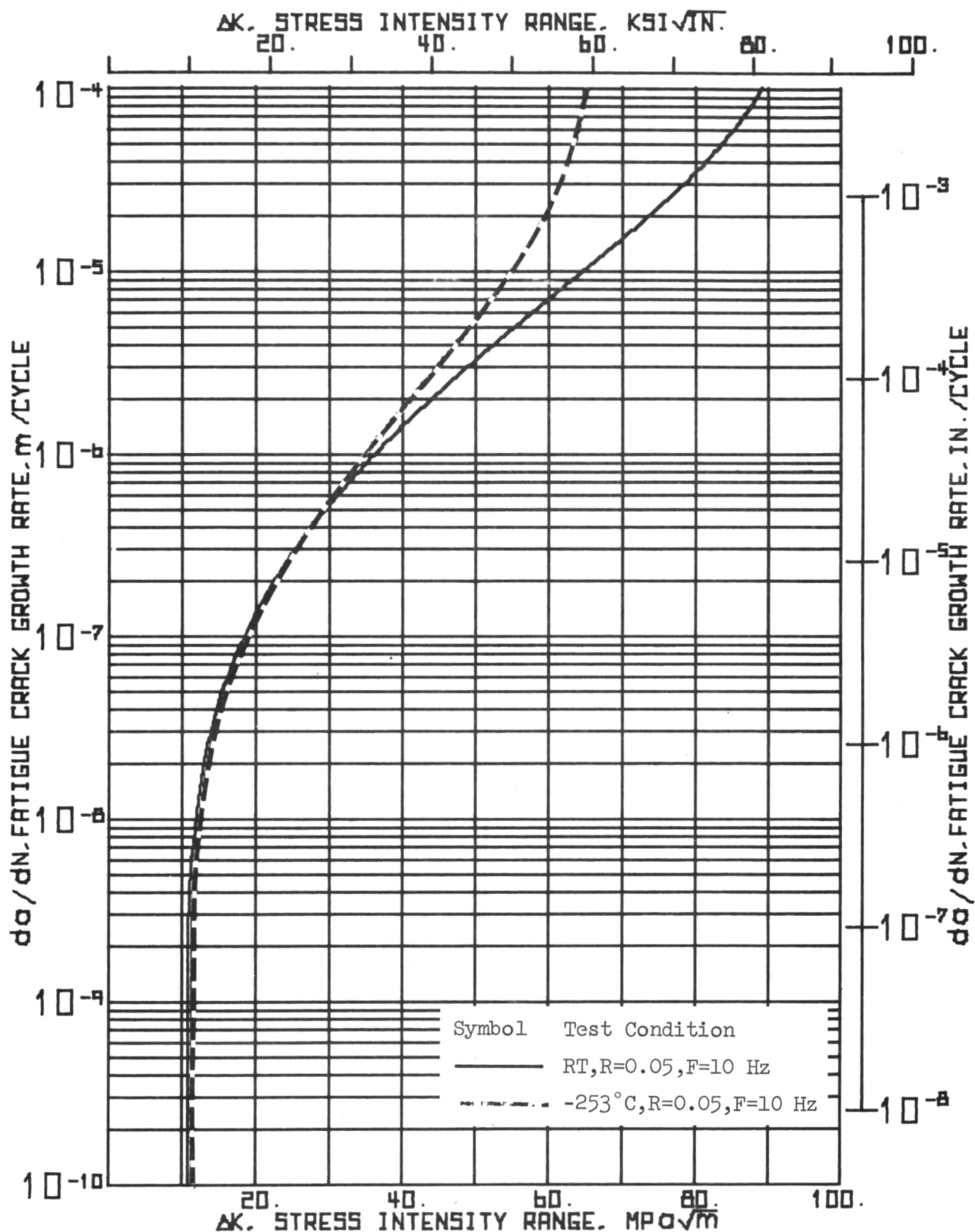


Figure 69.- Comparison of Suggested 1σ Design Curves for Ti-5Al-2.5 Sn (ELI) at Room Temperature and -253°C (-423°F), R = 0.05, F = 10 Hz

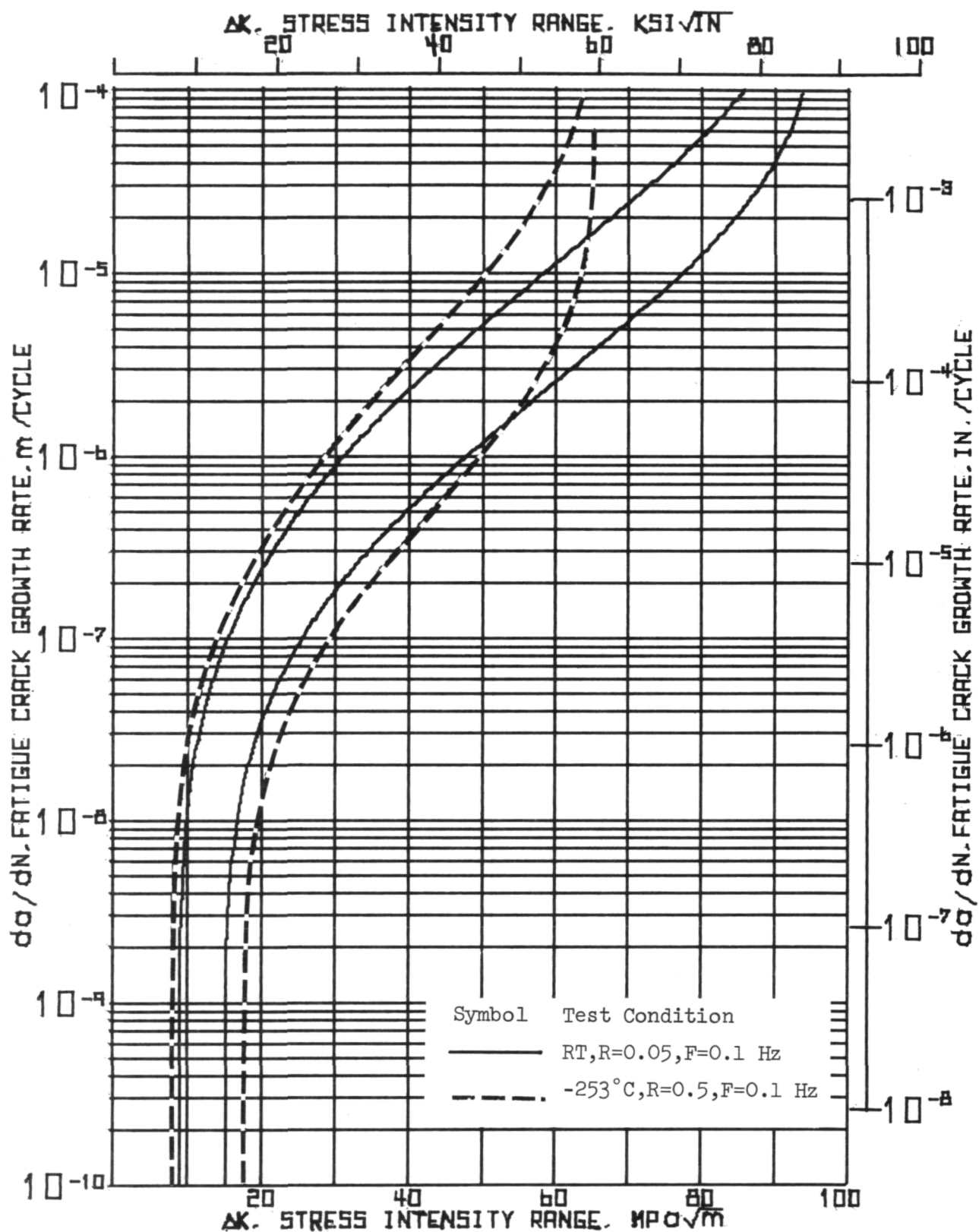


Figure 70.--Comparison of Fatigue Crack Propagation Behavior of Ti-5Al-2.5 Sn (ELI) at Room Temperature and -253°C (-423°F), R = 0.05, F = 0.1 Hz

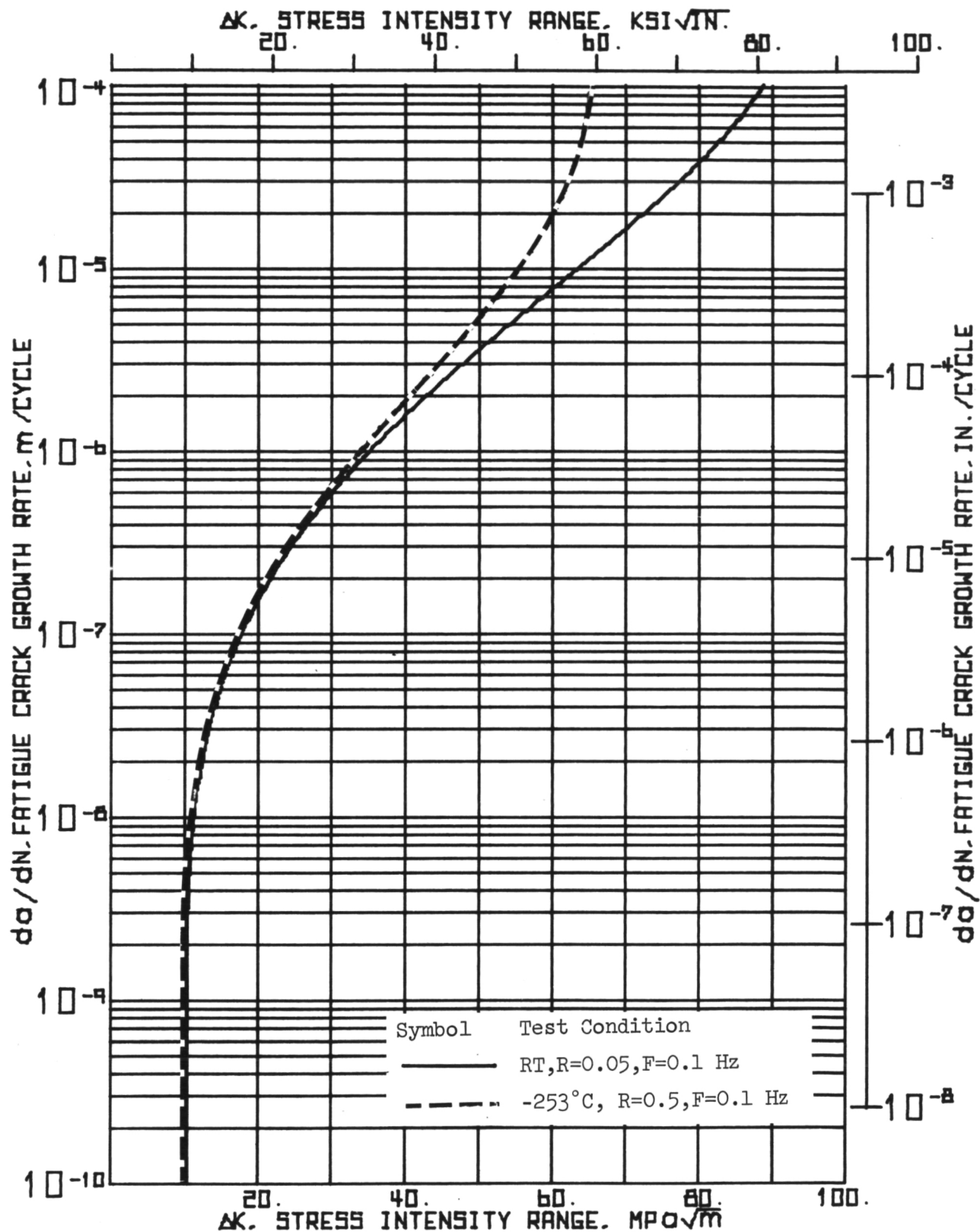


Figure 71.- Comparison of Suggested 1 σ Design Curves for Ti-5Al-2.5 Sn (ELI) at Room Temperature and -253°C (-423°F), R = 0.05, F = 0.1 Hz

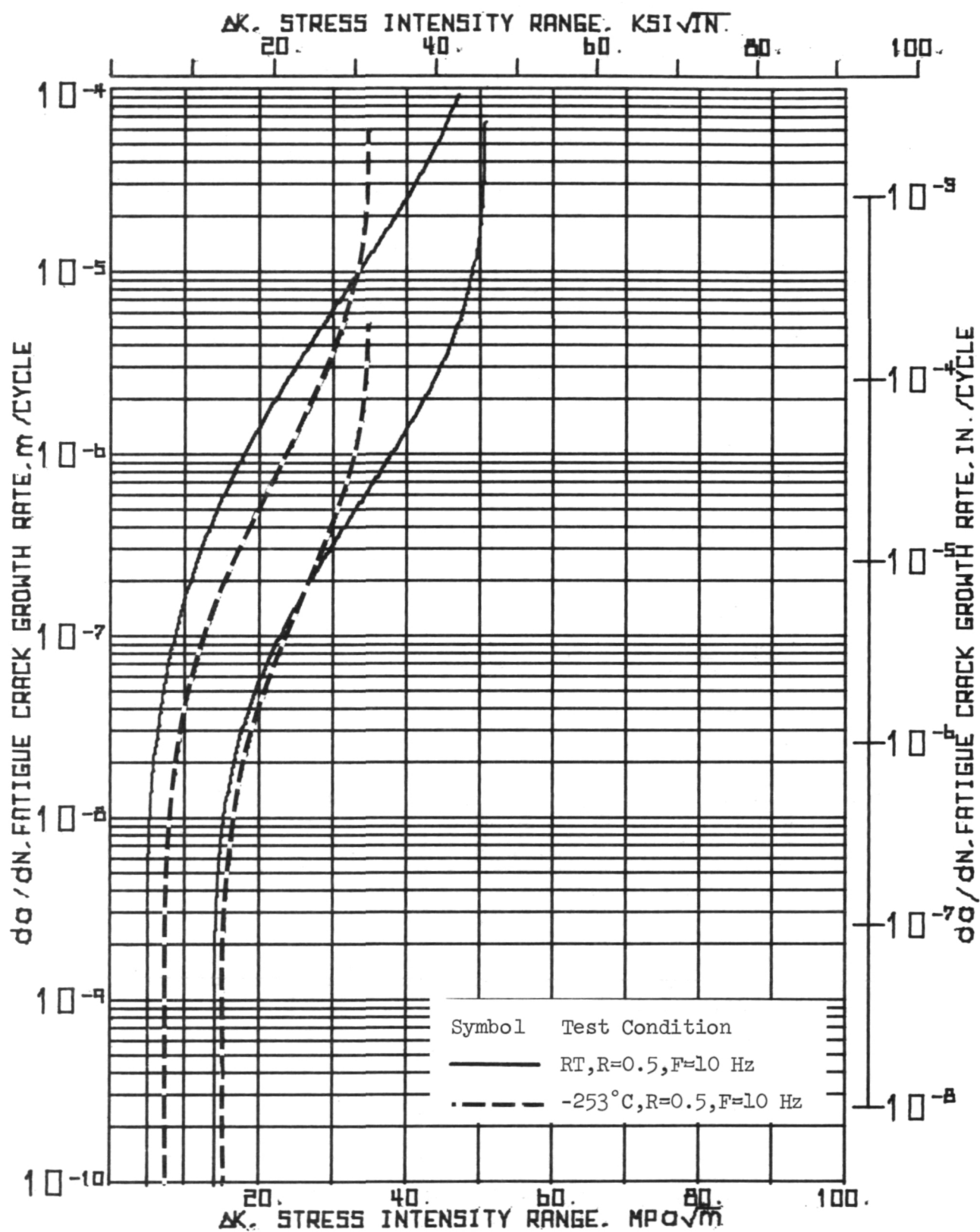


Figure 72.- Comparison of Fatigue Crack Propagation Behavior of Ti-5Al-2.5 Sn (ELI) at Room Temperature and -253°C (-423°F), R = 0.5, F = 10 Hz

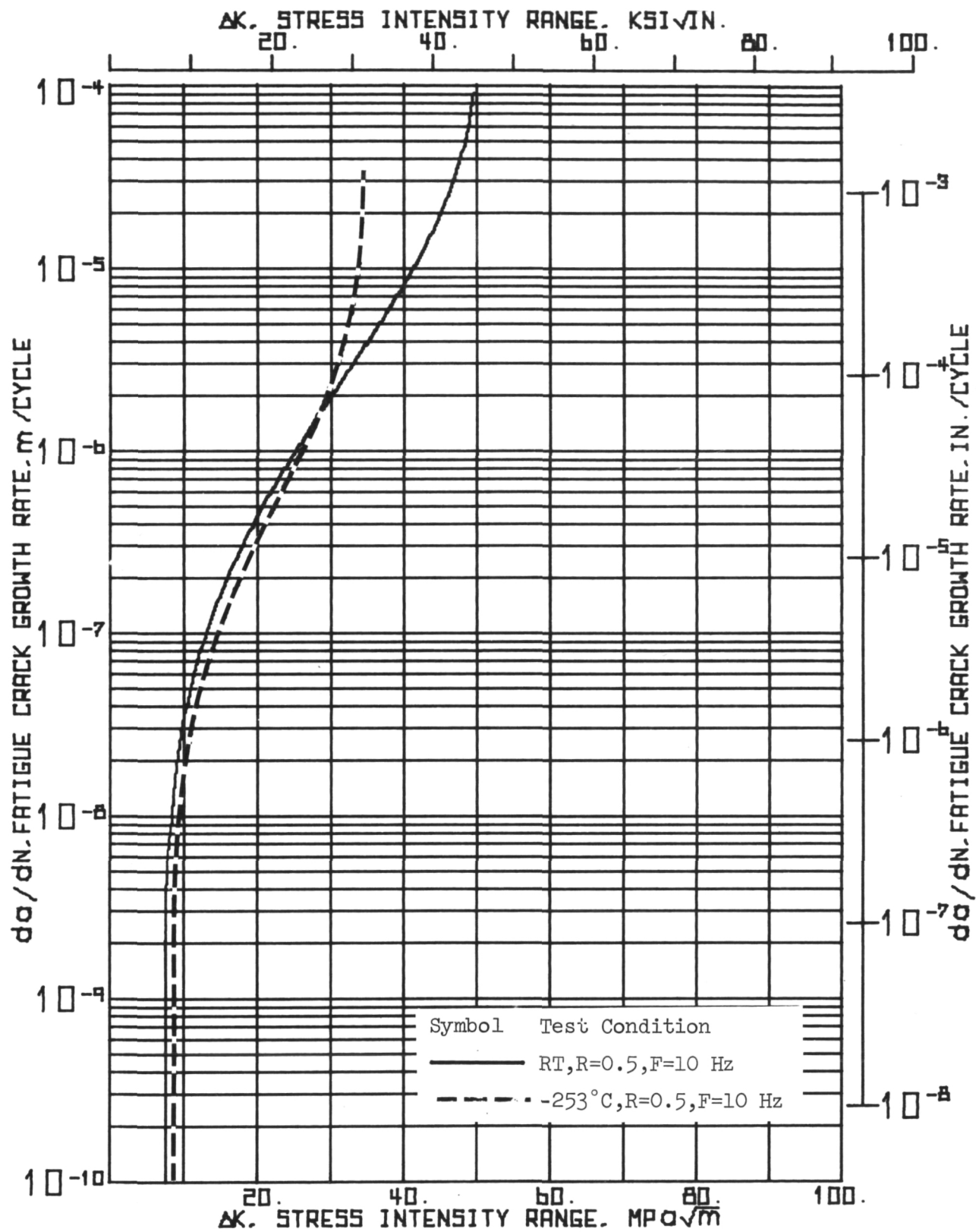


Figure 73.-Comparison of Suggested 1σ Design Curves for Ti-5Al-2.5 Sn (ELI) at Room Temperature and -253°C (-423°F), R = 0.5, F = 10 Hz

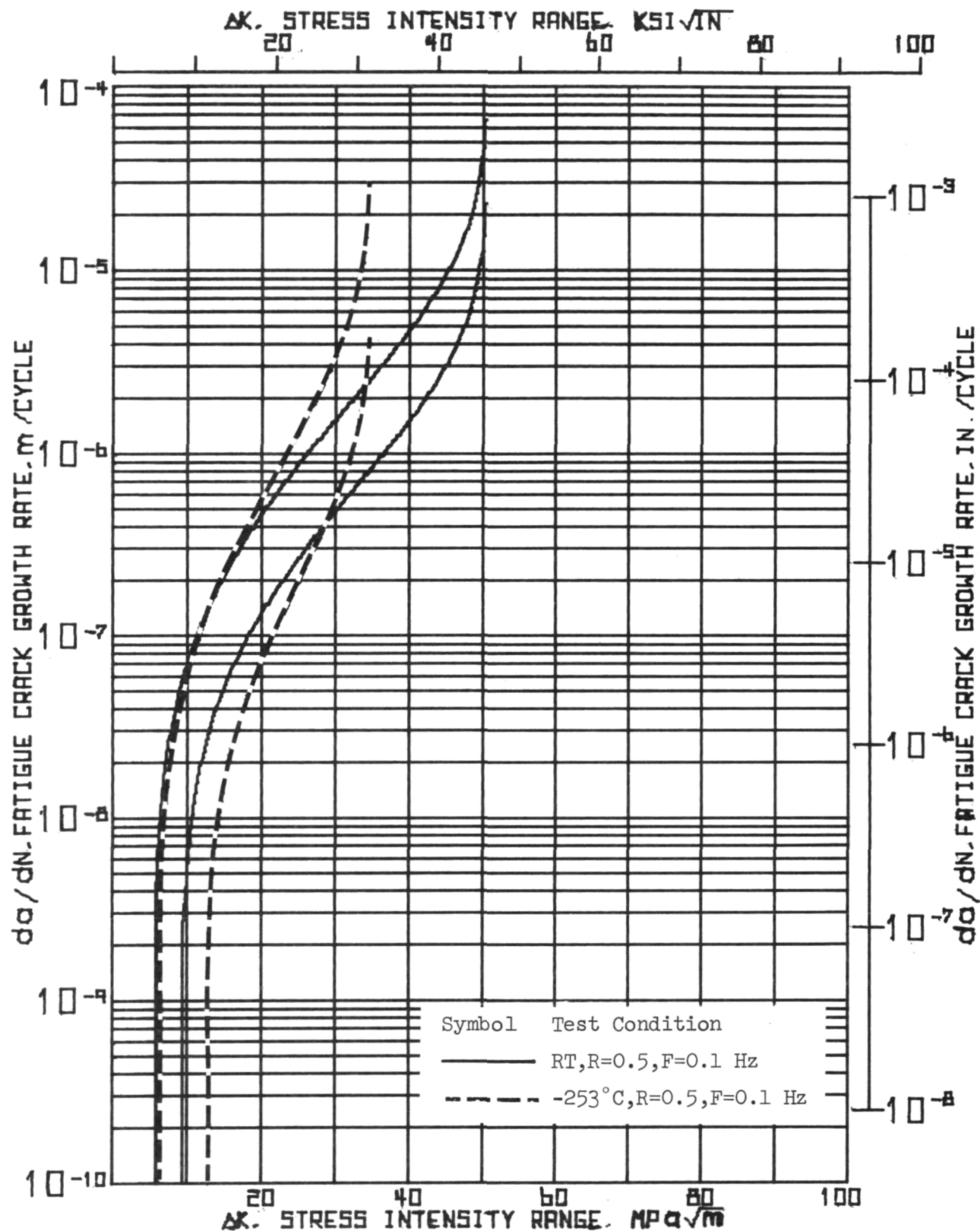


Figure 7⁴.- Comparison of Fatigue Crack Propagation Behavior of Ti-5Al-2.5 Sn (ELI) at Room Temperature and -253°C (-423°F), R = 0.5, F = 0.1 Hz

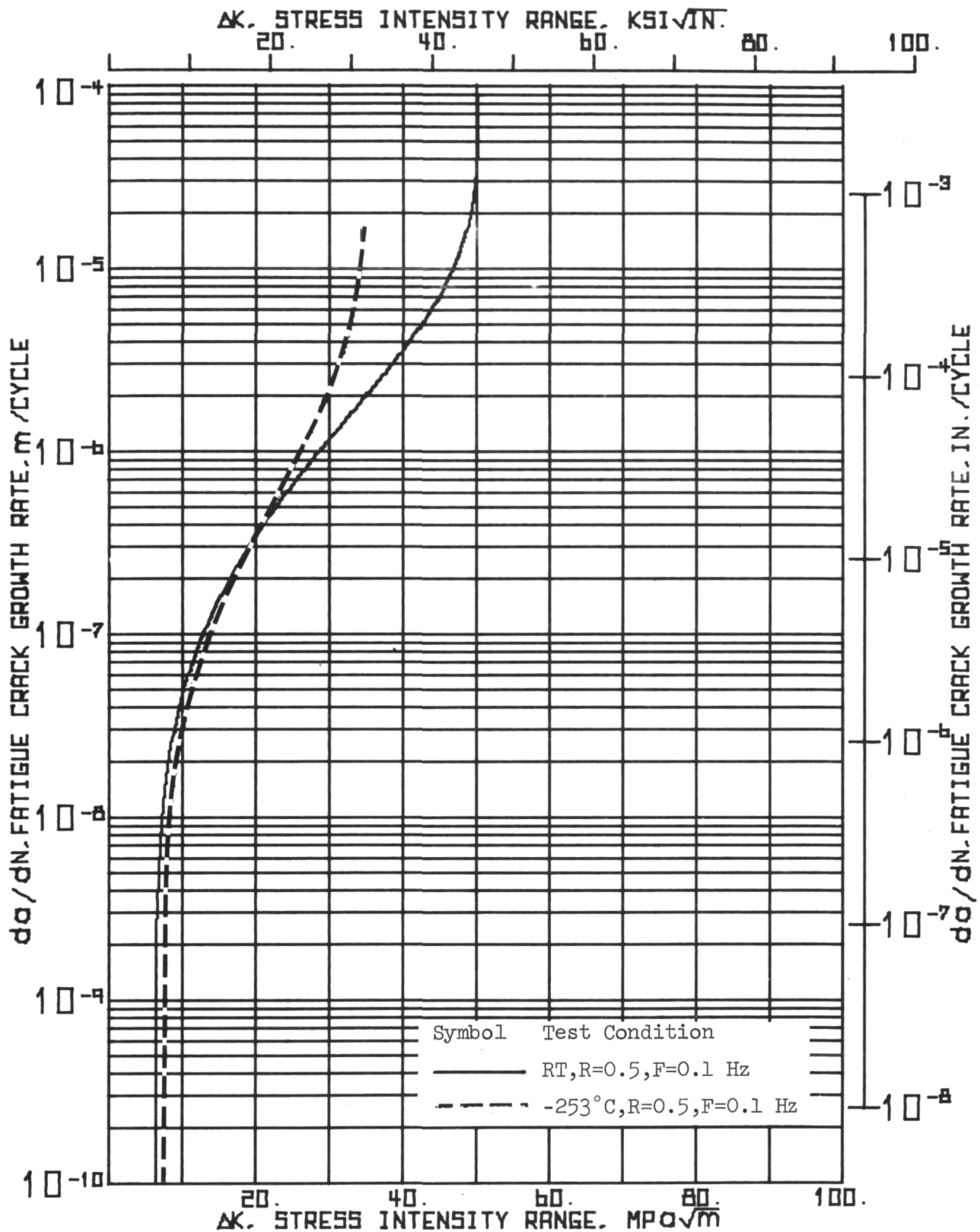


Figure 75.- Comparison of Suggested 1σ Design Curves for Ti-5Al-2.5 Sn (ELI) at Room Temperature and -253°C (-423°F), R = 0.5, F = 0.1 Hz

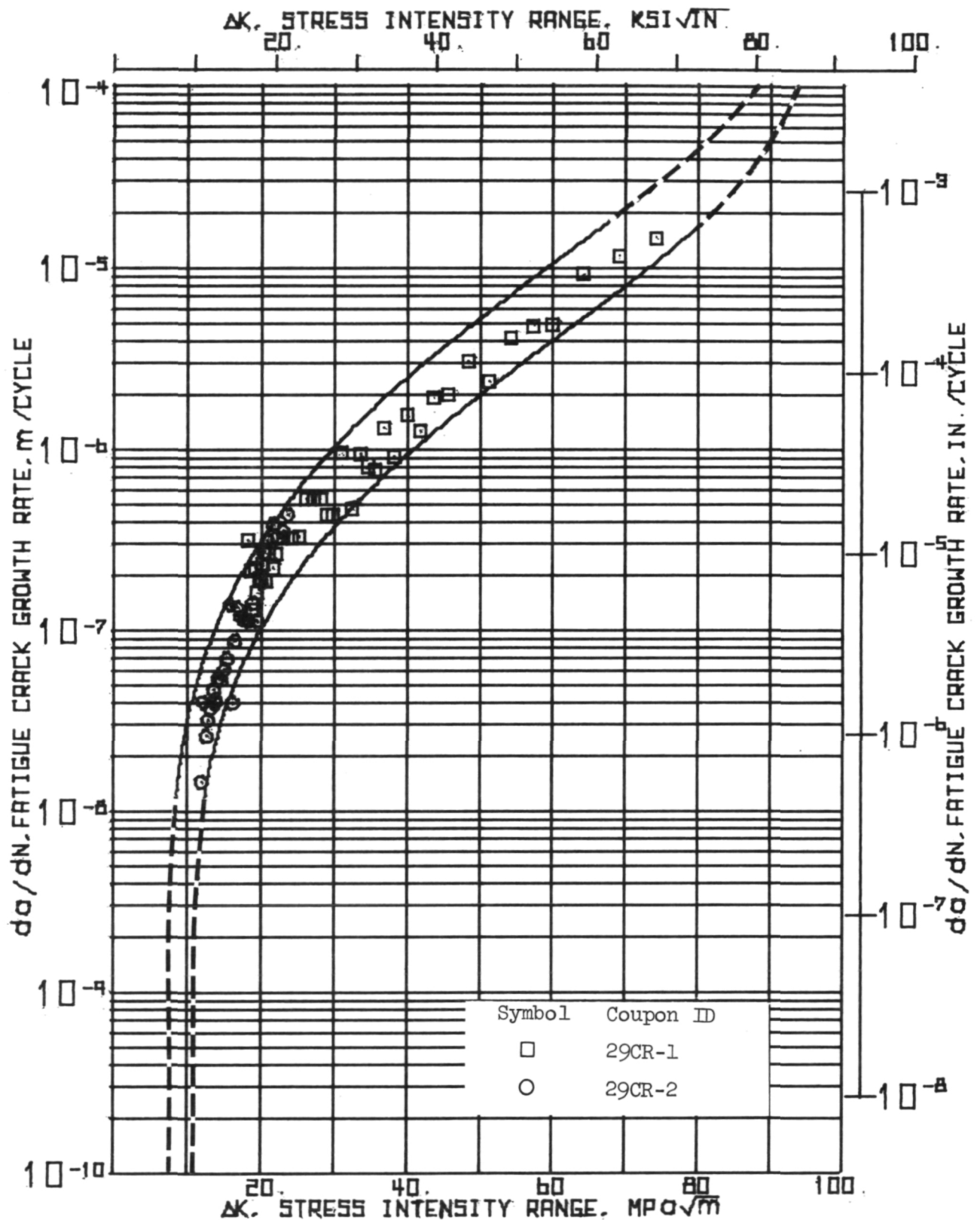


Figure 76.- Fatigue Crack Propagation Data for Ti-5Al-2.5 Sn (ELI) at Room Temperature, R = 0.05, F = 10 Hz, Disk 29

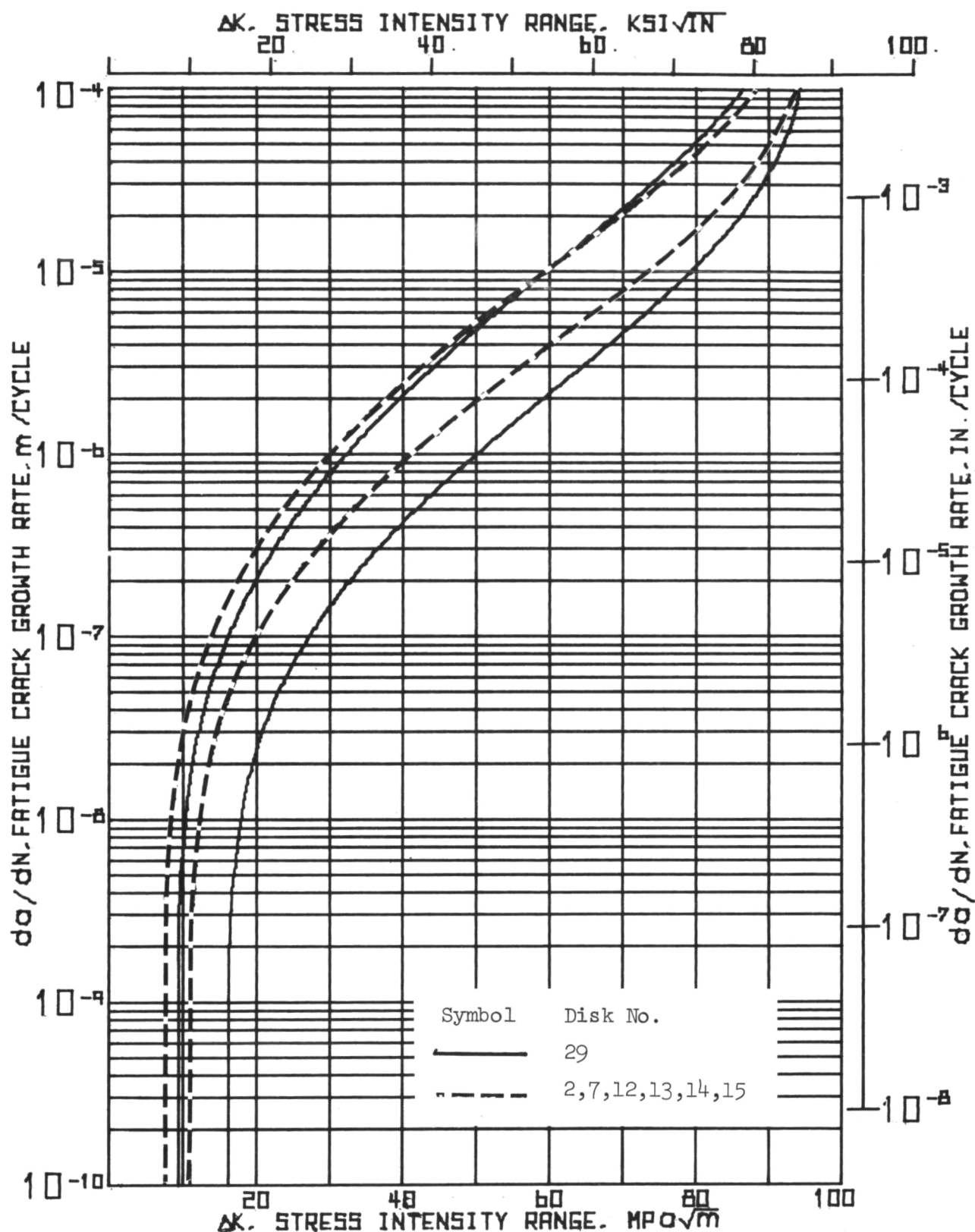


Figure 77.-Comparison of Fatigue Crack Propagation Data for Ti-5Al-2.5 Sn (ELI) Obtained from Pancake 29 and Pancakes 2, 7, 12, 13, 14 and 15, Room Temperature, R = 0.05, F = 10 Hz

Table 21 shows the K_d values which were used in Equations (8) and (14) to calculate the threshold stress intensity values and 2σ scatter band curves for the fatigue crack growth data. Also shown in the table are the risk function, r , (see Equation (15)), and corresponding stress intensity range for slow to fast growth transition, ΔK_{sf} in crack propagation rate. The constants α and μ varied for each data set. The values of α were in the range of -0.37 to -0.51 while μ varied between 2 and 7. Notice in Table 21 that the ratio of $\Delta K_{sf}/K_d$ did not vary significantly for the different test conditions.

4.7 Prediction of Life Analysis

A primary reason for collecting fatigue crack propagation data was to obtain the data necessary to perform a life prediction analysis for a rotating component. To accomplish this, the accuracy of the life prediction analysis procedure must be confirmed. Essentially the procedure consists of integrating the functional expression for da/dN (Equation 8) from the initial crack length, a_i , to the final crack length, a_f , to obtain the predicted life in cycles.

The life analysis computer program, previously developed at Calac [15 - 17] used in this study integrated da/dN by employing Simpson's rule [43] of integration. The program incrementally integrated over small Δa intervals so that the ΔK change remained small and summed the total number of cycles for each increment to obtain the predicted life. For WOL coupons, stress intensity was calculated using Equations (1) and (2). For rotating disks, K was calculated using Equation (17).

The best test for any such procedure is to check if the a versus N data of a WOL coupon can be duplicated by integration of the da/dN curve fit to this data. In general, small load steps could easily be accounted for in the program, providing that the step in K_{max} was not severe, approximately a factor of 2.5 or less, such that overload effects on crack growth did not occur. The accuracy of the resulting life prediction for a WOL specimen was dependent upon how closely the expression for da/dN , Equation (8), approximated the original data.

TABLE 21. TEST CONDITIONS AND NUMERICAL ANALYSIS SUMMARY

Fatigue Crack Growth Test Conditions		K _d , MPa $\sqrt{\text{in.}}$	Extrapolated Threshold Stress Intensity, ΔK_{th} , MPa $\sqrt{\text{in.}}$	Risk Function r	Slow to Fast Stress Intensity Range, ΔK_{sf} , MPa $\sqrt{\text{in.}}$	Ratio of $\Delta K_{sf}/K_d$
Temperature, °C	Range Ratio Frequency, Hz					
23 ^a	0.05 10	95.9 (87.27)	9.2 (8.4) ^c 10.6 (9.7) 12.2 (11.1) 16.0 (14.6)	.0752	61.9 (56.3)	.637
23 ^b	0.05 10	95.9 (87.27)	7.4 (6.7) 8.1 (7.4) 9.0 (8.2) 10.9 (9.9)	.0681	60.9 (55.4)	.635
23	0.05 0.1	95.9 (87.27)	8.7 (7.9) 10.1 (9.2) 11.6 (10.5) 15.0 (13.6)	.0748	61.0 (55.4)	.636
23	0.5 10	50.5 (45.9)	6.0 (5.5) 7.4 (6.7) 9.1 (8.3) 13.5 (12.3)	.1378	32.6 (29.7)	.646
23	0.5 0.1	50.5 (45.9)	5.5 (5.0) 6.3 (5.7) 7.2 (6.6) 9.7 (8.8)	.1100	32.7 (29.8)	.648
-253	0.05 10	65.9 (60.0)	9.3 (8.5) 11.2 (10.2) 13.4 (12.2) 19.1 (17.4)	.1103	42.8 (39.0)	.649
-253	0.05 0.1	65.9 (60.0)	7.8 (7.1) 9.7 (8.8) 11.9 (10.8) 17.8 (16.2)	.1023	42.7 (38.9)	.648
-253	0.5 10	34.7 (31.6)	6.8 (6.2) 8.3 (7.6) 10.1 (9.2) 14.6 (13.3)	.1923	23.8 (21.6)	.685
-253 ^d	0.5 0.1	34.7 (31.6)	6.0 (5.5) 7.3 (6.6) 8.8 (8.0) 12.6 (11.5)	.1744	23.5 (31.4)	.679

a. Convair data on pancakes 1 to 18, Lot 1

b. Calac data on pancake 29, Lot 2

c. The four entries are for extrapolated thresholds, respectively; left bound, 2 σ , curve; design curve; median curve; right bound, 2 σ , curve.

d. Specimen 5CR-2 data only

In this investigation, expressions for da/dN were developed based on the data collected for all coupons tested at each test condition. Table 22 shows the life prediction results versus the actual test results for WOL coupons 29CR-1 and 29CR-2 tested at room temperature, $R = 0.05$, $f = 10$ Hz. For these coupons, the α , μ values needed in Equation (8) were chosen as those which represented the data for just these two coupons.

In Table 22, the predicted life, based on the median curve, should be closest to N_A and in fact, N_M was 12.8% higher than N_A for 29CR-1 and 8.4% lower than N_A for 29CR-2. Although these are good fits, they would have been closer if the α and μ values for each specimen had been used rather than the constants for the combined data set. The suggested design predicted lives were both conservative as expected; the predicted lives being 13% and 34% lower than N_A for coupons 29CR-1 and 29CR-2, respectively.

For a case where α and μ are based on the results for a large number of coupons, values of N_M would be much higher than N_A for some coupons and lower for others. Therefore, as an alternative, the predicted life based on the l_G scatter band, suggested design curve was compared to N_A for all coupons tested by Convair at room temperature, $R = 0.05$, $f = 10$ Hz. The values of N_D would be expected to be approximately equal to or less than N_A for all coupons if the suggested design curve is a good, conservative predicted life approach. Results are shown in Table 23.

The predicted life, N_D , results of Table 23, based on the design curve, were lower than the actual life, N_A for 7 of the 10 coupons and less than 10% higher for the other three coupons. This result confirmed the distribution of lives expected for a data set of a large number of coupons. Except for coupons 12RS-2 and 13RS-2, the conservativeness in life prediction was not unreasonable. For the two RS direction coupons, N_A was significantly longer than N_D because these coupons had an apparently significantly higher threshold value than the other coupons.

TABLE 22

COMPARISON BETWEEN PREDICTED AND ACTUAL
FATIGUE LIVES FOR WOL COUPONS 29CR-1, 29CR-2

Specimen No.	Actual Life, N_A , Cycles	Predicted Life-Median, Curve N_M , Cycles	Predicted Life-Design Curve, N_D , Cycles
29CR-1	43,399	48,842	37,394
29CR-2 ^a	181,000	165,785	118,232

a Actual life shown is number of cycles between $a = 18.1$ mm (0.712 in.)
and failure.

TABLE 23

COMPARISON BETWEEN PREDICTED AND ACTUAL FATIGUE LIVES FOR
WOL COUPONS TESTED AT ROOM TEMPERATURE, $R = 0.05$, $f = 10$ Hz

Specimen No.	Actual Life, N_A , Cycles	Predicted Life Design Curve N_D , Cycles
7CR-1	155,403	169,772
7RC-1	154,950	155,367
2SR-1	275,819	169,969
7SR-1	159,203	103,830
2SC-1	125,650	132,899
7SC-1	154,200	142,749
12RS-2 ^a	373,321	41,560
13RS-2	332,750	43,326
14CS-2	16,630	11,763
15CS-2	19,636	11,705

^a Integrated from $a = 20.5$ mm (0.808 in.) to failure

The results given in Tables 22 and 23 confirm the expected accuracy of the analysis method for life prediction. In subsequent sections of this report, the procedure will be applied to life prediction for rotating components.

Page Intentionally Left Blank

5.0 ROTATIONAL DISK STUDY RESULTS

This section describes the results of the rotational disk spin pit study. Specific subsections describe burst, fatigue crack growth, and proof tests. Results are compared to laboratory WOL coupon data.

Prior to testing all disks (surface finish polished to 16rms or better) were visually inspected for surface crack length. Measured surface crack lengths were consistently underestimated due to the tight nature of the cracks and, presumably, the typical "smearing" of titanium which occurred during machining. Cracks in disks 19, 27, and 28, which contained no notches, were virtually impossible to be seen even under a 60x microscope. Eddy current inspection easily revealed the location of the cracks in these three, but, of course, gave no information as to crack length. Some disks were inspected using various dye penetrants, not harmful to titanium, which revealed no cracks.

After the first test cycle of a disk used for fatigue crack growth, cracks were easily observed since they had permanently opened and the crack tip was marked by a surface dimple. This result coupled with the limited visual inspection study prior to test, indicated that inspection of rotor components for cracks prior to service will be extremely difficult. The problem is compounded by the fact that in service the main flaws of concern will be axially oriented surface or imbedded flaws. Penetrants which etch the surface may be useful to reveal the surface flaws, but the question of damage to the component by the etchant could then be a problem. Alternatively, ultrasonic inspection could be used to inspect for flaws, but an extremely careful, precise, and expensive calibration of flaws in the actual rotor part would have to be undertaken. Even then flaws less than 1.27 mm (0.050 in.) would be nearly impossible to detect in any consistent, reliable fashion. This point will be discussed further in Section 6.

5.1 Burst Tests

Five of the ten disks were specifically used for determining burst speed as a function of crack length. Although the other five disks were used for crack growth or proof test studies, each of them either failed during testing or were burst after testing to provide burst speed data from all ten disks.

Burst test procedure, except for failures during the crack growth studies, was simply to slowly increase the speed of the disk until burst. Total test time to burst varied from 2 to 5 minutes depending on the burst speed obtained. Table 24 lists the results of all the burst tests in order of increasing crack length.

The first three burst tests listed contained short enough cracks that yielding began at the bore and progressed radially outwards prior to burst. Seven of the ten tests resulted in fracture of the disks, however, in disks 26, 27 and 21 extensive diametrical growth of the disks due to plastic growth of the bore (disks 26 and 27) or plastic hinge at a notch (disk 21) resulted in rotational instability and subsequent failure of the spin shaft. These tests were classified as burst tests with a burst speed equivalent to the speed at which shaft failure occurred. This classification was made because of the flat topped stress-strain response of the material similar to an elastic - perfectly plastic behavior and because burst is essentially caused by excessive plastic deformation [31]. Therefore, in situations where spin up was slow enough, deformation of the disk prior to burst was large enough to cause instability. The speed at which this occurred was undoubtedly close to the fracture burst speed [41].

Disk 26 contained no precrack and was presumed to be flaw free. The disk was originally spun up to 79,890 rpm before discontinuance of the test due to incipient shaft instability. The shaft was replaced when instability was found to be due to an undersized shaft. The disk was rerun to burst but large deformation caused instability and subsequent shaft failure at 99,540 rpm. Post test examination revealed that the bore diameter had grown from

TABLE 24

BURST SPEED STUDY

Disk No.	Crack Length at Burst mm (in.)	Burst Speed, N_B , rpm	Stress Intensity at Failure, K_{I_Q} , MPa \sqrt{m} (ksi $\sqrt{in.}$)	Plastic Radius, r_p , mm (in.)	Remarks
26	0	99,540 ^a	-	0.93	Plastic ^b
27	1.47 (.058)	96,480 ^a	-	0.92	Plastic
19	13.84 (.545)	84,240	-	0.82	Plastic
20	21.41 (.843)	69,290	107.0 (97.4)	-	-
21	27.18 (1.070)	66,850 ^a	108.1 (98.4)	-	-
28	32.00 (1.26)	64,300	104.4 (95.0)	-	-
25	34.98 (1.377)	59,320	90.1 (82.0)	-	-
24	35.03 (1.379)	55,740	75.5 (68.7)	-	-
22	35.51 (1.398)	54,350	76.3 (69.4)	-	-
23	37.36 (1.471)	52,650	74.4 (67.7)	-	-

Average K_{I_Q} for disks
21, 28, 25, 24, 22, 23

87.8 (79.9)

Average K_{I_Q} for Laboratory CR Orientation Specimens

87.5 (79.7)

Spread of Lab. Data, All Orientations

78.3 to 96.9 (71.3 to 88.2)

Average K_{I_Q} for CR Orientation Coupons

90.7 (82.6)

^a Instability speed.

^b The word plastic indicates that material from the bore outward plastically deformed.

25.4 mm (1.000 in.) to 26.16 mm (1.030 in.) and to 26.03 mm (1.025 in.) perpendicular to the 26.16 mm (1.030 in.) measurement. Maximum outer diameter growth was from 127.02 mm (5.001 in.) to 127.28 mm (5.011 in.). This large permanent deformation made further testing impossible and the burst speed was defined as occurring at 99,540 rpm. This result was compared to the predicted burst speed based on Equation 18 of 95,680 rpm, and that based on Equation (21) due to Robinson [29], of 100,703 rpm. The agreement between the test result and predicted burst speeds can be seen to have been excellent.

Unnotched disk 27 was spun to determine the effect of a small flaw, 1.47 mm (0.058 in.), wholly immersed in a plastic stress field, on burst speed. Figure 78 shows the shape of the fracture surface and the short flaw. Visible in Fig. 78 is the precrack region and the extent of crack growth which occurred during the burst test as well as the machine cut needed to pull the fracture surface open after test. Failure was due to rotational instability after 126 sec elapsed time at 96,480 rpm.

The effect on burst speed due to a longer crack, 13.85 mm (0.545 in.), imbedded in a plastic field was investigated using disk 19. This unnotched disk fractured in two places with one fracture zone containing the precracked flaw, see Fig. 79. The plane containing the flaw failed in a mode similar to the brittle fracture failure of K_{TQ} tests, see Fig. 80, while the other plane was a large ductile tear failure mode. The burst speed of 84,240 rpm was significantly lower than that for disks 28 and 27, as expected.

Disk 20 was spun to burst after being used for crack growth measurements. The disk contained symmetrical notches with a fatigue precrack at the end of one notch. For burst calculations, the disk was analyzed as a single flaw of length 21.41 mm (0.843 in.). Post test examination revealed that the unprecracked notch had initiated a fatigue crack during spin pit cycling of 1.42 mm (0.056 in.) average length. Failure of the disk occurred along a diametrical line containing the two notches. Failure zones appeared as K_{TQ} type brittle fractures except for the somewhat large shear lips. The burst speed of 69,290 rpm was slightly above the 68,805 rpm speed necessary

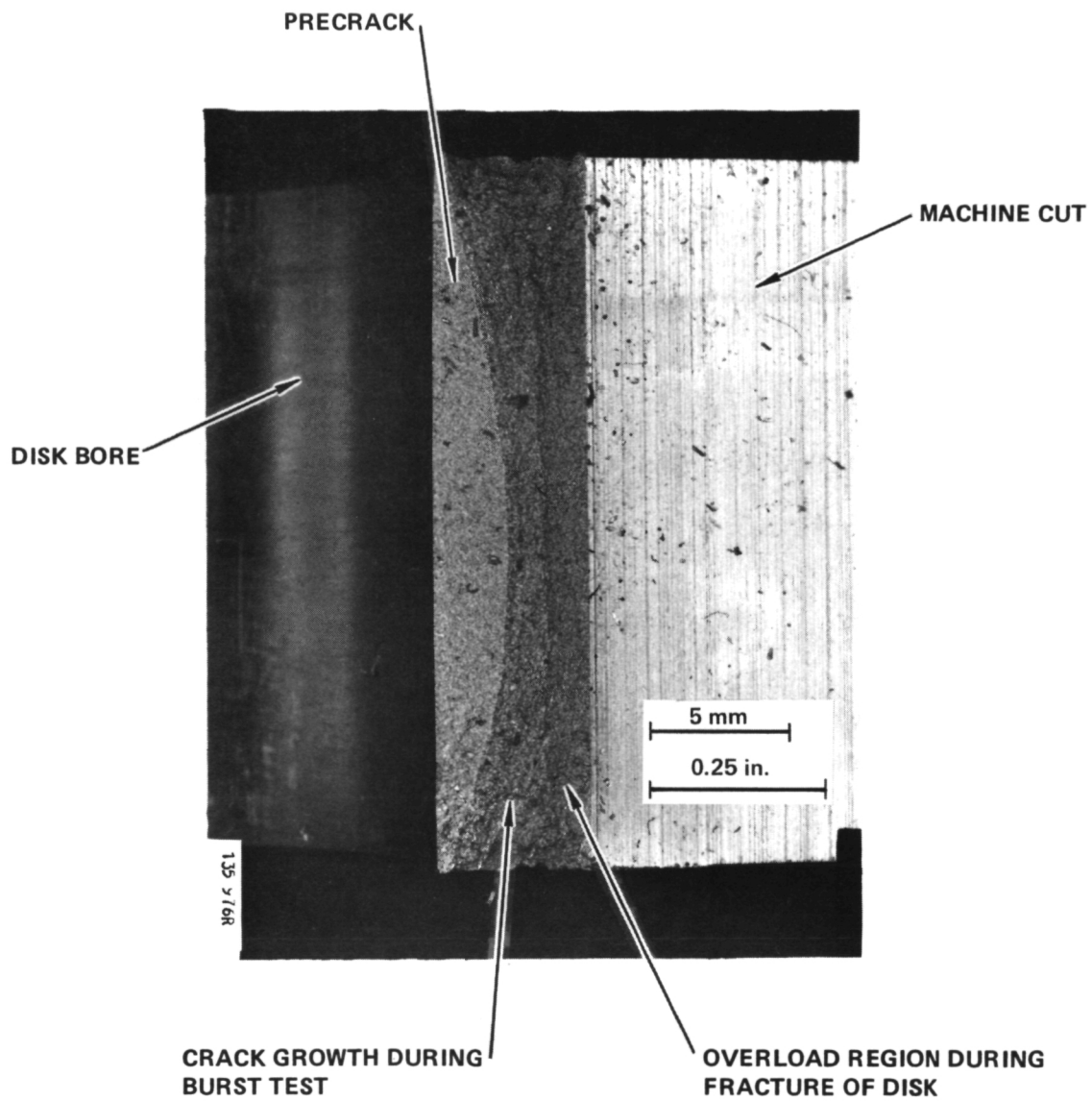


Figure 78. - Fracture Surface of Disk 27

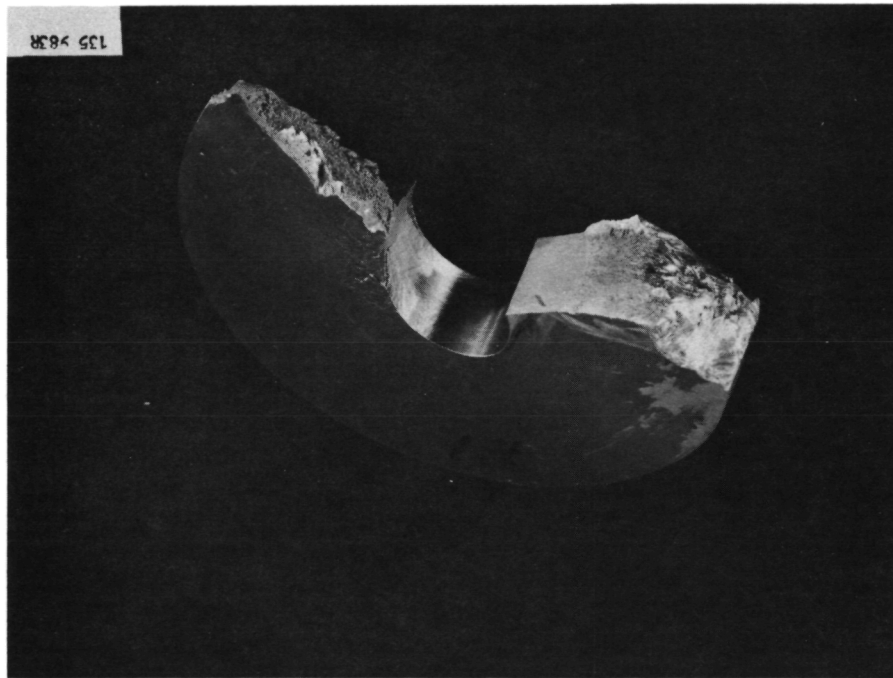


Figure 79.- Disk 19 After Burst Test

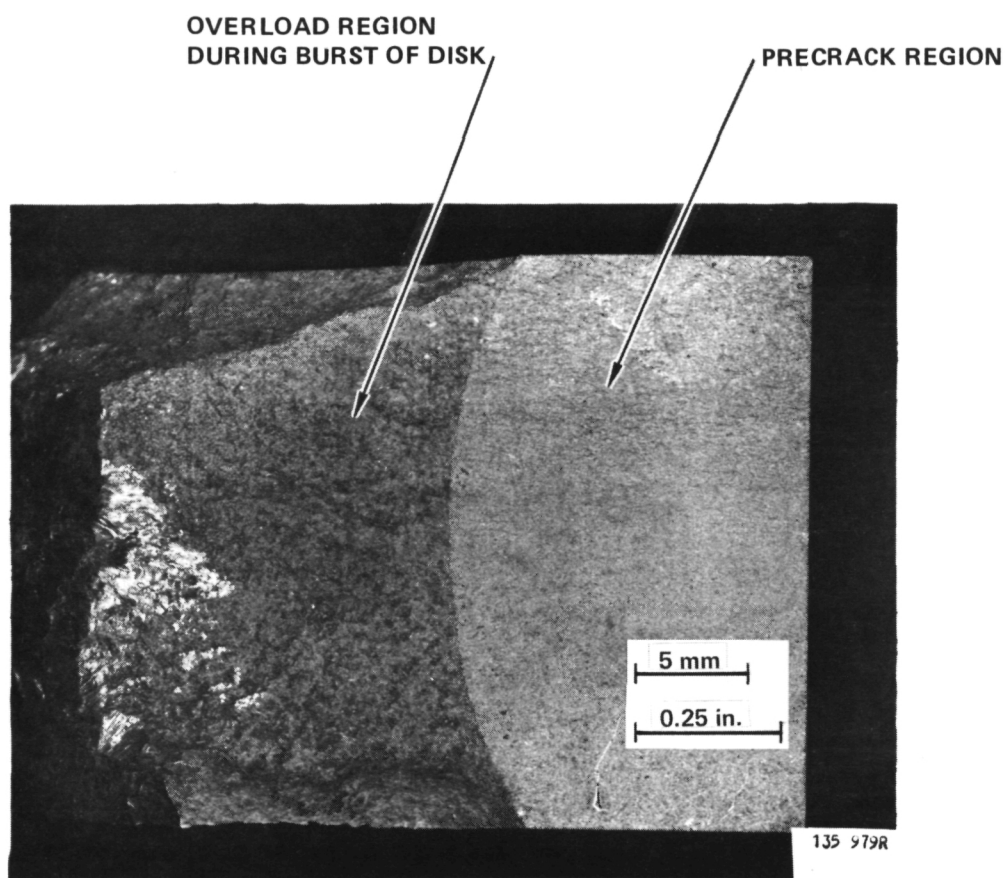


Figure 80. - Fracture Surface of Disk 19

for the onset of bore yielding based on the material's average yield strength. This means that failure possibly occurred with a small amount of plastic flow near the bore.

Disk 21 was spun to 66,850 before shaft failure due to excessive bore growth. The shaft was replaced and the disk spun to 65,350 rpm before removal due to instability again caused by bore growth. A third spin to 66,490 rpm failed to burst the disk and further testing was discontinued. Burst speed was defined as 66,850 rpm. Figure 81 shows the fracture surface of disk 21. The crack growth which occurred during each spin up is clearly visible.

Figure 82, a macro-photograph of disk 21 after test, clearly shows the notches, opened straight precrack and the dimpled plastic zone which occurred during test. Figures 83 to 86 show close-up details of the crack tip region. The shape of the plastic zone is clearly visible in these figures. Notice that the crack grew through the large plastic zone and then turned down the inside of one side of the plastic zone. For disk 21, K_{IQ} was calculated as $108.1 \text{ MPa } \sqrt{\text{m}}$ ($98.4 \text{ ksi } \sqrt{\text{in.}}$).

Disk 28 burst after 355 cycles at 64,300 rpm, 700 rpm below the maximum speed during the previous fatigue cycling. Failure crack length was 32.0 mm (1.26 in.) and K_{IQ} was calculated as $104.4 \text{ MPa } \sqrt{\text{m}}$ ($95.0 \text{ ksi } \sqrt{\text{in.}}$). Failure occurred before onset of bore yielding. Typical large shear lips were observed on the fracture surface. Disk 25 was spun to burst after surviving 400 fatigue cycles between 38,900 and 55,000 rpm. Burst speed was 59,320 rpm; crack length was found to be 34.98 mm (1.377 in.) and K_{IQ} calculated as $90.1 \text{ MPa } \sqrt{\text{m}}$ ($82.0 \text{ ksi } \sqrt{\text{in.}}$).

Disk 24 was burst without prior fatigue cycling. Figure 87 shows the typical damage inflicted on disk 24 caused by the burst while Fig. 88 shows the excellent preservation of the fracture surface despite the violence of burst. Disk 22 was intended as a proof test but the crack was longer than anticipated and burst occurred on the first cycle. Disk 23 burst after 42 fatigue cycles. The burst rpm and calculated K_{IQ} values for the above tests are tabulated in

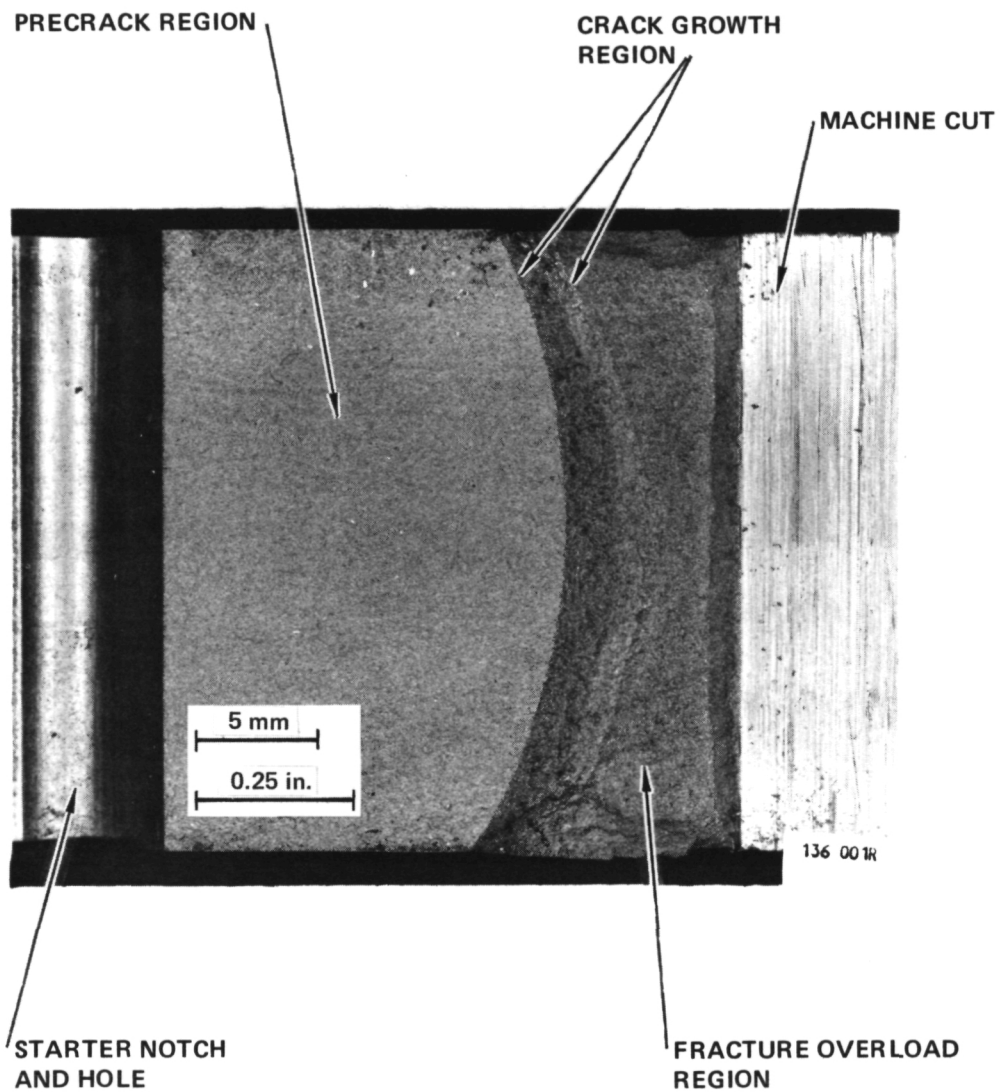


Figure 81. - Fracture Surface of Disk 21

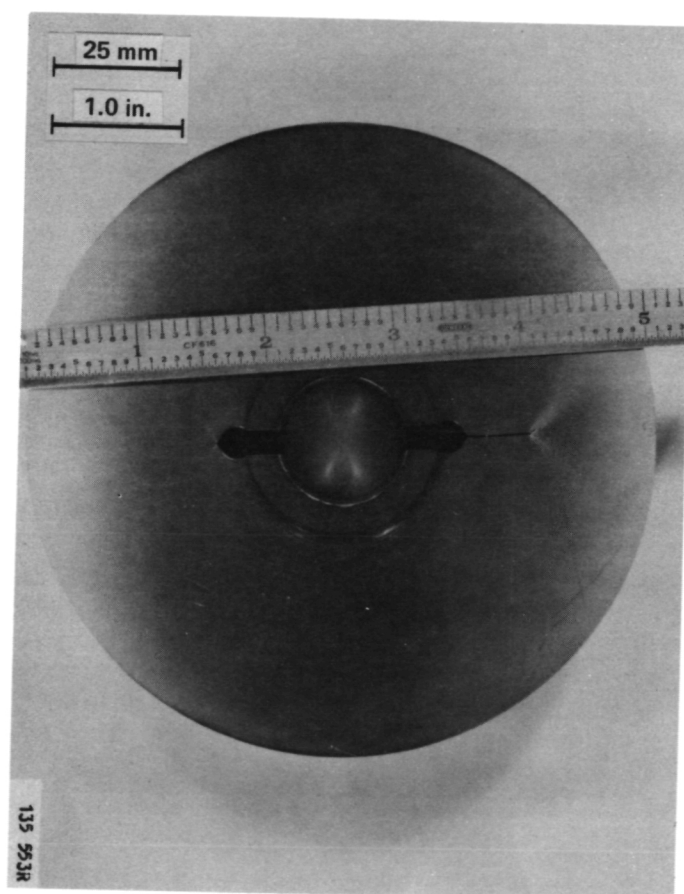


Figure 82. -Top Surface of Disk 21 After
Being Spun to 66,850 rpm

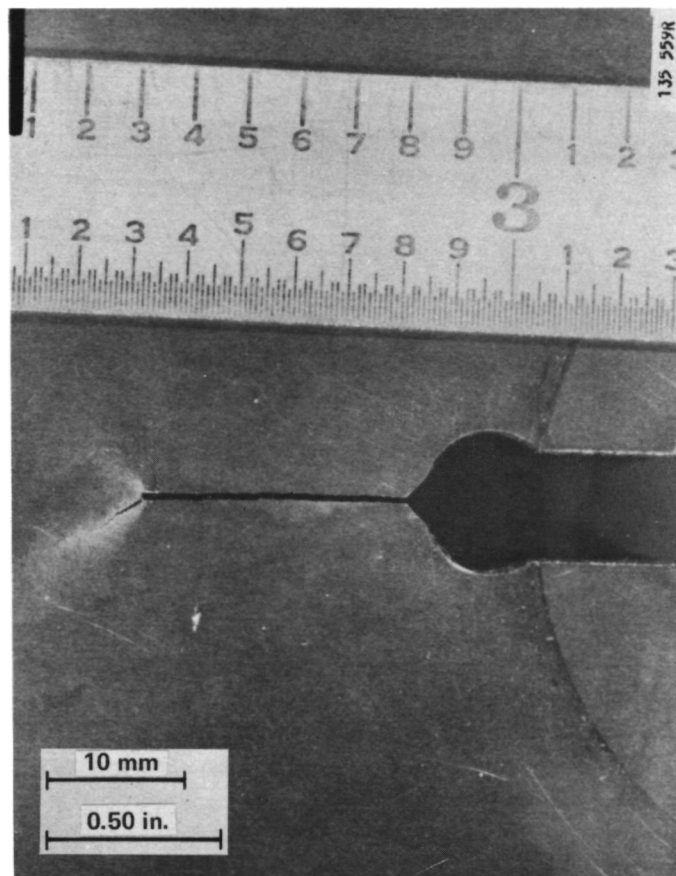


Figure 83. - Crack Tip on Top Surface of Disk 21 After Test

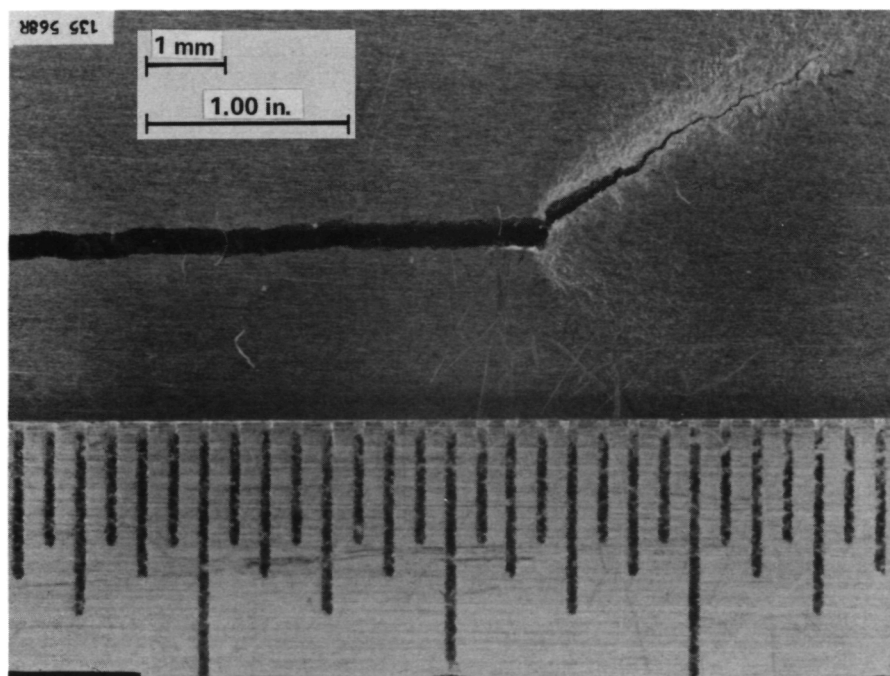


Figure 84.- Crack Tip on Top Surface of Disk 21 After Test

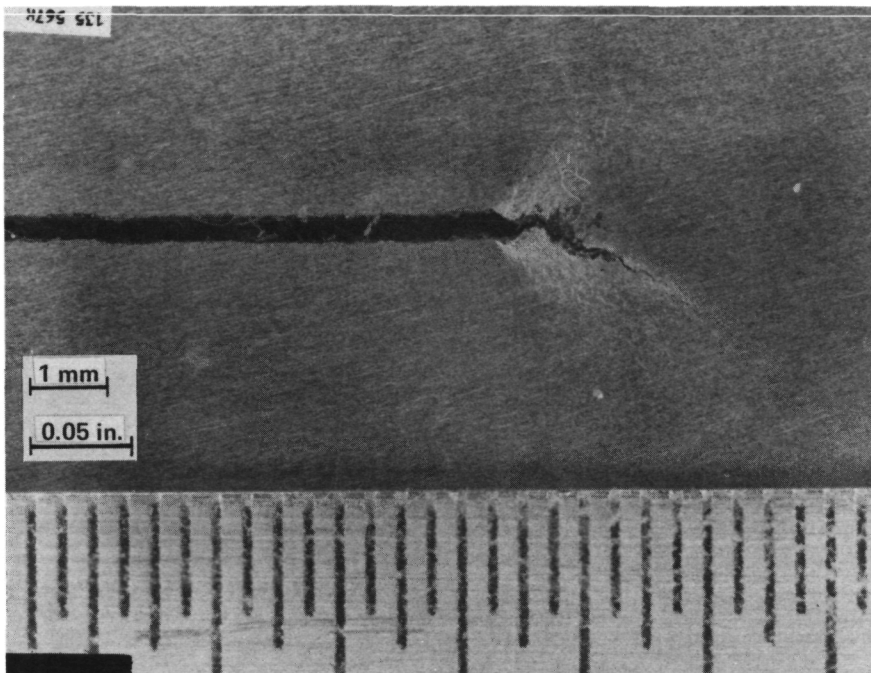


Figure 85. - Crack Tip on Bottom Surface of Disk 21 After Test

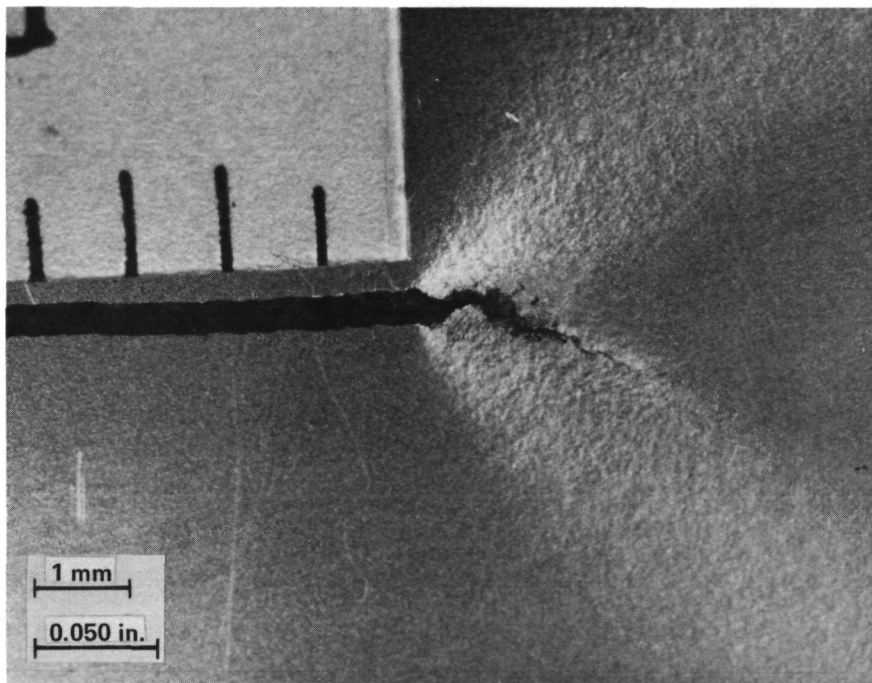


Figure 86. - Crack Tip on Bottom Surface of Disk 21 After Test



Figure 87. - One Half of Disk 24 After Burst

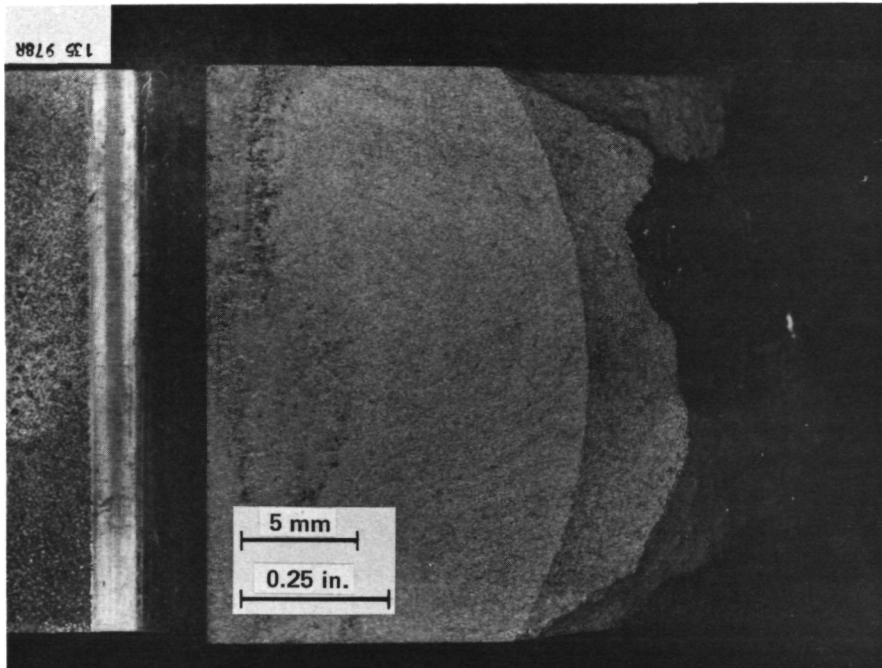


Figure 88. -Fracture Surface of Disk 24

Table 24. All three of these disks failed prior to the onset of bore yielding since burst speeds were well below 68,804 rpm.

In summary, Table 24 clearly shows that for all ten disks, burst speed decreased as crack length increased. The large drop in burst speed between disk 19 and disk 20 was due partially to the increase in crack length and partially to differences between disks with and without a plastically yielded bore.

The six disks in which no bore yield occurred had an average K_{IQ} of 87.8 MPa \sqrt{m} (79.9 ksi $\sqrt{in.}$) compared to the average of 87.5 MPa \sqrt{m} (79.7 ksi $\sqrt{in.}$) for the room temperature laboratory data for the six orientations of the WOL coupons. The two CR direction toughness samples average 90.7 MPa \sqrt{m} (82.6 ksi $\sqrt{in.}$) while the range of all toughness samples was 78.3 to 96.9 MPa \sqrt{m} (66.0 to 98.4 ksi $\sqrt{in.}$). All of the results and comparisons are shown in Table 24.

The toughness results for the disks did not, at first, appear to correlate well with the WOL laboratory data. In the CR direction, three WOL toughness coupons from three different pancakes were tested, see Section 3.3, and their K_{IQ} values ranged from 89.8 to 92.7 MPa \sqrt{m} (81.7 to 84.4 ksi $\sqrt{in.}$). However, the disks which burst before the onset of bore yielding had K_{IQ} values from 72.5 to 108.1 MPa \sqrt{m} (66.1 to 98.4 ksi $\sqrt{in.}$). In addition, Table 24 clearly shows that the disks with longer crack lengths at burst had lower K_{IQ} values. However, disks 25 and 24 had virtually the same crack lengths at failure, but quite disparate K_{IQ} values. Discussion of the explanation of these differences will be delayed until the end of this section after rotationally induced fatigue crack growth results have been reviewed.

5.2 Crack Growth Tests

Three disks (23, 25 and 28) were used to study the fatigue crack growth properties of this alloy in a rotational stress field. Test speeds were chosen such that significant crack growth would occur within the 400 cycle design life time. All testing was done at an R ratio of 0.5 and at a frequency of approximately 1 cycle/min.

Disk 23 had an initial crack length of 35.38mm (1.393 in.) and was cycled between 37,500 rpm and 53,000 rpm. The disk burst after 42 cycles at a final crack length of 39.24 mm(1.545 in.). The change in crack length was 3.86 mm (0.152 in.), equivalent to an average crack growth rate of 9.1×10^{-5} m/cycle (3.6×10^{-3} in./cycle), at an average ΔK of 36.4 MPa \sqrt{m} (66.2 ksi/in.).

Disk 25 was cycled between the speeds of 38,400 and 55,000 rpm. Table 25 shows the results of the crack growth testing. Note that ΔK and K_{max} varied only by a small amount throughout the crack growth testing. Normally, as a crack extends, crack growth rate tends to increase; however, for disk 25 the rate decreased. This result was attributed to the large plastic stress field generated during the first cycle of loading relative to the small plastic zone size after precracking.

This data suggested that possibly on the first fatigue cycle a large amount of crack growth occurred, essentially a tear, and was followed by subsequent decrease in the growth rate due to propagation of the crack through the large plastic zone. Support for this effect of the disk cycle history was found on the fracture surfaces of both disks 23 and 25, but was seen most clearly on disk 25 due to better post-burst preservation of the fracture surface, see Fig. 89. This figure shows a large tear immediately after the precrack of approximately 1 mm (0.040 in.) length followed by the region of crack growth. Note that the tear region was essentially not visible on the disk surface.

The fatigue crack growth results of Disk 28 are shown in Table 26. In this test, the disk failed after 355 cycles of testing between 46,000 and 65,000 rpm. Crack growth rates were faster than for those for disk 25 which correlates with the higher ΔK of disk 28. Only a small retardation in crack growth rate was observed after the first growth measurement. However, observation of the fracture surface revealed the same tear phenomenon as disks 23 and 25, see Fig. 90. This tear would have been visible on the surface if the test had been stopped after the first cycle. A greater retardation in growth rates would most likely have been observed if crack readings had been taken after 75 and 150 cycles as planned.

TABLE 25

FATIGUE CRACK GROWTH RESULTS FOR DISK 25

$$N_{\min} = 38,900 \text{ rpm}$$

$$N_{\max} = 55,000 \text{ rpm}$$

$$f \approx 1 \text{ cycle/min.}$$

Avg. Crack Length ^a Avg mm (in.)	Cycles N	Crack Growth Increment Δa , mm (in.)	Crack Growth Rate, $\Delta a/\Delta N$, m/cycle (in./cycle)	Max. Stress Intensity, K_{\max} , MPa \sqrt{m} (ksi $\sqrt{\text{in.}}$)	Stress Intensity, Range, ΔK , MPa \sqrt{m} (ksi $\sqrt{\text{in.}}$)
28.24 (1.112)	0				
		2.87 (.113)	3.81×10^{-5} (1.5×10^{-3})	75.0 (68.3)	37.6 (34.2)
31.12 (1.225)	75				
		3.40 (.134)	1.37×10^{-5} (5.4×10^{-4})	76.6 (69.7)	38.2 (34.8)
34.52 (1.359)	325				
		0.46 (.018)	6.1×10^{-6} (2.4×10^{-4})	77.2 (70.3)	38.7 (35.2)
34.98 (1.377)	400				
Avg. Values Over the Total Δa Increment	400	6.73 (.265)	1.68×10^{-5} (6.6×10^{-4})	75.9 (69.1)	37.9 (34.5)

Crack length at burst = 34.98 mm (1.377 in.)

Burst speed = 59,320 rpm

$$K_{\text{IQ}} = 90.1 \text{ MPa } \sqrt{m} \text{ (82.0 ksi } \sqrt{\text{in.}})$$

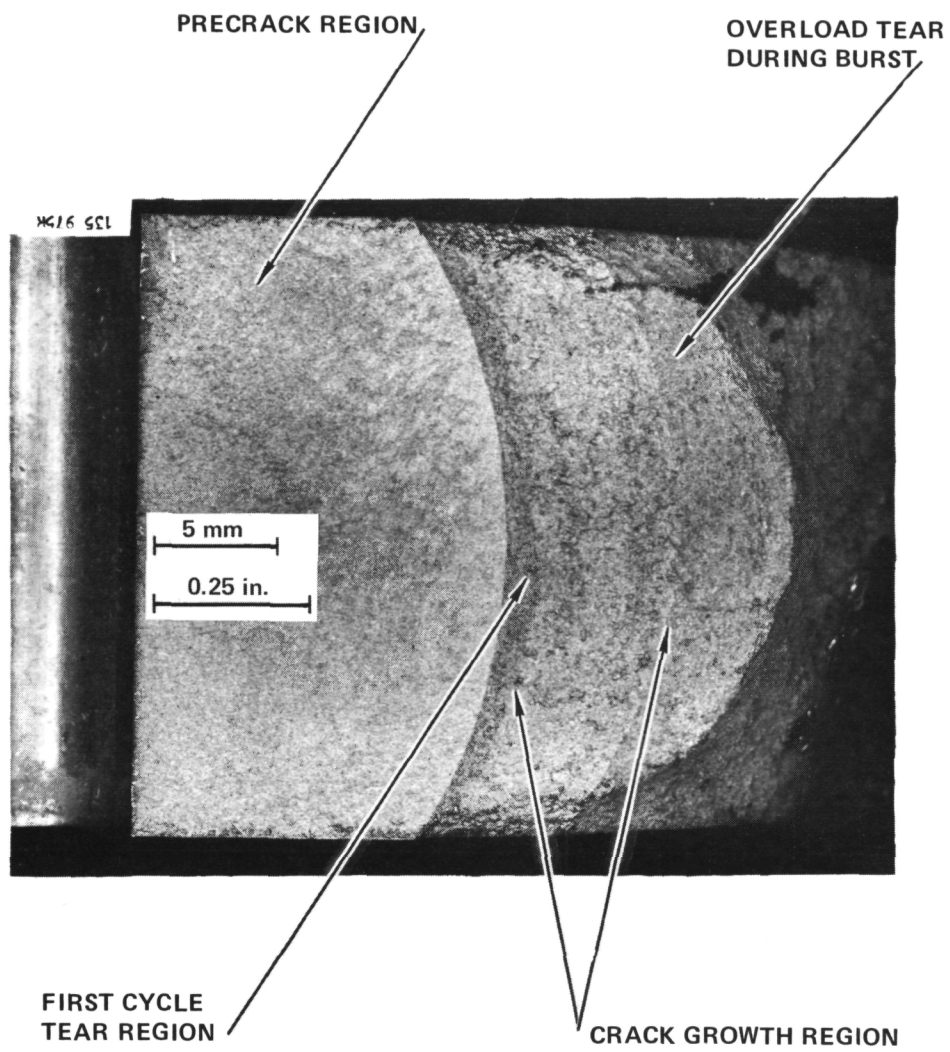


Figure 89. - Fracture Surface of Disk 25

TABLE 26

FATIGUE CRACK GROWTH RESULTS FOR DISK 28

$$N_{\min} = 46,000 \text{ rpm}$$

$$N_{\max} = 65,000 \text{ rpm}$$

$$f \approx 1 \text{ cycle/min.}$$

Avg. Crack Length, a_{Avg} mm (in.)	Cycles N	Crack Growth Increment Δa , mm (in.)	Crack Growth Rate, $\Delta a/\Delta N$ m/cycle (in./cycle)	Max. Stress Intensity K_{\max} MPa $\sqrt{\text{m}}$ (ksi $\sqrt{\text{in.}}$)	Stress Intensity, Range, ΔK MPa $\sqrt{\text{m}}$ (ksi $\sqrt{\text{in.}}$)
13.06 (0.614)	0	8.48 (.334)	4.3×10^{-5} (1.7×10^{-3})	87.7(79.8)	43.7(39.8)
21.54 (0.848)	200	4.04 (.159)	4.1×10^{-5} (1.6×10^{-3})	96.9(88.2)	48.5(44.1)
25.58 (1.007)	300	6.43 (.253)	1.2×10^{-4} (4.6×10^{-3})	103 (93.9)	51.5(46.9)
32.00 (1.260)	355				
Avg. Values Over the Total Δa Increment	355	18.95 (.746)	5.3×10^{-5} (2.1×10^{-3})	95.7(87.1)	47.8(43.5)

Crack length at burst = 32.00 mm (1.260 in.)

Burst speed = 64,300 rpm

$$K_{\text{IQ}} = 104 \text{ MPa } \sqrt{\text{m}} \text{ (95.0 ksi } \sqrt{\text{in.}})$$

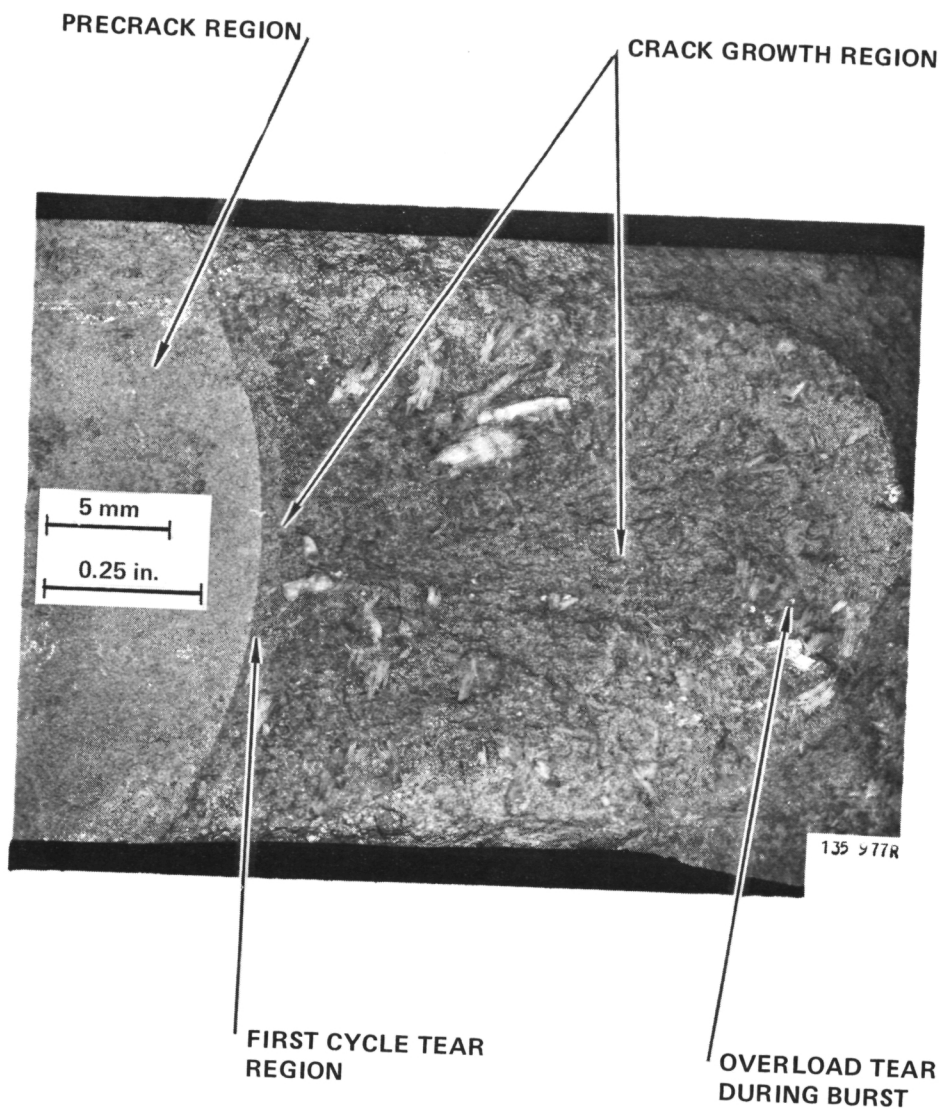


Figure 90. - Fracture Surface of Disk 28

Disk 22 was planned to be used for investigating the proof test concept. However, failure of the disk during spin up to the proof rpm, due to a longer crack than that anticipated, precluded use of this disk. Therefore, only disk 20 was available for proof testing.

Disk 20 was spun to a proof speed of 60,200 rpm for one cycle and returned to zero. This speed was sufficient to proof the disk for any crack length greater than 27.9 mm (1.1 in.); a nominal K_{TQ} of $87.8 \text{ MPa}\sqrt{\text{m}}$ ($80 \text{ ksi}\sqrt{\text{in.}}$) was used for this calculation. After the proof spin, the disk was cycled between 40,000 and 56,500 rpm for 400 cycles without failure. After cycling, the disk was spun to burst. Since no failure occurred prior to 400 cycles, the proof test concept was successfully proven in that flaws above 27.9 mm (1.1 in.) were screened which did insure a life of 400 cycles. At the stresses developed during cycling, growth would probably have continued for about another 300 cycles. Table 27 shows the results of the crack growth study.

Table 27 shows that as with disks 25 and 28, the fatigue crack propagation rate decreased for the second and third readings and increased on the fourth reading. Also, like disks 23, 25, and 28 the crack on disk 20 extended during the first cycle, in this case the proof cycle, see Fig. 91. The large initial crack extension and associated plastic zone caused the observed crack growth rate pattern.

The fatigue crack growth data points obtained under rotational cycling conditions are plotted in Fig. 92 along with the 2σ scatter bands for the 10 Hz. $R = 0.5$, room temperature, WOL data. The rotational crack growth data can be seen to be somewhat higher than the extrapolated data from the WOL coupons. The shape of the fatigue crack growth rate curve for the disks, see Fig. 92, is quite different than the WOL data curve and is difficult to explain without further investigation. Notice in this figure that all of this low cycle fatigue data was at or above ΔK_{sf} ($36.3 \text{ MPa}\sqrt{\text{m}}$ ($33 \text{ ksi}\sqrt{\text{in.}}$)) for the $R = 0.5$ room temperature WOL data as defined in Section 2.3.4. The low cycles to failure of these crack growth disks was entirely consistent with the definition of the risk function, r , and associated ΔK_{sf} definition.

TABLE 27

PROOF AND FATIGUE CRACK GROWTH TEST RESULTS FOR DISK 20

Original Crack Length = 18.24 mm (0.718 in.)

One proof cycle up to 60,200 rpm applied
with no apparent surface crack growth.

$$N_{\min} = 46,000 \text{ rpm}$$

$$N_{\max} = 56,500 \text{ rpm}$$

$$f \approx 1 \text{ cycle/min}$$

Avg. Crack Length ^a Avg mm (in.)	Cycles N	Crack Growth Increment Δa , mm (in.)	Crack Growth Rate, $\Delta a/\Delta N$ m/cycle (in./cycle)	Max. Stress Intensity, K_{\max} MPa \sqrt{m} (ksi $\sqrt{\text{in.}}$)	Stress Intensity Range, ΔK MPa \sqrt{m} (ksi $\sqrt{\text{in.}}$)
18.24 (.718)	0	1.37 (.054)	9.1×10^{-6} (3.6×10^{-4})	68.1 (62.0)	34.1 (31.0)
19.61 (.772)	150	0.584 (.023)	7.9×10^{-6} (3.1×10^{-4})	69.9 (63.6)	34.9 (31.8)
20.19 (.795)	225	0.406 (.016)	5.3×10^{-6} (2.1×10^{-4})	70.1 (63.8)	35.0 (31.9)
20.60 (.811)	300	0.813 (.032)	8.1×10^{-6} (3.2×10^{-4})	70.4 (64.1)	35.2 (32.0)
21.41 (.843)	400				
Avg. Values Over the Total Δa Increment	400	3.18 (.125)	7.9×10^{-6} (3.1×10^{-4})	69.7 (63.4)	34.8 (31.7)

Crack length at burst = 21.41 mm (0.843 in.)

Burst speed = 69,290 rpm

$$K_{IQ} = 107 \text{ MPa } \sqrt{m} \text{ (97.4 ksi } \sqrt{\text{in.}})$$

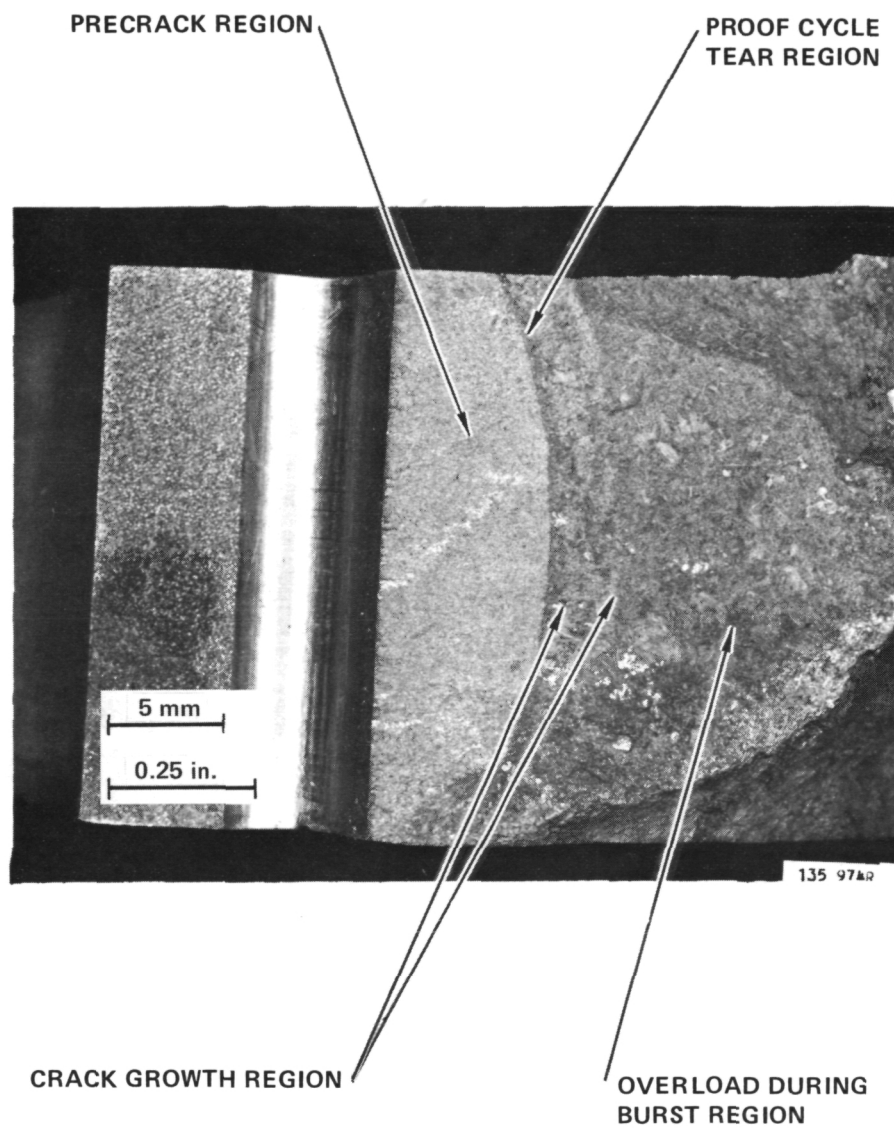


Figure 91.- Fracture Surface of Disk 20

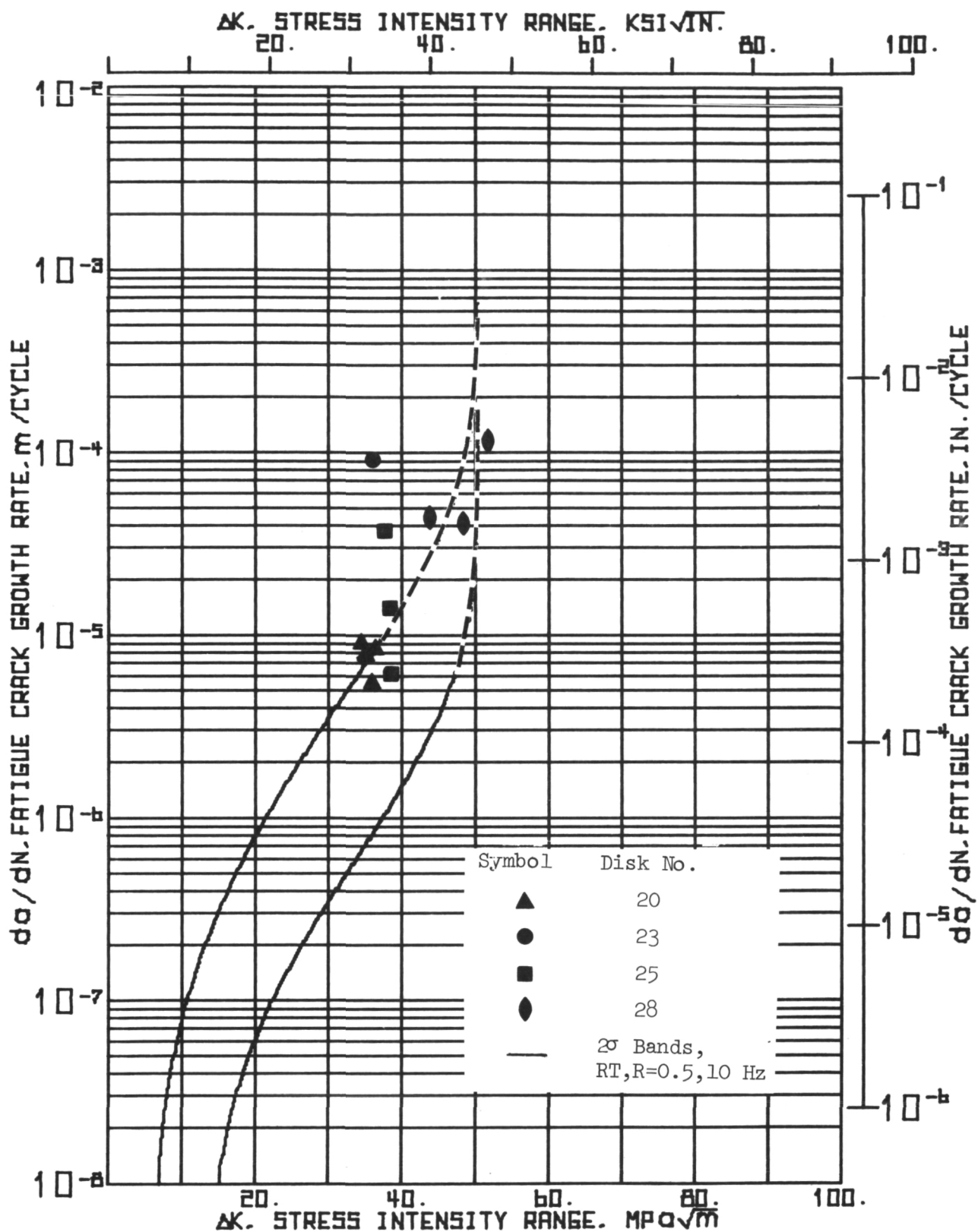


Figure 92.- Fatigue Crack Growth Rate Data for Disks Compared to WOL Coupon Data

Although there may be other unconsidered causes of the shape of the crack growth curve indicated in Fig. 89, three immediate possibilities are suggested as explanation: 1) the extrapolation of the WOL data curve above $\sim 5 \times 10^{-6}$ m/cycle (2×10^{-4} in./cycle) was incorrect and unconservative, 2) the first crack growth reading for each disk is incorrect due to initial uncertainty of the crack location, and 3) the initial cycle of rotationally induced loading caused a jump in crack length followed by retardation due to the large induced plastic zone. If the first possibility was true, the growth rates observed for the disks would correlate better, but the unusual curve shape of the data would be left to explain. The second possibility is eliminated by the fact that the original crack length before rotational loading was known accurately after fracture of the disk. The first crack length measured after the initial number of load cycles was as accurately known as subsequent measurements. The third possible cause of the rotationally induced crack growth curve appears the most likely explanation when combined with the first possibility.

5.3 Discussion

The possibility of an error in extrapolation of the $R = 0.5$, room temperature data was evaluated by testing coupon 5CR-2 at Calac in a room temperature, laboratory air environment at $F = 1$ Hz. The results of this test are shown in Fig. 93 where the data is compared to the previously obtained 2σ scatter bands for the $R = 0.5$, $f = 10$ Hz, room temperature WOL data. Figure 93 clearly showed that the fatigue crack growth rates for coupon 5CR-2 above 10^{-6} m/cycle laid to the right of the previously extrapolated curve. Notice that the first data point is significantly high after which the rate quickly decreased to the same rate as the previous WOL data. Subsequent fatigue crack growth rates started to follow the same curve as previous WOL data before deviating from the extrapolated curve. Thus, the results for 5CR-2 had some characteristics of the spin pit data as well as the prior WOL data. The results confirmed that the previously extrapolated curve was in error. Fatigue crack growth data for specimen 5CR-2 also deviated from previous WOL data in that the K_{\max} at fracture was $\sim 110 \text{ MPa } \sqrt{\text{m}}$ ($100 \text{ ksi } \sqrt{\text{in.}}$) which was

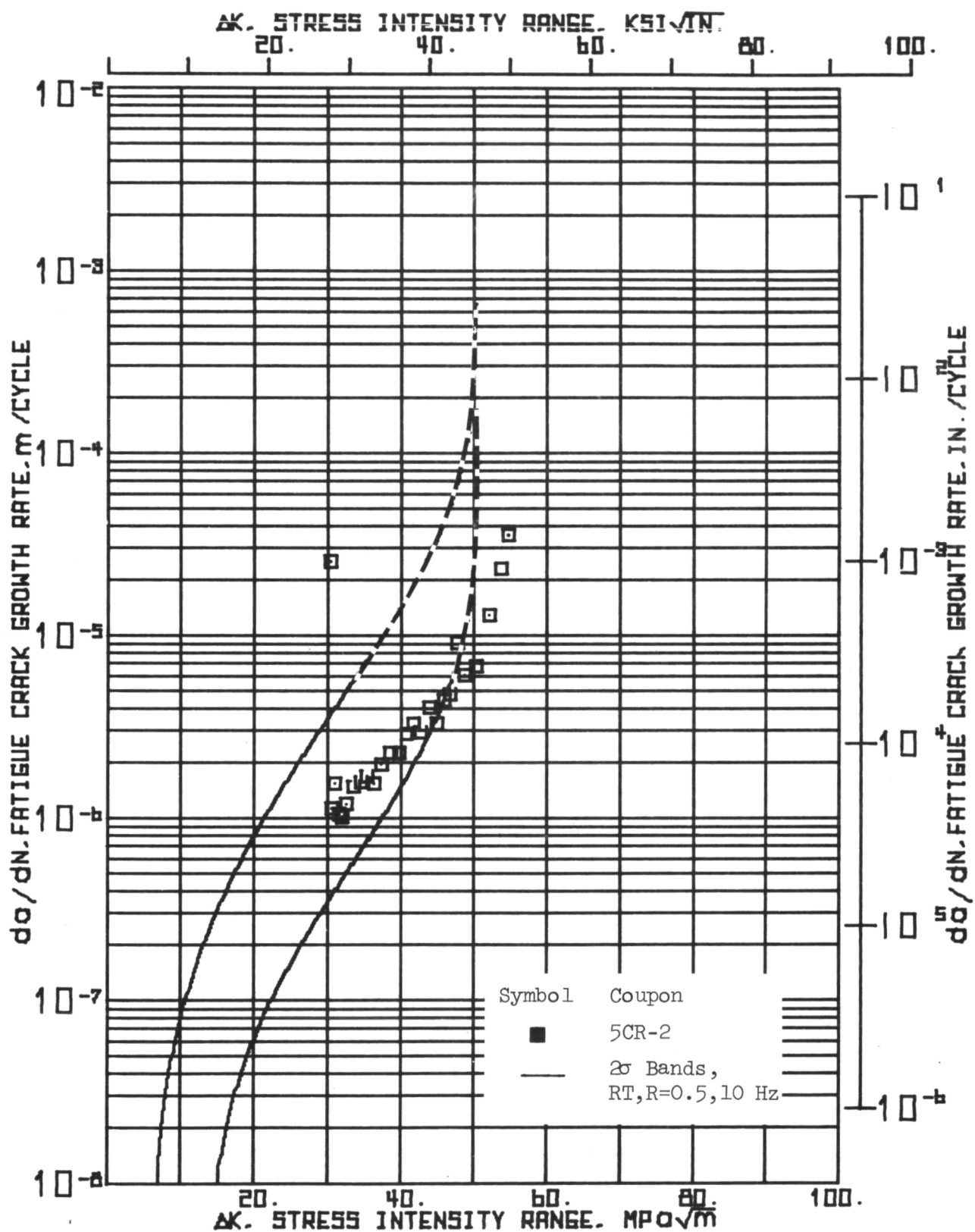


Figure 93. - Comparison of Data for Coupon 5CR-2 and Previously Extrapolated WOL Data

approximately 20% greater than the average K_{IQ} for this orientation, $90.1 \text{ MPa } \sqrt{\text{m}}$ ($82.0 \text{ ksi } \sqrt{\text{in.}}$). This result is not unusual for titanium alloys [42] and indicates the often encountered difficulty of rationalizing the relationship between K_{IQ} , or K_{Ic} , and K_{max} at fracture which occurs during fatigue cycling. Although K_{Ic} may be a useful number for comparing materials, the maximum stress intensity at fracture of a crack growth coupon may be a more meaningful number from a design viewpoint.

Figure 94 shows a view of the fracture surface of coupon 5CR-2. This fracture surface was similar to those observed for all of the other WOL coupons except that a small, but significant tear of the coupon was observed. This tear appeared to have occurred during the first cycle of applied load after pre-cracking.

Specimen 5CR-2 had a short initial crack length and failed at an a/w ratio of less than 0.6 eliminating the possibility that the data was influenced by a coupon end effect. The rate of increase in ΔK with Δa was similar for both the disk and coupon 5CR-2. In addition, comparison of the K_{max} of the sample to the proposed ASTM criteria [44] for maximum allowable K_{max} as a function of a/w showed that the data of Fig. 93 met this criteria up to a ΔK of $53 \text{ MPa } \sqrt{\text{m}}$ which included all but the last two data points. Essentially this criteria restricts the nominal stress in the uncracked ligament to be less than σ_{ys} . Based on this criteria, all four data points of disk 20 and the first two data points for disk 28 meet the restriction. Note in Fig. 92 that the data for disk 20 is similar to that for disk 23 and 25 which did not meet the proposed nominal stress criteria. Based on this discussion, the conclusion was made that the difference between the spin pit fatigue crack growth data and laboratory WOL coupon data probably could not be explained as being due to a difference in end effect; in the manner in which ΔK increased with Δa or to a difference in the amount of specimen plasticity.

The differences between the spin pit and WOL fatigue crack growth data may lie in the following explanation. The disks were precracked at approximately a K_{max} of less than $33 \text{ MPa } \sqrt{\text{m}}$ ($30 \text{ ksi } \sqrt{\text{in.}}$) and at a R ratio of approximately 0.15.

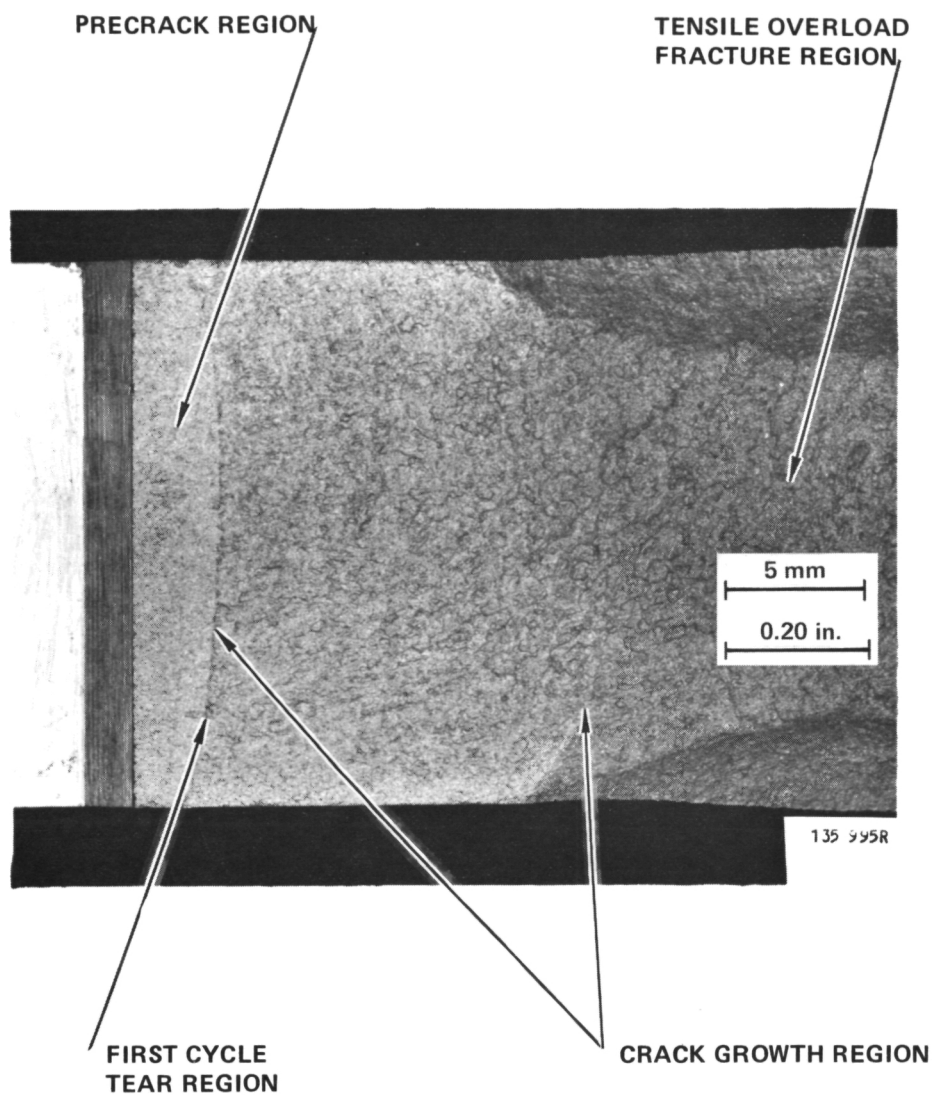


Figure 94. - Fracture Surface of WOL Coupon 5CR-2

During the first cycle of the rotational testing, disks were subjected to a K_{\max} in the range of 68 to 87 MPa \sqrt{m} (62 to 79 ksi $\sqrt{in.}$). This large K_{\max} resulted in large plastic zones visible on the disk surfaces after the first cycle and was associated with first cycle tearing as previously discussed.

Subsequent to such a change in K_{\max} , termed overload, crack growth rates often decrease [42, 45-49]; a result observed for the three easily analyzed disks; 20, 25, and 28. Similar to these disks, the only data point for disk 23 appears to be high. However, for this disk, failure occurred after 42 cycles at a K_{IQ} of 72.6 MPa \sqrt{m} (66.1 ksi $\sqrt{in.}$). Therefore, the high growth rate of disk 23 may simply have been due to the fact that the disk had a low K_{IQ} , due to a high a/R ratio and to material variations, and that crack growth testing was started near this K_{IQ} value. Recall that for all data, recorded measurements are average values and thus, like for disk 23, growth rates for cycles 40 to 42 may have been an order of magnitude, or more, faster than for cycles 10 to 12.

To investigate the effect on da/dN of the large change in ΔK and K_{\max} compared to the precrack values, WOL coupons 8CR-2 and 10CR-2 were fatigue cycled at $R = 0.5$ and at room temperature with an initial K_{\max} of 78.2 MPa \sqrt{m} (71.1 ksi $\sqrt{in.}$) and 81.6 MPa \sqrt{m} (74.2 ksi $\sqrt{in.}$) respectively, similar to the disks. In addition, the specimens were tested at a frequency of 0.0167 Hz (1 cycle/min) to simulate the spin pit cycling rate and thus check for any possible frequency effects.

The test results for 8CR-2 and 10CR-2 are compared to the 1 Hz data for 5CR-2 in Fig. 95. The crack growth rate curves for these two coupons can be seen to be similar to that for 5CR-2 which was tested at 1 Hz and at a lower starting K_{\max} of 60.6 MPa \sqrt{m} (55.3 ksi $\sqrt{in.}$). The first fatigue crack growth rate recorded for these two coupons was high after which the growth rate decreased and then increased. The K_{IQ} values at failure were similar for all three coupons. However, the curves were not identical, the growth rates for 8CR-2 being greater than those for 10CR-2 which were greater than for 5CR-2 between ~ 42 and 53 MPa \sqrt{m} (~ 46 and 58 ksi $\sqrt{in.}$).

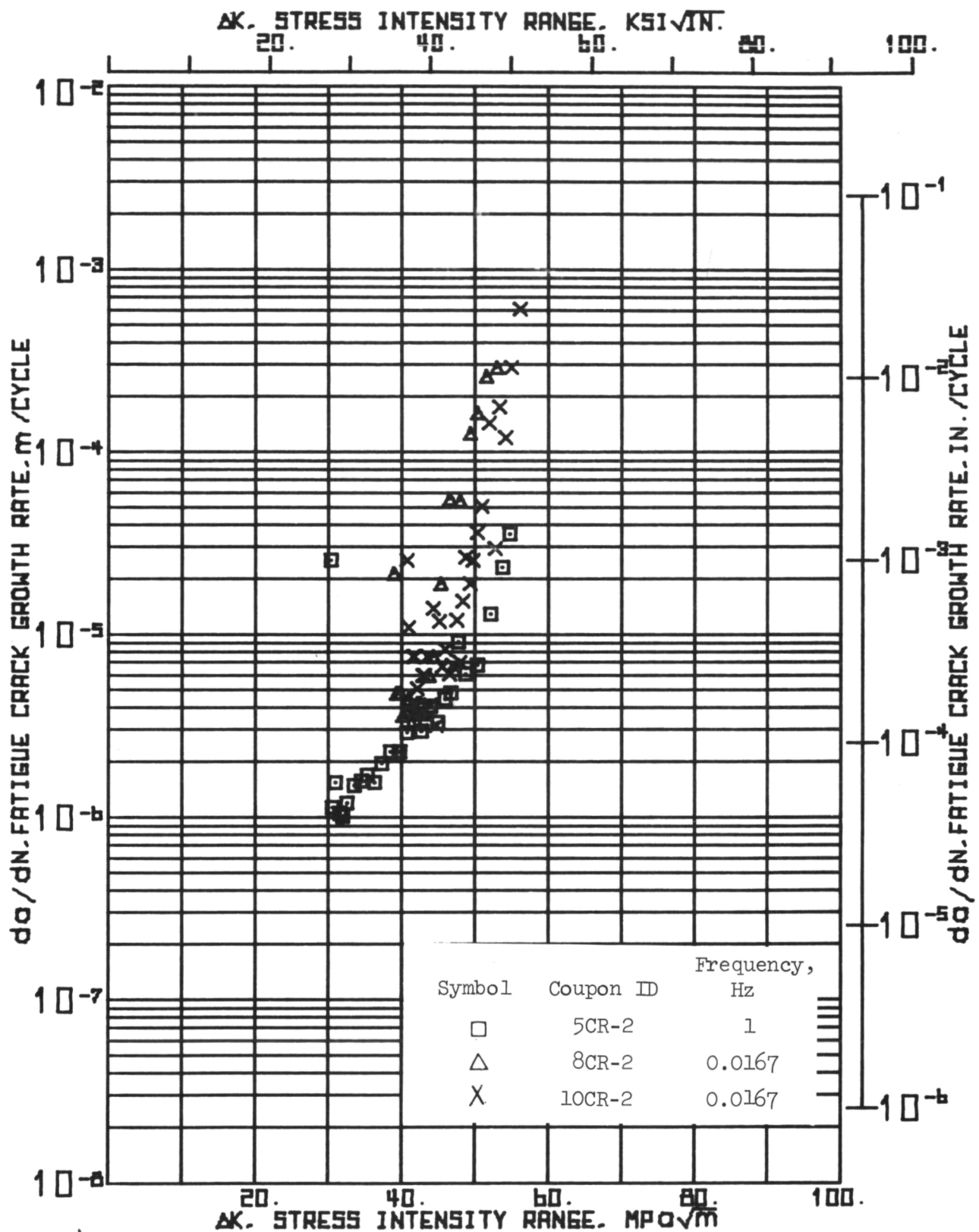


Figure 95.- High Stress Intensity Fatigue Crack Growth Rate Data for WOL Coupons at R = 0.5, Room Temperature

Figure 96 shows the data for 5CR-2, 8CR-2, and 10CR-2 as well as that for all of the other WOL coupons tested at $R = 0.5$, room temperature. The lines shown are curves which approximate the median crack growth history of all of the coupons under discussion. Except for the first data point, the data for 5CR-2 was a continuation of the data previously obtained at lower ΔK levels. This figure shows that the only significant difference between the previous data and that for these three coupons was the initial high growth rates. The differences in crack growth rates among the coupons above $\sim 42 \text{ MPa} \sqrt{\text{m}}$ ($38 \text{ ksi} \sqrt{\text{in.}}$) appear to have been due to coupon-to-coupon scatter.

Fatigue crack growth data from the disks are plotted in Fig. 97 together with the curve lines for 5CR, 8CR-2, and 10CR-2. The curves for the three WOL coupons showed a good correlation to the spin pit data. Thus, one can conclude that the WOL specimens properly and completely modeled the spin pit data. This conclusion is supported by Figs. 94, 98, and 99 which show the fracture surfaces of coupons 5CR-2, 8CR-2, and 10CR-2, respectively. Similar to all four disks used for fatigue crack growth studies, an initial first cycle tear occurred in these coupons followed by more stable crack growth and subsequent fracture. These fracture surfaces were identical to those observed on the disks, Figs. 89-91.

In summary, one can conclude that the fatigue crack growth behavior observed for the disks was exactly duplicated by the WOL coupons tested at high starting K_{max} levels. The reason for the shape of the crack growth curve for the disks, see Fig. 97, was understandable. During the first cycle, large subsurface crack growth occurred without observable surface growth and accompanied by a large plastic zone visible as surface dimpling. During subsequent cycles, the crack propagated, with the surface growth retarded at first, but quickly catching up so that a more uniform, less bowed crack front was achieved. As crack growth continued, the crack bowed more until fracture. This physical response of the disks resulted in an initially high crack growth rate which decreased over $\sim 2.5 \text{ mm}$ (0.1 in.) after which the crack grew in a more uniform manner until fracture.

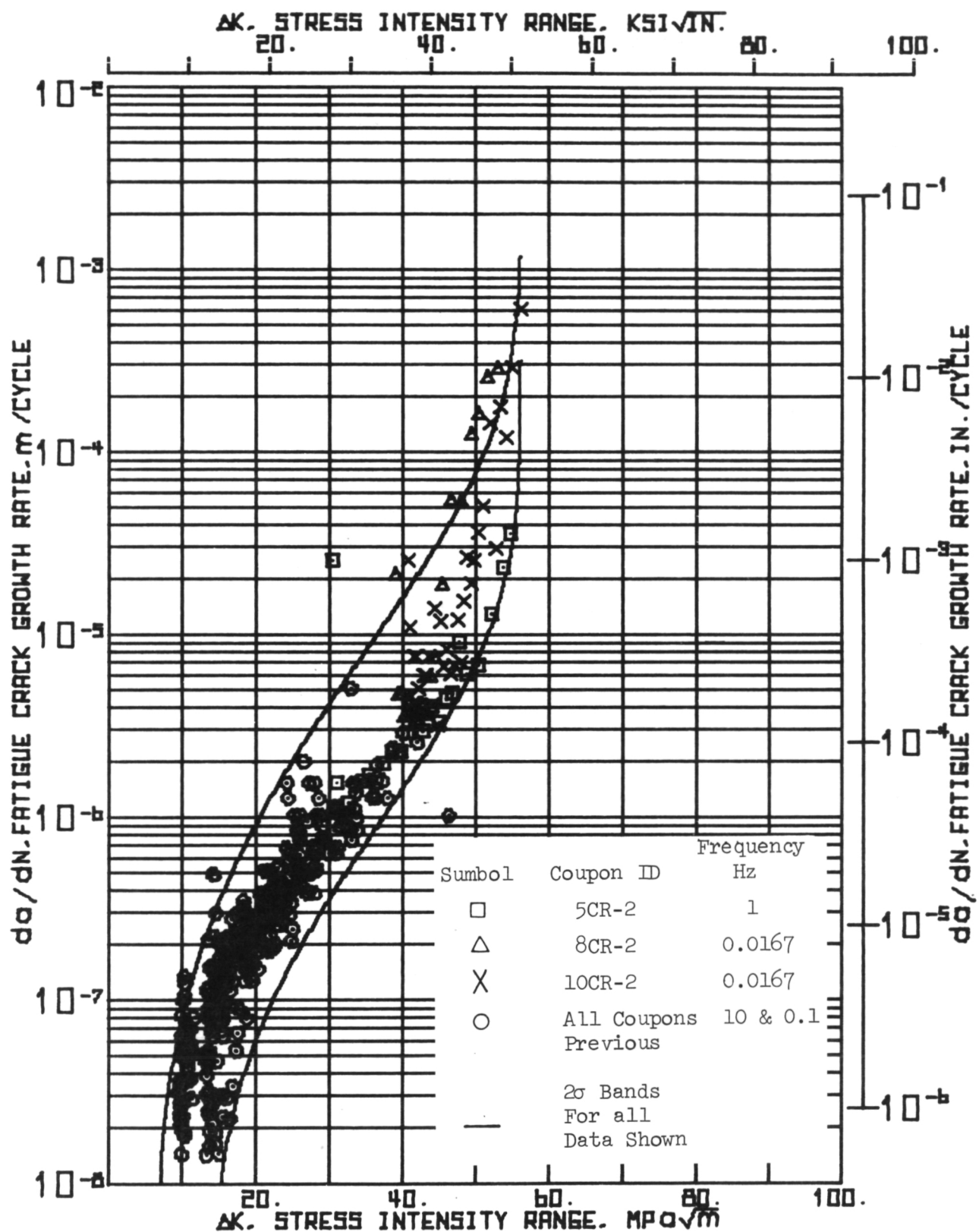


Figure 96.- Comparison of High Stress Intensity Fatigue Crack Growth Rate Data to Previously Extrapolated WOL Data at R = 0.5, Room Temperature

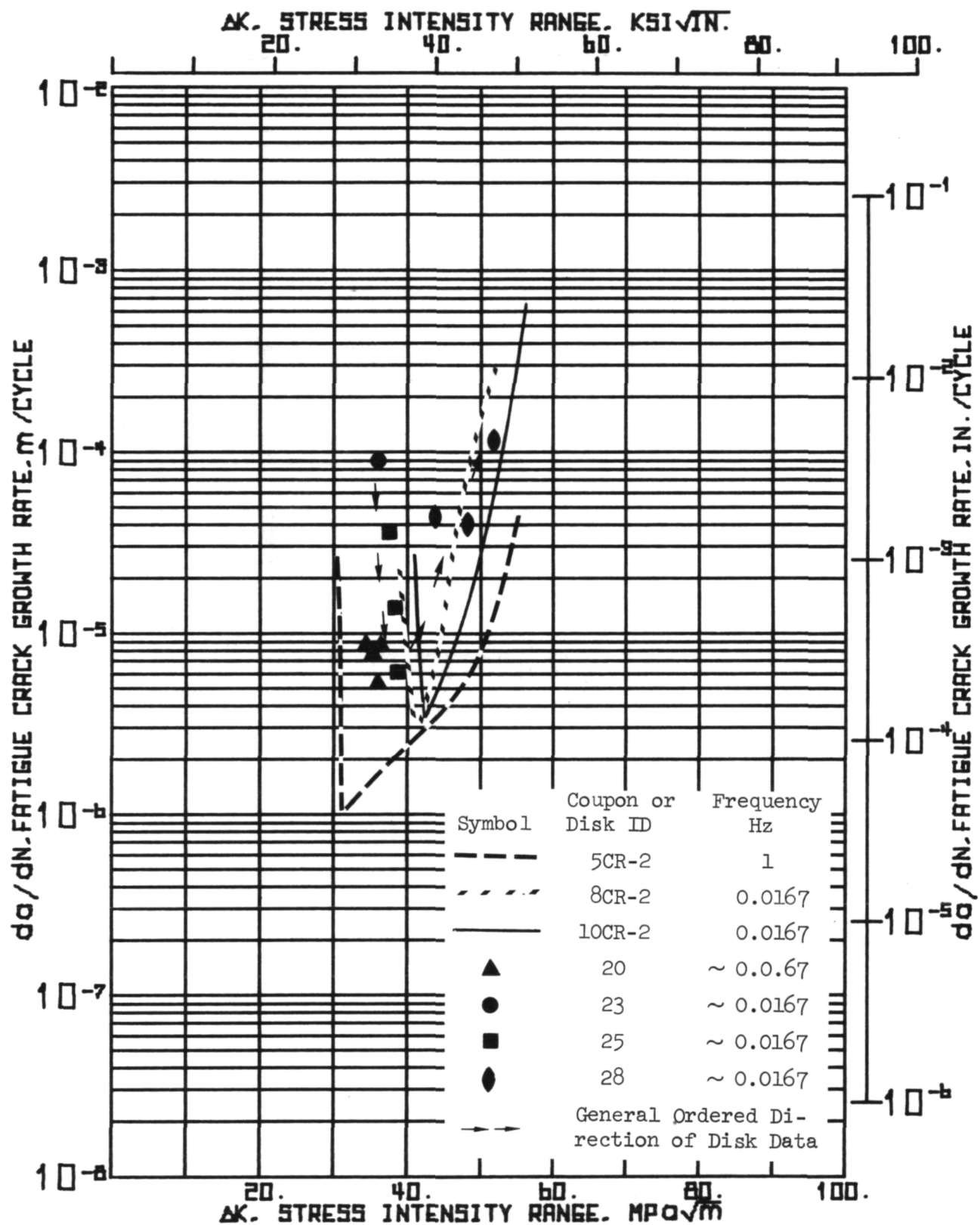


Figure 97.- Comparison of Ordered Fatigue Crack Growth Data for WOL Coupons to Rotating Disks

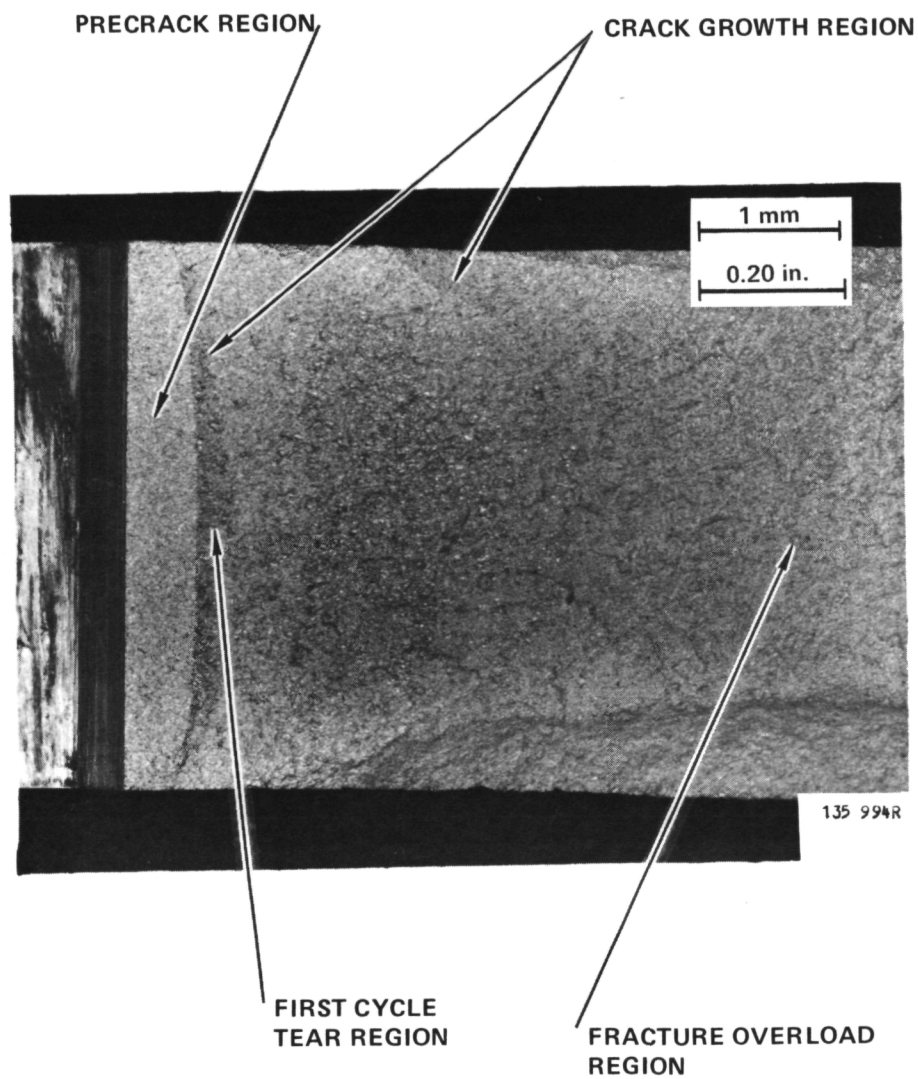


Figure 98. - Fracture Surface of WOL Coupon 8CR-2

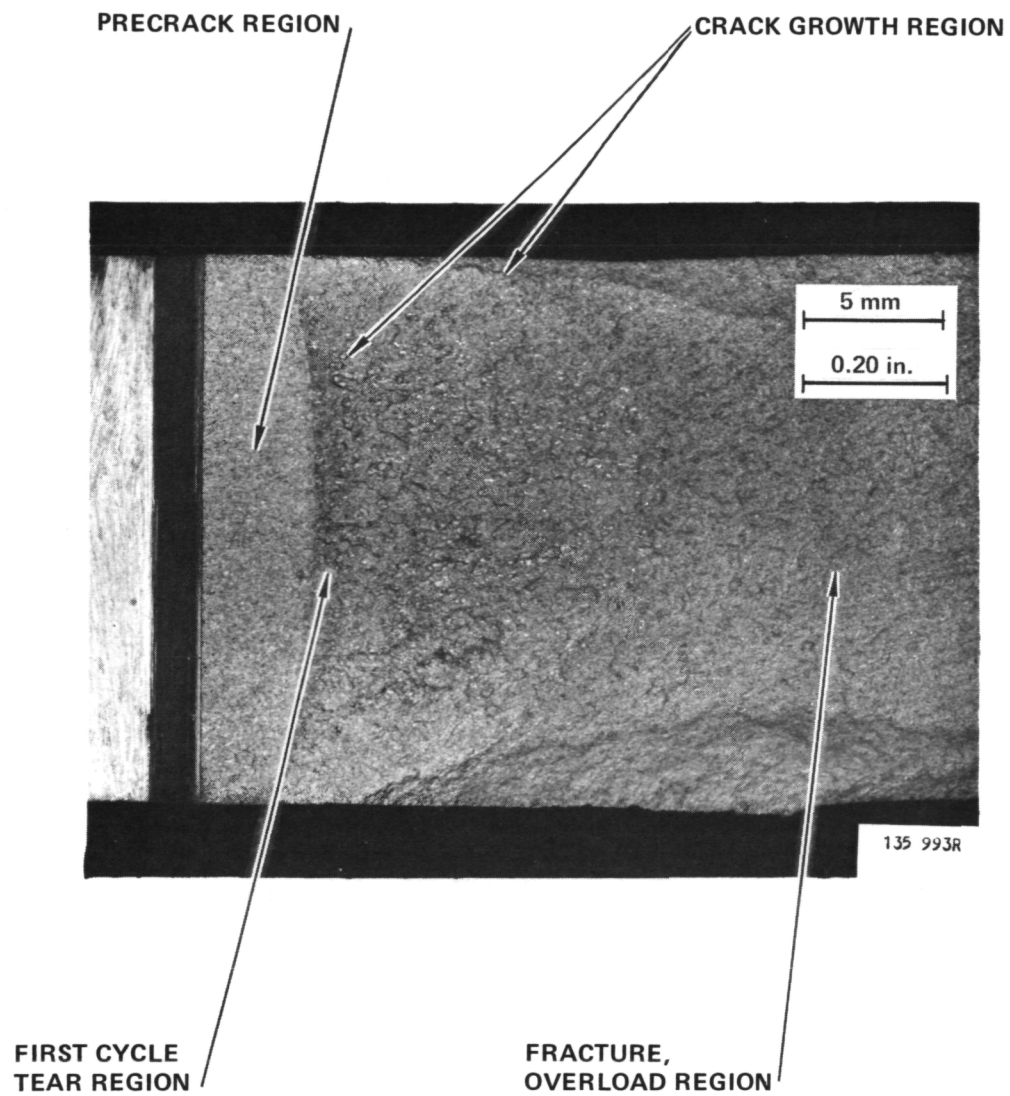


Figure 99. -Fracture Surface of WOL Coupon 10CR-2

Although the fatigue crack growth data and fracture surfaces of the disks were exactly duplicated by a simple test using a WOL coupon, the problem of choosing an appropriate life prediction curve remained. A simple curve fit to the data could have been chosen, but the model would have been clumsy at best due to the unusual curve shape of the actual data for the disks and those for the coupons. Therefore, an engineering design approach was taken in that a growth of 1.5 mm (0.060 in.) was assumed on the first cycle and subsequent growth rates were assumed to follow the conservatively chosen 2σ left bound scatter band curve shown in Fig. 13. Normally, the suggested 1σ life band would have been used as discussed in Section 4.7. However, for simplicity the life prediction analysis routine assumed that K_d was a constant which was not true as the WOL coupons showed. A more complex analysis for this high growth rate data would have taken the variation in K_d into account. The resulting 1σ band would be essentially equivalent to the 2σ band based on the present analysis. Tear regions were approximately 1.10 to 1.65 mm (0.045 to 0.065 in.) and 1.52 mm (0.060 in.) was chosen as a conservative compromise.

The results of the analysis are shown in Table 28. The predicted number of cycles for disk 20 was low because this disk was first subjected to a proof cycle overload and subsequent cycles had a lower maximum speed. This resulted in an expected retardation in growth rate which is commonly observed [42, 45-49]. The results of this life analysis together with the data plotted in Fig. 97 clearly showed that good correlation was found between crack growth data obtained from the disks and from the WOL coupons. A similar good correlation was found by Coles, Johnson and Papp [50] between crack growth data obtained from surface-flawed tensile bars and that from large bore diameter rotating disks of Inconel 718. As previously mentioned in Section 5.1, K_{IQ} values in this program did not appear to correlate as well as the crack data. This is shown by disk 23 whose cycle life could be adequately predicted, see Table 28, but whose early failure at an apparently low K_{IQ} value was not anticipated.

A reasonable hypothesis for explaining the early failure of disk 23 can be made with the aid of Fig. 100 which shows K_{IQ} values, 104.4 - 108.1 MPa \sqrt{m} (95.0-98.4 ksi $\sqrt{in.}$), correlated well with those from WOL coupons 5, 8 and

TABLE 28

COMPARISON BETWEEN PREDICTED AND OBSERVED DISK LIVES

Test Conditions: $R = 0.5$
 $f \approx 0.0167 \text{ Hz}$
 Room Temperature

Disk No.	Observed Spin Pit Cycles, N_o	Predicted Spin Pit Cycles, N_D	Remarks
20	400	62	Proof disk, no failure observed or predicted.
23	42	43	Disk failed due to net section stress rupture; not predicted.
25	400	445	No failure observed or predicted.
28	355	348	Failure observed and predicted.

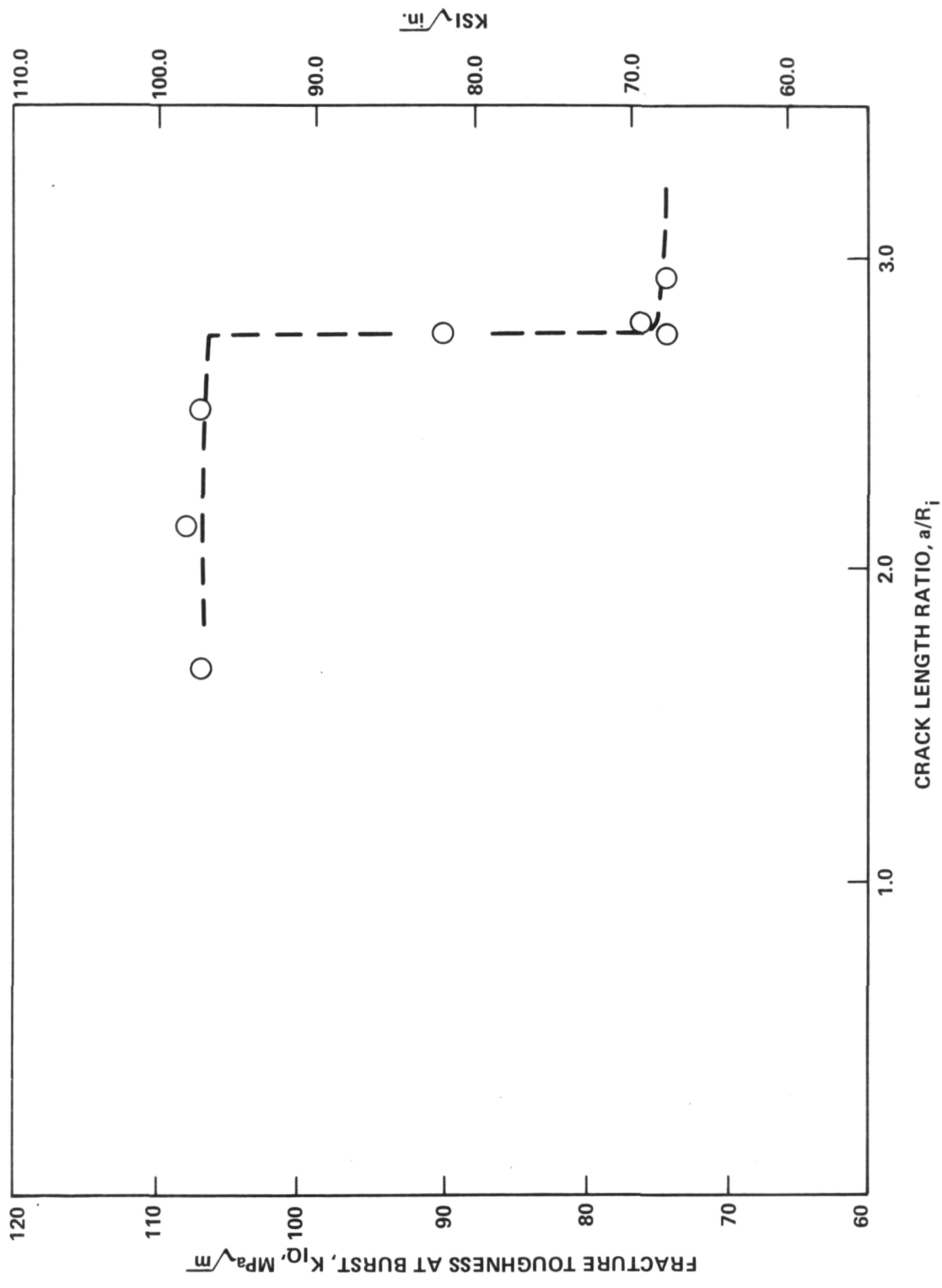


Figure 100. - Fracture Toughness at Burst as a Function of a/R_i

10CR-2: 106.2-112.6 MPa \sqrt{m} (96.6-102.5 ksi $\sqrt{in.}$). However, observed fatigue crack growth rates for disks whose K_{IQ} values varied from 107 to 74.4 MPa \sqrt{m} (97.4 to 67.7 ksi $\sqrt{in.}$) all correlated with WOL coupons 5, 8, and 10CR-2. The conclusion was that at all a/R_i values, the fracture mechanics assumption (that cracks in different geometries, but with the same K_I will respond the same), held for fatigue crack growth but not for fracture.

The reason for the change in K_{IQ} values appears to have been stress rupture. The stress field perpendicular to the crack propagation direction is quite different for the disk as compared to the WOL coupon. This made little difference for correlating crack growth data, as expected. Burst of a disk, however, occurred essentially when the net section stress ahead of the flaw equals the yield strength as discussed in Section 3. Therefore, if cracks are short enough, K_{IQ} will be reached before the net section stress equals σ_{ys} , but if the crack is long enough, net section stress will occur and the disk will burst before K_{IQ} is reached. This stress rupture condition for this disk geometry was at an a/R_i of approximately 2.6 to 2.8. A specific example was disk 23 which grew at a rate correlatable to the WOL coupons, but failed at a reduced K_{IQ} value due to stress rupture.

From a practical design point, this condition is probably not of great importance since long flaws are not encountered. Therefore, in Section 6 on Prediction of Disk Life, the da/dN curve for $R = 0.5$ was chosen as the left hand 2σ scatter band and K_d from the data of Fig. 96 and for $R = 0.05$ data the left hand 2σ scatter band curve and K_d from Fig. 44 were chosen. The K_d value for $R = 0.05$ data, 95.8 MPa \sqrt{m} (87.2 ksi $\sqrt{in.}$) was somewhat conservative compared to the $R = 0.5$ or disk K_{IQ} value. These K_d values will be reasonably reliable since in Section 6 all crack lengths chosen will be less than an a/R_i of 2.6. The initial tear of 1.0-1.5 mm (0.04-0.060 in.) will be taken into account.

A final problem remained in choosing appropriate curves for the $-253^{\circ}\text{C} (-423^{\circ}\text{F})$ data to be used in the life prediction analysis of Section 6. The effects of a -253°C Hz environment on the spin pit results must be considered. Large variations in K_{IQ} do not have to be accounted for because the disk thickness exceeded that necessary for constraint by a factor of approximately four. Disks would also have remained elastic up to burst for all cracks longer than 0.91 mm (0.072 in.) equivalent to burst speeds up to 91,295 rpm. Thus, short cracks could have been grown in high stress fields without onset of bore plasticity. Therefore, for use in analysis of life prediction procedures, Section 6, the left hand 2σ scatter band curves shown in Figs. 48 and 50 respectively, were chosen for the $-253^{\circ}\text{C} (-423^{\circ}\text{F})$ crack growth data. The K_d values associated with these curves should be conservative since they are equal to the fracture toughness K_{IC} values. No effect of frequency was assumed. The chosen design curves were somewhat arbitrarily chosen, but hopefully are conservative since they reflect the observations of the room temperature and $-253^{\circ}\text{C} (-423^{\circ}\text{F})$ data. Figures 101 and 102 show the differences between the curves chosen for the room temperature data and that for the $-253^{\circ}\text{C} (-423^{\circ}\text{F})$ data. The question of the amount of crack tear to account for on the first cycle at $-253^{\circ}\text{C} (-423^{\circ}\text{F})$ will be discussed in Section 6.

The correlation between the WOL and rotating disk data supported the validity of the stress analysis assumptions made for the disks in Section 2.4.1. These assumptions were: 1) only one crack, even though many disks had two notches, because of the longer length of this crack and associated sharp crack tip; 2) the geometry term in Equation (17), $f(a/R_1)$ is valid up to $a/R_1 \approx 2.8$ provided that net section plastic flow has not occurred. Correlation of the fatigue crack growth data supported both of these assumptions. The rotating disk burst test data also supported the two assumptions and, as was shown in Fig. 100, conclusively supported the lack of a large plastic flow condition associated with assumption 2.

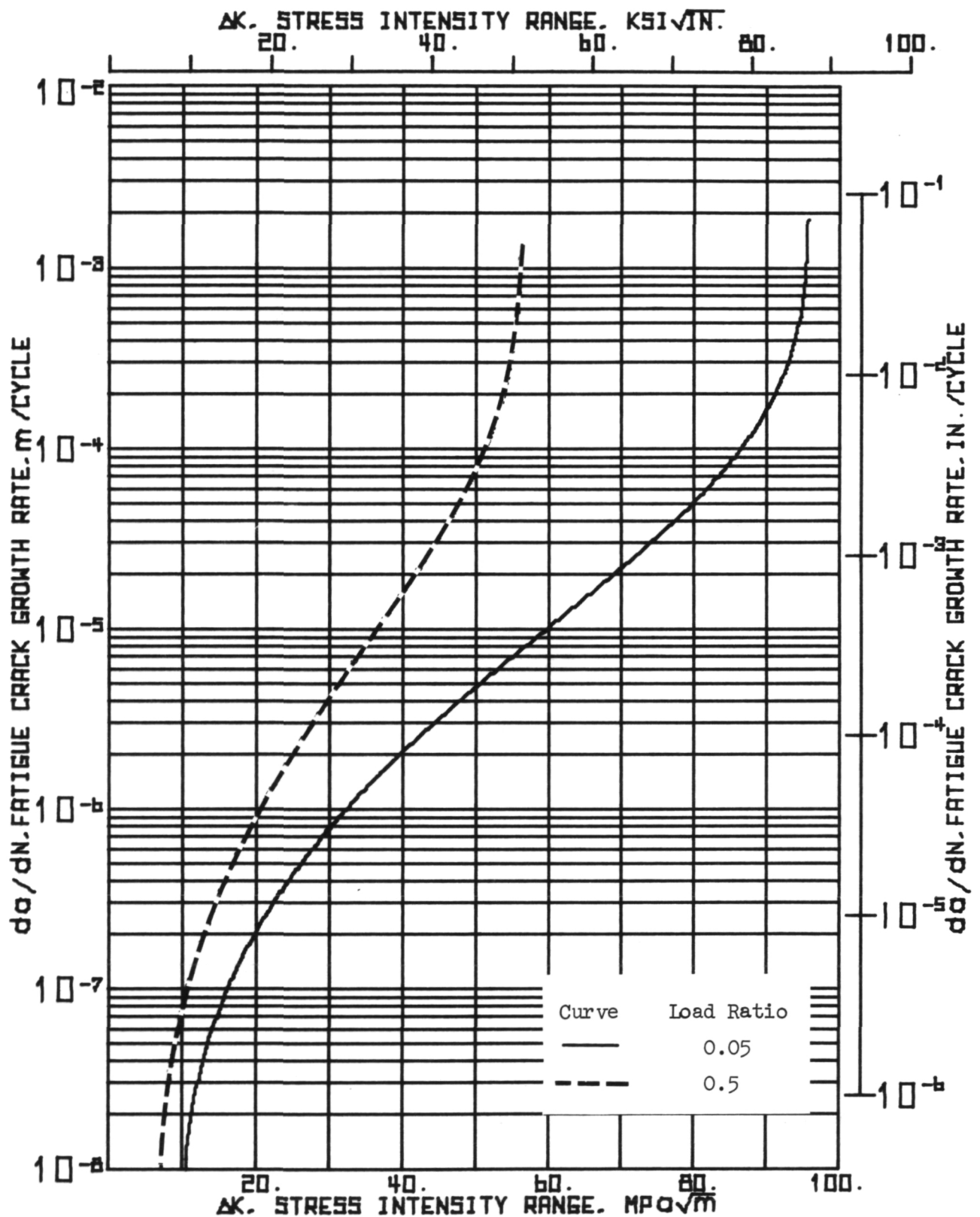


Figure 101.- Fatigue Crack Growth Curves at Room Temperature for Use in Predicting Disk Life

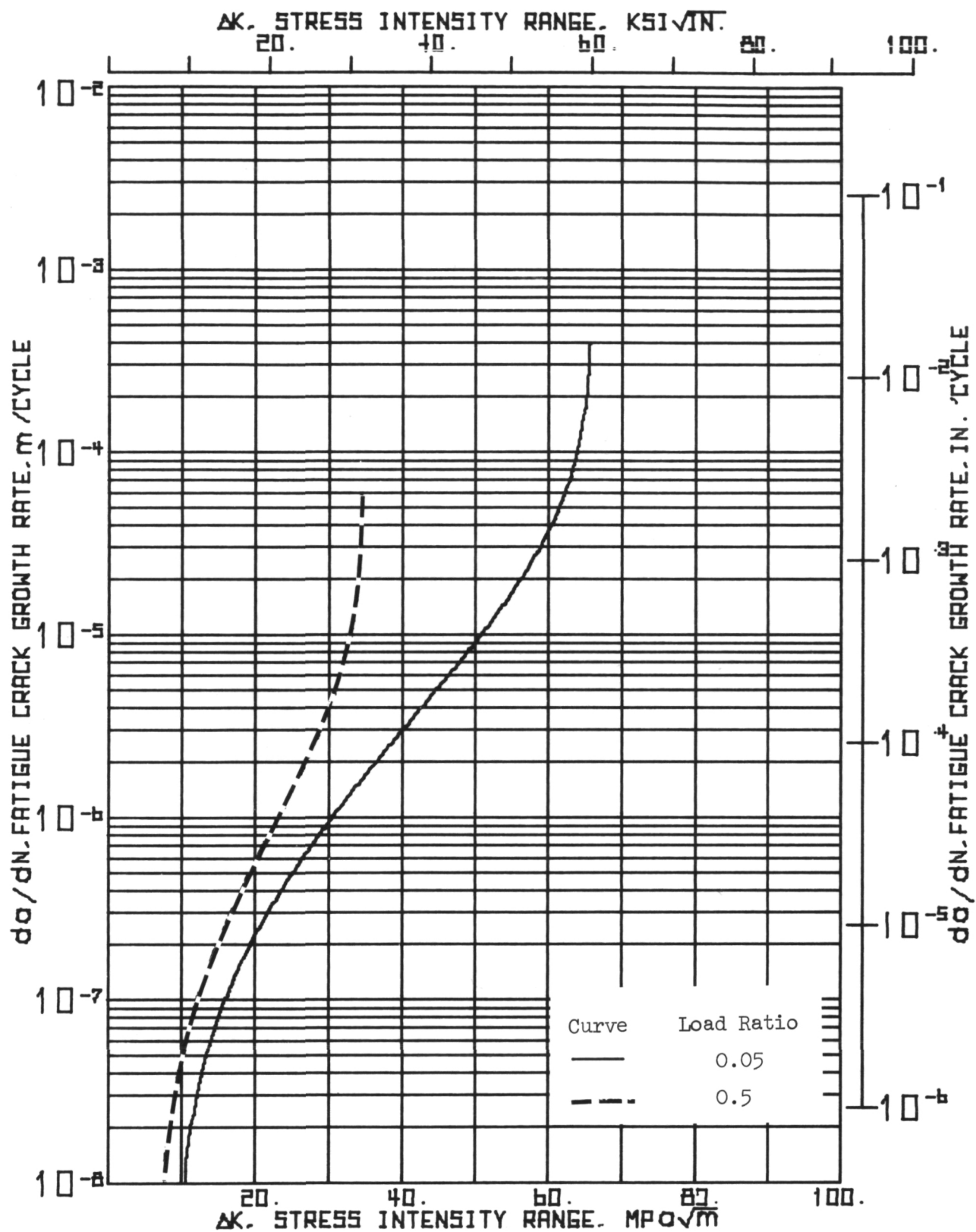


Figure 102.-Fatigue Crack Growth Curves at -253°C (-423°F)
for Use in Predicting Disk Life

6.0 PREDICTION OF DISK LIFE

6.1 Fracture Control Concepts

Fracture mechanics concepts assume flaws, discontinuities, inadvertent damage, corrosion pits, etc., are unavoidable in structural applications. These natural defects may nucleate cracks that grow due to application of static or cyclic stresses. After the growing crack attains a critical size, rapid and uncontrollable crack propagation results.

Traditional design criteria assume the fracture strength to be greater than the yield strength, usually equal to the ultimate strength and preceded by extensive plastic deformation. Based on this assumption, past experience can be used to determine safety factors that keep working loads below fracture loads. This is acceptable for ductile materials and most structures, since the size of flaw which reduces the fracture strength to less than the yield strength is readily detectable. However, the failure best described by fracture mechanics occurs at stresses below the elastic limit in brittle materials that fail after small amounts of plastic deformation or in ductile materials that are embrittled by environment, temperature, strain rate, triaxial stress or alternating stresses. In these instances, the flaw size which reduces the fracture strength below the yield strength is not easily detectable.

A detailed analysis of premature failures revealed that flaws or cracks existed in many parts prior to failure [51]. These defects may be present in mill products, may be imparted during processing, or may be imparted in service. In addition, there is a finite probability that defects will not be detected by post-fabrication or in-service inspection [52]. The effect that these defects have on the life of a flawed structure can often be estimated through application of fracture mechanics and fatigue crack growth concepts.

The application of fatigue crack growth knowledge to estimate service life of flawed components involves a sequence of operations as indicated in Table 29. Step 1 is establishment of the initial flaw size. Step 2 indicates that the failure criterion must be established which then leads to a definition of the critical flaw size. The examples shown in Step 2 are applicable for setting the critical flaw size at either a critical plane strain fracture condition or a critical plane stress fracture condition. If a failure criterion other than that of complete fracture is used, the calculation is affected (for example, the failure criterion could be defined as the first flaw that can be detected in a given level of field inspection).

In Step 3, the cycles required to grow from the initial flaw size a_i , to the critical (or inspectable) flaw size are determined as indicated. Basically, the calculation simply involves tracing the growth as a crack length versus cycles curve from a_i to a_c as shown. If basic information on the fatigue crack growth behavior is available, the calculation is accomplished by using an equation which relates da/dN to K_{max} or ΔK . The output from the calculation is either allowable operating stress level or life.

Once the flaw growth analysis has been completed, the inspection requirements can be established. The flaw detection level required by the flaw growth analysis may be too stringent for the type of NDI specified. Table 30 presents flaw detectability limits for some common NDI methods. These results were obtained under laboratory conditions, with some surface flaw locations known before the test. Flaw detection limits for production parts have been estimated to be twice the levels shown, and flaw detection limits for structure during maintenance inspections estimated to be three times the levels shown [53, 54]. Detection of 3 mm(0.120 in.) surface flaws by penetrant inspection should be routine. However, 3 mm(0.120 in.) long embedded flaws, especially those with small volume, will be difficult to detect, even by ultrasonic techniques.

6.2 Proof Test Concepts

If the required initial flaw dimensions for component life are such that

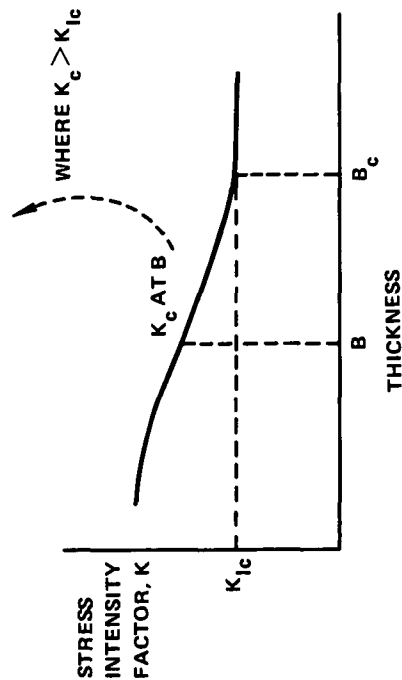
TABLE 29.- STEPS IN APPLYING FRACTURE MECHANICS CONCEPTS TO FATIGUE-CRACK PROPAGATION ANALYSIS

- I ESTABLISH INITIAL FLAW SIZE, a_i
 - a) MAXIMUM SIZE FLAW THAT CAN BE MISSED IN AN INSPECTION
 - b) ESTABLISH RELIABILITY, CONFIDENCE LEVEL
- II DEFINE FAILURE CRITERION AND DETERMINE CRITICAL FLAW SIZE FOR MATERIAL/THICKNESS/GEOMETRY COMBINATION
 - a) FROM K_{Ic} WITH THICKNESS (B) GREATER THAN B_c USE

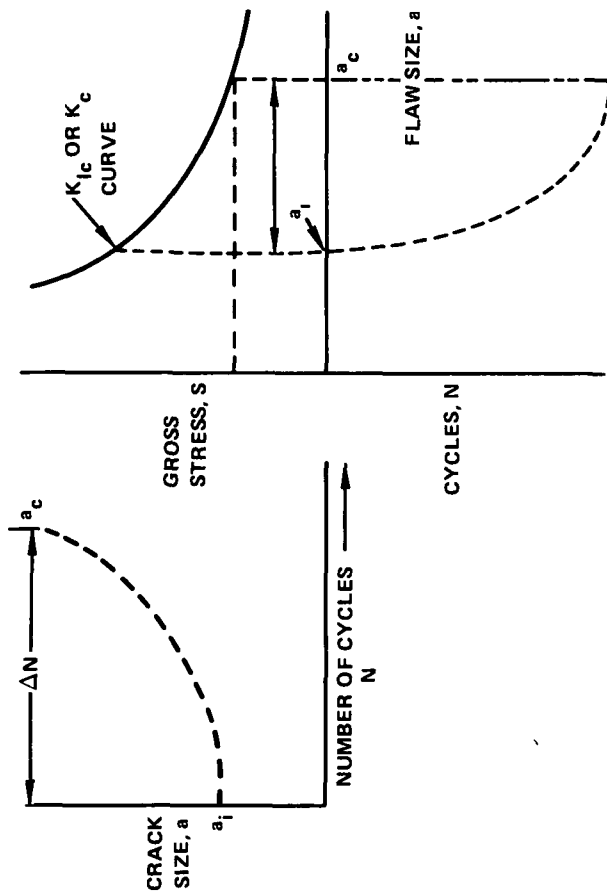
$$a_c = \frac{1}{\pi} \left(\frac{K_{Ic}}{S} \right)^2$$

- b) IF K_c GREATER THAN K_{Ic} FOR THE THICKNESS OF INTEREST USE

$$a_c = \frac{1}{\pi} \left(\frac{K_c}{S} \right)^2$$



- III CALCULATE CYCLES REQUIRED TO GROW CRACK FROM a_i TO a_c FROM FATIGUE-CRACK GROWTH LAW



INPUTS		OUTPUTS	
a_i, B K_{Ic} OR K_c a_c	ENVIRONMENT, TEMPERATURE OR CONTAMINANT (FREQUENCY, WAVE FORM) <u>BASIC MATERIAL PROPERTY DATA, C, N</u> STRESS (INCLUDING SPECTRUM) OR LIFE REQUIREMENT	PERFORM ANALYSIS TO YIELD OUTPUT $\frac{da}{dN} = f(\Delta K)$	OPERATING STRESS LEVEL (ALLOWABLE) OR LIFE

TABLE 30
FLAW DETECTABILITY LIMITS FOR VARIOUS NDT TECHNIQUES^a

Material	Inspection Technique				
	Visual ^b	Magnetic ^b Particle	Penetrant ^b	X-Ray ^c	Ultrasonic ^c Delta ^c Ultrasonic ^c
6.35 mm(0.25 in.) Extrusion ⁴⁶ 7075-T6511 4340 V	0.762(0.03) ^d 0.762(0.03)	- 7.62(0.30)	6.35 (0.25) 8.89 (0.35)	12.7(0.50) 12.7(0.50)	6.35(0.25) 5.08(0.20)
0.508 mm(0.020 in.) Plate ⁴⁷ 7075-T6 Ti-6Al-4V	- -	- -	1.02 (0.040) 0.813(0.032)	- 1.778(0.070)	- 1.27(0.050) 2.54(0.100)
3.2 mm(0.125 in.) Plate ⁴⁸ 7075-T6 Ti-6Al-4V	- -	- -	0.762(0.030) 1.27 (0.050)	- 3.30 (0.130)	- 2.29(0.090)
12.7 mm(0.500 in.) Plate ⁴⁸ 7075-T6 Ti-6Al-4V	- -	- -	0.889(0.035)	11.68 (0.460) -	7.37(0.290) 3.81(0.150)
					2.29(0.090)

a. 100 percent detection level in laboratory tests

b. Surface flaws of known location

c. Both known surface flaws and unknown embedded flaws

d. Crack lengths are in mm(in.)

reliable detection is not possible within the state-of-the-art of NDI, or if 100 percent reliability is required where NDI cannot be conducted, a proof test philosophy must be considered [56]. Proof testing is one method of detecting and eliminating small flaws which has found wide-spread use in assuring adequate life for spacecraft pressure vessels [57,58].

The first step in this method requires construction of a plot of flaw size versus estimated life, as shown in Fig. 103. If N_f is the desired design life in cycles, the initial flaw size must be $\leq a_i$ so that any crack-like defects will not grow to critical dimensions during the required design life. The absence of flaws larger than a_i can be guaranteed by application of a stress (σ_{OP}), since flaws of that size would produce failure during the proof cycle, Fig. 104.

6.3 Rotor Design Life Analysis Procedures

The above described life and proof test analysis procedures were used to establish the general procedures that should be used to ensure the design life of a rotor component. Because of the short life requirements, high stress fields and difficulties of inspection of a rotor, the proof test concept is considered the most likely to ensure rotor life. Therefore, the following procedure for ensuring rotor design life against bore failure by proof spinning is suggested:

- (1) Establish desired life in cycles, N_{DL} .
- (2) Obtain tensile properties, fracture toughness, and crack propagation data.
- (3) Define rotor operating conditions (particularly, predicted cycle history).
- (4) Define rotor stress distribution.
- (5) Based on Steps 1 to 4, calculate maximum allowable crack length, a_c , for the conditions of a surface flaw such that burst will not occur (assumes surface flaw crack propagation properties are the same as through crack).

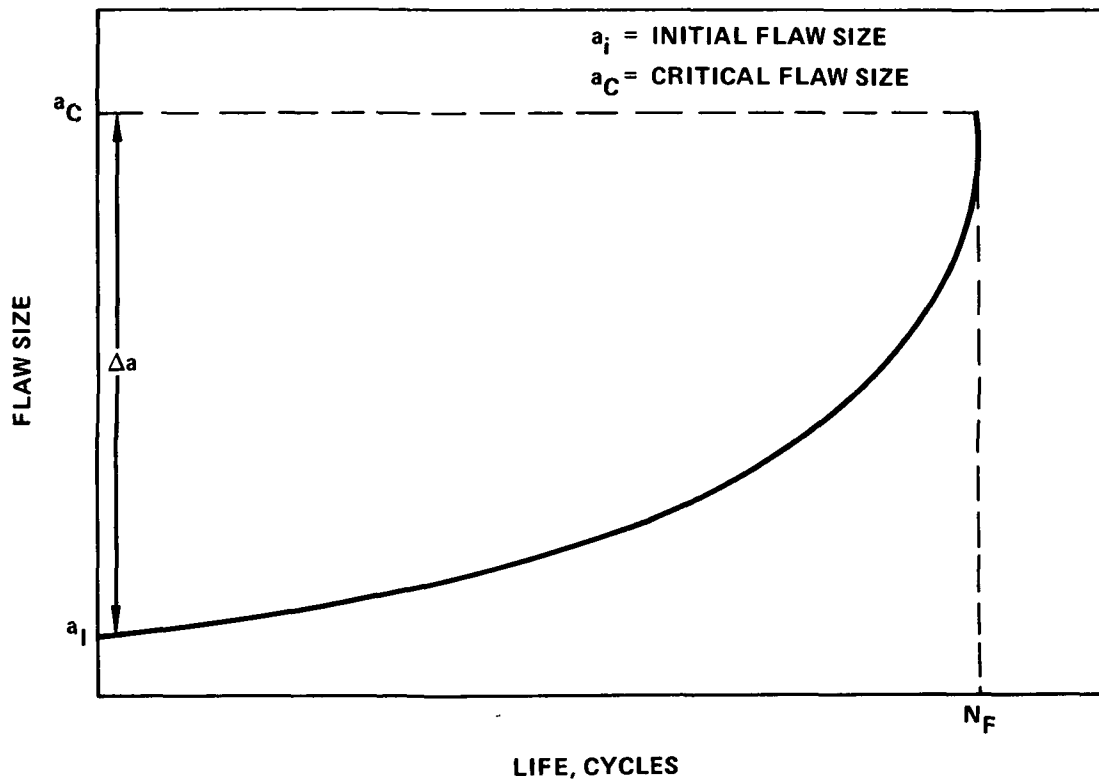


Figure 103. - Relationship Between Flaw Size and Estimated Life for an Assumed Maximum Operating Stress

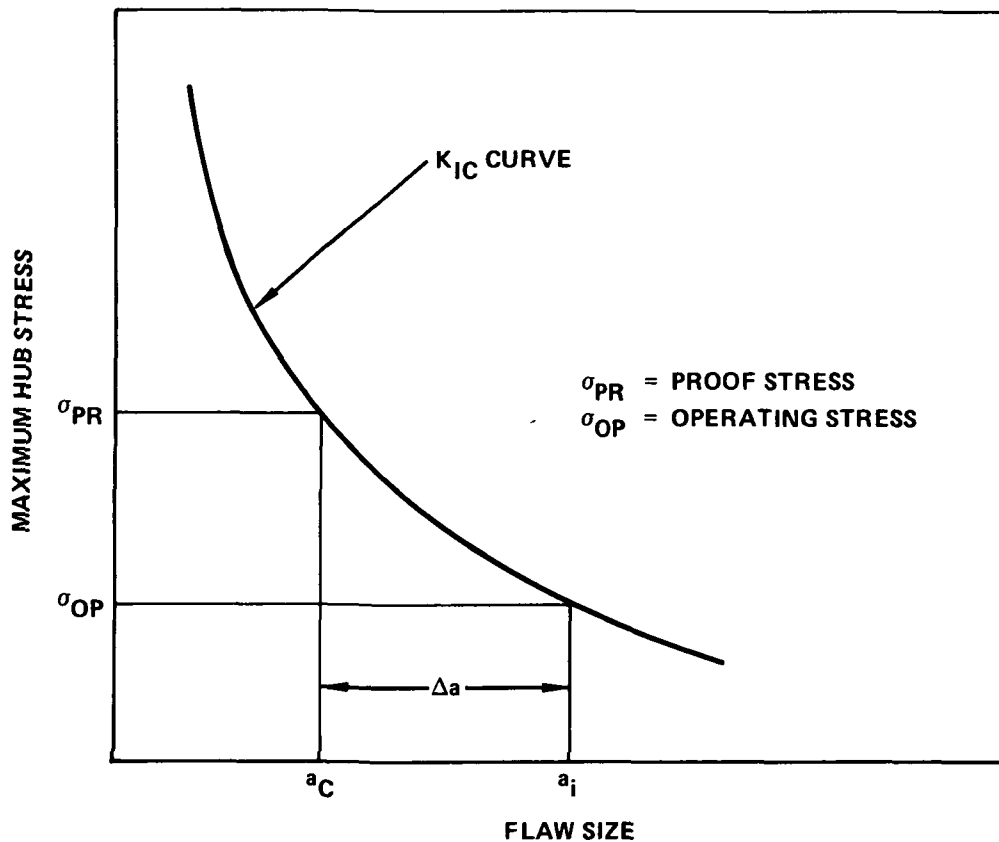


Figure 104. - Establishment of Minimum Flaw Size by Proof Testing

- (6) Based on Steps 1 to 4, calculate maximum allowable initial crack length to ensure rotor design life (this step must be performed for different $a/2c$ ratios if a surface flaw is assumed).
- (7) Establish proof spin test needed to screen a_i determined in Step 6.
- (8) Develop plots of rotor life, N , versus a_i (for different $a/2c$ ratios if a surface flaw is assumed).
- (9) Develop plots of proof stress, S_p , versus a_i (for different $a/2c$ ratios if a surface flaw is assumed).
- (10) Check to ensure rotor proof speed, N_p is less than rotor burst speed N_b , for maximum allowable flaw size, a_i .

6.4 Example of Rotor Design Life Analysis Procedure

Because the exact local bore stress distribution is not known for the liquid hydrogen rotor, an example of applying the life analysis procedure will be discussed using a parallel-sided thin disk. The disk will be assumed to be geometrically the same as those tested in this program. Critical flaw location will be assumed at the bore and crack shape as a through thickness crack propagating in the radial direction. The life analysis procedure will be described using each of the steps listed in Section 6.3.

Step 1. Design life will be assumed to be minimum of 400 cycles.

Step 2. Tensile, fracture toughness, and crack propagation properties have been previously determined at room temperature and $-253^{\circ}\text{C} (-423^{\circ}\text{F})$ in LH_2 , at two R ratios and various frequencies. Laboratory coupon results were compared to spin pit results (see Section 5).

Step 3. Rotor operating conditions are defined as $-253^{\circ}\text{C} (-423^{\circ}\text{F})$ in liquid hydrogen. Cycles will be assumed to be applied at irregular intervals and with various hold times up to a few minutes duration. No crack growth will be assumed to occur during shutdown and load ratio will be assumed as $R = 0.05$. Based on the data collected in Step 2,

frequency and hold time affects will be ignored as a variable. The fatigue crack growth curves of Section 5.3, Figs. 98 and 99, will be used in the life analysis.

Step 4. Since this example is for a parallel sided thin disk, the appropriate Timoshenko [24] stress distribution described in Section 2 will be used. Since the rotor is a low cycle life component, the maximum bore stress at $-253^{\circ}\text{C}(-423^{\circ}\text{F})$ must be high otherwise the life would be much longer than 400 cycles. Therefore, based on the limited literature data [59], a maximum operating bore stress equivalent to 0.9 times the σ_{ult} will be assumed for this example. This results in an assumed maximum bore stress at $-253^{\circ}\text{C}(-423^{\circ}\text{F})$ of 1310 MPa (190 ksi).

The assumed operating cycle representing a reasonable simplification of the disk cycle can now be described as: a sinusoidal wave of frequency 1 cycle/minute, R ratio of 0.05, maximum stress of 1310 MPa (190 ksi) and minimum stress of 58.6 MPa (8.5 ksi) equivalent to engine idle. This corresponds to a rotor speed variation between 88,983 rpm and 15,863 rpm.

Step 5. To calculate the critical crack length, a_c , at failure, Equation (17) must be used in the form:

$$f \sqrt{\pi a} = K / \rho \omega^2 R_i^2 \quad (23)$$

where f is defined as before and K is chosen as

$$K_c = 65.9 \text{ MPa} \sqrt{\text{m}} \quad (60 \text{ ksi} \sqrt{\text{in.}}).$$

Solving Equation (23) by trial and error resulted in an a_c of 0.775 mm (0.0305 in.).

Step 6. The maximum allowable initial flaw size, a_i , is calculated by integrating the da/dN vs. ΔK curve of Fig. 101 using the appropriate stress intensity analysis for the disk. The integration is started at a low enough a_i value such that the calculated life to a_c is equal to or greater than the design life. Calculation of life was conducted similar to that previously described in Section 4.7 for WOL

coupons except that the appropriate stress intensity expression for the disk was used. The initial crack length was found by an iterative procedure to be 0.057 mm (0.0022 in.) for the minimum design life of 400 cycles. To allow for a reasonable factor of safety, say 3, design life would be 1200 cycles and a_i becomes 0.019 mm (0.00076 in.).

Table 31 shows the effect of different maximum speed levels on a_i for an N_{DL} of 400 cycles and a safe life of 1200 cycles, N_{SL} . Comparing the a_i values of Table 31 with the flaw detectability limits of Table 30, maximum operating speeds of 60,000 rpm or higher preclude reliable detection of a_i for N_{SL} and of 70,000 rpm or higher for N_{DL} . This conclusion helps justify the proof test concept. However, the validity of the concept can be questioned by the fact that for speeds above 70,000 rpm, a_i is equal to or smaller than the grain size. The effect of a proof test on such small flaws is unknown. This is especially true as to the possibility and extent of a first cycle tear. Such a tear would decrease the initial flaws listed in Table 31, since this effect was not taken into account.

Step 7. The proof spin needed to assure the design life of this example rotor must now be established based upon the a_i determined in Step 6. The easiest type of proof test would be a room temperature proof spin. At room temperature, the onset of plastic flow at the bore would occur above 68,800 rpm. At this speed, the shortest crack which could be proofed would be 19.94 mm (0.785 in.) assuming a maximum K_{IQ} of 104.4 MPa \sqrt{m} (95 ksi $\sqrt{in.}$) for the disk at room temperature. Clearly, a flaw of this size precludes a room temperature proof for the a_i flaws listed in Table 31 for speeds greater than 50,000 rpm unless the bore of the disk is allowed to yield. However, such yielding would introduce a dimensional change in the rotor disk, a usually unacceptable practice.

Therefore, to proof cycle this example disk and thus guarantee no flaws $\geq a_i$, a cryogenic proof cycle must be employed. At -253°C (-423°F) onset of bore plastic flow does not occur until a speed of 91,295 rpm is reached. At this speed, using a K_Q of 66 MPa \sqrt{m} (60 ksi $\sqrt{in.}$), a flaw of 0.691 mm (0.0272 in.) or greater would cause

TABLE 31

EFFECT OF MAXIMUM ROTOR DESIGN OPERATING SPEED ON
INITIAL AND CRITICAL CRACK LENGTHS

Test Conditions: $R = 0.05$

$-253^{\circ}\text{C} (-423^{\circ}\text{F})$

Maximum Speed N_{max} , rpm	Maximum Tangential Bore Stress, σ_{Tmax} , MPa (ksi)	Initial Crack Length, a_i , mm(in.) ⁱ		Critical Crack Length, a_c , mm (in.) ^c
		Cycle Life		Cycle Life
		400 N_{DL}	1200 N_{SL}	400
90,000	1340 (194.4)	0.0508 (0.0020)	0.0178 (0.0007)	0.7366 (0.0290)
88,983	1310 (190.0)	0.0559 (0.0022)	0.0198 (0.00078)	0.7747 (0.0305)
80,000	1059 (153.6)	0.1422 (0.0056)	0.0432 (0.0017)	1.285 (0.0506)
70,000	810.8(117.6)	0.4572 (0.018)	0.1448 (0.0057)	2.705 (0.1065)
60,000	595.7(86.4)	3.150 (0.124)	0.9017 (0.0355)	11.07 (0.436)
50,000	413.7(60.0)	25.4 (1.0)	15.75 (0.620)	37.29 (1.468)

burst. Thus, to insure the minimum 400 cycle design life, a cryogenic proof cycle would be inadequate for maximum service speeds greater than 67,000 rpm or for a more conservative 1200 cycles, speeds greater than 61,000 rpm. These speeds correspond to maximum service bore tangential stresses of 742.6 MPa (107.7 ksi) and 615.7 MPa (89.3 ksi), respectively. These limits on the applicability of a proof cycle test will be reduced to even lower speeds if crack growth can occur during the proof cycle since the crack length after proof could be larger than that calculated based on the proof speed.

The primary conclusion for this example based on this analysis is that to insure a safe life of 1200 cycles for speeds greater than 61,000 rpm (maximum tangential bore stresses greater than 615.7 MPa (89.3 ksi)), the example disk cannot be proof cycled at room temperature or at cryogenic temperatures without plastically deforming the disk. The reasons for the inadequacy of the proof cycle at these two temperatures eliminates a proof cycle at any other temperature. Non-destructive examination of the disk prior to service will also not be adequately reliable for the same speed ranges. Interestingly, the minimum inspectable flaw size of 0.889 mm (0.035 in.) is extremely close to the minimum flaw size that can be guaranteed by a proof cycle (0.691 mm (0.0272 in.)) provided no crack growth occurs during the proof cycle. Finally, Table 31 indicates that periodic inspection of disks cycled at maximum speeds above 70,000 rpm is valueless because of the small a_c values.

For disks cycled at maximum speeds below 60,000 rpm, either a cryogenic proof cycle or adequate inspection techniques could be used to insure life. However, at these low speeds, maximum tangential bore stresses are so low compared to σ_{ys} that typical machining, forging, or other such defects are unlikely to be large enough to be of concern. In essence, at maximum operating speeds and stresses of normal concern in small disk service design ($> 60,000$ rpm, $> \sim 690$ MPa (100 ksi)), the life of this example disk cannot be ensured by either proof cycling or NDI techniques. At lower speeds, initial defects of normal size (~ 1.27 to 2.54 mm (0.050 to 0.10 in.)) are so short compared to a_c that disk life is in the 10^4 to 10^7 cycle range and proof testing is irrelevant and only simple NDI of concern.

The situation below 60,000 rpm is a stress and rpm range not usually of concern to small rotor design.

All of the above discussion pertained only to a load ratio of 0.05. Table 32 compares the effect on a_i and a_c of cycling the example disk at $R = 0.5$ instead of 0.05. Essentially, at $R = 0.5$, a_i is slightly longer than at $R = 0.05$, but a_c is significantly shorter. Thus, Δa for the same life is considerably shorter at $R = 0.5$ than at $R = 0.05$.

Based on Table 32 the conclusions described as to the inadequacy of a proof cycle or NDI at rotor speeds above 60,000 rpm remained the same.

A procedure suggested by Bowie [60] for insuring the design life of this example disk against failure due to a bore crack would be to perform a room temperature proof cycle prior to final machining at a speed in excess of the speed required for the onset of bore yielding. This proof cycle would result in a compressive residual stress field at the bore. If the compressive residual stress field was large enough, the maximum tangential bore stresses during subsequent cycling at -253°C would be reduced to a level such that the minimum initial flaw size needed to insure design life would be of an inspectable size. Alternatively, a test program could be conducted to determine the flaw size screened by a proof speed which causes plastic flow at the bore. In either case, final machining of the disk would have to be performed after the proof cycle. Of major concern in such an approach would be prevention of compressive yield during the proof cycle and the assumption that the disk would not show evidence of work softening or hardening during post-proof service cycles.

Applying the theory of elastic perfectly-plastic disks and assuming a Tresca yield criteria, Fig. 105 shows the tangential and radial stresses during a proof cycle at room temperature at 90,000 rpm. The stress distributions of Fig. 105 and the three following figures were calculated using the procedure of Bowie [61]. Figure 106 shows post-proof residual stresses. After the proof cycle, assume that the disk was subjected to the same load cycle discussed in Step 4. Figure 107 shows tangential and radial stress at -253°C at the assumed speed of 88,983 rpm without a prior proof cycle. Stresses after the above described proof cycle are

TABLE 32

EFFECT OF LOAD RANGE RATIO, R, ON INITIAL AND CRITICAL CRACK LENGTHS

Operating Conditions: $-253^{\circ}\text{C}(-423^{\circ}\text{F})$
 $N_{DL} = 400 \text{ cycles}$

Maximum Rotor Speed, N_{max} , rpm	Maximum Tangential Bore Stress, $\sigma_{\theta \text{ max}}$, MPa.(ksi)	Initial Crack Length, a_i , mm(in.) R = 0.05	Critical Crack Length, a_c , mm(in.) R = 0.05	Critical Crack Length, a_c , mm(in.) R = 0.5
90,000	1340 (194.4)	0.0508(0.0020)	0.1041(0.0041)	0.7366(0.0290)
80,000	1059 (153.6)	0.1422(0.0056)	0.2083(0.0082)	1.285 (0.0506)
70,000	810.8(117.6)	0.4572(0.018)	0.4318(0.0170)	2.705 (0.1065)
60,000	596.7(86.4)	3.150 (0.124)	0.9728(0.0383)	11.07 (0.436)
50,000	413.7(60.0)	25.4 (1.00)	2.875 (0.1132)	37.29 (1.468)
				0.1880(0.0074)
				0.3048(0.0120)
				0.5410(0.0213)
				1.095 (0.0431)
				3.005 (0.1183)

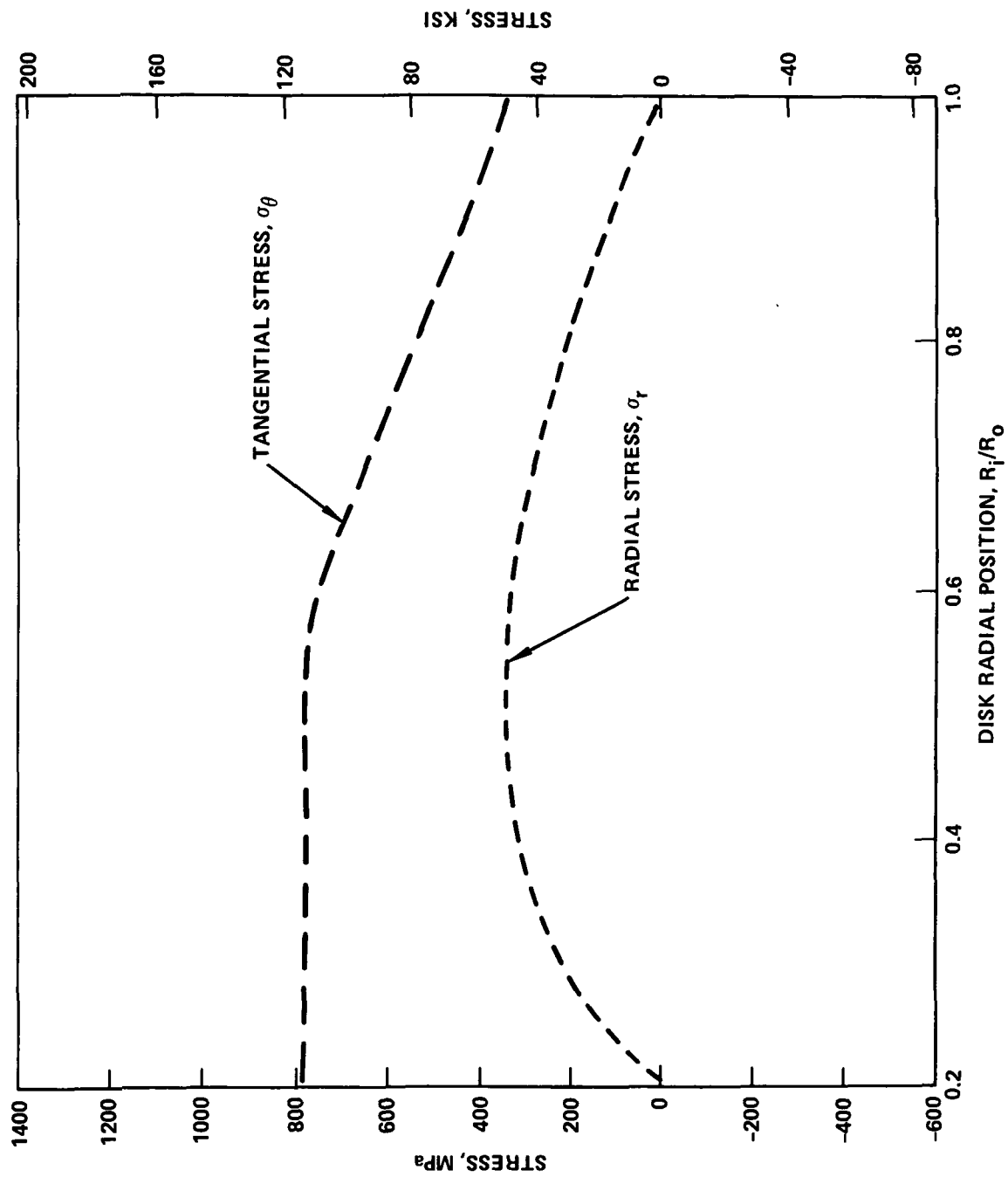


Figure 105. - Tangential and Radial Stress Distributions of Example Disk During Room Temperature Proof Cycle at 90,000 rpm

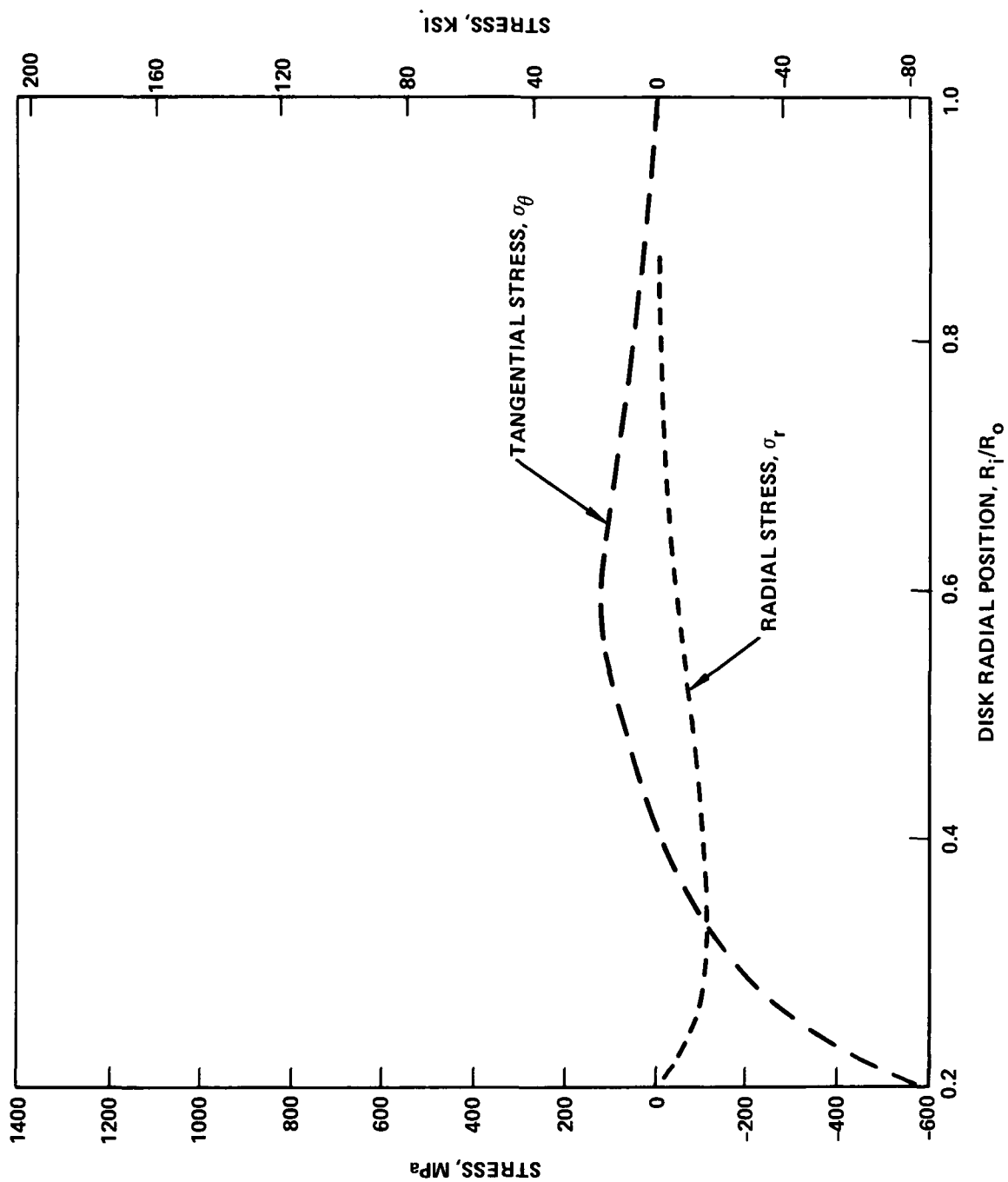


Figure 106. - Tangential and Radial Stress Distribution of Example Disk at 0 rpm After Proof Cycle

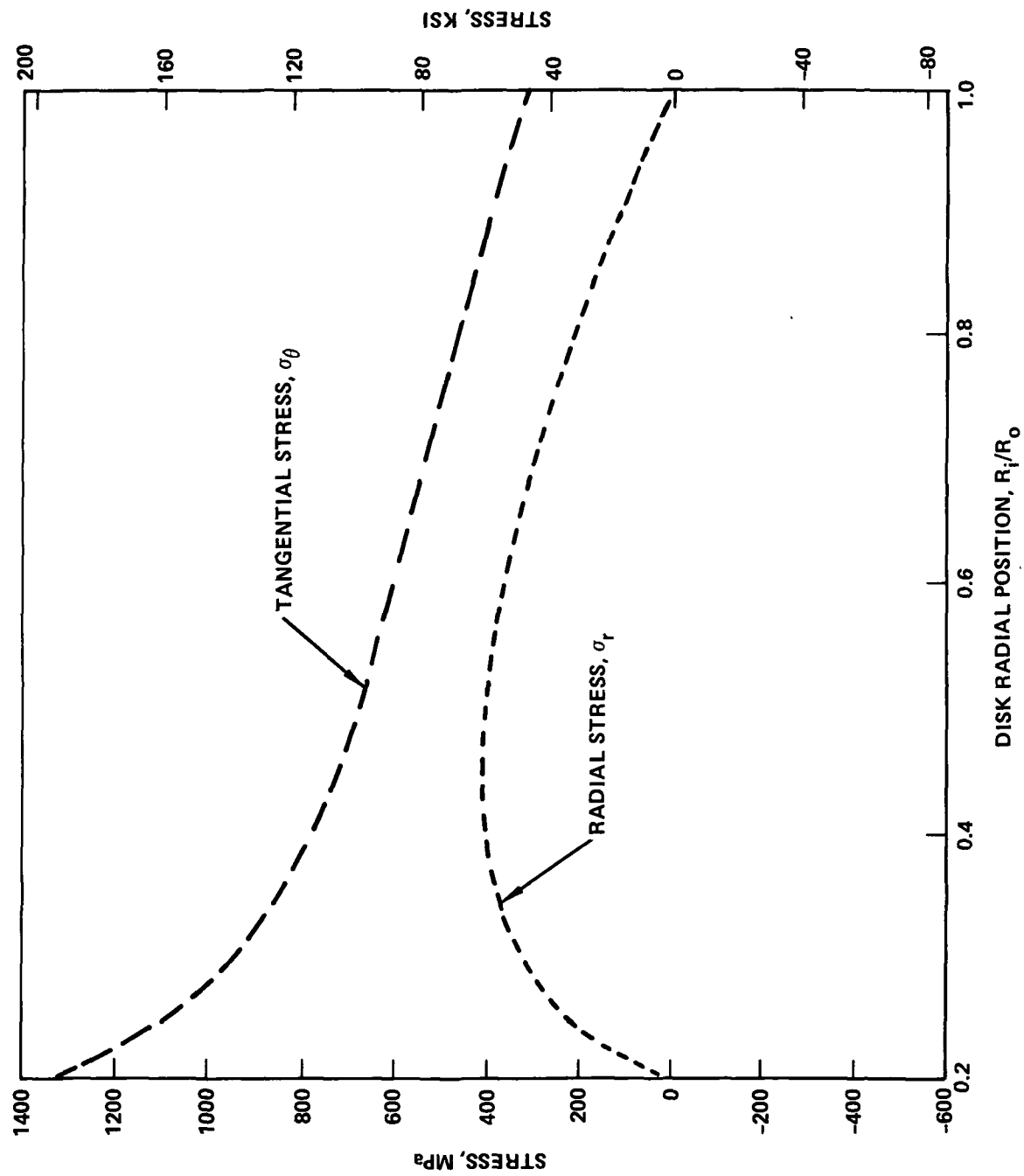


Figure 107. - Tangential and Radial Stress Distributions of Example Disk at -253°C (-423°F) and at 88,983 rpm Without Prior Proof Cycle

shown in Fig. 108. The stress distribution during service can be seen in Fig. 108 to be greatly changed by the proof cycle. Any crack growth analysis would have to take this new stress field into account during calculation of an expression for stress intensity. The reduced bore stresses of Fig. 108 due to the proof cycle are low enough that quite possibly the minimum a_1 has reached a size that can be reliably inspected.

During the proof cycle discussed above for the example disk, an unnotched spin test specimen would experience a hoop stress virtually equal to the nominal yield stress from the 12.7 mm (0.5 in.) radius bore outward to a radius of 37.4 mm (1.458 in.). Therefore, extreme importance is given to determining whether present fracture mechanics test techniques applied to disks are suitable for prediction of the amenability of the disk material to initial flaw screening in a nominal stress field at the yield condition. The key question is: given a reasonable critical flaw size at the bore of the spin test specimen, does the disk material have sufficient fracture toughness in a uniform stress field at the yield condition such that rapid crack propagation would not occur during the proof cycle?

Step 8,
9 & 10. Since a proof speed could not be found for the example service disk at speeds of normal interest, the application of these steps will be ignored. : .

6.5 Applications to Practical Rotor Design

Practical disk geometry is normally of variable thickness. This fact is the primary difference which affects bore stresses between disks designed for service and the example parallel sided disk discussed in Section 6.4. Thickness variations can drastically change the radial and tangential stress distribution. In normal practice, bore stresses are reduced because disk thickness decreases from the bore to the rim. The only effect of a different bore to rim stress distribution on the concepts presented in

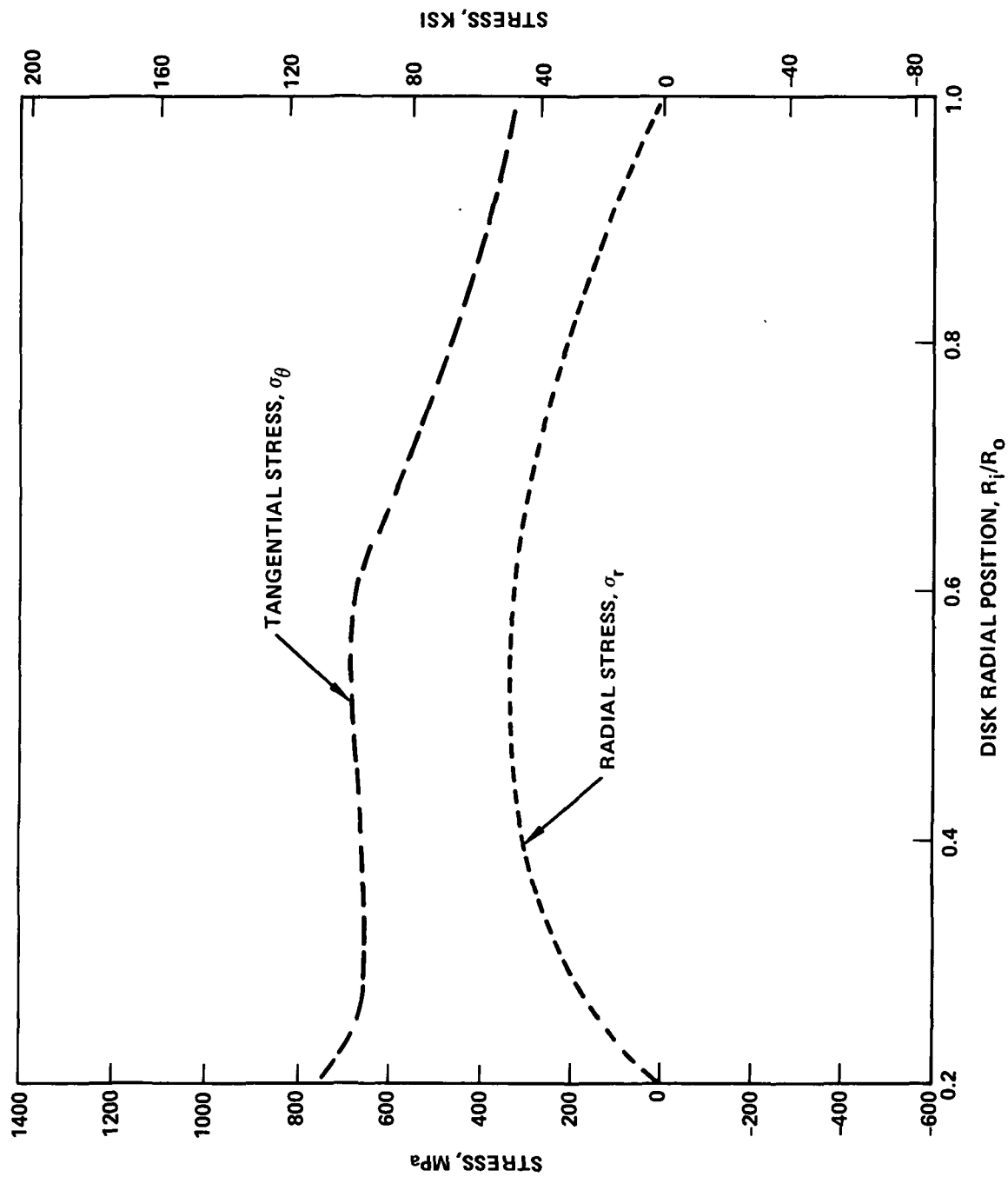


Figure 108. - Tangential and Radial Stress Distributions of Example Disk at -253°C (-423°F) and at 88,983 rpm after Prior Proof Cycle at 90,000 rpm at Room Temperature

Sections 6.1 to 6.4 is that a new stress intensity analysis must be undertaken for a variable thickness disk. If the superposition analysis method of Grandt [25] is used, the result would be unique for each disk geometry. In general, such an analysis is not a particularly formidable task.

The stress intensity calculation for a service disk would also be affected by the fact that the flaws of interest are surface cracks or imbedded flaws. Stress intensity analyses of some validity have been conducted for such flaws [62-65]. They would, of course, have to be used when applying the concepts discussed in Sections 6.1 to 6.4 to a service rotor.

Despite the necessity of a new stress intensity expression for a variable thickness disk, the conclusions of Section 6.4 remain the same for a disk designed for the -253°C (-423°F) liquid hydrogen environment. These conclusions are: (1) for maximum service bore stresses of normal interest ($\sigma_{\text{max}}/\sigma_{\text{ys}} > 0.5$), design life cannot be adequately insured by: (a) a proof cycle at room temperature, (b) a proof cycle at 253°C ; (c) NDI, unless flaws less than ~ 0.9 mm (0.035 in.) can be detected with better than 95% reliability and 90% confidence; (2) a room temperature proof cycle at the proper speed in excess of that necessary to insure the onset of bore plasticity may be adequate to insure design life; (3) if $\sigma_{\text{max}}/\sigma_{\text{ys}}$ is < 0.5 then a proof cycle is probably not needed to insure design life and a simple NDI detection of flaws 2.54 mm (0.1 in.) or larger would be adequate.

There have been rotor designs in which allowable initial flaw sizes were of a size such that they could be reliably found by inspection or could be proofed by a proof cycle [63-65]. However, these were specific cases of large diameter turbine generator rotors where for the stress levels normally encountered a_i was fairly large (> 7.6 mm (0.3 in.)). Such a situation was shown in Section 6.4 not to be the case for the small rotors designed for cryogenic service environment considered in this program.

Page Intentionally Left Blank

7.0 CONCLUSIONS AND RECOMMENDATIONS

7.1 Conclusions

Based on the results of this program, several major conclusions have been drawn. Conclusions pertaining to concepts of proof cycling and NDI for flaw screening apply specifically to the bore region of relatively small diameter rotors for cryogenics applications. However, with proper concern for operating environment differences, the procedures and results on which the conclusions are based are pertinent to much larger disks and other operating environments. The conclusions are:

- o Consistent homogeneous forgings were made from the Ti-5Al-2.5Sn(ELI) alloy. The major problem of future concern is prevention of die-lock and associated cracking.
- o Tensile and fracture toughness properties were excellent, met all specifications and were consistent with data available in the literature.
- o The experimental compliance calibration results of the WOL geometry was unchanged at -253°C (-423°F) when compared to the results at room temperature.
- o At room temperature and at -253°C (-423°F) in liquid hydrogen, no discernable effect of frequency or coupon orientation within the pancakes on fatigue crack propagation behavior was observed.
- o An increase in load ratio, R , increased fatigue crack growth rates.
- o Fatigue crack growth rates at -253°C (-423°F) were similar to room temperature growth rates at low ΔK levels, but faster at high ΔK levels due to the decrease in fracture toughness.

- o Results of burst tests of rotating disks were consistent for unflawed and flawed disks. Toughness values for disks with intermediate crack lengths and which remained elastic until failure correlated closely to WOL coupon data. Disks with long cracks failed due to stress rupture with lower K_{IQ} values than WOL coupons.
- o Fatigue crack growth data for rotating disks closely matched data for WOL coupons provided they were tested at similar initial K_{max} levels.
- o The fatigue cycle life of rotating disks could be predicted from WOL data only by accounting for the large initial crack growth rate caused by the first cycle of load. This initial high growth rate was caused by a large tear on the first cycle of load and occurred on each disk used for crack growth study and on all three WOL coupons used to simulate the disk data.
- o A proof cycle, if successfully applied, can retard subsequent growth due to the large plastic zone induced and in spite of the associated tear in crack length.
- o The probability of a tear during proof or first service load cycle is extremely high at room temperature and must be assumed to occur with equal probability at -253°C (-423°F). This problem in itself may preclude any elastic proof cycle.
- o Rotor disks of the type considered in this program, designed for use at cryogenic temperatures, and operating at stresses normally encountered ($\sigma_{max}/\sigma_{ys} > 0.5$) cannot be proof cycled without plasticity at room temperature and still adequately insure design life. Such disks also cannot be advantageously proof cycled without plasticity at cryogenic temperatures.
- o The reasons for failure of the proof cycle concept are:
 - (1) minimum flaw size determined by the proof cycle is likely to be greater than that needed to insure life; (2) high probability of crack tear during proof.

- o Guarantee of design life by NDI flaw screening is probably inadequate.
- o The apparent failure of NDI to insure design life is due to the probability that the minimum reliably detectable flaw size is greater than that needed to insure design life.
- o The only type of proof cycle which may be adequate to insure design life is one in which compressive residual stresses at the bore are induced after the cycle. Such a proof cycle would have to be followed by final machining of the disk due to dimensional changes during the proof cycle. This plastic proof cycle would have to be adequately examined to insure validity.

7.2 Recommendations

Based on the conclusions of Section 7.1, the following recommendations are offered for rotors of the type considered in this program and designed for use at cryogenic temperatures.

- o Reliably determine that the maximum bore stress, σ_{\max} , of the rotor of interest is or is not in excess of $0.5 \sigma_{ys}$.
- o If σ_{\max} is $< 0.5 \sigma_{ys}$, adequate assurance of design life should be made by instituting NDI screening for flaws. Flaws of concern will be in excess of 0.1 in. and probably much larger.
- o If σ_{\max} is $> 0.5 \sigma_{ys}$, adequate assurance of design life should be attempted by commencing a program to intensively study the plastic proof cycle concept. Such a study should be both analytical and experimental and carefully consider the effects of such a proof cycle on possible changes in rotor design concepts. If this study is not undertaken, then assurance of design life can only be attempted by being based on an extremely conservative low cycle fatigue analysis founded on a large statistically adequate data base.

Page Intentionally Left Blank

APPENDIX

The fatigue crack propagation data developed during the course of this program using WOL coupons is presented in the following sections. The data is presented in tabular as well as graphical form for each test coupon. Hopefully this will permit ready use of the data in subsequent investigations. Test methods, data reduction procedures, and coupon identification codes were presented in preceding sections of this report.

Data is presented in the following sections in the order listed below:

Section A1	RT, $R = 0.05$, $f = 10$ Hz
Section A2	RT, $R = 0.05$, $f = 0.1$ Hz
Section A3	RT, $R = 0.5$, $f = 10$ Hz
Section A4	RT, $R = 0.5$, $f = 0.1$ Hz
Section A5	RT, $R = 0.5$, $f = 1$ Hz & 0.0167
Section A6	-253°C , $R = 0.05$, $f = 10$ Hz
Section A7	-253°C , $R = 0.05$, $f = 0.1$ Hz
Section A8	-253°C , $R = 0.5$, $f = 10$ Hz
Section A9	-253°C , $R = 0.5$, $f = 0.1$ Hz

A complete listing of test conditions is shown at the top of each data sheet and at the bottom of each figure. For all coupons, data listed is based on optical crack length readings, but is followed by a listing comparing optical to compliance results. The crack bow correction listed just above each data tabulation refers to the extent of crack length added to the average of the optically based measurement to account for the bow in the crack front. Details of the reasons for and extent of this correction are discussed in Section 2.3.4 of the text of this report. The 2σ scatter bands shown on the figures are those for the entire data set tested at the conditions listed on the bottom of the figure.

Except for Coupon 7CR-2, the room temperature apparent modulus of elasticity was used to calculate the normalized compliance term for comparing compliance based a/w calculations to optical based a/w measurements. This room temperature E value was used because all compliance measurements were taken at room temperature except for coupon 7CR-2.

SECTION A1

This section of the Appendix includes all fatigue crack growth data obtained from WOL coupons tested at room temperature, at a range ratio of 0.05, and at a frequency of 10 Hz.

(W8)1SPEC.7CR-1 Y1-5AL-2.5SN(EL) R0.05 F10 HZ * * * * * W E D G E * * * * * L 0 A D * * * * * P R O G R A M * * * * * 11108 AUG 18, 1976

INPUT CONSTANTS:

RANGE RATIO(R) * * * * * .05
 TEST FREQUENCY(HZ) * * * * * 10.0
 SPECIMEN WIDTH(W) * * * * * 51.003 MM(2.008 IN.)
 SPECIMEN THICKNESS(B) * * * * * 19.976 MM(.747 IN.)
 CRACK BOW CORRECTION * * * * * 1.270 MM(.050 IN.)

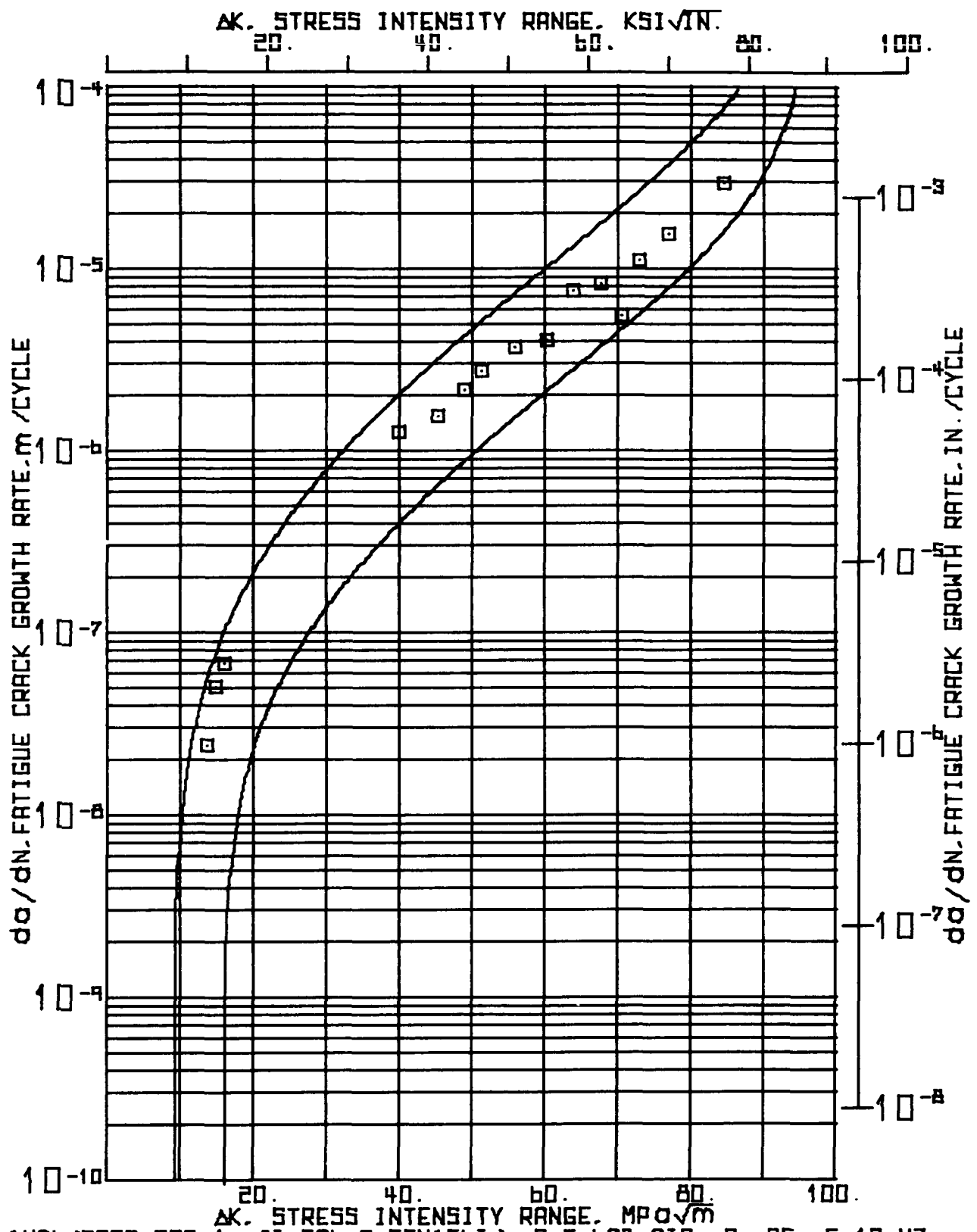
NUMBER OF CYCLES	P KN	MAXIMUM LOAD KIPS	SIDE 1		SIDE 2		CORRECTED AVERAGE CRACK LENGTH		CHANGE IN CRACK LENGTH		CHANGE IN CYCLES		CRACK GROWTH RATE DA / DN		STRESS INTENSITY RANGE	
			MM	INCH	MM	INCH	MM	INCH	MM	INCH	MM	INCH	MM	INCH	MPA X 1000.5	KSI X 1000.5
*000	8.01	1.80	16.59	.653	16.71	.658	17.92	.705	2.807	.110	100.000	28.07	1.10	13.61	12.39	
100.000	8.01	1.80	20.12	.792	18.80	.740	20.73	.816	.864	.034	25.000	34.54	1.36	14.83	13.50	
125.000	8.01	1.80	20.83	.820	19.81	.780	21.59	.850	1.689	.066	25.000	67.56	2.66	15.78	14.36	
150.000	8.01	1.80	22.38	.881	21.64	.852	23.28	.916								
150.000	17.79	4.00	22.38	.881	21.64	.852	23.28	.916	2.197	.086	2.000	1098.55	43.25	38.72	35.24	
152.000	17.79	4.00	24.66	.971	23.75	.935	25.48	1.003	2.273	.089	1.500	1515.53	59.67	43.73	39.80	
153.500	17.79	4.00	27.03	1.064	25.93	1.021	27.75	1.092	1.676	.066	1.000	1676.40	66.00	49.08	44.67	
154.500	17.79	4.00	29.36	1.156	26.95	1.061	29.43	1.158	2.400	.095	.500	4800.60	189.00	55.81	50.79	
155.000	17.79	4.00	31.34	1.234	29.77	1.172	31.83	1.253	.241	.009	.052	4640.38	182.69	61.01	55.52	
155.052	17.79	4.00	31.57	1.243	30.02	1.182	32.07	1.262	.305	.012	.051	5976.47	235.29	62.19	56.59	
155.103	17.79	4.00	31.90	1.256	30.30	1.193	32.37	1.274	.673	.027	.100	6731.00	265.00	64.39	58.60	
155.203	17.79	4.00	32.61	1.284	30.94	1.218	33.05	1.301	.864	.034	.100	8636.00	340.00	68.12	61.93	
155.303	17.79	4.00	33.55	1.321	31.72	1.249	33.91	1.335	1.194	.047	.100	11938.00	470.00	73.71	67.08	
155.403	17.79	4.00	34.72	1.367	32.94	1.297	35.10	1.382								

(WOL)SPEC.7CR-1 T1-5AL-2.5SN(ELI) R.T.LAB AIR R=05 F=10 HZ 11108 AUG 18, 1976

INPUT CONSTANTS

ELASTIC MODULUS(E) = $118.590E+03$ MPA($17.200E+06$ PSI)

NUMBER OF CYCLES N	CRACK MOUTH COMPLIANCE CER	ABAR / W OPTICAL BASE	COMPLIANCE BASE
X 1000			
.000	37.7472	.351	.365
100.000	44.1723	.406	.402
125.000	51.4005	.423	.438
150.000	56.2193	.456	.459
152.000	67.4631	.500	.501
153.500	81.9195	.544	.544
154.500	102.8010	.577	.592
155.000	118.8636	.624	.621
155.052	122.0761	.629	.626
155.103	126.6949	.635	.634
155.203	135.7294	.648	.647
155.303	148.0795	.665	.663
155.403	172.6735	.688	.690



(WOL) SPEC. 7RC-1 (I-SAL-2.55N(ELI) R T. LAB AIR R= 05 F=10 4Z

(W01)SPEC.7RC-1 T1-5AL-2.5SN(ELI) R.T.LAB AIR R0.05 F=10 HZ * * W E D G E * O P E N * L B A D * P R O G R A M * * 11108 AUG 18, '76

INPUT CONSTANTS:

RANGE RATIO(R) * .05
 TEST FREQUENCY(HZ) * 10.0
 SPECIMEN WIDTH(W) * 50.800 MM(2.000 IN.)
 SPECIMEN THICKNESS(B) * 19.014 MM(.749 IN.)
 CRACK 394 CORRECTION * 1.270 MM(.050 IN.)

NUMBER OF CYCLES	MAXIMUM LOAD	SIDE 1 CRACK LENGTH		SIDE 2 CRACK LENGTH		CORRECTED AVERAGE CRACK LENGTH		CHANGE IN CRACK LENGTH		CHANGE IN CYCLES		CRACK GROWTH RATE DA / DN MICR0 IN.		STRESS INTENSITY RANGE DELTA K	
		MM	INCH	MM	INCH	MM	INCH	MM	INCH	DN	X 1000	NANO- METER	PER CYCLE	MPA X 400.5	KSI X 1000.5
N	P	KN	KIPS												
000	8.01	1.80	17.07	.672	16.84	.663	18.22	.717	2.438	.096	100.000	24.38	.96	13.74	12.50
100.000	8.01	1.80	19.89	.783	18.90	.744	20.66	.813	1.257	.049	25.000	50.29	1.98	14.99	13.64
125.000	8.01	1.80	21.08	.830	20.22	.796	21.92	.863	1.689	.066	25.000	67.56	2.66	16.12	14.67
150.000	8.01	1.80	22.68	.893	22.00	.866	23.61	.929							
150.000	17.79	4.00	22.68	.893	22.00	.866	23.61	.929	2.527	.099	2.000	1263.65	49.75	39.96	36.37
152.000	17.79	4.00	25.07	.987	24.66	.971	26.14	1.029	2.019	.079	1.300	1553.31	61.15	45.36	41.28
153.300	17.79	4.00	27.05	1.065	26.72	1.052	28.16	1.108	.546	.021	.250	2184.40	86.00	48.95	44.54
153.550	17.79	4.00	27.64	1.088	27.23	1.072	28.70	1.130	1.092	.043	.400	2730.50	107.50	51.48	46.85
153.950	17.79	4.00	28.73	1.131	28.32	1.115	29.79	1.173	1.486	.058	.400	3714.75	146.25	55.93	50.90
154.350	17.79	4.00	30.28	1.192	29.74	1.171	31.28	1.231	.813	.032	.200	4064.00	160.00	60.45	55.01
154.550	17.79	4.00	31.04	1.222	30.61	1.205	32.09	1.263	.762	.030	.100	7620.00	300.00	63.90	58.16
154.650	17.79	4.00	31.80	1.252	31.37	1.235	32.85	1.293	.825	.032	.100	8255.00	325.00	67.73	61.64
154.750	17.79	4.00	32.61	1.284	32.21	1.264	33.68	1.326	.279	.011	.050	5588.00	220.00	70.62	64.27
154.800	17.79	4.00	32.89	1.295	32.49	1.279	33.96	1.337	.559	.022	.050	11176.00	440.00	72.96	66.40
154.850	17.79	4.00	33.40	1.315	33.10	1.303	34.52	1.359	.775	.030	.050	15494.00	610.00	76.95	70.03
154.900	17.79	4.00	34.19	1.346	33.86	1.333	35.29	1.389	1.473	.058	.050	29464.00	1160.00	84.56	76.96
154.950	17.79	4.00	35.79	1.409	35.20	1.386	36.77	1.447							

11108 AUG 18, '76

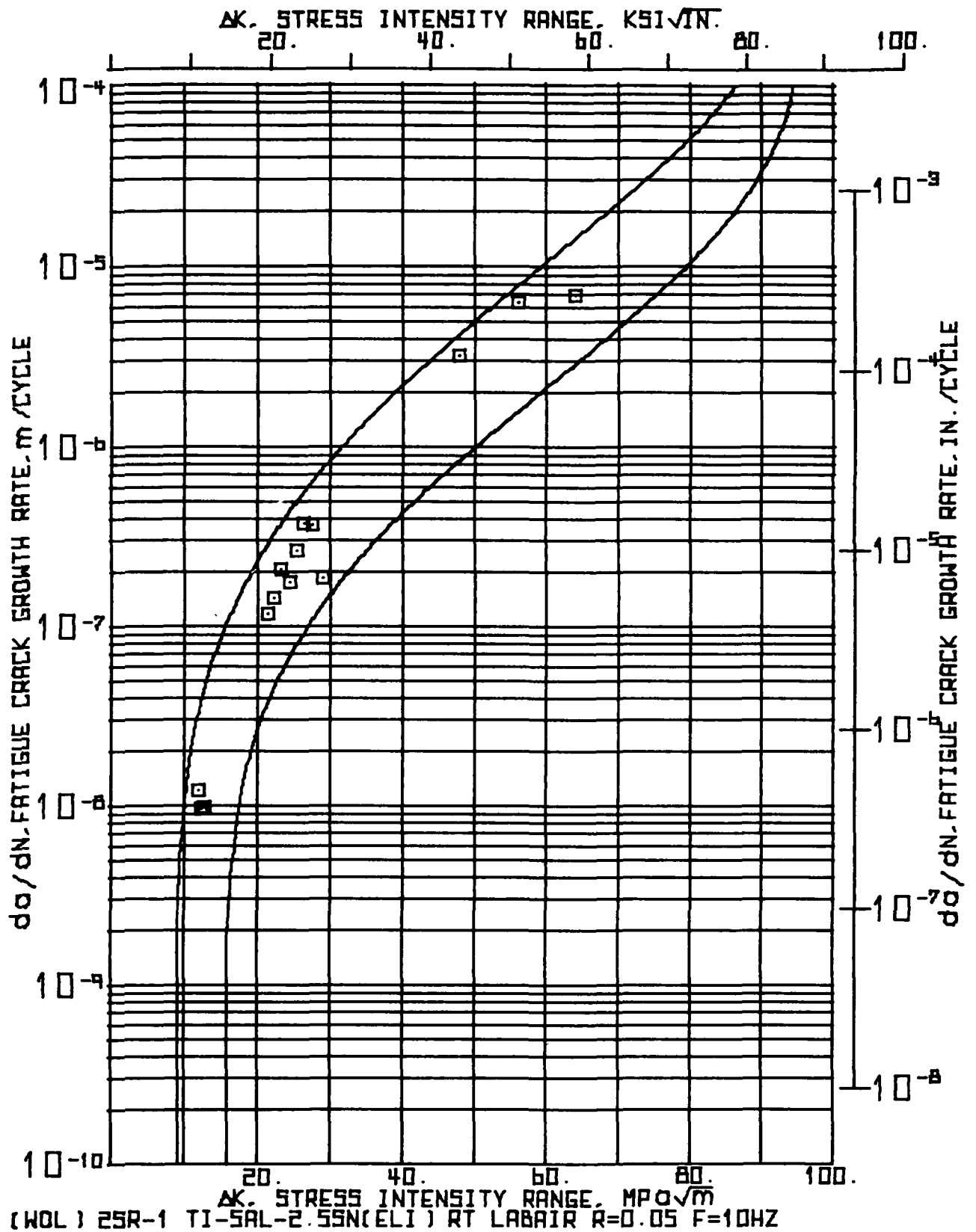
(W8L)SPEC.7RC-1 T1-5AL-2-55N(EL) R-1.LAB AIR R-05 F-10 HZ

INPUT CONSTANTS

ELASTIC MODULUS(E) = 118.590E+03 MPA(17.200E+06 PSI)

NUMBER CRACK MOUTH ABAR / W
OF COMPLIANCE OPTICAL COMPLIANCE
CYCLES BASE
N CEB

X 1000				
.000	37.0230	.359		.365
100.000	45.0657	.407		.407
125.000	49.1894	.431		.427
150.000	58.7464	.465		.469
152.000	70.8176	.514		.512
153.300	85.3030	.554		.553
153.550	90.1314	.565		.565
153.950	98.9836	.586		.584
154.350	112.6643	.616		.611
154.550	123.1260	.632		.628
154.650	131.9782	.647		.641
154.750	144.0494	.663		.658
154.800	149.6826	.668		.665
154.850	161.7537	.679		.678
154.900	184.2866	.695		.701
154.950	226.1333	.724		.733



(HBL) 255-1 T1-SAL-2.55SN(EL) RT LABAIR R0.05 F.10HZ * * W E D G E * 0 P E N * L 0 A D * P R 0 G R A M * * 1108 AUG 18, 1976

INPUT CONSTANTS:

RANGE RATIO(R) * .05
 TEST FREQUENCY(HZ) * 10.0
 SPECIMEN WIDTH(W) * 50.902 MM(2.004 IN.)
 SPECIMEN THICKNESS(B) * 18.961 MM(.746 IN.)
 CRACK 99A CORRECTION * 1.270 MM(.050 IN.)

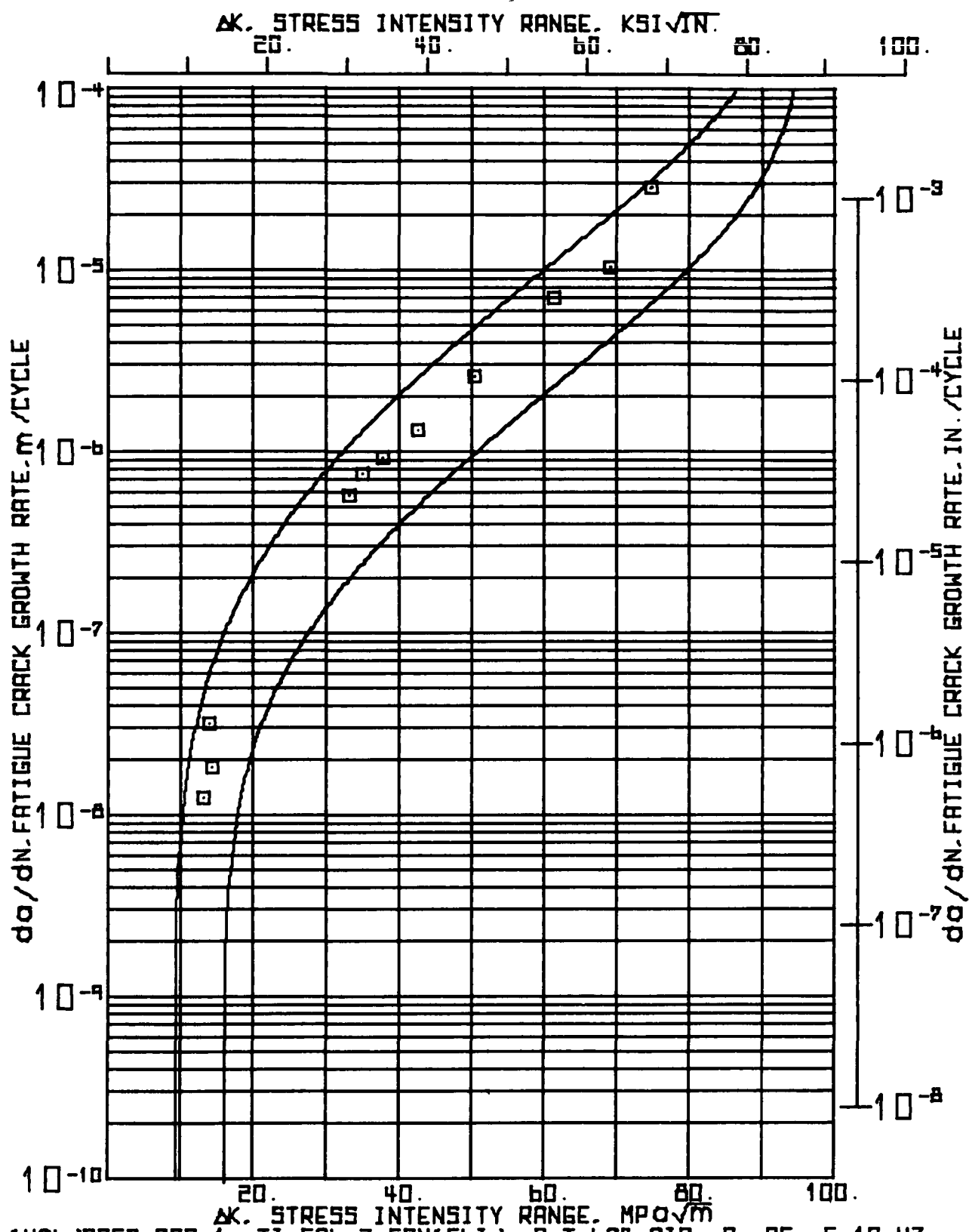
NUMBER OF CYCLES	MAXIMUM LOAD	SIDE 1 CRACK LENGTH		SIDE 2 CRACK LENGTH		CORRECTED AVERAGE CRACK LENGTH		CHANGE IN CRACK LENGTH		CHANGE IN CYCLES		CRACK GROWTH RATE		STRESS INTENSITY RANGE	
		KN	KIPS	MM	INCH	MM	INCH	MM	INCH	MM	INCH	DN X 1000	DA / DN MICR8 IN.	MPA X 1000.5	DELTA K IN00.5
N X 1000	P			A1	A2	ADAR									
.000	7.56 1.70	16.64	.655	16.64	.655	17.91 .705		.940	.037	80.000	11.75	.46	12.36	11.25	
80.000	7.56 1.70	17.45	.687	17.70	.697	18.85 .742		.737	.029	80.000	9.21	.36	12.84	11.68	
160.000	7.56 1.70	18.19	.716	18.44	.726	19.58 .771		.762	.030	80.120	9.51	.37	13.29	12.09	
240.120	7.56 1.70	18.95	.746	19.20	.756	20.35 .801									
240.120	12.01 2.70	18.95	.746	19.20	.756	20.35 .801		.762	.030	6.700	113.73	4.48	21.87	19.91	
246.820	12.01 2.70	19.71	.776	19.96	.786	21.11 .831		.762	.030	5.500	138.55	5.45	22.69	20.65	
252.320	12.01 2.70	20.47	.806	20.73	.816	21.87 .861		1.016	.040	5.000	203.20	8.00	23.70	21.57	
257.320	12.01 2.70	21.49	.846	21.74	.856	22.89 .901		.762	.030	4.500	169.33	6.67	24.78	22.55	
261.820	12.01 2.70	22.25	.876	22.50	.886	23.65 .931		.762	.030	3.000	254.00	10.00	25.77	23.46	
264.820	12.01 2.70	23.01	.906	23.27	.916	24.41 .961		.762	.030	2.100	362.86	14.29	26.83	24.42	
266.920	12.01 2.70	23.77	.936	24.03	.946	25.17 .991		.889	.035	2.500	355.60	14.00	28.06	25.53	
269.420	12.01 2.70	24.54	.966	25.04	.986	26.06 1.026		.902	.035	5.000	180.34	7.10	29.49	26.84	
274.420	12.01 2.70	25.68	1.011	25.70	1.012	26.96 1.061									
274.420	17.79 4.00	25.68	1.011	25.70	1.012	26.96 1.061		2.489	.098	.800	3111.50	122.50	48.22	43.88	
275.220	17.79 4.00	28.17	1.109	28.19	1.110	29.45 1.159		2.477	.098	.400	6191.25	243.75	56.37	51.30	
275.620	17.79 4.00	30.63	1.206	30.68	1.208	31.93 1.257		1.346	.053	.200	6731.00	265.00	64.31	58.52	
275.620	17.79 4.00	30.84	1.214	33.17	1.306	33.27 1.310									

(WBL) 2SR-1 T1.5AL-2.5SN(EL) RT LABAIR R-0.05 F-10HZ 11108 AUG 18, '76

INPUT CONSTANTS

ELASTIC MODULUS(E) = $118.590E+03$ MPA($17.200E+06$ PSI)

NUMBER OF CYCLES	CRACK MBUTM COMPLIANCE CEB	ABAK / W OPTICAL BASE	COMPLIANCE BASE
0.000	34.1800	.352	.341
80.000	34.3231	.370	.346
160.000	37.8952	.385	.365
240.120	41.6105	.400	.388
248.820	46.0687	.415	.412
252.320	47.5348	.430	.420
257.320	52.0131	.450	.441
261.420	54.9853	.465	.454
264.820	59.4435	.480	.472
268.920	63.1587	.495	.486
269.420	67.6170	.512	.502
274.420	80.2487	.530	.540
275.220	98.0818	.579	.563
275.620	127.0605	.627	.634
275.820	154.5531	.654	.670



(W01)SPEC-7SR.1 T1-SAL-2.5SN(ELI) R.T.LAB AIR Re:05 F010 HZ * * * * * 11:08 AUG 18, 1976

INPUT CONSTANTS:

RANGE RATIO(R) * .05
 TEST FREQUENCY(HZ) * 10.0
 SPECIMEN WIDTH(W) * 50.927 MM(2.005 IN.)
 SPECIMEN THICKNESS(B) * 18.986 MM(.747 IN.)
 CRACK B0.4 CORRECTION * 1.270 MM(.050 IN.)

NUMBER OF CYCLES	MAXIMUM LOAD	SIDE 1 CRACK LENGTH	SIDE 2 CRACK LENGTH	CORRECTED AVERAGE CRACK LENGTH	CHANGE IN CRACK LENGTH DA	CHANGE IN CYCLES	CRACK GROWTH RATE DA / DN MICRO IN.	STRESS INTENSITY RANGE DELTA K MPA X KSI X MM ^{3/2} X IN ^{3/2}
N X 1000	P KN	A1 MM	A2 MM	ABAR MM	INCH MM	DN X 1000	METER PER CYCLE	
000	8.01 1.80	17.04	16.69	16.87	1.245	0.049 100.000	12.45	13.29 12.09
100.000	8.01 1.80	18.14	18.08	18.11	.800	0.031 25.000	32.00	13.92 12.67
125.000	8.01 1.80	19.25	18.57	18.91	.457	0.018 25.000	18.29	14.34 13.05
150.000	8.01 1.80	19.56	19.18	19.37	1.156	0.045 2.000	577.85	33.10 30.12
152.000	17.79 4.00	20.62	20.42	20.52	1.143	0.045 1.500	762.00	35.01 31.86
153.500	17.79 4.00	21.77	21.56	21.67	1.854	0.073 2.000	927.10	37.77 34.38
155.500	17.79 4.00	23.62	23.42	23.52	2.642	0.104 2.000	1320.80	42.62 38.79
157.500	17.79 4.00	26.34	25.98	26.16	3.124	0.123 1.200	2603.50	50.46 45.92
158.700	17.79 4.00	29.36	29.21	29.29	2.819	0.111 0.400	7048.50	61.31 55.79
159.100	17.79 4.00	32.18	32.03	32.11	.533	0.021 0.051	10458.82	69.24 63.02
159.151	17.79 4.00	32.77	32.51	32.64	1.486	0.059 0.052	28575.00	74.88 68.15
159.203	17.79 4.00	34.29	33.96	34.13				

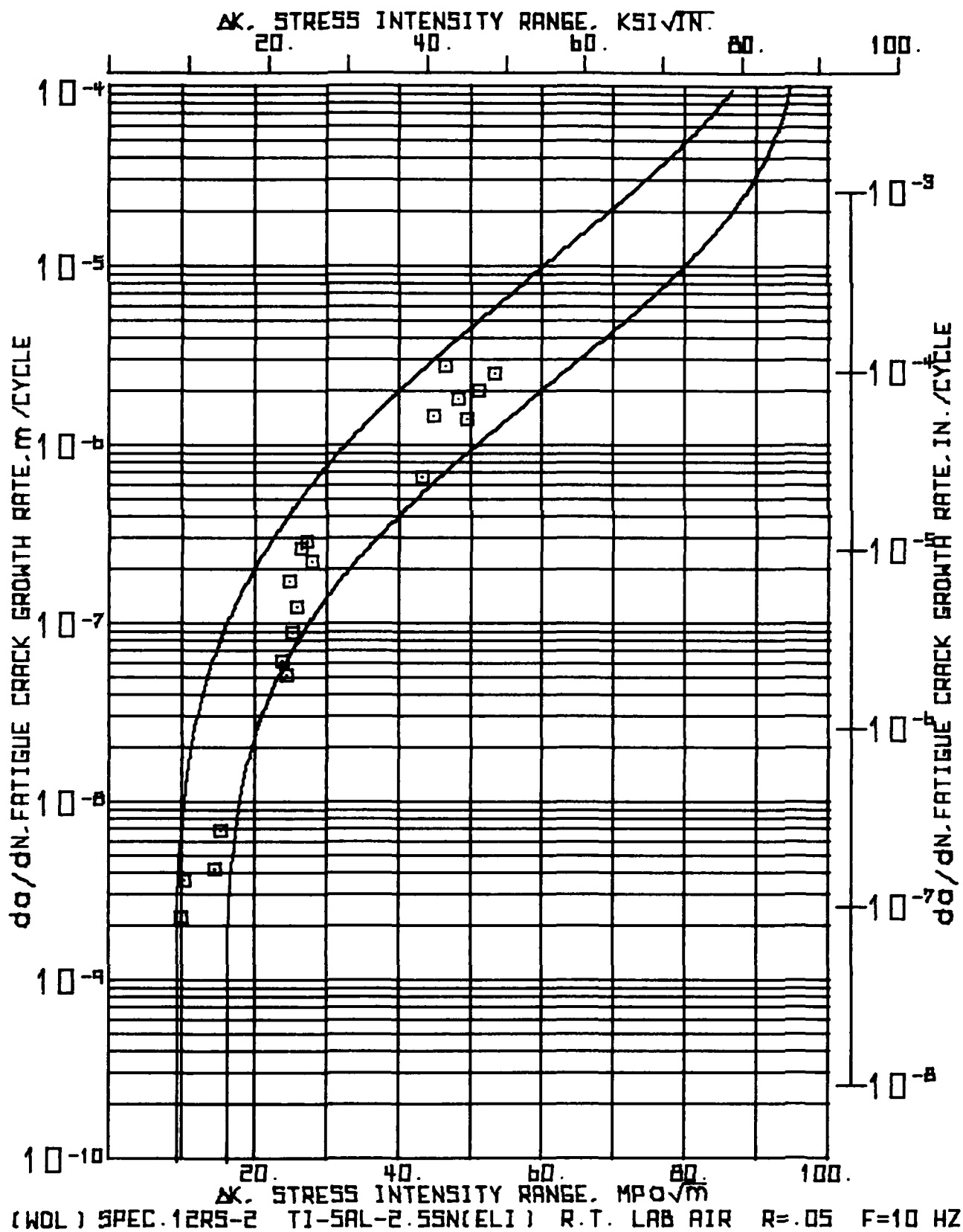
11108 AUG 18, '76

(M0L)SPEC.75R-1 Y1-SAL-2-55N(ELI) R.T.LAB AIR R=05 F=10 HZ

INPUT CONSTANTS

ELASTIC MODULUS(E) = 118.890E+03 MPA(17.200E+06 PSI)

NUMBER OF CYCLES	CRACK MOUTH COMPLIANCE	ABAR / W OPTICAL COMPLIANCE	BASE
N	CEB	BASE	BASE
X 1000			
.000	36.1603	.356	.354
100.000	41.7852	.381	.389
125.000	44.1959	.396	.402
150.000	44.9995	.405	.407
152.000	50.0244	.428	.434
153.500	54.6422	.450	.452
155.500	63.4814	.487	.487
157.500	80.3562	.539	.540
158.700	106.0702	.600	.599
159.100	139.4199	.655	.652
159.151	153.4804	.666	.669
159.203	186.4265	.695	.703



INPUT CONSTANTS:

RANGE RATIO(R) * .05
 TEST FREQUENCY(HZ) * 10.0
 SPECIMEN WIDTH(W) * 50.698 MM(1.996 IN.)
 SPECIMEN THICKNESS(B) * 19.012 MM(.748 IN.)
 CRACK B9% CORRECTION * 1.270 MM(.050 IN.)

NUMBER OF CYCLES	MAXIMUM LOAD	SIDE 1 CRACK LENGTH	SIDE 2 CRACK LENGTH	CORRECTED AVERAGE CRACK LENGTH	CHANGE IN CRACK LENGTH		CHANGE IN CYCLES		CRACK GROWTH RATE		STRESS INTENSITY RANGE	
					MM	INCH	MM	INCH	MM	INCH	MPA X KSI X IN ^{3/2}	DELTA K
N x 1000	P KN	A1 MM	A2 MM	ABAR MM	DA MM	DN INCH	DA MM	DN INCH	NANB. METER PER CYCLE	DA / DN MICR9 IN.	MPA X KSI X IN ^{3/2}	
000	6.34 1.42	16.43	16.43	17.70	.697		.660	.026 288.000	2.29	.09	10.23 9.31	
288.000	6.34 1.42	17.09	17.09	18.36	.723		.635	.025 172.699	3.68	.14	10.53 9.59	
460.699	6.34 1.42	17.73	17.73	19.00	.748							
000	8.01 1.80	19.51	19.00	20.52	.808		1.143	.045 267.608	4.27	.17	14.89 13.55	
267.608	8.01 1.80	20.52	20.27	21.67	.853		.508	.020 71.661	7.09	.28	15.50 14.11	
339.269	8.01 1.80	20.78	21.03	22.17	.873							
339.269	12.01 2.70	20.78	21.03	22.17	.873		.635	.025 10.000	63.50	2.50	23.92 21.77	
349.269	12.01 2.70	21.03	22.05	22.61	.898		.318	.013 6.000	52.92	2.08	24.51 22.30	
355.269	12.01 2.70	21.16	22.56	23.13	.910		.445	.018 2.500	177.80	7.00	24.99 22.74	
357.769	12.01 2.70	21.79	22.41	23.57	.928		.318	.013 3.500	90.71	3.57	25.49 23.19	
361.269	12.01 2.70	22.05	23.19	23.89	.940		.381	.015 3.000	127.00	5.00	25.96 23.62	
364.269	12.01 2.70	22.30	23.73	24.27	.955		.571	.022 2.100	272.14	10.71	26.62 24.22	
366.369	12.01 2.70	23.06	24.08	24.84	.978		.444	.017 1.500	296.33	11.67	27.36 24.90	
367.869	12.01 2.70	23.44	24.59	25.29	.995		.571	.022 2.500	228.60	9.00	28.13 25.60	
370.369	12.01 2.70	23.57	25.60	25.86	1.018							
370.369	17.79 4.00	23.57	25.60	25.86	1.018		.889	.035 1.300	683.85	26.92	43.40 39.50	
371.669	17.79 4.00	24.59	26.37	26.75	1.053		.444	.017 .297	1496.63	58.92	45.09 41.03	
371.966	17.79 4.00	24.97	26.87	27.19	1.070		.698	.027 .244	2862.70	112.70	46.62 42.43	
372.210	17.79 4.00	25.86	27.38	27.89	1.098		.508	.020 .272	1867.65	73.53	48.33 43.98	
372.482	17.79 4.00	26.37	27.89	28.40	1.118							

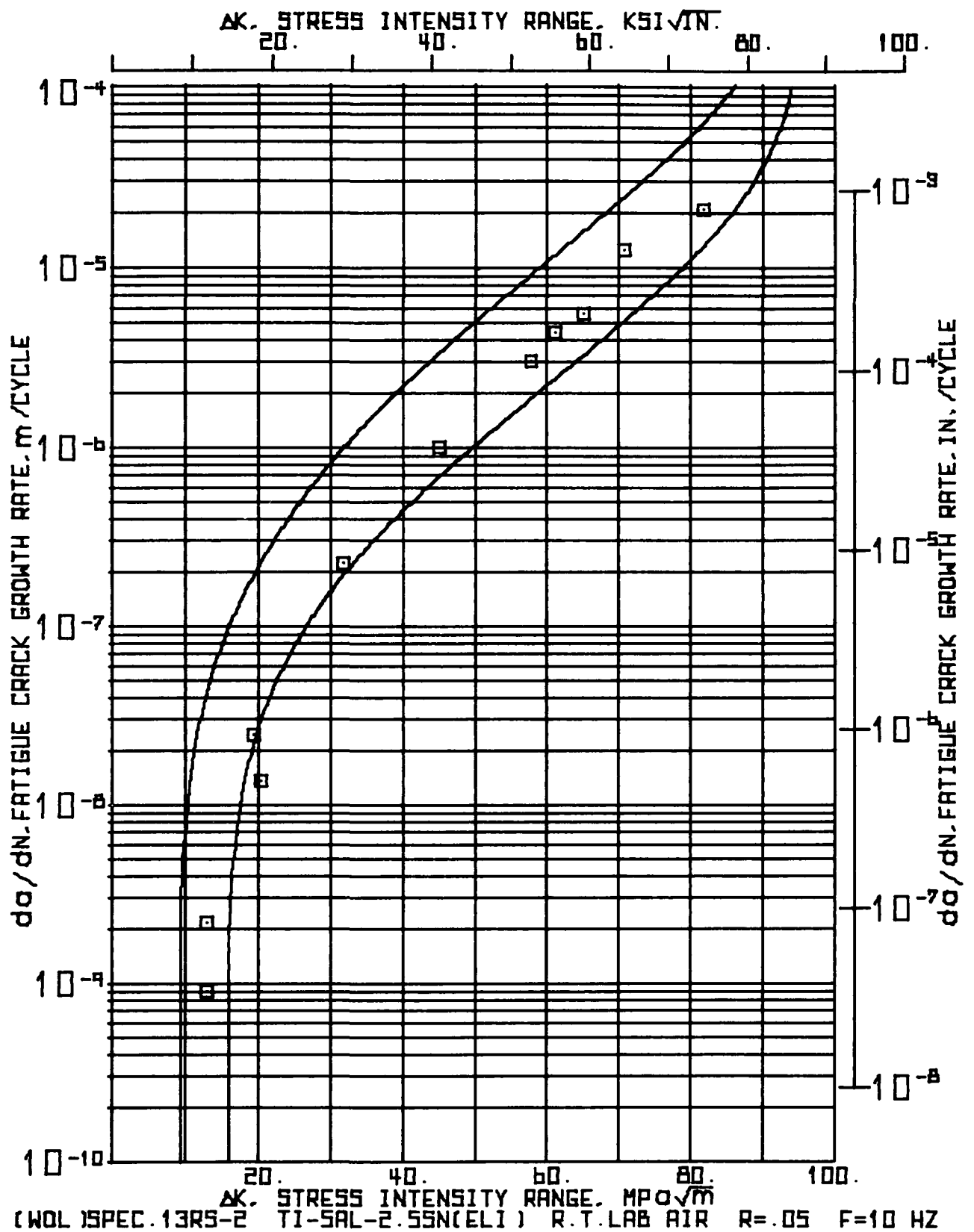
(28L) SPEC-12RS-2 T1-5AL-2-55N(ELL) R-7. LAB AIR R-05 F-10 HZ										11:08 AUG 18, 1976				PAGE 2	
NUMBER OF CYCLES	MAXIMUM LOAD	SIDE 1 CRACK LENGTH		SIDE 2 CRACK LENGTH		CORRECTED AVERAGE CRACK LENGTH		CHANGE IN CRACK LENGTH		CHANGE IN CYCLES		CRACK GROWTH RATE		STRESS INTENSITY RANGE	
		A1 MM	INCH	A2 MM	INCH	MM	INCH	MM	INCH	MM	INCH	DA MM	DN INCH	DA / DN MICRO METER PER CYCLE	MPA X 1000 KSI X 1000
372.482	17.79 KN	26.37	1.038	27.89	1.098	28.40	1.118	.381	.015	.264	.015	1443.18	56.82	49.65	45.19
372.746	17.79 KN	26.62	1.048	28.40	1.118	28.78	1.133	.635	.025	.306	.025	2075.16	81.70	51.24	46.63
373.052	17.79 KN	27.38	1.078	28.91	1.138	29.41	1.158	.699	.028	.270	.028	2587.04	101.85	53.45	48.64
373.322	17.79 KN	28.27	1.113	29.41	1.158	30.11	1.185								

(WBL) SPEC.12RS-2 T1-SAL-2-SSN(EL) R.T. LAB AIR R=05 F=10 HZ 11:08 AUG 18, 1976

INPUT CONSTANTS

ELASTIC MODULUS(E) = 118.590E+03 MPa(17.200E+06 PSI)

NUMBER OF CYCLES N	CRACK MOUTH COMPLIANCE CEB	ABAR / W OPTICAL BASF	COMPLIANCE BASE
280.000	36.2385	.349	.355
460.000	38.6226	.362	.370
640.000	40.0531	.375	.379
820.000	41.9604	.405	.390
1000.000	52.3273	.450	.445
349.269	54.3577	.456	.451
355.269	55.3114	.465	.455
357.769	58.1723	.471	.467
361.269	61.0332	.479	.478
364.269	63.4174	.490	.487
366.369	63.8542	.499	.489
367.569	68.6624	.510	.505
370.369	76.7684	.536	.530
371.366	83.9207	.550	.549
372.210	85.6280	.560	.554
372.482	91.0730	.568	.567
376.746	96.3181	.580	.579
373.052	105.8545	.594	.598
373.322			



(T001)SPEC.138522 T15AL-2.55N(ELI) R.T.LAB AIR R0.05 P.10 MZ ***** W E D G E * * 8 P E N * L B A D * P R 8 G R A M * * * 14:22 AUG 03, 1976

INPUT CONSTANTS:

RANGE RATIO(R) ■ .05
 TEST FREQUENCY(HZ) ■ 10.0
 SPECIMEN WIDTH(W) ■ 50.800 MM(2.000 IN.)
 SPECIMEN THICKNESS(T) ■ 13.850 MM(.744 IN.)
 CRACK R9A CORRECTION ■ 1.270 MM(.050 IN.)

NUMBER OF CYCLES	MAXIMUM LOAD	SIDE 1 CRACK LENGTH	SIDE 2 CRACK LENGTH	CORRECTED AVERAGE CRACK LENGTH	CHANGE IN CRACK LENGTH	CHANGE IN CYCLES	CRACK GROWTH RATE DA / DN	STRESS INTENSITY RANGE
X 1000	KN	MM	MM	MM	MM	DN X 1000	MM PER CYCLE	MPA X 1000
0.00	8.01	16.09	16.71	17.97	.089	.003 100.000	.89	12.96
100.000	8.01	16.74	16.84	18.06	.216	.008 100.000	2.16	11.80
200.000	8.01	16.54	17.17	18.28				11.68
200.000	11.57	21.60	18.63	18.28	1.206	.048 50.000	24.13	17.71
250.000	11.57	21.60	18.03	19.44	.673	.026 50.000	13.46	18.49
300.000	11.57	21.60	18.23	20.15				
300.000	15.57	31.50	19.48	20.15	5.499	.216 25.000	219.96	28.91
325.000	15.57	31.50	23.49	25.65	6.909	.272 7.000	986.97	40.91
332.000	15.57	31.50	31.01	32.06	.597	.203	2984.50	117.50
332.000	15.57	31.50	31.70	33.16	.864	.200	4318.00	170.00
332.000	15.57	31.50	32.64	34.02	.813	.150	5418.67	213.33
332.000	15.57	31.50	33.48	34.84	1.219	.100	12192.00	450.00
332.000	15.57	31.50	34.62	36.06	2.057	.100	20574.00	810.00
332.000	15.57	31.50	36.84	38.11				

14:22 AUG 03, 1976

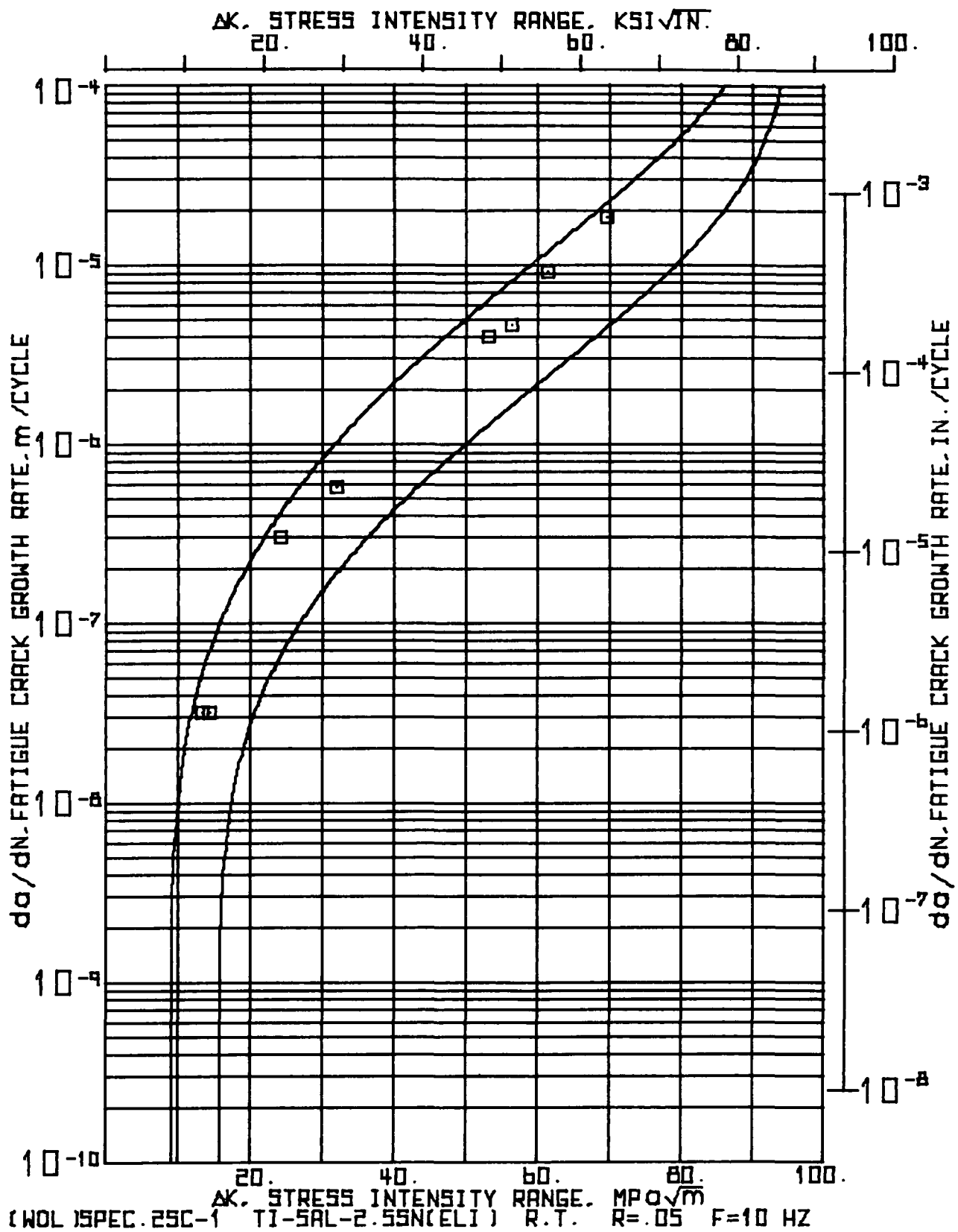
(KPLISPEC) 13KS-2 T1-5AL-2.5SN(ELL) R-T-LAB AIR R-05 F-10 MZ

INPUT CONSTANTS

ELASTIC MODULUS(E) = 118.590E+03 MPa(17.200E+06 PSI)

NUMBER OF CYCLES	CRACK MOUTH COMPLIANCE CLE	ABAR / W OPTICAL BASE	CUMPLIANCE BASE
100	35.1770	.354	.348
100.000	36.7760	.355	.358
200.000	37.3754	.360	.363
300.000	40.7734	.383	.383
400.000	43.1718	.397	.397
500.000	67.1561	.505	.500
600.000	127.3164	.641	.633
700.000	139.1091	.653	.651
800.000	152.7302	.670	.668
900.000	170.2887	.696	.687
1000.000	192.3715	.710	.711
1100.000	261.4161	.750	.765

X 1000



*(NUL)SPEC.2SC.1 TIOAL-2.6SN(ELI) R.T. R.05 F.10 MZ * * * * *
 * * * * * W E D G E * * B P E N * * L O A D * * P R O G R A M * * *

10:22 AUG 03, 1976

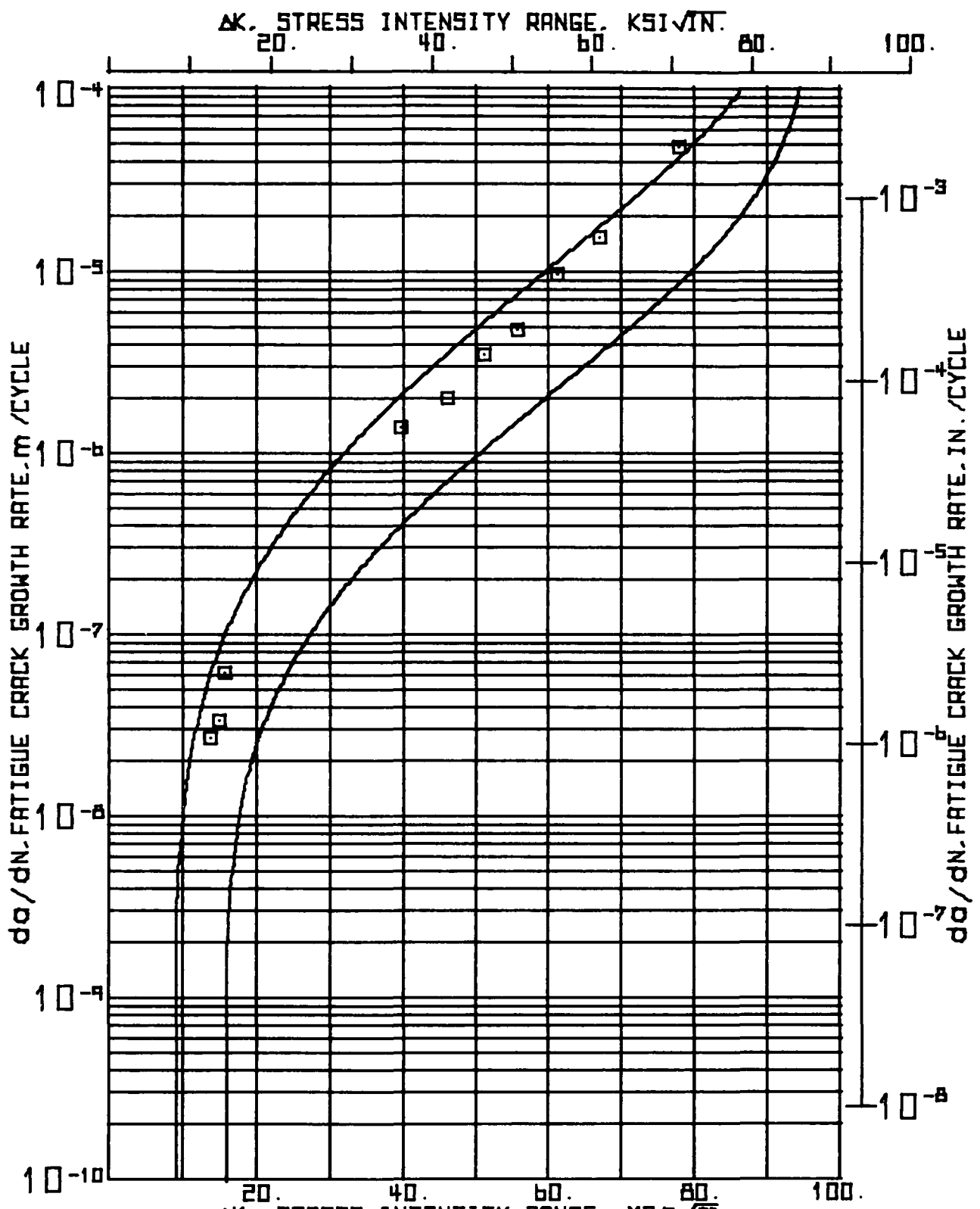
INPUT CONSTANTS:

RANGE RATIO(R) * * .05
 TEST FREQUENCY(HZ) * * 10.0
 SPECIMEN WIDTH(W) * * 51.105 MM(2.012 IN.)
 SPECIMEN THICKNESS(B) * * 18.999 MM(.748 IN.)
 CRACK BG. CORRECTION * * 1.270 MM(.050 IN.)

NUMBER OF CYCLES	MAXIMUM LOAD	SIDE 1 CRACK LENGTH	SIDE 2 CRACK LENGTH	CORRECTED AVERAGE CRACK LENGTH	CHANGE IN CRACK LENGTH	CHANGE IN DA	CHANGE IN CYCLES	CRACK GROWTH RATE DA / DN MICR9 IN.	STRESS INTENSITY RANGE DELTA K MPA X KSI X M00.5 IN00.5
N X 1000	P KN KIPS	A1 MM INCH	A2 MM INCH	ADAR N.1 INCH	MM	INCH	DN X 1000	METER PER CYCLE	
300	8.01 1.80	17.27 .680	17.17 .676	18.49 .728	1.880	.074	60.500	31.07	1.22 13.63 12.40
600	8.01 1.80	19.35 .762	18.85 .742	20.37 .802	1.245	.049	39.500	31.51	1.24 14.65 13.33
1000	8.01 1.80	20.70 .815	19.99 .787	21.62 .851					
1000	11.57 2.60	20.70 .815	19.99 .787	21.62 .851	4.432	.175	15.000	295.49	11.63 24.35 22.16
1100	11.57 2.60	25.17 .991	24.38 .960	26.05 1.025	5.601	.220	10.000	560.07	22.05 32.23 29.33
1200	11.57 2.60	30.71 1.209	30.05 1.183	31.05 1.246					
1200	15.57 3.50	30.71 1.209	30.05 1.183	31.65 1.246	.787	.031	.200	3937.00	155.00 53.39 48.58
1200	15.57 3.50	31.50 1.240	30.84 1.214	32.44 1.277	.902	.035	.200	4508.50	177.50 56.67 51.58
1200	15.57 3.50	32.38 1.275	31.75 1.250	33.34 1.312	1.340	.053	.150	8974.67	303.33 61.60 56.06
1200	15.57 3.50	33.78 1.330	33.05 1.301	34.68 1.365	1.791	.071	.100	17907.00	705.00 69.78 63.51
1200	15.57 3.50	35.56 1.400	34.85 1.372	36.47 1.436					

(MULTISPEC.2SC.1 TI-5AL-2.5SN(ELI) S.T. R.05 F.10.MZ 14:22 AUG 03, '76
 INPUT CONSTANTS

ELASTIC MODULUS(E) = 118.59UE+03 MPA(17.200E+06 PSI)				
NUMBER OF CYCLES	CRACK COMPLIANCE	ABAR / W OPTICAL BASE	COMPLIANCE BASE	
X 1000				
000	41.0091	.362	.364	
60.000	45.3337	.399	.411	
100.000	52.2665	.423	.442	
110.000	73.1731	.510	.519	
120.000	117.3926	.619	.619	
125.000	125.2437	.635	.633	
125.400	139.1093	.652	.651	
125.850	164.3364	.679	.681	
125.850	212.2824	.714	.723	



(WOL) SPEC. 75C-1 TI-5AL-2.55N(ELI) R.T. R= 05 F=10 HZ

IMPLICIT CONSTANTS:

TEST FREQUENCY (Hz)	SPECIMEN WIDTH (in.)	SPECIMEN THICKNESS (in.)	RANGE RATIO (K)
10.0	51.003	2.008	0.05
19.045	19.045	0.750	0.05
1.270	1.270	0.050	0.05

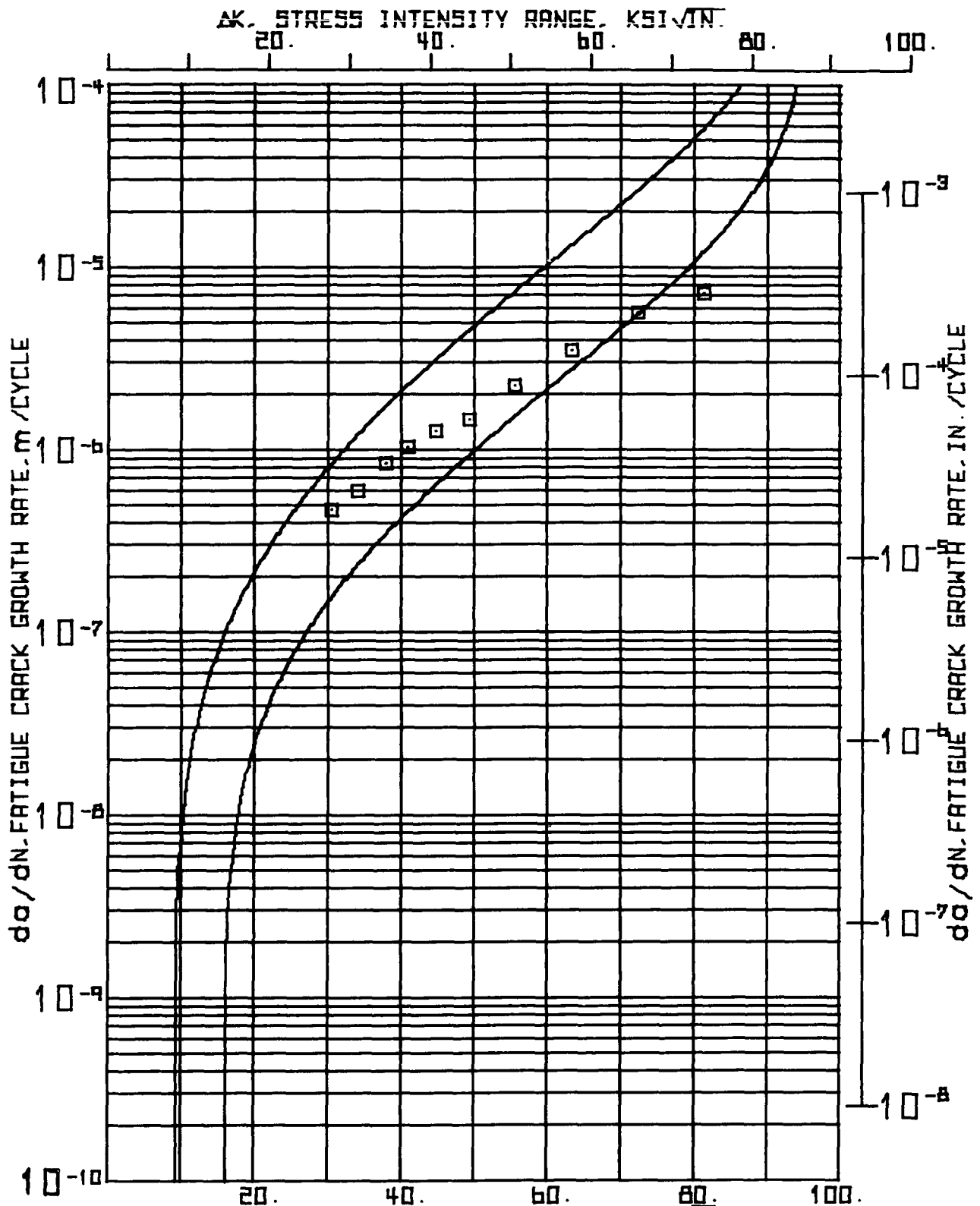
NUMBER OF CYCLES	MAXIMUM LOAD	SIDE 1		SIDE 2		CORRECTED		CHANGE		CRACK GRWTH		STRESS	
		CRACK LENGTH	MM	CRACK LENGTH	MM	AVERAGE CRACK LENGTH	MM	INCH	INCH	DA / DN	RATE	INTENSITY RANGE DELTA X	
N	P	A1	A2	A1	A2	MM	INCH	MM	INCH	DN	MEIER	MPA X	KSI X
X 1000	KN	KIPS	MM	INCH	MM	INCH	MM	INCH	INCH X 1000	PER CYCLE	IN.	4000.5	1000.5
100	8.01	1.80	17.27	.680	17.35	.683	18.58	.731	2.654	.104	100.000	26.54	1.04
100	8.01	1.80	19.96	.786	19.96	.786	21.23	.836	.826	.033	25.000	33.02	1.30
125	8.61	1.80	20.65	.813	20.93	.824	22.06	.868	1.511	.060	25.000	60.45	2.38
150	8.01	1.80	22.30	.878	22.30	.878	23.57	.928	2.743	.108	2.000	1371.60	54.00
150	17.79	4.00	22.30	.878	22.30	.878	23.57	.928	2.563	.101	1.300	1973.38	77.69
152	17.79	4.00	25.07	.967	25.02	.985	26.31	1.036	.864	.034	.250	3454.40	136.00
153	17.79	4.00	27.66	1.069	27.56	1.085	28.68	1.137	1.892	.075	.400	4730.75	186.25
153	17.79	4.00	29.45	1.120	28.50	1.122	29.74	1.171	.952	.037	.100	9525.00	375.00
153	17.79	4.00	30.30	1.193	30.43	1.198	31.64	1.245	1.511	.059	.100	15113.00	595.00
154	17.79	4.00	31.32	1.233	31.32	1.233	32.59	1.263	2.337	.092	.050	46736.00	1840.00
154	17.79	4.00	32.79	1.291	32.87	1.294	34.10	1.342	36.44	1.436			
154	17.79	4.00	33.05	1.380	35.28	1.389	36.44	1.436					

(MULTISPEC7SC-1 T1-SAL-2.5SN(EL)) R.T. R=05 F=10 MZ 14123 AUG 03, 1976

INPUT CONSTANTS

ELASTIC MODULUS(E) = $118.590E+03$ MPA($17.200E+06$ PSI)

NUMBER OF CYCLES	CRACK GROWTH COMPLIANCE N	ABAR / W	
		OPTICAL BASF	COMPLIANCE BASF
x 1000	CEU		
100	35.0097	.404	.370
125	47.0561	.416	.420
150	50.7802	.433	.435
175	58.0345	.442	.447
200	70.1250	.516	.510
225	89.4699	.506	.503
250	90.3363	.503	.503
275	118.0871	.620	.621
300	128.0656	.639	.637
325	154.7547	.609	.671
350	224.0838	.714	.732



(WOL) SPEC 14CS-2 TI-5AL-2.55N(ELI) R.T. R=.05 F=10 HZ

(KOL)SPEC.1*CS=2 T1=5AL=2.5SN(ELI) R=7. R=05 F=10 HZ 14123 AUG 03,176

INPUT CONSTANTS

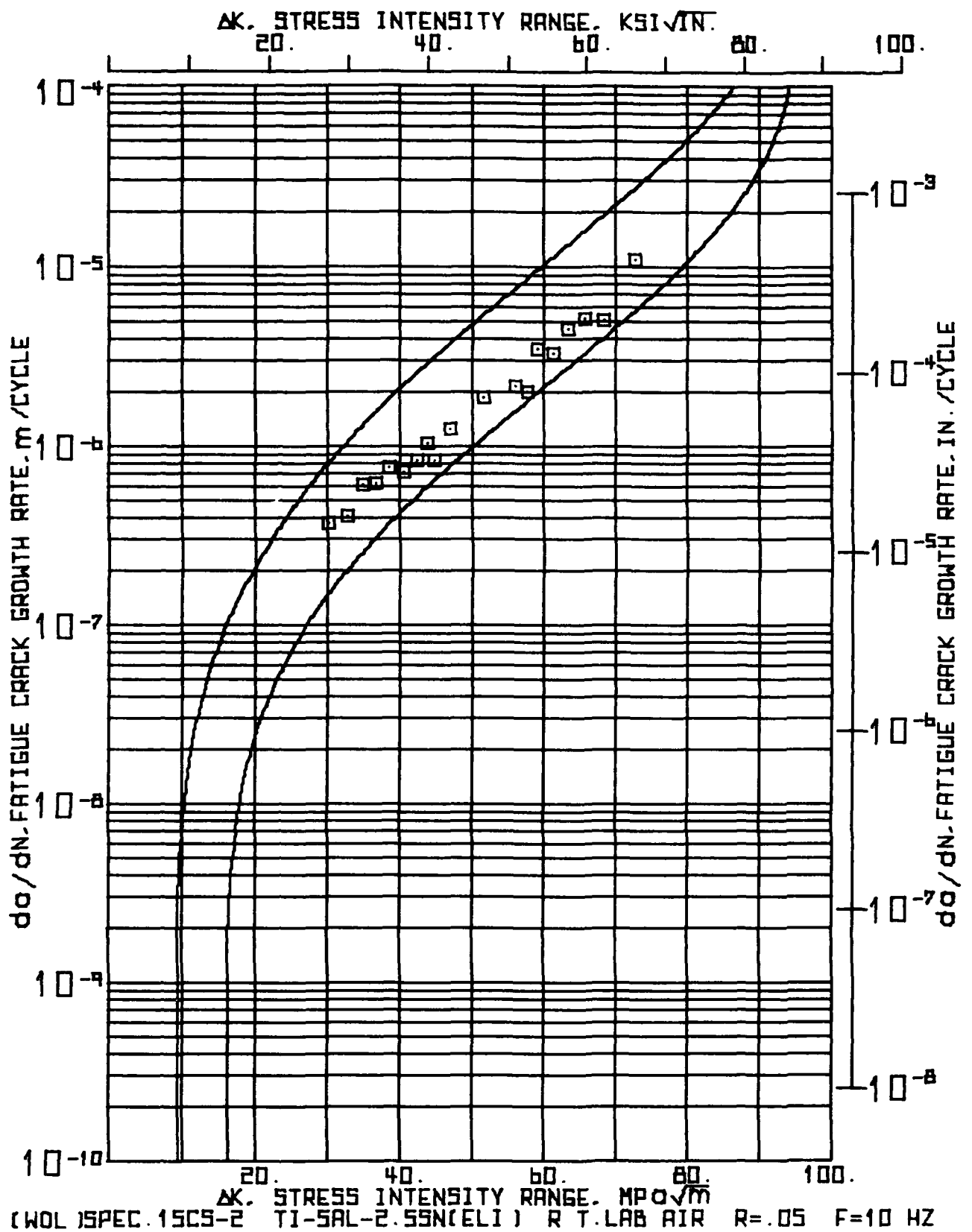
ELASTIC MODULUS(E) = 110599E+03 MPa(17.200E+06 PSI)

NUMBER OF CYCLES	CRACK MOUTH COMPLIANCE	ADAR / A OPTICAL BASE	COMPLIANCE BASE
------------------------	---------------------------	-----------------------------	--------------------

A

X 1000

000	40.2910	.361	.380
5000	47.3434	.408	.420
9000	56.6249	.455	.470
11000	66.772	.488	.496
12000	73.3296	.512	.520
13700	85.4169	.530	.533
14700	94.5984	.578	.580
15700	110.2614	.622	.622
16150	141.0185	.653	.654
16500	174.4746	.692	.694
16630	181.3317	.711	.713



(W9L)SPFC-15CS-2 T1-5AL-2.55N(ELI) R.T.LAB AIR R.05 F.10 WZ * * * * * 14:24 AUG 03,176

INPUT CONSTANTS:

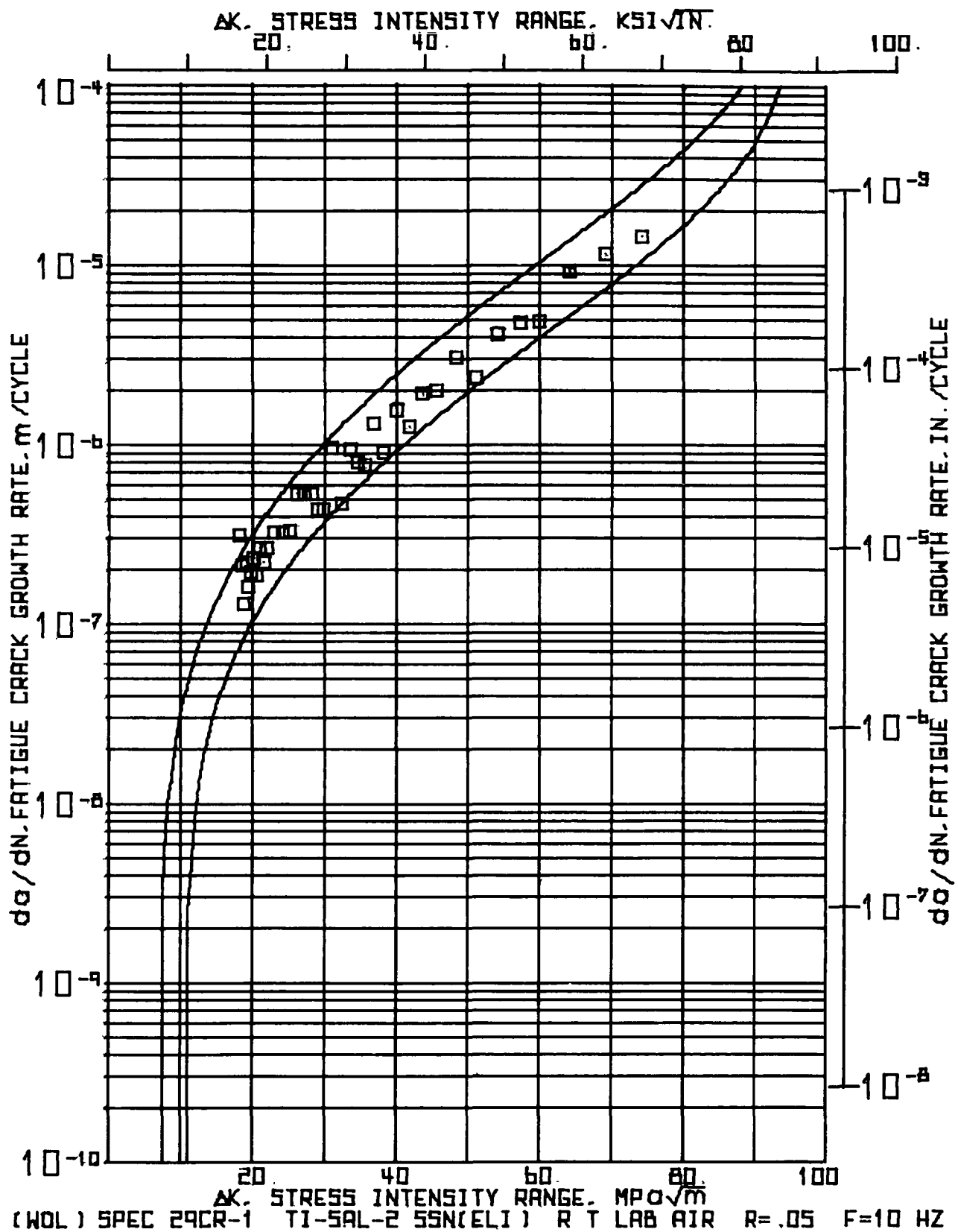
RANGE RATIO(R) * .05
 TEST FREQUENCY(HZ) * 10.0
 SPECIMEN WIDTH(W) * 50.927 MM(2.005 IN.)
 SPECIMEN THICKNESS(B) * 18.951 MM(.746 IN.)
 CRACK IN. CORRECTION * 1.270 MM(.050 IN.)

NUMBER OF CYCLES	MAXIMUM LOAD P	SIDE 1		SIDE 2		CONNECTED AVERAGE CRACK LENGTH		CHANGE IN CRACK LENGTH		CHANGE IN CYCLES		CRACK GROWTH RATE DA / DN		STRESS INTENSITY RANGE DELTA K	
		KN	KIPS	MM	INCH	MM	INCH	MM	INCH	MM	INCH	MM	INCH	MPA X 1000	KSI X 1000
1	17.79	4.00	17.04	.671	16.94	.667	16.26	.719	1.854	.073	5.000	370.84	14.60	30.17	27.46
5	17.79	4.00	18.67	.743	18.82	.741	20.12	.792	1.613	.063	4.000	403.22	15.87	32.70	29.76
9	17.79	4.00	20.60	.811	20.32	.800	21.73	.855	1.206	.047	2.000	603.25	23.75	35.02	31.87
11	17.79	4.00	21.64	.852	21.63	.854	22.94	.903	.749	.029	1.200	624.42	24.58	36.79	33.48
12	17.79	4.00	22.40	.882	22.43	.883	23.69	.932	1.130	.044	1.500	753.53	29.67	38.62	35.14
13	17.79	4.00	23.55	.927	23.55	.927	24.82	.977	.724	.029	1.000	723.90	28.50	40.57	36.92
14	17.79	4.00	24.28	.956	24.26	.955	25.54	1.005	.826	.033	1.000	825.50	32.50	42.33	38.52
15	17.79	4.00	25.25	.994	24.94	.982	26.37	1.038	.470	.018	.450	1044.22	41.11	43.89	39.94
16	17.79	4.00	25.60	1.008	25.53	1.005	26.84	1.056	.292	.011	.350	834.57	32.86	44.85	40.82
16	17.79	4.00	25.66	1.018	25.66	1.018	27.13	1.068	1.257	.050	1.000	1257.30	49.50	46.92	42.70
17	17.79	4.00	27.10	1.067	27.13	1.068	28.38	1.117	1.680	.074	1.000	1879.60	74.00	51.60	46.96
18	17.79	4.00	28.93	1.139	29.06	1.144	30.26	1.191	.711	.028	.330	2155.15	54.85	56.07	51.03
18	17.79	4.00	29.64	1.167	29.77	1.172	30.94	1.219	.203	.008	.100	2032.00	50.00	57.80	52.60
18	17.79	4.00	29.67	1.176	29.95	1.179	31.18	1.227	.521	.021	.150	3471.33	136.67	59.23	53.90
19	17.79	4.00	30.43	1.198	30.43	1.198	31.70	1.248	.495	.019	.150	3302.00	140.00	61.34	55.83
19	17.79	4.00	30.64	1.214	31.01	1.221	32.19	1.267	.470	.019	.103	4562.14	179.61	63.47	57.76
19	17.79	4.00	31.59	1.256	31.39	1.236	32.66	1.286	.533	.021	.103	5178.64	213.88	65.80	59.89
19	17.79	4.00	31.88	1.255	31.98	1.259	33.20	1.307	.508	.020	.100	5080.00	200.00	68.39	62.24
19	17.79	4.00	32.33	1.273	32.54	1.261	33.71	1.327	1.103	.043	.100	11049.00	435.00	72.73	66.19
19	17.79	4.00	33.48	1.318	33.60	1.323	34.01	1.370							

(W6)SPEC:15CS-2 Y1.5AL-2.5SN(ELL) R.T.LAB AIR R=.05 F=10 HZ 14124 AUG 03.76

INPUT CONSTANTS

ELASTIC MODULUS(E) = 118.590E+03 MPa(17.200E+06 PSI)					
NUMBER OF CYCLES	CRACK MBUTH CEFFICIENCY	ABAR / W OPTICAL COMPLIANCE BASE	BASE	BASE	
N	CEP				
X 100					
1.000	36.0946	.359		.359	
5.000	42.0090	.395		.393	
9.000	46.7276	.427		.430	
11.000	52.9358	.450		.445	
12.000	57.7481	.465		.465	
13.000	61.7584	.487		.481	
14.000	65.6708	.501		.498	
15.000	70.0911	.518		.511	
16.000	74.0913	.527		.524	
16.500	74.1955	.533		.528	
17.000	77.4243	.557		.534	
18.000	104.1675	.594		.595	
18.130	104.1819	.608		.606	
18.930	113.0922	.612		.613	
19.080	115.7045	.622		.621	
19.130	120.3292	.632		.636	
19.333	136.7457	.641		.645	
19.436	142.7662	.652		.656	
19.536	154.7971	.652		.671	
19.636	174.0405	.684		.691	



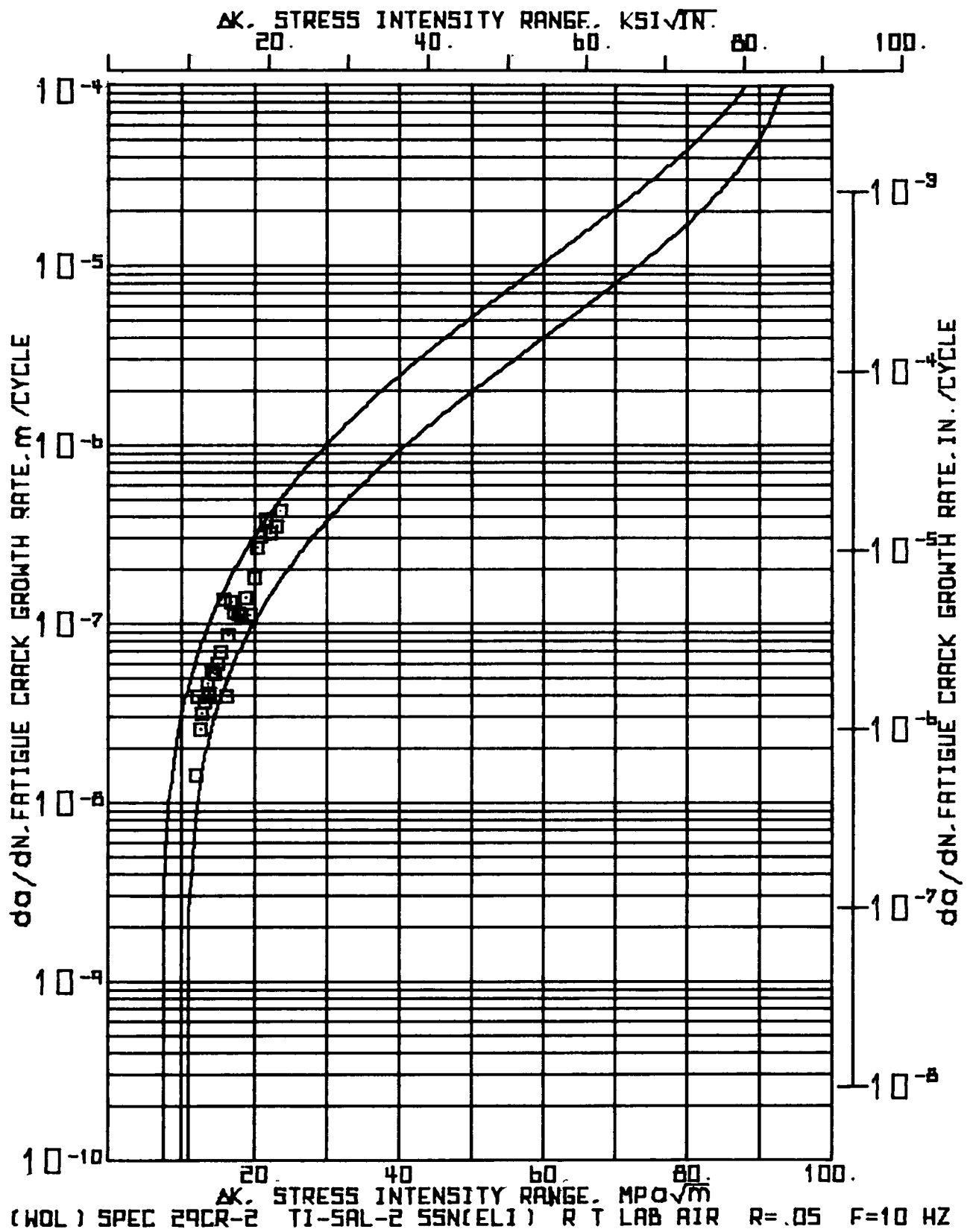
11135 AUG 05, 1976

INPUT CONSTANTS:

RANGE RATIO(R) = .05
 TEST FREQUENCY(HZ) = 10.0
 SPECIMEN WIDTH(W) = 50.876 MM(2.003 IN.)
 SPECIMEN THICKNESS(B) = 19.083 MM(.751 IN.)
 CRACK BE. CORRECTION = 16.383 MM(.645 IN.)

NUMBER OF CYCLES	MAXIMUM LOAD	SIDE 1 CRACK LENGTH	SIDE 2 CRACK LENGTH	CORRECTED AVERAGE CRACK LENGTH	CHANGE IN CRACK LENGTH	CHANGE IN CYCLES	CRACK GROWTH RATE DA / DN	STRESS INTENSITY RANGE DELTA K
A X 1000	F KIPS	MM	MM	MM	MM	DN X 1000	IN. PER CYCLE	MPA X 10.05
000	11.12 2.50	1.70 .067	1.83 .072	18.15 .714	.610 .024	2.000	304.80 12.00	18.14 16.51
2000	11.12 2.50	2.57 .101	2.18 .086	18.76 .738	.419 .017	2.000	209.55 8.25	18.56 16.89
4000	11.12 2.50	3.00 .118	2.59 .102	19.18 .755	.254 .010	2.000	127.00 5.00	18.85 17.15
6000	11.12 2.50	3.25 .126	2.84 .112	19.43 .765	.432 .017	2.000	215.90 8.50	19.15 17.43
8000	11.12 2.50	3.73 .147	3.23 .127	19.66 .782	.318 .013	2.000	158.75 6.25	19.48 17.73
10000	11.12 2.50	4.11 .162	3.48 .137	20.18 .794	.381 .015	2.000	190.50 7.50	19.80 18.02
12000	11.12 2.50	4.47 .176	3.69 .153	20.56 .809	.457 .018	2.000	228.60 9.00	20.20 18.38
14000	11.12 2.50	5.05 .199	4.22 .166	21.02 .827	.368 .014	2.000	184.15 7.25	20.62 18.75
16000	11.12 2.50	5.36 .211	4.65 .183	21.39 .842	.521 .020	2.000	260.35 10.25	21.05 19.16
18000	11.12 2.50	5.99 .236	5.05 .199	21.91 .862	.432 .017	2.000	215.90 8.50	21.55 19.61
20000	11.12 2.50	6.40 .252	5.51 .217	22.34 .879	.521 .020	2.000	260.35 10.25	22.06 20.08
22000	11.12 2.50	6.91 .272	6.05 .238	22.66 .900	1.283 .051	4.000	320.67 12.63	23.09 21.02
24000	11.12 2.50	6.28 .326	7.24 .285	24.14 .950	.630 .025	2.000	317.50 12.50	24.28 22.09
26000	11.12 2.50	8.84 .348	7.95 .313	24.78 .975	.813 .032	2.500	325.12 12.80	25.24 22.97
30000	11.12 2.50	9.60 .378	8.81 .347	25.59 1.007	.521 .021	1.000	520.70 20.50	26.17 23.82
31000	11.12 2.50	10.19 .401	9.27 .365	26.11 1.028	.787 .031	1.500	524.93 20.67	27.15 24.71
33000	11.12 2.50	11.02 .434	10.01 .394	26.50 1.059	.521 .020	1.000	520.70 20.50	28.18 25.65
34000	11.12 2.50	11.63 .458	10.44 .411	27.42 1.079	.432 .017	1.000	431.80 17.00	28.98 26.37
35000	11.12 2.50	12.19 .480	10.74 .423	27.65 1.096	.432 .017	1.000	431.80 17.00	29.73 27.05
36000	11.12 2.50	12.45 .490	11.35 .447	28.28 1.113				

NUMBER OF CYCLES	MAXIMUM LOAD	P	SIDE 1 CRACK LENGTH		SIDE 2 CRACK LENGTH		CORRECTED AVERAGE		CHANGE IN		CRACK GROWTH RATE		STRESS INTENSITY RANGE	
			A1 INCH	A1 MM	A2 INCH	A2 MM	MM	INCH	INCH	MM	DA INCH	DN CYCLES	MPA X 1000	DELTA X 1000
36000	11.12 2.50	12.45	490	11.35	447	20.28	1.113	.952	.037	1.000	952.50	37.50	31.00	28.21
37000	11.12 2.50	13.16	518	12.55	494	29.24	1.151	.457	.018	1.000	457.20	18.00	32.35	29.47
38000	11.12 2.50	13.72	543	12.70	500	29.69	1.169	.643	.026	.700	925.29	36.43	33.54	30.53
39000	11.12 2.50	14.00	575	13.31	524	30.34	1.194	.394	.015	.500	767.40	31.00	34.70	31.58
39000	11.12 2.50	14.29	590	13.72	540	30.73	1.210	.341	.015	.500	762.00	30.00	35.60	32.40
39700	11.12 2.50	15.32	603	14.15	557	31.11	1.225	.646	.025	.500	1295.40	51.00	36.86	33.55
40000	11.12 2.50	15.95	628	14.81	583	31.76	1.250	.444	.017	.500	809.00	35.00	38.28	34.84
40700	11.12 2.50	16.48	649	15.16	597	32.21	1.268	.762	.030	.500	1524.00	60.00	39.96	36.36
41000	11.12 2.50	17.02	678	15.95	626	32.97	1.298	.490	.020	.400	1238.25	46.75	41.83	38.07
41600	11.12 2.50	17.36	703	16.31	642	33.46	1.317	.571	.022	.300	1905.00	75.00	43.55	39.63
41900	11.12 2.50	17.89	720	17.02	670	34.04	1.340	.597	.023	.300	1909.67	78.33	45.56	41.46
42000	11.12 2.50	18.52	745	17.53	692	34.63	1.363	.902	.036	.300	3005.67	118.33	48.38	44.02
42500	11.12 2.50	19.04	781	18.47	727	35.53	1.399	.470	.019	.200	2349.50	92.50	51.22	46.61
42700	11.12 2.50	20.17	794	19.08	751	36.00	1.417	.613	.032	.200	4064.00	160.00	54.15	49.28
42900	11.12 2.50	21.13	832	19.74	777	36.82	1.449	.470	.018	.100	4699.00	185.00	57.37	52.21
43000	11.12 2.50	21.56	849	20.24	797	37.29	1.468	.463	.019	.100	4826.00	190.00	59.98	54.56
43100	11.12 2.50	22.15	872	20.62	812	37.77	1.487	.914	.036	.100	9144.00	360.00	64.18	58.41
43200	11.12 2.50	22.34	903	21.67	853	38.68	1.523	.572	.023	.050	11430.00	450.00	69.24	63.01
43200	11.12 2.50	23.65	931	22.10	870	39.26	1.545	.711	.028	.050	14224.00	560.00	74.19	67.51
43300	11.12 2.50	24.18	952	22.99	905	39.97	1.573							



(N) * WEDGEBEN * LBAD * PRogram *
 TI=5AL=2.5SN(EL) R.TOLAB AIR R.05 F=10 HZ
 SPEC.29CR=2

INPUT CONSTANTS:

RANGE RATIO(α)	■ .05
TEST FREQUENCY (Hz)	■ 10.0
SPECIMEN WIDTH (in.)	■ 50.863 MM
SPECIMEN THICKNESS (in.)	■ 19.126 MM
CRACK BG. CORRECTION	■ 16.485 MM

[illegible]

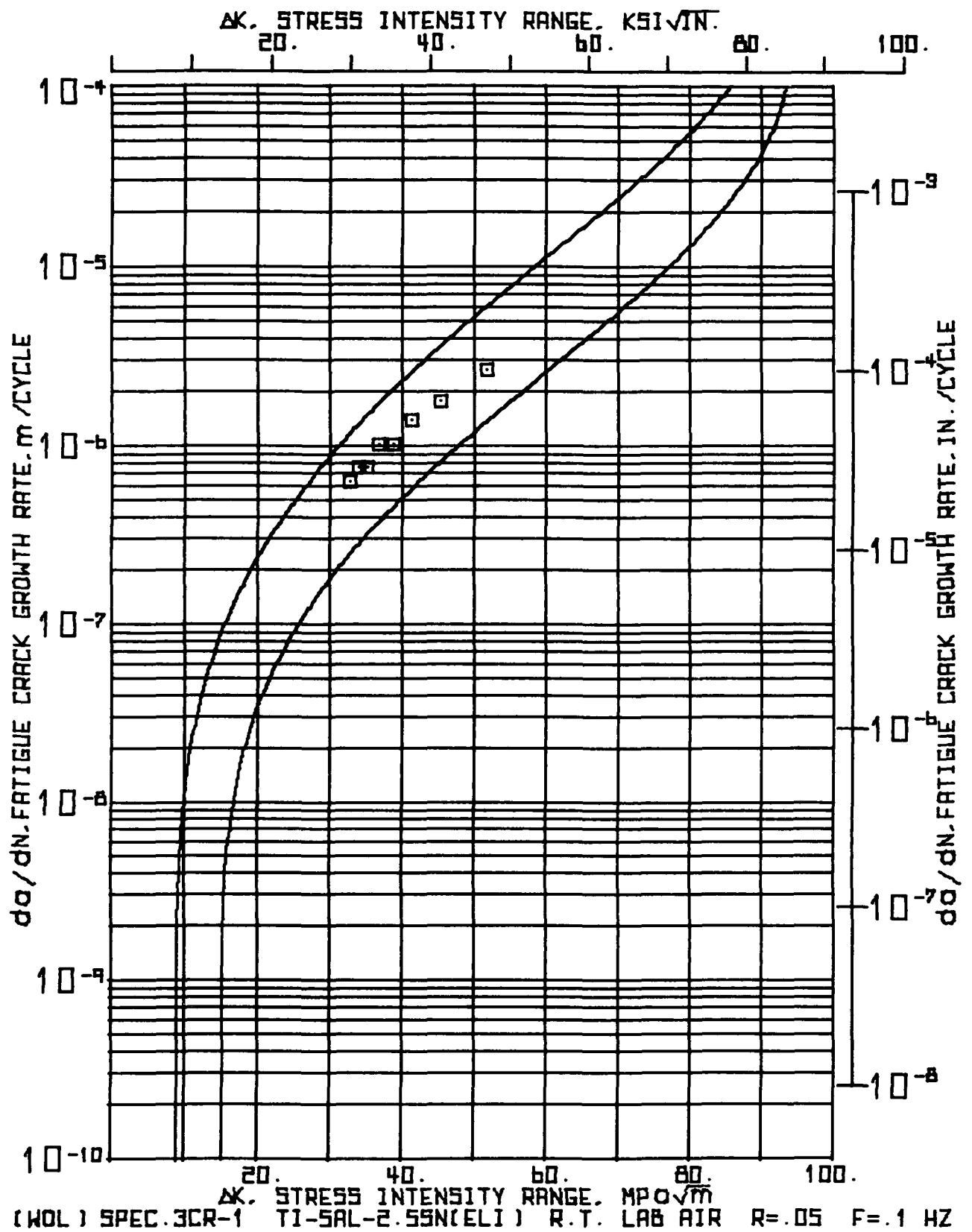
11:36 AUG 05, 1976

(481) SPEC-25CR-2 II-5AL-2-55NUE11 R-I-LAB AIR R-05 F=10 HZ

NUMBER PF	MAXIMUM LOAD	SIDE 1 CRACK LENGTH		SIDE 2 CRACK LENGTH		CORRECTED AVERAGE		CHANGE IN		CHANGE IN		CRACK GROWTH RATE		STRESS INTENSITY		
		MM	INCH	MM	INCH	MM	INCH	MM	INCH	CRACK LENGTH DA	CYCLES	MM	INCH	DA / DN METER PER CYCLE	MICR8 IN.	DELTA K MPA X KSI X M00.5 IN00.5
CYCLES	P	A1	A2													
250.300	7.56 1.70	9.78	.385	9.37	.369	26.06	1.026	.559	.022	5.000	111.76	4.40	18.26	16.62		
255.300	7.56 1.70	10.31	.406	9.96	.392	26.62	1.048	.622	.025	4.500	138.29	5.44	18.88	17.18		
259.800	7.56 1.70	11.05	.435	10.46	.412	27.24	1.072	.444	.017	4.000	111.12	4.37	19.47	17.72		
263.500	7.56 1.70	11.58	.456	10.82	.426	27.69	1.090	.508	.020	2.800	181.43	7.14	20.03	18.23		
266.600	7.56 1.70	12.09	.476	11.33	.446	28.19	1.110	.267	.011	1.000	266.70	10.50	20.50	18.65		
267.600	7.56 1.70	12.45	.490	11.51	.453	28.46	1.120	.368	.014	1.200	306.92	12.08	20.90	19.02		
269.500	7.56 1.70	12.75	.502	11.94	.470	28.83	1.135	.572	.023	1.500	381.00	15.00	21.51	19.57		
270.300	7.56 1.70	13.21	.520	12.62	.497	29.40	1.157	.483	.019	1.500	321.73	12.67	22.23	20.23		
271.000	7.56 1.70	13.72	.540	13.08	.515	29.88	1.176	.521	.020	1.500	347.13	13.67	22.96	20.89		
273.300	7.56 1.70	14.25	.561	13.59	.535	30.40	1.197	.432	.017	1.000	431.80	17.00	23.69	21.55		
274.300	7.56 1.70	14.78	.582	13.92	.548	30.84	1.214									

SECTION A2

This section of the Appendix includes all fatigue crack growth data obtained from WOL coupons tested at room temperature, at a range ratio of 0.05, and at a frequency of 0.1 Hz.



INPUT CONSTANTS:

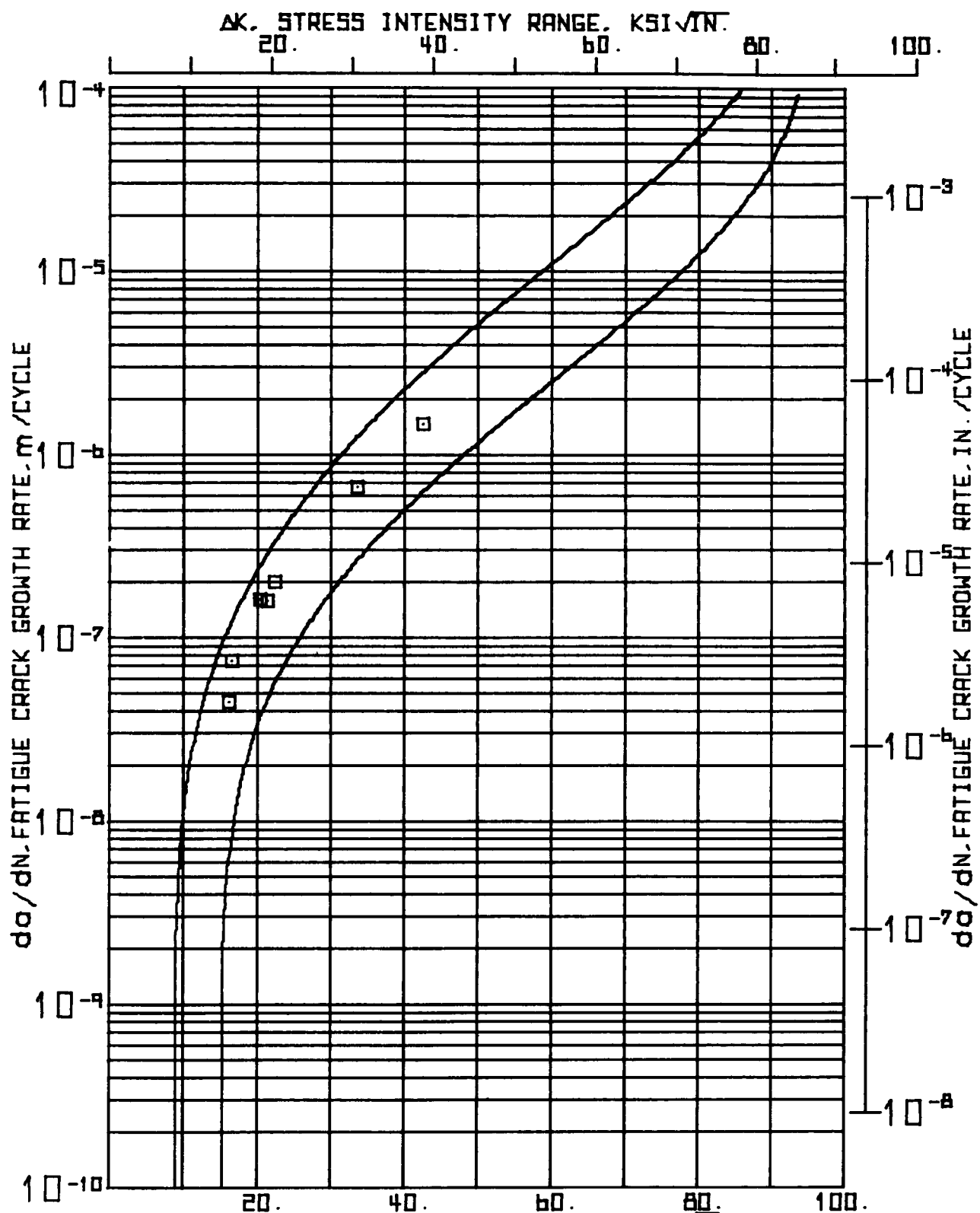
RANGE RATIO(R) .05
 TEST FREQUENCY(HZ) .1
 SPECIMEN WIDTH(W) 50.902 MM(2.004 IN.)
 SPECIMEN T-THICKNESS(B) 18.959 MM(.746 IN.)
 CRACK BR. CORRECTION 1.270 MM(.050 IN.)

NUMBER OF CYCLES	P KN	MAXIMUM LOAD KIPS	SIDE 1		SIDE 2		CORRECTED AVERAGE CRACK LENGTH		CHANGE IN CRACK LENGTH MM	CHANGE IN CYCLES	CRACK GROWTH RATE DA / DN MICRONS PER CYCLE	STRESS INTENSITY RANGE DELTA K			
			A1 INCH	MM	A2 INCH	MM	MM	INCH				MPA X 1000	ksi X 1000		
1000	17.79	4.00	19.41	.764	19.41	.764	20.08	.814	.635	.025	1.000	635.00	25.00	32.82	29.87
1000	17.79	4.00	19.91	.784	20.17	.794	21.31	.839	.762	.030	1.000	762.00	30.00	33.95	30.90
2000	17.79	4.00	20.42	.804	21.18	.834	22.07	.869	.762	.030	1.000	762.00	30.00	35.25	32.08
3000	17.79	4.00	21.18	.834	21.95	.864	22.83	.899	1.016	.040	1.000	1016.00	40.00	36.86	33.55
4000	17.79	4.00	21.95	.864	23.22	.914	23.85	.939	1.016	.040	1.000	1016.00	40.00	38.86	35.36
5000	17.79	4.00	22.56	.904	24.23	.954	24.87	.979	1.397	.055	1.000	1397.00	55.00	41.46	37.73
6000	17.79	4.00	24.49	.964	25.50	1.004	26.26	1.034	1.778	.070	1.000	1778.00	70.00	45.32	41.25
7000	17.79	4.00	26.52	1.044	27.03	1.064	28.04	1.104	2.667	.105	1.000	2667.00	105.00	51.80	47.14
8000	17.79	4.00	29.06	1.144	29.62	1.174	30.71	1.209							

(K9L) SPEC.3CR-1 T1-5AL-2.5SN(ELI) R.T. LAB AIR R.05 F.1.MZ --- 11:50 AUG 03, '76

INPUT CONSTANTS

ELASTIC MODULUS(E) = 118.590E+03 MPA(17.200E+06 PSI)				
NUMBER	CRACK NGUTM	OPTICAL	COMPLIANCE	
OF		BASE	BASE	
CYCLES				
N	CEP			
X 1000				
100	45.0527	.406	.410	
1000	45.3444	.419	.414	
2000	51.1863	.434	.437	
3000	53.7531	.449	.449	
4000	57.4117	.469	.464	
5000	62.7453	.489	.485	
6000	69.1707	.516	.507	
7000	81.0214	.551	.543	
8000	103.0643	.603	.593	



(WOL) SPEC. BCR-1 TI-5AL-2.55N(ELI) R.T. LAB AIR R=.05 F=.1 HZ

(40L) SPEC.8CB-1 T1-SAL-2.55N(ELT) R.T.LAB AIR R.05 F.0.1 HZ * * W E D G E * * B P E N * L B A D * P R B G R A M * *

11:51 AUG 03, '76

INPUT CONSTANTS:

RANGE RATIO(R) * .05
 TEST FREQUENCY(HZ) * .1
 SPECIMEN WIDTH(W) * 51.003 MM(2.008 IN.)
 SPECIMEN THICKNESS(B) * 19.007 MM(.748 IN.)
 CRACK DIS. CORRECTION * 1.270 MM(.050 IN.)

NUMBER FF CYCLES	MAXIMUM LOAD P	SIDE 1		SIDE 2		CORRECTED AVERAGE CRACK LENGTH		CHANGE IN CRACK LENGTH DA		CHANGE IN CYCLES		CRACK GROWTH RATE DA / DN		STRESS INTENSITY RANGE DELTA K	
		MM	INCH	MM	INCH	MM	INCH	MM	INCH	DN	X 1000	METER	IN.	MPA X 10 ⁻³	IN ³ /2
1000	9.79	2.20	16.94	.667	17.37	.684	18.43	.725	.553	.022	12.500	44.70	1.76	16.15	14.70
12.500	9.79	2.20	17.40	.685	18.03	.710	18.99	.747	.552	.022	7.500	74.51	2.93	16.57	15.08
20.000	9.79	2.20	17.88	.704	18.67	.735	19.55	.769							
20.000	11.57	2.60	17.88	.704	18.67	.735	19.55	.769	1.219	.048	7.500	162.56	6.43	20.40	18.56
27.500	11.57	2.60	19.25	.758	19.74	.777	20.76	.817	.788	.031	5.000	157.48	6.20	21.39	19.46
32.500	11.57	2.60	20.04	.769	20.52	.804	21.55	.848	1.016	.040	5.000	203.20	8.00	22.34	20.33
37.500	11.57	2.60	21.06	.829	21.54	.848	22.57	.868							
37.500	15.57	3.50	21.06	.829	21.54	.848	22.57	.868	3.353	.132	5.000	670.56	26.40	33.59	30.57
42.500	15.57	3.50	24.38	.960	24.92	.981	25.92	1.020	5.143	.202	3.487	1475.05	58.07	42.63	38.80
45.887	15.57	3.50	23.39	1.157	30.20	1.189	31.06	1.223							

1.001 SPEC-8CR-1 71-5AL-2-SSN(ELI) R.T.LAB.AIR R=0.5 F=0.1 M2 11:51 AUG 03, '76

INPUT CONSTANTS

ELASTIC MODULUS(E) = 118.590E+03 MPA(17.200E+06 PSI)				
NUMBER OF CYCLES	CRACK COMPLIANCE	ADAR / BASE	OPTICAL COMPLIANCE BASE	
N	CcB			
X 1000				
000	41.0255	.361		.364
12.000	43.4388	.372		.398
20.000	45.0477	.383		.407
27.000	46.2698	.407		.427
34.000	52.2875	.423		.442
37.500	56.5096	.442		.459
42.600	72.3980	.508		.517
45.957	112.0191	.609		.611

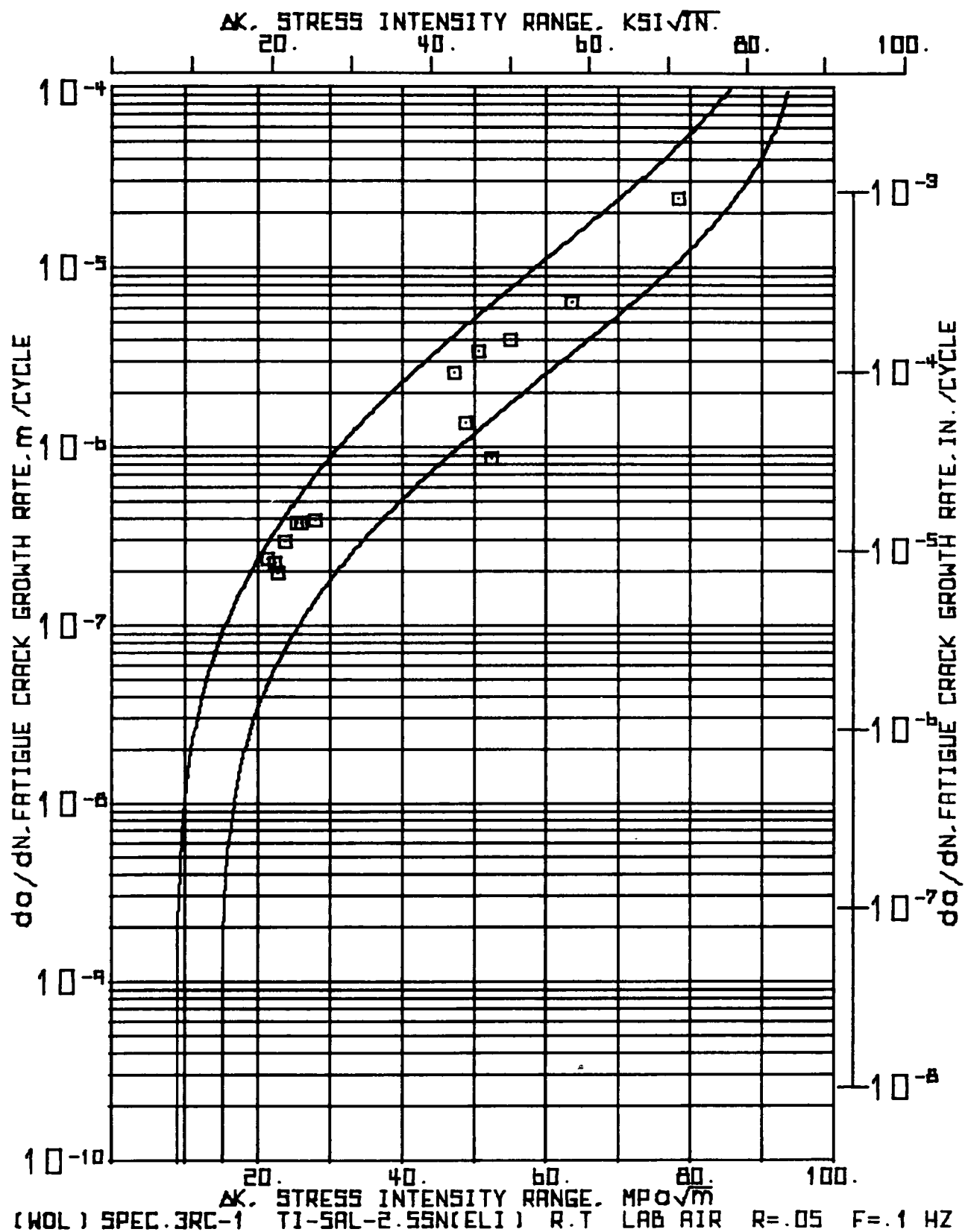


TABLE SPEC-3PC-1 TT-5AL-2-55N(ELT) R.T. LAB AIR R-05 F-0.1 Hz 11:51 AUG 03, '76

INPUT CONSTANTS:

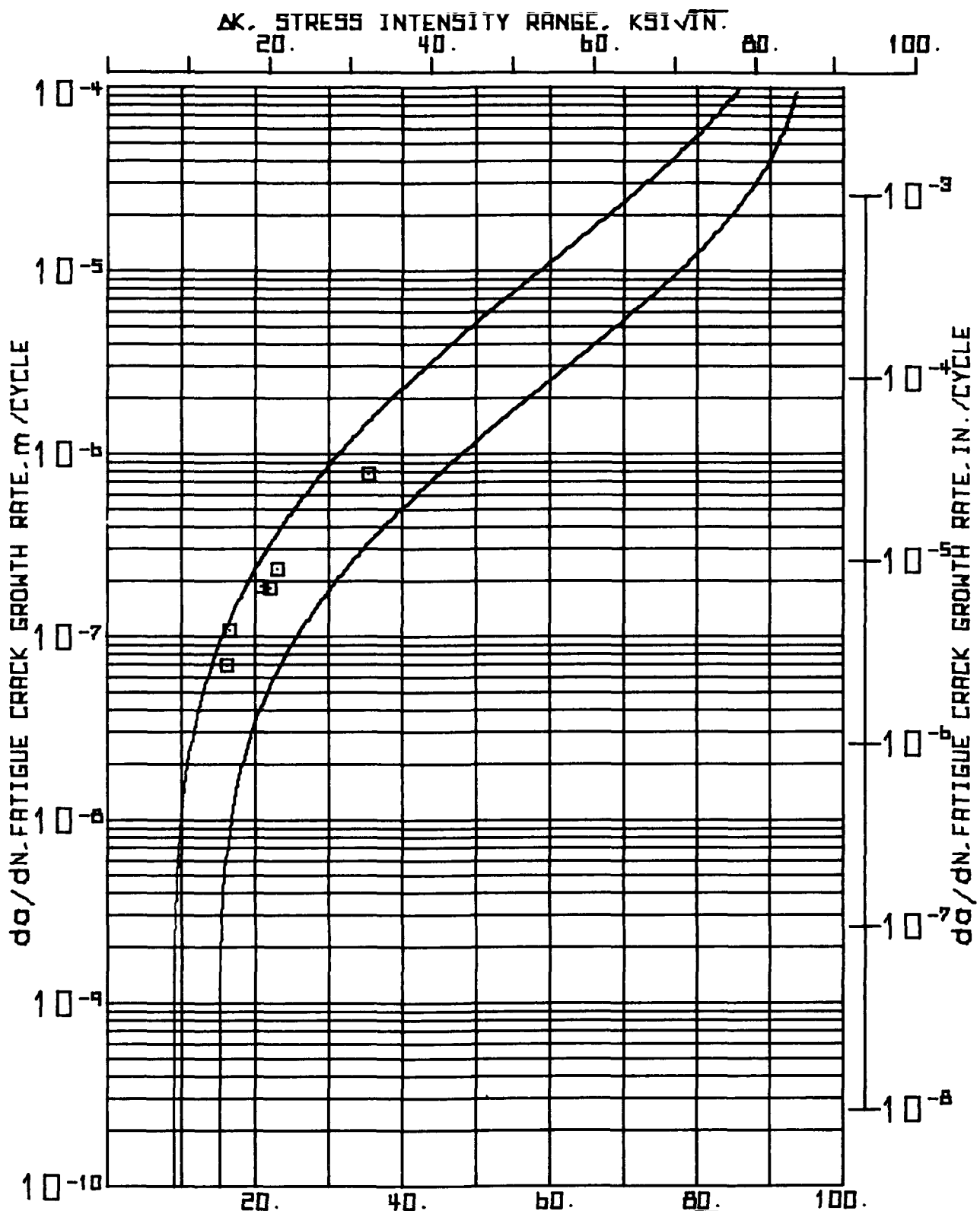
RANGE RATIO (R) .05
 TEST FREQUENCY (Hz) .1
 SPECIMEN WIDTH (in) 50.902 MM (2.004 in.)
 SPECIMEN THICKNESS (B) 18.948 MM (.746 in.)
 CRACK BA CORRECTION 1.270 MM (.050 in.)

NUMBER OF CYCLES	MAXIMUM LOAD	SIDE 1		SIDE 2		CORRECTED AVERAGE CRACK LENGTH		CHANGE IN CRACK LENGTH		CHANGE IN CYCLES		CRACK GROWTH RATE		STRESS INTENSITY RANGE	
		A1	INCH	A2	INCH	MM	INCH	MM	INCH	DN	INCH X 1000	MM	INCH	MPA X 1000	KSI X 1000
1	12.07 2.71	14.16	.715	18.16	.715	19.43	.765	1.600	.063	6.691	239.16	9.42	21.50	19.56	
6.691	12.07 2.71	19.76	.778	19.76	.778	21.03	.828	.254	.010	1.125	225.74	8.89	22.46	20.44	
7.816	12.07 2.71	20.02	.788	20.02	.788	21.29	.838	.254	.010	1.280	198.44	7.81	22.74	20.69	
9.096	12.07 2.71	20.27	.798	20.27	.798	21.54	.848	1.778	.070	6.030	294.86	11.61	23.30	21.75	
15.126	12.07 2.71	22.05	.868	22.05	.868	23.32	.918	.508	.020	1.350	376.30	14.81	25.32	23.04	
16.476	12.07 2.71	22.56	.888	22.56	.888	23.83	.938	.504	.020	1.350	376.30	14.81	25.39	23.66	
17.826	12.07 2.71	23.06	.908	23.06	.908	24.33	.958	2.280	.090	5.876	389.04	15.32	28.01	25.49	
23.702	12.07 2.71	25.35	.998	25.35	.998	26.62	1.048								
23.702	18.68 4.20	25.35	.998	25.35	.998	26.62	1.048	.762	.030	.292	2609.59	102.74	47.20	42.95	
25.994	18.68 4.20	26.11	1.028	26.11	1.028	27.38	1.078	.381	.015	.278	1370.50	53.96	48.79	44.40	
24.272	18.68 4.20	26.49	1.043	26.49	1.043	27.76	1.093	.889	.035	.260	3419.23	134.62	50.66	46.10	
24.532	18.68 4.20	27.38	1.078	27.38	1.078	28.65	1.128	.254	.010	.293	866.89	34.13	52.45	47.73	
24.225	14.68 4.20	27.64	1.088	27.64	1.088	28.91	1.138	1.270	.050	.320	3968.75	156.25	54.99	50.04	
25.145	18.68 4.20	28.31	1.138	28.31	1.138	30.18	1.168	3.170	.125	.495	6414.14	252.53	63.69	57.96	
25.640	18.68 4.20	32.08	1.263	32.08	1.263	33.35	1.313								
25.740	18.68 4.20	34.49	1.358	34.49	1.358	35.76	1.408	2.413	.095	.100	24130.00	950.00	78.32	71.27	

(A0L) SPEC3PC-1 T1-5AL-2-5SN(ELI) R.T. LAB AIR R=05 F=1.14Z. ... 11151 AUG 03, '76

INPUT CONSTANTS

ELASTIC MODULUS(E) = 118.590E+03 MPA(17.200E+06 PSI)						
NUMBER OF CYCLES	CRACK WIDTH COMPLIANCE	ABAR / W OPTICAL BASE	COMPLIANCE BASE			
N	CEB					
X 1000						
1.00	42.3355	.382	.396			
6.691	40.3459	.413	.414			
7.416	40.9943	.418	.427			
9.736	40.0943	.423	.427			
15.126	55.0151	.458	.457			
16.474	56.3393	.468	.462			
17.526	60.2497	.478	.475			
23.702	71.5051	.523	.514			
23.994	76.5015	.548	.530			
24.272	75.7851	.545	.536			
24.532	83.4227	.563	.548			
24.525	92.0296	.568	.569			
24.145	94.6506	.593	.594			
25.640	141.0240	.655	.654			
25.740	195.0770	.703	.711			



(WOL) SPEC. BRC-1 TI-SAL-2.55N(ELI) R.T. LAB AIR R=.05 F=.1 HZ

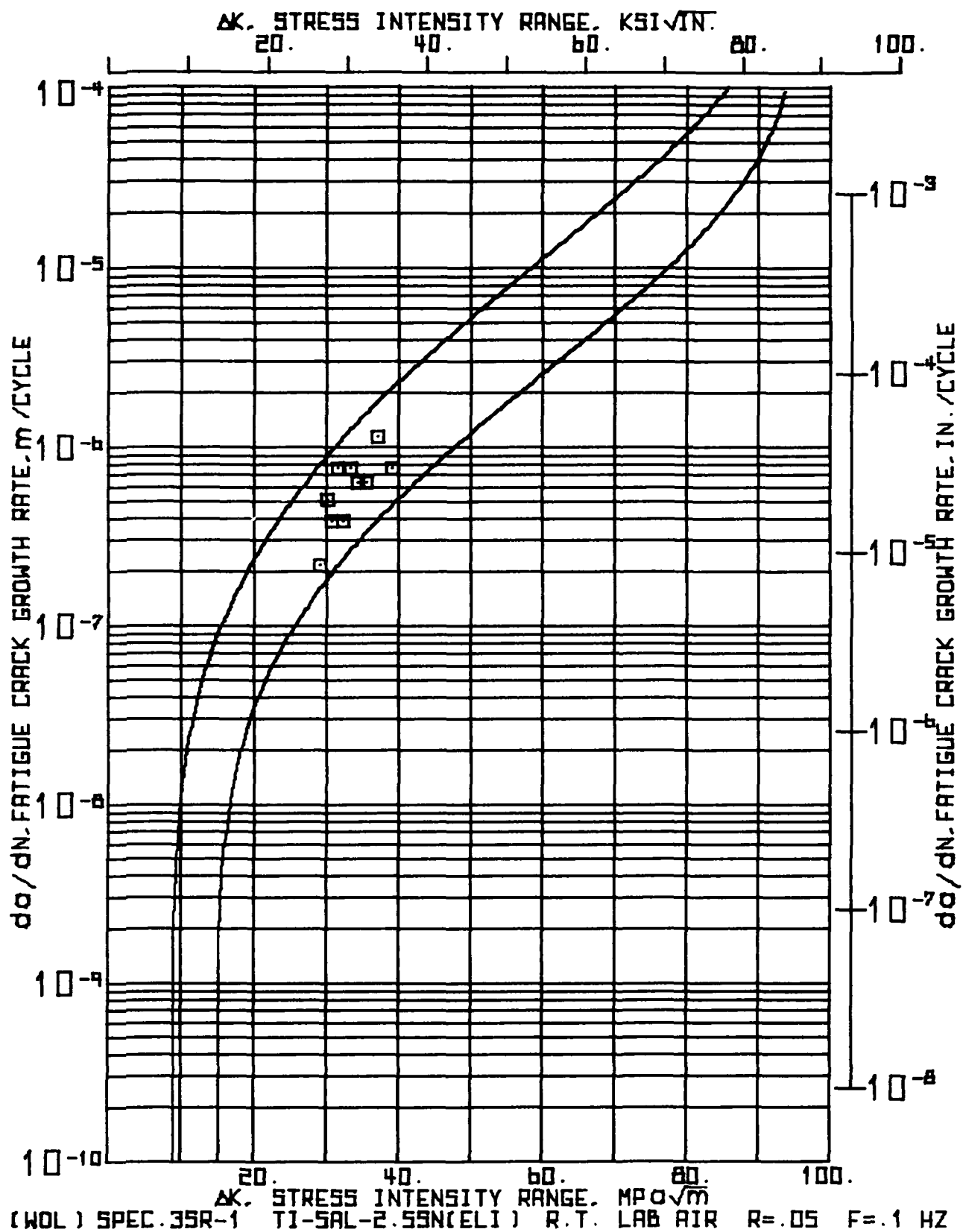
INPUT CONSTANTS:

NUMBER OF CYCLES	P KN	MAXIMUM LOAD KIPS	SIDE 1 CRACK LENGTH		SIDE 2 CRACK LENGTH		CORRECTED AVERAGE LENGTH	CHANGE IN CRACK LENGTH	CHANGE IN CYCLES	CRACK GROWTH RATE DA / DN MICR9 IN9	STRESS INTENSITY RANGE	
			A1 MM	INCH	A2 MM	INCH					MPA X 400.5	ksi X IN00.5
15000	9.79	2.20	10.52	.729	18.72	.737	13.09	.783				
3000	9.79	2.20	17.25	.679	17.32	.682	10.55	.730				
7500	9.79	2.20	17.68	.696	17.53	.706	15.08	.751				
15000	9.79	2.20	10.52	.729	18.72	.737	13.09	.783				
15000	11.57	2.60	10.52	.729	18.72	.737	19.89	.783				
22500	11.57	2.60	20.04	.789	20.02	.788	21.30	.838				
27500	11.57	2.60	20.98	.826	20.90	.823	22.21	.874				
32500	11.57	2.60	22.10	.870	22.12	.871	23.38	.920				
32500	15.57	3.50	22.10	.870	22.12	.871	23.38	.920				
37500	15.57	3.50	25.78	1.015	26.21	1.032	27.27	1.073				

(MPL) SPEC:8NC-1 11-5AL-2.5SN(ELI) R-Y-LAB AIR R=05 F=1 HZ 11:52 AUG 03, 1976

INPUT CONSTANTS

ELASTIC MODULUS(E) = 113.590E+03 MPa (17.200E+06 PSI)				
NUMBER OF CYCLES	CRACK INPUT COMPLIANCE	ABAR / IN	OPTICAL COMPLIANCE	BASE BASE
N	CL3			
X 1000				
500	40.2426	.363	.340	
7500	43.4620	.373	.398	
12500	45.6766	.389	.411	
22500	53.9251	.417	.449	
27500	54.7300	.434	.453	
32500	61.1688	.457	.479	
37500	79.8804	.533	.538	



(MEL) SPEC.3SR-1 YI-BAL-2.55N(EL) R.1. LAB AIR R.05 F.01 HZ * * * * * 11:52 AUG 03, 1976

INPUT CONSTANTS:

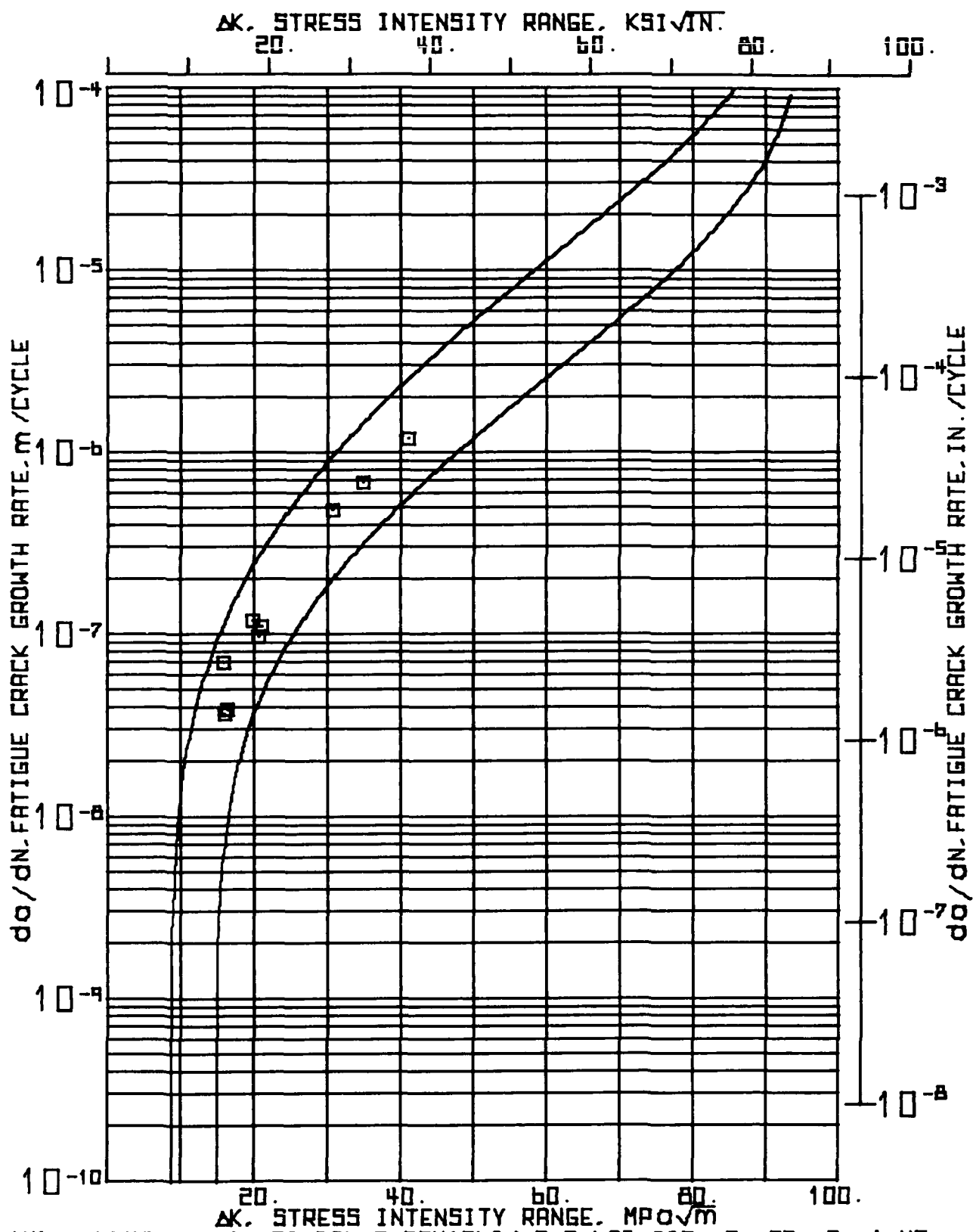
RANGE RATIO(R) .05
TEST FREQUENCY(HZ) .1
SPECIMEN WIDTH(W) 50.902 MM(2.004 IN.)
SPECIMEN THICKNESS(B) 18.989 MM(.748 IN.)
CRACK BR. CORRECTION 1.270 MM(.050 IN.)

NUMBER OF CYCLES	MAXIMUM LOAD	SIDE 1 CRACK LENGTH	SIDE 2 CRACK LENGTH	CORRECTED AVERAGE CRACK LENGTH	CHANGE IN CRACK LENGTH	CHANGE IN DA	INCH X 1000	CRACK GROWTH RATE DA / DN	STRESS INTENSITY RANGE
N	P	A1	A2	ABAR	MM	MM	DN	NANOMETER	MPA X 1000.5
X 1000	KN	MM	MM	MM	INCH	INCH	INCH X 1000	PER CYCLE	IN000.5
000	17.79	4.00	16.74	.659	16.61	.654	17.95	.706	
4500	17.79	4.00	17.65	.695	17.65	.695	16.92	.745	29.12
5500	17.79	4.00	18.16	.715	18.16	.715	19.43	.765	30.11
6500	17.79	4.00	18.67	.735	18.41	.725	19.81	.760	30.73
7500	17.79	4.00	19.43	.765	19.18	.755	20.57	.810	31.56
8500	17.79	4.00	19.68	.775	19.63	.775	20.95	.825	32.42
9500	17.79	4.00	20.45	.805	20.45	.805	21.72	.855	33.32
10500	17.79	4.00	20.95	.825	21.21	.835	22.35	.860	34.47
11500	17.79	4.00	21.46	.845	21.97	.865	22.99	.905	35.57
12500	17.79	4.00	22.73	.895	22.99	.905	24.13	.950	37.21
13500	17.79	4.00	23.49	.925	23.75	.935	24.89	.960	39.11
									35.59

(KUL) SPEC-3SR-1 11-5AL-2-53N(ELI) R-T LAB AIR R=05 F=1 HZ 11:52 AUG 03, 1976

INPUT CONSTANTS

ELASTIC MODULUS(E) = 118.590E+03 MPa(17.200E+06 PSI)				
NUMBER OF CYCLES	CRACK INBTM COMPLIANCE	ABAR / W OPTICAL COMPLIANCE	BASF	
N	CEB			
X 1500				
4500	43.1601	.372	.357	
5000	43.9042	.382	.401	
6000	46.1366	.369	.412	
7000	47.6249	.434	.420	
8000	48.5690	.412	.424	
9000	52.0837	.427	.441	
10000	55.0563	.439	.454	
11000	58.0725	.452	.467	
12000	62.0077	.474	.484	
13000	66.3725	.489	.499	



(WOL) SPEC. 85R-1 TI-5AL-2.55N(ELI) R.T. LAB AIR R=.05 F=.1 HZ

*** W E D G E * O P E N * L 0 A D * P R 8 G R A M * * * 11:53 AUG 03, 1976

*** (108L) SPEC:8SR-1 T1-5AL-2.55N(ELI) R.1.LAB AIR R=05 F=0.1 HZ

INPUT CONSTANTS:

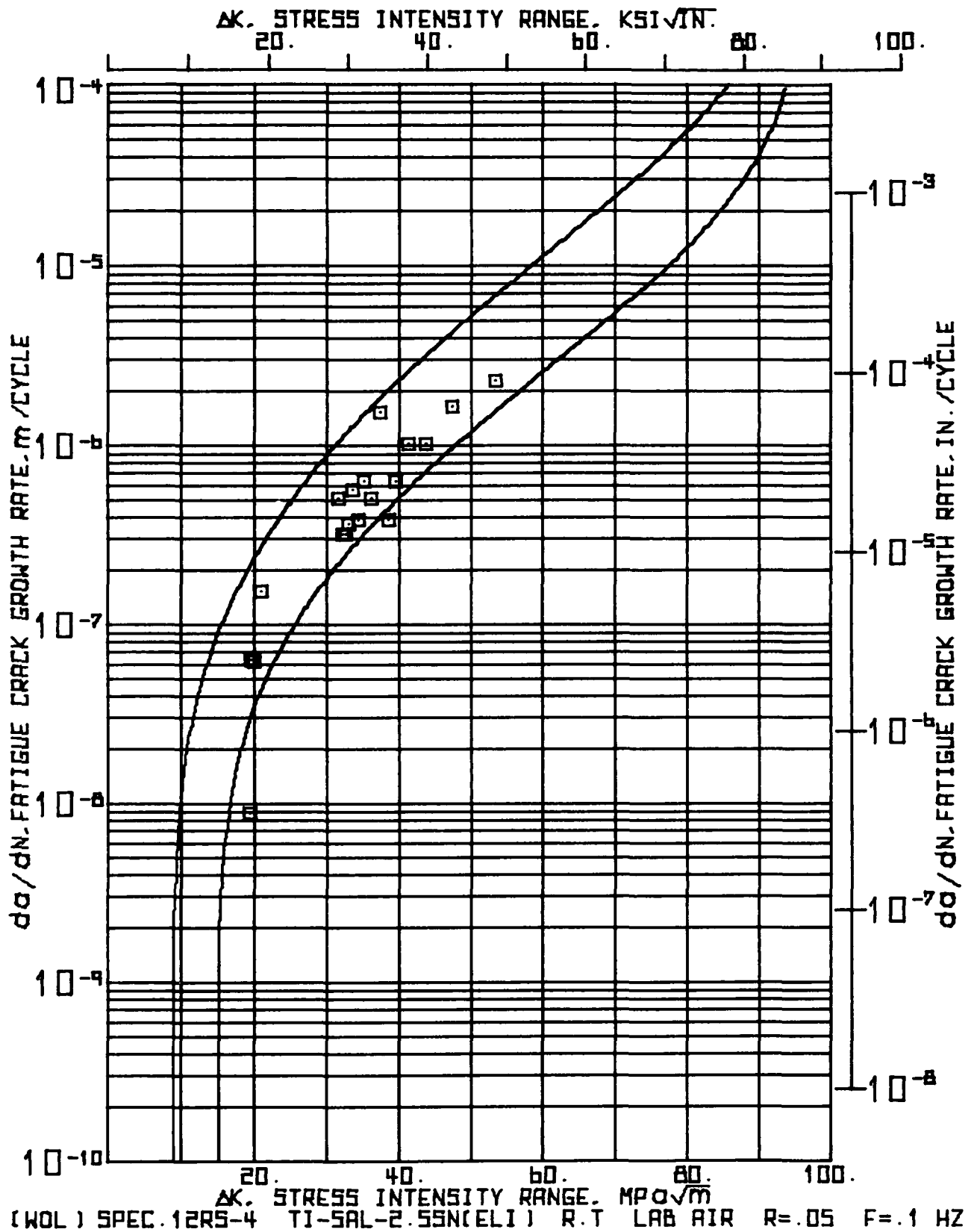
RANGE, RATIO(M) * .05
 TEST FREQUENCY(HZ) * .1
 SPECIMEN WIDTH(M) * 51.029 MM(2.009 IN.)
 SPECIMEN THICKNESS(B) * 19.014 MM(.749 IN.)
 CRACK DIA. CORRECTION * 1.270 MM(.050 IN.)

NUMBER OF CYCLES	P KIPS	MAXIMUM LOAD	SIDE 1		SIDE 2		CORRECTED AVERAGE CRACK LENGTH		CHANGE IN CRACK LENGTH		CHANGE IN CYCLES		CRACK GROWTH RATE DA / DN		STRESS INTENSITY RANGE	
			MM	INCH	MM	INCH	MM	INCH	MM	INCH	MM	INCH	MM	INCH	MPA X 100.5	KSI X 14.5
1000	4N	9.79	2.20	16.97	.668	17.35	.683	18.43	.725	.350	.014	5.000	71.12	2.80	16.07	14.62
5000	9.79	2.20	17.40	.685	17.63	.694	18.78	.739	.279	.011	7.500	37.25	1.47	16.30	14.83	
12500	9.79	2.20	17.78	.700	17.81	.701	19.06	.750	.292	.012	7.500	38.95	1.53	16.51	15.02	
20000	9.79	2.20	18.29	.720	17.88	.704	19.35	.762								
26000	11.57	2.60	18.29	.720	17.88	.704	19.35	.762	.902	.035	7.500	120.23	4.73	20.05	18.24	
27500	11.57	2.60	19.28	.759	18.69	.736	20.26	.797	.495	.020	5.000	99.06	3.90	20.71	18.85	
32500	11.57	2.60	19.94	.785	19.02	.749	20.75	.817	.553	.022	5.000	111.76	4.40	21.23	19.32	
37500	11.57	2.60	20.57	.810	19.51	.766	21.31	.839								
37500	15.57	3.50	20.57	.810	19.51	.768	21.31	.839	2.438	.096	5.000	487.68	19.20	30.74	27.98	
42500	15.57	3.50	23.06	.908	21.89	.862	23.75	.935	2.680	.106	3.887	689.40	27.14	35.08	31.93	
46387	15.57	3.50	25.43	1.001	24.89	.940	26.43	1.040	3.023	.119	2.500	1209.04	47.60	41.19	37.48	
48887	15.57	3.50	28.37	1.117	27.99	1.102	29.45	1.159								

(*01) SPEC:8SR-1 T1-5AL-2-55NIELI) R-1-LAB-AIR R-05 F-01-MZ 11:53 AUG 03,176

INPUT CONSTANTS

ELASTIC MODULUS(E) = 110.590E+03 MPA(17.200E+06 PSI)				
NUMBER OF CYCLES	CRACK MOUTH COMPLIANCE	ADAR / W OPTICAL COMPLIANCE	BASE BASE	
N				
K 1500				
000	39.4325	.361	.375	
5000	47.2372	.368	.380	
12500	41.7420	.374	.385	
20000	43.4562	.379	.398	
27500	45.657	.397	.407	
35000	47.400	.407	.419	
37500	50.0289	.418	.435	
40000	53.511	.465	.472	
45367	74.6365	.518	.522	
45687	97.3741	.577	.591	



(A0L) 5PLC-12RS-4 T1-5AL-2-55N(EL) R.T. LAB AIR R-05 F-01 HZ 11153 AUG 03, 1976 PAGE 2

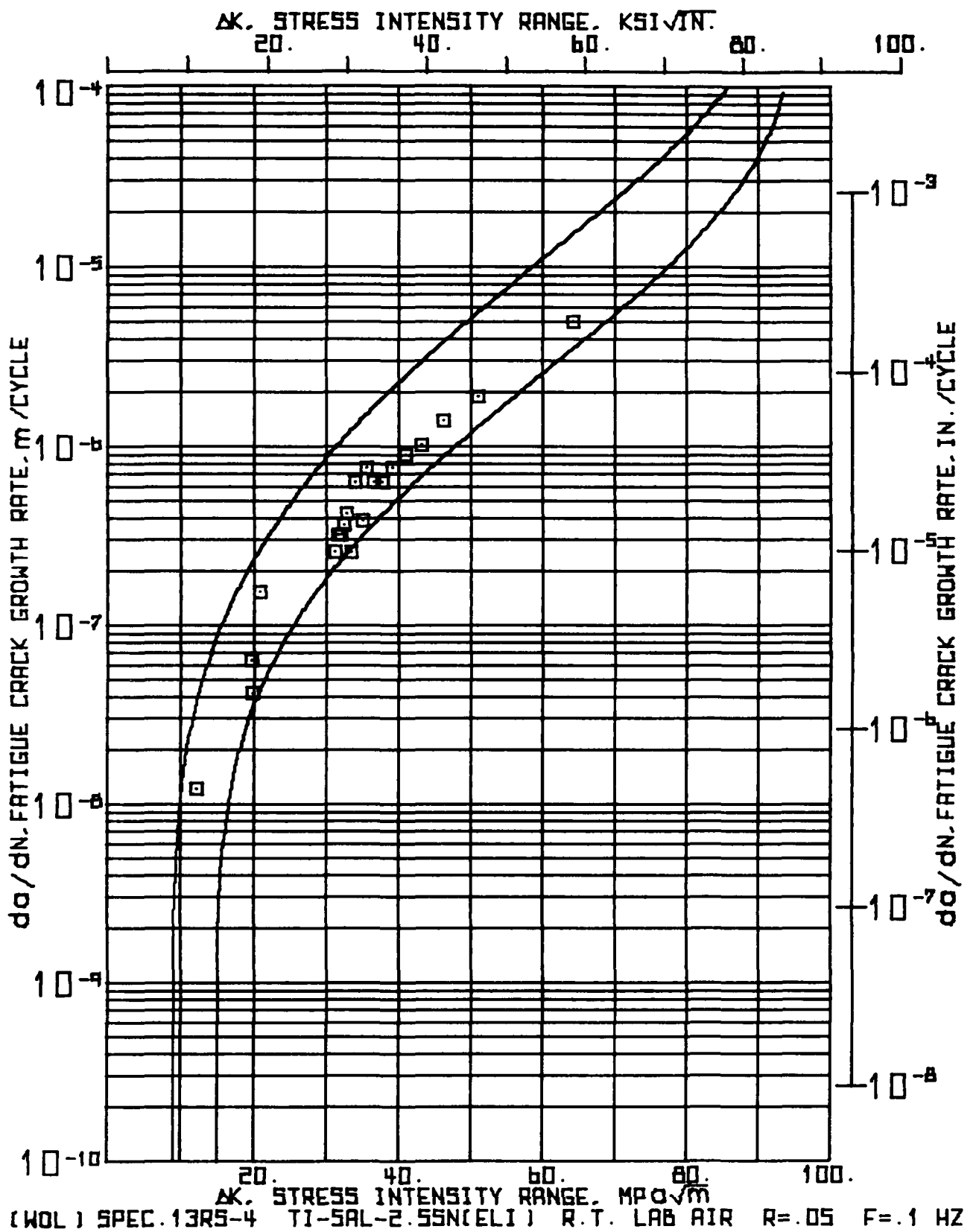
NUMBER OF CYCLES	MAXIMUM LOAD	P	SIDE 1		SIDE 2		CORRECTED AVERAGE CRACK LENGTH	CHANGE IN CRACK LENGTH		CHANGE IN CYCLES	CRACK GROWTH RATE		STRESS INTENSITY RANGE
			MM	INCH	MM	INCH	MM	MM	INCH		DA / DN METER PER CYCLE	MICR3 IN.	MPA X 1000 KSI X 1000
N			A1		A2								DELTA K
X 1000	KN	KIPS	MM	INCH	MM	INCH	MM	MM	INCH	DN X 1000			
13.350	17.79	4.00	25.53	1.005	26.03	1.025	27.05	1.065	1.651	.065	1.000	1651.00	65.00
													47.33
14.350	17.79	4.00	27.05	1.065	27.81	1.095	28.70	1.130	2.286	.090	1.000	2286.00	90.00
													53.50
15.350	17.79	4.00	29.34	1.155	30.10	1.185	30.99	1.220					46.68

11153 AUG 03, 1976

1001) 5P2C012RS44 Y1-5AL-2.35N(ELI) M.F. LAB AIR R=0.05 F=0.1 MZ

INPUT CONSTANTS

ELASTIC MODULUS(E) * 110.590E+03 MPa (17.200E+06 PSI)									
NUMBER	CRACK	NUMBER	ABAR	/	W				
OF	COMPLIANCE	OPTICAL	COMPLIANCE						
CYCLES	BASE	BASE	BASE						
N	CEP								
* 1000									
1.000	35.7J43	.354	.351						
2.000	36.4402	.360	.356						
3.000	37.9359	.365	.366						
4.000	38.0737	.372	.370						
5.000	4.16164	.387	.379						
6.000	43.1427	.392	.396						
7.000	43.0506	.402	.401						
8.000	45.1181	.407	.412						
9.000	44.0619	.412	.416						
10.000	47.3426	.417	.424						
11.000	48.0373	.427	.431						
12.000	51.3200	.435	.438						
13.000	53.0525	.447	.448						
14.000	57.2757	.457	.463						
15.000	58.0195	.472	.466						
16.000	6.4943	.480	.478						
17.000	65.4573	.492	.494						
18.000	71.4067	.512	.514						
19.000	75.1042	.542	.534						
20.000	8.03170	.505	.561						
21.000	11.0584	.610	.606						



(16L) SPEC:13RS-4 T1-5AL-2-55N(ELI) R.T. LAB AIR R-05 F-0.1 MZ 12103 AUG 03,176

INPUT CONSTANTS:

RANGE RATIO(R) .05
 TEST FREQUENCY(HZ) .1
 SPECIMEN WIDTH(A) 50.851 MM(2.002 IN.)
 SPECIMEN THICKNESS(B) 18.971 MM(.747 IN.)
 CRACK BR. CORRECTION 1.270 MM(.050 IN.)

NUMBER OF CYCLES	MAXIMUM LOAD	SIDE 1 CRACK LENGTH		SIDE 2 CRACK LENGTH		CORRECTED AVERAGE CRACK LENGTH		CHANGE IN CRACK LENGTH		CHANGE IN CYCLES		CRACK GROWTH RATE DA / DN		STRESS INTENSITY RANGE DELTA K	
		INCH	MM	INCH	MM	INCH	MM	MM	INCH	DN X 1000	NANG. METER PER CYCLE	MICRS IN, PER CYCLE	MPA X 1000	KSI X 1000	
X 1000	KN	KIPS	INCH	MM	INCH	MM	INCH	MM	INCH	X 1000					
000	7.56	1.70	16.56	652	16.41	646	17.75	.699	.381	.015	31.525	12.09	.48	12.14	11.05
31.525	7.56	1.70	16.99	669	16.74	659	18.14	.714							
31.525	12.01	2.70	16.99	669	16.74	659	18.14	.714	.254	.010	4.017	63.23	2.49	19.55	17.79
35.542	12.01	2.70	17.25	679	16.99	669	18.39	.724	.254	.010	6.175	41.13	1.62	19.77	18.00
41.717	12.01	2.70	17.50	689	17.25	679	18.64	.734							
000	12.01	2.70	18.01	709	18.52	729	19.53	.769	.254	.010	1.650	153.94	6.06	20.83	18.96
1.650	12.01	2.70	18.26	719	18.77	739	19.79	.779							
1.650	17.79	4.00	18.26	719	18.77	739	19.79	.779	.254	.010	1.000	254.00	10.00	31.22	28.41
2.650	17.79	4.00	18.52	729	19.02	749	20.04	.789	.254	.010	.800	317.50	12.50	31.59	28.75
3.450	17.79	4.00	18.77	739	19.28	759	20.29	.799	.254	.010	.800	317.50	12.50	31.97	29.10
4.250	17.79	4.00	19.02	749	19.53	769	20.55	.809	.254	.010	.700	362.86	14.29	32.36	29.45
4.950	17.79	4.00	19.28	759	19.79	779	20.80	.819	.381	.015	.900	423.33	16.67	32.85	29.90
5.850	17.79	4.00	19.53	769	20.29	799	21.18	.834	.254	.010	1.000	254.00	10.00	33.36	30.36
6.850	17.79	4.00	19.79	779	20.55	809	21.44	.844	.635	.025	1.000	635.00	25.00	34.08	31.02
7.850	17.79	4.00	20.29	799	21.31	839	22.07	.869	.381	.015	1.000	381.00	15.00	34.95	31.80
8.850	17.79	4.00	20.80	819	21.56	849	22.45	.884	.381	.015	.500	762.00	30.00	35.62	32.41
9.350	17.79	4.00	21.31	839	21.82	859	22.83	.899	.635	.025	1.000	635.00	25.00	36.54	33.26
10.350	17.79	4.00	21.82	859	22.53	889	23.47	.924	.635	.025	1.000	635.00	25.00	37.75	34.36
11.350	17.79	4.00	22.58	889	23.09	909	24.10	.949	.762	.030	1.000	762.00	30.00	39.15	35.64
12.350	17.79	4.00	23.34	919	23.85	939	24.87	.979							

(INCL) SPEC. 13RS-4 T1-SAL-2.55N(ELI) R.T. LAB AIR R-05 F-01 HZ 12103 AUG 03, '76 PAGE 2															
NUMBER OF CYCLES	MAXIMUM LOAD	SIDE 1 CRACK LENGTH		SIDE 2 CRACK LENGTH		CORRECTED AVERAGE LENGTH		CHANGE IN LENGTH		CHANGE IN CYCLES		CRACK GROWTH RATE		STRESS INTENSITY RANGE	
		N	P	A1	A2	MM	INCH	MM	INCH	MM	INCH	DN	INCH	DA / DN METER PER CYCLE	MPA X M00.5
12.350	17.79	4.00	23.34	.919	23.85	.939	24.37	.979	.887	.035	1.000	859.00	35.00	40.94	37.25
13.350	17.79	4.00	24.36	.959	24.61	.969	25.76	1.014	1.016	.040	1.000	1016.00	40.00	43.15	39.27
14.350	17.79	4.00	25.37	.999	25.63	1.009	26.77	1.054	1.397	.055	1.000	1397.00	55.00	46.23	42.07
15.350	17.79	4.00	26.38	1.049	27.15	1.069	28.17	1.109	1.905	.075	1.000	1905.00	75.00	51.07	46.48
16.350	17.79	4.00	28.68	1.129	28.93	1.139	30.07	1.184	4.953	.195	1.000	4953.00	195.00	64.22	58.44
17.350	17.79	4.00	33.50	1.319	34.01	1.339	35.03	1.379							

INPUT CONSTANTS

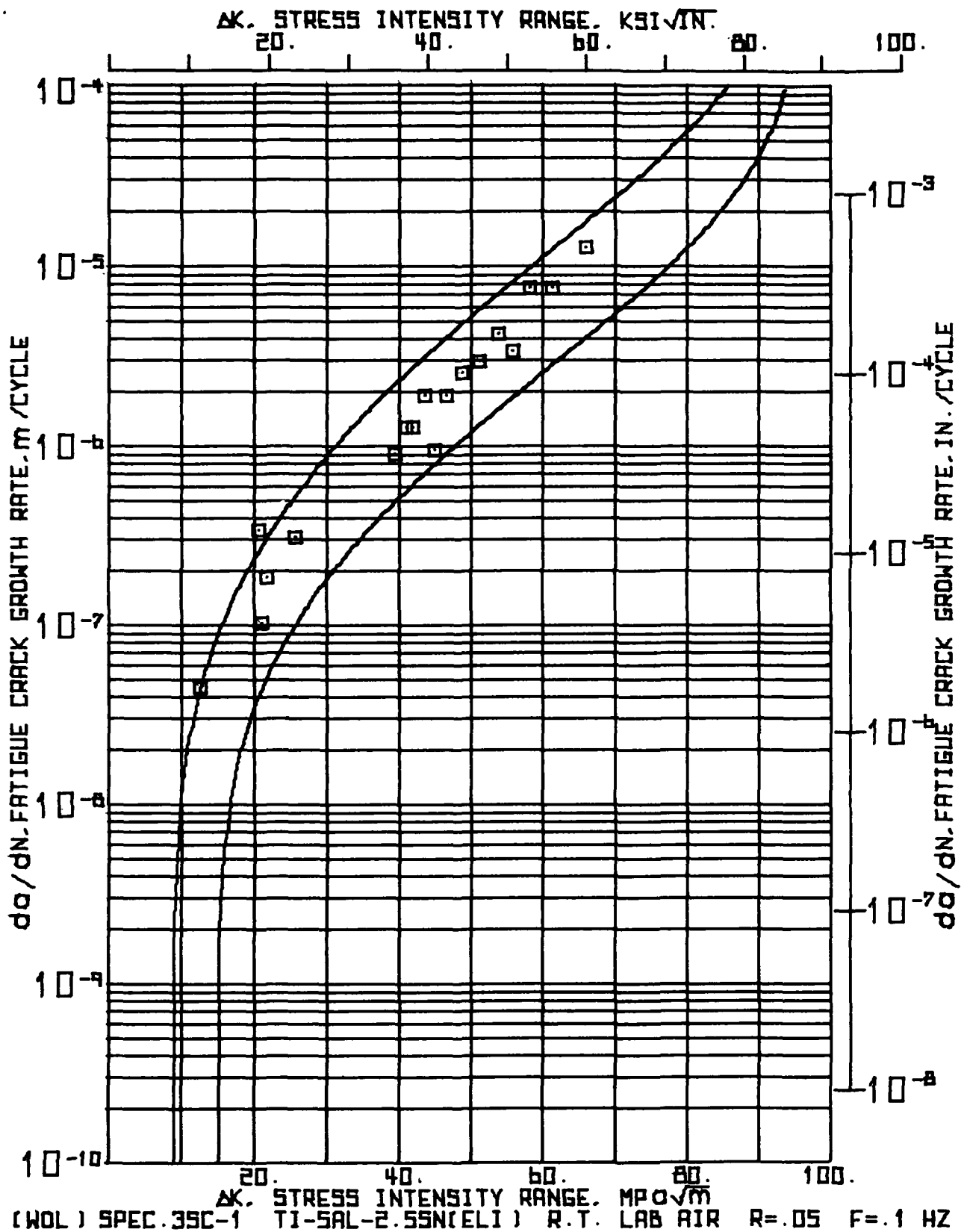
ELASTIC MODULUS(E) = 118.590E+03 MPA(17.200E+06 PSI)

NUMBER CRACK MOUTH ABAR / 4
OF COMPLIANCE OPTICAL COMPLIANCE
CYCLES BASE BASE

N CEB

X 1000

.000	34.1983	.349	.341
31.025	34.5418	.357	.346
35.542	35.0052	.362	.351
41.717	36.4287	.367	.356
.000	36.4287	.364	.375
1.050	40.1459	.389	.379
2.050	41.0328	.394	.388
3.050	43.1156	.399	.396
4.050	43.0631	.404	.400
4.950	44.0060	.409	.404
5.050	46.5369	.417	.416
6.050	49.0672	.422	.427
7.050	51.2975	.434	.438
8.050	54.0271	.442	.451
9.050	53.0271	.449	.448
10.050	55.7542	.462	.457
11.050	54.7319	.474	.469
12.050	62.4451	.479	.483
13.050	66.7098	.506	.499
14.050	73.5003	.526	.521
15.050	83.2655	.554	.548



(K9L) SPEC:35C71 T1-5AL-2.5SN(ELT) R.T. LAB AIR R=0.05 F=1 HZ 12:12 AUG 03, 196

INPUT CONSTANTS:

RANGE RATIO(R) .05
 TEST FREQUENCY(HZ) .1
 SPECIMEN WIDTH(W) 50.978 MM(2.007 IN.)
 SPECIMEN THICKNESS(B) 19.004 MM(.748 IN.)
 CRACK 50% CRACK LENGTH 1.270 MM(.050 IN.)

NUMBER OF CYCLES	MAXIMUM LOAD	SIDE 1 CRACK LENGTH	SIDE 2 CRACK LENGTH	CORRECTED AVERAGE CRACK LENGTH	CHANGE IN CRACK LENGTH	CHANGE IN CYCLES	CRACK GROWTH RATE DA / DN	STRESS INTENSITY RANGE
N	KIPS	MM	MM	MM	MM	DN X 1000	NANO METER PER CYCLE	MPA X 1000
1000	7.56	1.70	16.87	.664	17.12	.674	10.26	.719
24070	7.56	1.70	17.93	.706	18.19	.716	19.33	.761
24370	12.01	2.70	17.93	.706	18.19	.716	19.33	.761
25590	12.01	2.70	18.44	.726	18.69	.736	19.84	.781
26087	12.01	2.70	18.69	.736	18.95	.746	20.09	.791
34262	12.01	2.70	19.71	.776	20.22	.796	21.23	.836
4000	12.01	2.70	21.74	.856	23.27	.916	23.77	.936
1650	12.01	2.70	22.25	.876	23.77	.936	24.28	.956
1650	17.79	4.00	22.25	.876	23.77	.936	24.28	.956
2650	17.79	4.00	23.01	.906	24.79	.976	25.17	.991
3050	17.79	4.00	23.52	.926	25.30	.996	25.68	1.011
3450	17.79	4.00	24.03	.946	25.81	1.016	26.19	1.031
3850	17.79	4.00	24.79	.976	26.57	1.046	26.95	1.061
4250	17.79	4.00	25.30	.996	26.82	1.056	27.33	1.076
4650	17.79	4.00	26.06	1.026	27.58	1.086	28.09	1.106
4950	17.79	4.00	26.62	1.056	28.35	1.116	28.85	1.136
5250	17.79	4.00	27.58	1.086	29.36	1.156	29.74	1.171
5400	17.79	4.00	28.35	1.116	29.87	1.176	30.38	1.196
5550	17.79	4.00	24.85	1.136	30.38	1.196	30.89	1.216
5650	17.79	4.00	29.62	1.166	31.14	1.226	31.65	1.246

12112 AUG 03, 1976

(PWL) SPEC-3SC-1 T1-5AL-2-SSN(ELI) R.T. LAB AIR R-05 F-1 MZ

NUMBER OF CYCLES	MAXIMUM LOAD	SIDE 1		SIDE 2		CORRECTED AVERAGE		CHANGE IN		CHANGE IN		CRACK GROWTH RATE		STRESS INTENSITY	
		CRACK LENGTH	MM	CRACK LENGTH	MM	CRACK LENGTH	MM	CRACK LENGTH	MM	CRACK LENGTH	MM	DA	IN.	MPA X DELTA K	KSI X DELTA K
N	P	A1	MM	A2	MM	ABAR	MM	DA	MM	DN	INCH	METER	PER CYCLE		
X 1000	KIPS														
5.650	17.79	4.00	29.02	1.166	31.14	1.226	31.05	1.246	.762	.030	.100	7620.00	300.00	61.36	55.84
5.750	17.79	4.00	30.48	1.196	31.90	1.256	32.41	1.276	1.270	.050	.100	12700.00	500.00	65.95	60.04
5.850	17.79	4.00	31.65	1.246	33.17	1.306	33.68	1.326							

INPUT CONSTANTS

ELASTIC MODULUS(E) = 118.590E+03 MPA(17.200E+06 PSI)				
NUMBER OF CYCLES	CRACK MOUTH COMPLIANCE	ABAR / W OPTICAL BASE	COMPLIANCE BASE	
X 1000				
.000	47.9605	.358	.384	
2.570	42.4500	.379	.393	
25.530	43.3394	.389	.401	
25.587	44.0842	.394	.405	
38.662	43.1526	.417	.427	
.000	55.3342	.466	.470	
1.650	61.0131	.476	.481	
2.850	69.2605	.494	.507	
3.250	71.9447	.504	.514	
3.450	74.7736	.514	.523	
3.650	77.4520	.529	.532	
4.250	82.0657	.536	.546	
4.650	88.0236	.551	.561	
4.950	94.5815	.566	.575	
5.250	104.631	.583	.595	
5.450	108.7315	.596	.604	
5.550	117.6683	.606	.619	
5.650	124.709	.621	.630	
5.750	136.2507	.636	.647	
5.850	160.4630	.661	.677	

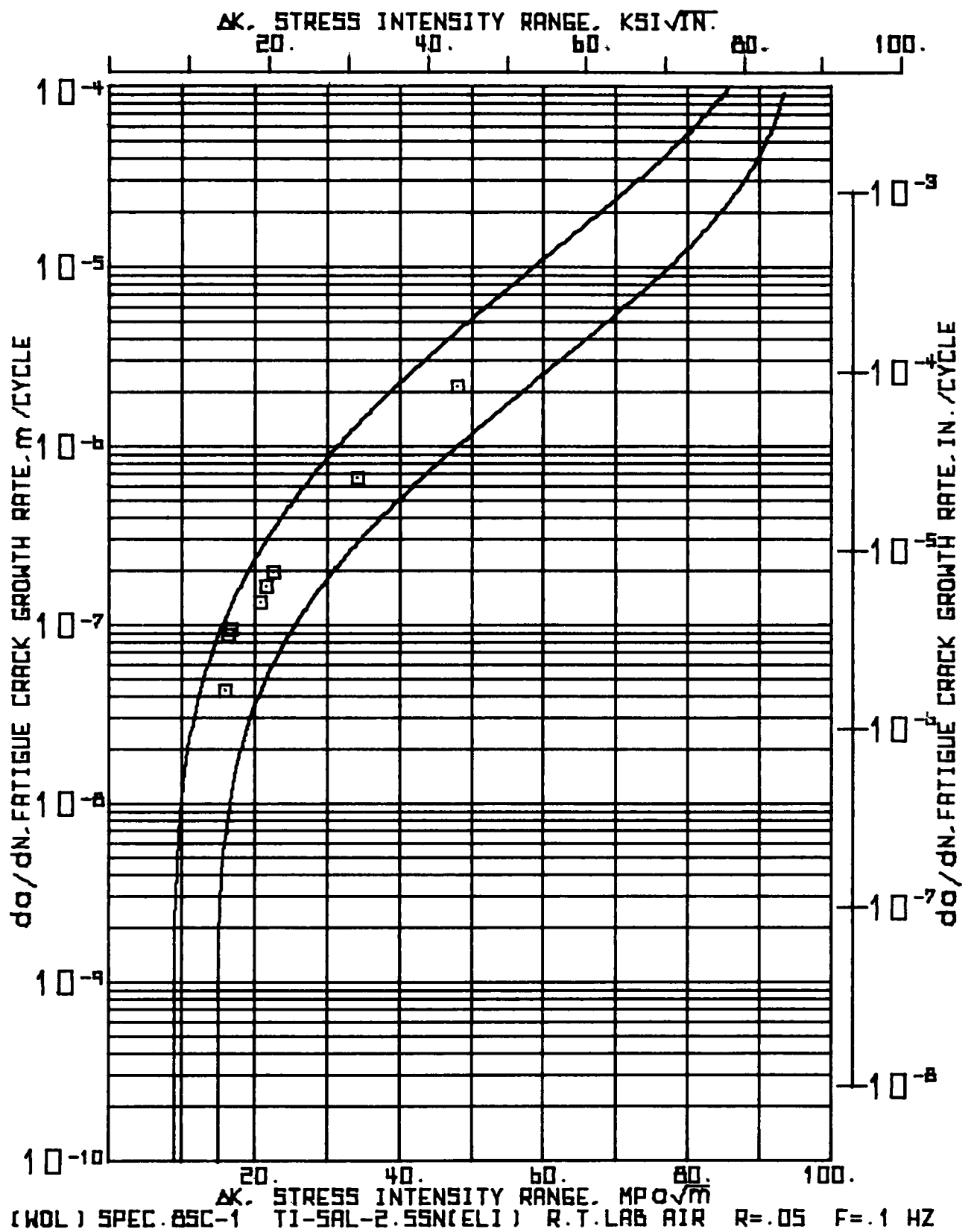


TABLE SPEC-85C-1 T1-5AL-2.55N(ELT) R.T.LAB AIR R-05 F-0.1 HZ 12:21 AUG 03, 1976

INPUT CONSTANTS:

RANGE RATIO(K) .05
 TEST FREQUENCY(HZ) .1
 SPECIMEN WIDTH(W) 50.927 MM(2.005 IN.)
 SPECIMEN THICKNESS(B) 19.004 MM(.748 IN.)
 CRACK BIA CORRECTION 1.270 MM(.050 IN.)

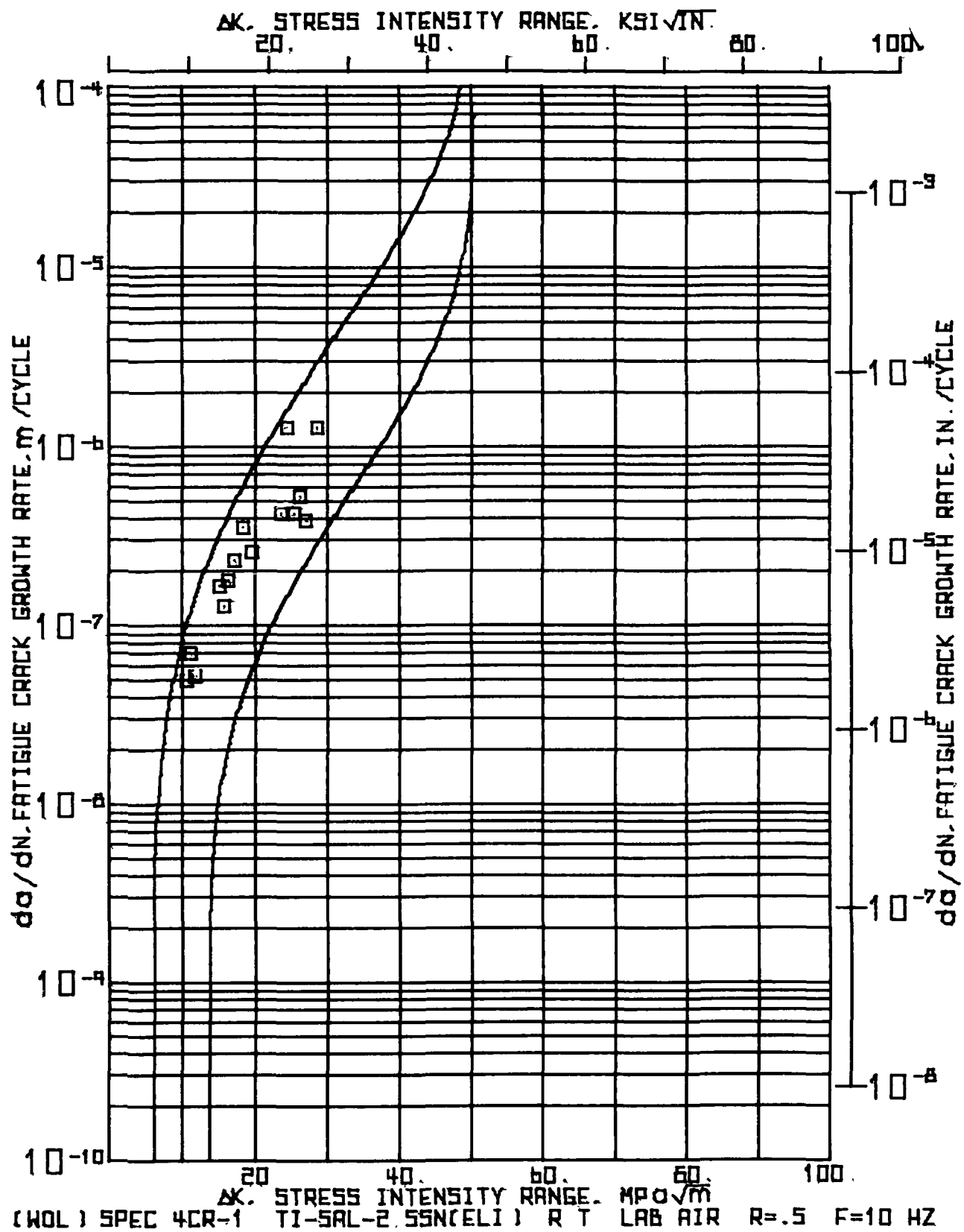
NUMBER OF CYCLES	MAXIMUM LOAD		SIDE 1 CRACK LENGTH		SIDE 2 CRACK LENGTH		CORRECTED AVERAGE CRACK LENGTH		CHANGE IN CRACK LENGTH		CHANGE IN CYCLES	CRACK GROWTH RATE DA / DN MICR9 METER		STRESS INTENSITY RANGE DELTA K	
	N	P	A1	A2	MM	INCH	MM	INCH	MM	INCH		DN X 1000	PER CYCLE	MPA X KSI X	IN ^{3/2}
X 1000	KN	KIPS	MM	INCH	MM	INCH	MM	INCH	MM	INCH					
000	9.79	2.20	17.17	.676	17.07	.672	16.39	.724	.216	.009	5.000	43.18	1.70	16.04	14.60
500	9.79	2.20	17.48	.688	17.20	.677	18.61	.732	.660	.026	7.500	88.05	3.47	16.36	14.89
12500	9.79	2.20	16.19	.716	17.81	.701	19.27	.758	.711	.028	7.500	94.83	3.73	16.83	15.36
20000	9.79	2.20	16.07	.735	18.75	.738	19.98	.786							
20000	11.57	2.60	16.67	.735	18.75	.738	19.98	.786	1.016	.040	7.500	135.47	5.33	20.76	18.90
27500	11.57	2.60	19.74	.777	19.71	.776	20.99	.826	.825	.033	5.000	165.10	6.50	21.69	19.74
32500	11.57	2.60	20.65	.813	20.45	.805	21.82	.859	.991	.039	5.000	198.12	7.80	22.68	20.64
37500	11.57	2.60	21.62	.851	21.46	.845	22.81	.898							
37500	15.57	3.50	21.62	.851	21.46	.845	22.81	.898	3.340	.132	5.000	668.02	26.30	34.10	31.04
42500	15.57	3.50	24.74	.974	25.02	.985	26.15	1.029	6.420	.332	3.887	2166.22	85.28	48.10	43.77
46387	15.57	3.50	33.05	1.301	33.55	1.321	34.57	1.361							

(*8L) SPEC.8SC-1 YI-SAL-2.5SNIELJ) R.T.LAB AIR R=.05 F=.1 HZ 12121 AUG 03,176
 INPUT CONSTANTS

ELASTIC MODULUS(E) = 116.590E+03 MPa(17.200E+06 PSI)				
NUMBER OF CYCLES	CRACK COMPLIANCE	ABAR / W OPTICAL BASf	COMPLIANCE BASf	
N X 1000	CEB			
1000	40.2157	.361	.360	
5000	41.2201	.365	.364	
12500	41.9027	.378	.387	
25000	45.3416	.392	.407	
27500	48.2589	.412	.423	
32500	51.4762	.428	.438	
37500	56.3920	.448	.459	
42500	73.9970	.513	.522	
46587	172.1234	.679	.689	

SECTION A3

This section of the Appendix includes all fatigue crack growth data obtained from WOL coupons tested at room temperature, at a range ratio of 0.5, and at a frequency of 10 Hz.



(WBL) SPEC-4CR-1 11-5AL-2.5SN(ELI) R.T. LAB AIR R.5 F.10 HZ 15102 AUG 03, 176

INPUT CONSTANTS:

RANGE RATIO(R) • .50
 TEST FREQUENCY(HZ) • 10.0
 SPECIMEN WIDTH(W) • 50.876 MM(2.003 IN.)
 SPECIMEN THICKNESS(B) • 18.920 MM(.745 IN.)
 CRACK BR. CORRECTION • 1.270 MM(.050 IN.)

NUMBER OF CYCLES	MAXIMUM LOAD	P KN	SIDE 1 CRACK LENGTH		SIDE 2 CRACK LENGTH		CORRECTED AVERAGE CRACK LENGTH	CHANGE IN CRACK LENGTH	CHANGE IN CYCLES	CRACK GROWTH RATE DA / DN MICRO METER PER CYCLE	STRESS INTENSITY RANGE DELTA K				
			MM	INCH	MM	INCH									
X 1000															
• 300	12.01	2.70	16.54	.651	17.73	.700	18.43	.725	1.181	.046	24.360	48.49	1.91	10.67	9.71
24.360	12.01	2.70	17.96	.707	18.72	.737	19.61	.772	1.143	.045	16.500	69.27	2.73	11.25	10.24
40.660	12.01	2.70	19.23	.757	19.74	.777	20.75	.817	.571	.022	11.000	51.95	2.05	11.72	10.66
51.660	12.01	2.70	19.35	.762	20.75	.817	21.32	.839							
51.660	15.12	3.40	19.35	.762	20.75	.817	21.32	.839	.825	.032	5.000	165.10	6.50	15.26	13.89
56.660	15.12	3.40	20.75	.817	21.01	.827	22.15	.872	.504	.020	4.000	127.00	5.00	15.77	14.35
60.660	15.12	3.40	21.26	.837	21.51	.847	22.66	.892	.889	.035	5.000	177.80	7.00	16.34	14.87
65.660	15.12	3.40	21.51	.847	23.04	.907	23.55	.927	1.143	.045	5.000	228.60	9.00	17.21	15.67
70.660	15.12	3.40	23.29	.917	23.55	.927	24.69	.972	1.397	.055	4.000	349.25	13.75	18.42	16.75
74.660	15.12	3.40	24.56	.967	25.07	.987	26.09	1.027	.762	.030	3.000	254.00	10.00	19.56	17.83
77.660	15.12	3.40	25.58	1.007	25.58	1.007	26.85	1.037							
77.660	17.79	4.00	25.58	1.007	25.58	1.007	26.85	1.057	.254	.010	.600	423.33	16.67	23.68	21.55
78.660	17.79	4.00	25.83	1.017	25.83	1.017	27.10	1.067	.762	.030	.600	1270.00	50.00	24.39	22.20
79.660	17.79	4.00	26.59	1.047	26.59	1.047	27.86	1.097	.504	.020	1.200	423.33	16.67	25.32	23.05
80.660	17.79	4.00	27.10	1.067	27.10	1.067	28.37	1.117	.635	.025	1.200	529.17	20.83	26.21	23.86
81.660	17.79	4.00	27.61	1.087	27.86	1.097	29.01	1.142	.381	.015	1.000	361.00	15.00	27.05	24.62
82.660	17.79	4.00	27.86	1.097	28.37	1.117	29.39	1.157	1.270	.050	1.000	1270.00	50.00	28.50	25.94
83.660	17.79	4.00	29.39	1.157	29.39	1.157	30.66	1.207							

(HDL) SPEC:4CR-1 T1-5AL-2.5SN(ELT) R.T. LAB AIR R=5 F=10 HZ 15:02 AUG 03,176

INPUT CONSTANTS

ELASTIC MODULUS(E) = 118.590E+03 MPA(17.200E+06 PSI)					
NUMBER OF CYCLES	CRACK MOUTH COMPLIANCE	ABAR / W	OPTICAL BASE	COMPLIANCE BASE	
N	CEB				
X 1000					
56.560	52.9574	.435	.445	.445	
60.560	54.2387	.445	.451	.451	
65.560	57.6553	.463	.465	.465	
70.560	61.7260	.485	.482	.482	
74.560	69.1863	.513	.507	.507	
77.460	73.4571	.528	.520	.520	
78.460	77.3008	.533	.532	.532	
79.060	79.4361	.548	.538	.538	
80.260	85.4152	.558	.553	.553	
81.460	90.7672	.570	.567	.567	
82.460	98.0546	.578	.564	.564	
83.460	108.4773	.603	.603	.603	

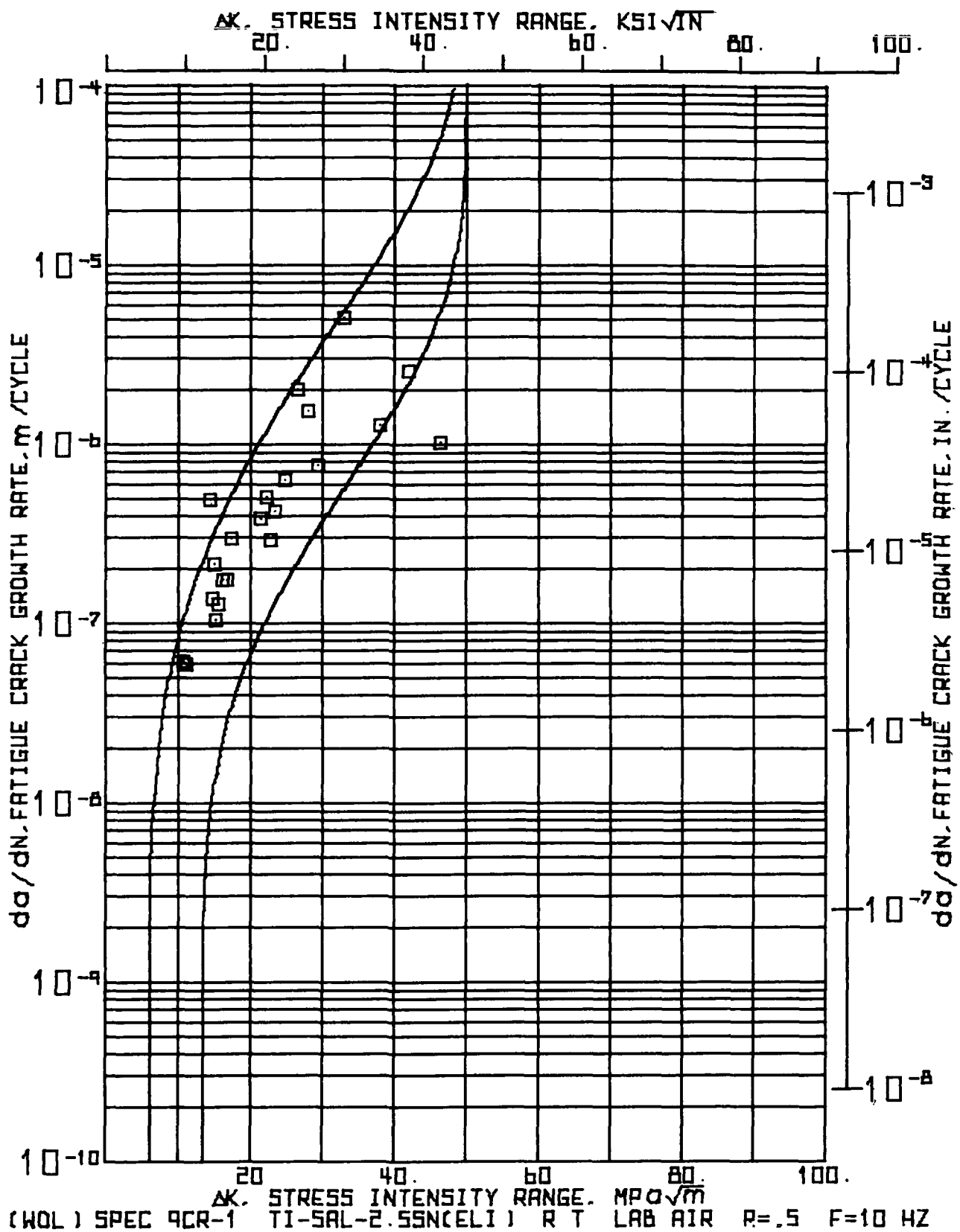


TABLE SPEC9CR-1 TEST 5AL-2:SSN(ELT) R.T. LAB AIR R=5 F=10 HZ 15:03 AUG 03, 196

INPUT CONSTANTS:

RANGE RATIO(R) .50
 TEST FREQUENCY(HZ) 10.0
 SPECIMEN WIDTH(W) 51.054 MM(2.010 IN.)
 SPECIMEN THICKNESS(B) 18.908 MM(.744 IN.)
 CRACK 39% CORRECTION 1.270 MM(.050 IN.)

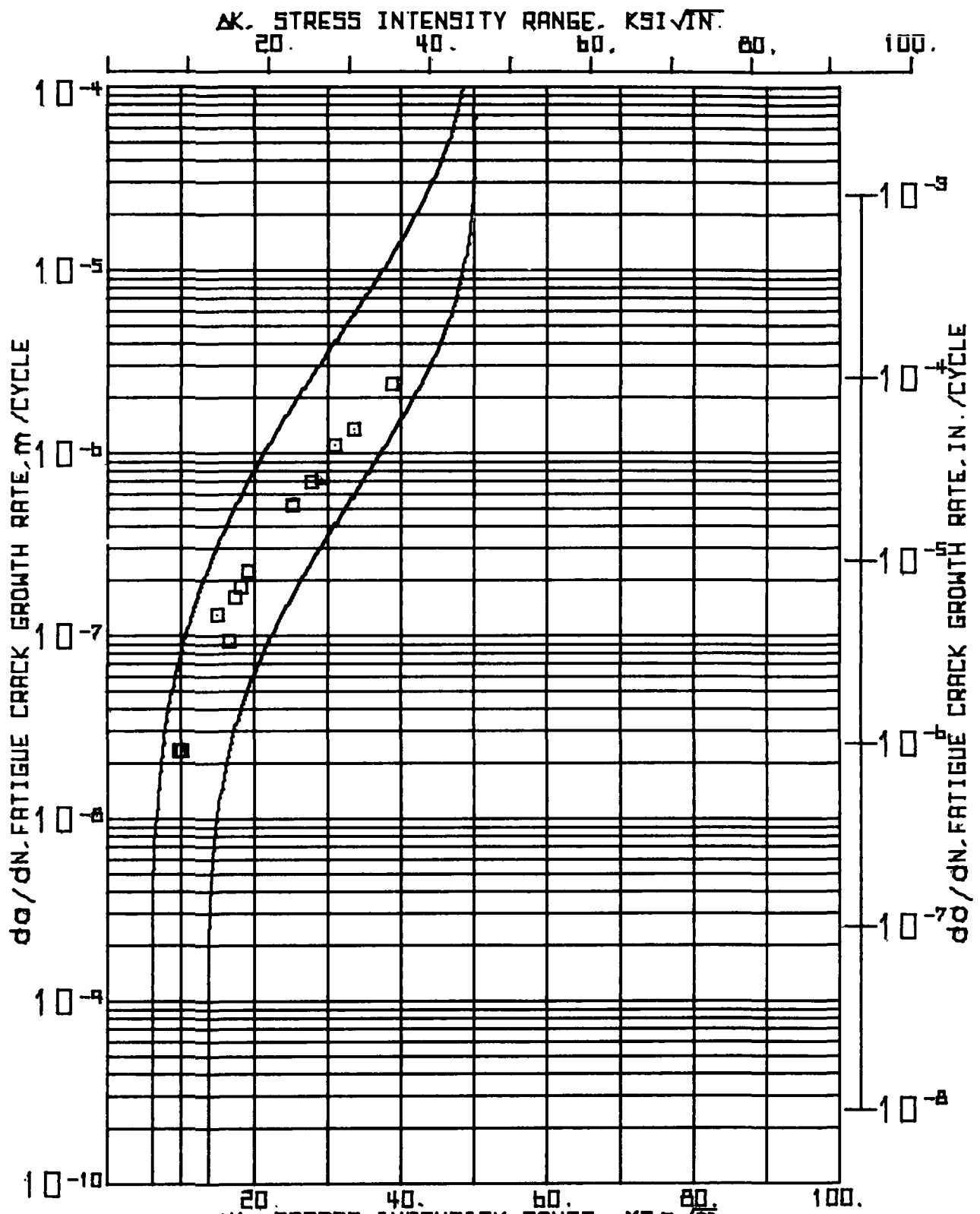
NUMBER OF CYCLES	MAXIMUM LOAD KIPS	SIDE 1 CRACK LENGTH		SIDE 2 CRACK LENGTH		CORRECTED AVERAGE CRACK LENGTH		CHANGE IN CRACK LENGTH		CHANGE IN CYCLES		CRACK GROWTH RATE DA / DN		STRESS INTENSITY RANGE DELTA K	
		A1 MM	INCH	A2 MM	INCH	MM	INCH	MM	INCH	DN X 1000	METER PER CYCLE	MICR0 IN.	MPA X 100.5	KSI X 14.5	
000	12.01	2.70	17.70	.697	17.70	.697	18.97	.747	.635	.025	10.500	60.48	2.38	10.76	9.79
10.500	12.01	2.70	18.34	.722	18.34	.722	19.61	.772	.762	.030	13.000	58.62	2.31	11.11	10.11
23.500	12.01	2.70	19.10	.752	19.10	.752	20.37	.802							
23.500	15.12	3.40	19.10	.752	19.10	.752	20.37	.802	.508	.020	1.050	483.81	19.05	14.41	13.11
24.550	15.12	3.40	19.61	.772	19.61	.772	20.88	.822	.381	.015	2.800	136.07	5.36	14.71	13.39
27.350	15.12	3.40	19.86	.782	20.12	.792	21.26	.837	.317	.012	1.500	211.67	8.33	14.96	13.61
28.650	15.12	3.40	20.12	.792	20.50	.807	21.58	.849	.571	.022	5.500	103.91	4.09	15.28	13.91
34.350	15.12	3.40	20.62	.812	21.13	.832	22.15	.872	.508	.020	4.000	127.00	5.00	15.69	14.28
38.350	15.12	3.40	21.39	.842	21.39	.842	22.66	.892	.699	.028	4.000	174.63	6.88	16.17	14.72
42.350	15.12	3.40	22.02	.867	22.15	.872	23.36	.919	.699	.028	4.000	174.63	6.88	16.76	15.25
46.350	15.12	3.40	22.66	.892	22.91	.902	24.05	.947	.889	.035	3.000	296.33	11.67	17.46	15.89
49.350	15.12	3.40	23.67	.932	23.67	.932	24.94	.982							
49.350	17.79	4.00	23.67	.932	23.67	.932	24.94	.982	.762	.030	2.000	381.00	15.00	21.47	19.54
51.350	17.79	4.00	24.43	.962	24.43	.962	25.70	1.012	.508	.020	1.000	508.00	20.00	22.23	20.23
52.350	17.79	4.00	24.94	.982	24.94	.982	26.21	1.032	.381	.015	1.300	293.08	11.54	22.78	20.73
53.650	17.79	4.00	25.20	.992	25.45	1.002	26.59	1.047	.635	.025	1.500	423.33	16.67	23.45	21.34
55.150	17.79	4.00	25.96	1.022	25.96	1.022	27.23	1.072	1.270	.050	2.000	635.00	25.00	24.77	22.55
57.150	17.79	4.00	27.23	1.072	27.23	1.072	28.50	1.122	1.016	.040	.500	2032.00	80.00	26.54	24.15
57.650	17.79	4.00	28.24	1.112	28.24	1.112	29.51	1.162	.762	.030	.500	1524.00	60.00	28.05	25.53
58.150	17.79	4.00	29.01	1.142	29.01	1.142	30.28	1.192							

NUMBER OF CYCLES	MAXIMUM LOAD	P	SIDE 1 CRACK LENGTH		SIDE 2 CRACK LENGTH		CONNECTED AVERAGE		CHANGE IN		CHANGE IN		CRACK GRWTH RATE		STRESS INTENSITY	
			M1	INCH	A1	MM	INCH	MM	INCH	MM	INCH	X 1000	DA / DN METER PER CYCLE	IN / IN	MPA X 1000.5	KSI X 1000.5
55.150	17.79	4.00	29.01	1.142	29.01	1.142	30.24	1.192	.762	.030	1.000	.500	762.00	30.00	29.47	26.82
55.150	17.79	4.00	29.77	1.172	29.77	1.172	31.04	1.222	2.540	.100	.500	.500	5080.00	200.00	32.96	30.00
59.050	17.79	4.00	32.31	1.272	32.31	1.272	33.58	1.322	1.270	.050	1.000	.500	1270.00	50.00	37.94	34.52
60.650	17.79	4.00	33.08	1.322	33.08	1.322	34.85	1.372	1.270	.050	.500	.500	2540.00	100.00	41.99	38.21
61.150	17.75	4.00	34.85	1.372	34.85	1.372	36.12	1.422	1.016	.040	1.000	1.000	1016.00	40.00	46.30	42.14
62.150	17.79	4.00	35.86	1.412	35.86	1.412	37.13	1.462								

(WEL) SPEC:9CR-1 T1-5AL-2.5SN(EL) R-T- LAB AIR R=5 F=10 HZ 15:03 AUG 03, 1976

INPUT CONSTANTS

ELASTIC MODULUS(E) = 118.590E+03 MPa(17.200E+06 PSI)				
NUMBER OF CYCLES N	CRACK MOUTH COMPLIANCE CEU	ABAR / W OPTICAL BASE	COMPLIANCE BASE	
X 1000				
.000	43.1182	.372	.379	
13.500	42.6789	.384	.394	
23.500	45.6665	.399	.410	
24.550	45.8799	.409	.411	
27.350	46.2932	.416	.412	
28.450	46.5468	.423	.417	
34.350	50.3611	.434	.433	
36.350	51.0415	.444	.439	
40.350	54.0290	.457	.452	
45.350	55.3526	.471	.456	
45.350	62.6041	.489	.477	
51.350	67.4327	.503	.501	
52.350	71.7006	.513	.515	
53.650	72.7610	.521	.519	
57.150	89.0258	.558	.564	



(WOL) SPEC 4RC-1 TI-SAL-2.55N(ELI) R.T. LAB AIR R=.5 F=10 HZ

15104 AUG 03, '76

INPUT CONSTANTS:

[illegible]

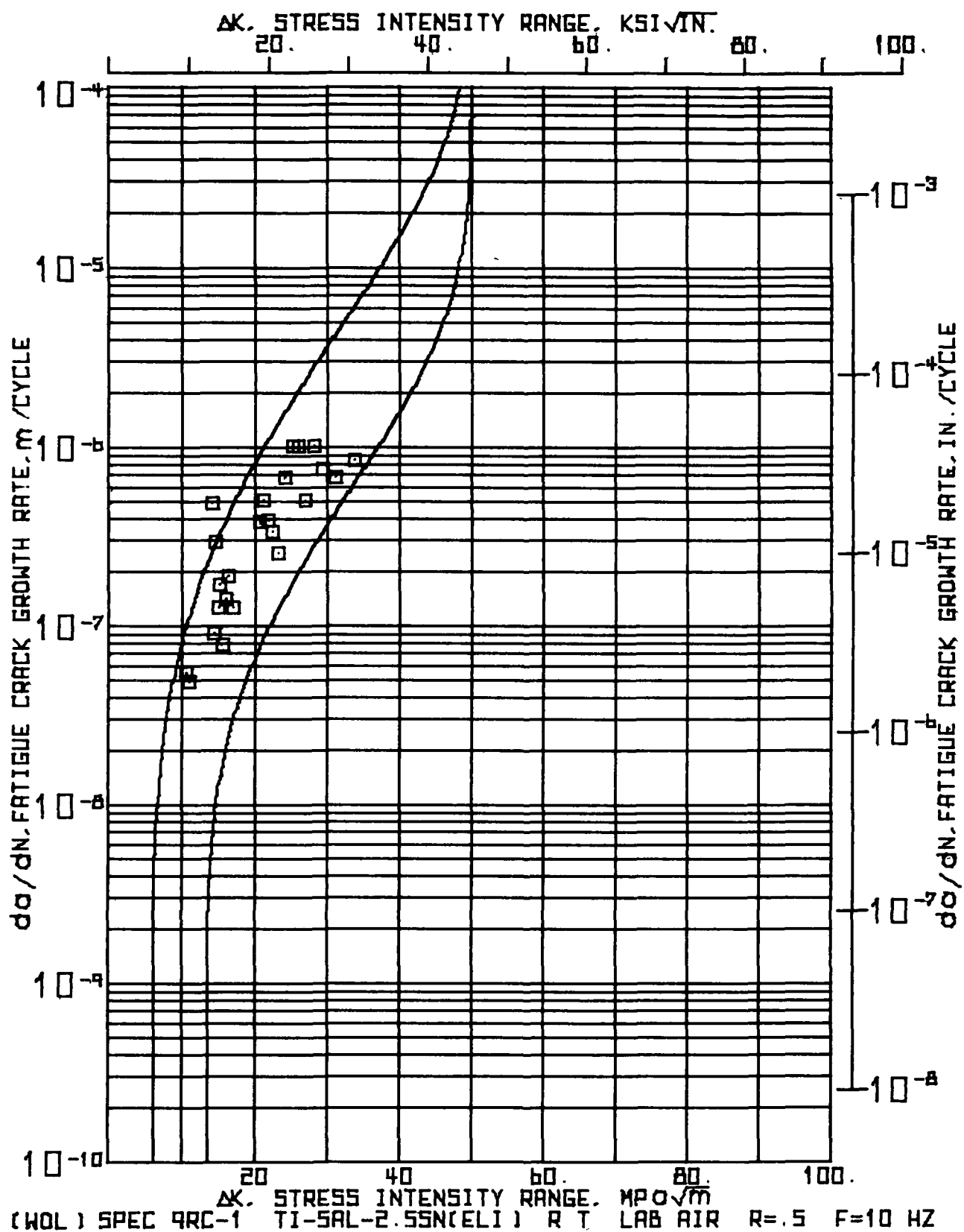
15104 AUG 03, '76

(46L)SPEC.4RC.1 T1=5AL=2.5SN(ELI) R.T.LAB AIR R=.5 F=10 HZ

INPUT CONSTANTS

ELASTIC MODULUS(E) = 118.590E+03 MPa(17.200E+06 PSI)

NUMBER OF CYCLFS	CRACK MBUTM COMPLIANCE	ABAR / W OPTICAL COMPLIANCE BASE	
N	CEP		
x 1000			
200	40.1459	.356	.379
20000	42.5546	.365	.393
70000	45.7663	.368	.411
95000	53.7955	.452	.449
105000	59.4159	.471	.472
110000	63.4305	.466	.467
115000	70.5567	.504	.512
120000	75.4742	.526	.526
125000	95.5472	.577	.577
126000	101.9705	.590	.591
127000	107.5909	.605	.601
129000	121.6405	.626	.625
129000	138.0047	.632	.651
130000	183.6652	.699	.699



(49L) SPEC-9RC-1 T1-5AL-2-5SN(EL) R.T. LAB AIR R=0.5 F=10 HZ 15:08 AUG 03, 1976

INPUT CONSTANTS:

RANGE RATIO(M) .50
 TEST FREQUENCY(HZ) 10.0
 SPECIMEN WIDTH(W) 50.927 MM(2.005 IN.)
 SPECIMEN THICKNESS(B) 18.933 MM(.745 IN.)
 CRACK BR. CORRECTION 1.270 MM(.050 IN.)

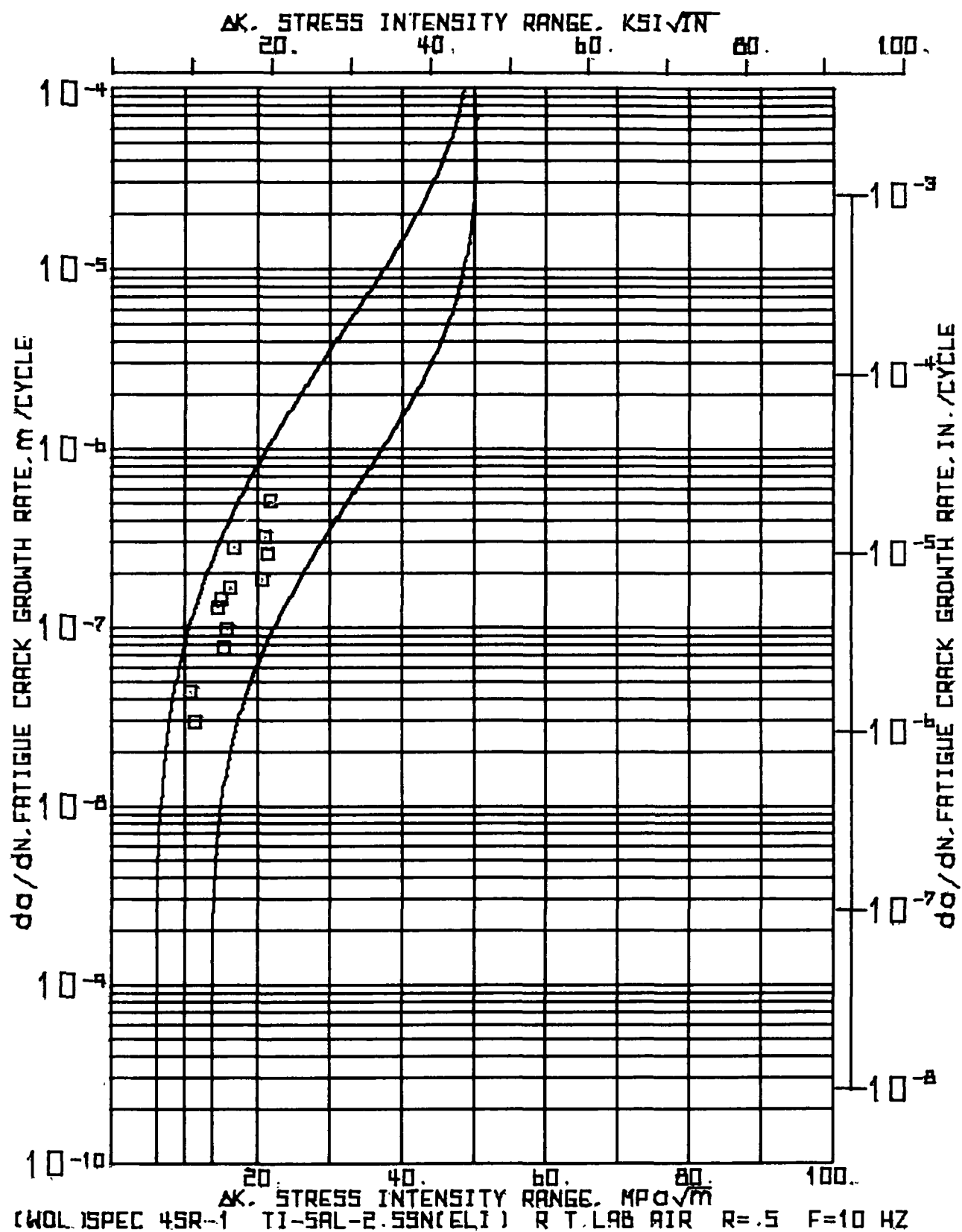
NUMBER OF CYCLES	MAXIMUM LOAD	SIDE 1 CRACK LENGTH	SIDE 2 CRACK LENGTH	CORRECTED AVERAGE CRACK LENGTH	CHANGE IN CRACK LENGTH	CHANGE IN CYCLES	CRACK GROWTH RATE DA / DN	STRESS INTENSITY RANGE DELTA K
N X 1000	KN	MM	MM	MM	MM	DN X 1000	METER IN.	MPA X 1000 KSI X 1000
000	12.01	2.70	17.45	.667	17.58	.692	18.78	.739
10.500	12.01	2.70	17.96	.707	18.21	.717	19.35	.762
23.500	12.01	2.70	18.59	.732	18.85	.742	19.99	.757
23.500	15.12	3.40	18.59	.732	18.85	.742	19.99	.767
24.550	15.12	3.40	19.23	.757	19.23	.757	20.50	.807
27.350	15.12	3.40	19.35	.762	19.61	.772	20.75	.817
28.850	15.12	3.40	19.66	.782	19.99	.787	21.20	.834
31.350	15.12	3.40	20.24	.797	20.24	.797	21.51	.847
34.350	15.12	3.40	20.75	.817	20.75	.817	22.02	.867
36.350	15.12	3.40	20.88	.822	21.26	.837	22.34	.879
42.350	15.12	3.40	21.26	.837	22.02	.867	22.91	.902
46.350	15.12	3.40	22.25	.877	22.53	.887	23.67	.932
49.350	15.12	3.40	22.53	.887	23.04	.907	24.05	.947
49.350	17.79	4.00	22.53	.887	23.04	.907	24.05	.947
51.350	17.79	4.00	23.55	.927	23.55	.927	24.82	.977
52.350	17.79	4.00	24.05	.947	24.05	.947	25.32	.997
53.650	17.79	4.00	24.56	.967	24.56	.967	25.83	1.017
55.150	17.79	4.00	25.07	.987	25.07	.987	26.34	1.037
57.150	17.79	4.00	25.58	1.007	25.58	1.007	26.85	1.057
58.650	17.79	4.00	26.59	1.047	26.59	1.047	27.86	1.097

NUMBER OF CYCLES	MAXIMUM LOAD	SIDE 1 CRACK LENGTH		SIDE 2 CRACK LENGTH		CORRECTED AVERAGE CRACK LENGTH ABAR		CHANGE IN CRACK LENGTH DA		CHANGE IN CYCLES DN X 1000	CRACK GROWTH RATE DA / DN MICR9 IN. PER CYCLE	STRESS INTENSITY RANGE DELTA K			
		MM	INCH	MM	INCH	MM	INCH	MM	INCH			MPA X 1000	MPA X 1000	INCH X 1000	
59.650	17.79	4.00	26.53	1.047	26.53	1.047	27.66	1.097	.508	.020	.500	1016.00	40.00	25.25	22.98
59.150	17.79	4.00	27.10	1.067	27.10	1.067	28.37	1.117	.508	.020	.500	1016.00	40.00	26.04	23.70
59.650	17.79	4.00	27.61	1.087	27.61	1.087	28.88	1.137	.762	.030	1.500	508.00	20.00	27.03	24.64
61.150	17.79	4.00	28.37	1.117	28.37	1.117	29.64	1.167	.508	.020	.500	1016.00	40.00	28.18	25.65
62.650	17.79	4.00	29.64	1.167	29.64	1.167	30.91	1.217	.762	.030	1.000	762.00	30.00	29.37	26.72
64.150	17.79	4.00	30.66	1.207	30.66	1.207	31.93	1.257	1.016	.040	1.500	677.33	26.67	31.16	28.36
65.650	17.79	4.00	31.93	1.257	31.93	1.257	33.20	1.307	1.270	.050	1.500	846.67	33.33	33.76	30.72

INPUT CONSTANTS

ELASTIC MODULUS(E) = 118.590E+03 MPA(17.200E+06 PSI)

NUMBER OF CYCLES N	CRACK MOUTH COMPLIANCE C ₀	ADAR / W OPTICAL BASE	COMPLIANCE BASE
10.500	40.1721	.369	.379
10.500	41.4815	.380	.389
23.000	43.1636	.393	.397
24.550	43.0910	.402	.399
27.350	44.0184	.417	.401
26.050	44.2320	.416	.402
31.550	45.7278	.422	.410
34.350	46.0625	.432	.415
35.350	46.2920	.439	.423
42.350	51.2635	.450	.438
46.350	52.1940	.465	.445
49.350	55.0571	.472	.456
51.550	60.0855	.467	.477
52.350	61.9676	.497	.462
53.650	65.0139	.507	.495
55.150	67.5233	.517	.501
57.150	70.3611	.527	.523



INPUT CONSTANTS:

TEST FREQUENCY (HZ)	SPECIMEN WIDTH (IN.)	SPECIMEN THICKNESS (IN.)	RANGE RATIO (R)
50.902	2.004	.745	10.0
18.915	1.270	.050	50

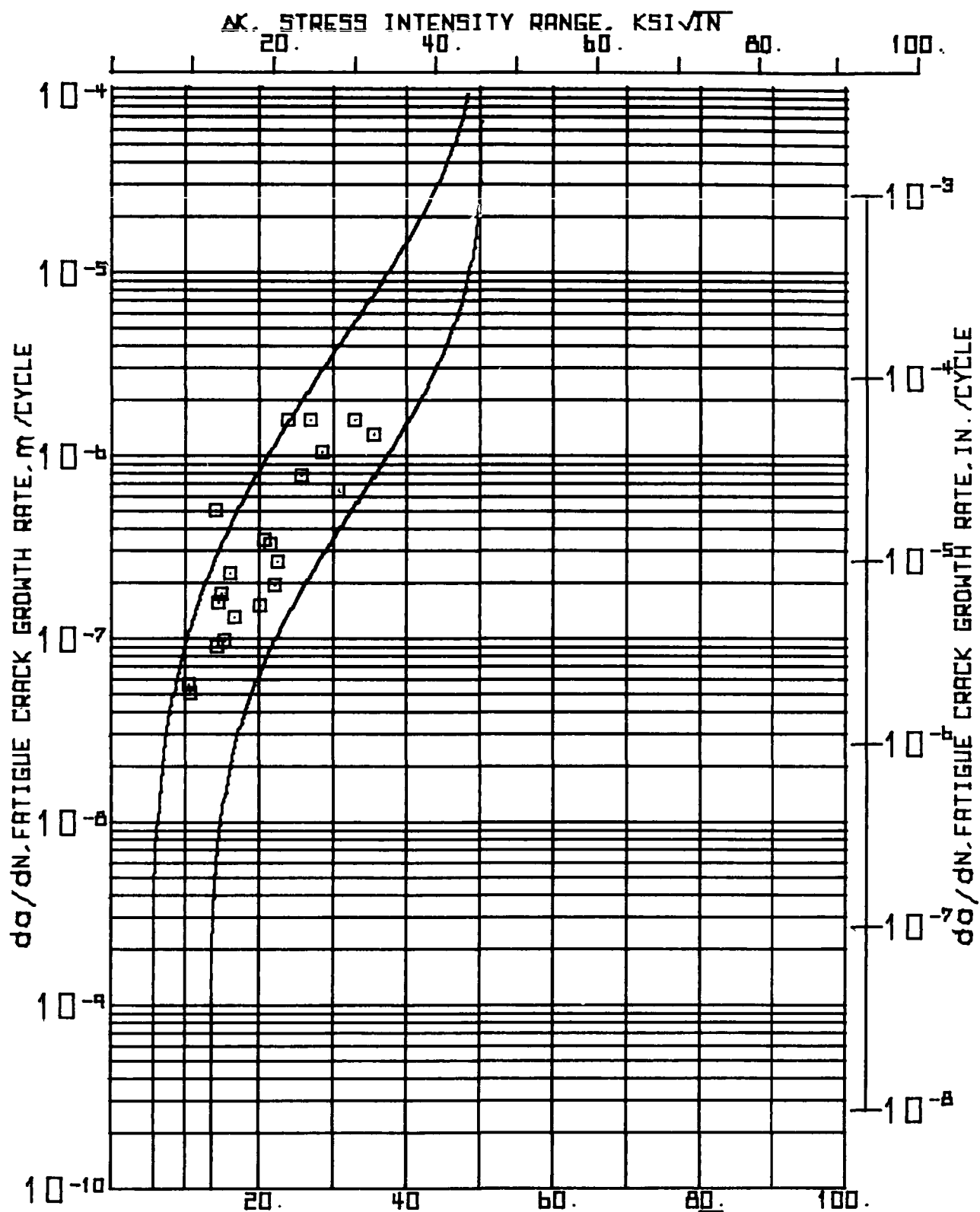
[illegible]

(W0L)SPEC+SR-1 77-5AL-2-55N(EL) R-T-LAB AIR R-0.5 F-10 HZ 11109 AUG 18, 1976

INPUT CONSTANTS

ELASTIC MODULUS(E) = 118.590E+03 MPa (17.200E+06 PSI)

NUMBER OF CYCLES	CRACK MOUTH COMPLIANCE	ABAR / W OPTICAL BASE	COMPLIANCE BASE
56.900	47.3927	.417	.419
60.900	48.2466	.428	.423
70.900	52.0893	.445	.441
74.900	54.6511	.458	.452
77.900	55.9319	.474	.458
80.300	59.7746	.483	.473
81.500	63.6172	.491	.488
82.500	65.1790	.496	.497
83.500	68.7408	.505	.505



(WOL) SPEC. 45R-1 T1-SAL-2.55N(ELI) R.T. LAB AIR R=.5 F=10 HZ.

11:09 AUG 18 '76

INPUT CONSTANTS:

RANGE RATIO(R)	• .50
TEST FREQUENCY(HZ)	• 10.0
SPECIMEN WIDTH(W)	• 51.054 MM(
SPECIMEN THICKNESS(B)	• 18.928 MM(
CRACK BGA CORRECTION	• 1.270 MM(
	• .050 IN.)
	• .745 IN.)
	• 2.010 IN.)

NUMBER OF CYCLES	MAXIMUM LOAD		SIDE 1 CRACK LENGTH		SIDE 2 CRACK LENGTH		CORRECTED AVERAGE CRACK LENGTH		CHANGE IN CRACK LENGTH MM	CHANGE IN CYCLES	CRACK GROWTH RATE DA / DN MICR METER IN.		STRESS INTENSITY RANGE DELTA K		
	N X 1000	P KN	A1 MM	INCH	A2 MM	INCH	ABAR MM	INCH			DN X 1000	MANB. METER	MPA X Mmm.5	KSI X INmm.5	
000	12.01	2.70	17.60	.693	17.98	.708	19.06	.750	.572	.023	10.500	54.43	2.14	10.77	9.80
10.500	12.01	2.70	18.11	.713	18.62	.733	19.63	.773	.635	.025	13.000	48.85	1.92	11.07	10.08
23.500	12.01	2.70	18.62	.733	19.38	.763	20.27	.798							
23.500	15.12	3.40	18.62	.733	19.38	.763	20.27	.798	.508	.020	1.050	483.81	19.05	14.32	13.03
24.550	15.12	3.40	19.38	.763	19.63	.773	20.78	.818	.381	.015	4.300	88.60	3.49	14.62	13.31
28.850	15.12	3.40	19.63	.773	20.14	.793	21.16	.833	.381	.015	2.500	152.40	6.00	14.89	13.55
31.350	15.12	3.40	19.89	.783	20.65	.813	21.54	.848	.508	.020	3.000	169.33	6.67	15.22	13.85
34.350	15.12	3.40	20.40	.803	21.16	.833	22.05	.868	.762	.030	8.000	95.25	3.75	15.70	14.29
42.350	15.12	3.40	21.41	.843	21.67	.853	22.81	.898	.889	.035	4.000	222.25	8.75	16.36	14.89
46.350	15.12	3.40	22.17	.873	22.68	.893	23.70	.933	.381	.015	3.000	127.00	5.00	16.30	15.38
49.350	15.12	3.40	22.68	.893	22.94	.903	24.08	.948							
49.350	17.79	4.00	22.68	.893	22.94	.903	24.08	.948	.635	.025	4.300	147.67	5.81	20.42	18.58
53.650	17.79	4.00	23.19	.913	23.70	.933	24.71	.973	.508	.020	1.500	338.67	13.33	21.04	19.15
55.150	17.79	4.00	23.70	.933	24.21	.953	25.22	.993	.635	.025	2.000	317.50	12.50	21.70	19.75
57.150	17.79	4.00	24.46	.963	24.71	.973	25.86	1.018	.381	.015	2.000	190.50	7.50	22.31	20.31
59.150	17.79	4.00	24.97	.983	24.97	.983	26.24	1.033	.508	.020	2.000	254.00	10.00	22.87	20.82
61.150	17.79	4.00	25.48	1.003	25.48	1.003	26.75	1.053	1.524	.060	1.000	1524.00	60.00	24.24	22.06
62.150	17.79	4.00	27.00	1.063	27.00	1.063	28.27	1.113	.762	.030	1.000	762.00	30.00	25.94	23.61
63.150	17.79	4.00	27.76	1.093	27.76	1.093	29.03	1.143	.762	.030	.500	1524.00	60.00	27.18	24.74
63.650	17.79	4.00	28.52	1.123	28.52	1.123	29.79	1.173							

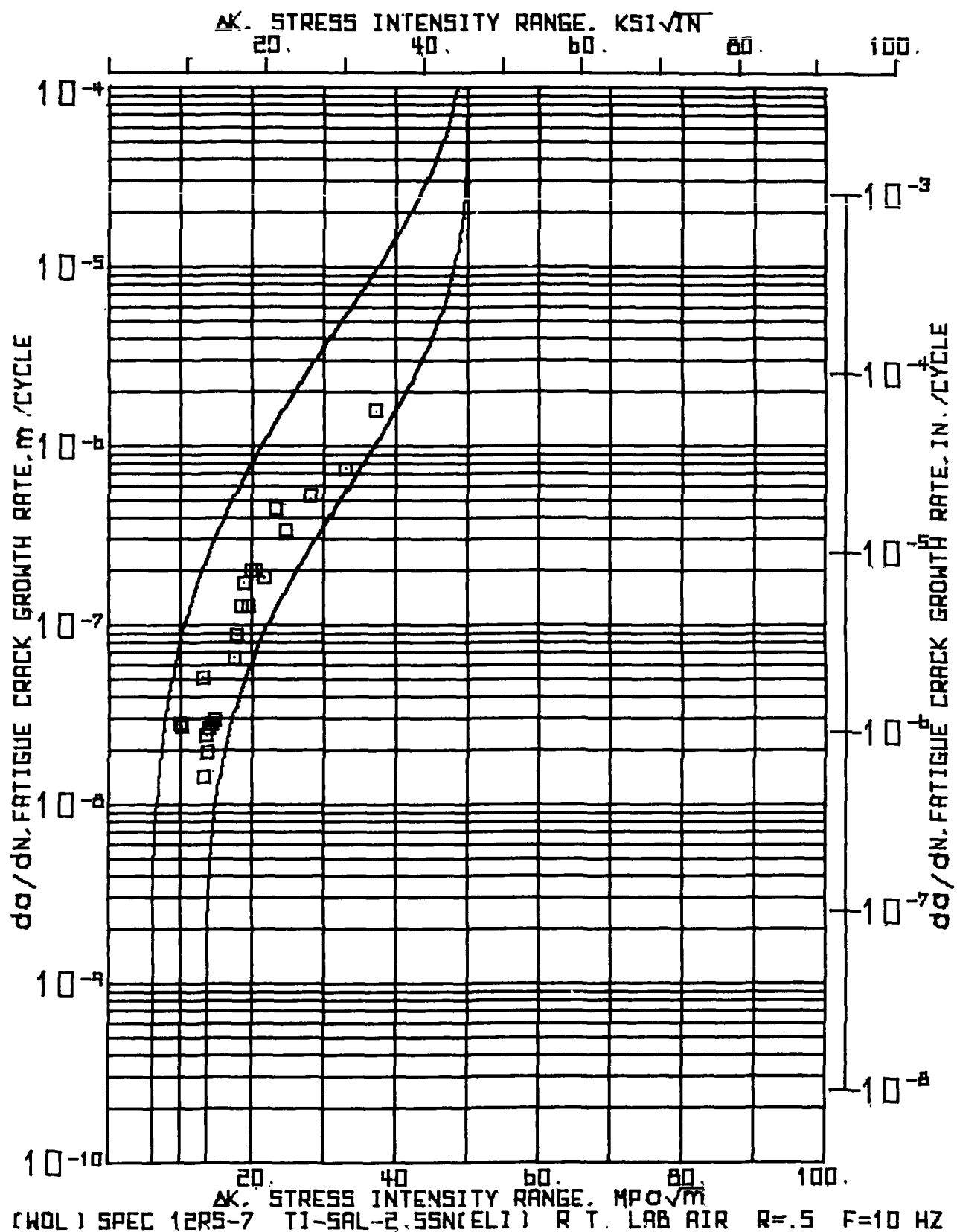
(WOL) SPEC.9SR-1 T1-5AL-2.55N(EL1) R.T. LAB AIR R-5 F=10 HZ										11:09 AUG 18, '76	PAGE 2
NUMBER OF CYCLES	MAXIMUM LOAD	SIDE 1 CRACK LENGTH	SIDE 2 CRACK LENGTH	CORRECTED AVERAGE LENGTH	CHANGE IN LENGTH	CRACK LENGTH DA	CHANGE IN CYCLES	CRACK GRGTH RATE DA / DN METER PER CYCLE	STRESS INTENSITY RANGE DELTA K MPA X KSI X 1000.5		
N X 1000	P KN KIPS	A1 MM INCH	A2 MM INCH	MM INCH	MM INCH	MM	DN X 1000				
63.650	17.79 4.00	28.52 1.123	28.52 1.123	29.79 1.173	1.016	0.040	1.000	1016.00 40.00	28.76 26.17		
64.650	17.79 4.00	29.54 1.163	29.54 1.163	30.61 1.213	1.270	0.050	2.000	635.00 25.00	31.02 28.23		
66.650	17.79 4.00	30.81 1.213	30.81 1.213	32.08 1.263	.762	0.030	.500	1524.00 60.00	33.29 30.29		
67.150	17.79 4.00	31.57 1.243	31.57 1.243	32.84 1.293	1.270	0.050	1.000	1270.00 50.00	35.84 32.61		
68.150	17.79 4.00	32.84 1.293	32.84 1.293	34.11 1.343							

(K9L) SPEC:9SR-1 Y1-SAL=2.55N(E1) R.T. LAB AIR R=5 F=10 MZ 11109 AUG 18, 1976

INPUT CONSTANTS

ELASTIC MODULUS(E) = 118.590E+03 MPa 17.200E+06 PSI

NUMBER OF CYCLES N	CRACK MOUTH COMPLIANCE CEB	ABAR / W OPTICAL BASE	COMPLIANCE BASE
1000	40.5886	.373	.382
10.500	41.4431	.385	.387
23.500	42.7248	.397	.394
24.550	42.9384	.407	.395
28.550	43.1520	.414	.397
31.350	44.0065	.422	.401
34.350	46.1428	.432	.412
42.350	48.7063	.447	.425
46.350	50.4425	.464	.435
49.350	52.5515	.472	.443
53.650	60.6692	.484	.477
55.150	64.0872	.494	.489
57.150	67.5052	.506	.501



(WLC) SPEC. 12RS-7 T1-SAL-2-SN(ELT) R.O.T. LAB ATR R=5 F=10 HZ * * * * * 14:11 AUG 04, '76

INPUT CONSTANTS:

RANGE RATIO(R) * .50
TEST FREQUENCY(HZ) * 10.0
SPECIMEN WIDTH(W) * 50.851 MM(2.002 IN.)
SPECIMEN THICKNESS(T) * 18.964 MM(.747 IN.)
CRACK 99, CORRECTION * 1.270 MM(.050 IN.)

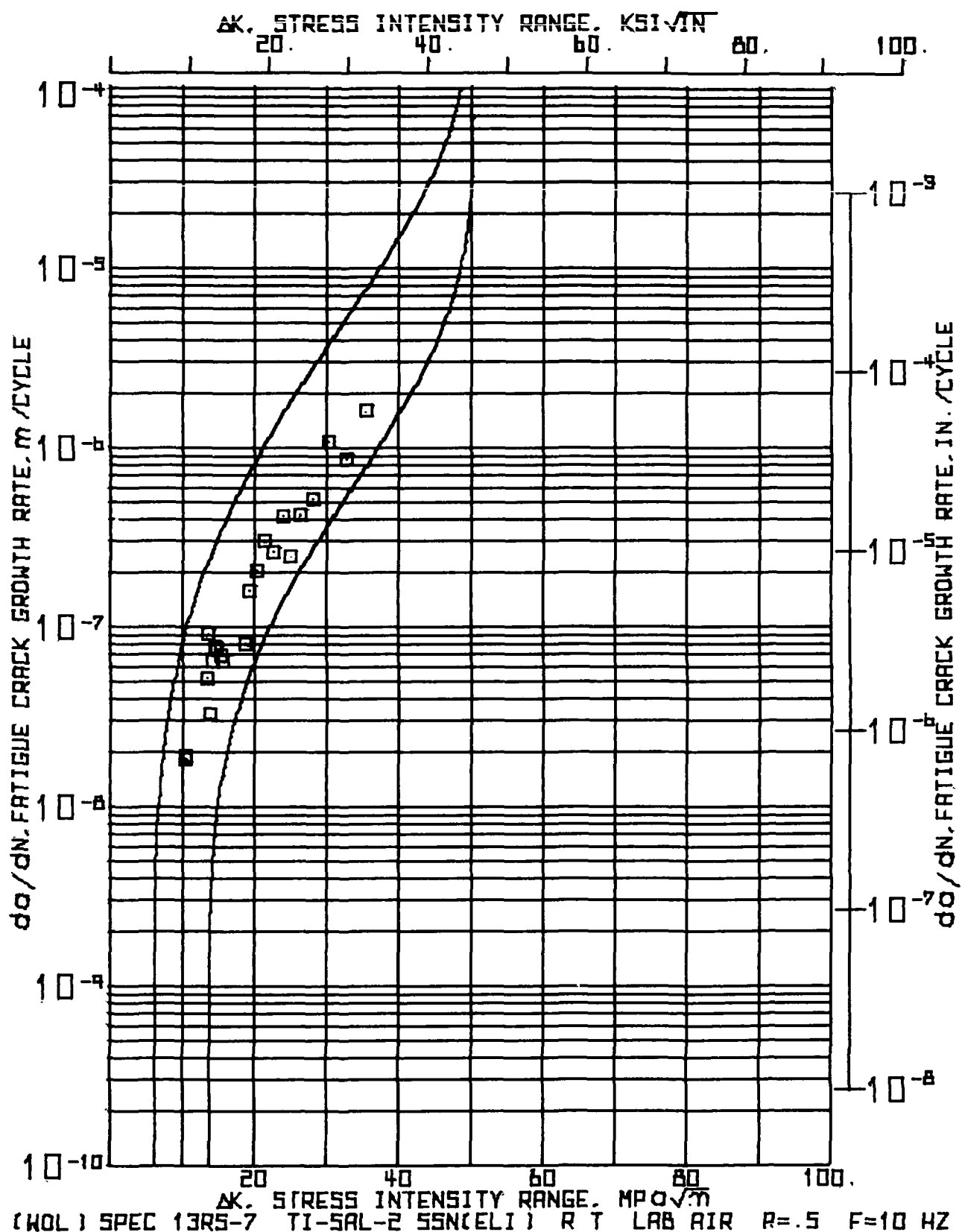
NUMBER OF CYCLES	MAXIMUM LOAD	SIDE 1 CRACK LENGTH		SIDE 2 CRACK LENGTH		CORRECTED AVERAGE CRACK LENGTH		CHANGE IN CRACK LENGTH		CHANGE IN CYCLES		CRACK GROWTH RATE DA / DN		STRESS INTENSITY RANGE DELTA K	
		A1 INCH	MM	A2 INCH	MM	MM ABR	INCH	MM DA	INCH DN	MM DA	INCH DN	NANOMETER PER CYCLE	MICRONS PER CYCLE	MPA X METER	MPA X METER
1200	KN	KIPS													
1200	12.01	2.70	16.26	.640	16.51	.650	17.05	.695	.381	.015	13.600	28.01	1.10	10.09	9.19
13600	12.01	2.70	16.76	.660	16.76	.660	18.03	.710	.381	.015	14.000	27.21	1.07	10.27	9.34
27600	12.01	2.70	17.02	.670	17.27	.680	18.41	.725							
27600	15.12	3.40	17.02	.670	17.27	.680	18.41	.725	.254	.010	5.000	50.80	2.00	13.11	11.93
32600	15.12	3.40	17.27	.680	17.53	.690	18.67	.735	.381	.015	26.750	14.24	.56	13.30	12.12
59350	15.12	3.40	17.76	.700	17.78	.700	19.05	.750	.318	.013	13.000	24.42	.96	13.51	12.30
72350	15.12	3.40	18.03	.710	18.16	.715	19.37	.762	.445	.018	23.000	19.33	.76	13.75	12.51
95350	15.12	3.40	18.54	.730	18.54	.730	19.81	.780	.508	.020	19.000	26.74	1.05	14.06	12.79
114350	15.12	3.40	19.05	.750	19.05	.750	20.32	.800	.508	.020	18.000	28.22	1.11	14.40	13.10
132350	15.12	3.40	19.56	.770	19.56	.770	20.83	.820	.508	.020	17.200	29.53	1.16	14.75	13.42
149350	15.12	3.40	20.07	.790	20.07	.790	21.34	.840							
149350	17.79	4.00	20.07	.790	20.07	.790	21.34	.840	.254	.010	3.860	65.80	2.59	17.67	16.08
153410	17.79	4.00	20.32	.800	20.32	.800	21.59	.850	.508	.020	5.800	87.59	3.45	18.01	16.39
159210	17.79	4.00	20.57	.810	21.08	.830	22.10	.870	.635	.025	5.000	127.00	5.00	18.52	16.85
164210	17.79	4.00	21.34	.840	21.59	.850	22.73	.895	.508	.020	3.000	169.33	6.67	19.06	17.35
167210	17.79	4.00	21.84	.860	22.10	.870	23.24	.915	.508	.020	4.000	127.00	5.00	19.56	17.80
171210	17.79	4.00	22.35	.880	22.61	.890	23.75	.935	.508	.020	2.500	203.20	8.00	20.08	18.28
173710	17.79	4.00	22.86	.900	23.11	.910	24.26	.955	.508	.020	2.500	203.20	8.00	20.63	18.77
176210	17.79	4.00	23.37	.920	23.62	.930	24.76	.975	1.651	.065	9.000	183.44	7.22	21.86	19.89
185210	17.79	4.00	25.15	.990	25.15	.990	26.42	1.040							

(WCL) SPEC. 1295-7 71-5AL-2-55N(ELI) R.T. LAB AIR H=5 F=10 HZ																						14:11 AUG 04, '76		PAGE 2	
NUMBER OF CYCLES		MAXIMUM LOAD		P		SIDE 1 CRACK LENGTH		SIDE 2 CRACK LENGTH		CORRECTED AVERAGE CRACK LENGTH		CHANGE IN CRACK LENGTH		CHANGE IN CYCLES		CRACK GROWTH RATE DA / DN		STRESS INTENSITY RANGE		MANS- METER PER CYCLE					
N	X 1000	KN	MM	INCH	A1	MM	INCH	A2	MM	INCH	MM	INCH	MM	INCH	DN	X 1000	DN	MICRS	MPA X 1000	KGSI X 1000	DELTA K				
185.210	17.79	4.00	25.15	.990	25.15	.990	26.42	1.040	.889	.035	2.000	444.50	17.50	23.47	21.36										
187.210	17.79	4.00	25.91	1.020	26.16	1.030	27.30	1.075	1.010	.040	3.000	338.67	13.33	24.81	22.58										
190.210	17.79	4.00	26.92	1.060	27.18	1.070	28.32	1.115	3.175	.125	6.000	529.17	20.83	28.23	25.69										
195.210	17.79	4.00	23.97	1.180	30.44	1.200	31.50	1.240	1.524	.060	2.030	750.74	29.56	33.08	30.10										
198.240	17.79	4.00	31.24	1.240	32.26	1.270	33.02	1.300	1.651	.065	1.050	1572.38	61.90	37.19	33.84										
199.290	17.79	4.00	33.27	1.310	33.53	1.320	34.67	1.365																	

(KJL) SPEC:1295-7 T1-5AL-2-55N(ELI) K.T. LAB AIR Re-5 F=10 HZ 14111 AUG 04,176

INPUT CONSTANTS

ELASTIC MODULUS(E) = 118.590E+03 MPA(17.200E+06 PSI)				
NUMBER OF CYCLES	CRACK MOUTH COMPLIANCE	ABAR /" OPTICAL BASE	COMPLIANCE BASE	
N	CEJ			
X 1000				
.000	33.2725	.347		.334
13.600	34.4068	.355		.342
27.600	35.1630	.362		.348
36.500	35.3411	.367		.350
53.350	36.2973	.375		.359
72.350	36.6754	.381		.368
98.350	39.2220	.390		.374
115.350	40.0344	.400		.383
132.350	44.8990	.410		.406
149.550	46.2635	.420		.412
153.410	47.2621	.425		.418
155.210	49.0344	.435		.427
165.210	50.5067	.447		.435
167.210	53.1638	.457		.446
171.210	54.3421	.467		.454
173.710	56.7145	.477		.461
176.210	55.776	.467		.471
185.210	69.7115	.519		.508



(WOL) SPEC.13RS-7 T1=5AL-2.55N(ELI) R.T. LAB AIR No.5 F=10 HZ * * W.E.D.G.E.* B.P.E.N.* L.B.A.D.* P.R.G.R.A.M.* * 14:11 AUG 04, 1976

INPUT CONSTANTS:

RANGE RATIO(M) * .50
 TEST FREQUENCY(HZ) * 10.0
 SPECIMEN WIDTH(M) * 50.800 MM(2.000 IN.)
 SPECIMEN THICKNESS(B) * 18.979 MM(.747 IN.)
 CRACK SBA CORRECTION * 1.270 MM(.050 IN.)

NUMBE OF CYCLFS	MAXIMUM LOAD	SIDE 1 CRACK LENGTH	SIDE 2 CRACK LENGTH	CORRECTED AVERAGE CRACK LENGTH	CHANGE IN CRACK LENGTH	CHANGE IN CYCLES	CRACK GROWTH RATE DA / DN MICRO INCH PER CYCLE	STRESS INTENSITY RANGE DELTA K MPA X KSL X
N X 1000	KN	MM	MM	MM	MM	DN X 1000	MEIER INCH PER CYCLE	MPA X KSL X
000	12.01	2.70	16.99	.669	16.99	.719		
13.600	12.01	2.70	17.25	.679	18.52	.729	.74	10.35 9.43
27.600	12.01	2.70	17.50	.689	18.77	.739	.71	10.44 9.53
27.600	15.12	3.40	17.50	.689	18.77	.739		
32.600	15.12	3.40	17.75	.699	19.02	.749		
35.550	15.12	3.40	18.01	.709	19.28	.759		
59.350	15.12	3.40	18.77	.739	20.04	.769		
67.350	15.12	3.40	19.28	.759	20.55	.809		
72.550	15.12	3.40	19.66	.774	20.93	.824		
80.650	15.12	3.40	20.29	.799	21.56	.849		
88.350	15.12	3.40	20.80	.819	22.07	.869		
95.350	15.12	3.40	21.31	.839	22.52	.866		
95.350	17.79	4.00	21.31	.839	22.52	.866		
99.210	17.79	4.00	21.56	.849	22.82	.898		
105.010	17.79	4.00	22.83	.899	23.72	.934		
110.010	17.79	4.00	23.34	.919	24.74	.974		
113.010	17.79	4.00	24.10	.949	25.63	1.009		
117.010	17.79	4.00	25.12	.989	26.64	1.049		
119.510	17.79	4.00	26.14	1.029	27.66	1.089		
122.010	17.79	4.00	26.64	1.049	28.27	1.113		

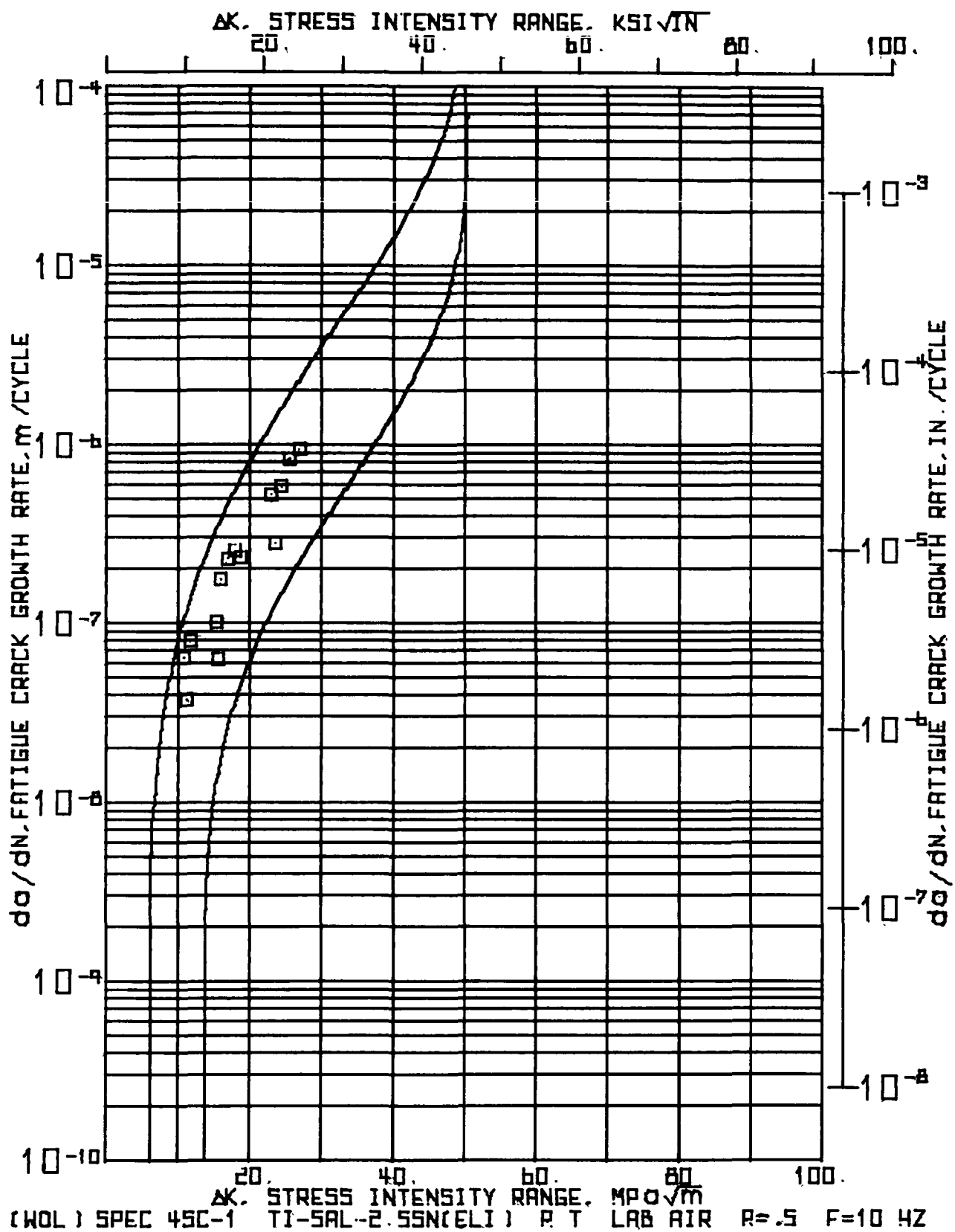
NUMBER OF CYCLES	MAXIMUM LOAD	SIDE 1		SIDE 2		CORRECTED AVERAGE	CHANGE IN		CHANGE IN CYCLES	CRACK GROWTH RATE		STRESS INTENSITY RANGE		
		CRACK LENGTH	INCH	CRACK LENGTH	MM		CRACK LENGTH	MM		INCH	MM	DA / DN	MPA X 1000.5	KSI X 1000.5
122.010	17.79 KN	26.64	1.049	27.36	1.077	28.27	1.113	1.041	.041	2.520	413.25	16.27	26.39	24.01
124.530	17.79 KN	27.31	1.099	28.17	1.109	29.31	1.154	1.016	.040	2.000	508.00	20.00	28.15	25.62
126.530	17.79 KN	28.93	1.159	29.18	1.149	30.33	1.194	1.270	.050	1.200	1058.33	41.67	30.34	27.61
127.730	17.79 KN	30.20	1.189	30.45	1.199	31.60	1.244	1.016	.040	1.200	846.67	33.33	32.82	29.87
128.930	17.79 KN	31.22	1.229	31.47	1.239	32.61	1.284	1.270	.050	.800	1567.50	62.50	35.66	32.46
129.730	17.79 KN	32.49	1.279	32.74	1.289	33.84	1.334							

(A2L) JFC-013RS-7 TYPAL-2155N(ELI) K.T. LAB AIR R=15 F=10 HZ 14111 AUG 04, 1976

INPUT CONSTANTS

ELASTIC MODULUS(E) = 110.590E+03 MPa (17.200E+06 PSI)

NUMBER OF CYCLES	CRACK DEPTH COMPLIANCE	ABAR / W OPTICAL BASF	COMPLIANCE BASE
N	CLD		
X 1000			
000	37.4215	.359	.362
11.500	35.1775	.364	.367
27.500	33.0895	.369	.377
32.400	40.0075	.374	.379
35.450	47.2565	.379	.380
57.350	41.2015	.394	.385
67.350	42.3355	.404	.392
72.350	43.4695	.412	.398
60.550	44.5034	.424	.404
80.350	45.4934	.434	.414
90.350	46.1394	.443	.427
97.210	51.3744	.449	.441
105.010	50.1057	.457	.459
110.110	61.4242	.467	.460
113.010	60.3679	.504	.493
117.010	77.5741	.524	.512
119.510	75.3951	.544	.527
122.010	81.5032	.576	.543
124.530	90.3645	.577	.565



TEST FREQUENCY (HZ)	RANGE RATIO (K)	SPECIMEN WIDTH (K)	SPECIMEN THICKNESS (B)	CRACK BG. CORRECTION
10.0	50	50.876 MM	2.003 IN.	0.748 IN.
18.992	50	18.992 MM	0.748 IN.	0.050 IN.
1.270	50	1.270 MM	0.050 IN.	

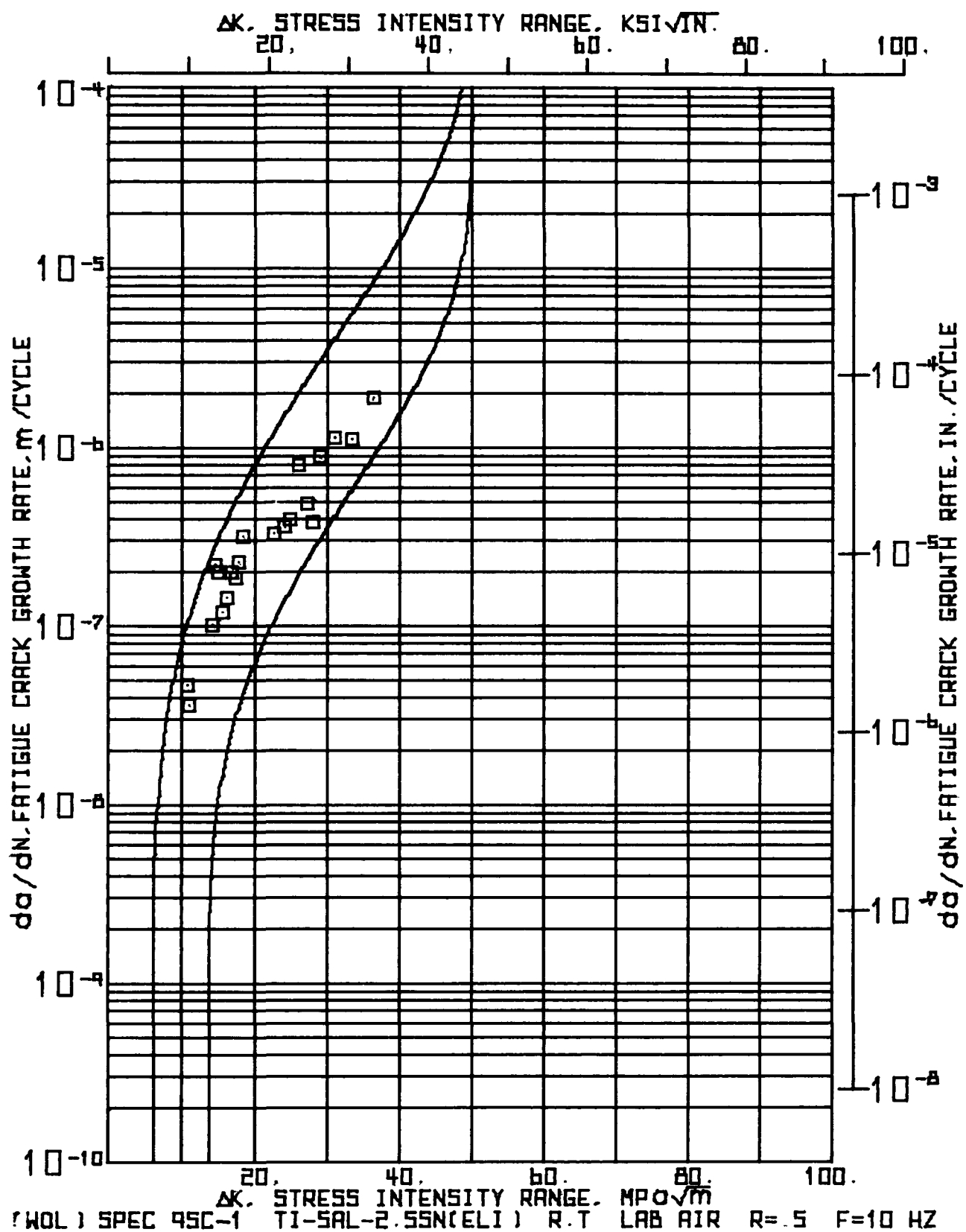
NUMBER OF CYCLES	MAXIMUM LOAD	SIDE 1 CRACK LENGTH		SIDE 2 CRACK LENGTH		CORRECTED AVERAGE CRACK LENGTH		CHANGE IN CRACK LENGTH		CHANGE IN CYCLES		CRACK GROWTH RATE DA / DN		STRESS INTENSITY RANGE DELTA K	
		P	A1	A2	MM	INCH	MM	INCH	MM	INCH	DN	X 1000	NANO- METER	MICRO- IN.	MPA X 1000
N	KIPS	MM	INCH	MM	INCH	MM	INCH	MM	INCH	DN	X 1000	METER	IN.	MPA X 1000	KSI X 1000
X 1000	KN	MM	INCH	MM	INCH	MM	INCH	MM	INCH	DN	X 1000	METER	IN.	MPA X 1000	KSI X 1000
.000	12.01	2.70	17.48	.688	.700	18.90	.744	.762	.030	11.785	64.66	2.55	10.75	9.79	
11.785	12.01	2.70	18.24	.718	.730	19.66	.774	1.118	.044	29.900	37.38	1.47	11.23	10.22	
41.685	12.01	2.70	19.13	.753	.783	20.78	.818	.889	.035	11.000	80.82	3.18	11.78	10.72	
52.685	12.01	2.70	20.40	.803	.803	21.67	.853								
52.685	15.12	3.40	20.40	.803	.803	21.67	.853	.508	.020	5.000	101.60	4.00	15.34	13.96	
57.685	15.12	3.40	20.65	.813	.833	22.17	.873	.254	.010	4.000	63.50	2.50	15.63	14.23	
61.685	15.12	3.40	20.90	.823	.843	22.43	.883	.889	.035	5.000	177.80	7.00	16.09	14.64	
66.685	15.12	3.40	21.67	.853	.883	23.32	.918	1.143	.045	5.000	228.60	9.00	16.95	15.42	
71.685	15.12	3.40	23.19	.913	.913	24.46	.963	1.016	.040	4.000	254.00	10.00	17.94	16.33	
75.685	15.12	3.40	24.46	.963	.943	25.48	1.003	.698	.027	3.000	232.83	9.17	18.80	17.11	
78.685	15.12	3.40	24.97	.983	.978	26.17	1.030								
.000	17.79	4.00	24.97	.983	.993	26.37	1.038	.317	.012	.600	529.17	20.83	23.00	20.93	
.600	17.79	4.00	25.35	.998	.943	26.68	1.050	.508	.020	1.800	282.22	11.11	23.54	21.43	
2.400	17.79	4.00	25.98	1.023	.918	27.19	1.070	.699	.028	1.200	562.08	22.92	24.38	22.19	
3.600	17.79	4.00	26.75	1.053	.943	27.89	1.098	.825	.032	1.000	825.50	32.50	25.51	23.22	
4.600	17.79	4.00	27.51	1.083	.978	28.71	1.130	.953	.038	1.000	952.50	37.50	26.94	24.51	
5.600	17.79	4.00	28.27	1.113	.918	29.67	1.168								

14:12 AUG 04, '76

(MPL) SPEC=SC=1 YI=5AL=2.55N(ELI) R=1 LAB AIR R=5 F=10 HZ

INPUT CONSTANTS

ELASTIC MODULUS(E) = 110.590E+03 MPA(17.200E+06 PSI)					
NUMERICAL	CRACK WIDTH	BEAR / "	OPTICAL COMPLIANCE	BEAR / "	OPTICAL COMPLIANCE
OF	COMPLIANCE	BASE	BASE	BASE	BASE
CYCLES					
N	CEB				
X 1.00					
57.685	51.0131	.436	.436	.436	.436
61.685	51.2274	.441	.441	.437	.437
65.685	54.4425	.458	.458	.452	.452
71.685	60.9154	.461	.461	.474	.474
75.685	64.5022	.501	.501	.490	.490
76.685	67.3330	.514	.514	.501	.501
.000	71.1611	.516	.516	.513	.513
.600	71.1611	.524	.524	.513	.513
2.400	77.5913	.534	.534	.532	.532
3.600	83.1642	.548	.548	.548	.548
4.800	87.5797	.564	.564	.559	.559
5.600	95.1673	.583	.583	.576	.576



CODE * P E N * L O A D * P R O G R A M *

INPUT CONSTANTS:

TEST FREQUENCY (HZ)	SPECIMEN WIDTH (IN.)	SPECIMEN THICKNESS (B)	CRACK SIZE CORRECTION
50	2.004	.743	.050
10.0	2.004	.743	.050
50.902	2.004	.743	.050
18.882	2.004	.743	.050
1.270	2.004	.743	.050

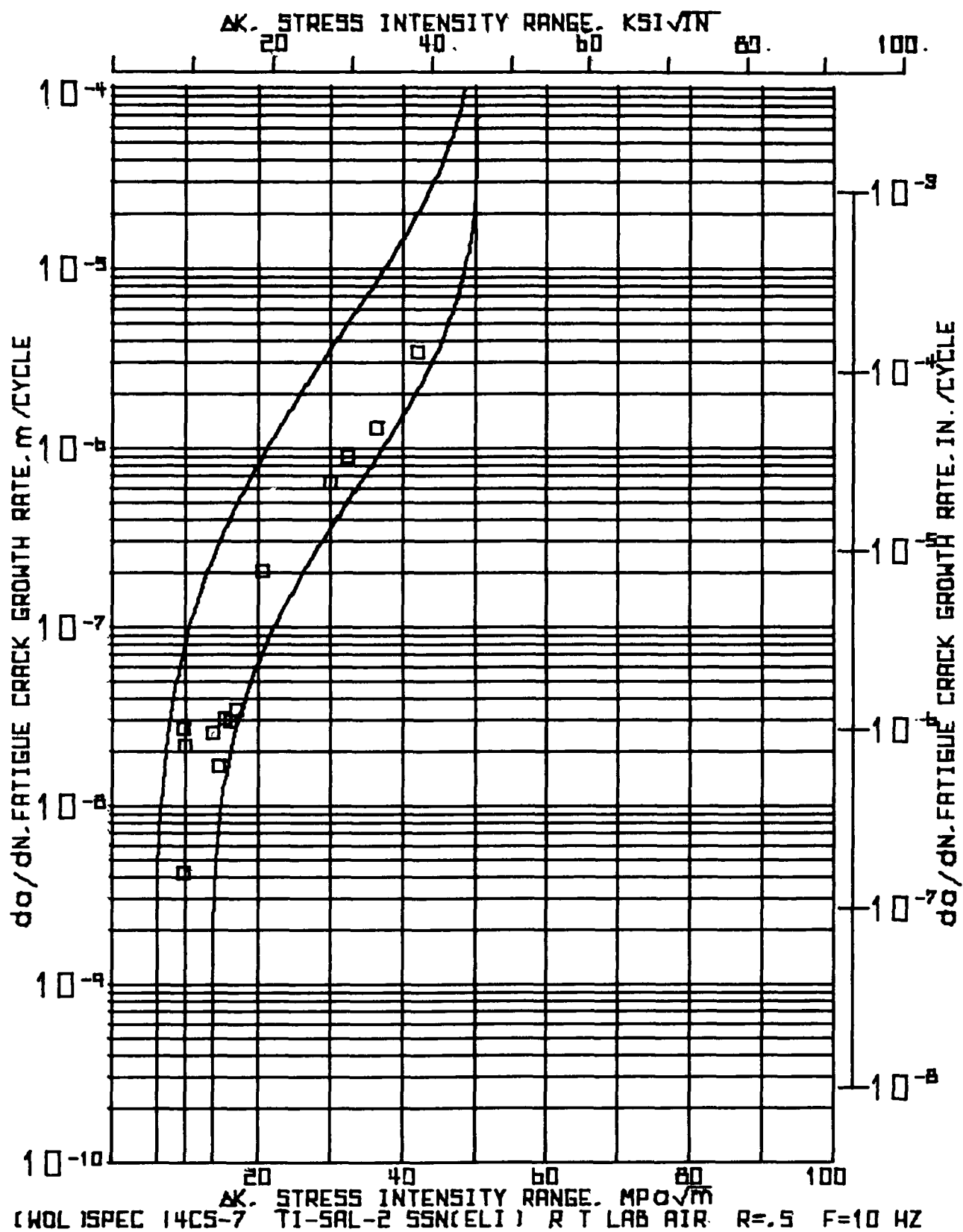
NUMBER OF CYCLES	MAXIMUM LOAD P	SIDE 1 CRACK LENGTH		SIDE 2 CRACK LENGTH		CORRECTED AVERAGE CRACK LENGTH ABAR	CHANGE IN CRACK LENGTH DA		CHANGE IN CYCLES	CRACK GROWTH RATE		STRESS INTENSITY RANGE DELTA K		
		MM	INCH	MM	INCH		MM	INCH		DN X 1000	DA / DN MICRO IN. PER CYCLE	NANO- METER	MPA X 1000	ksi X 1000
1000	12.01	2.70	17.42	6.86	17.68	6.96	.741	.635	.025	13.600	46.69	1.84	10.74	9.77
15000	12.01	2.70	17.93	7.06	18.44	7.26	.766	.504	.020	14.000	36.29	1.43	11.02	10.03
20000	12.01	2.70	18.44	7.26	18.95	7.46	.766	.635	.025	2.850	222.81	8.77	14.60	13.22
25000	12.01	2.70	18.44	7.26	18.95	7.46	.766	.504	.020	5.000	101.60	4.00	14.21	12.94
30000	12.01	2.70	18.44	7.26	18.95	7.46	.766	.635	.025	2.850	222.81	8.77	14.60	13.22
35000	12.01	2.70	18.44	7.26	18.95	7.46	.766	.504	.020	2.500	203.20	8.00	15.01	13.65
40000	12.01	2.70	18.44	7.26	18.95	7.46	.766	.635	.025	7.400	120.14	4.73	15.53	14.13
45000	12.01	2.70	18.44	7.26	18.95	7.46	.766	.504	.020	4.400	144.32	5.68	16.13	14.68
50000	12.01	2.70	18.44	7.26	18.95	7.46	.766	.635	.025	3.800	200.53	7.89	16.71	15.21
55000	12.01	2.70	18.44	7.26	18.95	7.46	.766	.504	.020	3.400	186.76	7.35	17.33	15.77
60000	12.01	2.70	18.44	7.26	18.95	7.46	.766	.635	.025	2.200	230.91	9.09	17.86	16.25
65000	12.01	2.70	18.44	7.26	18.95	7.46	.766	.504	.020	1.600	317.50	12.50	18.35	16.70
70000	12.01	2.70	18.44	7.26	18.95	7.46	.766	.635	.025	3.860	329.02	12.95	22.67	20.63
75000	12.01	2.70	18.44	7.26	18.95	7.46	.766	.504	.020	1.750	362.86	14.29	23.93	21.78
80000	12.01	2.70	18.44	7.26	18.95	7.46	.766	.635	.025	1.600	396.88	15.63	24.84	22.60
85000	12.01	2.70	18.44	7.26	18.95	7.46	.766	.504	.020	1.100	808.15	31.82	26.00	23.66
90000	12.01	2.70	18.44	7.26	18.95	7.46	.766	.635	.025	1.050	463.81	19.05	27.14	24.70
95000	12.01	2.70	18.44	7.26	18.95	7.46	.766	.504	.020	1.000	381.00	15.00	27.91	25.40

NUMBER OF CYCLES	MAXIMUM LOAD	SIDE 1		SIDE 2		CORRECTED AVERAGE LENGTH	CHANGE		CHANGE IN CYCLES	CRACK GROWTH RATE		STRESS INTENSITY RANGE				
		CRACK LENGTH	MM	INCH	CRACK LENGTH		MM	INCH		CRACK LENGTH	MM		INCH	DA / DN METER PER CYCLE	NANO METER IN.	MPA X DELTA K INCH X INCH
N	P	KN	MM	INCH	MM	INCH	MM	INCH	DN X 1000							
X 1000																
71,110	17.79	4.00	23.60	1.126	26.60	1.126	29.07	1.176		.889	.035	1.000	889.00	35.00	29.07	26.45
72,110	17.79	4.00	29.36	1.156	29.62	1.166	30.76	1.211		1.143	.045	1.000	1143.00	45.00	31.10	28.30
73,110	17.79	4.00	30.63	1.206	30.63	1.206	31.90	1.256		.889	.035	.800	1111.25	43.75	33.37	30.37
73,910	17.79	4.00	31.05	1.246	31.39	1.236	32.79	1.291		1.524	.060	.800	1905.00	75.00	36.46	33.18
74,710	17.79	4.00	33.17	1.306	32.92	1.296	34.32	1.351								

(K2L) SPEC-95C-1 TI-5AL-2.5SN(EL) R.T. LAP AIR R=0.5 F=10 MZ 14:12 AUG 04,176

INPUT CONSTANTS

ELASTIC MODULUS(E) = 118.590E+03 MPA(17.200E+06 PSI)				
NUMBER OF CYCLES	CRACK MOUTH COMPLIANCE	ABAR / W OPTICAL BASE	COMPLIANCE BASE	
X 1000				
0.00	39.4877	.370	.375	
13.600	40.0155	.382	.382	
27.200	42.0723	.392	.395	
40.800	44.5766	.402	.403	
54.400	46.0570	.415	.413	
68.000	47.3852	.425	.419	
81.600	51.1459	.442	.437	
95.200	54.1545	.455	.450	
108.800	57.0392	.470	.465	
122.400	60.7239	.482	.476	
136.000	62.5281	.492	.483	
149.600	64.0065	.502	.490	
163.200	71.1013	.527	.513	
176.800	73.0022	.539	.527	
190.400	80.0031	.552	.540	
204.000	85.0040	.569	.553	
217.600	88.0173	.579	.563	
231.200	95.7811	.587	.578	
244.800	103.4201	.604	.593	
258.400	112.0343	.627	.610	



(WBL)SPEC-14CS-7 YI-5AL-25SSN(ELI) R.T.LAB AIR R.S F=10 HZ W E D G E S B P E N L B A U P R B G R A M S S 14112 AUG 04, '76

INPUT CONSTANTS:

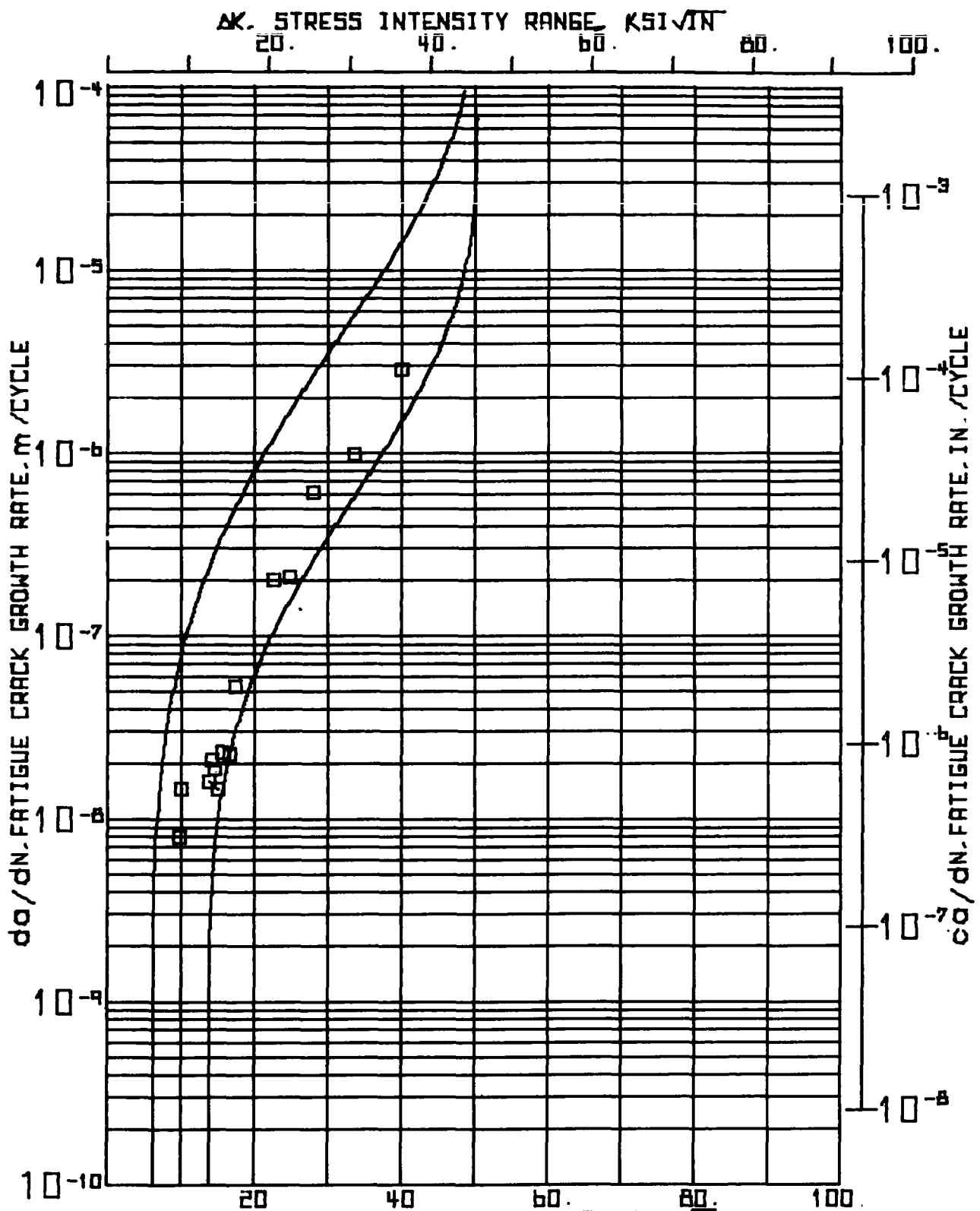
RANGE RATIO(K) .50
 TEST FREQUENCY(HZ) 10.0
 SPECIMEN WIDTH(IN) 51.054 MM(2.010 IN.)
 SPECIMEN THICKNESS(B) 19.017 MM(.749 IN.)
 CRACK 99% CORRECTION 1.270 MM(.050 IN.)

NUMBER OF CYCLES	MAXIMUM LOAD	SIDE 1 CRACK LENGTH	SIDE 2 CRACK LENGTH	CORRECTED AVERAGE CRACK LENGTH	CHANGE IN CRACK LENGTH DA	CHANGE IN CYCLES DN	CRACK GROWTH RATE DA / DN	STRESS INTENSITY RANGE DELTA K
N X 1000	KV	MM	MM	MM	MM	INCH X 1000	METER PER CYCLE	MPA X 1000
000	11.34 2.55	17.22	17.09	18.43	.725	.010	10.000	26.67 1.05 9.77 8.89
10.000	11.34 2.55	17.40	17.45	18.69	.736	.007	40.000	4.13 .16 9.87 8.98
50.000	11.34 2.55	17.53	17.63	18.86	.742	.025	30.000	21.17 .83 10.05 9.14
80.000	11.34 2.55	17.66	18.01	19.49	.767	.030	30.000	24.98 .96 13.83 12.58
110.000	15.12 3.40	18.97	18.97	20.24	.797	.058	90.000	16.37 .64 14.57 13.26
200.000	15.12 3.40	20.80	20.09	21.72	.855	.036	30.000	30.06 1.18 15.43 14.04
230.000	15.12 3.40	21.62	21.08	22.62	.890	.035	30.000	29.21 1.15 16.12 14.67
260.000	15.12 3.40	22.30	22.15	23.49	.925	.040	30.000	33.87 1.33 16.92 15.40
290.000	15.12 3.40	25.10	21.39	24.51	.965	.237	30.000	200.24 7.88 20.51 18.67
320.000	15.12 3.40	29.92	1.178	30.52	1.201	.037	1.500	635.00 25.00 29.96 27.26
350.000	17.79 4.00	30.73	1.210	31.47	1.239	.052	1.500	880.53 34.67 32.37 29.46
380.000	17.79 4.00	31.95	1.258	32.79	1.291	.075	1.500	1270.00 50.00 36.39 33.12
410.000	17.79 4.00	33.73	1.328	34.70	1.366	.066	.500	3352.80 132.00 41.92 38.15
440.000	17.79 4.00	35.51	1.398	36.37	1.432			

(MUL)SPFC-1,CS-7 T1-5AL-2.5SN(EL1) R-T-LAB AIR R-0.5 F=10. HZ 14:12 AUG 04, 1976

INPUT CONSTANTS

ELASTIC MODULUS(E) • 118.590E+03 MPa(17.200E+06 PSI)					
NUMBER OF CYCLES	CRACK NGUM COMPLIANCE	ABAR / W OPTICAL COMPLIANCE	BASE	BASE	
N	CE0				
x 1000					
1000	37.0281	.361	.365		
10000	35.0329	.366	.370		
50000	39.0378	.369	.375		
50000	40.2426	.382	.380		
110000	42.0572	.397	.394		
200000	47.0563	.425	.419		
230000	47.3009	.443	.431		
260000	54.7300	.460	.453		
290000	66.0028	.450	.499		
320000	103.0211	.598	.593		
321000	110.0939	.616	.615		
323000	127.0710	.642	.635		
324500	162.0802	.660	.679		
325000	213.2859	.712	.724		



(WOL) SPEC 15C5-7 TI-5AL-2 55N(ELI) R T LAB AIR R=.5 F=10 HZ

(AL)SPEC.15CS-7 11-SAL-2155NIELT) R.T.LAB AIR R=5 F=10 HZ * * * * * W E D G E * B P E N * L B A D * P R B G R A H * * * * * 14112 AUG 04, 1976

INPUT CONSTANTS:

RANGE RATIO(R) * .50
 TEST FREQUENCY(HZ) * 10.0
 SPECIMEN WIDTH(W) * 50.902 MM(2.004 IN.)
 SPECIMEN THICKNESS(B) * 18.805 MM(.743 IN.)
 CRACK B9% CORRECTION * 1.270 MM(.050 IN.)

NUMBER OF CYCLES	MAXIMUM LOAD	SIDE 1		SIDE 2		CORRECTED AVERAGE CRACK LENGTH		CHANGE IN CRACK LENGTH		CHANGE IN CYCLES		CRACK GROWTH RATE DA / DN		STRESS INTENSITY RANGE DELTA K	
		MM	INCH	MM	INCH	MM	INCH	MM	INCH	DN	X 1000	METER	MICR9 IN.	MPA X M=0.5	KSI X IN=0.5
000	11.34 2.55	18.99	.669	16.94	.667	18.24	.718	.317	.012	40.000		7.94	.31	9.82	8.94
40.000	11.34 2.55	17.45	.687	17.12	.674	18.55	.730	.432	.017	30.000		14.32	.57	9.99	9.09
70.000	11.34 2.55	18.08	.712	17.35	.683	18.99	.747								
70.000	15.12 3.40	18.08	.712	17.35	.683	18.99	.747	.952	.037	60.000		15.87	.62	13.74	12.50
130.000	15.12 3.40	19.25	.758	18.08	.712	19.94	.785	.622	.024	30.000		20.74	.82	14.25	12.97
160.000	15.12 3.40	19.94	.785	18.64	.734	20.56	.809	.559	.022	30.000		18.63	.73	14.65	13.33
190.000	15.12 3.40	20.65	.813	19.05	.750	21.12	.831	.432	.017	30.000		14.39	.57	15.00	13.65
220.000	15.12 3.40	21.46	.845	19.10	.752	21.55	.848	1.372	.054	60.000		22.86	.90	15.68	14.27
280.000	15.12 3.40	23.01	.906	20.29	.799	22.92	.902	.673	.027	30.000		22.44	.88	16.50	15.02
310.000	15.12 3.40	23.98	.944	20.68	.814	23.60	.929	1.588	.063	30.000		52.92	2.08	17.50	15.92
340.000	15.12 3.40	25.27	.995	22.56	.888	25.18	.991								
340.000	17.79 4.00	25.27	.995	22.56	.888	25.18	.991	2.007	.079	10.000		200.66	7.90	22.70	20.65
350.000	17.79 4.00	26.92	1.060	24.92	.981	27.19	1.070	1.041	.041	5.000		208.28	8.20	24.77	22.54
355.000	17.79 4.00	27.20	1.071	26.72	1.052	28.23	1.111	3.048	.120	5.000		609.60	24.00	28.07	25.54
360.000	17.79 4.00	30.48	1.200	29.54	1.163	31.28	1.231	2.337	.092	2.400		973.67	38.33	33.65	30.62
362.400	17.79 4.00	32.69	1.287	32.00	1.260	33.62	1.323	2.273	.090	.800		2841.63	111.88	40.06	36.45
363.200	17.79 4.00	35.31	1.390	33.93	1.336	35.89	1.413								

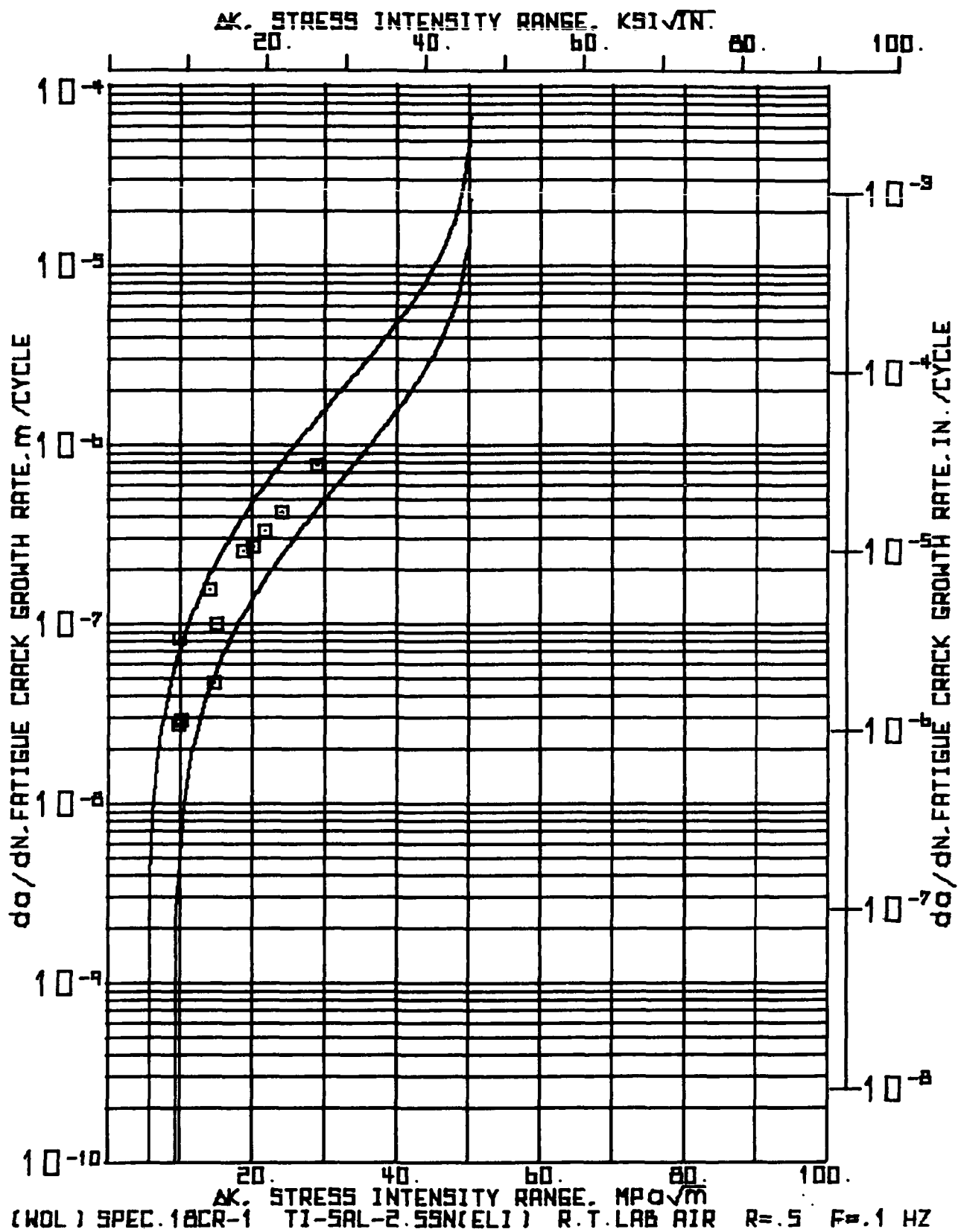
... (MPL) SPEC: 15CS-7 T1-5AL-2-5SN(ELI) R.T. LAB AIR R=5 F=10 HZ 1+112 AUG 04, 1976

INPUT CONSTANTS

ELASTIC MODULUS(E) = 110.590E+03 MPA(17.200E+06 PSI)				
NUMBER OF CYCLES	CRACK LENGTH COMPLIANCE	ADAR / W OPTICAL BASE	COMPLIANCE BASE	
N	C _{ED}			
X 1000				
000	37.0249	.358	.363	
40.000	39.1217	.365	.373	
70.000	39.9201	.373	.378	
100.000	42.3153	.392	.392	
160.000	43.1137	.404	.396	
190.000	44.3073	.415	.413	
220.000	47.1057	.423	.417	
260.000	53.4930	.450	.447	
310.000	55.6593	.464	.454	
340.000	62.2754	.495	.463	
350.000	73.4530	.534	.520	
355.000	84.0307	.555	.551	
360.000	107.7843	.615	.602	
362.400	142.1106	.660	.655	
363.200	184.4310	.705	.701	

SECTION A4

This section of the Appendix includes all fatigue crack growth data obtained from WOL coupons tested at room temperature, at a range ratio of 0.5, and at a frequency of 0.1 Hz.



(WGL) SPEC. ICR=1 YI=5AL*2.5SN(ELI) RT.LAB AIR R=5 F=1 HZ
 * * * * * WEDGE * * * * * OPEN * * * * * L Q A D * * * * * P R O G R A M * * * * *

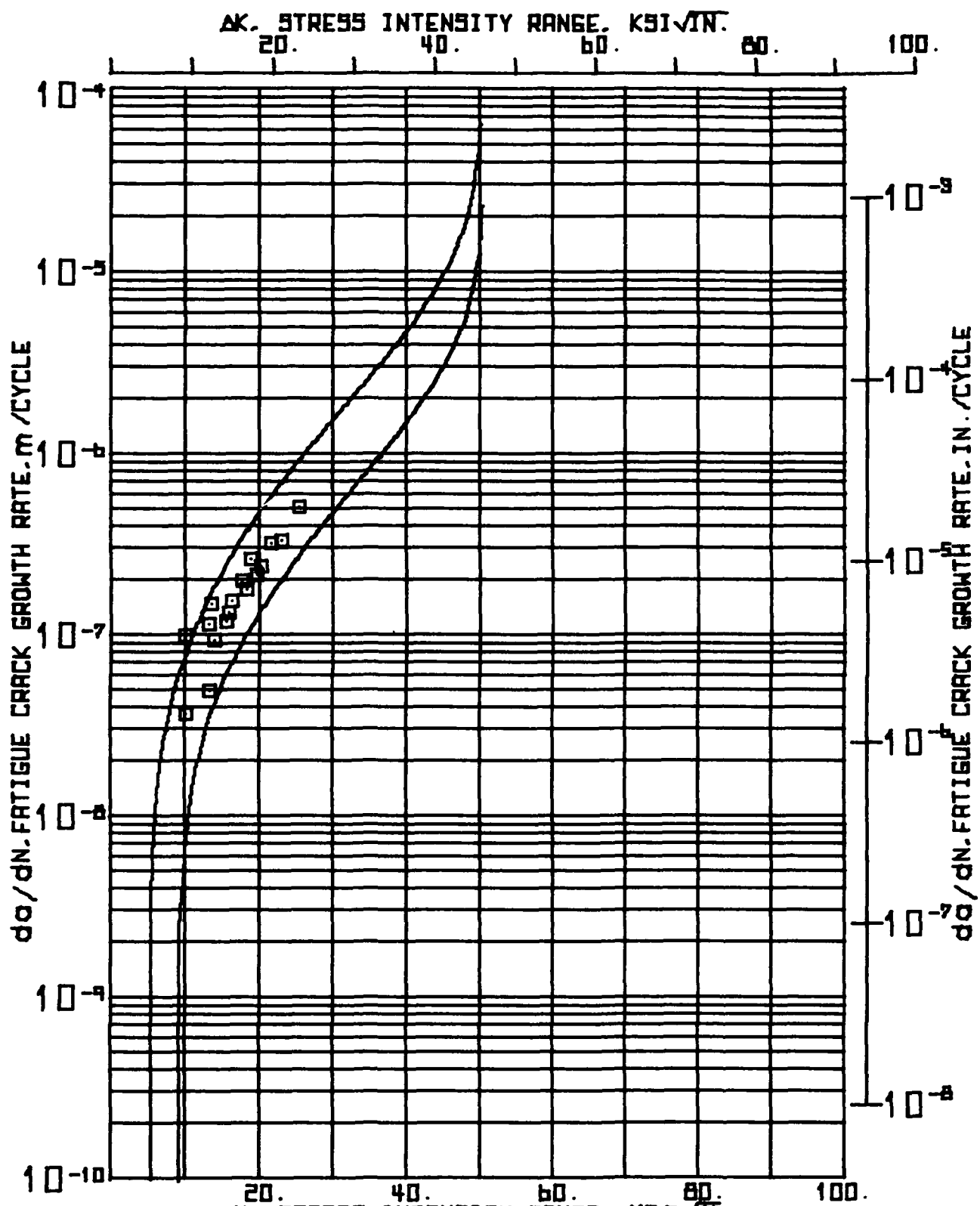
INPUT CONSTANTS:

RANGE RATING(M) .50															
TEST FREQUENCY(HZ) .1															
SPECIMEN WIDTH(M) 50.927 MM(2.005 IN.)															
SPECIMEN THICKNESS(B) 18.959 MM(.746 IN.)															
CRACK B9, CORRECTION 1.270 MM(.050 IN.)															
NUMBER OF CYCLES	MAXIMUM LOAD	SIDE 1 CRACK LENGTH		SIDE 2 CRACK LENGTH		CORRECTED AVERAGE LENGTH		CHANGE IN CRACK LENGTH		CHANGE IN CYCLES		CRACK GROWTH RATE DA / DN		STRESS INTENSITY RANGE	
		MM	INCH	MM	INCH	MM	INCH	MM	INCH	MM	INCH	NANO- METER	MICRO IN.	MPA X 1000	KSI X 1000
X 1000	KN	P	A1	A2											
000	11.34 2.55		17.35	.683	16.69	.657	18.29	.720	.254	.010	9.465	26.84	1.06	9.77	8.89
9.465	11.34 2.55		17.86	.703	16.69	.657	18.54	.730	.737	.029	9.050	81.39	3.20	9.99	9.09
16.515	11.34 2.55		18.08	.712	17.93	.706	19.28	.759	.483	.019	16.930	28.51	1.12	10.27	9.35
35.445	11.34 2.55		18.95	.746	18.03	.710	19.76	.778							
35.445	15.12 3.40		18.95	.746	18.03	.710	19.76	.778	1.295	.051	8.450	153.30	6.04	14.27	12.99
43.895	15.12 3.40		20.07	.790	19.51	.768	21.06	.829	.356	.014	7.700	46.18	1.82	14.84	13.51
51.595	15.12 3.40		20.42	.804	19.86	.782	21.41	.843	.762	.030	7.700	98.96	3.90	15.25	13.83
59.295	15.12 3.40		20.98	.826	20.83	.820	22.17	.873							
59.295	17.79 4.00		20.38	.856	20.83	.820	22.17	.873	1.257	.050	5.000	251.46	9.90	18.86	17.17
64.295	17.79 4.00		22.22	.875	22.10	.870	23.43	.922	1.334	.053	5.000	266.70	10.50	20.16	18.34
69.295	17.79 4.00		23.52	.926	23.47	.924	24.76	.975	1.613	.064	5.000	322.58	12.70	21.81	19.84
74.295	17.79 4.00		25.32	.997	24.89	.980	26.38	1.038	2.070	.082	5.000	414.02	16.30	24.19	22.02
79.295	17.79 4.00		27.00	1.063	27.36	1.077	28.45	1.120	3.610	.150	5.000	762.00	30.00	28.99	26.38
84.295	17.79 4.00		30.73	1.210	31.24	1.230	32.26	1.270							

(MOL) SPEC-18CR-1 T1-SAL-2-SSN(ELI) R.T.LAB_AIR Re.5 F=0.1 HZ 14112 AUG 04.176

INPUT CONSTANTS

ELASTIC MODULUS(E) = 118.590E+03 MPA(17.200E+06 PSI)					
NUMBER OF CYCLES	CRACK MOUTH COMPLIANCE	OPTICAL BASF	ABAK / W	COMPLIANCE BASE	
N	CEP				
X 1000					
100	40.9214	.359		.384	
500	41.7238	.364		.388	
1000	43.4285	.379		.397	
1500	44.1309	.388		.402	
2000	47.3404	.413		.419	
5100	50.5499	.420		.434	
5900	54.5618	.435		.452	
6000	59.3761	.460		.472	
6900	65.7952	.486		.495	
7400	75.4237	.518		.526	
7900	89.3666	.559		.564	
8000	127.5784	.633		.635	



(WOL) SPEC 10CR-1 T1 5AL-2.55N(FL1) PT LAB AIR P-0 5 F=0.1 42

(49L) SPEC:1UCR-1 T1-5AL-2.55N(ELI) RT LAB AIR R0.5 P0.1 HZ 14:13 AUG 06, 1976

INPUT CONSTANTS:

RANGE RATIO(R) .50
TEST FREQUENCY(HZ) .1
SPECIMEN WIDTH(W) 50.952 MM(2.006 IN.)
SPECIMEN THICKNESS(B) 18.933 MM(.745 IN.)
CRACK DBA CORRECTION 1.270 MM(.050 IN.)

NUMBER OF CYCLES	MAXIMUM LOAD	LOAD KIPS	SIDE 1 CRACK LENGTH	SIDE 2 CRACK LENGTH	CORRECTED AVERAGE CRACK LENGTH	CHANGE IN CRACK LENGTH	CHANGE IN CYCLES	CRACK GRGTH RATE DA / DN	STRESS INTENSITY RANGE DELTA K
N	P	KIPS	MM	MM	MM	MM	INCH X 1000	DA / DN MICR9 IN PER CYCLE	MPA X 100.5 IN0.5
1000	12.01	2.70	16.66	16.66	16.66	16.66	16.66	16.66	16.66
3500	12.01	2.70	17.22	16.97	16.36	16.36	16.36	16.36	16.36
10500	12.01	2.70	17.48	17.22	16.78	16.78	16.78	16.78	16.78
15500	15.12	3.40	17.46	17.22	16.78	16.78	16.78	16.78	16.78
21000	15.12	3.40	17.98	17.73	16.98	16.98	16.98	16.98	16.98
24000	15.12	3.40	18.26	18.03	17.10	17.10	17.10	17.10	17.10
30000	15.12	3.40	19.25	19.05	17.50	17.50	17.50	17.50	17.50
30000	15.68	3.75	19.25	19.05	17.50	17.50	17.50	17.50	17.50
33000	16.68	3.75	19.61	19.41	17.64	17.64	17.64	17.64	17.64
36000	16.68	3.75	19.94	19.86	17.82	17.82	17.82	17.82	17.82
39000	16.68	3.75	20.35	20.37	18.02	18.02	18.02	18.02	18.02
39000	17.79	4.00	20.35	20.37	18.02	18.02	18.02	18.02	18.02
42000	17.79	4.00	20.95	20.95	18.25	18.25	18.25	18.25	18.25
45000	17.79	4.00	21.39	21.59	18.50	18.50	18.50	18.50	18.50
45000	17.79	4.00	22.35	22.17	18.73	18.73	18.73	18.73	18.73
51000	17.79	4.00	22.91	22.89	19.01	19.01	19.01	19.01	19.01
54000	17.79	4.00	23.70	23.52	19.26	19.26	19.26	19.26	19.26
59000	17.79	4.00	25.25	25.15	19.90	19.90	19.90	19.90	19.90
61000	17.79	4.00	25.93	25.78	19.015	19.015	19.015	19.015	19.015

PAGE 2

14113 AUG 04, '76

5 F90.1 HZ.

RT LAB AIR

1-5AL-2-55N

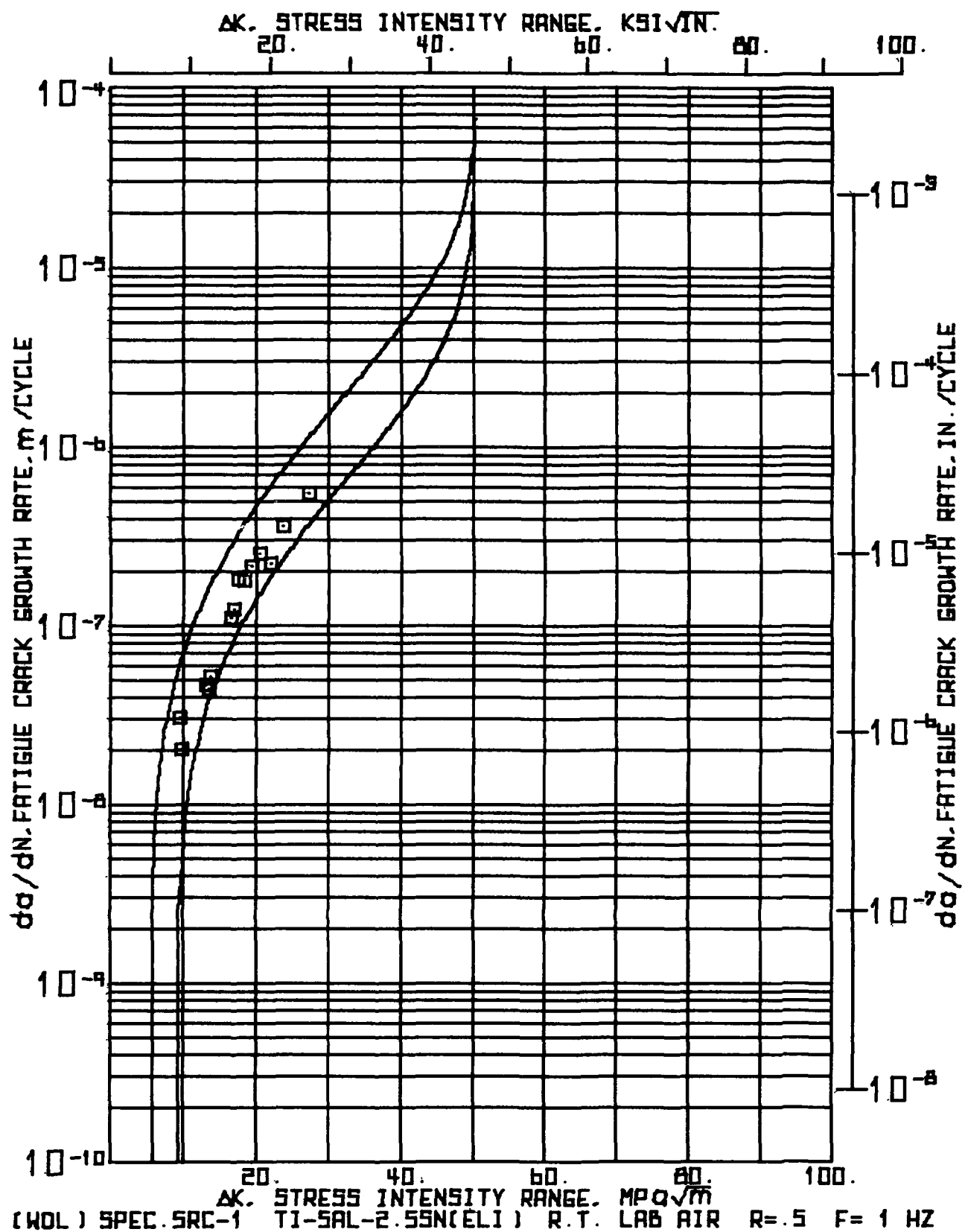
FD-302 (Rev. 10-6-95)

NUMBER OF CYCLES	MAXIMUM LOAD	SIDE 1		SIDE 2		CORRECTED		CHANGE IN CRACK LENGTH	CHANGE IN CYCLES	CRACK GROWTH RATE DA / DN MICR9 IN. PER CYCLE	STRESS INTENSITY RANGE MPA X 400.5
		CRACK LENGTH	CRACK LENGTH	CRACK LENGTH	CRACK LENGTH	CRACK LENGTH	CRACK LENGTH				
61.000	17.79 4.00	25.23 1.021	25.78 1.015	27.13 1.068	2.781	.110	5.450	510.33	20.09	25.84	23.51
66.450	17.79 4.00	28.70 1.130	28.57 1.125	29.91 1.177							

(WOL) SPEC:1CCR-1 TI-5AL-2.55N(ELI) RI LAB AIR R=0.5 F=0.1 HZ 14:13 AUG 04, 1976

INPUT CONSTANTS

ELASTIC MODULUS(E) = 118.590E+03 MPa (17.200E+06 PSI)					
NUMBER OF CYCLES	CRACK MOUTH COMPLIANCE	ABAR / W	OPTICAL BASE	COMPLIANCE BASE	
N	CEB				
x 1000					
900	39.2639	.354		.374	
1000	40.0652	.360		.379	
10500	40.6666	.365		.384	
15000	41.6879	.375		.388	
21000	42.4692	.381		.393	
24000	44.0718	.390		.402	
30000	45.6744	.401		.410	
33000	46.4757	.408		.414	
36000	48.0783	.416		.422	
39000	50.4822	.424		.434	
42000	52.4861	.436		.445	
45000	53.6874	.447		.448	
48000	56.0913	.462		.459	
51000	59.2966	.474		.471	
54000	64.1044	.488		.489	
59000	71.3161	.519		.514	
61000	76.1240	.532		.528	
60050	96.0579	.587		.580	



(W01) SPEC.SRC-1 T1-SAL-2.55N(ELI) R.T. LAB AIR R-0.5 F-0.1 HZ * * * * * 14113 AUG 04, '76

INPUT CONSTANTS:

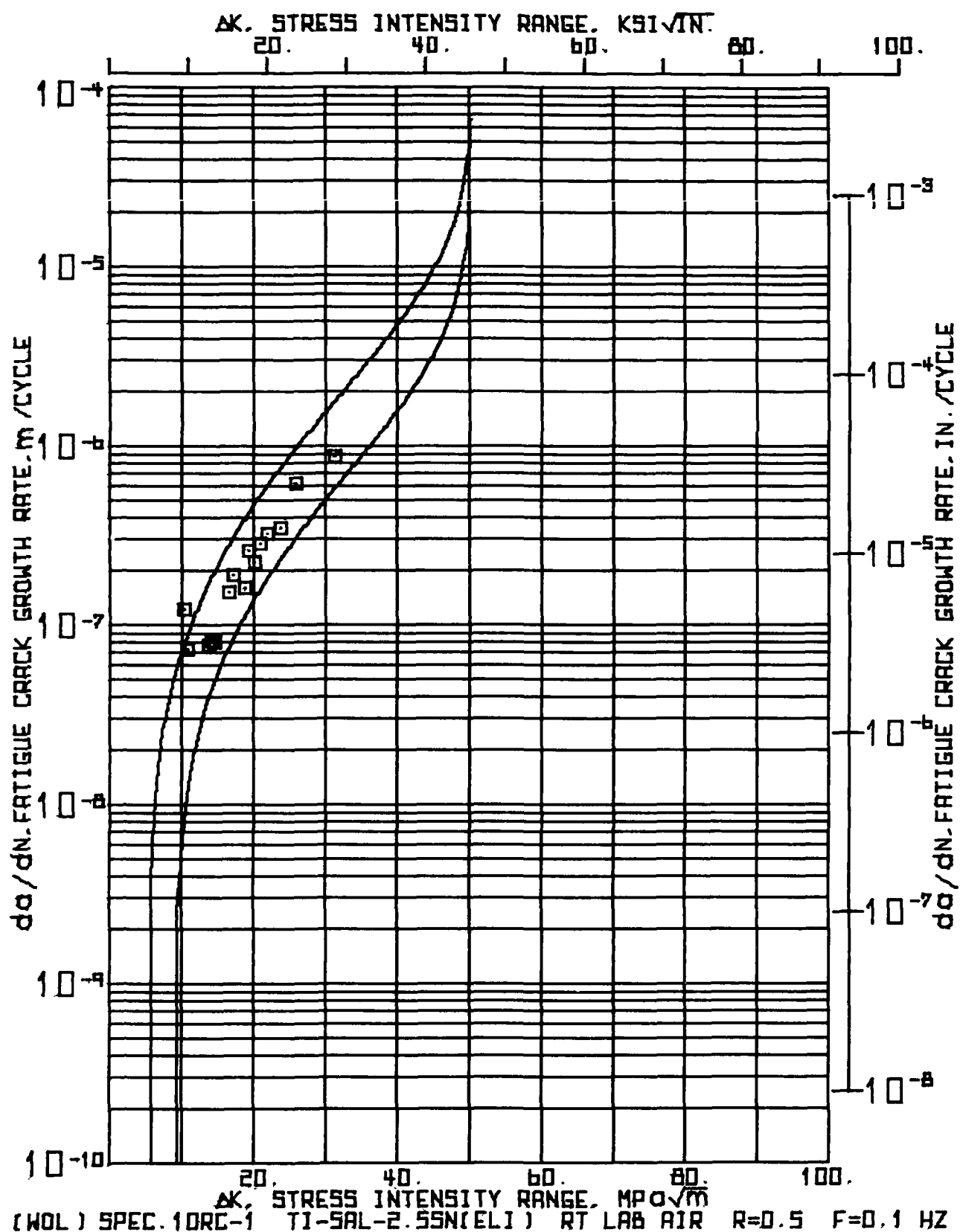
RANGE RATIO(R) = .50
 TEST FREQUENCY(HZ) = .1
 SPECIMEN WIDTH(W) = 50.952 MM(2.006 IN.)
 SPECIMEN THICKNESS(B) = 18.974 MM(.747 IN.)
 CRACK BG. CORRECTION = 1.270 MM(.050 IN.)

NUMBER OF CYCLES	P KN	MAXIMUM LOAD	SIDE 1 CRACK LENGTH		SIDE 2 CRACK LENGTH		CORRECTED AVERAGE CRACK LENGTH	CHANGE IN LENGTH		CHANGE IN CYCLES	CRACK GROWTH RATE DA / DN		STRESS INTENSITY RANGE DELTA K
			MM	INCH	MM	INCH	MM	MM	INCH		MM	INCH	
1000	KN	KIPS	A1		A2			DA	DN		METER	MICRO IN.	MPA X 10 ⁻⁵
													10 ⁻⁵
000	11.34	2.55	16.64	.655	16.59	.653	17.88	.704					
9.465	11.34	2.55	16.47	.664	16.94	.667	18.17	.715	.292	.012	9.465	30.86	1.22 9.59 8.73
35.445	11.34	2.55	17.25	.679	17.63	.694	18.71	.736	.534	.021	25.980	20.53	.81 9.77 8.89
35.445	15.12	3.40	17.25	.679	17.63	.694	18.71	.736	.394	.016	8.450	46.59	1.83 13.30 12.10
43.495	15.12	3.40	17.41	.701	17.86	.703	19.10	.752	.343	.013	7.700	44.53	1.79 13.52 12.31
51.595	15.12	3.40	18.21	.717	18.14	.714	19.44	.765	.406	.016	7.700	52.78	2.08 13.76 12.52
59.295	15.12	3.40	18.64	.734	18.52	.729	19.85	.781					
59.295	17.79	4.00	13.04	.734	18.52	.729	19.85	.781	.552	.022	5.000	111.76	4.40 16.55 15.06
64.295	17.79	4.00	19.23	.767	19.05	.750	20.41	.803	.622	.024	5.000	124.46	4.90 17.01 15.48
69.295	17.79	4.00	19.31	.784	19.61	.772	21.03	.828	.914	.036	5.000	182.88	7.20 17.65 16.06
74.295	17.79	4.00	20.68	.814	20.68	.814	21.95	.864	.902	.035	5.000	180.34	7.10 18.43 16.79
79.295	17.79	4.00	21.59	.850	21.56	.849	22.85	.899	1.079	.042	5.000	215.90	8.50 19.40 17.65
84.295	17.79	4.00	22.68	.893	22.63	.891	23.93	.942	1.283	.051	5.000	256.54	10.10 20.62 18.77
89.295	17.79	4.00	23.98	.944	23.90	.941	25.21	.992	1.113	.044	5.000	223.52	8.80 22.00 20.02
94.295	17.79	4.00	24.94	.982	25.17	.991	26.33	1.036	1.803	.071	5.000	360.68	14.20 23.89 21.74
99.295	17.79	4.00	26.67	1.050	27.05	1.065	28.13	1.107	2.756	.109	5.000	551.18	21.70 27.41 24.94
104.295	17.79	4.00	29.41	1.158	29.82	1.174	30.89	1.216					

(MOL) SPEC.5KC-1 T1-SAL-2.5SN(EL1) R.T. LAB AIR R=5 F=1 M2 14113 AUG 04, '76

INPUT CONSTANTS

ELASTIC MODULUS(E) = 118.590E+03 MPA(17.200E+06 PSI)					
NUMBER OF CYCLES	CRACK GOUTH COMPLIANCE	ABAR / W	OPTICAL BASE	COMPLIANCE BASE	
N 1000					
X 1000					
9.465	33.7270	.351	.338	.338	
30.445	36.5301	.357	.343	.343	
43.395	36.1301	.367	.354	.354	
51.535	36.9391	.375	.359	.359	
59.295	38.6452	.382	.370	.370	
64.235	40.1512	.390	.379	.379	
69.295	42.5603	.401	.393	.393	
74.295	44.9694	.413	.406	.406	
79.235	48.3845	.431	.427	.427	
84.235	51.3936	.448	.436	.436	
89.295	55.4087	.470	.456	.456	
94.295	61.5329	.495	.481	.481	
99.295	67.4541	.517	.501	.501	
104.295	70.4995	.532	.518	.518	
	103.0902	.606	.594	.594	



(WOL) SPEC.10RC-1 TISSAL-2.5SN(ELI) RT LAB AIR R0.5 F0.1 MZ 14113 AUG 04, 1976

INPUT CONSTANTS:

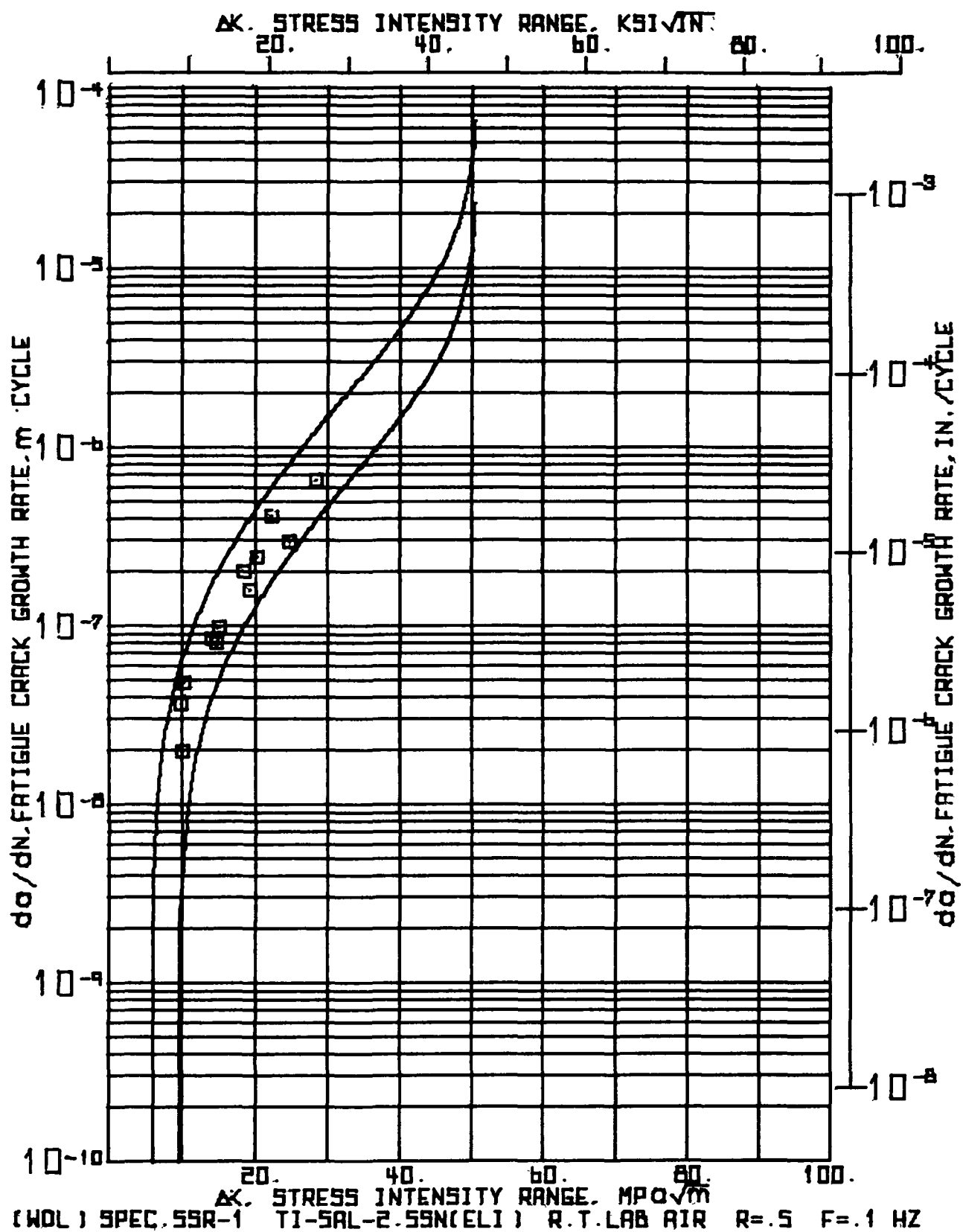
RANGE RATIO(R) 0.50
 TEST FREQUENCY(HZ) 0.1
 SPECIMEN WIDTH(W) 51.054 MM(2.010 IN.)
 SPECIMEN THICKNESS(B) 18.951 MM(.746 IN.)
 CRACK BR. CORRECTION 1.270 MM(.050 IN.)

NUMBER OF CYCLES	MAXIMUM LOAD	SIDE 1		SIDE 2		CORRECTED AVERAGE		CHANGE IN CRACK LENGTH		CHANGE IN CYCLES		CRACK GROWTH RATE		STRESS INTENSITY RANGE	
		MM	INCH	MM	INCH	MM	INCH	MM	INCH	MM	INCH	DA / DN MICR9	IN. / CYCLE	MPA X 10 ⁻⁵	ksi X 10 ⁻⁵
1000	KN	A1		A2		ABAR		DA		DN					
000	12.01 2.70	17.55	.691	16.99	.669	18.54	.730	.432	.017	3.500		123.37	4.86	10.48	9.53
3500	12.01 2.70	18.08	.712	17.32	.682	18.97	.747	.508	.020	7.000		72.57	2.86	10.70	9.74
10500	12.01 2.70	18.34	.722	18.09	.712	19.48	.767								
10500	15.12 3.40	18.34	.722	18.08	.712	19.48	.767	.584	.023	7.500		77.89	3.07	13.81	12.57
18000	15.12 3.40	19.05	.750	18.54	.730	20.07	.790	.737	.029	9.000		81.84	3.22	14.24	12.96
27000	15.12 3.40	19.58	.771	19.48	.767	20.80	.819	.241	.009	3.000		80.43	3.17	14.58	13.27
30000	16.68 3.75	19.81	.780	19.74	.777	21.04	.828								
36000	16.68 3.75	20.70	.815	20.68	.814	21.96	.864	.914	.036	6.000		152.40	6.00	16.53	15.04
39000	16.68 3.75	21.34	.840	21.18	.834	22.53	.887	.572	.023	3.000		190.50	7.50	17.14	15.59
39000	17.79 4.00	21.34	.840	21.18	.834	22.53	.887								
42000	17.79 4.00	21.79	.858	21.69	.854	23.01	.906	.483	.019	3.000		160.87	6.33	18.76	17.08
45000	17.79 4.00	22.56	.888	22.50	.886	23.80	.937	.787	.031	3.000		262.47	10.33	19.37	17.63
46000	17.79 4.00	23.24	.915	23.16	.912	24.47	.963	.673	.027	3.000		224.37	8.83	20.12	18.31
51000	17.79 4.00	24.10	.949	24.03	.946	25.34	.997	.864	.034	3.000		287.87	11.33	20.95	19.06
54000	17.79 4.00	25.04	.986	25.04	.986	26.31	1.036	.978	.039	3.000		325.97	12.83	22.02	20.04
59000	17.79 4.00	26.85	1.057	26.75	1.053	28.07	1.105	1.753	.069	5.000		350.52	13.80	23.77	21.63
61000	17.79 4.00	28.32	1.115	27.74	1.092	29.30	1.153	1.232	.048	2.000		615.95	24.25	25.96	23.62
66450	17.79 4.00	33.17	1.306	32.44	1.277	34.07	1.341	4.775	.188	5.450		876.18	34.50	31.50	28.66

(W9L) SPEC:10RC-1 T1=5AL-2.5SN(EL1) RT LAB AIR R=0.5 F=0.1 MZ 14113 AUG 04, '76

INPUT CONSTANTS

ELASTIC MODULUS(E) = 118.59UE+03 MPA(17.200E+06 PSI)				
NUMBER OF CYCLES	CRACK MOUTH COMPLIANCE	ABAR / W OPTICAL BASE	COMPLIANCE BASE	
N	CEP			
X 1000				
3.000	39.1008	.363	.374	
3.500	40.1029	.372	.379	
10.000	40.9049	.382	.384	
18.000	44.1132	.393	.402	
27.000	47.5214	.407	.418	
30.000	48.1234	.412	.422	
35.000	52.9356	.430	.445	
39.000	53.7379	.441	.449	
42.000	56.1440	.451	.459	
43.000	59.3523	.466	.472	
48.000	62.0603	.479	.484	
51.000	64.1749	.496	.503	
54.000	72.1852	.515	.516	
59.000	45.6202	.550	.554	
61.000	53.5407	.574	.573	
66.500	150.7666	.667	.666	



(W6L) SPEC.5SR-1 T1-5AL-2.55(SNIEL) R.1-LAB AIR R.5 F.1 HZ * * W E D G E * 0 P E N * L 0 A D * P R 0 G R A M * * 10113 AUG 04, 1976

INPUT CONSTANTS:

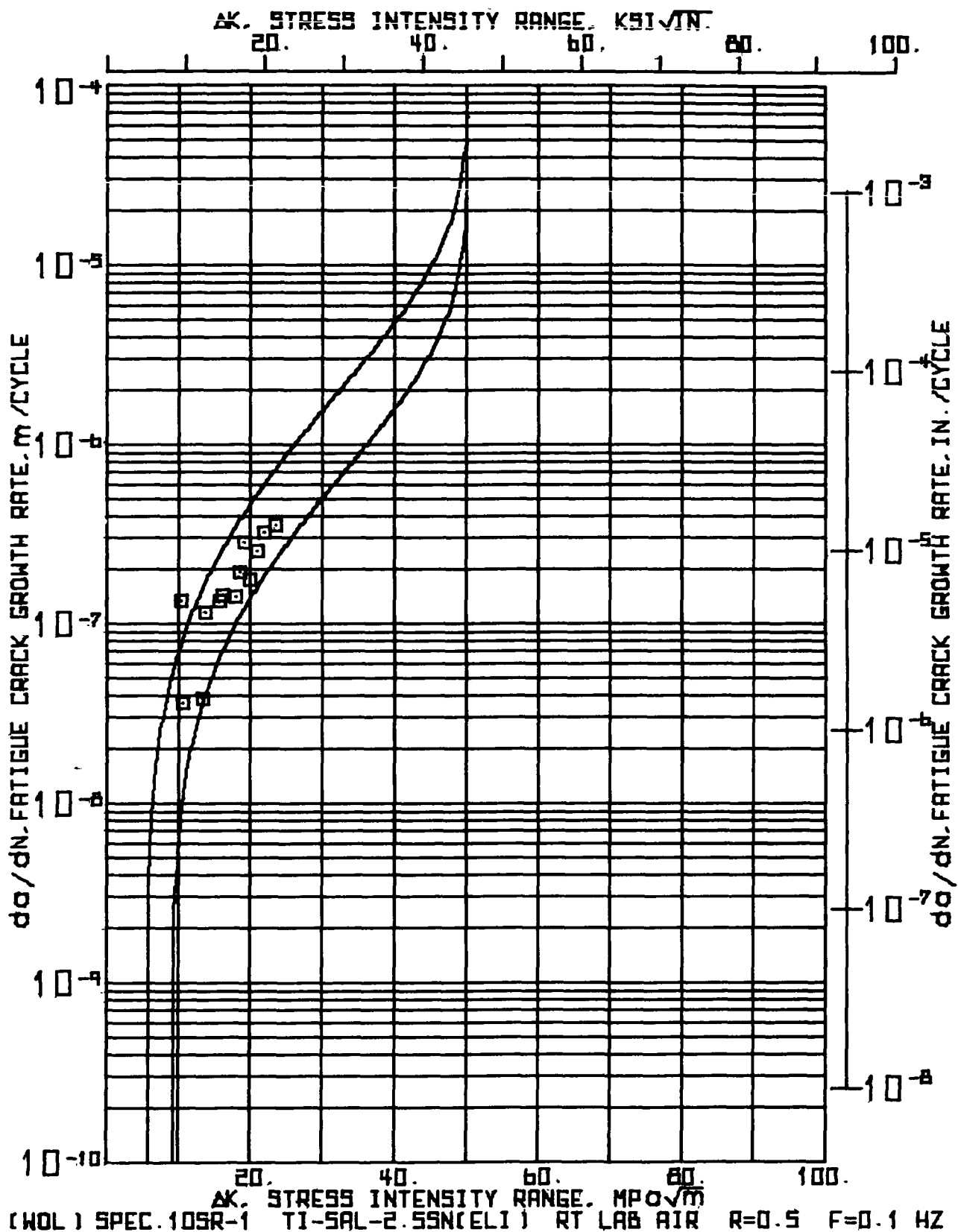
RANGE RATIO(R) * .50
 TEST FREQUENCY(HZ) * .1
 SPECIMEN WIDTH(W) * 50.952 MM(2.006 IN.)
 SPECIMEN THICKNESS(B) * 18.956 MM(.746 IN.)
 CRACK BRW CORRECTION * 1.270 MM(.050 IN.)

NUMBER OF CYCLES	MAXIMUM LOAD	SIDE 1 CRACK LENGTH	SIDE 2 CRACK LENGTH	CORRECTED AVERAGE CRACK LENGTH	CHANGE IN CRACK LENGTH	CHANGE IN DA	CHANGE IN CYCLES	CRACK GROWTH RATE DA / DN	STRESS INTENSITY RANGE
X 1000	KN	MM	MM	MM	MM	MM	DN X 1000	MM PER CYCLE	MPA X 10 ⁻³ IN ^{-3/2}
000	11.34	2.55	17.17	.676	17.09	.673	18.40	.724	
9.465	11.34	2.55	17.48	.688	17.46	.686	18.75	.738	
18.515	11.34	2.55	17.73	.698	17.58	.692	18.92	.745	
35.445	11.34	2.55	18.64	.734	18.29	.720	19.74	.777	
35.445	15.12	3.40	18.64	.734	18.29	.720	19.74	.777	
43.895	15.12	3.40	19.35	.762	19.00	.748	20.45	.805	
51.595	15.12	3.40	20.09	.791	19.51	.768	21.07	.829	
59.295	15.12	3.40	20.75	.817	20.37	.802	21.63	.859	
59.295	17.79	4.00	20.75	.817	20.37	.802	21.83	.859	
64.295	17.79	4.00	21.54	.848	21.59	.850	22.83	.899	
69.295	17.79	4.00	22.53	.887	22.17	.873	23.62	.930	
74.295	17.79	4.00	23.67	.932	23.47	.924	24.84	.978	
79.295	17.79	4.00	25.20	.992	26.09	1.027	26.91	1.059	
84.295	17.79	4.00	27.13	1.068	27.10	1.067	28.38	1.117	
89.295	17.79	4.00	30.40	1.197	30.43	1.196	31.69	1.247	

(HDL) SPEC.5SR.1 Y1.5AL-2.5SNIEL1) R.T.LAB_AIR R.5 F.5 F.5.1 MZ 14113 AUG 04.176

INPUT CONSTANTS

ELASTIC MODULUS(E) = 118.590E+03 MPA(17.200E+06 PSI)					
NUMBER OF CYCLES	CRACK MOUTH COMPLIANCE	ABAR / W	OPTICAL BASE	COMPLIANCE BASE	
N	CE3				
x 1000					
.000	38.5091	.361		.369	
9.465	39.3114	.368		.374	
16.515	40.9159	.371		.384	
35.445	42.5204	.387		.393	
43.595	44.1250	.401		.402	
51.595	47.3341	.414		.419	
59.295	48.3366	.428		.426	
65.295	53.7523	.448		.449	
65.295	56.9613	.464		.462	
74.295	63.3795	.468		.487	
79.295	71.4023	.528		.514	
84.295	81.5318	.557		.544	
89.295	112.3161	.622		.610	



(K0L) SPEC10SR-1 TT-5AL-2.55N(TL1) RT LAB AIR R0.05 F0.01 HZ * * * * * W E D G E * 0 P E N * L 0 A D * P R 0 G R A M * * * 14113 AUG 04, 1976

INPUT CONSTANTS:

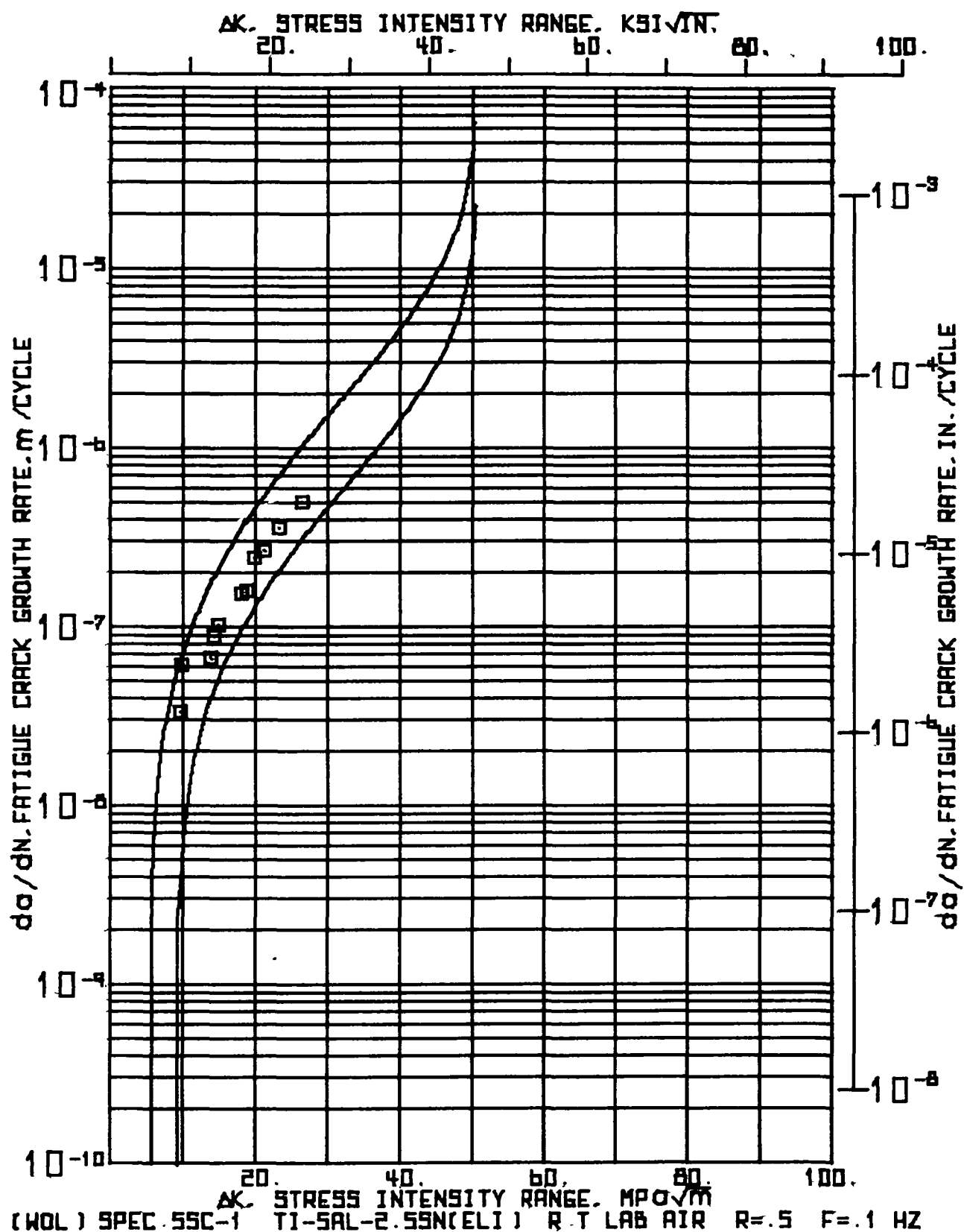
RANGE RATIO(R) * .50
 TEST FREQUENCY(HZ) * .1
 SPECIMEN LENGTH(IN) * 50.952 MM(2.006 IN.)
 SPECIMEN THICKNESS(B) * 18.943 MM(.746 IN.)
 CRACK BGA CORRECTION * 1.270 MM(.050 IN.)

NUMBER OF CYCLES	MAXIMUM LOAD KIPS	SIDE 1 CRACK LENGTH		SIDE 2 CRACK LENGTH		CORRECTED AVERAGE CRACK LENGTH		CHANGE IN CRACK LENGTH		CHANGE IN CYCLES		CRACK GROWTH RATE DA / DN MICRO INCH PER CYCLE		STRESS INTENSITY RANGE DELTA K	
		A1 MM	INCH	A2 MM	INCH	MM	INCH	MM	INCH	DN X 1000	DA X 1000	METER PER CYCLE	INCH PER CYCLE	MPA X M0.05	KSI X IN0.05
000	12.01	2.70	16.81	.662	16.94	.667	18.15	.714	.470	.018	3.500	134.26	5.29	10.33	9.40
3500	12.01	2.70	17.48	.688	17.22	.678	18.62	.733	.254	.010	7.000	36.29	1.43	10.50	9.56
10500	12.01	2.70	17.48	.688	17.73	.696	18.87	.743							
10500	15.12	3.40	17.48	.688	17.73	.694	18.87	.743	.521	.021	13.500	38.57	1.52	13.46	12.25
24000	15.12	3.40	17.93	.706	18.31	.721	19.39	.763	.699	.028	6.000	116.42	4.58	13.84	12.59
30000	15.12	3.40	18.75	.738	18.90	.744	20.09	.791							
30000	16.68	3.75	18.75	.748	18.90	.744	20.09	.791	.800	.031	6.000	133.35	5.25	15.81	14.38
36000	16.68	3.75	19.68	.775	19.56	.770	20.89	.822	.432	.017	3.000	143.93	5.67	16.27	14.81
39000	16.68	3.75	20.04	.789	20.07	.790	21.32	.839							
39000	17.79	4.00	20.04	.789	20.07	.790	21.32	.839	.851	.033	6.000	141.82	5.58	17.90	16.29
45000	17.79	4.00	20.83	.820	20.98	.826	22.17	.873	.584	.023	3.000	194.73	7.67	18.55	16.88
48000	17.79	4.00	21.46	.845	21.51	.847	22.76	.896	.864	.034	3.000	267.87	11.33	19.23	17.50
51000	17.79	4.00	22.28	.877	22.43	.883	23.62	.930	.533	.021	3.000	177.80	7.00	19.94	18.14
54000	17.79	4.00	22.61	.898	22.96	.904	24.16	.951	1.283	.051	5.000	256.54	10.10	20.91	19.03
59000	17.79	4.00	24.00	.945	24.33	.958	25.44	1.001	.648	.026	2.000	323.85	12.75	22.03	20.05
61000	17.79	4.00	24.69	.972	24.94	.982	26.09	1.027	1.943	.076	5.453	356.34	14.03	23.69	21.56
66453	17.79	4.00	26.62	1.048	26.90	1.059	28.03	1.103							

(A9L) SPEC:1USR-1 T1-5AL-2-55N(EL) RT LAB AIR R=0.5 F=0.1 MZ 14113 AUG 04, 1976

INPUT CONSTANTS

ELASTIC MODULUS(E) = 118.590E+03 MPA(17.200E+06 PSI)				
NUMBER OF CYCLES N	CRACK ROUTE COMPLIANCE CE ₃	ABAR / W OPTICAL COMPLIANCE BASE	BASE	
x 1000				
37.000	37.0815	.356	.364	
37.500	37.4833	.365	.369	
38.000	37.8850	.370	.374	
38.500	38.2868	.375	.378	
39.000	38.6885	.380	.382	
39.500	39.0902	.385	.387	
40.000	39.4919	.390	.392	
40.500	39.8936	.395	.397	
41.000	40.2953	.400	.402	
41.500	40.6970	.405	.407	
42.000	41.0987	.410	.412	
42.500	41.5004	.415	.417	
43.000	41.9021	.420	.422	
43.500	42.3038	.425	.427	
44.000	42.7055	.430	.432	
44.500	43.1072	.435	.437	
45.000	43.5089	.440	.442	
45.500	43.9106	.445	.447	
46.000	44.3123	.450	.452	
46.500	44.7140	.455	.457	
47.000	45.1157	.460	.462	
47.500	45.5174	.465	.467	
48.000	45.9191	.470	.472	
48.500	46.3208	.475	.477	
49.000	46.7225	.480	.482	
49.500	47.1242	.485	.487	
50.000	47.5259	.490	.492	
50.500	47.9276	.495	.497	
51.000	48.3293	.500	.502	
51.500	48.7310	.505	.507	
52.000	49.1327	.510	.512	
52.500	49.5344	.515	.517	
53.000	49.9361	.520	.522	
53.500	50.3378	.525	.527	
54.000	50.7395	.530	.532	
54.500	51.1412	.535	.537	
55.000	51.5429	.540	.542	
55.500	51.9446	.545	.547	
56.000	52.3463	.550	.552	
56.500	52.7480	.555	.557	
57.000	53.1497	.560	.562	
57.500	53.5514	.565	.567	
58.000	53.9531	.570	.572	
58.500	54.3548	.575	.577	
59.000	54.7565	.580	.582	
59.500	55.1582	.585	.587	
60.000	55.5599	.590	.592	
60.500	55.9616	.595	.597	
61.000	56.3633	.600	.602	
61.500	56.7650	.605	.607	
62.000	57.1667	.610	.612	
62.500	57.5684	.615	.617	
63.000	57.9701	.620	.622	
63.500	58.3718	.625	.627	
64.000	58.7735	.630	.632	
64.500	59.1752	.635	.637	
65.000	59.5769	.640	.642	
65.500	59.9786	.645	.647	
66.000	60.3803	.650	.652	
66.500	60.7820	.655	.657	
67.000	61.1837	.660	.662	
67.500	61.5854	.665	.667	
68.000	61.9871	.670	.672	
68.500	62.3888	.675	.677	
69.000	62.7905	.680	.682	
69.500	63.1922	.685	.687	
70.000	63.5939	.690	.692	
70.500	63.9956	.695	.697	
71.000	64.3973	.700	.702	
71.500	64.7990	.705	.707	
72.000	65.2007	.710	.712	
72.500	65.6024	.715	.717	
73.000	66.0041	.720	.722	
73.500	66.4058	.725	.727	
74.000	66.8075	.730	.732	
74.500	67.2092	.735	.737	
75.000	67.6109	.740	.742	
75.500	68.0126	.745	.747	
76.000	68.4143	.750	.752	
76.500	68.8160	.755	.757	
77.000	69.2177	.760	.762	
77.500	69.6194	.765	.767	
78.000	70.0211	.770	.772	
78.500	70.4228	.775	.777	
79.000	70.8245	.780	.782	
79.500	71.2262	.785	.787	
80.000	71.6279	.790	.792	
80.500	72.0296	.795	.797	
81.000	72.4313	.800	.802	
81.500	72.8330	.805	.807	
82.000	73.2347	.810	.812	
82.500	73.6364	.815	.817	
83.000	74.0381	.820	.822	
83.500	74.4398	.825	.827	
84.000	74.8415	.830	.832	
84.500	75.2432	.835	.837	
85.000	75.6449	.840	.842	
85.500	76.0466	.845	.847	
86.000	76.4483	.850	.852	
86.500	76.8500	.855	.857	
87.000	77.2517	.860	.862	
87.500	77.6534	.865	.867	
88.000	78.0551	.870	.872	
88.500	78.4568	.875	.877	
89.000	78.8585	.880	.882	
89.500	79.2602	.885	.887	
90.000	79.6619	.890	.892	
90.500	80.0636	.895	.897	
91.000	80.4653	.900	.902	
91.500	80.8670	.905	.907	
92.000	81.2687	.910	.912	
92.500	81.6704	.915	.917	
93.000	82.0721	.920	.922	
93.500	82.4738	.925	.927	
94.000	82.8755	.930	.932	
94.500	83.2772	.935	.937	
95.000	83.6789	.940	.942	
95.500	84.0806	.945	.947	
96.000	84.4823	.950	.952	
96.500	84.8840	.955	.957	
97.000	85.2857	.960	.962	
97.500	85.6874	.965	.967	
98.000	86.0891	.970	.972	
98.500	86.4908	.975	.977	
99.000	86.8925	.980	.982	
99.500	87.2942	.985	.987	
100.000	87.6959	.990	.992	



INPUT CONSTANTS:

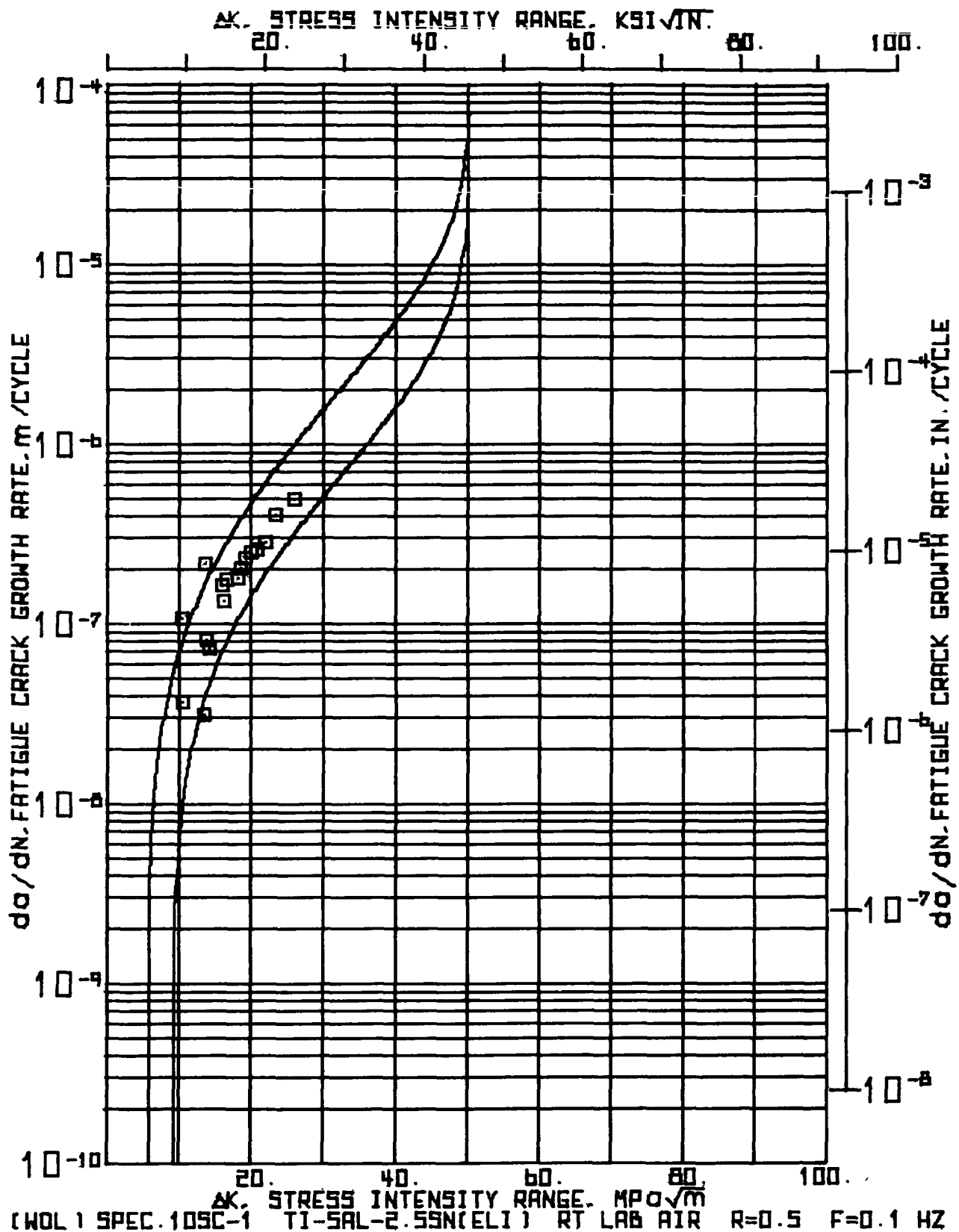
RANGE RATIO(R) * .50
 TEST FREQUENCY(HZ) * .1
 SPECIMEN WIDTH(W) * 51.054 MM(2.010 IN.)
 SPECIMEN THICKNESS(B) * 18.981 MM(.747 IN.)
 CRACK Bg. CORRECTION * 1.270 MM(.050 IN.)

NUMBER OF CYCLES	MAXIMUM LOAD	SIDE 1 CRACK LENGTH	SIDE 2 CRACK LENGTH	CORRECTED AVERAGE CRACK LENGTH	CHANGE IN CRACK LENGTH	CHANGE IN CYCLES	CRACK GROWTH RATE DA / DN	STRESS INTENSITY RANGE
N X 1000	P KN	A1 MM	A2 MM	MM	MM	DN X 1000	MM PER CYCLE	MPA X 10 ^{-0.5}
000	11.34 2.55	17.17 .676	17.09 .673	18.40 .724				
9.250	11.34 2.55	17.75 .699	17.12 .674	18.71 .736	.305 .012	9.050	33.68 1.33	9.79 8.91
25.980	11.34 2.55	18.72 .737	18.26 .719	19.76 .778	1.054 .042	16.930	62.26 2.45	10.09 9.18
25.940	15.12 3.40	18.72 .737	18.26 .719	19.76 .778	.571 .022	8.450	67.63 2.66	13.97 12.71
34.430	15.12 3.40	19.41 .764	18.72 .737	20.33 .800	.686 .027	7.700	89.06 3.51	14.38 13.09
42.130	15.12 3.40	20.22 .796	19.23 .759	21.02 .827	.800 .032	7.700	103.91 4.09	14.90 13.56
49.830	15.12 3.40	21.01 .827	20.09 .791	21.82 .859				
49.830	17.79 4.00	21.01 .827	20.09 .791	21.82 .859	.775 .031	5.000	154.94 6.10	18.22 16.58
54.530	17.79 4.00	21.92 .863	20.73 .816	22.59 .839	.800 .032	5.000	160.02 6.30	18.94 17.24
59.830	17.79 4.00	22.66 .892	21.53 .850	23.39 .921	1.232 .049	5.000	246.38 9.70	19.95 18.16
64.830	17.79 4.00	23.70 .933	23.01 .906	24.63 .969	1.359 .054	5.000	271.78 10.70	21.37 19.44
69.830	17.79 4.00	24.99 .984	24.43 .962	25.98 1.023				
74.830	17.79 4.00	26.72 1.052	26.31 1.036	27.79 1.094	1.803 .071	5.000	360.68 14.20	23.32 21.22
79.830	17.79 4.00	29.16 1.148	28.93 1.139	30.31 1.133	2.527 .100	5.000	505.46 19.90	26.51 24.12

... (WBL) SPEC:SSC=1 _T1=5AL=2.5SN(E) _R=T, LAB_AIR _R=5 _F=1 _HZ _ _ _ _ _ 10:13 AUG 04, '76

INPUT CONSTANTS

ELASTIC MODULUS(E) = 118.590E+03 MPa(17.200E+06 PSI)					
NUMBER OF CYCLES	CRACK GOUTH COMPLIANCE	ABAR / " OPTICAL BASE	COMPLIANCE BASE		
N	CE3				
X 1000					
9.000	39.3640	.360	.375		
9.050	40.1674	.366	.379		
25.980	42.5774	.387	.393		
34.430	44.1841	.398	.402		
42.130	46.3942	.412	.415		
49.530	49.6075	.427	.431		
54.830	53.0243	.443	.449		
59.530	57.5410	.458	.466		
64.630	62.6611	.482	.484		
69.630	69.0879	.509	.506		
74.630	80.3347	.544	.540		
79.630	104.4352	.594	.595		



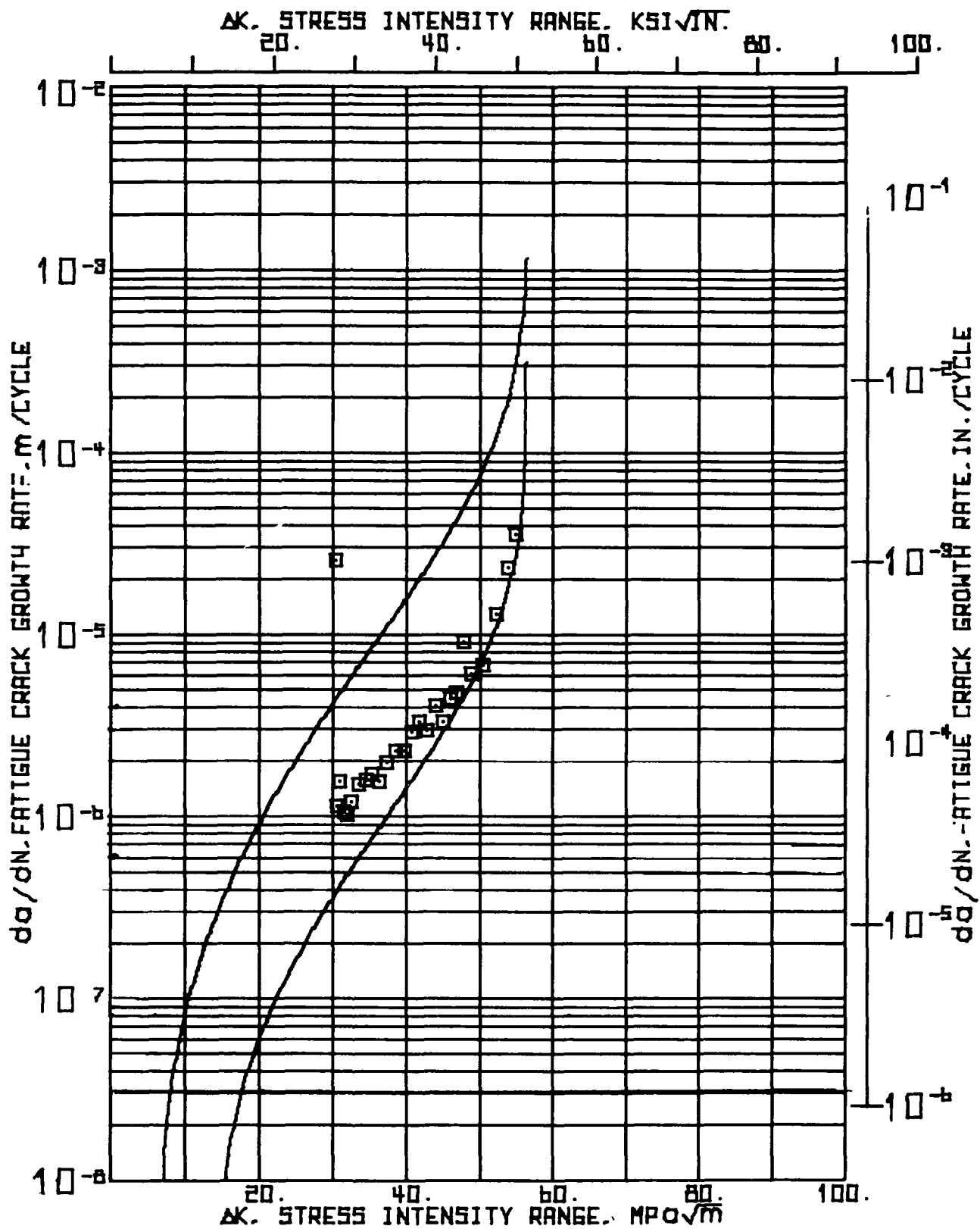
(.9L) SPEC:10SC=1 T1=5AL+2.55N(ELI) RT LAB AIR R=0.5 F=0.1 MZ 10114 AUG 04, '76

INPUT CONSTANTS

ELASTIC MODULUS(E) = 118.590E+03 MPA(17.200E+06 PSI)				
NUMBER OF CYCLES	CRACK MOUTH COMPLIANCE	ABAR / W OPTICAL COMPLIANCE BASE		
N	CES			
X 1000				
1000	35.3440	.356	.368	
1500	33.1428	.364	.373	
10500	40.7405	.369	.383	
16000	41.5393	.373	.387	
21000	43.1370	.385	.396	
24000	43.9358	.390	.401	
30000	45.5323	.399	.413	
35000	47.1311	.408	.418	
36000	47.7299	.416	.422	
37000	50.5264	.426	.433	
42000	53.5218	.437	.448	
45000	55.1194	.448	.454	
46000	57.5159	.462	.464	
51000	61.5101	.476	.480	
54000	65.5031	.491	.497	
59000	73.4926	.519	.520	
61000	75.2856	.534	.534	
66433	91.2564	.566	.563	

SECTION A5

This section of the Appendix includes all fatigue crack growth data obtained from WOL coupons tested at room temperature, at a range ratio of 0.5, and at a frequency of 1 Hz and 0.0167.



(WOL) SPEC 5CR-2 TI-5AL-2SN(ELI) RT LAB AIR R = 0.5 F = 1 HZ

(WEL) SPEC.5CR-2 T1-5AL-2.5SN(EL) ROOM TEMP LAB AIR R=5 F=1 HZ

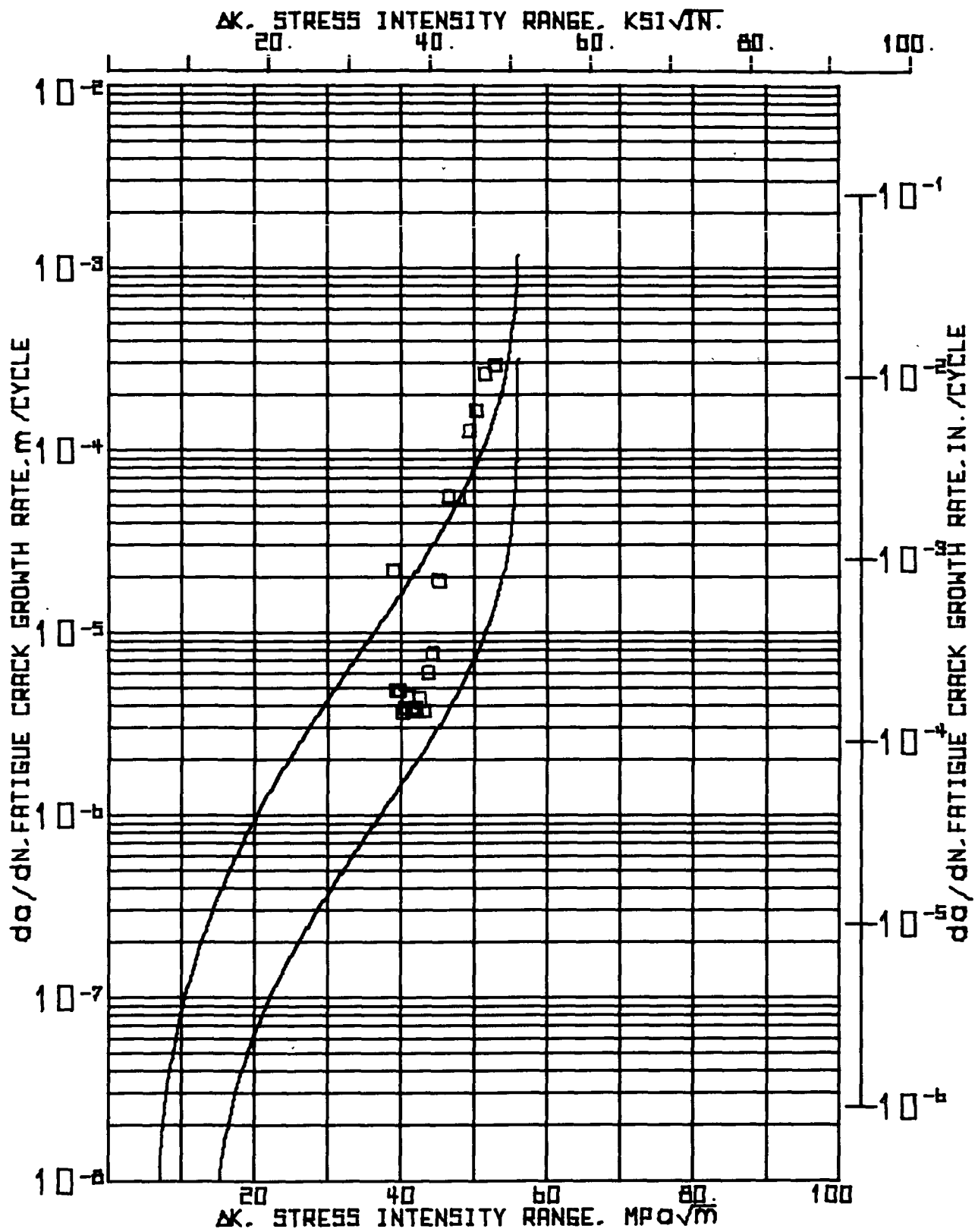
15:47 SEP 28, 1976

INPUT CONSTANTS:

RANGE RATIO(R) .50
 TEST FREQUENCY(HZ) 1.0
 SPECIMEN WIDTH(W) 50.952 MM(2.006 IN.)
 SPECIMEN THICKNESS(B) 19.025 MM(.749 IN.)
 CRACK RA. CORRECTION 1.270 MM(.050 IN.)

NUMBER OF CYCLES	N	X 1000	P	MAXIMUM LOAD KIPS	SIDE 1		SIDE 2		CORRECTED AVERAGE LENGTH		CHANGE IN CRACK LENGTH		CHANGE IN CYCLES		CRACK GROWTH RATE DA / DN MICRØ IN. METER		STRESS INTENSITY RANGE DELTA K	
					MM	INCH	MM	INCH	MM	INCH	MM	INCH	DN	X 1000	INCH	X 1000	MPA X 10 ^{3.5}	KSI X 10 ^{3.5}
		.000	35.59	8.00	16.37	.668	16.74	.659	18.12	.713	.254	.010	.010	.010	25400.00	1000.00	30.31	27.58
		.010	35.59	8.00	17.09	.673	17.12	.674	18.38	.723	.114	.004	.100	.100	1143.00	45.00	30.56	27.81
		.110	35.59	8.00	17.27	.680	17.17	.676	18.49	.728	.470	.018	.300	.300	1566.33	61.67	30.96	28.17
		.410	35.59	8.00	17.75	.699	17.63	.694	18.96	.746	.318	.013	.300	.300	1058.33	41.67	31.51	28.63
		.710	35.59	8.00	18.08	.712	17.93	.706	19.28	.759	.406	.016	.400	.400	1016.00	40.00	32.04	29.16
		1.110	35.59	8.00	18.52	.729	18.31	.721	19.68	.775	.483	.019	.400	.400	1206.50	47.50	32.70	29.75
		1.510	35.59	8.00	19.00	.748	18.80	.740	20.17	.794	.597	.023	.400	.400	1492.25	58.75	33.53	30.52
		1.910	35.59	8.00	19.63	.773	19.35	.762	20.76	.817	.635	.025	.400	.400	1567.50	62.50	34.53	31.42
		2.310	35.59	8.00	20.40	.803	19.86	.782	21.40	.842	.508	.020	.300	.300	1693.33	66.67	35.49	32.30
		2.610	35.59	8.00	20.80	.819	20.47	.806	21.91	.862	.470	.019	.300	.300	1566.33	61.67	36.35	33.08
		2.910	35.59	8.00	21.34	.840	20.83	.822	22.38	.831	.597	.023	.300	.300	1989.67	78.33	37.32	33.97
		3.210	35.59	8.00	21.95	.864	21.46	.845	22.97	.904	.686	.027	.300	.300	2286.00	90.00	38.55	35.08
		3.510	35.59	8.00	22.71	.894	22.07	.869	23.66	.931	.457	.018	.200	.200	2286.00	90.00	39.70	36.13
		3.710	35.59	8.00	23.19	.913	22.50	.886	24.12	.949	.584	.023	.200	.200	2921.00	115.00	40.80	37.13
		3.910	35.59	8.00	23.60	.937	23.06	.908	24.70	.972	.330	.013	.100	.100	3302.00	130.00	41.80	38.04
		4.010	35.59	8.00	24.10	.949	23.42	.922	25.03	.985	.597	.023	.200	.200	2984.50	117.50	42.85	39.00
		4.210	35.59	8.00	24.71	.973	24.00	.945	25.63	1.009	.406	.016	.100	.100	4064.00	160.00	44.04	40.08
		4.310	35.59	8.00	25.10	.988	24.43	.962	26.03	1.025	.330	.013	.100	.100	3302.00	130.00	44.95	40.91
		4.410	35.59	8.00	25.50	1.004	24.69	.972	26.37	1.038	.445	.018	.100	.100	4445.00	175.00	45.94	41.81
		4.510	35.59	8.00	25.93	1.021	25.15	.990	26.81	1.055								

(M8L) SPEC:5CR-2										T1-5AL-2.5SN(EL1)										R80M TEMP LAB. AIR R-0.5 F-1 HZ										15:47 SEP 28, 1976										PAGE 2									
NUMBER OF CYCLES		MAXIMUM LOAD		SIDE 1 CRACK LENGTH		SIDE 2 CRACK LENGTH		CORRECTED AVERAGE CRACK LENGTH		CHANGE IN CRACK LENGTH		CHANGE IN CYCLES		CRACK GROWTH RATE		STRESS INTENSITY RANGE																																	
N	X 1000	P	KN	KIPS	MM	INCH	MM	INCH	MM	INCH	MM	INCH	MM	INCH	DA	DN	NANB- METER	MICR8 IN.	MPA X 1000	KSI X 1000																													
4.510	35.59	8.00	25.93	1.021	25.15	.990	26.81	1.055	.241	.009	.050	4.826.00	190.00	46.84	42.63																																		
4.560	35.59	8.00	26.26	1.034	25.30	.996	27.05	1.065	.457	.018	.050	9144.00	360.00	47.80	43.50																																		
4.610	35.59	8.00	26.52	1.044	25.96	1.022	27.51	1.083	.305	.012	.050	6096.00	240.00	48.87	44.47																																		
4.660	35.59	8.00	26.87	1.058	26.21	1.032	27.81	1.095	.673	.027	.100	6731.00	265.00	50.30	45.75																																		
4.760	35.59	8.00	27.66	1.089	26.77	1.054	28.49	1.121	.521	.020	.040	13017.50	512.50	52.15	47.46																																		
4.800	35.59	8.00	28.24	1.112	27.23	1.072	29.01	1.142	.470	.019	.020	23495.00	925.00	53.77	48.93																																		
4.820	35.59	8.00	28.80	1.134	27.61	1.087	29.48	1.160	.178	.007	.005	35560.00	1400.00	54.87	49.93																																		
4.825	35.59	8.00	28.98	1.141	27.79	1.094	29.65	1.167																																									



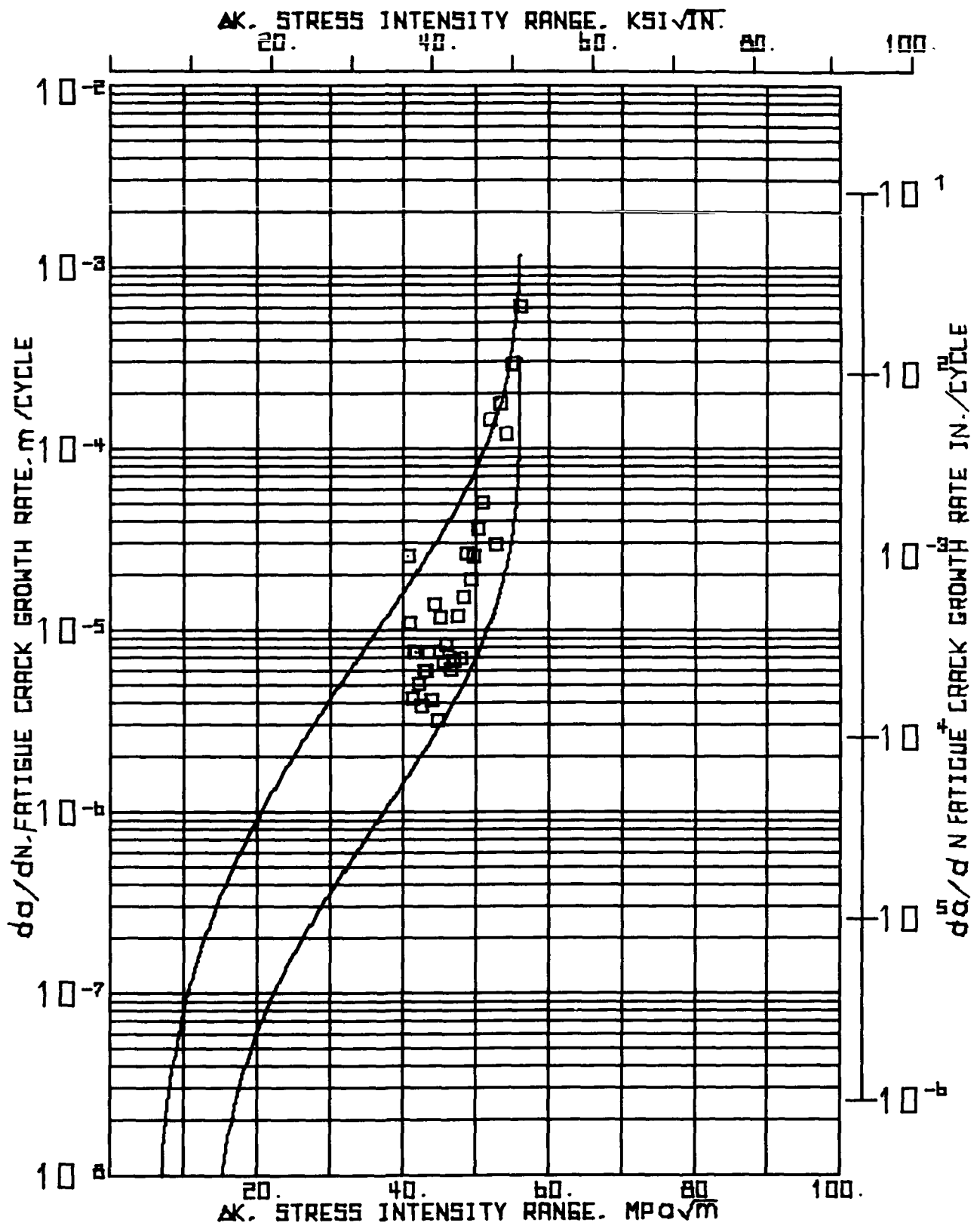
(WOL) SPEC 8CR-2 TI-5AL-2.5SN(ELI) RT LAB AIR R = 0.5 F = 0.0167 HZ

15:48 SEP 28 '76

INPUT CONSTANTS:

RANGE RATIO(R)	• .50
TEST FREQUENCY(HZ)	• .0167
SPECIMEN WIDTH(W)	• 51.105 MM(2.012 IN.)
SPECIMEN THICKNESS(B)	• 19.101 MM(.752 IN.)
CRACK 99A CONNECTION	• 1.270 MM(.050 IN.)

NUMBER OF CYCLES	N	X 1000	MAXIMUM LOAD	P KN	KIPS	SIDE 1 CRACK LENGTH		SIDE 2 CRACK LENGTH		CORRECTED AVERAGE CRACK LENGTH		CHANGE IN CRACK LENGTH		CHANGE IN CYCLES		CRACK GROWTH RATE		STRESS INTENSITY RANGE				
						A1	MM	INCH	A2	MM	INCH	ADAR	MM	INCH	MM	INCH	DN	X 1000	NANO- METER	MICRONS IN.	MPA X 1000.5	KSI X 1000.5
						MM	INCH	MM	INCH	MM	INCH	MM	INCH	MM	INCH	MM	INCH	MM	INCH	MM	INCH	MM
						16.81	.662	16.92	.666	18.14	.714	.216	.009	.010	21590.00	850.00	39.06	35.56				
						17.07	.672	17.09	.673	18.35	.722	.190	.007	.040	4762.50	187.50	39.43	35.89				
						17.30	.681	17.25	.679	18.54	.730	.190	.007	.040	4762.50	187.50	39.77	36.19				
						17.45	.687	17.48	.688	18.73	.737	.216	.009	.060	3598.33	141.67	40.13	36.52				
						17.68	.696	17.68	.696	18.95	.746	.229	.009	.060	3810.00	150.00	40.53	36.89				
						18.16	.715	18.19	.716	19.44	.765	.267	.010	.060	4445.00	175.00	40.99	37.30				
						18.54	.730	18.47	.727	19.77	.778	.330	.013	.090	3668.89	144.44	41.55	37.81				
						18.77	.739	18.69	.736	20.00	.787	.229	.009	.060	3810.00	150.00	42.09	38.30				
						19.08	.751	18.90	.744	20.26	.797	.254	.010	.060	4233.33	166.67	42.56	38.73				
						19.38	.763	19.25	.758	20.59	.810	.330	.013	.090	3668.89	144.44	43.14	39.26				
						19.76	.778	19.53	.771	20.94	.824	.356	.014	.060	5926.67	233.33	43.84	39.90				
						19.96	.786	19.84	.781	21.17	.833	.229	.009	.030	7620.00	300.00	44.45	40.45				
						20.75	.817	20.19	.795	21.74	.856	.571	.022	.030	19050.00	750.00	45.31	41.23				
						21.36	.841	20.90	.823	22.40	.882	.660	.026	.012	55033.33	2166.67	46.68	42.48				
						22.10	.870	21.26	.837	22.95	.903	.546	.021	.010	54610.00	2150.00	48.09	43.77				
						22.68	.893	21.69	.854	23.46	.923	.508	.020	.004	127000.00	5000.00	49.38	44.94				
						23.01	.906	22.02	.867	23.79	.936	.330	.013	.002	165100.00	6500.00	50.44	45.91				
						23.37	.920	22.71	.894	24.31	.957	.521	.021	.002	260350.00	10250.00	51.56	46.92				
						24.21	.953	23.04	.907	24.69	.980	.584	.023	.002	292100.00	11500.00	53.07	48.30				

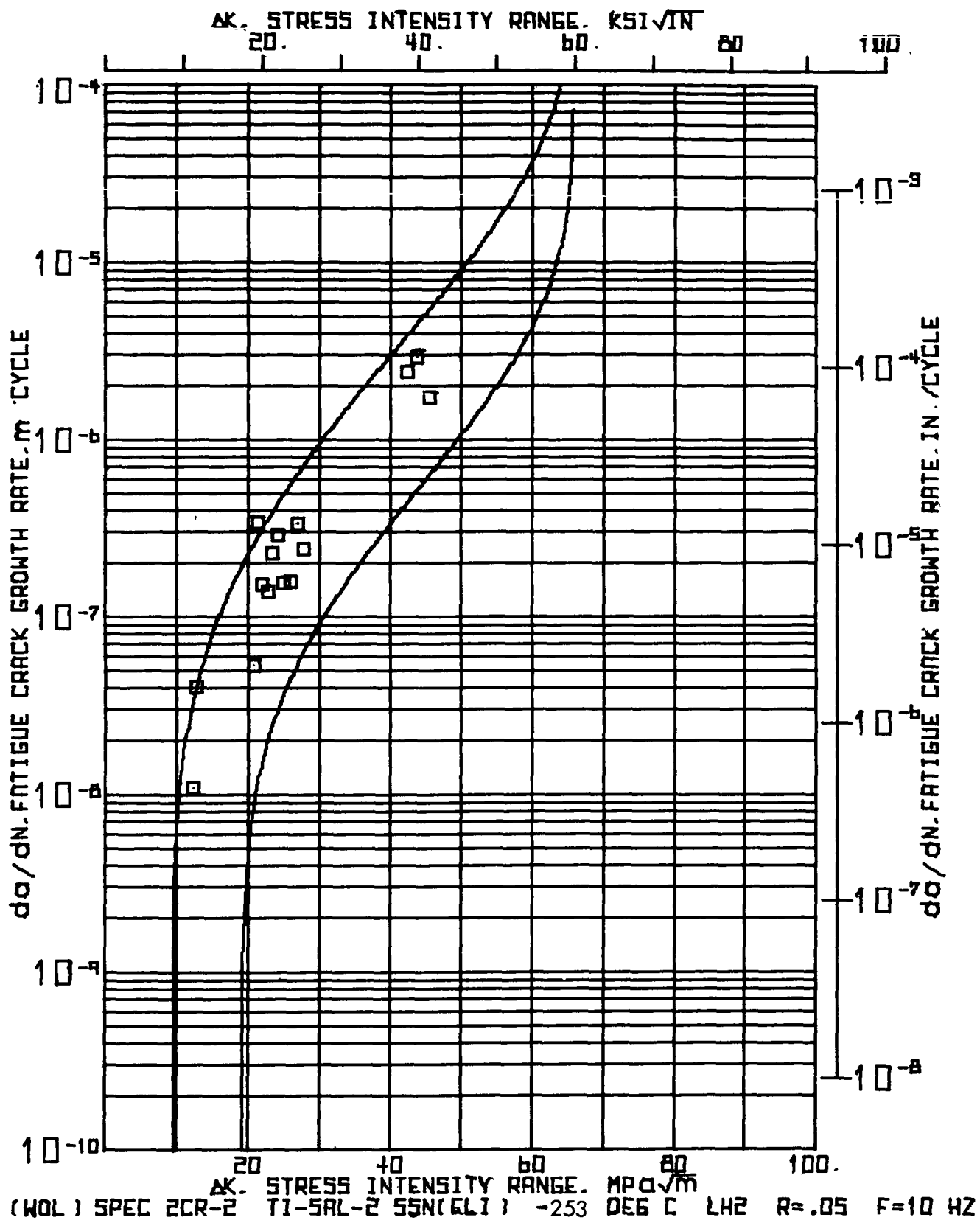


(WOL) 10CR-2 TI-5AL-2.5SN(ELI) RT LAB AIR R = 0.5 F = 0.0167 HZ

NUMBER OF CYCLES	MAXIMUM LOAD	SIDE 1 CRACK LENGTH			SIDE 2 CRACK LENGTH			CORRECTED AVERAGE CRACK LENGTH			CHANGE IN CRACK LENGTH DA			CHANGE IN CYCLES			CRACK GRWT RATE			STRESS INTENSITY RANGE		
		MM	INCH	A1	MM	INCH	A2	MM	INCH	MM	INCH	MM	INCH	DN	X 1000	NANO- METER PER CYCLE	DA / DN	MICR- IN.	MPA X 1000	DELTA K KSI X 1000		
N X 1000	P	KN	KIPS																			
	.517	46.2610.40	20.50	.807	21.69	.854	22.36	.880	.140	.006	.020	6985.00	275.00						46.02	43.73		
	.537	46.2610.40	20.68	.814	21.79	.858	22.50	.866	.152	.006	.010	15240.00	600.00					49.37	44.02			
	.547	46.2610.40	20.83	.820	21.95	.864	22.66	.892	.267	.011	.010	26670.00	1050.00					48.88	44.43			
	.557	46.2610.40	21.06	.829	22.25	.876	22.92	.902	.191	.008	.010	19050.00	750.00					49.44	44.99			
	.567	46.2610.40	21.31	.839	22.38	.881	23.11	.910	.152	.006	.006	25400.00	1000.00					49.87	45.38			
	.573	46.2610.40	21.44	.844	22.56	.888	23.27	.916	.216	.008	.006	35933.33	1416.67					50.34	45.81			
	.579	46.2610.40	21.64	.852	22.78	.897	23.48	.924	.305	.012	.006	50800.00	2000.00					51.01	46.42			
	.585	46.2610.40	21.79	.858	23.24	.915	23.79	.936	.432	.017	.003	143933.33	5666.67					51.99	47.31			
	.588	46.2610.40	22.33	.879	23.57	.924	24.22	.953	.089	.003	.003	29633.33	1166.67					52.70	47.96			
	.591	46.2610.40	22.38	.881	23.70	.933	24.31	.957	.356	.014	.002	177800.00	7000.00					53.32	48.52			
	.593	46.2610.40	22.81	.898	23.98	.944	24.66	.971	.241	.010	.002	120650.00	4750.00					54.17	49.29			
	.595	46.2610.40	22.96	.904	24.31	.957	24.90	.980	.292	.011	.001	292100.00	11500.00					54.94	50.00			
	.596	46.2610.40	23.16	.912	24.69	.972	25.20	.992	.610	.024	.001	609600.00	24000.00					56.30	51.23			
.597	46.2610.40	23.75	.935	25.32	.997	25.81	1.016															

SECTION A6

This section of the Appendix includes all fatigue crack growth data obtained from WOL coupons tested at -253°C , at a range ratio of 0.05, and at a frequency of 10 Hz.



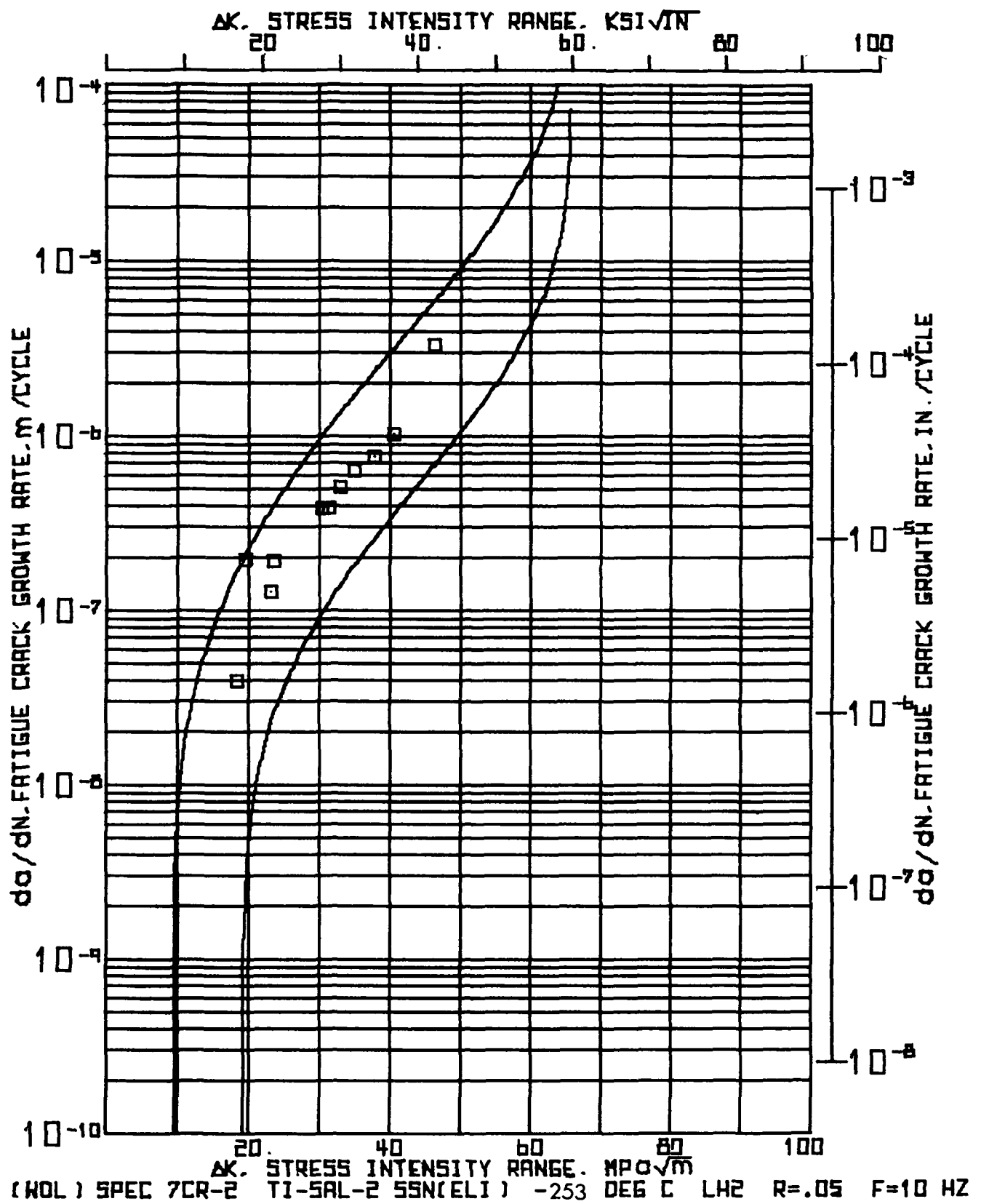
INPUT CONSTANTS:

RANGE RATIO(R)															.05														
TEST FREQUENCY(HZ)															10.0														
SPECIMEN WIDTH(W)															50.927 MM(2.005 IN.)														
SPECIMEN THICKNESS(B)															18.976 MM(.747 IN.)														
CRACK & CORRECTION															1.27C MM(.050 IN.)														
NUMBER OF CYCLES	MAXIMUM LOAD	SIDE 1			SIDE 2			CORRECTED AVERAGE CRACK LENGTH			CHANGE IN CRACK LENGTH			CHANGE IN CYCLES			CRACK GROWTH RATE			STRESS INTENSITY RANGE									
		P	KN	MM	A1	INCH	MM	A2	INCH	MM	INCH	MM	DA	INCH	MM	DN	INCH	MM	NANO-METER	DA / DN	IN. PER CYCLE	MPA X 10 ⁻⁵	DELTA K	IN. X 10 ⁻⁵					
600	7.56	1.70	16.79	.661	17.17	.676	18.25	.718	.508	.020	46.600	10.90	.43	12.42	11.30														
600	7.56	1.70	17.30	.681	17.63	.696	18.76	.738	.622	.025	15.400	40.41	1.59	12.74	11.59														
600	7.56	1.70	17.98	.708	18.24	.718	19.38	.763																					
600	12.01	2.70	17.98	.708	18.24	.718	19.38	.763	.508	.020	9.500	53.47	2.11	20.76	18.89														
700	12.01	2.70	19.25	.758	19.51	.768	20.65	.813	.762	.030	2.200	346.36	13.64	21.38	19.45														
700	12.01	2.70	19.76	.778	20.02	.788	21.16	.833	.508	.020	3.300	153.94	6.06	22.03	20.04														
800	12.01	2.70	20.52	.808	20.78	.818	21.92	.863	.762	.030	5.500	138.55	5.45	22.71	20.67														
800	12.01	2.70	21.03	.828	21.29	.838	22.43	.883	.508	.020	2.200	230.91	9.09	23.42	21.32														
800	12.01	2.70	21.79	.858	22.05	.868	23.19	.913	.762	.030	2.600	293.08	11.54	24.18	22.00														
900	12.01	2.70	22.30	.878	22.56	.888	23.70	.933	.508	.020	3.250	156.31	6.15	24.97	22.72														
900	12.01	2.70	23.32	.918	23.57	.928	24.71	.973	1.016	.040	6.400	158.75	6.25	25.97	23.64														
900	12.01	2.70	24.03	.938	24.08	.948	25.22	.993	.508	.020	1.500	338.67	13.33	27.04	24.61														
1000	12.01	2.70	24.33	.958	24.59	.968	25.73	1.013	.508	.020	2.100	241.90	9.52	27.79	25.29														
1000	17.79	4.00	24.33	.958	24.59	.968	25.73	1.013	.508	.020	.210	2419.05	95.24	42.34	38.53														
1000	17.79	4.00	24.84	.978	25.10	.988	26.24	1.033	.762	.030	.260	2930.77	115.38	43.88	39.93														
1010	17.79	4.00	25.60	1.008	25.86	1.018	27.00	1.063	.508	.020	.290	1751.72	68.97	45.50	41.41														
1010	17.79	4.00	26.11	1.028	26.37	1.038	27.51	1.083																					

(MOL) SPEC-2CR-2 T1-5AL-2-5SN(ELI) = 293 DEG.C. LH2 R=.05 F=.10 HZ 15149 AUG 05, '76

INPUT CONSTANTS

ELASTIC MODULUS(E) = 11×10^5 PSI (17.200E+06 PSI)				
NUMBER OF CYCLES	CRACK COMPLIANCE	ABAR / IN OPTICAL BASE	COMPLIANCE BASE	
N	CEB			
X 1000				
.000	39.5535	.358	.374	
62.000	41.7629	.361	.369	



(46L) SPEC. 7CR-2 T1-SAL-2.55N(ELI) - 253 DEG.C. LM2 M=0.5 F=10 HZ - 15:50 AUG 05, 1976

INPUT CONSTANTS:

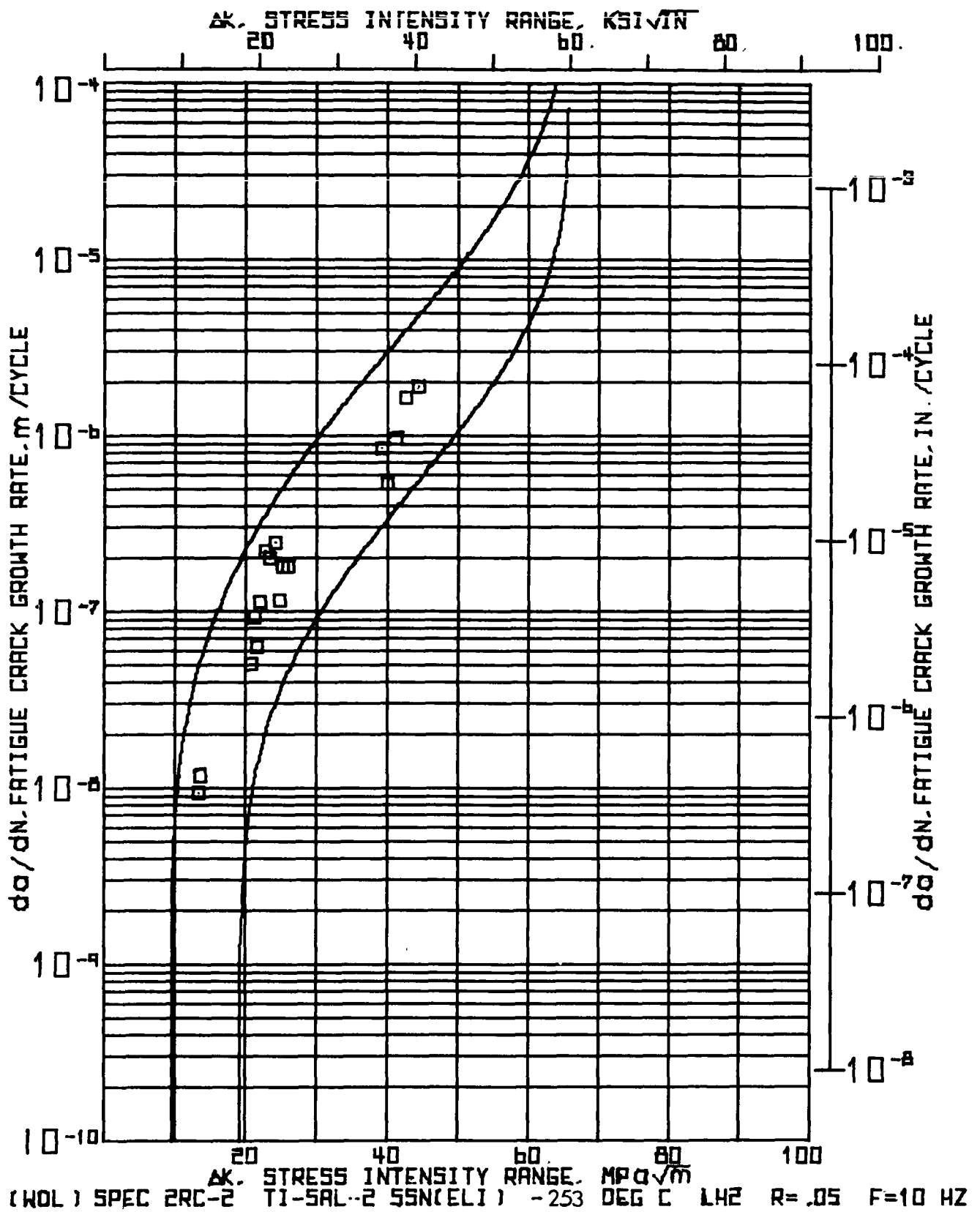
RANGE RATIO(R) = .05
 TEST FREQUENCY(HZ) = 10.0
 SPECIMEN WIDTH(W) = 50.978 MM(2.007 IN.)
 SPECIMEN THICKNESS(B) = 18.984 MM(.747 IN.)
 CRACK B/W CORRECTION = 1.270 MM(.050 IN.)

NUMBER OF CYCLES	N	MAXIMUM LOAD	P KN	SIDE 1 CRACK LENGTH		SIDE 2 CRACK LENGTH		CORRECTED AVERAGE CRACK LENGTH MM	INCH	MM	CHANGE IN CRACK LENGTH DA	INCH	X 1000	CHANGE IN CYCLES	CRACK GROWTH RATE DA / DN	NANO- METER	MICRONS IN.	PER CYCLE	STRESS INTENSITY RANGE		
				A1 MM	INCH	A2 MM	INCH												MPA X	KSI X	IN ^{3/2}
000		11.12	2.50	16.92	.666	16.92	.666	14.19	.716												
26000		11.12	2.50	17.93	.706	17.93	.706	19.20	.756	1.016	.040	26.000		39.04	1.54	18.33				16.73	
36000		11.12	2.50	19.39	.783	19.39	.783	21.16	.833	1.956	.077	10.000		195.58	7.72	19.67				17.92	
36000		12.46	2.80	19.69	.763	19.69	.783	21.16	.833												
36000		12.46	2.80	20.14	.793	20.14	.793	21.41	.843	.254	.010	2.000		127.00	5.00	23.22				21.13	
40000		12.46	2.80	20.52	.808	20.52	.805	21.79	.858	.381	.015	2.000		190.50	7.50	23.58				21.45	
40000		15.57	3.50	20.52	.808	20.52	.808	21.79	.858												
42000		15.57	3.50	21.29	.838	21.29	.836	22.56	.868	.762	.030	2.000		381.00	15.00	30.30				27.58	
44000		15.57	3.50	22.05	.863	22.05	.864	23.32	.918												
46000		15.57	3.50	23.06	.908	23.06	.908	24.33	.958	1.016	.040	2.000		508.00	20.00	32.94				29.97	
48000		15.57	3.50	24.33	.968	24.33	.958	25.60	1.008	1.270	.050	2.000		635.00	25.00	34.98				31.83	
50000		15.57	3.50	25.86	1.018	25.86	1.018	27.14	1.068	1.524	.060	2.000		762.00	30.00	37.76				34.36	
51000		15.57	3.50	26.87	1.058	26.87	1.058	28.14	1.108	1.016	.040	1.000		1016.00	40.00	40.61				36.95	
52000		15.57	3.50	30.18	1.188	30.18	1.184	31.45	1.238	1.302	.130	1.000		3302.00	130.00	46.32				42.15	

--- (MIL) SPEC 07CR-2 TJ-5AL-245SN(ELI) --- 253 DE60C LH2 K0005 F010 HZ --- 15150 AUG 05, 1976

INPUT CONSTANTS

ELASTIC MODULUS(E) = 130.311E+03 MPa(18.900E+06 PSI)					
NUMBER OF CYCLES	CRACK NGUTH COMPLIANCE	ABAR / W		OPTICAL COMPLIANCE	
		BASE	BASE	BASE	BASE
N	CEP				
x 1000					
40000	51.9910	.428	.441		
42000	58.6577	.442	.470		
44000	59.8387	.457	.474		
46000	66.7054	.502	.499		
50000	76.3151	.532	.529		
51000	90.2405	.552	.565		
52000	106.9249	.617	.600		



*** W E D G E * B P E N * L B A D * P R B G R A M * * * 15150 AUG 05, 1976

*** (A9L) SPEC-2RC-2 T1-5AL-2, SSN(ELT) -253 DEG.C. LM2 R4.05 F.10 HZ

INPUT CONSTANTS:

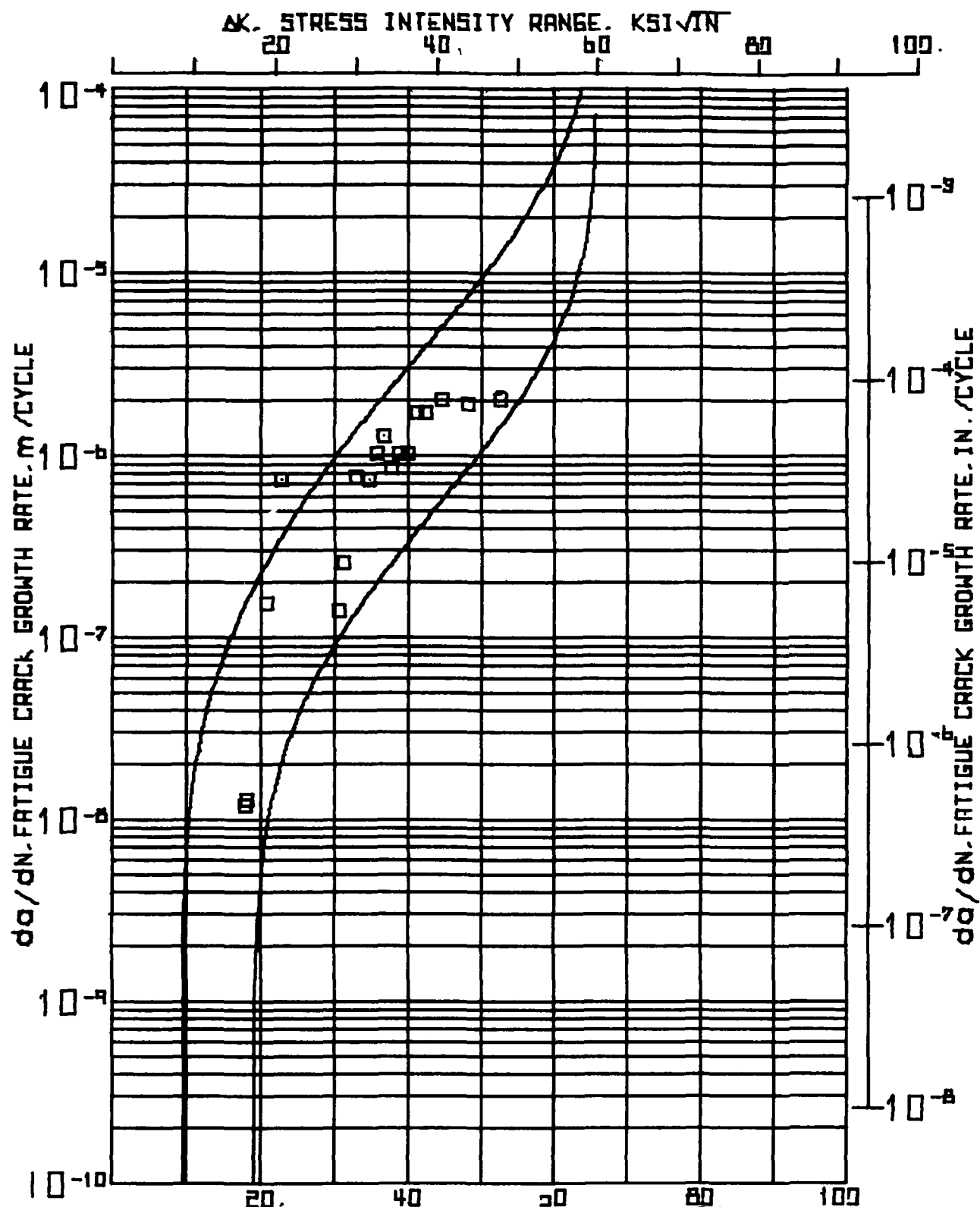
RANGE RATIO(R) * .05
 TEST FREQUENCY(HZ) * 10.0
 SPECIMEN WIDTH(W) * 51.079 MM(2.011 IN.)
 SPECIMEN THICKNESS(B) * 18.956 MM(.746 IN.)
 CRACK BGA CORRECTION * 1.276 MM(.050 IN.)

NUMBER OF CYCLES	P	MAXIMUM LOAD	SIDE 1		SIDE 2		CORRECTED AVERAGE LENGTH		CHANGE IN CRACK LENGTH		CHANGE IN CYCLES		CRACK GRGTH RATE DA / DN		STRESS INTENSITY RANGE DELTA K	
			MM	INCH	MM	INCH	MM	INCH	MM	INCH	MM	INCH	MM	INCH	MPA K	KSI X
N	X 1000	KN	KIPS	A1	A2						DN	DA	METER	IN.	4...5	1N...5
											X 1000		PER CYCLE			
000	0.00	8.01	1.80	17.68	.696	17.68	.696	10.95	.746	.254	.010	26.700	9.51	.37	13.45	12.24
26.700	26.700	8.01	1.80	17.93	.706	17.93	.706	19.20	.756	.254	.010	21.500	11.81	.47	13.60	12.38
46.200	46.200	8.01	1.80	18.19	.716	18.19	.716	19.46	.766							
48.200	48.200	12.01	2.70	18.19	.716	18.19	.716	19.46	.766	.508	.020	10.000	50.80	2.00	20.76	18.90
50.200	50.200	12.01	2.70	18.09	.736	18.09	.736	19.96	.766	.508	.020	5.500	92.36	3.64	21.26	19.34
63.700	63.700	12.01	2.70	19.20	.756	19.20	.756	20.47	.806	.254	.010	4.000	63.50	2.50	21.64	19.69
67.700	67.700	12.01	2.70	19.46	.766	19.46	.766	20.73	.816	.508	.020	4.500	112.89	4.44	22.03	20.05
72.200	72.200	12.01	2.70	19.96	.786	19.96	.786	21.23	.836	.762	.030	3.460	220.23	8.67	22.71	20.67
75.660	75.660	12.01	2.70	20.73	.816	20.73	.816	22.00	.866	.508	.020	2.500	203.20	8.00	23.43	21.32
79.160	79.160	12.01	2.70	21.23	.836	21.23	.836	22.50	.866	.762	.030	3.100	245.81	9.68	24.18	22.00
81.260	81.260	12.01	2.70	22.00	.866	22.00	.866	23.27	.916	.254	.010	2.200	115.45	4.55	24.82	22.57
83.460	83.460	12.01	2.70	22.25	.876	22.25	.876	23.52	.926	.508	.020	2.800	181.43	7.14	25.29	23.02
86.260	86.260	12.01	2.70	22.76	.896	22.76	.896	24.03	.946	.508	.020	2.800	181.43	7.14	25.97	23.63
89.060	89.060	12.01	2.70	23.27	.916	23.27	.916	24.54	.966							
89.060	89.060	17.79	4.00	23.27	.916	23.27	.916	24.54	.966	.254	.010	.300	846.67	33.33	39.25	35.71
89.360	89.360	17.79	4.00	23.52	.926	23.52	.926	24.79	.976	.508	.020	.950	534.74	21.05	40.05	36.45
90.310	90.310	17.79	4.00	24.03	.946	24.03	.946	25.30	.996	.508	.020	.530	958.49	37.74	41.16	37.46
90.540	90.540	17.79	4.00	24.54	.966	24.54	.966	25.81	1.016	.762	.030	.460	1656.52	65.22	42.62	38.79
91.300	91.300	17.79	4.00	25.30	.996	25.30	.996	26.57	1.046	.762	.030	.400	1905.00	75.00	44.49	40.48
91.700	91.700	17.79	4.00	26.06	1.026	26.06	1.026	27.33	1.076							

(AEL) SPEC24C-2 YI-5AL-2-SSN(ELI) - 253.DEU.C. LH2 R-05 F-10.HZ 15:50 AUG 05.176

INPUT CONSTANTS

ELASTIC MODULUS(E) = 110.590E+03 MPa(17.200E+06 PSI)			
NUMBER	CRACK INPUT	ASAR / "	
OF	COMPLIANCE	OPTICAL	COMPLIANCE
CYCLES		BASE	
N	CEB		
x 1000			
75.060	42.1363	.431	.423



(WOL) SPEC 7RC-2 T1-5AL-2,55N(ELI) -253 DEG C LH2 R=.05 F=10 HZ

(WBL) SPEC. 7RC-2 T1-5AL-2.55N(ELI) - 253 DEG.C. LH2 R.05 F.10 MZ														15:50 AUG 05, 1976		PAGE 2	
NUMBER OF CYCLES	MAXIMUM LOAD	SIDE 1 CRACK LENGTH		SIDE 2 CRACK LENGTH		CORRECTED AVERAGE CRACK LENGTH		CHANGE IN CRACK LENGTH		CHANGE IN CYCLES		CRACK GRWTH RATE		STRESS INTENSITY RANGE			
		MM	INCH	MM	INCH	MM	INCH	MM	INCH	MM	INCH	DA / DN METER PER CYCLE	DA / DN METER PER CYCLE	MPA X 1000	DE-TA X KSI X 1000		
56.100	15.57 KN	30.00	1.181	30.00	1.181	31.27	1.231	1.016	.040	.500	2032.00	80.00	52.53	47.81			
56.600	15.57 KN	31.01	1.221	31.01	1.221	32.28	1.271										

15:50 AUG 05, '76

(MOL) SPEC,74C-2 T1-5AL-2.55N(ELL) =253 DEG.C. LH2 R=0.05 F#10 MZ

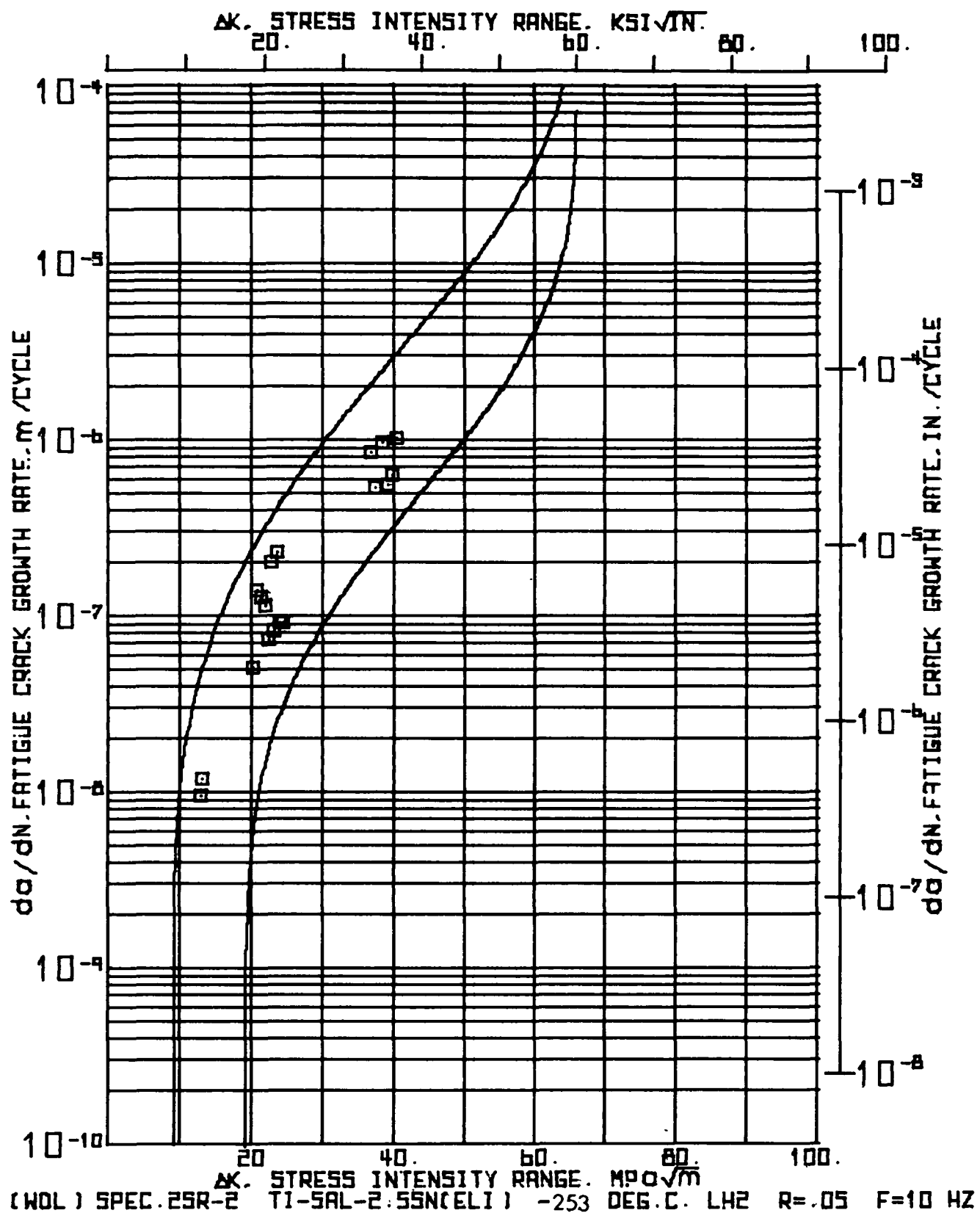
INPUT CONSTANTS

ELASTIC MODULUS(E) = 118.590E+03 MPA(17.200E+06 PSI)

NUMBER	CRACK MOUTH	ABAR / W	
OF	COMPLIANCE	OPTICAL	COMPLIANCE
CYCLES		BASE	

N	CE3
X	1.000

45.000	51.4830	.456	.438
--------	---------	------	------



15:51 AUG 05, '76

(.001) SPEC,2SR=2 T1=5AL=2.55N(ELI) = 253.DEG.C. LH2 R=.05 F=10 HZ

INPUT CONSTANTS

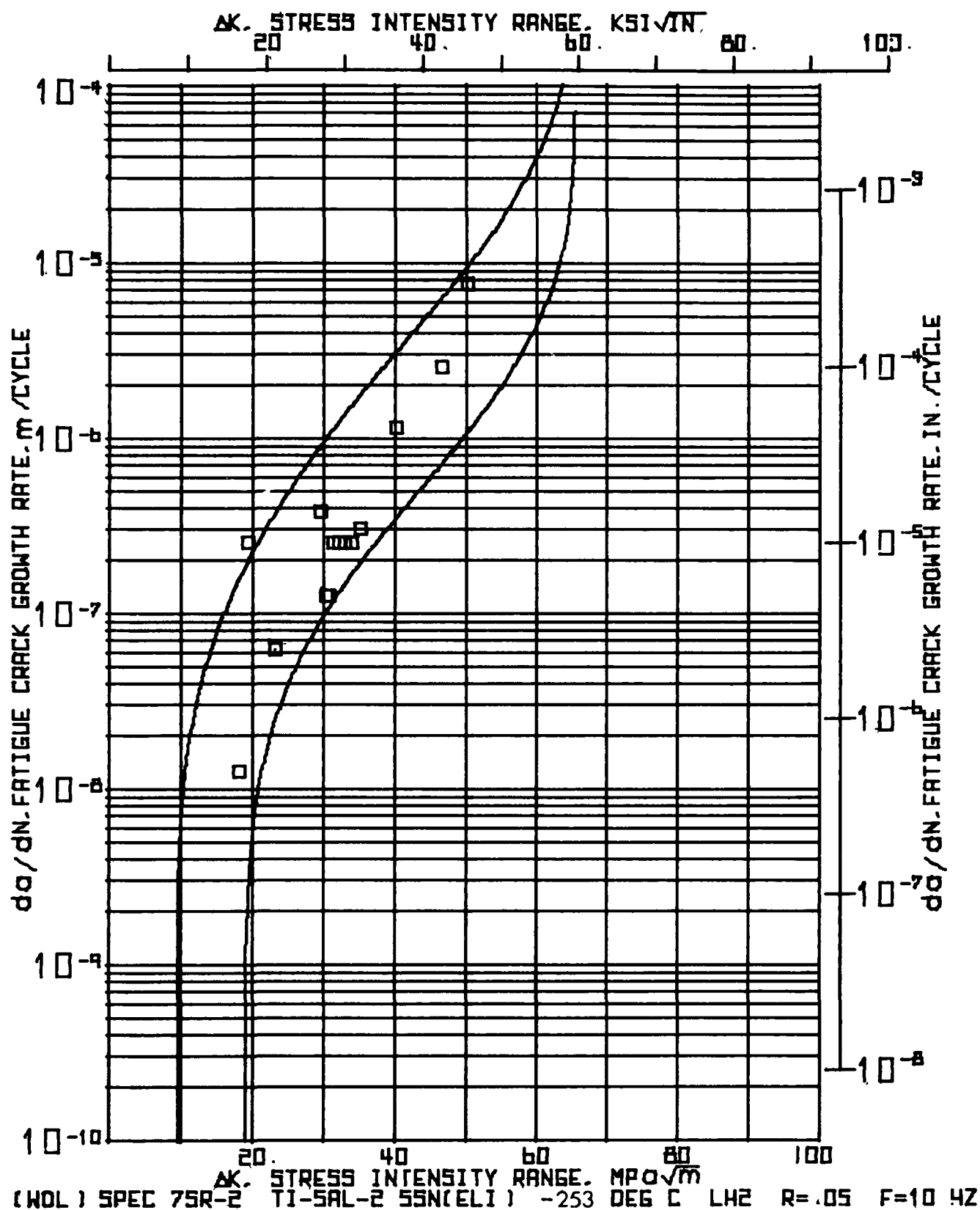
ELASTIC MODULUS(E) = $116.590E+03$ MPA($17.200E+06$ PSI)

NUMBER	CRACK WIDTH	ADAK / W
8F	COMPLIANCE	OPTICAL COMPLIANCE
CYCLES	BASE	BASE

CLD

X 1000

75.060	44.2373	423	402
--------	---------	-----	-----



(40E) SPEC:7SR-2 T1-5AL-2.55N(TL1) -253 DEG.C. LK2 R4.05 F.10 W7
 * * * * * E D G E * R P E N * L B A D * P R 8 G R A M * * *
 16:43 AUG 05.176

INPUT CONSTANTS:

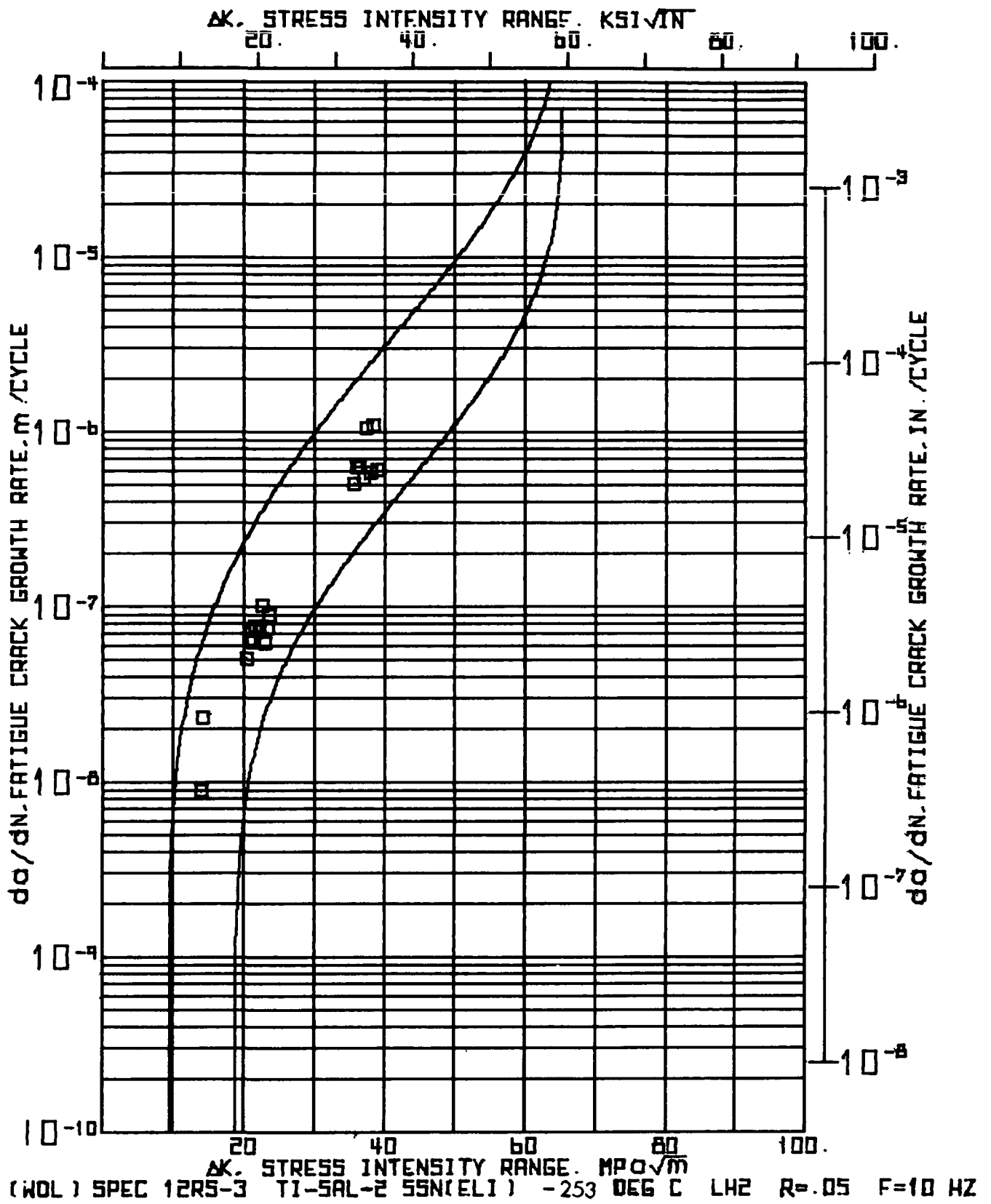
RANGE RATIO(M) * .05
 TEST FREQUENCY(HZ) * 10.0
 SPECIMEN WIDTH(W) * 50.952 MM(2.006 IN.)
 SPECIMEN THICKNESS(B) * 19.002 MM(.748 IN.)
 CRACK BD. CORRECTION * 1.270 MM(.050 IN.)

NUMBER OF CYCLES	MAXIMUM LOAD	SIDE 1		SIDE 2		CORRECTED AVERAGE CRACK LENGTH		CHANGE IN CRACK LENGTH		CHANGE IN CYCLES		CRACK GROWTH RATE DA / DN MICR9 METER PER CYCLE		STRESS INTENSITY RANGE DELTA K MPA X 1000		
		KN	MM	KN	INCH	MM	INCH	MM	INCH	MM	INCH	DA	DN	INCH	X 1000	
000	11.12 2.50	16.97	.668	16.97	.668	18.24	.718	.330	.013	26.000		12.70	.50		18.14	16.51
26.000	11.12 2.50	17.30	.681	17.30	.681	18.57	.731	2.540	.100	10.000		254.00	10.00		19.36	17.62
30.000	11.12 2.50	19.84	.781	19.84	.781	21.11	.831									
36.000	12.46 2.80	19.84	.781	19.84	.781	21.11	.831	.254	.010	4.000		63.50	2.50		23.16	21.07
40.000	12.46 2.80	20.09	.791	20.09	.791	21.36	.841									
40.000	15.57 3.50	20.09	.791	20.09	.791	21.36	.841	.762	.030	2.000		381.00	15.00		29.67	27.00
42.000	15.57 3.50	20.85	.821	20.85	.821	22.12	.871	.254	.010	2.000		127.00	5.00		30.41	27.68
44.000	15.57 3.50	21.11	.831	21.11	.831	22.38	.881	.254	.010	2.000		127.00	5.00		30.82	28.03
46.000	15.57 3.50	21.36	.841	21.36	.841	22.63	.891	.504	.020	2.000		254.00	10.00		31.39	28.57
48.000	15.57 3.50	21.87	.861	21.87	.861	23.14	.911	.504	.020	2.000		254.00	10.00		32.21	29.31
50.000	15.57 3.50	22.38	.881	22.38	.881	23.65	.931	.504	.020	2.000		254.00	10.00		33.06	30.09
52.000	15.57 3.50	22.89	.901	22.89	.901	24.16	.951	.504	.020	2.000		254.00	10.00		33.95	30.90
54.000	15.57 3.50	23.39	.921	23.39	.921	24.66	.971	.762	.030	2.500		304.80	12.00		35.12	31.96
56.000	15.57 3.50	24.16	.951	24.16	.951	25.43	1.001	4.064	.160	3.500		1161.14	45.71		40.13	36.58
60.000	15.57 3.50	25.22	1.011	25.22	1.011	29.49	1.161	.762	.030	.300		2540.00	100.00		46.55	42.37
60.300	15.57 3.50	26.38	1.041	26.38	1.041	30.25	1.191	1.524	.060	.200		7620.00	300.00		50.16	45.65
60.500	15.57 3.50	30.51	1.201	30.51	1.201	31.78	1.251									

(KBL) SPEC.75R-2 T1-5AL-2.55N(ELI) - 253 DEG.C. L#2 R-05 F#10 HZ 16143 AUG 05,176

INPUT CONSTANTS

ELASTIC MODULUS(E) = 118.590E+03 MPA(17.200E+06 PSI)			
NUMBER	CRACK	YOUTH	ABAR / W
8F	COMPLIANCE	OPTICAL	COMPLIANCE
CYCLES	BASE	BASE	BASE
N	CEB		
X 1000			
40.000	41.0146	0.419	0.384



11881) SPEC12RS-3 TISSAL-255NIELI) -253 DEG.C. LM2 M=05 F=10 HZ 16144 AUG 05, 1976

INPUT CONSTANTS:

RANGE RATIO(K) ■ .05
 TEST FREQUENCY(HZ) ■ 10.0
 SPECIMEN WIDTH(W) ■ 50.800 MM(2.000 IN.)
 SPECIMEN THICKNESS(B) ■ 19.014 MM(.749 IN.)
 CRACK 39A CORRECTION ■ 1.270 MM(.050 IN.)

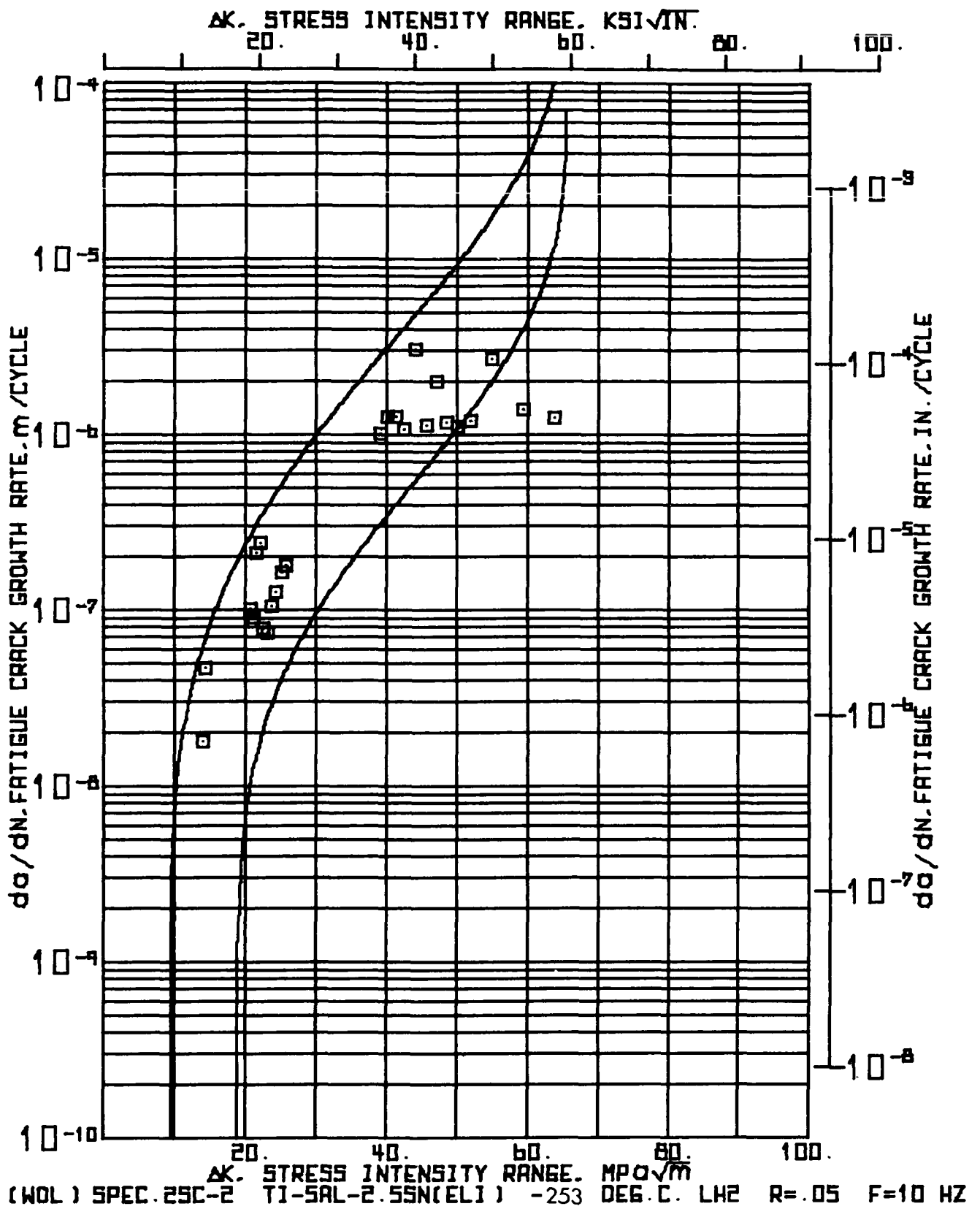
NUMBER OF CYCLES	MAXIMUM LOAD	SIDE 1 CRACK LENGTH	SIDE 2 CRACK LENGTH	CORRECTED AVERAGE CRACK LENGTH	CHANGE IN CRACK LENGTH DA	CHANGE IN CYCLES	CRACK GROWTH RATE DA / DN	STRESS INTENSITY RANGE DELTA K
N X 1000	KN	MM	MM	MM	MM	DN X 1000	NANO- METER PER CYCLE	MPA X 10 ⁻⁰⁵ IN ⁻⁰⁵
300	8.45 1.90	17.40 .685	17.40 .685	10.67 .735	.254	.010 28.400	8.94 .35	14.08 12.81
20.400	8.45 1.90	17.65 .695	17.65 .695	18.92 .745	.254	.010 10.950	23.20 .91	14.24 12.96
39.350	8.45 1.90	17.91 .705	17.91 .705	19.18 .755				
39.350	12.01 2.70	17.91 .705	17.91 .705	19.18 .755	.254	.010 5.000	50.80 2.00	20.47 18.63
44.350	12.01 2.70	18.16 .715	18.16 .715	19.43 .765	.254	.010 3.850	65.97 2.60	20.71 18.85
49.200	12.01 2.70	18.41 .725	18.41 .725	19.68 .775	.254	.010 3.400	74.71 2.94	20.96 19.07
51.600	12.01 2.70	18.67 .735	18.67 .735	19.94 .785	.254	.010 4.000	83.50 2.50	21.21 19.30
55.600	12.01 2.70	18.92 .745	18.92 .745	20.19 .795	.508	.020 6.550	77.56 3.05	21.59 19.65
62.150	12.01 2.70	19.43 .765	19.43 .765	20.70 .815	.508	.020 6.900	73.62 2.90	22.12 20.13
69.050	12.01 2.70	19.94 .785	19.94 .785	21.21 .835	.508	.020 5.000	101.60 4.00	22.67 20.63
74.350	12.01 2.70	20.45 .805	20.45 .805	21.72 .855	.254	.010 4.100	61.95 2.44	23.09 21.01
76.150	12.01 2.70	20.70 .815	20.70 .815	21.97 .865	.254	.010 3.350	75.82 2.99	23.38 21.28
81.500	12.01 2.70	20.95 .825	20.95 .825	22.22 .875	.254	.010 2.850	89.12 3.51	23.68 21.55
84.300	12.01 2.70	21.21 .835	21.21 .835	22.48 .885				
84.350	17.79 4.00	21.21 .835	21.21 .835	22.48 .885	.254	.010 .500	508.00 20.00	35.53 32.33
84.350	17.79 4.00	21.46 .845	21.46 .845	22.73 .895	.254	.010 .400	635.00 25.00	35.98 32.75
85.250	17.79 4.00	21.72 .855	21.72 .855	22.99 .905	.254	.010 .400	635.00 25.00	36.45 33.17
85.650	17.79 4.00	21.97 .865	21.97 .865	23.24 .915	.254	.010 .470	540.43 21.28	36.93 33.60
85.120	17.79 4.00	22.22 .875	22.22 .875	23.49 .925	.254	.010 .240	1058.33 41.67	37.41 34.05
86.360	17.79 4.00	22.48 .885	22.48 .885	23.75 .935				

NUMBER OF CYCLES	MAXIMUM LOAD	SIDE 1 CRACK		SIDE 2 CRACK		CORRECTED AVERAGE LENGTH	CHANGE IN CRACK LENGTH	CHANGE IN CYCLES	CRACK GROWTH		STRESS INTENSITY RANGE				
		LENGTH	MM	LENGTH	MM				RATE	DA / DN METER PER CYCLE					
	P	A1	A2												
	KN	MM	MM	INCH	INCH	MM	MM	INCH X 1000	DN	MICR9	MPA X 1000.5	INCH X 1000.5			
	KIPS	MM	MM	INCH	INCH	MM	MM	INCH X 1000	DN	METER	MPA X 1000.5	INCH X 1000.5			
80.360	17.79	4.00	22.43	.885	22.48	.885	.23.75	.935	.254	.010	.430	590.70	23.26	37.91	34.50
80.790	17.79	4.00	22.73	.895	22.73	.895	24.00	.945	.254	.010	.230	1104.35	43.48	38.42	34.96
87.020	17.79	4.00	22.99	.905	22.99	.905	24.26	.955	.254	.010	.420	604.76	23.81	38.93	35.43
87.440	17.79	4.00	23.24	.915	23.24	.915	24.51	.965	.254	.010	.420	604.76	23.81	38.93	35.43

(*9L) SPEC:12RS-3 T1-5AL-2.5SN(ELI) - 253 DEG.C LHZ R=05 F=10 HZ 16144 AUG 05,176

INPUT CONSTANTS

ELASTIC MODULUS(E) = 118.59CE+03 MPA(17.200E+06 PSI)					
NUMBER	CRACK	MOUTH	ABAR / W	OPTICAL	COMPLIANCE
OF	COMPLIANCE				
CYCLES				BASE	BASE
X 1000					
55.000	31.0278		.397	.370	
37.440	43.4562		.482	.398	

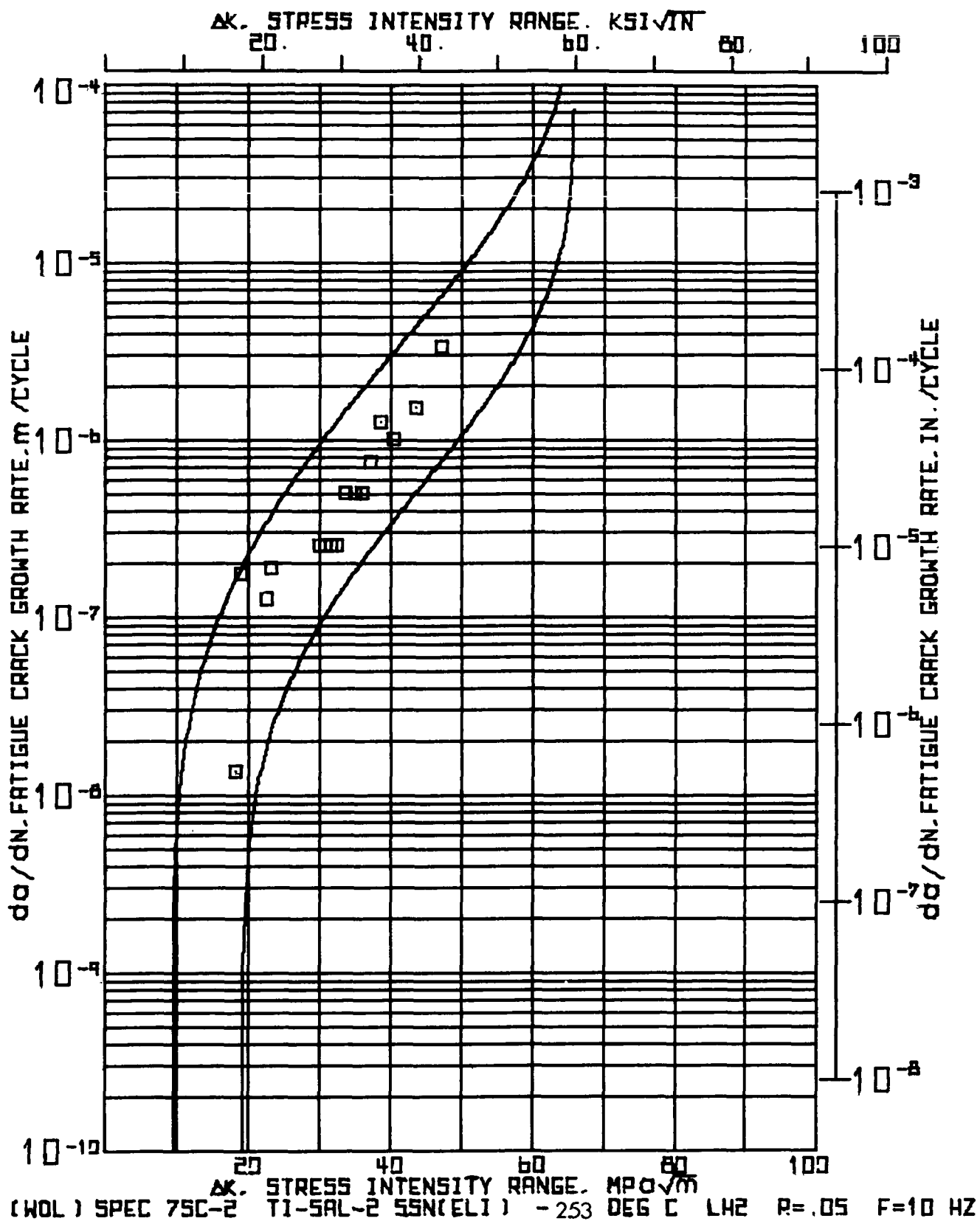


RANGE RATIO(R)														
TEST FREQUENCY(HZ)														
SPECIMEN WIDTH(W)														
SPECIMEN THICKNESS(B)														
CRACK BGA CORRECTION														
RANGE RATIO(R)														
TEST FREQUENCY(HZ)														
SPECIMEN WIDTH(W)														
SPECIMEN THICKNESS(B)														
CRACK BGA CORRECTION														
RANGE RATIO(R)														
TEST FREQUENCY(HZ)														
SPECIMEN WIDTH(W)														
SPECIMEN THICKNESS(B)														
CRACK BGA CORRECTION														
RANGE RATIO(R)														
TEST FREQUENCY(HZ)														
SPECIMEN WIDTH(W)														
SPECIMEN THICKNESS(B)														
CRACK BGA CORRECTION														
RANGE RATIO(R)														
TEST FREQUENCY(HZ)														
SPECIMEN WIDTH(W)														
SPECIMEN THICKNESS(B)														
CRACK BGA CORRECTION														
RANGE RATIO(R)														
TEST FREQUENCY(HZ)														
SPECIMEN WIDTH(W)														
SPECIMEN THICKNESS(B)														
CRACK BGA CORRECTION														
RANGE RATIO(R)														
TEST FREQUENCY(HZ)														
SPECIMEN WIDTH(W)														
SPECIMEN THICKNESS(B)														
CRACK BGA CORRECTION														
RANGE RATIO(R)														
TEST FREQUENCY(HZ)														
SPECIMEN WIDTH(W)														
SPECIMEN THICKNESS(B)														
CRACK BGA CORRECTION														
RANGE RATIO(R)														
TEST FREQUENCY(HZ)														
SPECIMEN WIDTH(W)														
SPECIMEN THICKNESS(B)														
CRACK BGA CORRECTION														
RANGE RATIO(R)														
TEST FREQUENCY(HZ)														
SPECIMEN WIDTH(W)														
SPECIMEN THICKNESS(B)														
CRACK BGA CORRECTION														
RANGE RATIO(R)														
TEST FREQUENCY(HZ)														
SPECIMEN WIDTH(W)														
SPECIMEN THICKNESS(B)														
CRACK BGA CORRECTION														
RANGE RATIO(R)														
TEST FREQUENCY(HZ)														
SPECIMEN WIDTH(W)														
SPECIMEN THICKNESS(B)														
CRACK BGA CORRECTION														
RANGE RATIO(R)														
TEST FREQUENCY(HZ)														
SPECIMEN WIDTH(W)														
SPECIMEN THICKNESS(B)														
CRACK BGA CORRECTION														
RANGE RATIO(R)														
TEST FREQUENCY(HZ)														
SPECIMEN WIDTH(W)														
SPECIMEN THICKNESS(B)														
CRACK BGA CORRECTION														
RANGE RATIO(R)														
TEST FREQUENCY(HZ)														
SPECIMEN WIDTH(W)														
SPECIMEN THICKNESS(B)														
CRACK BGA CORRECTION														
RANGE RATIO(R)														
TEST FREQUENCY(HZ)														
SPECIMEN WIDTH(W)														
SPECIMEN THICKNESS(B)														
CRACK BGA CORRECTION														
RANGE RATIO(R)														
TEST FREQUENCY(HZ)														
SPECIMEN WIDTH(W)														
SPECIMEN THICKNESS(B)														
CRACK BGA CORRECTION														
RANGE RATIO(R)														
TEST FREQUENCY(HZ)														
SPECIMEN WIDTH(W)														
SPECIMEN THICKNESS(B)														
CRACK BGA CORRECTION														
RANGE RATIO(R)														
TEST FREQUENCY(HZ)														
SPECIMEN WIDTH(W)														
SPECIMEN THICKNESS(B)														
CRACK BGA CORRECTION														
RANGE RATIO(R)														
TEST FREQUENCY(HZ)														
SPECIMEN WIDTH(W)														
SPECIMEN THICKNESS(B)														
CRACK BGA CORRECTION														
RANGE RATIO(R)														
TEST FREQUENCY(HZ)														
SPECIMEN WIDTH(W)														
SPECIMEN THICKNESS(B)														
CRACK BGA CORRECTION														
RANGE RATIO(R)														
TEST FREQUENCY(HZ)														
SPECIMEN WIDTH(W)														
SPECIMEN THICKNESS(B)														
CRACK BGA CORRECTION														
RANGE RATIO(R)														
TEST FREQUENCY(HZ)														
SPECIMEN WIDTH(W)														
SPECIMEN THICKNESS(B)														
CRACK BGA CORRECTION														
RANGE RATIO(R)														
TEST FREQUENCY(HZ)														
SPECIMEN WIDTH(W)														
SPECIMEN THICKNESS(B)														
CRACK BGA CORRECTION														
RANGE RATIO(R)														
TEST FREQUENCY(HZ)														
SPECIMEN WIDTH(W)														
SPECIMEN THICKNESS(B)														
CRACK BGA CORRECTION														
RANGE RATIO(R)														
TEST FREQUENCY(HZ)														
SPECIMEN WIDTH(W)														
SPECIMEN THICKNESS(B)														
CRACK BGA CORRECTION														
RANGE RATIO(R)														
TEST FREQUENCY(HZ)														
SPECIMEN WIDTH(W)														
SPECIMEN THICKNESS(B)														
CRACK BGA CORRECTION														
RANGE RATIO(R)														
TEST FREQUENCY(HZ)														
SPECIMEN WIDTH(W)														
SPECIMEN THICKNESS(B)														
CRACK BGA CORRECTION														
RANGE RATIO(R)														
TEST FREQUENCY(HZ)														
SPECIMEN WIDTH(W)														
SPECIMEN THICKNESS(B)														
CRACK BGA CORRECTION														
RANGE RATIO(R)														
TEST FREQUENCY(HZ)														
SPECIMEN WIDTH(W)														
SPECIMEN THICKNESS(B)														
CRACK BGA CORRECTION														
RANGE RATIO(R)														
TEST FREQUENCY(HZ)														
SPECIMEN WIDTH(W)														
SPECIMEN THICKNESS(B)														
CRACK BGA CORRECTION														
RANGE RATIO(R)														
TEST FREQUENCY(HZ)														
SPECIMEN WIDTH(W)														
SPECIMEN THICKNESS(B)														
CRACK BGA CORRECTION														
RANGE RATIO(R)														
TEST FREQUENCY(HZ)														
SPECIMEN WIDTH(W)														
SPECIMEN THICKNESS(B)														
CRACK BGA CORRECTION														
RANGE RATIO(R)														
TEST FREQUENCY(HZ)														
SPECIMEN WIDTH(W)														
SPECIMEN THICKNESS(B)														
CRACK BGA CORRECTION														
RANGE RATIO(R)														
TEST FREQUENCY(HZ)														
SPECIMEN WIDTH(W)														
SPECIMEN THICKNESS(B)														
CRACK BGA CORRECTION														
RANGE RATIO(R)														
TEST FREQUENCY(HZ)														
SPECIMEN WIDTH(W)														
SPECIMEN THICKNESS(B)														
CRACK BGA CORRECTION														
RANGE RATIO(R)														
TEST FREQUENCY(HZ)														
SPECIMEN WIDTH(W)														
SPECIMEN THICKNESS(B)														
CRACK BGA CORRECTION														
RANGE RATIO(R)														
TEST FREQUENCY(HZ)														
SPECIMEN WIDTH(W)														
SPECIMEN THICKNESS(B)														
CRACK BGA CORRECTION														
RANGE RATIO(R)														
TEST FREQUENCY(HZ)														
SPECIMEN WIDTH(W)														
SPECIMEN THICKNESS(B)														
CRACK BGA CORRECTION														
RANGE RATIO(R)														
TEST FREQUENCY(HZ)														
SPECIMEN WIDTH(W)														
SPECIMEN THICKNESS(B)														
CRACK BGA CORRECTION														
RANGE RATIO(R)														
TEST FREQUENCY(HZ)														
SPECIMEN WIDTH(W)														
SPECIMEN THICKNESS(B)														
CRACK BGA CORRECTION														
RANGE RATIO(R)														
TEST FREQUENCY(HZ)														
SPECIMEN WIDTH(W)														
SPECIMEN THICKNESS(B)														
CRACK BGA CORRECTION														
RANGE RATIO(R)														
TEST FREQUENCY(HZ)														
SPECIMEN WIDTH(W)														
SPECIMEN THICKNESS(B)														
CRACK BGA CORRECTION														
RANGE RATIO(R)														
TEST FREQUENCY(HZ)														
SPECIMEN WIDTH(W)														
SPECIMEN THICKNESS(B)														
CRACK BGA CORRECTION														
RANGE RATIO(R)														
TEST FREQUENCY(HZ)														
SPECIMEN WIDTH(W)														
SPECIMEN THICKNESS(B)														
CRACK BGA CORRECTION														
RANGE RATIO(R)														
TEST FREQUENCY(HZ)														
SPECIMEN WIDTH(W)														
SPECIMEN THICKNESS(B)														
CRACK BGA CORRECTION														
RANGE RATIO(R)														
TEST FREQUENCY(HZ)														
SPECIMEN WIDTH(W)														
SPECIMEN THICKNESS(B)														
CRACK BGA CORRECTION														
RANGE RATIO(R)														
TEST FREQUENCY(HZ)														
SPECIMEN WIDTH(W)														
SPECIMEN THICKNESS(B)														
CRACK BGA CORRECTION														
RANGE RATIO(R)														
TEST FREQUENCY(HZ)														
SPECIMEN WIDTH(W)														
SPECIMEN THICKNESS(B)														
CRACK BGA CORRECTION														
RANGE RATIO(R)														
TEST FREQUENCY(HZ)														
SPECIMEN WIDTH(W)														
SPECIMEN THICKNESS(B)														
CRACK BGA CORRECTION														
RANGE RATIO(R)														
TEST FREQUENCY(HZ)														
SPECIMEN WIDTH(W)														
SPECIMEN THICKNESS(B)														

(49L) SPEC.25C-2 TJ-5AL-2.55NIELI) ... 253 DEG.C. LH2 R=05 F=10 HZ 16144 AUG 05, '76

INPUT CONSTANTS

ELASTIC MODULUS(E) = 118.590E+03 MPA(17.200E+06 PSI)			
NUMBER	CRACK WIDTH	ABAR / IN	
OF	COMPLIANCE	OPTICAL	COMPLIANCE
CYCLES	BASE	BASE	BASE
N	CEB		
X 1000			
51.500	41.365	.418	.364



(MFL) SPEC.75C-2 11-SAL-2.55N(EL1) - 253 DEG.C. LH2 RA.05 F.10 HZ * * * * * 16145 AUG 05.176

INPUT CONSTANTS:

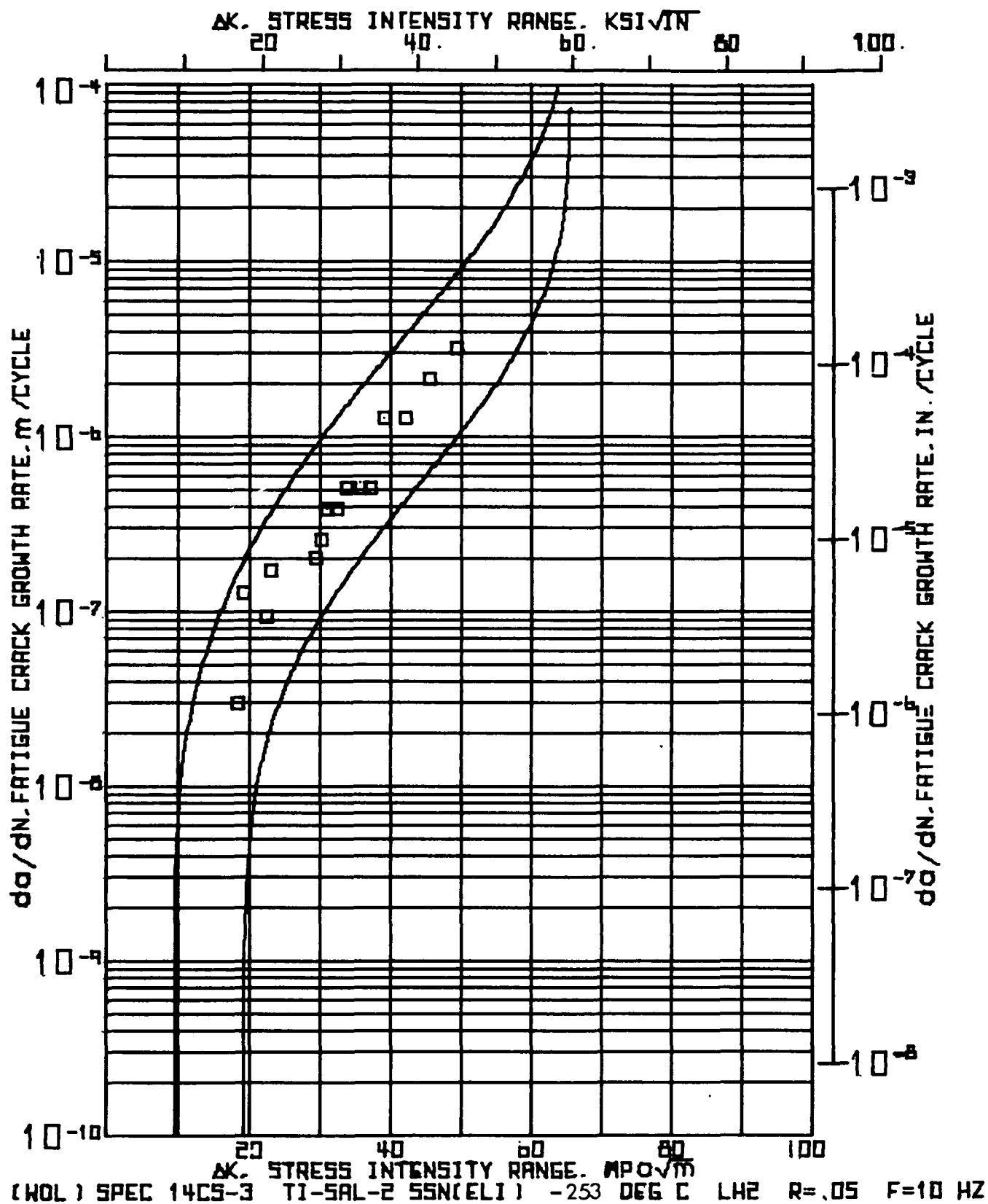
RANGE RATIO(M) * .05
 TEST FREQUENCY(HZ) * 10.0
 SPECIMEN ALTH(M) * 50.902 MM(2.004 IN.)
 SPECIMEN THICKNESS(B) * 19.004 MM(.748 IN.)
 CRACK 23A CORRELATION * 1.270 MM(.050 IN.)

NUMBER OF CYCLES	MAXIMUM LOAD	SIDE 1 CRACK LENGTH		SIDE 2 CRACK LENGTH		CORRECTED AVERAGE CRACK LENGTH		CHANGE IN CRACK LENGTH	CHANGE IN CYCLES	CRACK GRWTH RATE DA / DN MICRS IN.	STRESS INTENSITY RANGE DELTA K MPA X KSI X IN.0.5 IN.0.5
		MM	INCH	MM	INCH	MM	INCH				
1000	11.12	2.50	16.59	.669	16.99	.669	18.26	.719			
26000	11.12	2.50	17.35	.683	17.35	.683	18.62	.733			
30000	11.12	2.50	19.13	.753	19.13	.753	20.40	.803			
36000	12.46	2.80	19.13	.753	19.13	.753	20.40	.803			
40000	12.46	2.80	19.63	.773	19.63	.773	20.90	.823			
44000	12.46	2.80	20.40	.803	20.40	.803	21.67	.853			
44000	15.57	3.50	20.40	.803	20.40	.803	21.67	.853			
46000	15.57	3.50	20.90	.823	20.90	.823	22.17	.873			
46000	15.57	3.50	21.41	.843	21.41	.843	22.68	.893			
50000	15.57	3.50	21.92	.863	21.92	.863	23.19	.913			
52000	15.57	3.50	22.43	.883	22.43	.883	23.70	.933			
54000	15.57	3.50	23.44	.923	23.44	.923	24.71	.973			
55000	15.57	3.50	23.95	.943	23.95	.943	25.22	.993			
56000	15.57	3.50	24.46	.963	24.46	.963	25.73	1.013			
57000	15.57	3.50	25.22	.993	25.22	.993	26.49	1.043			
57000	15.57	3.50	25.73	1.013	25.73	1.013	27.00	1.063			
58000	15.57	3.50	26.75	1.053	26.75	1.053	28.02	1.103			
59000	15.57	3.50	28.27	1.113	28.27	1.113	29.54	1.163			
59000	15.57	3.50	29.29	1.153	29.29	1.153	30.56	1.203			

(MDL) SPEC7SC-2 T1-5AL-2-5SN(ELI) -253 DEB-C- LH2 R-05 F-10 HZ 16145 AUG 05, '76

INPUT CONSTANTS

ELASTIC MODULUS(E) = 11.59E+03 MPA(17.200E+06 PSI)			
NUMBER	CRACK MOUTH	ABAR / W	
OF	COMPLIANCE	OPTICAL	COMPLIANCE
CYCLES	BASE	BASE	BASE
N	CEB		
X 1000			
44.000	41.0244	.426	.309

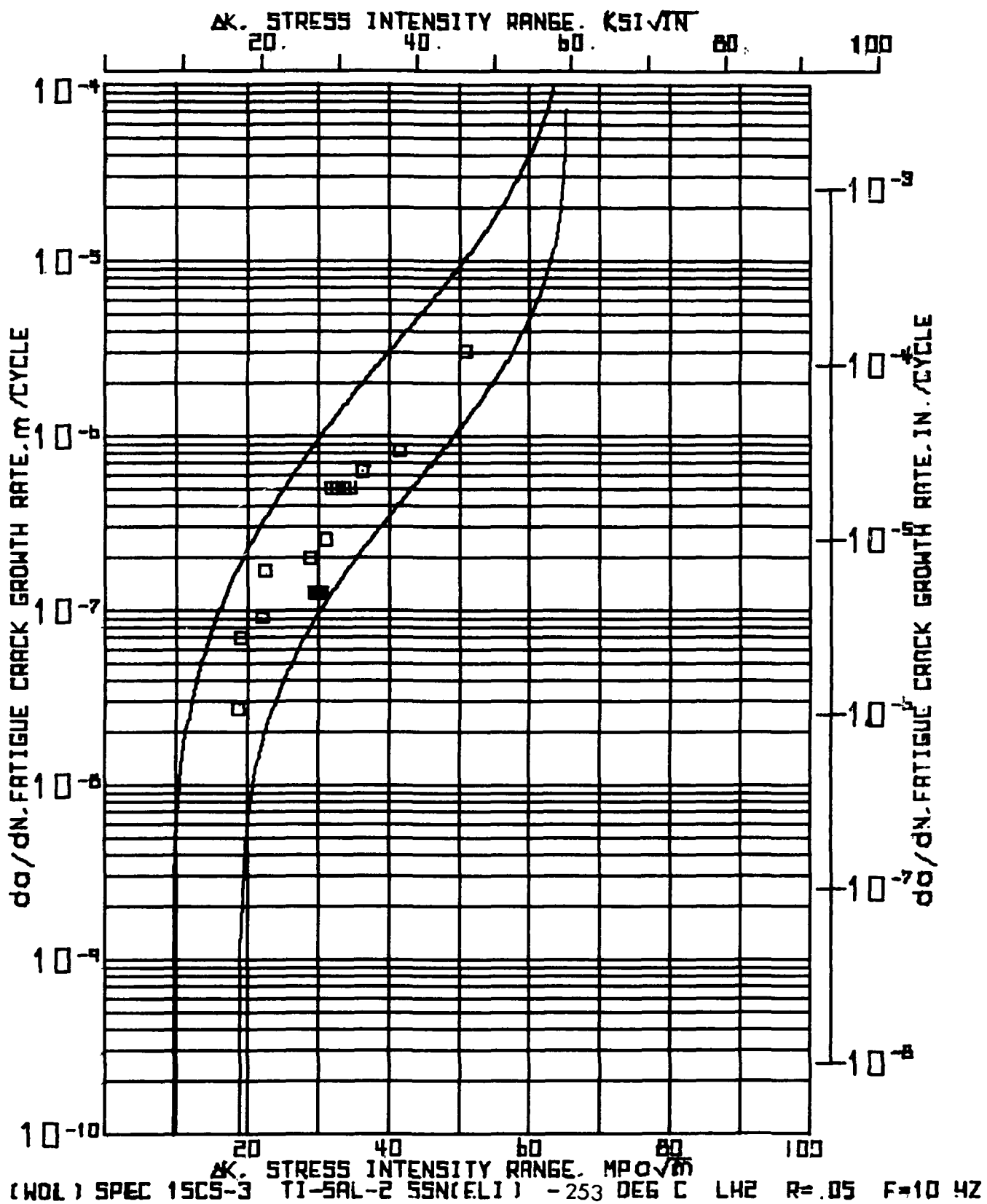


(A9L) SPEC.14CS-3 T1-SAL-2.55N(ELT) -253 DEG.C. LM2 R.05 P.10 HZ 16145 AUG 05, '76

INPUT CONSTANTS:

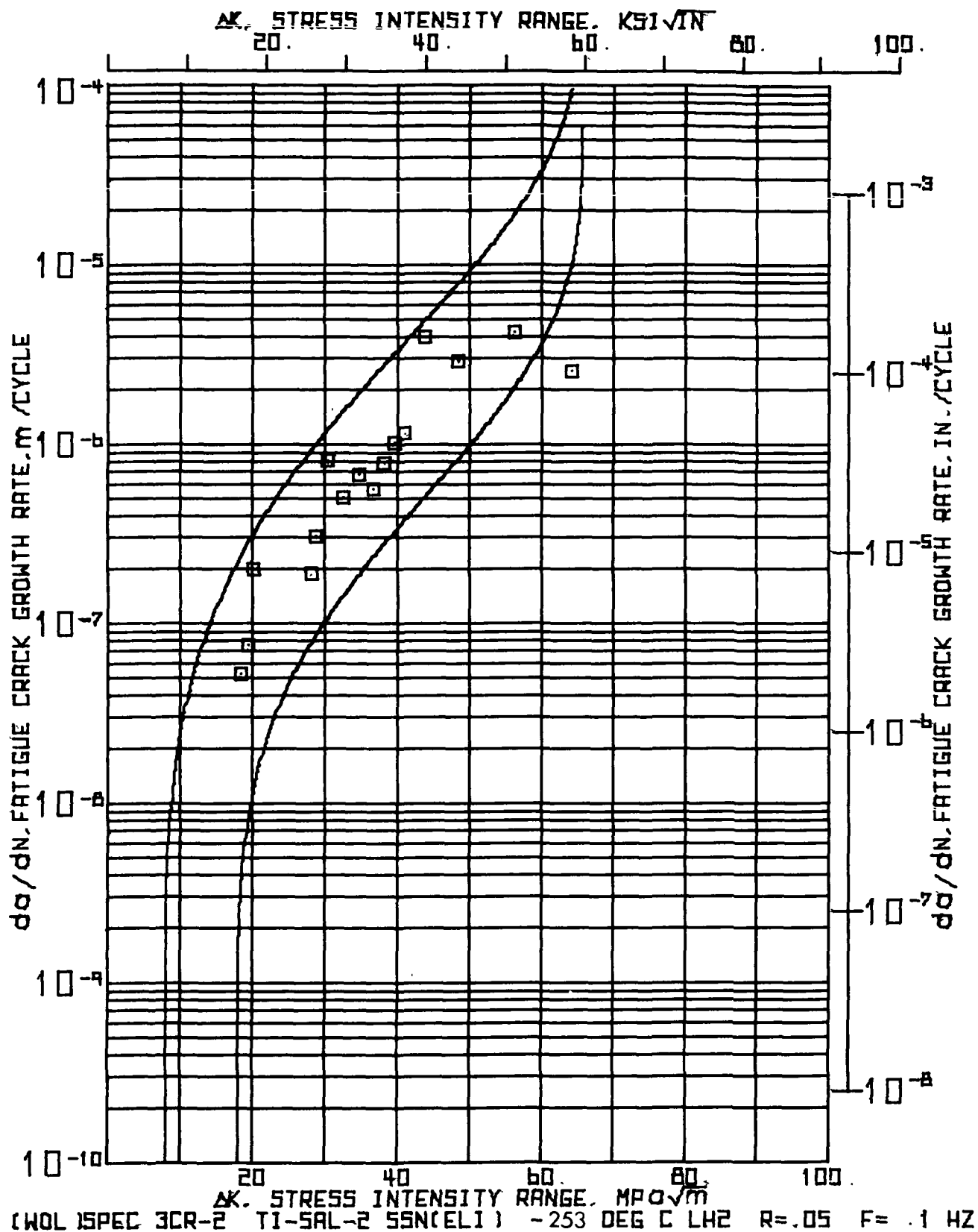
RANGE RATIO(R) .05
 TEST FREQUENCY(HZ) 10.0
 SPECIMEN WIDTH(W) 50.978 MM(2.007 IN.)
 SPECIMEN THICKNESS(B) 10.581 MM(.747 IN.)
 CRACK 99% CORRECTION 1.270 MM(.050 IN.)

NUMBER OF CYCLES	MAXIMUM LOAD	P KN	SIDE 1 CRACK LENGTH		SIDE 2 CRACK LENGTH		CORRECTED AVERAGE CRACK LENGTH	CHANGE IN CRACK LENGTH	CHANGE IN CYCLES	CRACK GROWTH RATE		STRESS INTENSITY RANGE	DELTA K
			MM	INCH	MM	INCH				NANO- METER	PER CYCLE		
1000	11.12	2.50	17.12	.674	17.12	.674	10.39	.724					
2000	11.12	2.50	17.86	.703	17.86	.703	19.13	.753					
3000	11.12	2.50	19.00	.748	19.00	.748	20.27	.798					
3400	12.46	2.80	19.00	.748	19.00	.748	20.27	.798					
3900	12.46	2.80	19.51	.768	19.51	.768	20.78	.818					
4200	12.46	2.80	20.02	.783	20.02	.783	21.29	.838					
42500	15.57	3.50	20.02	.788	20.02	.788	21.29	.838					
45000	15.57	3.50	20.52	.808	20.52	.808	21.79	.868					
47000	15.57	3.50	21.03	.828	21.03	.828	22.30	.878					
49000	15.57	3.50	21.79	.858	21.79	.858	23.06	.908					
51000	15.57	3.50	22.56	.888	22.56	.888	23.83	.938					
53000	15.57	3.50	23.57	.928	23.57	.928	24.84	.978					
55000	15.57	3.50	24.59	.968	24.59	.968	25.86	1.018					
56000	15.57	3.50	25.10	.988	25.10	.988	26.37	1.038					
57000	15.57	3.50	26.37	1.038	26.37	1.038	27.64	1.068					
58000	15.57	3.50	27.64	1.088	27.64	1.088	28.91	1.138					
58600	15.57	3.50	28.91	1.138	28.91	1.138	30.18	1.188					
59000	15.57	3.50	30.18	1.188	30.18	1.188	31.45	1.238					



SECTION A7

This section of the Appendix includes all fatigue crack growth data obtained from WOL coupons tested at -253°C , at a range ratio of 0.05, and at a frequency of 0.1 Hz.



11136 AUG 05, 1976

INPUT CONSTANTS:

RANGE RATIO(R) .05
TEST FREQUENCY(HZ) .1
SPECIMEN WIDTH(IN) 2.004 IN.
SPECIMEN THICKNESS(MM) 19.035 MM(.749 IN.)
CRACK 20% CORRECTION 1.270 MM(.050 IN.)

NUMBER OF CYCLES	MAXIMUM LOAD	SIDE 1 CRACK LENGTH	SIDE 2 CRACK LENGTH	CORRECTED AVERAGE CRACK LENGTH	CHANGE IN CRACK LENGTH	INCH X 1000	DA / DN CYCLES	CRACK GROWTH RATE	STRESS INTENSITY RANGE DELTA K					
N	P	A1	A2	MM	INCH	MM	INCH	DA / DN CYCLES	MPA X 1000					
274.300	11.12 2.50	17.22	17.22	17.22	.678	18.49	.728	.457	.018	8.668	52.75	2.08	18.39	16.74
282.968	11.57 2.60	17.68	17.68	17.68	.696	18.95	.746							
288.638	11.57 2.60	17.96	17.96	17.96	.707	19.23	.757	.279	.011	3.670	76.13	3.00	19.45	17.70
292.663	11.57 2.60	19.18	19.18	19.18	.755	20.45	.805	1.219	.048	6.025	202.36	7.97	20.13	18.32
292.663	15.57 3.50	19.18	19.18	19.18	.755	20.45	.805							
294.663	15.57 3.50	19.56	19.56	19.56	.770	20.83	.820	.381	.015	2.000	190.50	7.50	28.13	25.60
296.713	15.57 3.50	20.19	20.19	20.19	.795	21.46	.845	.635	.025	2.050	309.76	12.20	28.82	26.22
296.713	15.57 3.50	21.34	21.34	21.34	.860	23.11	.910	1.651	.065	2.030	813.30	32.02	30.47	27.73
300.758	15.57 3.50	22.66	22.66	22.66	.900	24.13	.950	1.016	.040	2.015	504.22	19.85	32.59	29.66
302.633	15.57 3.50	24.26	24.26	24.26	.955	25.53	1.005	1.397	.055	2.075	673.25	26.51	34.72	31.59
304.183	15.57 3.50	25.02	25.02	25.02	.985	26.29	1.035	.762	.030	1.350	564.44	22.22	36.82	33.51
304.943	15.57 3.50	25.65	25.65	25.65	1.010	26.92	1.060	.635	.025	.800	793.75	31.25	38.29	34.84
305.463	15.57 3.50	26.16	26.16	26.16	1.030	27.43	1.080	.504	.020	.500	1016.00	40.00	39.56	36.00
306.113	15.57 3.50	26.92	26.92	26.92	1.060	28.19	1.110	.762	.030	.660	1154.55	45.45	41.05	37.36
308.493	15.57 3.50	28.32	28.32	28.32	1.115	29.59	1.165	1.397	.055	.350	3991.43	157.14	43.81	39.87
307.103	15.57 3.50	30.10	30.10	30.10	1.185	31.37	1.235	1.778	.070	.610	2914.75	114.75	48.46	44.10
307.703	15.57 3.50	32.64	32.64	32.64	1.285	33.91	1.335	2.540	.100	.600	4233.33	166.67	56.20	51.15
308.103	15.57 3.50	33.65	33.65	33.65	1.325	34.92	1.375	1.016	.040	.400	2540.00	100.00	64.26	58.48

(WBL)SPEC.3CK.2 77-5AL-2.55V(EL1) .253 DEG.C.LH2 R=.05 F=.1 HZ 11136 AUG 05, '76

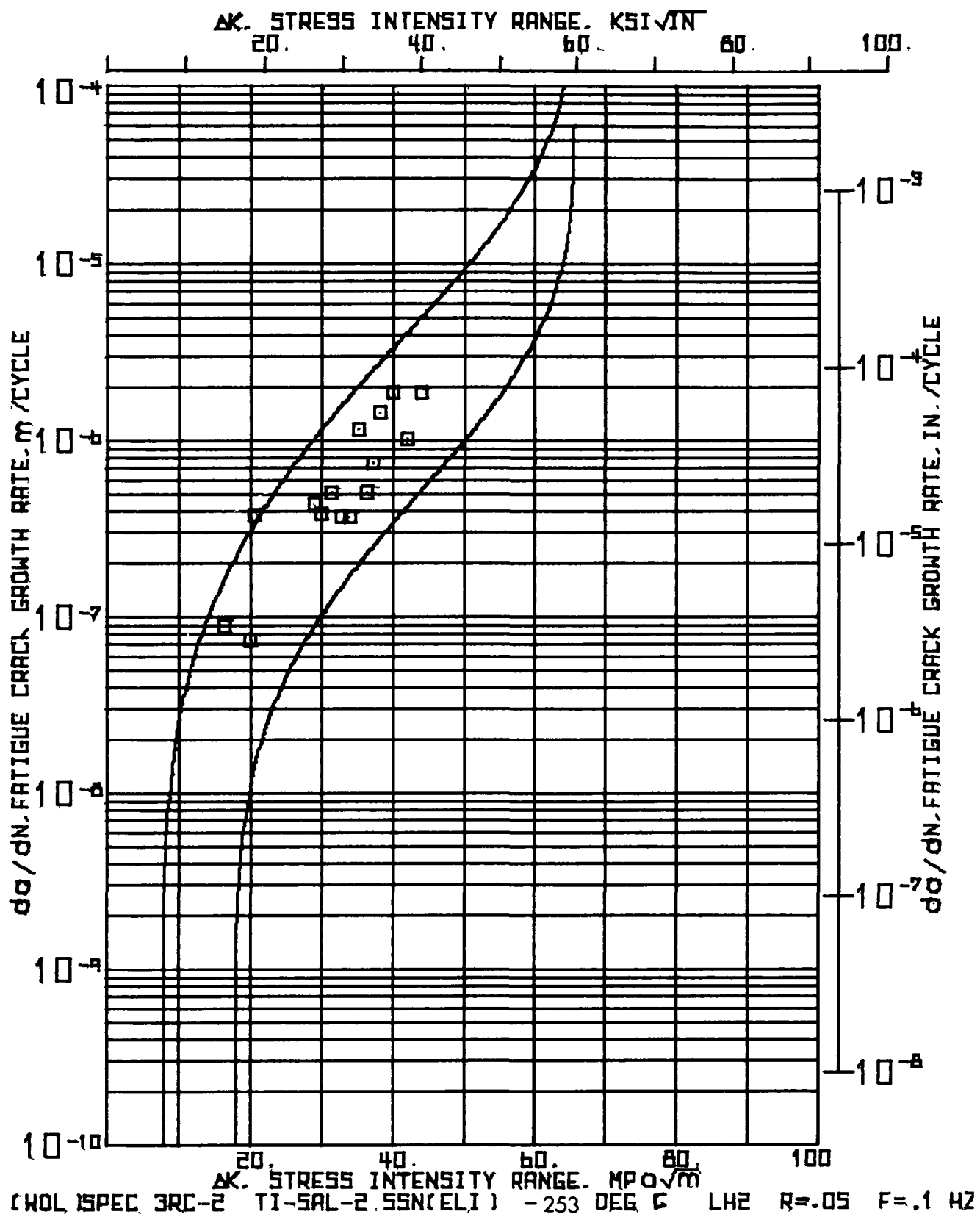
INPUT CONSTANTS

ELASTIC MODULUS(E) = 118.590E+03 MPa(17.200E+06 PSI)

NUMBER	CRACK MBUTM	ABAR / W	OPTICAL COMPLIANCE	BASF
OF	COMPLIANCE			
CYCLES				

X 1000

29.063	48.333	.409	.424
302.033	66.0652	.501	.499



11:36 AUG 05 '76

INPUT CONSTANTS:

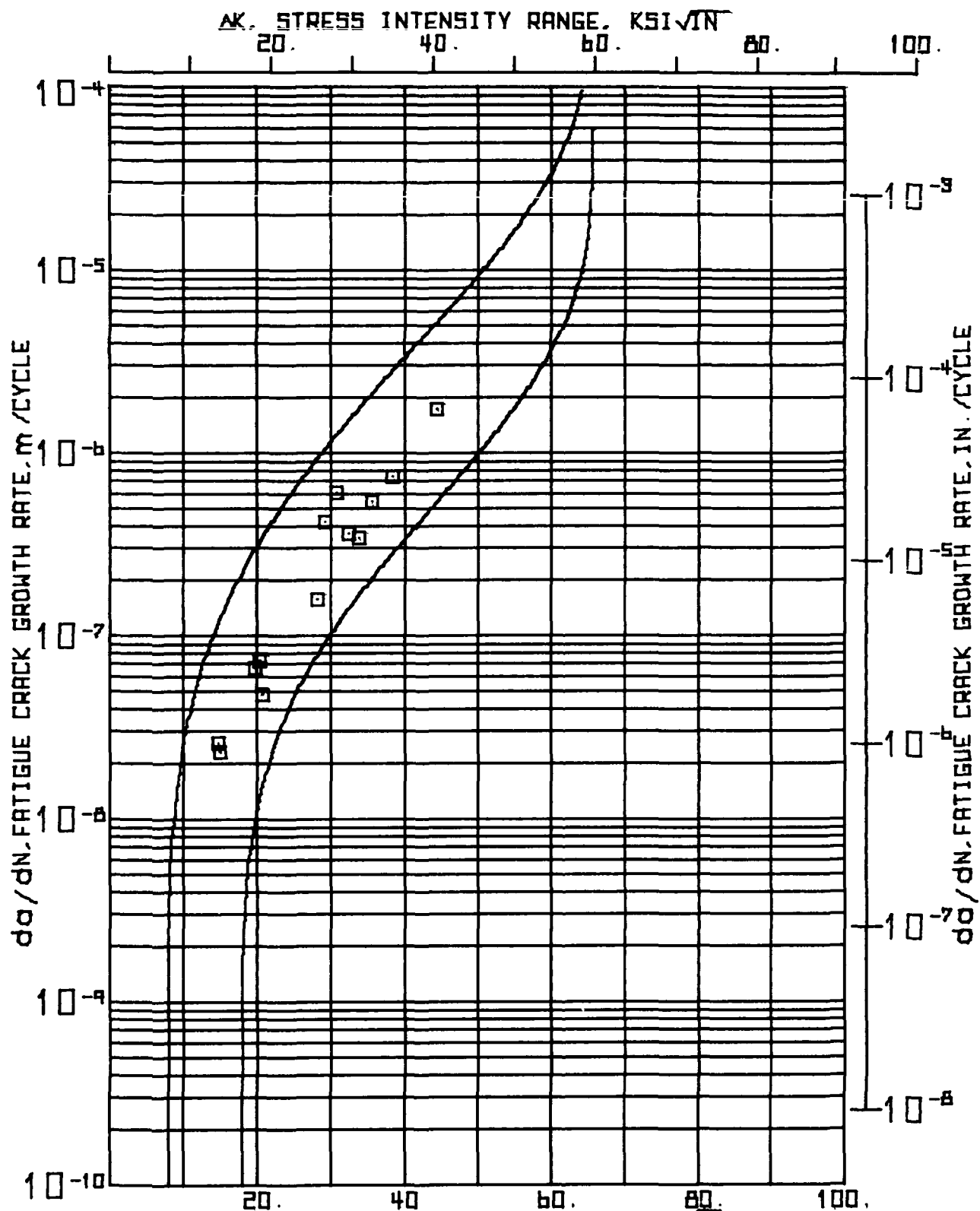
RANGE RATIO(R)	• .05
TEST FREQUENCY(HZ)	• 1
SPECIMEN WIDTH(W)	• 50.801 MM (2.002 IN.)
SPECIMEN THICKNESS(B)	• 18.887 MM (.744 IN.)
CRACK RES. CORRECTION	• 1.270 MM (.050 IN.)

NUMBER OF CYCLES	MAXIMUM LOAD	SIDE 1 CRACK LENGTH		SIDE 2 CRACK LENGTH		CORRECTED AVERAGE CRACK LENGTH		CHANGE IN CRACK LENGTH		CHANGE IN CYCLES		CRACK GROWTH RATE DA / DN		STRESS INTENSITY RANGE	
		KN	IN	MM	IN	MM	IN	MM	DA	DN	INCH X 1000	METER	MICR8 IN.	MPA X 1000.5	KSI X 1000.5
000	9.79	2.20	17.07	.672	17.07	.672	18.34	.722	.762	.030	8.660	87.99	3.46	16.33	14.86
8.660	9.79	2.20	17.63	.702	17.83	.702	19.10	.752							
8.660	11.57	2.60	17.63	.702	17.83	.702	19.10	.752							
18.335	11.57	2.60	18.54	.730	18.54	.730	19.81	.780	.711	.028	9.675	73.51	2.89	19.96	18.15
20.355	11.57	2.60	19.30	.760	19.30	.760	20.57	.810	.762	.030	2.020	377.23	14.85	20.65	18.79
20.355	15.57	3.50	19.30	.760	19.30	.760	20.57	.810							
22.405	15.57	3.50	20.19	.795	20.19	.795	21.46	.845	.889	.035	2.050	433.66	17.07	28.91	26.31
22.405	15.57	3.50	20.95	.825	20.95	.825	22.22	.875	.762	.030	2.000	381.00	15.00	30.09	27.38
22.405	15.57	3.50	21.97	.865	21.97	.865	23.24	.915	1.016	.040	2.020	502.97	19.80	31.44	28.62
22.405	15.57	3.50	22.73	.895	22.73	.895	24.00	.945	.762	.030	2.077	366.88	14.44	32.90	29.94
22.405	15.57	3.50	23.24	.915	23.24	.915	24.51	.965	.508	.020	1.365	372.16	14.65	34.01	30.95
30.632	15.57	3.50	24.13	.950	24.13	.950	25.40	1.000	.883	.035	.765	1162.09	45.75	35.29	32.12
31.132	15.57	3.50	24.36	.960	24.36	.960	25.65	1.010	.254	.010	.500	508.00	20.00	36.40	33.13
31.132	15.57	3.50	24.89	.980	24.89	.980	26.16	1.030	.506	.020	.680	747.06	29.41	37.18	33.63
32.162	15.57	3.50	25.40	1.000	25.40	1.000	26.67	1.050	.503	.020	.350	1451.43	37.14	38.25	34.81
32.772	15.57	3.50	26.34	1.045	26.34	1.045	27.61	1.095	1.143	.045	.610	1873.77	73.77	40.10	36.49
33.272	15.57	3.50	27.05	1.065	27.05	1.065	28.32	1.115	.506	.020	.500	1016.00	40.00	42.09	38.31
33.272	15.57	3.50	28.07	1.105	28.07	1.105	29.34	1.155	1.016	.040	.540	1881.48	74.07	44.08	40.12

... (MOL) SPEC. SRC=2 T1=5AL=2.55N(EL1) -253 DEG.C. LM2 R=05 F=01 HZ 11:36 AUG 05, '76

INPUT CONSTANTS

ELASTIC MODULUS(E) = 110.590E+03 MPA(17.200E+06 PSI)			
NUMBER OF CYCLES	CRACK MOUTH COMPLIANCE	ABAR / W OPTICAL COMPLIANCE	BASE BASE
N	CE3		
x 1000			
20.355	46.3635	.405	.414
20.002	59.1534	.472	.471
33.012	94.3257	.577	.574



(WOL) SPEC 35R-2 TI-5AL-2 55N(ELI) -253 DEG C LH2 R=.05 F= 1 HZ

INPUT C6\STAVTS:

RANGE MATI9(K)														
TEST FREQUENCY(MZ)														
SPECIMEN WIDTH(M)														
SPECIMEN THICKNESS(B)														
CRACK 39A CORRECTION														
.05														
.1														
50.676 MM(
18.938 MM(
1.270 MM(
.050 IN.)														
NUMBER OF CYCLES	MAXIMUM LOAD	SIZE 1 CRACK LENGTH	SIZE 2 CRACK LENGTH	SIZE 1 MM	SIZE 1 INCH	SIZE 2 MM	SIZE 2 INCH	CORRECTED AVERAGE LENGTH	CHARGE IN CRACK LENGTH	CHANGE IN CYCLES	CRACK GROWTH RATE DA / DN	STRESS INTENSITY RANGE		
N	P	A1	A2	MM	INCH	MM	INCH	MM	INCH	MM	INCH	MPA X 1000	DA X 1000	IN X 1000
300	8.90	2.00	17.30	.681	17.30	.681	18.57	.731	.152	.006	5.825	26.16	1.03	13.42
5.625	4.90	2.00	17.45	.687	17.45	.687	18.72	.737	.406	.016	17.300	23.49	.92	13.59
23.125	5.90	2.00	17.86	.703	17.86	.703	19.13	.753						
23.125	11.57	2.60	17.86	.703	17.86	.703	19.13	.753	.508	.020	7.600	66.84	2.63	18.04
30.725	11.57	2.60	18.36	.723	18.36	.723	19.63	.773	.639	.025	8.650	73.41	2.89	18.52
35.375	11.57	2.60	19.00	.743	19.00	.743	20.27	.798	.127	.005	2.650	47.92	1.89	18.85
42.025	11.57	2.60	19.13	.753	19.13	.753	20.40	.803						
42.025	15.57	3.50	19.13	.753	19.13	.753	20.40	.803	.381	.015	2.400	158.75	6.25	25.68
44.425	15.57	3.50	19.51	.768	19.51	.768	20.78	.818	1.016	.040	2.400	423.33	16.67	26.56
46.425	15.57	3.50	20.52	.808	20.52	.808	21.79	.858	1.270	.050	2.100	604.76	23.81	28.08
48.925	15.57	3.50	21.79	.858	21.79	.858	23.06	.908	.762	.030	2.100	382.86	14.29	29.56
51.025	15.57	3.50	22.56	.888	22.56	.888	23.83	.938	.762	.030	2.200	346.36	13.64	30.75
53.225	15.57	3.50	23.32	.918	23.32	.918	24.59	.968	1.143	.045	2.100	544.29	21.43	32.35
55.325	15.57	3.50	24.46	.963	24.46	.963	25.73	1.013	1.651	.065	2.200	750.45	29.55	34.95
57.525	15.57	3.50	26.11	1.028	26.11	1.028	27.38	1.078	3.302	.130	1.900	1737.89	68.42	40.47
59.425	15.57	3.50	29.41	1.158	29.41	1.158	30.68	1.238						

(K9L) SPEC.359-2 YI-SAL-2.55N(ELI) - 253 DEG.C. LH2 R=05 F=1 MZ 11:37 AUG 05, '76

INPUT CONSTANTS

ELASTIC MODULUS(E) = $110.590E+03$ MPA($17.200E+06$ PSI)

NUMBER	CRACK WIDTH	ACAR / W
OF	COMPLIANCE	OPTICAL COMPLIANCE
CYCLES	BASF	BASF

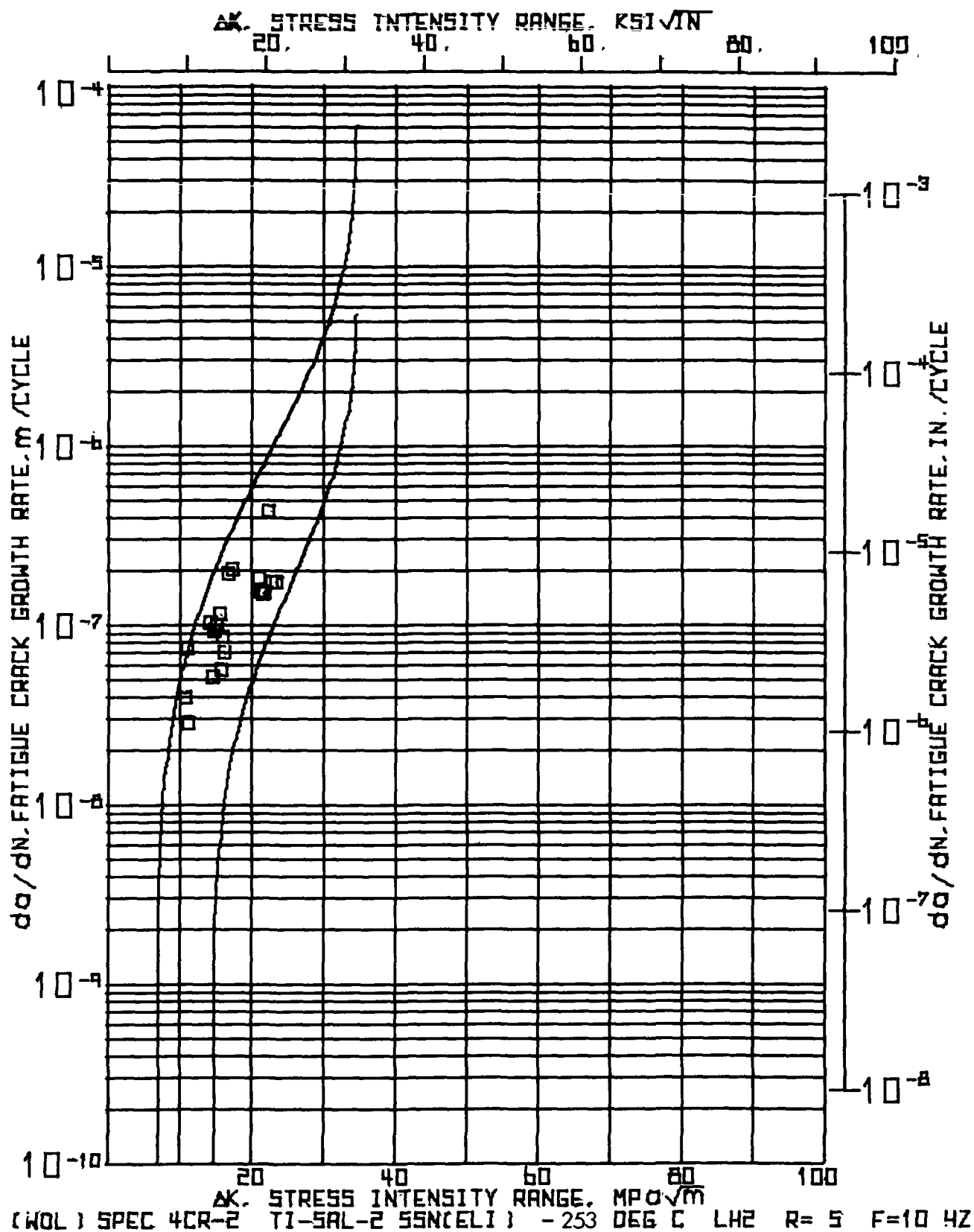
A
CEB

X 1000

42.025	45.0866	0.01	0.410
--------	---------	------	-------

SECTION A8

This section of the Appendix includes all fatigue crack growth data obtained from WOL coupons tested at -253°C , at a range ratio of 0.5, and at a frequency of 10 Hz.



(1681) SPEC. 4CR-2 T1-5AL-2.55N(ELT) * 253 DEUC. LM2 R=0.5 F=10 HZ * * * * * 16140 AUG 04, 1976

INPUT CONSTANTS:

RANGE RATIO(M) * 50
 TEST FREQUENCY(HZ) * 10.0
 SPECIMEN ATTH(M) * 50.902 MM(2.004 IN.)
 SPECIMEN THICKNESS(B) * 10.890 MM(.744 IN.)
 CRACK EA CORRECTION * 1.270 MM(.050 IN.)

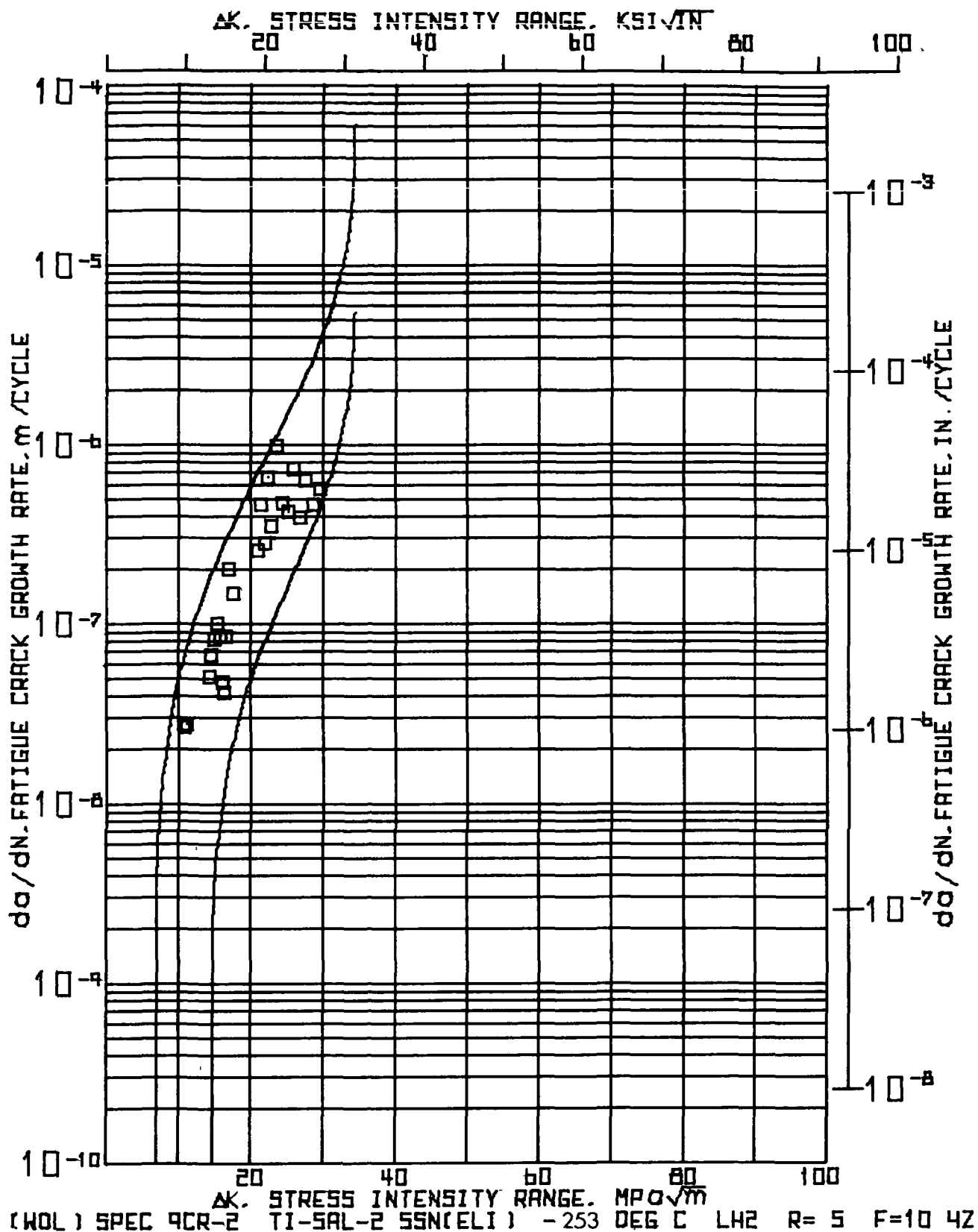
NUMBER RF CYCLES	MAXIMUM LOAD	P	SIDE 1		SIDE 2		CONNECTED AVERAGE CRACK LENGTH		CHANGE IN CRACK LENGTH		CHANGE IN CYCLES		CRACK GRBATH RATE DA / DN		STRESS INTENSITY RANGE	
			MM	INCH	MM	INCH	MM	INCH	MM	INCH	MM	INCH	MM	INCH	MPA X 10 ³	KSI X 10 ³
13.000	12.01	2.70	17.55	.691	17.55	.691	16.82	.741	.508	.020	13.000		39.08	1.54	10.70	9.74
20.000	12.01	2.70	18.57	.731	18.57	.731	19.84	.781	.508	.020	7.000		72.57	2.86	10.96	9.97
29.000	12.01	2.70	18.82	.741	18.82	.741	20.09	.791	.254	.010	9.000		28.22	1.11	11.15	10.15
34.000	15.12	3.40	19.33	.761	19.33	.761	20.60	.811	.508	.020	5.000		101.60	4.00	14.29	13.01
39.000	15.12	3.40	19.58	.771	19.58	.771	20.85	.821	.254	.010	5.000		50.80	2.00	14.55	13.24
44.000	15.12	3.40	20.09	.791	20.09	.791	21.36	.841	.508	.020	5.600		90.71	3.57	14.82	13.49
49.000	15.12	3.40	20.60	.811	20.60	.811	21.67	.861	.508	.020	5.200		97.69	3.85	15.19	13.82
54.000	15.12	3.40	21.11	.831	21.11	.831	22.36	.881	.254	.010	4.500		112.89	4.44	15.57	14.17
59.000	15.12	3.40	21.36	.841	21.36	.841	22.63	.891	.254	.010	4.600		55.22	2.17	15.87	14.44
64.000	15.12	3.40	21.62	.851	21.62	.851	22.89	.901	.254	.010	3.000		84.67	3.33	16.07	14.62
69.000	15.12	3.40	21.87	.861	21.87	.861	23.14	.911	.254	.010	3.700		68.65	2.70	16.28	14.81
74.000	15.12	3.40	22.89	.901	22.89	.901	24.16	.951	1.016	.040	5.300		191.70	7.55	16.81	15.30
79.000	15.12	3.40	23.39	.921	23.39	.921	24.66	.971	.508	.020	2.500		203.29	8.00	17.49	15.92
84.000	17.79	4.00	23.39	.921	23.39	.921	24.66	.971	.254	.010	1.400		181.43	7.14	21.00	19.11
89.000	17.79	4.00	23.65	.931	23.65	.931	24.92	.981	.254	.010	1.665		152.55	6.01	21.29	19.37
94.000	17.79	4.00	23.90	.941	23.90	.941	25.17	.991	.254	.010	1.720		147.67	5.81	21.58	19.64
99.000	17.79	4.00	24.41	.961	24.41	.961	25.68	1.011	.254	.010	1.685		150.74	5.93	21.88	19.91

CYCLES	N	X 1000	P	KV	KIPS	SIDE 1		SIDE 2		CORRECTED		CHANGE		CHANGE		CRACK GROWTH		STRESS	
						MM	INCH	MM	INCH	MM	INCH	MM	INCH	MM	INCH	DA / DN	IN.	MPA X 1000	KSI X 1000
						A1		A2		LENGTH		LENGTH		LENGTH		METER			
																PER CYCLE			
79.870	17.79	4.00	24.91	.981	.261	25.68	1.011	.508	.020	1.175	432.34	17.02	22.35	20.34					
81.045	17.79	4.00	24.92	.981	24.92	.981	26.19	1.031	.254	.010	1.500	169.33	6.67	22.83	20.77				
82.545	17.79	4.00	25.17	.991	25.17	.991	26.44	1.041	.508	.020	3.000	169.33	6.67	23.32	21.22				
85.545	17.79	4.00	25.68	1.011	25.68	1.011	26.95	1.061											

```

(NDL) SPEC+ACR+2  T1=5AL+2+5SN(ELI)  =253 DEG.C. LHR  H=5.5 F=10.MZ  ...  16140 AUG 04,176
INPUT CONSTANTS
-----
ELASTIC MODULUS(E) = 118.590E+03 MPA( 17.200E+06 PSI)
-----
NUMBER  CRACK WIDTH  ABAR / "  -----
BF  COMPLIANCE  OPTICAL  COMPLIANCE  -----
CYCLES  BASE  BASE
N  C/D
x 1000
5+300  61.5598  .440  .440

```



WELDGE-8 P E N L O A D P R O G R A M * *
 16141 AUG 04, 1976

INPUT CONSTANTS:

RANGE RATIO(R) * .50
 TEST FREQUENCY(HZ) * 10.0
 SPECIMEN WIDTH(W) * 51.003 MM(2.008 IN.)
 SPECIMEN THICKNESS(B) * 18.981 MM(.747 IN.)
 CRACK 99% CORRECTION * 1.270 MM(.050 IN.)

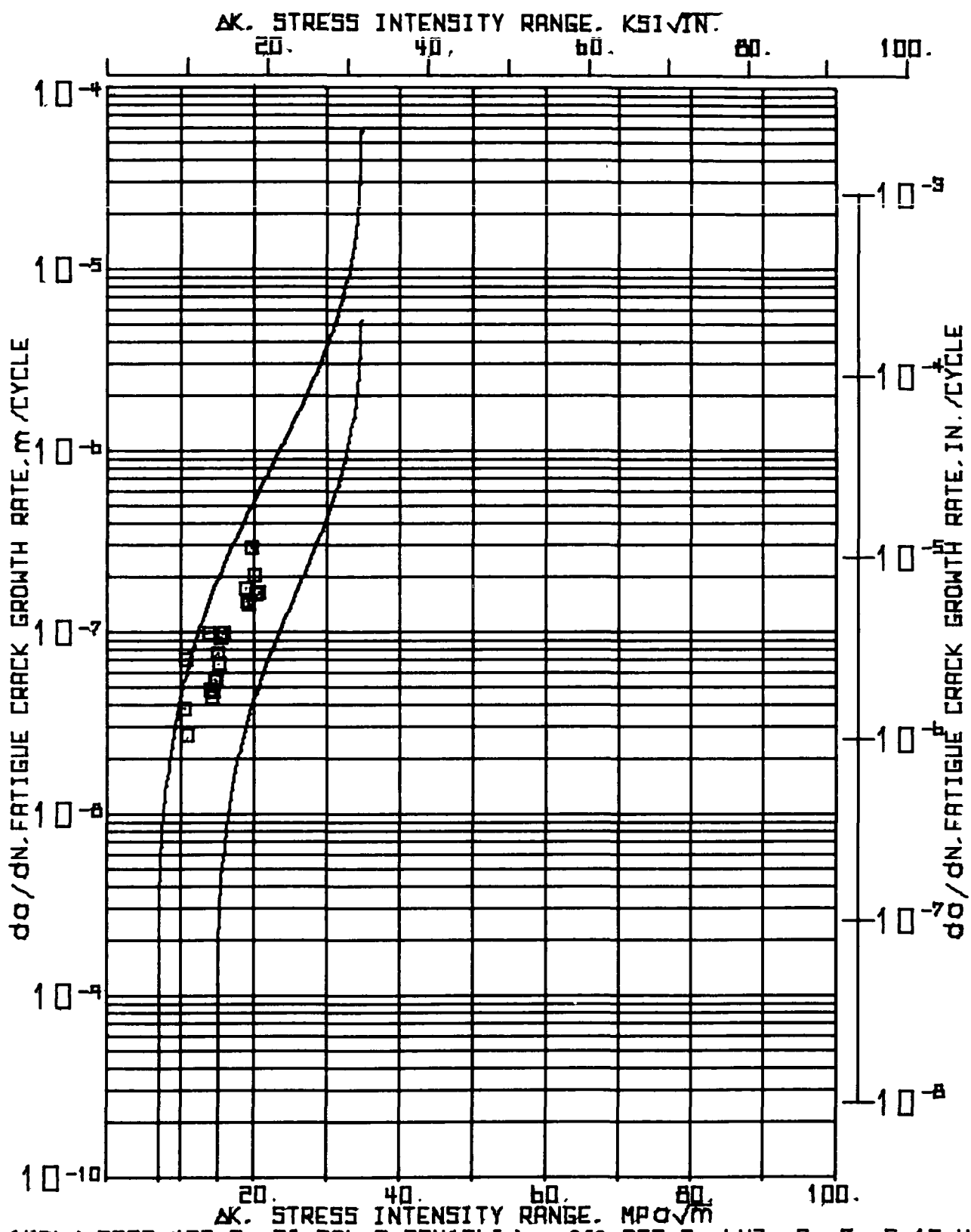
NUMBER OF CYCLES	P KN	MAXIMUM LOAD KIPS	SIDE 1 CRACK LENGTH		SIDE 2 CRACK LENGTH		CORRECTED AVERAGE CRACK LENGTH		CHANGE IN CRACK LENGTH		CHANGE IN CYCLES		CRACK GROWTH RATE DA / DN MICR METER IN.		STRESS INTENSITY RANGE DELTA K MPA X KSI X IN ^{3/2}	
			MM	INCH	MM	INCH	MM	INCH	MM	INCH	DN X 1000	PER CYCLE				
000	12.01	2.70	14.01	.709	18.01	.709	19.24	.759	.508	.020	19.000		26.74	1.05	10.85	9.87
19.000	12.01	2.70	14.02	.729	18.52	.729	19.79	.779	.508	.020	18.500		27.46	1.08	11.10	10.11
37.500	12.01	2.70	19.02	.749	19.02	.749	20.29	.799								
37.500	15.12	3.40	19.02	.749	19.02	.749	20.29	.799	.508	.020	10.100		50.30	1.98	14.32	13.03
47.800	15.12	3.40	19.53	.769	19.53	.769	20.80	.819	.508	.020	7.600		66.84	2.63	14.67	13.35
55.200	15.12	3.40	20.04	.789	20.04	.789	21.31	.839	.508	.020	6.200		81.94	3.23	15.03	13.68
61.400	15.12	3.40	20.55	.809	20.55	.809	21.82	.859	.508	.020	5.100		99.61	3.92	15.41	14.02
66.500	15.12	3.40	21.06	.829	21.06	.829	22.33	.879	.508	.020	6.000		84.67	3.33	15.80	14.38
72.500	15.12	3.40	21.56	.849	21.56	.849	22.83	.899	.254	.010	5.400		47.04	1.85	16.10	14.65
77.900	15.12	3.40	21.82	.859	21.82	.859	23.09	.909	.254	.010	6.100		41.64	1.64	16.31	14.84
84.000	15.12	3.40	22.07	.869	22.07	.869	23.34	.919	.508	.020	6.000		84.67	3.33	16.63	15.12
90.500	15.12	3.40	22.56	.889	22.56	.889	23.85	.939	.508	.020	2.500		203.20	8.00	17.07	15.54
92.500	15.12	3.40	23.09	.909	23.09	.909	24.36	.959	.508	.020	3.480		145.98	5.75	17.53	15.96
95.240	15.12	3.40	23.00	.929	23.00	.929	24.47	.979	.254	.010						
95.960	17.79	4.00	23.60	.929	23.60	.929	24.87	.979	.254	.010	1.000		254.00	10.00	21.05	19.16
96.960	17.79	4.00	23.65	.939	23.65	.939	25.12	.989	.508	.020	1.100		461.82	18.18	21.49	19.55
98.080	17.79	4.00	24.36	.959	24.36	.959	25.63	1.009	.254	.010	.900		282.22	11.11	21.94	19.96
98.960	17.79	4.00	24.01	.969	24.01	.969	25.88	1.019	.508	.020	.775		655.48	25.81	22.40	20.39
99.755	17.79	4.00	25.12	.989	25.12	.989	26.39	1.039	.254	.010	.720		352.78	13.89	22.89	20.83
100.475	17.79	4.00	25.37	.999	25.37	.999	26.64	1.049								

16141 AUG 04, 1976																	PAGE 2	
11-5AL-2-55N(EL1) - 253 DEG.C. LH2 R=5 F=10 HZ																		
NUMBER OF CYCLES	MAXIMUM LOAD	P	SIDE 1 CRACK LENGTH		SIDE 2 CRACK LENGTH		CORRECTED AVERAGE CRACK LENGTH		CHANGE IN CRACK LENGTH		CHANGE IN CYCLES	CRACK GROWTH RATE		STRESS INTENSITY RANGE				
			MM	INCH	MM	INCH	MM	INCH	MM	INCH		MM	INCH	MM	INCH	MPA X 1000	DELTA K IN	
100.075	17.79	4.00	26.37	.999	25.37	.999	26.64	1.049	.762	.030	.770	989.61	38.96	23.56	21.44			
101.245	17.79	4.00	26.14	1.029	26.14	1.029	27.41	1.079	.504	.020	1.080	470.37	18.52	24.44	22.24			
102.325	17.79	4.00	26.64	1.049	26.64	1.049	27.91	1.099	.504	.020	1.200	423.33	16.67	25.14	22.92			
103.025	17.79	4.00	27.15	1.069	27.15	1.069	28.42	1.119	.504	.020	.700	725.71	28.57	25.96	23.63			
104.225	17.79	4.00	27.66	1.089	27.66	1.089	28.93	1.139	.504	.020	1.300	390.77	15.34	26.79	24.38			
105.525	17.79	4.00	28.17	1.109	28.17	1.109	29.44	1.159	.504	.020	.800	635.00	25.00	27.65	25.16			
106.325	17.79	4.00	28.68	1.129	28.68	1.129	29.95	1.179	.504	.020	1.100	461.82	18.18	28.56	25.99			
107.425	17.79	4.00	29.18	1.149	29.18	1.149	30.45	1.199	.504	.020	.900	564.44	22.22	29.52	26.87			
108.325	17.79	4.00	29.69	1.169	29.69	1.169	30.96	1.219										

(*BL) SPEC.9CR-2 T1-5AL-2.5SN(ELI) - 253 DEG.C. LM2 R-15 F-10 MZ ----- 16141 AUG 04, 1976

INPUT CONSTANTS

ELASTIC MODULUS(E) = 115.590E+03 MPA(17.200E+06 PSI)				
NUMBER	CRACK MBUTM	ABAK / "		
OF	COMPLIANCE	OPTICAL	COMPLIANCE	
CYCLES	BASE	BASE	BASE	
N	CEB			
X 1000				
61.000	43.5808	.424	.398	



(WOL) SPEC 4RC-2 T1-SAL-2.55N(ELI) -253 DEG C LH2 R=.5 F=10 HZ

(ASLT) SPECIMEN C-2 T1-5AL-2.5SN(ELT) -253 DEG.C. LW2 K=0.5 F=10 HZ 16:41 AUG 04, 1976

INPUT CONSTANTS:

RANGE RATIO(R) ■ .50
 TEST FREQUENCY(HZ) ■ 10.0
 SPECIMEN WIDTH(W) ■ 50.876 MM(2.003 IN.)
 SPECIMEN THICKNESS(B) ■ 18.561 MM(.746 IN.)
 CRACK BSW CORRECTION ■ 1.270 MM(.050 IN.)

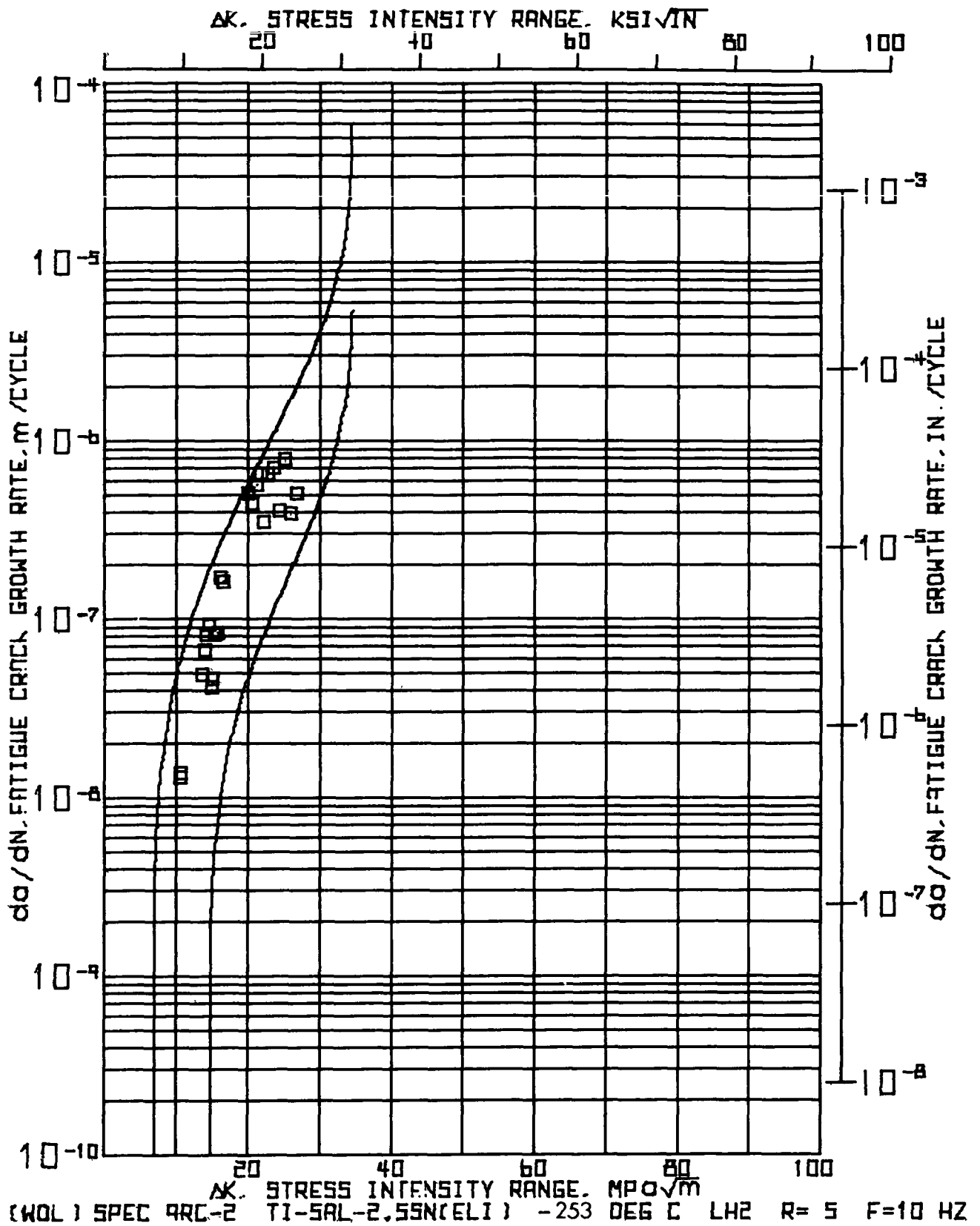
NUMBER OF CYCLES	P KN	MAXIMUM LOAD KIPS	SIDE 1 CRACK LENGTH		SIDE 2 CRACK LENGTH		CORRECTED AVERAGE CRACK LENGTH		CHANGE IN CRACK LENGTH		CHANGE IN CYCLES		CRACK GROWTH RATE DA / DN MICRONS IN.		STRESS INTENSITY RANGE MPA X DELTA K KSI X	
			A1 MM	INCH	A2 MM	INCH	MM	INCH	MM	INCH	DN X 1000	PER CYCLE	IN.	IN.	400.5	1000.5
X 1.00	1.00	1.00	16.92	.666	16.92	.666	18.19	.716	.508	.020	13.000	39.08	1.54	10.37	9.44	
13.000	12.01	2.70	17.42	.686	17.42	.686	18.69	.736	.508	.020	7.000	72.57	2.86	10.61	9.66	
20.000	12.01	2.70	17.93	.706	17.93	.706	19.20	.756	.254	.010	9.000	28.22	1.11	10.80	9.82	
29.000	12.01	2.70	18.19	.716	18.19	.716	19.46	.766	.508	.020	5.000	101.60	4.00	13.83	12.59	
34.000	15.12	3.40	18.69	.736	18.69	.736	19.96	.786	.254	.010	5.100	49.80	1.96	14.08	12.81	
35.100	15.12	3.40	18.95	.746	18.95	.746	20.22	.796	.254	.010	5.600	45.36	1.79	14.25	12.97	
44.700	15.12	3.40	19.20	.756	19.20	.756	20.47	.806	.254	.010	5.200	48.85	1.92	14.42	13.12	
45.900	15.12	3.40	19.46	.766	19.46	.766	20.73	.816	.254	.010	4.500	56.44	2.22	14.60	13.28	
54.400	15.12	3.40	19.71	.776	19.71	.776	20.98	.826	.254	.010	4.600	55.22	2.17	14.77	13.45	
53.000	15.12	3.40	19.96	.786	19.96	.786	21.23	.836	.254	.010	3.200	79.37	3.12	14.96	13.61	
62.200	15.12	3.40	20.22	.796	20.22	.796	21.49	.846	.254	.010	3.700	68.65	2.70	15.14	13.78	
65.900	15.12	3.40	20.47	.806	20.47	.806	21.74	.856	.508	.020	5.300	95.85	3.77	15.43	14.04	
71.200	15.12	3.40	20.98	.826	20.98	.826	22.25	.876	.254	.010	2.500	101.60	4.00	15.72	14.31	
73.700	15.12	3.40	21.23	.836	21.23	.836	22.50	.886	.254	.010	1.400	181.43	7.14	18.73	17.04	
73.700	17.79	4.00	21.23	.836	21.23	.836	22.50	.886	.254	.010	1.670	152.10	5.99	18.97	17.26	
75.100	17.79	4.00	21.49	.846	21.49	.846	22.76	.896	.254	.010	1.740	145.98	5.75	19.21	17.49	
76.770	17.79	4.00	21.74	.856	21.74	.856	23.01	.906	.508	.020	1.680	302.38	11.90	19.59	17.83	
78.510	17.79	4.00	22.00	.866	22.00	.866	23.27	.916								
80.130	17.79	4.00	22.50	.886	22.50	.886	23.77	.936								

NUMBER OF CYCLES	MAXIMUM LOAD	SIDE 1		SIDE 2		CORRECTED AVERAGE		CHANGE IN		CHANGE IN		CRACK GRWTH RATE		STRESS INTENSITY	
		CRACK LENGTH	MM	CRACK LENGTH	MM	CRACK LENGTH	MM	CRACK LENGTH	MM	CRACK LENGTH	DA	DA / DN	DA / DN	MPA X DELTA K	INCH X INCH
N	P	A1	MM	A2	MM	ABAR	MM	DA	MM	DN	INCH X 1000	NANO- METER	MICRON IN.		
X 1000	KIPS														
80,190	17.79	22.50	.886	22.50	.886	23.77	.936	.254	.010	1.190		213.45	8.40	19.95	18.18
81,360	17.79	22.76	.896	22.76	.896	24.03	.946	.254	.010	1.520		167.11	6.58	20.25	18.43
82,500	17.79	23.01	.906	23.01	.906	24.28	.956	.508	.020	3.000		169.33	6.67	20.66	18.80
83,500	17.79	23.52	.926	23.52	.926	24.79	.976								

(#BL) SPEC. #RC-2 T1-SAL-2.55N(ELI) - 253 DEUC. LM2 R#5 F#10 MZ 16141 AUG 04, '76

INPUT CONSTANTS

ELASTIC MODULUS(E) = 110.590E+03 MPA(17.200E+06 PSI)			
NUMBER	CRACK MOUTH	ABAR / W	
OF	COMPLIANCE	OPTICAL	COMPLIANCE
CYCLES	BASE	BASE	
N	CEP		
x 1000			
85.900	52.1617	.087	.442



(148L) SPEC:9AC-2 T1-SAL-2.55N(ELI) - 253 DEG.C. LM2 N=0.5 F=10 HZ - 16:42 AUG 04, 1976

INPUT CONSTANTS:

RANGE RATIO(R) = .50
 TEST FREQUENCY(HZ) = 10.0
 SPECIMEN WIDTH(W) = 51.054 MM(2.010 IN.)
 SPECIMEN THICKNESS(B) = 18.915 MM(.745 IN.)
 CRACK BV. CORRECTION = 1.270 MM(.050 IN.)

NUMBER OF CYCLES	MAXIMUM LOAD	SIDE 1 CRACK LENGTH	SIDE 2 CRACK LENGTH	CORRECTED AVERAGE CRACK LENGTH	CHANGE IN CRACK LENGTH	CHANGE IN CYCLES	CRACK GROWTH RATE DA / DN	STRESS INTENSITY RANGE DELTA K
N	P	A1	A2	ADAR	MM	DN	METER IN.	MPA X KSI X IN ^{3/2}
X 1000	KIPS	MM	MM	MM	INCH	X 1000	PER CYCLE	
600	12.01 2.70	17.42	17.42	.686	.736	.254	.010 19.500	13.03 .51 10.53 9.58
19.500	12.01 2.70	17.00	17.68	.696	.746	.254	.010 18.600	13.66 .54 10.65 9.69
30.100	12.01 2.70	17.93	17.93	.706	.756			
36.100	15.12 3.40	17.93	17.93	.706	.756	.508	.020 10.500	48.38 1.90 13.64 12.41
40.600	15.12 3.40	18.44	18.44	.726	.776	.508	.020 7.650	66.41 2.61 13.96 12.71
56.250	15.12 3.40	18.95	18.95	.746	.796	.504	.020 6.250	81.28 3.20 14.30 13.01
62.500	15.12 3.40	19.46	19.46	.766	.816	.504	.020 5.500	92.36 3.64 14.64 13.33
68.000	15.12 3.40	19.96	19.96	.786	.836	.254	.010 6.100	41.64 1.64 14.91 13.57
74.100	15.12 3.40	20.22	20.22	.796	.846	.254	.010 5.500	46.18 1.82 15.10 13.74
79.600	15.12 3.40	20.47	20.47	.806	.856	.504	.020 6.200	81.94 3.23 15.38 13.99
85.800	15.12 3.40	20.98	20.98	.826	.876	.504	.020 6.100	83.28 3.28 15.77 14.35
91.900	15.12 3.40	21.49	21.49	.846	.896	.504	.020 3.000	169.33 6.67 16.17 14.72
94.900	15.12 3.40	22.00	22.00	.866	.916	.559	.022 3.450	161.97 6.38 16.62 15.12
98.350	15.12 3.40	22.56	22.56	.886	.936			
96.350	17.79 4.00	22.56	22.56	.888	.938	.504	.020 1.000	508.00 20.00 20.09 18.29
99.350	17.79 4.00	23.06	23.06	.904	.958	.504	.020 1.150	441.74 17.39 20.64 18.78
100.500	17.79 4.00	23.57	23.57	.928	.978	.504	.020 .900	564.44 22.22 21.20 19.29
101.400	17.79 4.00	24.08	24.08	.948	.998	.504	.020 .770	659.74 25.97 21.79 19.83
102.170	17.79 4.00	24.59	24.59	.968	1.018	.254	.010 .720	352.78 13.89 22.25 20.25
102.590	17.79 4.00	24.64	24.64	.974	1.028			

NUMBER OF CYCLES	MAXIMUM LOAD	SIDE 1 CRACK LENGTH		SIDE 2 CRACK LENGTH		CORRECTED AVERAGE LENGTH		CHANGE IN CRACK LENGTH		CHANGE IN CYCLES		CRACK GROWTH RATE		STRESS INTENSITY RANGE	
		MM	INCH	MM	INCH	MM	INCH	MM	INCH	DN X 1000	DA METER	DA / DN PER CYCLE	MPA X 1000	DELTA K IN005	KSI X 1000
102090	17.79	24.84	.978	24.84	.978	26.11	1.028	.508	.020	.775	.655.48	25.81	22.73	20.68	
103665	17.79	25.35	.998	25.35	.998	26.62	1.048	.762	.030	1.085	702.30	27.65	23.56	21.44	
104750	17.79	26.11	1.028	26.11	1.028	27.34	1.078	.508	.020	1.250	406.40	16.00	24.44	22.24	
106200	17.79	26.62	1.048	26.62	1.048	27.89	1.098	.508	.020	.650	781.54	30.77	25.18	22.91	
106650	17.79	27.13	1.068	27.13	1.068	28.40	1.118	.508	.020	1.300	390.77	15.38	25.96	23.62	
107350	17.79	27.64	1.088	27.64	1.088	28.91	1.138	.508	.020	1.000	508.00	20.00	26.78	24.37	
108950	17.79	28.14	1.108	28.14	1.108	29.41	1.158								

```

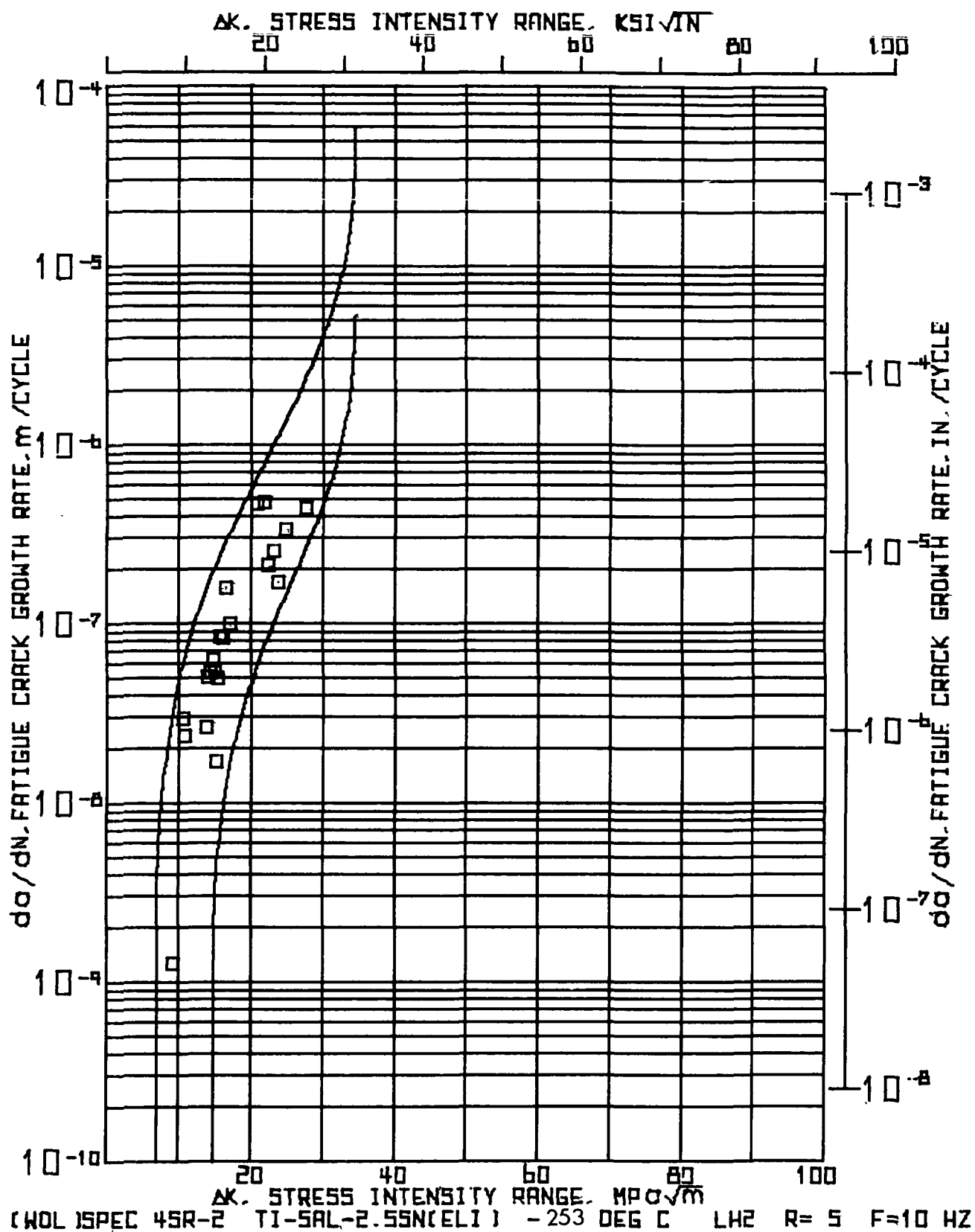
(101) SPEC,9RC=2  T1=5AL=2.55SN(EL1)  = 253 DEG.C LM2  R=0.5  F=10 M7
16142 AUG 04,176

INPUT CONSTANTS

ELASTIC MODULUS(E) = 110.590E+03 MPA( 17.200E+06 PSI)

NUMBER  CRACK 00UTM  ABAR / W
----- BF  COMPLIANCE  OPTICAL  COMPLIANCE
CYCLES  BASE  BASE
N
x 1000
----- 62.500  .. 43.2298  .. 0.06  .. 0.397

```



[illegible]

NUMBER OF CYCLES	MAXIMUM LOAD	SIDE 1 CRACK LENGTH	SIDE 2 CRACK LENGTH	CORRECTED AVERAGE CRACK LENGTH	CHANGE IN CRACK LENGTH	CHANGE IN CYCLES	CRACK GRWTH RATE DA / DN	STRESS INTENSITY RANGE
	P	A1	A2	MM	MM	DN	NANO METER	MPA X KST X INCH X INCH X INCH X
225.972	17.79 4.00	24.56	.967	24.56	.967	25.63	1.017	22.48
231.370	17.79 4.00	25.07	.987	25.07	.987	26.34	1.037	20.46
233.370	17.79 4.00	25.58	1.007	25.58	1.007	26.85	1.057	23.13
235.370	17.75 4.00	26.09	1.027	26.09	1.027	27.36	1.077	21.05
239.370	17.79 4.00	27.10	1.067	27.10	1.067	28.37	1.117	23.81
244.470	17.79 4.00	29.39	1.157	29.39	1.157	30.66	1.207	21.67
								22.66
								24.90
								27.54
								25.06

1.0015PEC+SR=2 T1=3AL=2.55V(EL1) = 253 DEG.C. LM2 M=5 F=10 Hz 16:42 AUG 04, '76

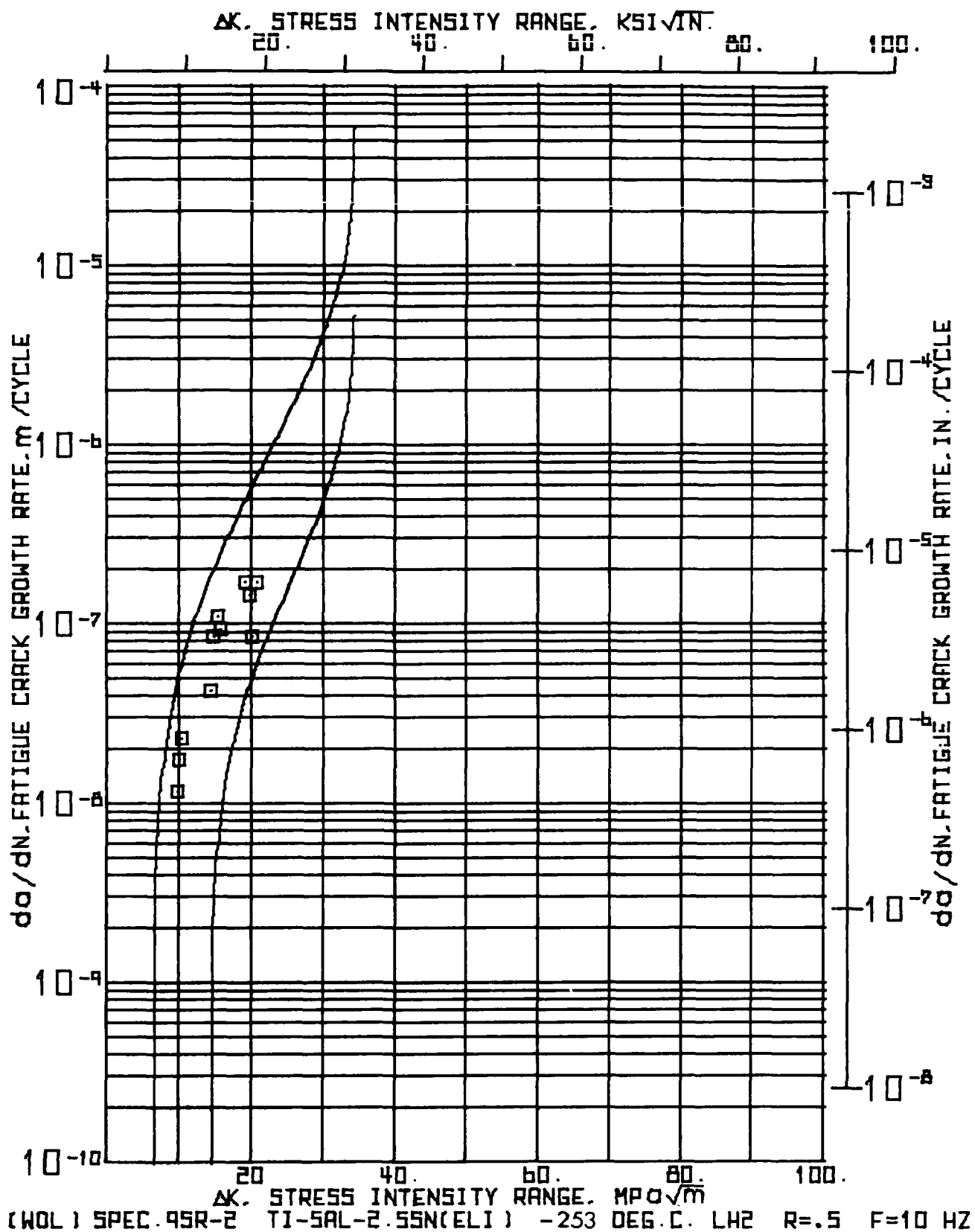
INPUT CONSTANTS

ELASTIC MODULUS(E) = 118.59CE+03 MPA(17.200E+06 PSI)

NUMBER	CRACK MOUTH	ABAR / W	OPTICAL COMPLIANCE
OF	COMPLIANCE	BASE	BASE
CYCLES			
N	CEB		

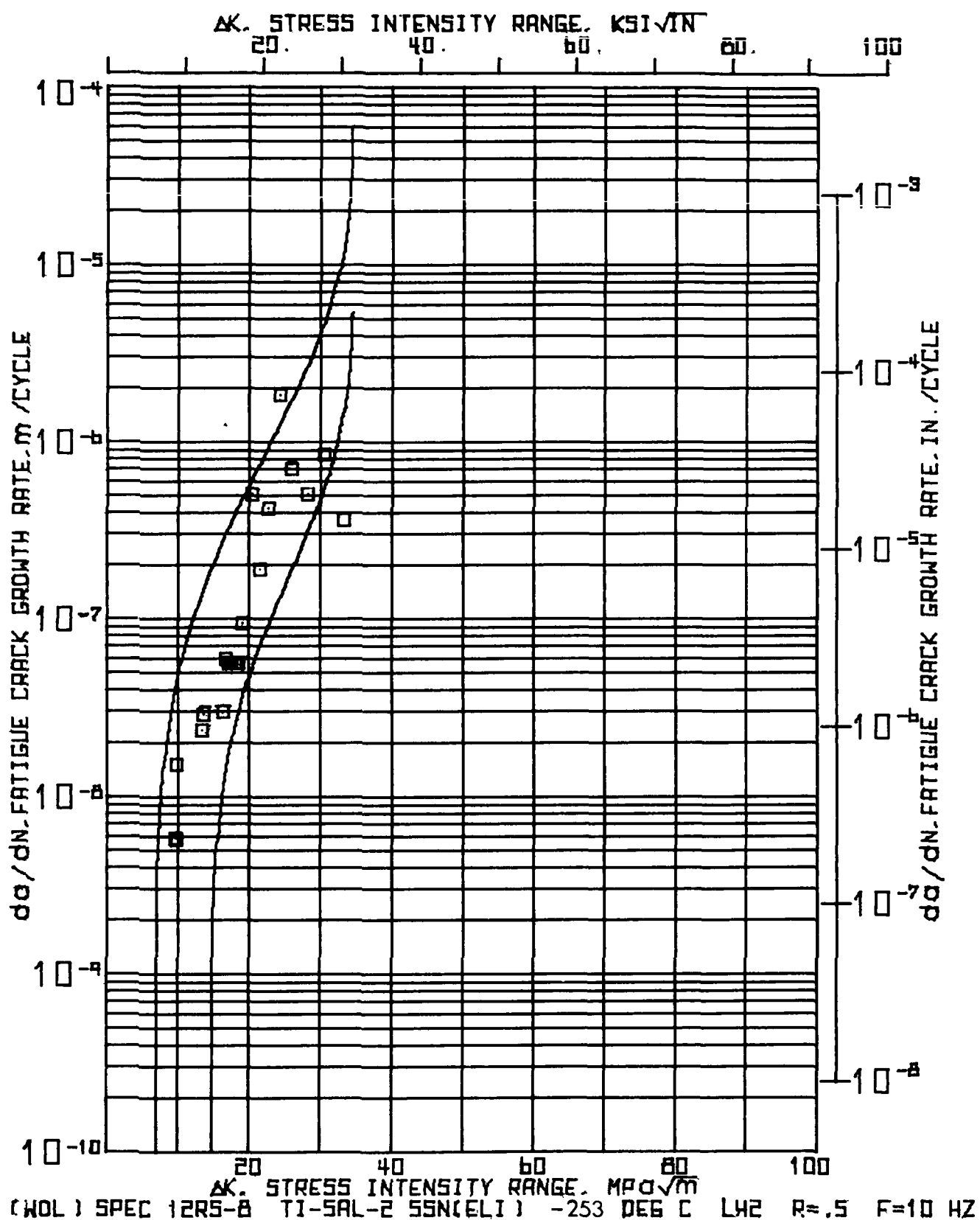
X 1000

160.050	47.2833	.423	.416
---------	---------	------	------



INPUT CONSTANTS:

RANGE RATIO(R)																
TEST FREQUENCY(HZ)																
SPECIMEN WIDTH(W)																
SPECIMEN THICKNESS(B)																
CRACK BR. CORRECTION																
.50																
10.0																
51.079 MM(2.011 IN.)																
18.893 MM(.744 IN.)																
1.270 MM(.050 IN.)																
NUMBER OF CYCLES	MAXIMUM LOAD	P	SIDE 1 CRACK LENGTH		SIDE 2 CRACK LENGTH		CONNECTED AVERAGE CRACK LENGTH		CHANGE IN CRACK LENGTH	CHANGE IN CYCLES	CRACK GROWTH RATE DA / DN	STRESS INTENSITY RANGE				
N	KN	KIPS	A1	MM	A2	INCH	MM	INCH	MM	INCH X 1000	NANO METER	MICRONS IN.	MPA X DELTA X			
X 1000											PER CYCLE		INCHES			
1000	11.34	2.55	17.73	.698	17.73	.698	19.00	.748	.508	.020	43.500	11.68	10.14			
43.500	11.34	2.55	18.24	.718	18.24	.718	19.51	.768	.762	.030	44.000	17.32	10.44			
87.500	11.34	2.55	19.00	.748	19.00	.748	20.27	.798	.762	.030	33.200	22.95	10.82			
125.700	11.34	2.55	19.76	.778	19.76	.778	21.03	.828					9.84			
125.700	15.12	3.40	19.76	.778	19.76	.778	21.03	.828	.508	.020	12.000	42.33	14.86			
152.700	15.12	3.40	20.27	.798	20.27	.798	21.54	.848	.508	.020	6.000	84.67	15.23			
135.700	15.12	3.40	20.78	.818	20.78	.818	22.05	.868	.762	.030	7.000	108.86	15.71			
145.700	15.12	3.40	21.54	.848	21.54	.848	22.81	.898	.508	.020	5.500	92.36	16.22			
151.200	15.12	3.40	22.05	.868	22.05	.868	23.32	.918					14.76			
151.200	17.79	4.00	22.05	.868	22.05	.868	23.32	.918	.508	.020	3.000	169.33	19.58			
155.200	17.79	4.00	22.56	.888	22.56	.888	23.83	.948	.508	.020	3.500	145.14	20.10			
157.700	17.79	4.00	23.06	.908	23.06	.908	24.33	.958	.254	.010	3.000	84.67	20.50			
160.700	17.79	4.00	23.32	.918	23.32	.918	24.59	.968	1.016	.040	6.000	169.33	21.21			
166.700	17.79	4.00	24.33	.958	24.33	.958	25.60	1.008					19.30			



(MUL) SPEC.12RS-8 T1-5AL-2-SSN(EL1) -253 DFG.C. LH2 R-0.5 F-10 MZ
 10:15 AUG 05, 1976

INPUT CONSTANTS:

RANGE RATIO(M) • .50
 TEST FREQUENCY(HZ) • 10.0
 SPECIMEN WIDTH(W) • 50.724 MM(1.997 IN.)
 SPECIMEN THICKNESS(B) • 19.017 MM(.749 IN.)
 CRACK BGA CORRECTION • 1.270 MM(.050 IN.)

NUMBER OF CYCLES	MAXIMUM LOAD	SIDE 1 CRACK LENGTH	SIDE 2 CRACK LENGTH	CRACK AVERAGE LENGTH	CHANGE IN CRACK LENGTH	CHANGE IN CYCLES	CRACK GROWTH RATE DA / DN	STRESS INTENSITY RANGE
X 1000	KN	MM	MM	MM	MM	DN X 1000	METER INCH	MPA X KSI X INCH ^{3/2}
000	11.34 2.55	16.59	.653	16.59	.653	17.06	.703	
43.500	11.34 2.55	16.84	.663	16.84	.663	18.11	.713	9.61 8.74
57.500	11.34 2.55	17.09	.673	17.09	.673	18.36	.723	9.72 8.84
120.500	11.34 2.55	17.60	.693	17.60	.693	18.07	.743	9.88 8.99
120.500	15.12 3.40	17.60	.693	17.60	.693	18.67	.743	
138.500	15.12 3.40	17.98	.708	17.98	.708	19.25	.758	13.45 12.24
149.700	15.12 3.40	18.36	.723	18.36	.723	19.63	.773	13.68 12.45
149.700	17.79 4.00	18.36	.723	18.36	.723	19.63	.773	
166.500	17.79 4.00	18.87	.743	18.87	.743	20.14	.793	16.43 14.95
175.000	17.79 4.00	19.38	.763	19.38	.763	20.65	.813	16.83 15.32
184.000	17.79 4.00	19.89	.783	19.89	.783	21.16	.833	17.24 15.69
193.000	17.79 4.00	20.40	.803	20.40	.803	21.67	.853	17.67 16.08
202.000	17.79 4.00	20.90	.823	20.90	.823	22.17	.873	18.11 16.48
211.000	17.79 4.00	21.41	.843	21.41	.843	22.68	.893	18.53 16.90
219.000	17.79 4.00	22.17	.873	22.17	.873	23.44	.923	19.13 17.46
228.000	17.79 4.00	23.70	.933	23.70	.933	24.97	.983	20.35 18.52
228.000	17.79 4.00	24.46	.963	24.46	.963	25.73	1.013	21.64 19.69
229.000	17.79 4.00	25.73	1.013	25.73	1.013	27.00	1.063	22.90 20.84
229.500	17.79 4.00	26.64	1.049	26.64	1.049	27.91	1.099	24.39 22.19
231.000	17.79 4.00	27.91	1.099	27.91	1.099	29.18	1.149	26.04 23.69

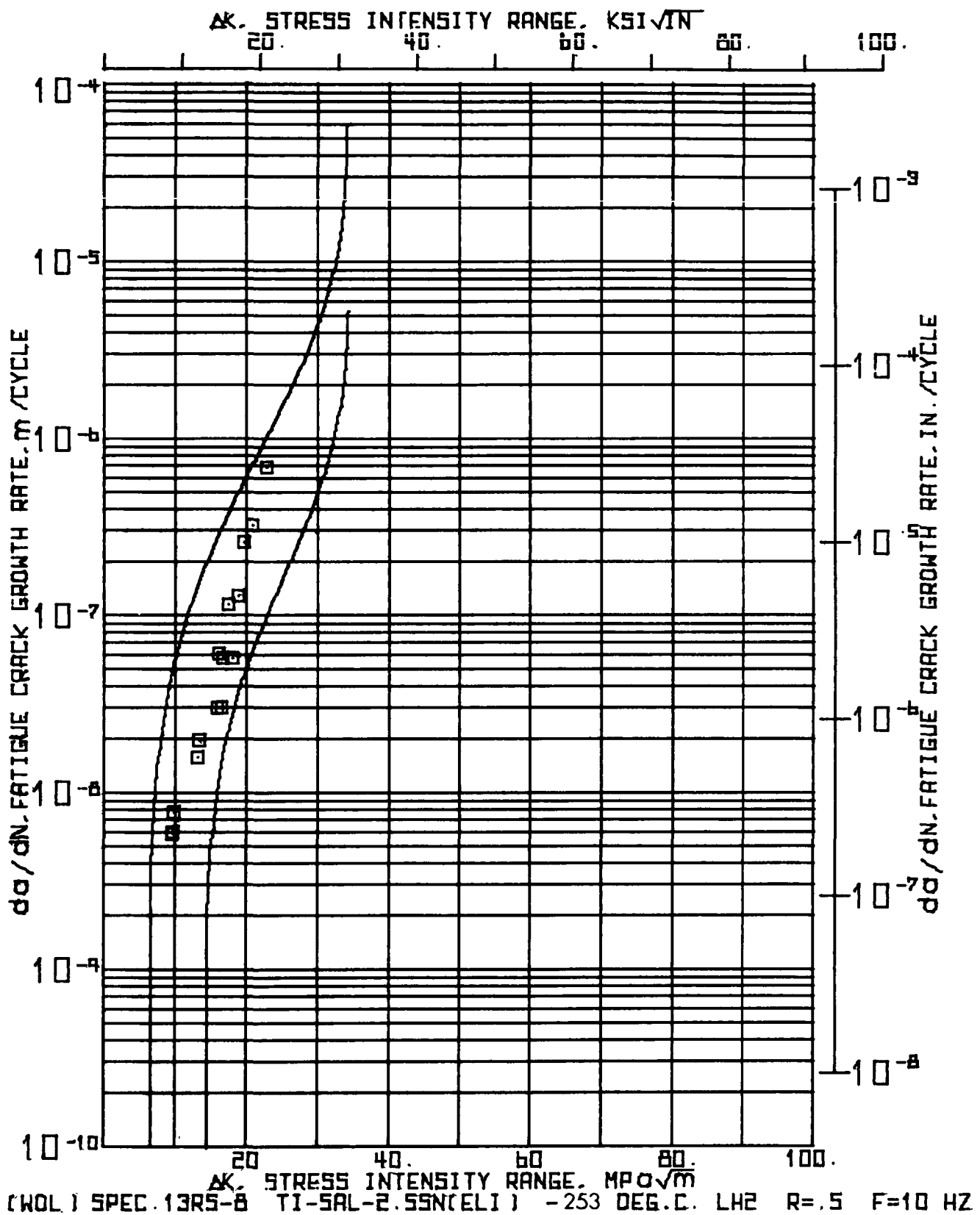
NUMBER OF CYCLES	MAXIMUM LOAD	SIDE 1 CRACK LENGTH	SIDE 2 CRACK LENGTH	CORRECTED AVERAGE		CHANGE IN		CHANGE IN		CRACK GROWTH RATE		STRESS INTENSITY RANGE	
		MM	INCH	MM	INCH	CRACK LENGTH	ASAR	CRACK LENGTH	DA	DN	DA / DN	MPA X 1000	KSI X 1000
231.300	17.79	27.91	1.099	27.91	1.099	29.18	1.149	1.270	0.50	2.500	508.00	28.19	25.66
233.000	17.79	29.18	1.149	29.14	1.149	30.45	1.199	1.270	0.50	1.500	846.67	33.33	27.90
235.300	17.79	30.45	1.199	30.45	1.199	31.72	1.249	1.270	0.50	3.500	362.86	14.29	30.48
238.000	17.79	31.72	1.249	31.72	1.249	32.99	1.299						

(NOL) SPEC.12RS-5 T1-SAL-2-5SN(ELI) -253 DEG.C. LM2 R-0.5 F-10 HZ 10:15 AUG 05, 1976

INPUT CONSTANTS

ELASTIC MODULUS(E) = 114.550E+03 MPa(17.200E+06 PSI)			
NUMBER	CRACK WIDTH	ABAR / W	
OF	COMPLIANCE	OPTICAL COMPLIANCE	
CYCLES	BASE	BASE	
N	CEP		
X 1000			

120.500	37.0232	.372	.360
---------	---------	------	------



INPUT CONSTANTS: 10:15 AUG 05, 1976

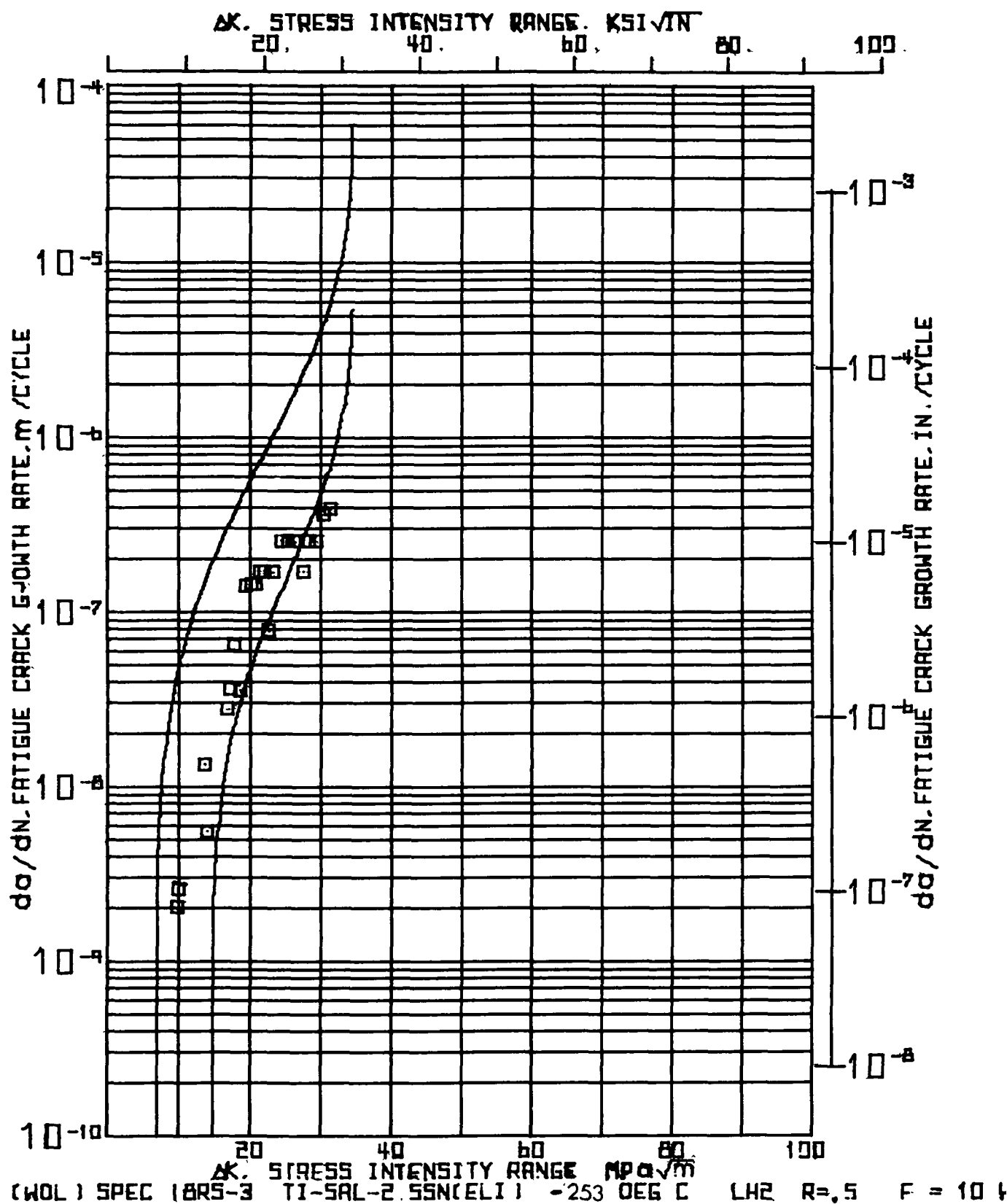
INPUT CONSTANTS:														
RANGE RATIO(R) .50 TEST FREQUENCY(HZ) 10.0 SPECIMEN WIDTH(W) 50.676 MM(.2003 IN.) SPECIMEN THICKNESS(B) 18.918 MM(.745 IN.) CRACK DB. (DIRECTION) 1.270 MM(.050 IN.)														
NUMBER OF CYCLES	MAXIMUM LOAD	SIDE 1 CRACK LENGTH	MM	INCH	MM	INCH	SIDE 2 CRACK LENGTH	MM	INCH	MM	INCH	CORRECTED AVERAGE LENGTH	MM	INCH
000	11.34	2.55	16.69	.665	16.69	.665	16.16	.715						
43.500	11.34	2.55	17.14	.675	17.14	.675	16.41	.725						
87.500	11.34	2.55	17.40	.685	17.40	.685	16.67	.735						
121.000	11.34	2.55	17.65	.695	17.65	.695	16.92	.745						
121.000	15.12	3.40	17.65	.695	17.65	.695	16.92	.745						
137.200	15.12	3.40	17.91	.705	17.91	.705	16.18	.755						
150.200	15.12	3.40	18.16	.715	18.16	.715	16.43	.765						
150.200	17.79	4.00	18.16	.715	18.16	.715	16.43	.765						
158.700	17.79	4.00	18.41	.725	18.41	.725	16.68	.775						
167.200	17.79	4.00	18.92	.745	18.92	.745	20.19	.795						
175.700	17.79	4.00	19.18	.755	19.18	.755	20.45	.805						
184.700	17.79	4.00	19.68	.775	19.68	.775	20.95	.825						
193.700	17.79	4.00	20.70	.815	20.70	.815	21.97	.865						
202.700	17.79	4.00	21.21	.835	21.21	.835	22.48	.885						
210.700	17.79	4.00	22.22	.875	22.22	.875	23.49	.925						
219.700	17.79	4.00	22.99	.905	22.99	.905	24.26	.955						
217.700	17.79	4.00	24.26	.955	24.26	.955	25.53	1.005						
221.700	17.79	4.00	26.29	1.035	26.29	1.035	27.56	1.085						

NUMBER OF CYCLES	MAXIMUM LOAD	CHANGE IN LENGTH	MM	INCH	CHANGE IN CRACK LENGTH	MM	INCH	CHANGE IN CYCLES	CRACK GROWTH RATE DA / DN	STRESS INTENSITY RANGE KSI X 10 ⁻⁵
000	11.34	2.55	16.69	.665	16.69	.665	16.16	.715		
43.500	11.34	2.55	17.14	.675	17.14	.675	16.41	.725		
87.500	11.34	2.55	17.40	.685	17.40	.685	16.67	.735		
121.000	11.34	2.55	17.65	.695	17.65	.695	16.92	.745		
121.000	15.12	3.40	17.65	.695	17.65	.695	16.92	.745		
137.200	15.12	3.40	17.91	.705	17.91	.705	16.18	.755		
150.200	15.12	3.40	18.16	.715	18.16	.715	16.43	.765		
150.200	17.79	4.00	18.16	.715	18.16	.715	16.43	.765		
158.700	17.79	4.00	18.41	.725	18.41	.725	16.68	.775		
167.200	17.79	4.00	18.92	.745	18.92	.745	20.19	.795		
175.700	17.79	4.00	19.18	.755	19.18	.755	20.45	.805		
184.700	17.79	4.00	19.68	.775	19.68	.775	20.95	.825		
193.700	17.79	4.00	20.70	.815	20.70	.815	21.97	.865		
202.700	17.79	4.00	21.21	.835	21.21	.835	22.48	.885		
210.700	17.79	4.00	22.22	.875	22.22	.875	23.49	.925		
219.700	17.79	4.00	22.99	.905	22.99	.905	24.26	.955		
217.700	17.79	4.00	24.26	.955	24.26	.955	25.53	1.005		
221.700	17.79	4.00	26.29	1.035	26.29	1.035	27.56	1.085		

(WDL) SPEC:13RS-A TI-5AL-2.5SN(ELI) - 253 DEG.C, LH2 R-5 F-10 HZ 10115 AUG 05, 1976

INPUT CONSTANTS

ELASTIC MODULUS(E) = 11e+590E+03 MPa(17.200E+06 PSI)			
NUMBER	CRACK	ADAM / W	
OF	ISUTM		
CYCLES	COMPLIANCE	OPTICAL COMPLIANCE	
	BASE	BASE	
N	CE3		
A 1700			
121+000	36+0304	0.372	0.359



(WOL) SPEC.10RS-3 TIAL-2-SSN(ELI) -253 DEG.C. LH2 R0.5 F 10 HZ

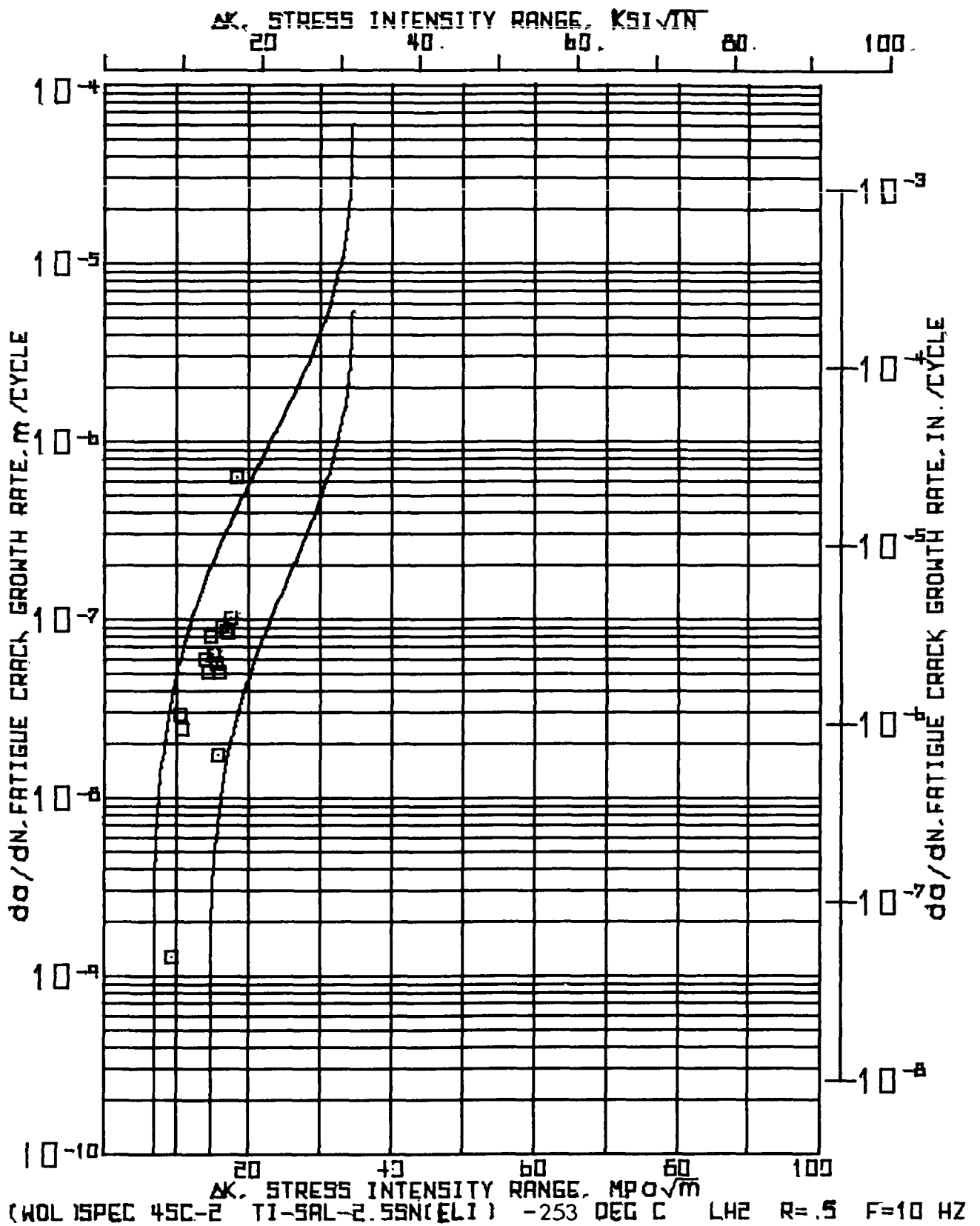
10:15 AUG 05,176

INPUT CONSTANTS:

RANGE RATIO(R) = .50
TEST FREQUENCY(HZ) = 10.0
SPECIMEN WIDTH(IN) = 50.902 MM(2.004 IN.)
SPECIMEN THICKNESS(B) = 18.928 MM(.745 IN.)
CRACK NO. CORRECTION = 1.270 MM(.050 IN.)

NUMBER OF CYCLES	MAXIMUM LOAD	SIDE 1 CRACK LENGTH	SIDE 2 CRACK LENGTH	CORRECTED AVERAGE CRACK LENGTH	CHANGE IN CRACK LENGTH	CHANGE IN CYCLES	CRACK GROWTH RATE DA / DN	STRESS INTENSITY RANGE MPA X DELTA K IN0.5	STRESS INTENSITY RANGE DELTA K IN0.5				
N	P	A1	A2	ABAR	MM	INCH	MM	INCH X 1000					
X 1000	KN	MM	MM	MM	MM	INCH	MM	INCH X 1000					
100	11.34	2.55	17.07	.672	18.34	.722	.254	.010	123.000	2.07	.08	9.82	8.93
123.000	11.34	2.55	17.32	.682	18.59	.732	.254	.010	98.000	2.59	.10	9.93	9.04
221.000	11.34	2.55	17.58	.692	18.85	.742							
221.000	15.12	3.40	17.58	.692	18.85	.742	1.118	.044	84.000	13.30	.52	13.66	12.43
305.000	15.12	3.40	18.09	.736	19.96	.766	.127	.005	23.000	5.52	.22	14.05	12.72
320.000	15.12	3.40	18.82	.741	20.09	.791							
320.000	17.79	4.00	18.82	.741	20.09	.791	.508	.020	18.000	28.22	1.11	16.78	15.27
346.000	17.79	4.00	19.33	.761	20.60	.811	.508	.020	14.000	36.29	1.43	17.19	15.64
362.000	17.79	4.00	19.84	.781	21.11	.831	1.016	.040	15.500	65.55	2.58	17.83	16.23
375.000	17.79	4.00	20.85	.821	22.12	.871	.508	.020	14.300	35.52	1.40	18.51	16.85
389.000	17.79	4.00	21.36	.841	22.63	.891	1.270	.050	9.000	141.11	5.56	19.36	17.62
392.000	17.79	4.00	22.63	.891	23.50	.941	.508	.020	3.500	145.14	5.71	20.27	18.44
402.000	17.79	4.00	23.14	.911	24.41	.961	.508	.020	3.500	145.14	5.71	20.82	18.94
405.000	17.79	4.00	23.65	.931	24.92	.981	.508	.020	3.000	169.33	6.67	21.39	19.47
406.000	17.79	4.00	24.16	.951	25.43	1.001	.508	.020	3.000	169.33	6.67	21.39	20.01
411.000	17.79	4.00	24.66	.971	25.93	1.021	.508	.020	6.500	78.15	3.08	22.62	20.58
416.000	17.79	4.00	25.17	.991	26.44	1.041	.508	.020	3.000	169.33	6.67	23.28	21.18
421.000	17.79	4.00	25.68	1.011	26.95	1.061	1.016	.040	4.000	254.00	10.00	24.32	22.13
425.000	17.79	4.00	26.70	1.051	27.97	1.101	.508	.020	2.000	254.00	10.00	25.44	23.15
427.000	17.79	4.00	27.20	1.071	28.47	1.121							

10:15 AUG 05, '76															PAGE 2	
(MPL) SPEC.18RS-3 T1-SAL-2-55N(ELI) -253 DEGC. LM2 M=5 F=10 HZ																
NUMBER OF CYCLES	MAXIMUM LOAD	P	SIDE 1		SIDE 2		CORRECTED AVERAGE LENGTH	CHANGE IN CRACK LENGTH	CHANGE IN CRACK LENGTH	CHANGE IN CYCLES	CRACK GRBATH RATE	STRESS INTENSITY				
			CRACK LENGTH	A1	CRACK LENGTH	A2						DA / DN	DELTA K			
N	KN	KIPS	MM	INCH	MM	INCH	MM	INCH	MM	INCH	DN X 1000	METER PER CYCLE	MPA X 1000	KSI X 1000		
427.300	17.79	4.00	27.20	1.071	27.20	1.071	26.47	1.021	.762	.030	3.000	254.00	10.00	26.44	24.06	
430.300	17.79	4.00	27.97	1.051	27.97	1.051	29.24	1.151	.505	.020	3.000	169.33	6.67	27.51	25.03	
435.300	17.79	4.00	28.47	1.021	28.47	1.021	29.74	1.171	.508	.020	2.000	254.00	10.00	28.41	25.85	
438.300	17.79	4.00	28.98	1.041	28.98	1.041	30.25	1.191	.504	.020	2.000	254.00	10.00	29.36	26.72	
437.300	17.79	4.00	29.49	1.061	29.49	1.061	30.76	1.211	.508	.020	1.400	362.86	14.29	30.37	27.64	
438.700	17.79	4.00	30.00	1.081	30.00	1.081	31.27	1.231	.508	.020	1.300	390.77	15.36	31.43	28.60	
440.000	17.79	4.00	30.51	1.201	30.51	1.201	31.78	1.251								



10126 AUG 05, 1976

INPUT CONSTANTS:

RANGE RATIO(R) .50
 TEST FREQUENCY(HZ) 10.0
 SPECIMEN WIDTH(W) 50.902 MM(2.004 IN.)
 SPECIMEN THICKNESS(B) 18.900 MM(.744 IN.)
 CRACK BRG CORRECTION 1.270 MM(.050 IN.)

NUMBER OF CYCLES	MAXIMUM LOAD	P KN	SIDE 1 CRACK LENGTH	A1 MM	INCH	MM	INCH	SIDE 2 CRACK LENGTH	A2 MM	INCH	CORRECTED AVERAGE CRACK LENGTH	MM	INCH	CHANGE IN		CHANGE IN CYCLES	CRACK GRWTH RATE DA / DN MICR0 METER PER CYCLE	STRESS INTENSITY RANGE DELTA K	
														DA MM	INCH			MPA X MM ^{3/2}	KSI X IN ^{3/2}
N	X 1000																		
000	10.68	2.40	17.30	.681	17.30	.681	18.57	.731	.127	.005	100.000	1.27	.05	9.32	8.48				
100.000	10.68	2.40	17.42	.686	17.42	.686	18.69	.736	.508	.020	17.550	28.95	1.14	10.64	9.68				
117.550	12.01	2.70	17.93	.706	17.93	.706	19.20	.756	.508	.020	21.000	24.19	.95	10.89	9.91				
134.550	12.01	2.70	18.44	.726	18.44	.726	19.71	.776	.762	.030	9.500	80.21	3.16	14.81	13.48				
151.550	15.12	3.40	20.22	.796	20.22	.796	21.49	.846	.508	.020	8.500	59.76	2.35	14.03	12.77				
168.550	15.12	3.40	20.73	.816	20.73	.816	22.00	.866	.508	.020	10.100	50.30	1.98	14.37	13.08				
185.550	15.12	3.40	20.98	.826	20.98	.826	22.25	.876	.254	.010	4.500	56.44	2.22	15.56	14.16				
202.550	15.12	3.40	21.23	.836	21.23	.836	22.50	.886	.254	.010	14.600	17.40	.68	15.76	14.34				
219.550	15.12	3.40	21.74	.856	21.74	.856	23.01	.906	.508	.020	10.000	50.80	2.00	16.06	14.62				
236.550	15.12	3.40	22.25	.876	22.25	.876	23.52	.926	.508	.020	5.600	90.71	3.57	16.48	15.00				
253.550	15.12	3.40	22.76	.896	22.76	.896	24.03	.946	.508	.020	5.200	86.10	3.32	16.91	15.32				
270.550	15.12	3.40	23.01	.906	23.01	.906	24.28	.956	.254	.010	3.000	84.67	3.33	17.25	15.70				
287.550	15.12	3.40	23.52	.926	23.52	.926	24.79	.976	.508	.020	5.000	101.60	4.00	17.60	16.02				
304.550	15.12	3.40	24.54	.966	24.54	.966	25.81	1.016	1.016	.040	1.600	635.00	25.00	18.33	16.62				

(A)USPEC:4SC-2 T1:5AL-2.5SN(EL1) - 253 DEG.C. LM2 R=5 F=10 HZ 10:26 AUG 05, 1976

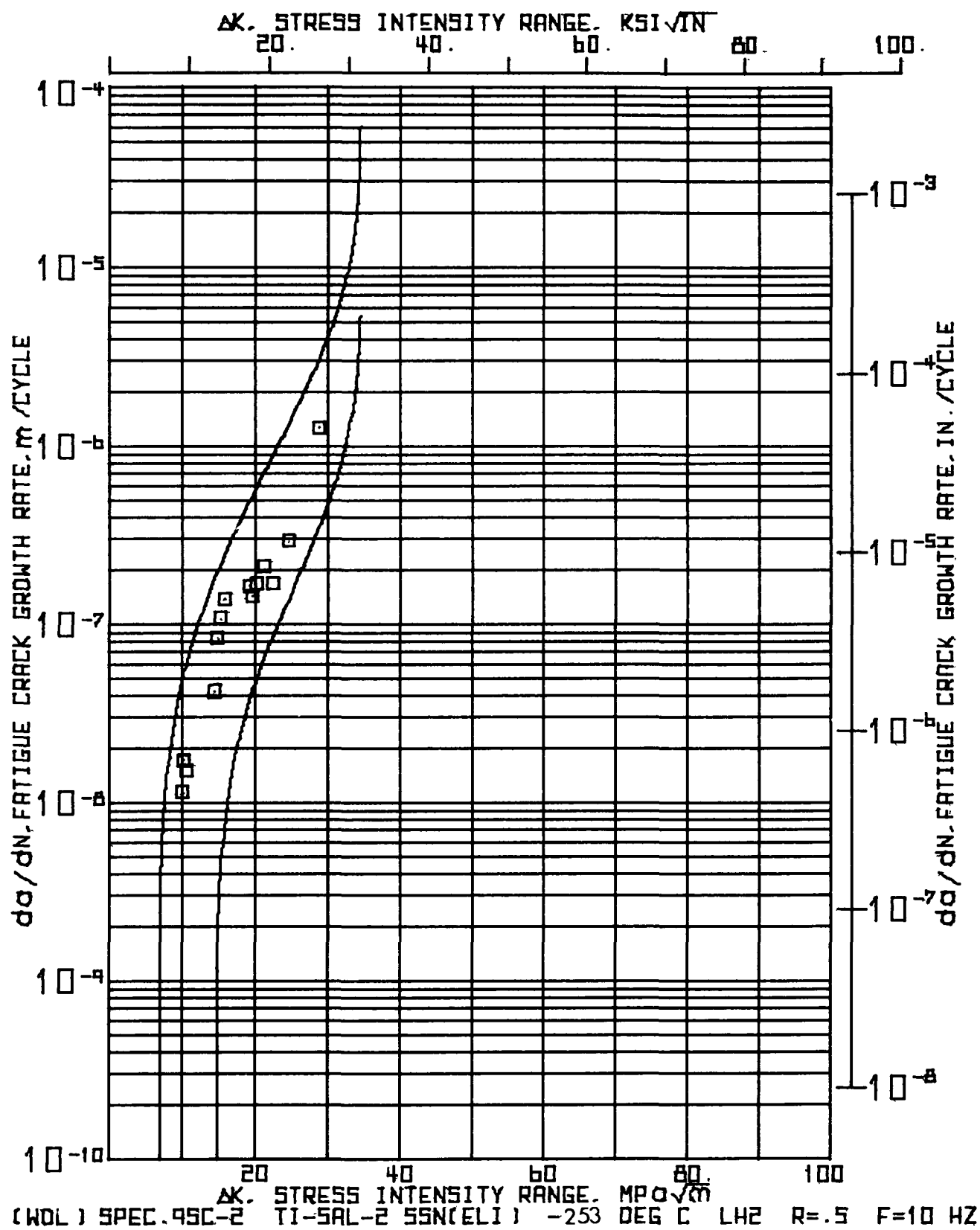
INPUT CONSTANTS

ELASTIC MODULUS(E) = 118.590E+03 HPA(17.200E+06 PSI)

NUMBER	CRACK MOUTH	ADAR / A
1	COMPLIANCE	OPTICAL COMPLIANCE
2	CYCLES	BASE
3	N	CEB

X 1000

179.200	47.945	0.37	0.422
---------	--------	------	-------



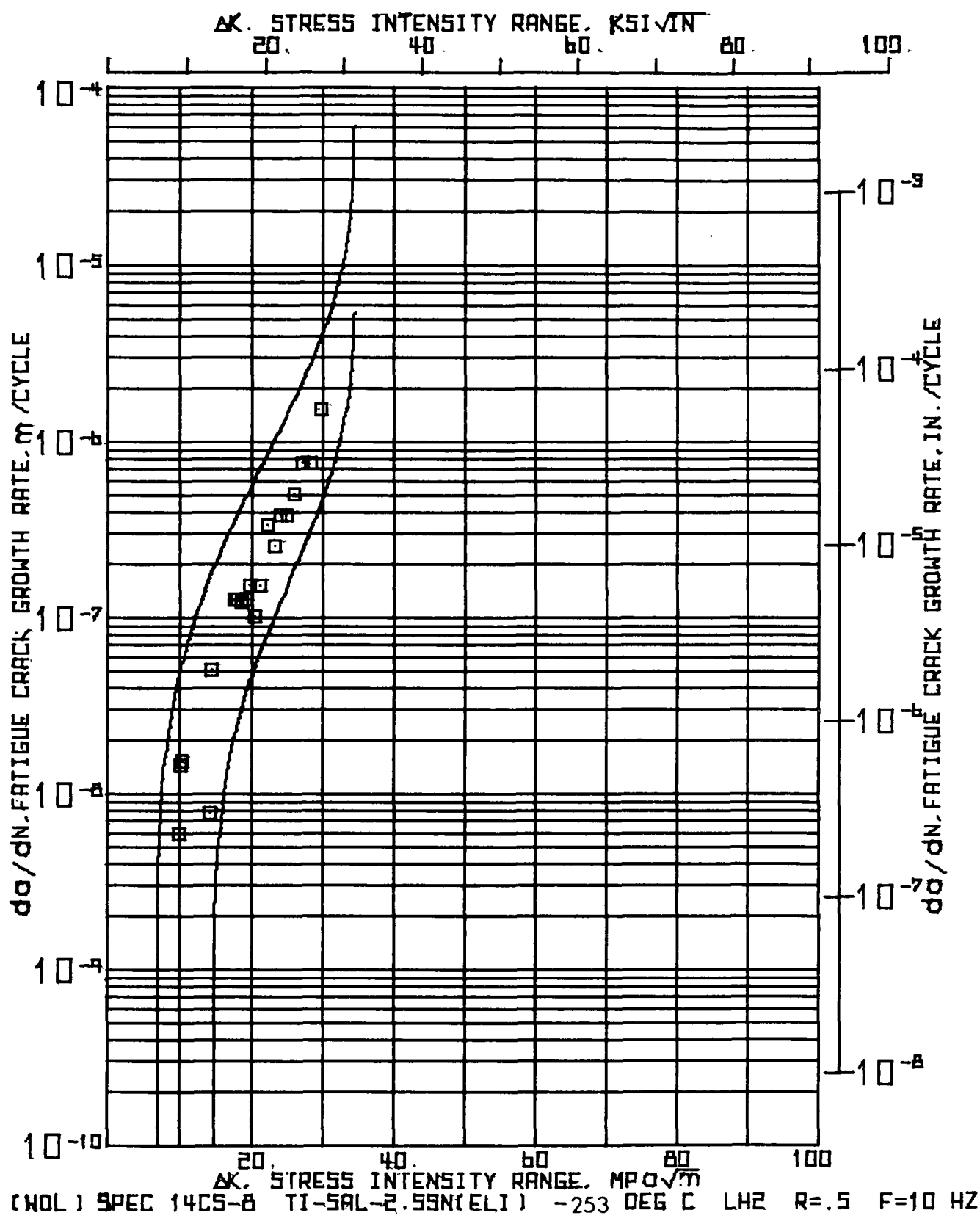
(A3L) SPEC.95C-2 T1-5AL-2.55N(ELT) -253 JEG.C. L#2 R#5 F#10 HZ * * * * *
 * * * * * W E D U E * * * P E N * L 0 A D * P R 0 G R A M * * * * *

10126 AUG 05, 1976

INPUT CONSTANTS:

RANGE RATIO(R) * * * * * .50
 TEST FREQUENCY(HZ) * * * * * 10.0
 SPECIMEN DIA.(IN) * * * * * 50.927 MM(2.005 IN.)
 SPECIMEN THICKNESS(D) * * * * * 18.921 MM(.746 IN.)
 CRACK COR. CORRECTION * * * * * 1.270 MM(.050 IN.)

NUMBER OF CYCLES	LOAD	MAXIMUM LOAD	SIDE 1 CRACK LENGTH	SIDE 2 CRACK LENGTH	CORRECTED AVERAGE CRACK LENGTH	CHANGE IN CRACK LENGTH	CHANGE IN CRACK LENGTH	CHANGE IN CRACK LENGTH	CRACK GRBATH RATE DA / DN	STRESS INTENSITY RANGE DELTA K
A	P	KIPS	MM	MM	MM	MM	MM	MM	IN. PER CYCLE	MPA X 10 ⁻⁵ KSI X 10 ⁻⁵
300	11.34	2.55	17.25	.679	17.25	.679	10.52	.729		
43.500	11.34	2.55	17.75	.699	17.75	.699	19.02	.749	.46	9.33 9.03
67.700	11.34	2.55	18.52	.729	18.52	.729	19.79	.779	.68	10.22 9.30
120.700	11.34	2.55	19.02	.749	19.02	.749	20.29	.799	.61	10.52 9.57
120.700	15.12	3.40	19.02	.749	19.02	.749	20.29	.799		
132.700	15.12	3.40	19.53	.769	19.53	.769	20.80	.819	1.67	14.37 13.07
136.700	15.12	3.40	20.04	.789	20.04	.789	21.31	.839	3.33	14.72 13.39
145.700	15.12	3.40	20.80	.819	20.80	.819	22.07	.869	4.29	15.17 13.81
151.200	15.12	3.40	21.56	.849	21.56	.849	22.83	.899	5.45	15.75 14.34
151.200	17.79	4.00	21.56	.849	21.56	.849	22.83	.899		
154.300	17.79	4.00	22.07	.869	22.07	.869	23.34	.919	6.45	19.13 17.41
157.600	17.79	4.00	22.58	.889	22.58	.889	23.85	.939	5.71	19.64 17.87
160.600	17.79	4.00	23.09	.909	23.09	.909	24.36	.959	6.67	20.16 18.35
166.600	17.79	4.00	24.36	.959	24.36	.959	25.63	1.009	8.33	21.13 19.23
172.800	17.79	4.00	25.37	.999	25.37	.999	26.04	1.049	6.67	22.49 20.47
179.700	17.79	4.00	27.41	1.079	27.41	1.079	28.68	1.129	11.59	24.54 22.33
182.100	17.79	4.00	30.48	1.200	30.48	1.200	31.75	1.250	50.42	28.72 26.14



(WBL) SPEC. 14CS-8 II-5AL-2-55N(ELL) - 253 DEG.C-1H2 R-05 F-10 HZ														10127 AUG 05, 1976	PAGE 2
NUMBR OF CYCLES	MAXIMUM LOAD	SIDE 1 CRACK LENGTH		SIDE 2 CRACK LENGTH		CORRECTED AVERAGE CRACK LENGTH		CHANGE IN CRACK LENGTH DA		CHANGE IN CYCLES		CRACK GROWTH RATE DA / DN		STRESS INTENSITY RANGE DELTA K	
		MM	INCH	MM	INCH	MM	INCH	MM	INCH	DN X 1000	NANOS METER	MICR9 IN.	PER CYCLE	MPA X M-0.5	KSI X IN-0.5
201-700	17.79 4.00	27.79	1.094	27.79	1.094	28.06	1.114	.762	.030	1.000	762.00	30.00	27.10	24.66	
202-700	17.79 4.00	28.55	1.124	28.55	1.124	29.82	1.174	.762	.030	1.000	762.00	30.00	28.44	25.88	
203-700	17.79 4.00	29.31	1.154	29.31	1.154	30.58	1.204	.762	.030	.500	1524.00	60.00	29.89	27.20	
204-200	17.79 4.00	30.07	1.184	30.07	1.184	31.34	1.234								

(*BL) SPEC=1*CS=8 T1=5AL=2*5SN(ELI) =253 DEG.C, LM2 R=.5 F*10.HZ 10:27 AUG 05, '76

INPUT CONSTANTS

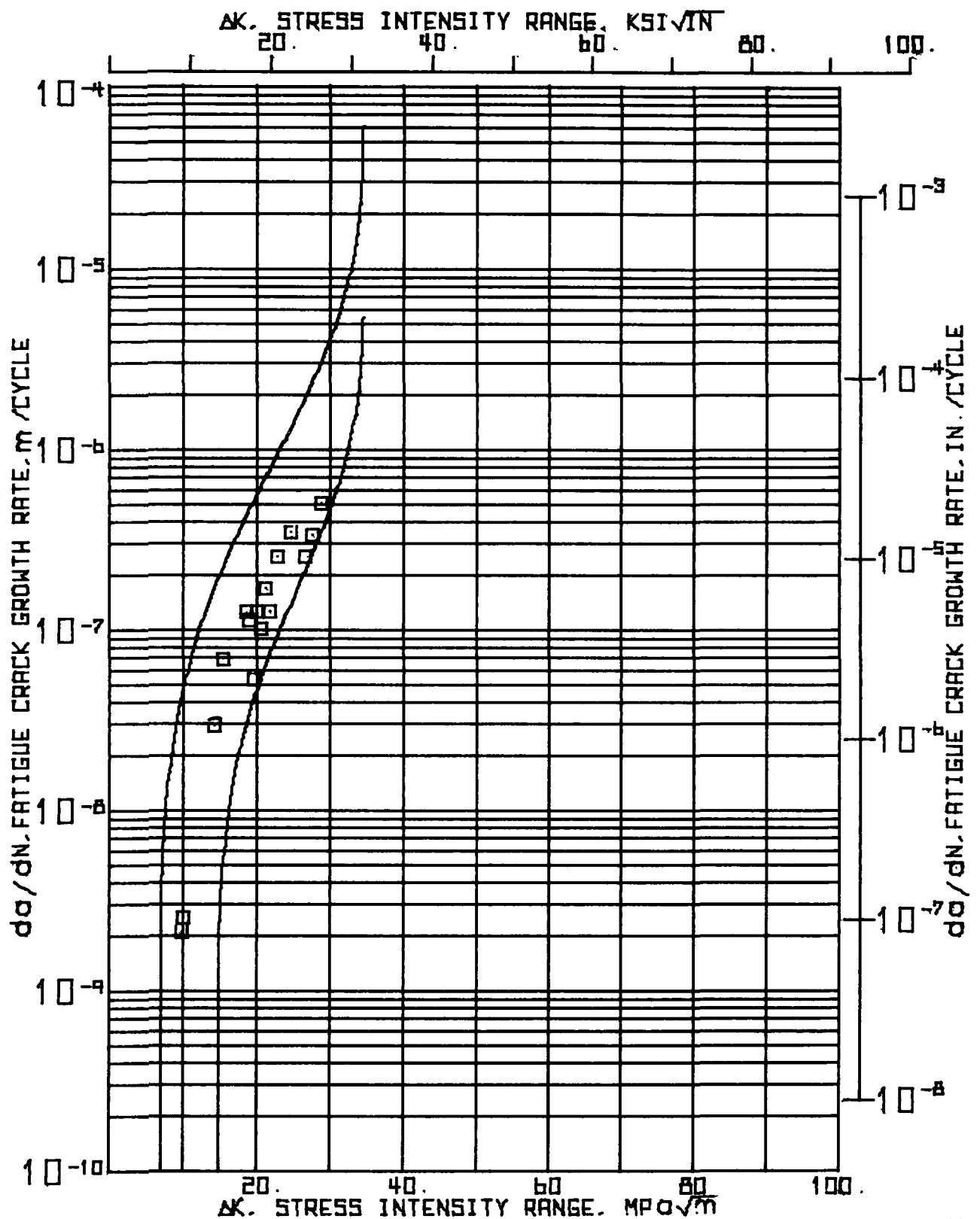
ELASTIC MODULUS(E) = 115.590E+03 MPa(17.200E+06 PSI)

NUMBER	CRACK MOUTH	OPTICAL	ABAK / A
9F	COMPLIANCE	BASE	COMPLIANCE
CYCLES	BASE	BASE	BASE

N CEB

* 1000

120.500	39.3*10	.396	.374
---------	---------	------	------



(49L) SPEC:16CS-8 T10SAL=2.55SN(ELI) -253 DEGC. LH2 R=5 F10 HZ 1012R AUG 05.176

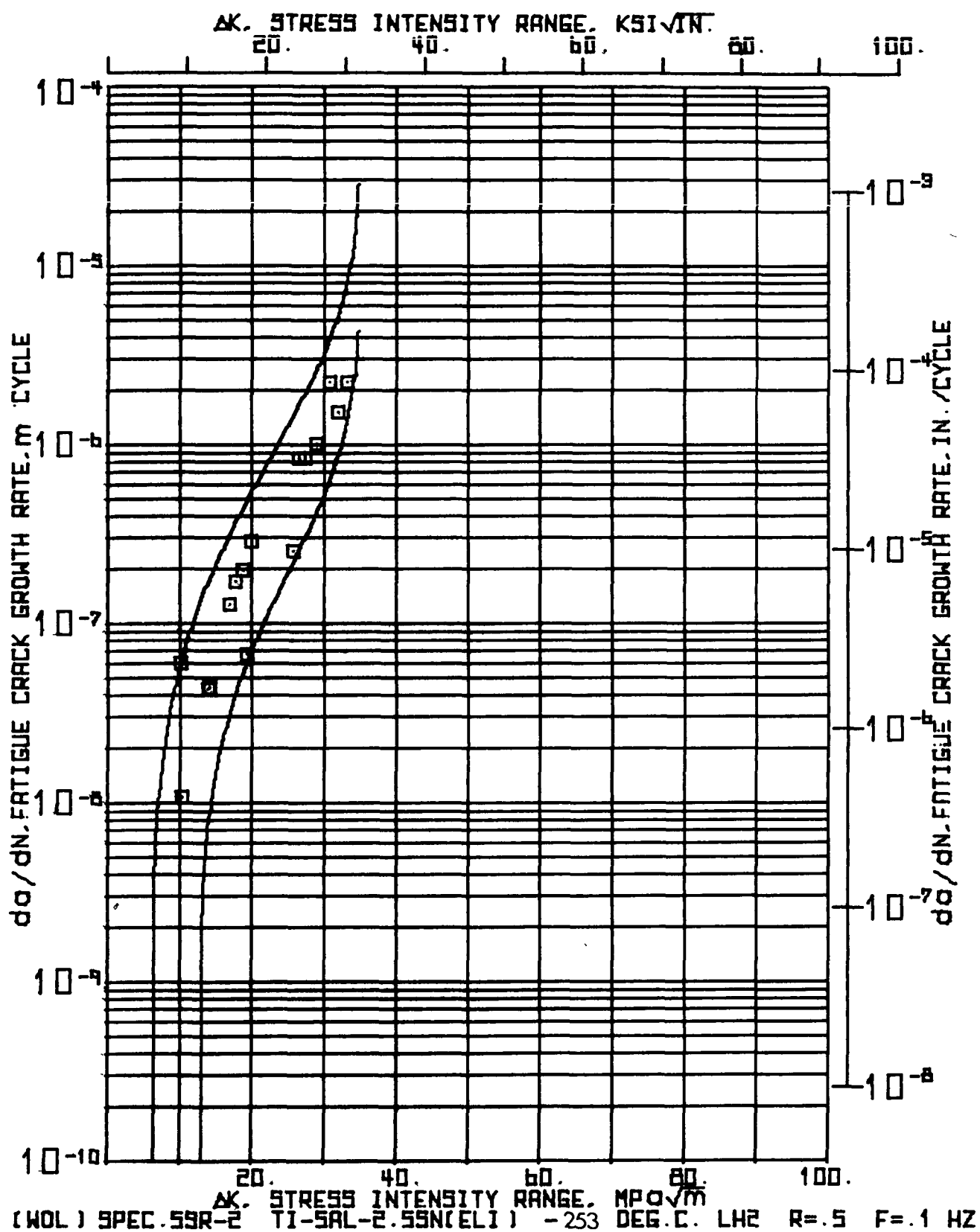
INPUT CONSTANTS:

RANGE RATIO(R) ■ .50
 TEST FREQUENCY(HZ) ■ 10.0
 SPECIMEN WIDTH(W) ■ 50.976 MM(2.007 IN.)
 SPECIMEN THICKNESS(B) ■ 18.933 MM(.745 IN.)
 CRACK 90A CORRECTION ■ 1.276 MM(.050 IN.)

NUMBER OF CYCLES	MAXIMUM LOAD	P	SIDE 1 CRACK LENGTH		SIDE 2 CRACK LENGTH		CORRECTED AVERAGE CRACK LENGTH		CHANGE IN CRACK LENGTH		CHANGE IN CYCLES		CRACK GROWTH RATE		STRESS INTENSITY RANGE	
			KN	INCH	MM	INCH	MM	INCH	MM	DA	DN	INCH X 1000	NANO-METER	DA / DN	MPA X 1000	INCH X 1000
X 1000																
000	11.34	2.55	17.22	.678	17.22	.678	15.49	.728	.254	.010	120.000	2.12	.08	9.86	8.97	
120.000	11.34	2.55	17.48	.688	17.48	.688	15.75	.738	.254	.010	98.500	2.58	.10	9.97	9.08	
240.000	11.34	2.55	17.73	.698	17.73	.698	19.00	.748								
360.000	15.12	3.40	17.73	.698	17.73	.698	19.00	.748	2.489	.098	84.000	29.63	1.17	14.16	12.89	
480.000	15.12	3.40	20.22	.796	20.22	.796	21.49	.846	.762	.030	11.000	69.27	2.73	15.30	13.93	
600.000	17.79	4.00	20.98	.826	20.98	.826	22.25	.876								
720.000	17.79	4.00	20.98	.826	20.98	.826	22.25	.876	.508	.020	4.000	127.00	5.00	18.58	16.91	
840.000	17.79	4.00	21.49	.846	21.49	.846	22.76	.896	.508	.020	4.500	112.89	4.44	19.06	17.34	
960.000	17.79	4.00	22.00	.866	22.00	.866	23.27	.916	.508	.020	9.500	53.47	2.11	19.55	17.80	
1080.000	17.79	4.00	22.50	.886	22.50	.886	23.77	.936	.508	.020	4.000	127.00	5.00	20.07	18.27	
1200.000	17.79	4.00	23.01	.906	23.01	.906	24.28	.956	.508	.020	5.000	101.60	4.00	20.62	18.76	
1320.000	17.79	4.00	23.52	.926	23.52	.926	24.79	.976	.508	.020	3.000	169.33	6.67	21.18	19.28	
1440.000	17.79	4.00	24.03	.946	24.03	.946	25.30	.996	.508	.020	4.000	127.00	5.00	21.77	19.81	
1560.000	17.79	4.00	24.54	.966	24.54	.966	25.81	1.016	1.016	.040	4.000	254.00	10.00	22.71	20.66	
1680.000	17.79	4.00	25.05	1.006	25.05	1.006	26.82	1.056	1.753	.069	5.000	350.52	13.80	24.58	22.37	
1800.000	17.79	4.00	27.30	1.075	27.30	1.075	28.57	1.125	.762	.030	3.000	254.00	10.00	26.51	24.12	
1920.000	17.79	4.00	28.07	1.105	28.07	1.105	29.34	1.155	.508	.020	1.500	338.67	13.33	27.58	25.10	
2040.000	17.79	4.00	28.57	1.125	28.57	1.125	29.84	1.175	.762	.030	1.500	508.00	20.00	28.72	26.13	
2160.000	17.79	4.00	29.34	1.155	29.34	1.155	30.61	1.205								

SECTION A9

This section of the Appendix includes all fatigue crack growth data obtained from WOL coupons tested at -253°C , at a range ratio of 0.5, and at a frequency of 0.1 Hz.



INPUT CONSTANTS:														
RANGE RATIO(R) 50 TEST FREQUENCY(MZ) 1 SPECIMEN WIDTH(W) 50.952 MM(2.006 IN.) SPECIMEN THICKNESS(B) 18.938 MM(.746 IN.) CRACK BG. CORRECTION 1.270 MM(.050 IN.)														
NUMBER OF CYCLES	P KN	MAXIMUM LOAD	SIDE 1 CRACK LENGTH		SIDE 2 CRACK LENGTH		CORRECTED AVERAGE LENGTH	CHANGE IN CRACK LENGTH DA	CHANGE IN CYCLES	CRACK GROWTH RATE DA / DN	STRESS INTENSITY RANGE	STRESS INTENSITY RANGE		
			A1 MM	INCH	A2 MM	INCH						MPA X 10 ⁻³	IN X 10 ⁻³	
000	11.34	2.55	17.07	.672	17.07	.672	18.34	.722						
100	11.34	2.55	17.93	.706	17.93	.706	19.20	.756						
200	11.34	2.55	18.06	.711	18.06	.711	19.33	.761						
250	15.12	3.40	18.06	.711	18.06	.711	19.33	.761						
300	15.12	3.40	18.44	.726	18.44	.726	19.71	.776						
400	15.12	3.40	18.82	.741	18.82	.741	20.09	.791						
500	17.79	4.00	18.82	.741	18.82	.741	20.09	.791						
600	17.79	4.00	19.58	.771	19.58	.771	20.65	.821						
700	17.79	4.00	20.60	.811	20.60	.811	21.67	.861						
800	17.79	4.00	21.74	.856	21.74	.856	23.01	.906						
900	17.79	4.00	22.12	.871	22.12	.871	23.39	.921						
1000	17.79	4.00	22.89	.901	22.89	.901	24.16	.951						
1100	22.24	5.00	22.89	.901	22.89	.901	24.16	.951						
1200	22.24	5.00	23.52	.926	23.52	.926	24.79	.976						
1300	22.24	5.00	24.03	.946	24.03	.946	25.30	.996						
1400	22.24	5.00	24.54	.966	24.54	.966	25.81	1.016						
1500	22.24	5.00	26.06	1.026	26.06	1.026	27.33	1.076						
1600	22.24	5.00	26.57	1.046	26.57	1.046	27.84	1.096						
1700	22.24	5.00	27.33	1.076	27.33	1.076	28.60	1.126						
1800	22.24	5.00	27.84	1.096	27.84	1.096	29.11	1.146						

REFERENCES

1. Van Stone, R. H.; Low, J. R.; and Shannon, J. L., Jr.: The Effect of Microstructure on the Fracture Toughness of Titanium Alloys. NASA, Lewis Research Center, Technical Report No. 2-Ti, December, 1974.
2. Titanium Alloys Handbook, Metals and Ceramics Information Center (Battelle), and Air Force Materials Laboratory, MCIC-HB-02, December, 1972.
3. Crossley, F. A.: Titanium-Rich End of the Titanium-Aluminum Equilibrium Diagram. Transactions of the Metallurgical Society of AIME, Vol. 236, August, 1966.
4. Bartlo, L. J.: The Effect of Microstructure on the Fatigue Properties of Ti-6Al-4V Bar. Reactive Metals, Inc.
5. Convair Astronautics; Report MRG 226, October 20, 1961.
6. McLerron, W. F.; and Foreman, C. R.: Design Data for Materials Subjected to Uniaxial and Multiaxial Stress Fields. AFML TR-65-140, May, 1965.
7. Hurlich, A.: Materials Requirements for Cryogenic Temperature Applications. Materials Science and Technology for Advanced Applications, Prentice-Hall, Inc., 1962.
8. Koehl, B. G.; Williams, D. N.; and Bartlett, E. S.: Investigation of the Reaction of Titanium with Hydrogen. NASA CR-92389, May 18, 1969.
9. Williams, D. N.; and Wood, R. A.: Investigation of the Reaction of 5Al-2.5Sn Titanium with Hydrogen at Subzero Temperature. Final Report on Contract No. NAS-9-12044, May 15, 1972.
10. Ryder, J. T.; Bowie, G. E.; and Pettit, D. E.: Recent Considerations in Experimental Compliance Calibration of the WOL Specimen. Accepted for publication in Engineering Fracture Mechanics, January, 1977.
11. Irwin, G. R.; and Kies, J. E.: Critical Energy Rate Analysis of Fracture Strength. Welding Journal, Vol. 33, 1954, pp. 193-198.

12. Wessel, E. T.: State-of-the-Art of the WOL Specimen for K_{Ic} Fracture Toughness Testing. Engineering Fracture Mechanics, Vol. 1, 1968, pp. 77-101.
13. Sandifer, J. P.; and Bowie, G. E.: Double Exponential Functions that Describe Crack Growth Rate Behavior. To be presented at the AIAA-ASME-SAE 18th Structural Dynamics and Materials Conference, San Diego, CA, March 21-23, 1977 and published in the conference proceedings.
14. Gumbel, E. J.: Statistics of Extremes. Columbia University Press, New York, 1958.
15. Bowie, G. E.; Pettit, D. E.; Ryder, J. T.; and Krupp, W. E.: NDI-Life Analysis Interface. Lockheed-California Company, LR 27013, September, 1974.
16. Pettit, D. E.; and Bowie, G. E.: Verification and Application of Compliance-Based Fatigue Crack Growth Data. Presented at ASM Material Testing and Quality Control Conference, November 11-13, 1975.
17. Pettit, D. E.; Ryder, J. T.; and Bowie, G. E.: Fracture of Engineering Materials. Lockheed-California Company Report, LR 27012, November 1975.
18. Bowie, G. E.: Private Communication, July, 1976.
19. Grandt, A. F., Jr.: Stress Intensity Factors for Some Thru-Cracked Fastener Holes. International Journal of Fracture, Vol. 11, No. 2, 1975.
20. Paris, P. C.; Gomez, M. P.; and Anderson, W. E.: A Rational Analytical Theory of Fatigue. The Trend in Engineering, Vol. 13, No. 1, January, 1961, University of Washington.
21. Emery, A. F.: Stress-Intensity Factors for Thermal Stresses in Thick Hollow Cylinders. Journal of Basic Engineering, Transactions of the ASME, Series D, Vol. 88, No. 1, March, 1966, pp. 45-53.
22. Emery, A. F.; Walker, G. E., Jr.; and Williams, J. A.: A Green's Function for the Stress Intensity Factors of Edge Cracks and Its' Application to Thermal Stresses. Journal of Basic Engineering, Transactions of the ASME, Series D, Vol. 91, No. 4, December, 1969, pp. 618-624.

23. Bueckner, H. F.: Weight Functions for the Notched Bar. *Zeitschrift fur Angewandte Mathematik and Mechanik*, Vol. 51, 1971, pp. 97-109.
24. Timoshenko, S.; and Goodier, J. N.: *Theory of Elasticity*. McGraw-Hill Book Co., Inc., New York, 1951, pp. 69-73.
25. Grandt, A. F., Jr.: Two Dimensional Stress Intensity Factor Solutions for Radially Cracked Rings. Air Force Materials Laboratory Report, TR-75-121, October, 1975.
26. Grandt, A. F., Jr.: Private Communication, February, 1976.
27. Bueckner, H. F.; and Giaever, I.: Stress Concentrations of a Notched Rotor Subjected to Centrifugal Forces. *Z. angew. Math. Mech.* Vol. 46, 1966, pp. 265-273.
28. Bowie, G. E.: Private Communication, Fall, 1975.
29. Robinson, E. L.: Bursting Tests on Steam Turbine Disc Wheels. *Trans. ASME*, Vol. 66, 1944, p. 373.
30. Hencky, H.: Zur Theorie Plastischer Deformationen und der heirdurch im Material hervorgerufenen Nachspannungen. *Z. angew. Math. Mech.*, Vol. 4, 1924, p. 323
31. Johnson, W.; and Mellor, P. B.: *Engineering Plasticity*. Van Nostrand Reinhold Co., London, 1973, pp. 270-278.
32. Clark, W. G.; and Aschini, L. J.: Fatigue Precracking of Spin-Burst Toughness Specimens. SESA Paper 1357. Presented at 1968 SESA Spring Meeting, Albany, N.Y., 1968.
33. *Handbook of Chemistry and Physics*. The Chemical Rubber Co., Cleveland, Ohio, 44th Edition, 1964, p. 145.
34. Van Orden, J.: Private Communication, Analysis of data supplied to G. Wald obtained from Reactive Metals, Inc., transmitted on March 12, 1975.
35. Buczek, M. J.; Hall, G. S.; Seagle, S. R.; and Bomberger, H. B.: Grain Refinement in Titanium Alloys. Air Force Materials Laboratory Report, AFML-TR-74-255, November, 1974.

36. The Mechanical Properties of Ti-6Al-4V, 2-Inch Thick Plate With and Without a Small Addition of Yttrium. Reactive Metals Inc., February, 1975.
37. Titanium Alloys Modified with a Trace of Yttrium. Reactive Metals, Inc., May 8, 1975.
38. Nachtigall, A. J.: Strain Cycling Fatigue Behavior of Ten Structural Metals Tested in Liquid Helium (4K), in Liquid Nitrogen (78K), and in Ambient Air (300K). NASA TN D-7532, February, 1974.
39. Sullivan, T. L.: Behavior of Ti-5Al-2.5Sn(ELI) Titanium Alloy Sheet Parent and Weld Metal in the Presence of Cracks at 20K. NASA TN D-6544, November, 1971.
40. Tiffany, C. F.; Masters, J. N.; and Hall, F. A.: Some Fracture Considerations in the Design and Analysis of Spacecraft Pressure Vessels. Presented at the 1966 National Metal Congress, McCormick Place, Chicago, Illinois.
41. Reuter, W. G.: Fracture Toughness of Ti-5Al-2.5Sn ELI Forging at -423°F. Aerojet Memoranda and Material RD Reports for October 30, 1969 - January 26, 1971.
42. Pettit, D. E.; Ryder, J. T.; Krupp, W. E.; and Hoepfner, D. W.: Investigation of the Effects of Stress and Chemical Environments on the Prediction of Fracture in Aircraft Structural Materials. AFML TR-74-183, December, 1974.
43. Kaplan, W.: Advanced Calculus. Addison-Wesley Publishing Company, Inc., Reading, Mass., 1952, pp. 171-174.
44. Hudak, S. J., Jr.; Bucci, R. J.; and Saxena, A.: Development of Standard Methods of Testing and Analyzing Fatigue Crack Growth Rate Data-Second Semi-Annual Report. AFML Contract F33615-75-C-5064, August, 1976.
45. Adzos, W. X.; Skat, A. C.; and Hillberry, B. M.: Effect of Single Overload/Underload Cycles on Fatigue Crack Propagation. Fatigue Crack Growth Under Spectrum Loads. ASTM STP 595, American Society for Testing and Materials, 1976, pp. 41-60.

46. Pernard, P. J.; Lindley, T. C.; and Richards, C. E.: Mechanisms of Overload Retardation During Fatigue Crack Propagation. Fatigue Crack Growth Under Spectrum Loads. ASTM STP 595, American Society for Testing and Materials, 1976, pp. 78-97.
47. Adetifa, O. A.; Gowda, C. V. B.; and Topper, T. H.: A Mode for Fatigue Crack Growth Delay Under Two-Level Block Loads. Fatigue Crack Growth Under Spectrum Loads. ASTM STP 595, American Society for Testing and Materials, 1976, pp. 142-156.
48. Bell, P. D.; and Wolfman, A.: Mathematical Modeling of Crack Growth Inter-Action Effects. Fatigue Crack Growth Under Spectrum Loads. ASTM STP 595 American Society for Testing and Materials, 1976, pp. 157-171.
49. Jacoby, G. H.; Nowack, H.; and von Lipzig, H. T. M.: Experimental Results and a Hypothesis for Fatigue Crack Propagation Under Variable-Amplitude Loading. Fatigue Crack Growth Under Spectrum Loads. ASTM STP 595, American Society for Testing and Materials, 1976, pp. 172-183.
50. Coles, A.; Johnson, R. E.; and Popp, H. G.: Utility of Surface-Flawed Tensile Bars in Cyclic Life Studies. Transactions of the ASME. The American Society of Mechanical Engineers, Journal of Engineering Materials and Technology, Vol. 98, Series H, No. 4, October 1976, pp. 305-315.
51. Hardrath, H. F.: Fatigue and Fracture Mechanics. AIAA Paper 70-512, Denver, Colorado, April 1970.
52. Packman, P.; et al: The Applicability of a Fracture Mechanics - Non-Destructive Testing Design Criterion. AFML-TR-68-32, 1968.
53. Leak, J. S.: Corrosion - A Study of Recent Air Force Experience. Materials Protection and Performance. January, 1971, pp. 17-20.
54. Lewis, W. F.; and Sproat, W. H.: A Review of Nondestructive Testing for Aerospace Applications. ER 11051, Lockheed-Georgia Company, Marietta, Georgia, January, 1971.

55. Hoepfner, D. W.; and Krupp, W. E.: Prediction of Component Life by Application of Fatigue Crack Growth Knowledge. Engineering Fracture Mechanics, Vol 6, 1974, pp. 47-70.
56. Krupp, W. E.; and Hoepfner, D. W.: Fracture Mechanics Applications in Materials Selection, Fabrication Sequencing and Inspection. Journal of Aircraft, Vol. 10, No. 11, November, 1973, pp. 672-688.
57. Glorioso, S.: Lunar Module Pressure Vessel Operating Criteria Specification. NASA-MSC-SE-V-0024, October 25, 1968.
58. Glorioso, S.; and Ecord, G.: Fracture Mechanics Analysis of Apollo Block I Titanium Alloy Pressure Vessels (Command and Service Modules). Apollo Working Paper No. 1325, 1969.
59. Schwartzberg, F. R.; Kiefer, T. F.; and Keys, R. D.: Determination of Low-Temperature Fatigue Properties of Structural Metal Alloys. Final Report, Martin Co., Martin-CR-64-74, April 1, 1962 - September 30, 1964 (Oct 1964), NASA George C. Marshall Space Flight Center Contract NAS8-2631.
60. Bowie, G. E.: Private Communication. February, 1973.
61. Bowie, G. E.: Elastic-Plastic Analysis of a Rotating Thin Disk; Tresca Conditions. The Boeing Company, Report No. O-R b-4/D4-3336, 1966.
62. Kobayashi, A. S.; Polvanich, N.; Emery, A. F.; and Love, W. J.: Stress Intensity Factor of a Surface Crack in a Pressurized Cylinder. Computational Fracture Mechanics. Presented at the Second National Congress on Pressure Vessels and Piping sponsored by ASME, San Francisco, CA, June 23-27, 1975.
63. Brandt, D. E.: The Development of a Turbine Wheel Design Criterion Based Upon Fracture Mechanics. ASME Paper No. 71-GT-10. Presented at the Gas Turbine Conference and Products Show, Houston, Texas, March 28 - April 1, 1971.

64. Greenburg, H. D.; Wessel, E. T.; and Pryle, W. H.: Fracture Toughness of Turbine-Generator Rotor Forgings. Engineering Fracture Mechanics, Vol. 1, 1970, pp. 653-674.
65. Greenberg, H. D.; Wessel, E. T.; Clark, W. D., Jr.; and Pryle, W. H.: Critical Flaw Sizes for Brittle Fracture of Large Turbine-Generator Rotor Forgings. Westinghouse Research Laboratories, Scientific Paper 69-1D9-MEMTL-P2, December 1, 1969.

DISTRIBUTION LIST

	<u>No. of Copies</u>
NASA-Lewis Research Center	
21000 Brookpark Road	
Cleveland, OH 44135	
Attn: Contracting Officer, MS 400-313	1
Technical Report Control Office, MS 5-5	1
Technical Utilization Office, MS 3-16	1
AFSC Liaison Office, MS 501-3	1
Library, MS 60-3	1
R. H. Johns, MS 49-3	1
G. T. Smith, MS 49-3	18
H. W. Douglass, MS 500-205	1
M&S Contract File, MS 49-1	1
J. C. Freche, MS 49-1	1
National Aeronautics & Space Administration	
Washington, DC 20546	
Attn: RPX/Chief, Liquid Experimental Engineering	1
KT/Technology Utilization Office	1
Library	1
RWS/D. A. Gilstad	1
NASA Scientific and Technical Information Facility	
Attn: Accessioning Department	
P. O. Box 8757	
Balt/Wash International Airport, MD 21240	10
NASA-Ames Research Center	
Moffett Field, CA 94035	
Attn: Library	1
D. Williams	1
NASA-Flight Research Center	
P. O. Box 273	
Edwards, CA 93523	
Attn: Library	1
NASA-Goddard Space Flight Center	
Greenbelt, MD 20771	
Attn: Library	1

DISTRIBUTION LIST (Continued)

	<u>No. of Copies</u>
NASA-John F. Kennedy Space Center Kennedy Space Center, FL 32931 Attn: Library	1
NASA-Langley Research Center Hampton, VA 23365 Attn: Library	1
R. W. Leonard	1
H. Hardrath	1
W. Elber	1
NASA-Manned Spacecraft Center Houston, TX 77001 Attn: Library	1
R. E. Johnson	1
S. V. Glorioso	1
NASA-Marshall Space Flight Center Marshall Space Flight Center, AL 35812 Attn: Library	1
S&E-ASTN/AA/C. Lifer	1
S&E-ASTN/ASR/C. Crockett	1
S&E-ASTN-AS/H. Coldwater	1
Air Force Office of Scientific Research Washington, DC 20333 Attn: Library	1
Air Force Rocket Propulsion Laboratory (RPM) Edwards, CA 93523 Attn: Library	1
Air Force Systems Command Aeronautical Systems Division Wright-Patterson AFB, OH 45433 Attn: Library	1
C. F. Tiffany, Code ENF	1
Air Force Systems Command Andrews Air Force Base Washington, DC 20332 Attn: Library	1

DISTRIBUTION LIST (Continued)

	<u>No. of Copies</u>
Air Force Systems Command Arnold Engineering Development Center Tallahoma, TN 37389 Attn: Library	1
Wright-Patterson Air Force Base Wright-Patterson Air Force Base, OH 45433 Attn: AFML Library D. M. Forney	1 1
Wright-Patterson Air Force Base Wright-Patterson Air Force Base, OH 45433 Attn: AFFDL H. A. Wood	1 1
Frankford Arsenal Philadelphia, PA 19137 Attn: 1320/Library C. Carman	1 1
Department of the Army U. S. Army Material Command Washington, DC 20315 Attn: AMCRD-RC	1
U. S. Army Missile Command Redstone Scientific Information Center Redstone Arsenal, AL 35808 Attn: Document Section	1
Commanding Officer U. S. Army Research Office (Durham) Box CM, Duke Station Durham, NC 27706 Attn: Library	1
Bureau of Naval Weapons Department of the Navy Washington, DC 20360 Attn: RRRE-6	1

DISTRIBUTION LIST (Continued)

	<u>No. of Copies</u>
Commander U. S. Naval Ordnance Laboratory White Oak Silver Springs, MD 20910 Attn: Library	1
Director, Code 6180 U. S. Naval Research Laboratory Washington, DC 20390 Attn: Library	1
H. W. Carhart	1
J. M. Krafft	1
Atomic Energy Commission Division of Reactor Development and Technology Washington, DC 20767	1
National Science Foundation Engineering Division 1800 G Street, NW Washington, DC 20540 Attn: Library	1
Battelle Memorial Institute 505 King Avenue Columbus, OH 43201 Attn: Library	1
E. Hulbert (Dr.)	1
G. Hahn (Dr.)	1
C. Federson	1
IIT Research Institute Technology Center Chicago, IL 60616 Attn: Library	1
Stanford Research Institute 3333 Ravenswood Ave. Menlo Park, CA 94025 Attn: Library	1

DISTRIBUTION LIST (Continued)

	<u>No. of Copies</u>
Brown University Providence, RI Attn: Technical Library	1
J. R. Rice (Dr.)	1
California Institute of Technology Pasadena, CA Attn: Technical Library	1
V. F. Zackay	1
Case Western Reserve University 10090 Euclid Ave. Cleveland, OH 44115 Attn: Technical Library	1
Carnegie Institute of Technology Department of Civil Engineering Pittsburgh, PA 15213 Attn: Library	1
Colorado State University Department of Mechanical Engineering Ft. Collins, CO 80521 Attn: F. Smith (Dr.)	1
Cornell University Department of Materials Science and Engineering Ithaca, NY 14830 Attn: Library	1
Pennsylvania State Univeristy State College, PA Attn: Library	1
University of Denver Denver Research Institute P. O. Box 10126 Denver, CO 80210 Attn: Security Office	1
Aerojet Liquid Rocket Company P. O. Box 15847 Sacramento, CA 95813 Attn: Technical Library, 2484-2115A	1

DISTRIBUTION LIST (Continued)

	<u>No. of Copies</u>
Aerospace Corp. 2400 E. El Segundo Blvd. Los Angeles, CA 90045 Attn: Library-Documents	1
Bell Aerosystems, Inc. Box 1 Buffalo, NY 14240 Attn: J. Davis	1
Brunswick Corp. Defense Products Division P. O. Box 4594 43000 Industrial Ave. Lincoln, NE Attn: Library	1
Chrysler Corp. Space Division P. O. Box 29200 New Orleans, LA 70129 Attn: P. Munafo Library	1 1
Del Research Corp. 427 Main St. Hellertown, PA 18055 Attn: P. Paris (Dr.)	1
Del West Associates, Inc. 6324 Variel Ave. Suite C Woodland Hill, CA 91364 Attn: M. Creager (Dr.)	1
Garrett Corp. Air Research Manufacturing Division 2525 West 190th St. Torrence, CA 90509	1
General American Transportation Corp. General American Research Division 7449 N. Natchez Ave. Niles, IL 60648 Attn: R. N. Johnson (Dr.)	1

DISTRIBUTION LIST (Continued)

	<u>No. of Copies</u>
General Dynamics P. O. Box 748 Ft. Worth, TX 76101 Attn: Library C. D. Little	 1 1
General Dynamics/Convair Aerospace P. O. Box 1128 San Diego, CA 92112 Attn: Library J. Jensen W. Witzel J. Haskins	 1 1 1 1
General Electric Co. Missiles and Space Systems Center Valley Forge Space Technology Center P. O. Box 8555 Philadelphia, PA 19101 Attn: Library	 1
Grumman Aircraft Engineering Corp. Bethpage, Long Island, NY Attn: Library	 1
Jet Propulsion Laboratory 4800 Oak Grove Dr. Pasadena, CA 91103 Attn: Library J. Lewis	 1 1
Ling-Temco-Vought Corp. P. O. Box 5907 Dallas, TX 75222 Attn: Library	 1
Lockheed Missiles and Space Co. P. O. Box 504 Sunnyvale, CA 94087 Attn: Library R. E. Lewis	 1 1

DISTRIBUTION LIST (Continued)

	<u>No. of Copies</u>
Martin-Marietta Corp.	
Denver Division	
P. O. Box 179	
Denver, CO 80201	
Attn: P. Lorenz, MS 0431	1
F. Schwartzberg, MS 0430	1
A. Holsten	1
McDonnell Douglas Aircraft Corp.	
P. O. Box 516	
Lambert Field, MO 63166	
Attn: Library	1
McDonnell Douglas Astronautics	
Western Division	
5301 Bolsa Ave.	
Huntington Beach, CA 92647	
Attn: Library	1
H. Babel	1
R. Rawe	1
North American Rockwell Space Division	
12214 Lakewood Blvd.	
Downey, CA 90241	1
Northrop Space Laboratories	
3401 West Broadway	
Hawthorne, CA	
Attn: Library	1
North American Rockwell, Inc.	
Rocketdyne Division	
6633 Canoga Ave.	
Canoga Park, CA 91304	
Attn: Library, Dept. 596-306	1
G. Vorman	1
North American Rockwell, Inc.	
Space and Information Systems Division	
12214 Lakewood Blvd.	
Downey, CA	
Attn: Library	1
J. Colipriest	1

DISTRIBUTION LIST (Continued)

	<u>No. of Copies</u>
Republic Aviation Fairchild Hiller Corp. Farmington, Long Island, NY Attn: Library	1
Thiokol Chemical Corp. Wasatch Division P. O. Box 524 Bringham City, UT 84302 Attn: Library Section	1
TRW Systems, Inc. One Space Park Redondo Beach, CA 90278 Attn: Technical Library, Document Acquisitions	1
United Aircraft Corp. Corporate Library 400 Main St. East Hartford, CT 06108 Attn: Library	1
United Aircraft Corp. Pratt and Whitney Division Florida Research and Development Center P. O. Box 2691 West Palm Beach, FL 33402 Attn: Library	1
Westinghouse Research Laboratories Beulah Rd., Churchill Borough Pittsburgh, PA 15235 Attn: Library	1
W. K. Wilson	1
G. T. Wessel	1
Massachusetts Institute of Technology Cambridge, MA Attn: Library	1

11 APR 83

Bull Frutberg E453/101 NM 5/74/21622

30

W. DONNELL DOUGLAS
RESEARCH & ENGINEERING LIBRARY

14 00

2 MAY 1977